



# Pervious Concrete Test Cells on MnROAD Low-Volume Road

Minnesota  
Department of  
Transportation

**RESEARCH  
SERVICES**

Office of  
Policy Analysis,  
Research &  
Innovation

Bernard Izevbekhai, Primary Author  
Minnesota Department of Transportation

**December 2011**

Research Project  
Final Report 2011-23

**MnROAD**  
Office of Materials

*Your Destination... Our Priority*



All agencies, departments, divisions and units that develop, use and/or purchase written materials for distribution to the public must ensure that each document contain a statement indicating that the information is available in alternative formats to individuals with disabilities upon request. Include the following statement on each document that is distributed:

To request this document in an alternative format, call Bruce Lattu at 651-366-4718 or 1-800-657-3774 (Greater Minnesota); 711 or 1-800-627-3529 (Minnesota Relay). You may also send an e-mail to [bruce.lattu@state.mn.us](mailto:bruce.lattu@state.mn.us). (Please request at least one week in advance).

## Technical Report Documentation Page

1. Report No. MN/RC 2011-23	2.	3. Recipients Accession No.	
4. Title and Subtitle Pervious Concrete Cells on MnROAD Low-Volume Road		5. Report Date December 2011	
		6.	
7. Author(s) Bernard Igbafen Izevbekhai, Alexandra Akkari		8. Performing Organization Report No.	
9. Performing Organization Name and Address Minnesota Department of Transportation 395 John Ireland Boulevard St Paul, MN 55155		10. Project/Task/Work Unit No.	
		11. Contract (C) or Grant (G) No. (c) LAB879	
12. Sponsoring Organization Name and Address Minnesota Department of Transportation Research Services Section 395 John Ireland Boulevard Mail Stop 330 St. Paul, Minnesota 55155		13. Type of Report and Period Covered Final Report	
		14. Sponsoring Agency Code	
15. Supplementary Notes <a href="http://www.lrrb.org/pdf/201123.pdf">http://www.lrrb.org/pdf/201123.pdf</a>			
16. Abstract (Limit: 250 words)  <p>Local agencies are interested in pervious pavements ability to reduce storm water runoff by allowing direct infiltration through the pavement structure. However, concerns about the ability of pervious pavements to perform in Minnesota's extreme climate, maintenance needs, and effect on groundwater quality needed to be understood.</p> <p>This report includes the design, construction, and early performance of three pervious concrete test cells construction at MnROAD in 2008. These cells were constructed to evaluate the performance of pervious concrete pavements on a low-volume road in a cold weather climate. The three cells discussed in this report are as follows: porous concrete overlay, pervious concrete on granular subgrade, pervious concrete on cohesive subgrade. This report has the following chapters, which uniquely discuss each phase of this project: research synthesis; mix design, concept design, and geotechnical exploration; construction sequence; initial testing; hydrologic evaluation; early two year performance; implementation; effect of sound absorption on OBSI; and acoustic properties of clogged pavements.</p>			
17. Document Analysis/Descriptors Pervious concrete pavement, Porous concrete, Concrete pavements		18. Availability Statement No restrictions. Document available from: National Technical Information Services, Alexandria, Virginia 22312	
19. Security Class (this report) Unclassified	20. Security Class (this page) Unclassified	21. No. of Pages 373	22. Price

# **Pervious Concrete Test Cells on MnROAD Low-Volume Road**

## **Final Report**

*Prepared by:*

Bernard Izevbekhai  
Alexandra Akkari

Minnesota Department of Transportation

**December 2011**

*Published by:*

Minnesota Department of Transportation  
Research Services Section  
395 John Ireland Boulevard, Mail Stop 330  
St. Paul, Minnesota 55155

This report represents the results of research conducted by the authors and does not necessarily represent the views or policies of the Local Road Research Board or the Minnesota Department of Transportation. This report does not contain a standard or specified technique.

The authors, the Local Road Research Board, and the Minnesota Department of Transportation do not endorse products or manufacturers. Any trade or manufacturers' names that may appear herein do so solely because they are considered essential to this report.

## **ACKNOWLEDGMENTS**

The authors acknowledge Keith Shannon and Maureen Jenson of the Minnesota Department of Transportation for their continued support of this type of research. LRRB is acknowledged for their support and funding of this research project. Dan Frentress and Fred Corrigan of ARM of Minnesota are also acknowledged for their help with this study. Finally, the authors express gratitude to both Bruce Holdhusen and Mark Maloney for providing administrative and technical assistance for this project.

# TABLE OF CONTENTS

<b>CHAPTER 1 INTRODUCTION.....</b>	<b>1</b>
<b>1.1 Report Overview .....</b>	<b>1</b>
1.1.1 Chapter 1: Synthesis .....	1
1.1.2 Chapter 2: Pervious Concrete at MnROAD.....	1
1.1.3 Chapter 3: Concept Design, Mix Design, and Geotechnical Exploration .....	1
1.1.4 Chapter 4: Initial Testing .....	1
1.1.5 Chapter 5: Hydrologic Evaluation .....	2
1.1.6 Chapter 6: Early Performance of Pervious Cells .....	2
1.1.7 Chapter 7: Implementation .....	2
1.1.8 Chapter 8: Effect of Sound Absorption on Tire Pavement Interaction Noise .....	2
1.1.9 Chapter 9: Acoustic Properties of Clogged Pervious Concrete Pavements.....	3
<b>1.2 Background .....</b>	<b>3</b>
1.2.1 Hypothesis.....	4
1.2.2 Research Matrix and Methods .....	4
<b>1.3 Synthesis.....</b>	<b>5</b>
1.3.1 Mechanical and Rheological Properties of Pervious Concrete Pavements .....	5
1.3.2 Mix Design & Structural Design of Pervious Concrete Pavements .....	7
1.3.3 Performance of Pervious Concrete .....	8
1.3.4 Tire-Pavement Acoustics of Pervious Concrete .....	10
1.3.5 Construction Issues Benefit-Over-Cost of Pervious Concrete.....	11
<b>CHAPTER 2 CONCEPT DESIGN, MIX DESIGN, AND GEOTECHNICAL EXPLORATION.....</b>	<b>15</b>
<b>2.1 Introduction and Initiative.....</b>	<b>15</b>
2.1.1 MnROAD Instrumentation and Surface Data Collection .....	15
<b>2.2 Research Matrix.....</b>	<b>16</b>
<b>2.3 Design of Pervious Concrete .....</b>	<b>18</b>
2.3.1 Design Process .....	18
2.3.2 Desired Performance Requirements .....	25
2.3.3 Trial Mixing Requirements.....	25
2.3.4 Strength and Gradation Requirements .....	26
2.3.5 Permeability and Porosity Performance Requirements .....	26

2.3.6	Mix Proportions .....	26
2.3.7	Sampling .....	27
<b>2.4</b>	<b>Design Guide Output of Pervious Cells .....</b>	<b>30</b>
2.4.1	Design Guide Output Summary Pervious on Sand.....	31
<b>2.5</b>	<b>Structural Analysis of Pervious Versus Normal Concrete Using I-Slab .....</b>	<b>33</b>
<b>2.6</b>	<b>Hydrological Infiltration Model for Pervious Concrete.....</b>	<b>34</b>
2.6.1	Vertical Pipe and Block Model (Bernard’s Tortuosity Model) .....	34
2.6.2	Reversed Draw Down Model (Bernard’s Concept of Reversed Drawdown).....	36
2.6.3	Hantush Mounding Model .....	36
2.6.4	Dynamic Hydraulic Conductivity Model.....	38
2.6.5	Conventional Green Ampt Infiltration Model .....	41
<b>2.7</b>	<b>Baseline Environmental Contamination and Conditions.....</b>	<b>41</b>
2.7.1	Introduction.....	41
2.7.2	Baseline Environmental .....	42
2.7.3	Baseline Contamination Levels .....	43
2.7.4	Planned Water Quality Testing.....	43
<b>2.8</b>	<b>Geotechnical Report .....</b>	<b>44</b>
2.8.1	Introduction.....	44
2.8.2	Sub-Surface Exploration Strategies .....	44
2.8.3	Subsurface Description .....	45
2.8.4	MnDOT Cone Penetrometer Test Probes .....	45
2.8.5	Foundation Borings.....	46
<b>CHAPTER 3</b>	<b>CONSTRUCTION OF CELL 39, 85 AND 89.....</b>	<b>56</b>
<b>CHAPTER 4</b>	<b>INITIAL TESTING .....</b>	<b>70</b>
<b>4.1</b>	<b>Texture Measurements.....</b>	<b>70</b>
<b>4.2</b>	<b>Friction Testing.....</b>	<b>73</b>
<b>4.3</b>	<b>Sound Absorption Characteristics of the Test Cells.....</b>	<b>76</b>
<b>4.4</b>	<b>On Board Sound Interaction (OBSI) Collection Process .....</b>	<b>80</b>
<b>4.5</b>	<b>Initial Ride Measurement.....</b>	<b>84</b>
<b>4.6</b>	<b>Hydraulic Conductivity Measurements in Pervious Concrete.....</b>	<b>88</b>
<b>4.7</b>	<b>Conclusion .....</b>	<b>92</b>
<b>CHAPTER 5</b>	<b>HYDROLOGIC EVALUATION .....</b>	<b>93</b>

<b>5.1</b>	<b>Introduction.....</b>	<b>93</b>
5.1.1	State of the Art.....	93
5.1.2	Objectives .....	94
<b>5.2</b>	<b>General Layout and Hydrologic Instrumentation.....</b>	<b>94</b>
5.2.1	General Layout.....	95
5.2.2	Transverse Drains .....	95
5.2.3	Piezometers.....	96
5.2.4	Abstraction Wells.....	96
5.2.5	Water Marks and Thermocouples.....	99
<b>5.3</b>	<b>Rainfall and Infiltration .....</b>	<b>99</b>
5.3.1	Rainfall Data .....	100
5.3.2	Infiltration Measurements from Perveameter .....	100
5.3.3	Freeze Thaw Characteristics .....	101
<b>5.4</b>	<b>Mounding Analysis .....</b>	<b>109</b>
5.4.1	Estimation of Aquifer Transmissivity (Not Based in Pumping).....	109
5.4.2	Monitoring Well Observation.....	110
5.4.3	Critical Flood Analysis .....	119
5.4.4	Future Hydrologic Monitoring.....	120
<b>5.5</b>	<b>Conclusion .....</b>	<b>121</b>
<b>CHAPTER 6</b>	<b>EARLY PERFORMANCE OF PERVIOUS CELLS.....</b>	<b>122</b>
<b>6.1</b>	<b>Introduction.....</b>	<b>122</b>
<b>6.2</b>	<b>Test Descriptions.....</b>	<b>122</b>
6.2.1	Ride Characteristics .....	123
6.2.2	Surface Characteristics.....	124
6.2.3	Noise Characteristics .....	126
6.2.4	Physical Properties.....	127
<b>6.3</b>	<b>Results .....</b>	<b>130</b>
6.3.1	Ride Results .....	131
6.3.2	Surface Results.....	134
6.3.3	Noise Results .....	138
6.3.4	Physical Property Results .....	148
<b>6.4</b>	<b>Analysis and Interpretation of Results .....</b>	<b>165</b>

6.4.1	Roughness Index and Surface Rating Discussion.....	165
6.4.2	Texture and Friction Discussion.....	166
6.4.3	Sound Absorption Analysis.....	167
6.4.4	Variation in Nuclear Density.....	168
6.4.5	Variation in Dissipated Volumetric Rate.....	172
6.4.6	FWD Trend Discussion.....	174
6.4.7	Temperature and Moisture Trends and Comparison.....	175
6.4.8	Environmental Versus Traffic Loading.....	175
<b>6.5</b>	<b>Auto-Regression Integrated Moving Average Modeling.....</b>	<b>176</b>
6.5.1	Time Series Analysis.....	176
<b>6.6</b>	<b>Chapter Summary.....</b>	<b>181</b>
6.6.1	Surface Characteristics.....	181
6.6.2	Noise Characteristics.....	182
6.6.3	Physical Properties.....	182
<b>CHAPTER 7</b>	<b>IMPLEMENTATION.....</b>	<b>183</b>
7.1	<b>Detroit Lakes.....</b>	<b>183</b>
7.2	<b>Shoreview.....</b>	<b>185</b>
7.3	<b>Relation of Sound Absorption to Permeability of Pervious Pavements.....</b>	<b>191</b>
<b>CHAPTER 8</b>	<b>EFFECT OF SOUND ABSORPTION COEFFICIENT ON TIRE PAVEMENT INTERACTION NOISE.....</b>	<b>193</b>
8.1	<b>Introduction.....</b>	<b>193</b>
8.2	<b>Porous Pavement Sound Absorption Theory.....</b>	<b>195</b>
8.3	<b>In-Situ Data Collection.....</b>	<b>196</b>
8.3.1	Objective.....	196
8.3.2	Definitions.....	196
8.4	<b>Results of Sound Absorption Testing.....</b>	<b>197</b>
8.5	<b>OBSI – Sound Absorption Correlation.....</b>	<b>198</b>
8.6	<b>Investigation of OBSI SA Correlation in 3<sup>rd</sup> Octave Frequency Domain.....</b>	<b>205</b>
8.7	<b>Components of the Sound Absorption Coefficient.....</b>	<b>205</b>
8.8	<b>Conclusions.....</b>	<b>207</b>
<b>CHAPTER 9</b>	<b>ACOUSTIC PROPERTIES OF CLOGGED PERVIOUS CONCRETE PAVEMENTS.....</b>	<b>209</b>

<b>9.1</b>	<b>Introduction.....</b>	<b>209</b>
<b>9.2</b>	<b>Research Significance .....</b>	<b>210</b>
<b>9.3</b>	<b>Description of Test Sections .....</b>	<b>210</b>
<b>9.4</b>	<b>Municipal Maintenance Strategies.....</b>	<b>211</b>
<b>9.5</b>	<b>Field Evaluation of Maintenance Strategy .....</b>	<b>212</b>
9.5.1	Infiltrometer .....	212
9.5.2	In-Situ Density Evaluation.....	213
9.5.3	In-Situ Sound Absorption Measurements.....	214
<b>9.6</b>	<b>Performance Evaluation of Clogged Test Cells.....</b>	<b>214</b>
<b>9.7</b>	<b>A Quantitative Evaluation of Maintenance Strategy .....</b>	<b>215</b>
<b>9.8</b>	<b>Field Evaluation and Analysis .....</b>	<b>216</b>
<b>9.9</b>	<b>Discussion.....</b>	<b>217</b>
<b>9.10</b>	<b>Conclusion and Recommendation .....</b>	<b>219</b>
<b>CHAPTER 10</b>	<b>FINAL CONCLUSIONS.....</b>	<b>231</b>
<b>REFERENCES.....</b>		<b>233</b>
<b>APPENDIX A: GEOTECH REPORT FROM FOUNDATIONS UNIT</b>		
<b>APPENDIX B: GLOSSARY</b>		
<b>APPENDIX C: ENVIRONMENTAL SAMPLING</b>		
<b>APPENDIX D: TEST WELL MEASUREMENTS AS OF 6/18/08</b>		
<b>APPENDIX E: EXCERPTS OF TESTING REPORT</b>		
<b>APPENDIX F: RELEVANT EXCERPT OF CONSTRUCTION ENGINEER'S NOTES</b>		
<b>APPENDIX G: MORE PICTURES</b>		
<b>APPENDIX H: ADDITIONAL RIDE DATA FOR PERVIOUS CELLS</b>		
<b>APPENDIX I: SA PLOTS WITH DATA FROM ALL EQUIPMENT</b>		
<b>APPENDIX J: TIME SERIES PLOTS FOR SA DATA</b>		
<b>APPENDIX K: RIDE CHARACTERISTIC DATA</b>		
<b>APPENDIX L: NOISE CHARACTERISTIC DATA</b>		
<b>APPENDIX M: PHYSICAL PROPERTY DATA</b>		

## LIST OF FIGURES

Figure 2.1: Aerial View of MnROAD, Showing the Pervious Cells 39, 85 and 89 the LVR .....	17
Figure 2.2: Pavement Design Layout.....	21
Figure 2.3: Crack Prediction for Pervious Pavement on Clay .....	32
Figure 2.4: Structural Analysis of Pervious Versus Normal Using ISlab.....	34
Figure 2.5: Bernard’s Block and Pipe Hydraulic Model .....	34
Figure 2.6: Hydraulic Conductivity Model (Perveammeter Design).....	38
Figure 2.7: Predicted Hydraulic Conductivity Model.....	40
Figure 2.8: A Green-Ampt Model .....	41
Figure 2.9: Borings for MW 1 2 3 & 4 Showing Soils Encountered.....	47
Figure 2.10: Layout of November 2007 Borings.....	48
Figure 2.11: Pervious Well 1 Completed Sand-and-Gravel-Packed, Bentonite-Slurried Cased and Capped .....	49
Figure 2.12: Saturated Sands Encountered.....	49
Figure 2.13: Well 2 Encountered Saturated Sands Up to 30 Ft Depth below Surface .....	50
Figure 2.14: Stiff Gray Clays Encountered at 32 to 36 ft Well 2 .....	50
Figure 2.15: Doug Lindenfelser, Chavonne Hopson and Jack Herndon Drilling Well #4 .....	51
Figure 2.16: In the Water Bearing/Saturated Layers, Auger Sample-Retention Was Minimal ...	51
Figure 2.17: CPT PROBE 1 .....	52
Figure 2.18: CPT Probe 2 .....	53
Figure 2.19: CPT Probe 3 .....	54
Figure 2.20: CPT Probe 4 .....	55
Figure 3.1: Cell 39 Sensor Layout .....	59
Figure 3.2: Sensor Layout in Cell 85 .....	60
Figure 3.3: Sensor Layout.....	61
Figure 3.4: Layout of Sensors in Cell 89 .....	62
Figure 3.5: Schematic Longitudinal Section though the Porous Overlay Cell.....	64
Figure 3.6: Porous Overlay Compaction .....	65
Figure 3.7: Porous Overlay Multi-Drum Screed Compactor.....	65
Figure 3.8: Porous Overlay Surface.....	66
Figure 3.9: Cell 89 Pervious Concrete on Clay and Cell 88 Porous Asphalt on Clay.....	66

Figure 3.10: Establishing 10 Ft Joints in Cells 85 and 89 .....	67
Figure 3.11: Cell 39 Looking NW Showing Porous Concrete Overlay, Bituminous Transition and French Drain Shouldering Aggregate .....	68
Figure 3.12: Cross Drain Construction between Porous Cell 86 and Control Cell 87 .....	69
Figure 4.1: CTM Display of a RWP Inside Lane Spot after 800 Cycles.....	70
Figure 4.2: CTM Display of a RWP Inside Lane Spot after 800 Cycles.....	71
Figure 4.3: CTM Display of a RWP Outside Lane Spot .....	71
Figure 4.4: CTM Display of a RWP Outside Lane Spot .....	72
Figure 4.5: CTM Display of a RWP Outside Lane Spot .....	72
Figure 4.6: Grip Tester.....	73
Figure 4.7: Initial Sound Absorption Test Results.....	77
Figure 4.8: Sound Absorption Factor for Each Cell .....	78
Figure 4.9: One Third Octave Frequency Response of 2 Sets of Microphones .....	80
Figure 4.10: Cells 85 and 86 Spectral Properties.....	81
Figure 4.11: LVR North Side OBSI .....	83
Figure 4.12: 2009 Spring OBSI Data.....	84
Figure 4.13: In-Situ Hydraulic Conductivity Measurement Device (Crude Perveammeter) .....	89
Figure 5.1: Enhanced X-Section through the Pavement.....	94
Figure 5.2: Transverse Drains in Cells 85-89 .....	96
Figure 5.3: Transverse Drain and Flow-Out Meters.....	97
Figure 5.4: Flow-Out Meter Partial Assembly .....	97
Figure 5.5: Drainable Railroad Ballast and Improvised Sensor Cage .....	98
Figure 5.6: Water Mark on Cell 85, Installed to 6 Ft below the Surface.....	99
Figure 5.7: December 2008 Watermark and Thermocouple Data for Cell 85.....	102
Figure 5.8: June 2009 Watermark and Thermocouple Data for Cell 85.....	103
Figure 5.9: December 2008 Thermocouple Data for Cell 85 .....	104
Figure 5.10: June 2009 Thermocouple Data for Cell 85 .....	105
Figure 5.11: December 2008 Watermark Data for Cell 85.....	105
Figure 5.12: June 2009 Watermark Data for Cell 85.....	106
Figure 5.13: Fluctuation of Top Water Level in the Observational Wells .....	113
Figure 5.14: Ensemble Mounding Analysis.....	114
Figure 5.15: Impulsive Mounding .....	116

Figure 5.16: Reservoir Routing Algorithm Derived for Each Layer .....	117
Figure 6.1: Lightweight Inertial Surface Analyzer .....	124
Figure 6.2: Digital Inspection Vehicle.....	124
Figure 6.3: (a) Circular Texture Meter and (b)Friction Trailer .....	125
Figure 6.4: (a) OBSI Intensity Meters and (b) Sound Absorption Tube .....	127
Figure 6.5: (a) Nuclear Density Meter and (b) Falling Head Permeability Device .....	129
Figure 6.6: (a) Relikor Vacuum Truck Assembly and (b) Dynatest FWD.....	130
Figure 6.7: Cell 39 IRI.....	131
Figure 6.8: Cell 85 IRI.....	132
Figure 6.9: Cell 89 IRI.....	132
Figure 6.10: Cell 39 SR .....	133
Figure 6.11: Cell 85 SR .....	133
Figure 6.12: Cell 89 SR .....	134
Figure 6.13: Cell 39 CTM.....	134
Figure 6.14: Cell 85 CTM.....	135
Figure 6.15: Cell 89 CTM.....	135
Figure 6.16: Cell 39 FN .....	136
Figure 6.17: Cell 85 FN .....	137
Figure 6.18: Cell 89 FN .....	137
Figure 6.19: Cell 39 OBSI .....	138
Figure 6.20: Cell 85-86 OBSI.....	139
Figure 6.21: Cell 88-89 OBSI.....	139
Figure 6.22: OBSI Spectrum – Cell 39 IL .....	140
Figure 6.23: OBSI Spectrum – Cell 39 OL.....	140
Figure 6.24: OBSI Spectrum – Cell 85 IL .....	141
Figure 6.25: OBSI Spectrum – Cell 85 OL.....	141
Figure 6.26: OBSI Spectrum – Cell 89 IL .....	142
Figure 6.27: OBSI Spectrum – Cell 89 OL.....	142
Figure 6.28: Difference in OBSI Octave Bands Between Runs – Cell 39 .....	143
Figure 6.29: OBSI Spectrum – All Cells Average.....	143
Figure 6.30: Cell 39 SA .....	147
Figure 6.31: Cell 85 SA .....	147

Figure 6.32: Cell 89 SA .....	148
Figure 6.33: Nuclear Density Results - All Cells .....	149
Figure 6.34: Mean Dissipated Volumetric Rate - All Cells.....	150
Figure 6.35: Difference in Sound Absorption after 2 <sup>nd</sup> Vacuum: Cells 39, 85 and 89.....	150
Figure 6.36: Difference in Dissipated Volumetric Rate after 2 <sup>nd</sup> Vacuum: Cells 39, 85 and 89	151
Figure 6.37: 2009 FWD Results – Cell 39 IL Slab 2 Center .....	153
Figure 6.38: 2009 FWD Results – Cell 39 OL Slab 2 Center.....	154
Figure 6.39: 2009 FWD Results – Cell 85 IL Slab 8 Center .....	155
Figure 6.40: 2009 FWD Results – Cell 85 OL Slab 8 Center.....	156
Figure 6.41: 2009 FWD Results – Cell 89 IL Slab 16 Center .....	157
Figure 6.42: 2009 FWD Results – Cell 89 OL Slab 16 Center.....	158
Figure 6.43: 2010 FWD Results – Cell 39 IL.....	159
Figure 6.44: 2010 FWD Results – Cell 39 OL .....	159
Figure 6.45: 2010 FWD Results – Cell 85 IL.....	160
Figure 6.46: 2010 FWD Results – Cell 85 OL .....	160
Figure 6.47: 2010 FWD Results – Cell 89 IL.....	161
Figure 6.48: 2010 FWD Results – Cell 89 OL .....	161
Figure 6.49: Cell 39 Thermocouple .....	162
Figure 6.50: Cell 85 Thermocouple .....	163
Figure 6.51: Cell 89 Thermocouple .....	163
Figure 6.52: Cell 87 Thermocouple .....	164
Figure 6.53: Cell 39 Watermark .....	164
Figure 6.54: Cell 85 Watermark .....	165
Figure 6.55: Ratio of Porous Versus Non-Porous SA – Bit and PCC .....	168
Figure 6.56: Density 95% Confidence Interval – Cell 39.....	169
Figure 6.57: Density 95% Confidence Interval – Cell 85.....	169
Figure 6.58: Density 95% Confidence Interval – Cell 89.....	170
Figure 6.59: Density – Inside Versus Outside Lane All Cells.....	171
Figure 6.60: Dissipated Volumetric Rate 95% CL – Cell 39 .....	173
Figure 6.61: Dissipated Volumetric Rate 95% CL – Cell 89 .....	173
Figure 6.62: Dissipated Volumetric Rate 95% CL – Cell 85 .....	174
Figure 6.63: Cell 39 IL Predictions.....	177

Figure 6.64: Cell 39 OL Predictions .....	178
Figure 6.65: Cell 85 IL Predictions.....	178
Figure 6.66: Cell 85 OL Predictions .....	179
Figure 6.67: Cell 89 IL Predictions.....	179
Figure 6.68: Cell 89 OL Predictions .....	180
Figure 7.1: Detroit Lakes Pervious Concrete.....	183
Figure 7.2: Detroit Lakes Pervious Concrete Surface .....	184
Figure 7.3: Detroit Lakes Pervious Concrete Permeability .....	184
Figure 7.4: Detroit Lakes Pervious Concrete Sound Absorption .....	185
Figure 7.5: Pervious Concrete in Shoreview .....	186
Figure 7.6: Pervious Concrete Surface in Shoreview .....	186
Figure 7.7: Shoreview Pervious Concrete Permeability .....	187
Figure 7.8: Shoreview Sound Absorption at 1000 Hz .....	189
Figure 7.9: Change in Shoreview SA from 2010 to 2011.....	190
Figure 7.10: Change in Permeability from 2010 to 2011 .....	191
Figure 7.11: Sound Absorption Versus Dissipated Volumetric Rate .....	192
Figure 8.1: Porous Concrete Cells .....	199
Figure 8.2: Comparison of Sound Absorption Coefficients of Porous and Non Porous Pavements .....	201
Figure 8.3: Line-Fit Plots for Porous and Non-Porous OBSI Versus Sound Absorption.....	203
Figure 9.1: Boat Ramp Pervious Filtration System Detroit Lakes Minnesota .....	223
Figure 9.2: General Structure of MnROAD Pervious Pavement.....	224
Figure 9.3: Vacuum Used on MnDOT Test Cells and Agents Collected at the Receptacle.....	225
Figure 9.4: MnDOT's Pervious Pavement Hydraulic Conductivity/ Infiltrometer Device.....	225
Figure 9.5: Nuclear Gage and BSWA 435 Sound Absorption Impedance Tube.....	226
Figure 9.6: Maintained Versus Unmaintained SA Trends.....	227
Figure 9.7: Sound Absorption of Clogged and Unclogged Locations in City of Shoreview .....	228
Figure 9.8: Accelerated Clogging Test .....	228
Figure 9.9: Results of Clogging Experiment .....	229
Figure 9.10: Section through Idealized Closely Packed Pervious Matrix .....	230

## LIST OF TABLES

Table 2.1: Location Allocation and Design Matrix for New Pervious Pavements.....	18
Table 2.2: Design ESALS for Current and Proposed LVR Cells.....	20
Table 2.3: Present Load Configurations .....	21
Table 2.4: Mix Design Process .....	22
Table 2.5: Permeability and Porosity Performance Range .....	26
Table 2.6: Mix Proportioning .....	27
Table 2.7: Mix Designs for Cell 64 .....	28
Table 2.8: Final Mix Designs for Cell 64 .....	29
Table 2.9: MnROAD Pervious Reliability Summary .....	31
Table 2.10: Prediction of Mounding for a Sustained 1in/hr Rain Using a VBA Model for the above Equation.....	37
Table 4.1: Initial friction Test (GRIP NUMBER) .....	75
Table 4.2: Summary Data for Sound Absorption on MnROAD Pavements .....	79
Table 4.3: OBSI of South Side of LVR .....	81
Table 4.4: OBSI Summary OBSI on North Side of LVR.....	82
Table 4.5: IRI of Test Cells Measured with the LWP Fall 2008 .....	85
Table 4.6: IRI of Test Cells Measured in Pervious Cells April 2009 .....	88
Table 4.7: Fall 2009 Flow Time for Porous Cells .....	91
Table 5.1: Rainfall Data Summary .....	100
Table 5.2: Comparison of Average Time of Discharge through a Porous Pavement.....	100
Table 5.3: Flow Measurements Concrete 1/23/09 .....	107
Table 5.4: Sample Flow Measurement on 1/23/09 .....	108
Table 5.5: Monitoring Well Observation with Respect to Time .....	111
Table 5.6: Mounding Analysis.....	112
Table 5.7: Comparison of 2008 to 2009 Well Observation Considering Rainfall Difference ...	115
Table 5.8: Approximate Transmissivity Deductions (6).....	120
Table 6.1: OBSI Spectrum Cell 39 .....	144
Table 6.2: OBSI Spectrum Cell 85 .....	145
Table 6.3: OBSI Spectrum Cell 89 .....	146
Table 6.4: Difference in Flow Time after 1 <sup>st</sup> Vacuum.....	151
Table 6.5: Mean Profile Depth Summary .....	166

Table 6.6: Friction Number Summary .....	167
Table 6.7: Mann Whitney Z-Test Density Results .....	172
Table 6.8: Environmental Versus Traffic Loading .....	176
Table 6.9: OBSI Autocorrelation Coefficients .....	181
Table 7.1: Shore Test Location Description and Permeability .....	188
Table 8.1: Descriptive Statistics Comparing Porous to Non-Porous Sound Absorption and OBSI .....	198
Table 8.2: Sound Absorption Ratios for Various Pavements .....	200
Table 8.3: Summary Output for OBSI of Porous and Non-Porous Pavements .....	204
Table 8.4: Component Absorption Coefficients $\alpha$ (f) Obtained from all MnROAD Pavements	206
Table 9.1: MnDOT and Municipal Pervious Concrete Projects and Test Sections.....	221
Table 9.2: Flow Times Before and After Vacuuming .....	222

## EXECUTIVE SUMMARY

This report includes the design, construction, and early performance of three pervious concrete test cells construction at MnROAD in 2008. These cells were constructed to evaluate the performance of pervious concrete pavements on a low-volume road in a cold weather climate. MnROAD research facility, located in Monticello, Minnesota, is one of the largest outdoor, real-time and real-life pavement testing facilities in the world. Opened in 1994, the facility is made up of the mainline that is a 3.5-mile, two-lane section carrying west-bound Interstate Highway 94 traffic and a 2.5 mile-long low-volume road “loop” that is trafficked by an 18-wheel truck. The facility is made up of approximately 50 test cells consisting in 80 sub-cells of experimental rigid or flexible pavements of various mechanical, environmental and structural and surface factorials.

The three cells discussed in this report are as follows:

- Cell 39 (low-volume loop) porous concrete overlay
- Cell 85 (low-volume loop) pervious concrete on granular subgrade
- Cell 85 (low-volume loop) pervious concrete on cohesive subgrade

Many significant findings resulted from this study that will contribute to the design and maintenance of pervious concrete pavements. Only a few of these conclusions are listed below:

- The pervious test cells show improved sound absorption compared to typical PCC pavement.
- Dissipated volumetric rate varied significantly throughout cells, suggesting uneven material consistency. This flow rate was generally higher in cell 85 (granular base) than cell 89 (clay base).
- Temperature and moisture sensors show a reduced temperature gradient throughout the pavement, base, and subgrade, and possibly a reduced amount of freeze thaw cycles for full-depth pervious concrete.
- Vacuuming more than two times a year has shown promising results and improved performance compared to the original lighter maintenance schedule. Pervious pavements can be maintained over time with this amount of effort.
- The frequent raveling of the pervious cells is suspected to be from freeze-thaw distress. Keeping the pavement unclogged can likely lessen the chances for this freeze-thaw damage to happen, and therefore reduce raveling.
- Predicting OBSI from sound absorption does not seem feasible at this point. This is likely because sound relief in pervious pavements comes from air compression instead of the conventional methods found in normal concrete.
- It is evident the sound absorption is related to the porosity of pervious pavements.
- The infiltration methods used in the pervious concrete cells can be maintained over time if proper maintenance activities are performed.
- Evaluation of the pervious test cells over the years has shown FWD deflection results higher than other typical concrete pavements. It is unsure how this can translate into

durability. However, a relationship between the two is very likely and this matter should be a subject of further study.

# CHAPTER 1 INTRODUCTION

## 1.1 Report Overview

Pervious pavement provides a solution for many highly developed urban areas where an excessive amount of contaminated water is diverted into storm and sewer systems and left untreated before entering natural water sources such as rivers and streams. By allowing water to flow through the pavement surface and infiltrate the underlying soil, pervious pavements can reduce the amount of this pollution. The test cells at MnROAD will be monitored for drainability to evaluate the possibility of using pervious pavements to mitigate this problem. Other important criteria influencing the performance of pervious concrete in pavements will also be monitored, including mechanical and structural properties, surface characteristics, noise, and durability.

This report has seven chapters which uniquely discuss each phase of this project.

### *1.1.1 Chapter 1: Synthesis*

This chapter presents the literature review done on the design, construction, and performance of pervious concrete pavements completed in other regions and by other agencies. The purpose of this literature review was to aid in the design, construction, evaluation process and experimental design of the three pervious concrete cells at MnROAD.

### *1.1.2 Chapter 2: Pervious Concrete at MnROAD*

This chapter includes a description of the mix design and pavement design for the pervious concrete cells at MnROAD. It also includes a discussion of the geotechnical evaluation and conditions at the MnROAD site done prior to construction.

### *1.1.3 Chapter 3: Concept Design, Mix Design, and Geotechnical Exploration*

This chapter is simply a detailed construction report documenting all phases of work involved in constructing cells 39, 85, and 89. Many photographs are also included for better representation of the completed activities and pavement throughout the construction process.

### *1.1.4 Chapter 4: Initial Testing*

This chapter provides the results from the initial performance evaluation completed soon after construction of the three pervious test cells in 2008. This evaluation included the following tests to measure many of the important properties used to determine overall performance.

- Texture Measurement ASTM E-2157 using the Circular Track Meter method
- In-Situ Sound Absorption Measurement using the prescribed ISO standard (NCAT Device)
- In-Situ (Dynamic) OBSI measurements using the provisional AASHTO standard
- Ride measurement using the MnDOT LISA Light Weight Profiler
- Friction Measurement using MnDOT Dynatest Friction Lock Wheel Skid trailer ASTM E-274

- Friction Measurement using FHWA Grip Tester from the FHWA Loans Program
- Indirect Hydraulic Conductivity tests

### ***1.1.5 Chapter 5: Hydrologic Evaluation***

The full-depth porous cells were designed as detention and retention systems that would ultimately infiltrate ground water. This chapter evaluates the concept, instrumentation, and general rainwater infiltration and transmission in the five porous full-depth cells. It analyzes the likelihood of flood after computing the rate of filling of each layer, which is a stepped function that may be likely. The equations are thus developed for each layer. Pumping tests were not performed for the determination of transmissivity of the aquifer. An estimation of the transmissivity of the aquifer was therefore performed. There was not sufficient precipitation since the fall of 2008 to provide reliable sufficient sub surface response data. However, there was sufficient evidence from the downstream monitoring wells that there was increased water elevation in the water bearing subgrade after construction of the porous systems.

### ***1.1.6 Chapter 6: Early Performance of Pervious Cells***

This chapter discusses the two year performance of the three pervious concrete test cells to evaluate the possible benefits of pervious concrete in pavements, such as increased durability, sound absorption, and drainability. This report describes the test methods conducted on cells 39, 85 and. The international roughness index, surface rating, surface texture, friction number, on board sound intensity, sound absorption, nuclear density, dissipated volumetric rate, falling weight deflection, clogging characteristics, temperature and moisture conditions were evaluated. All data collected from this evaluation during the first two years of testing is included in this chapter. The data was analyzed using statistical tests and time series analysis. Finally, all major trends and observations made during the first two years were discussed. Continued monitoring of the test cells will develop an understanding of the long-term performance for more effective and efficient design of permeable pavements.

### ***1.1.7 Chapter 7: Implementation***

This chapter presents two paving projects in the region where pervious concrete has been implemented. Photographs, sound absorption and permeability test methods and results are provided. Analysis of the relation between sound absorption and permeability for pervious concrete is also included.

The appendix of this report houses additional valuable materials and test results related to the pervious test cells. Relevant reports which complement the information in this report are also included.

### ***1.1.8 Chapter 8: Effect of Sound Absorption on Tire Pavement Interaction Noise***

This chapter provides the results of a study done to evaluate the relationship between sound absorption and OBSI for pervious pavements. SA and OBSI testing was done on the pervious cells at MnROAD and at other project sites. Sound absorption coefficients of porous pavement are generally higher than those of non-porous pavements. Of the 304 sound absorption test conducted over a period of 12 months, and the corresponding OBSI measured, there was no clear

correlation between sound absorption coefficient and OBSI. Ninety percent of the OBSI for porous pavements were less than 100-dBA, the typical industrial pivot for porous pavements. However, of the non-porous pavements, 25 percent of the measured OBSI was less than 100-dBA. Comparable OBSI was obtained between porous pavements and the innovative grinding where 90% of the measurements were less than 100-dBA as well.

Generally, the process of ascertaining if relationship exists between OBSI and sound absorption in the spatial and spectral domain are discussed. It is concluded that sound absorption is not the mechanism by which porous concrete pavements reduce noise. Since porous pavements are generally quiet, the mechanism of relief air compression is a tenable porous concrete pavement quietness mechanism.

### ***1.1.9 Chapter 9: Acoustic Properties of Clogged Pervious Concrete Pavements***

This chapter uses data collected since 2005 of properties of pervious concrete pavements at MnROAD and other project sites to evaluate how clogging can effect acoustic properties.

Paradoxically, non pervious pavements are similar to pervious pavements in their requirements for drainability for durability. However pervious concrete requires that the voids should be connected and free of clogging agents for durability of conductive and acoustic properties. The effect of clogging and the characteristics of pervious concrete clogged with various agents are examined.. Desirable acoustic absorption and hydraulic conductivity are reduced when pervious concrete is clogged and may be restored with adequate maintenance practices.

## **1.2 Background**

This section discusses the ramifications of current research and practice of pervious concrete in pavement and water engineering. It elucidates the existing best practices and accentuates research findings that are germane to this study. To achieve this objective, the section is divided into the following subsections.

- Mechanical and rheological properties of pervious concrete
- Mix design and structural design of pervious concrete pavements
- Performance of pervious concrete
- Tire –Pavement Acoustics of pervious concrete pavements
- Benefit/cost of Using Pervious Portland Cement Concrete Pavements

Ordinarily storm water run-off necessitates expensive design and construction of storm water structures that include detention or infiltration ponds. Intuitively, there is a huge saving in cost if the paved surface in pervious and conducts the storm water directly to the ground. The Pervious concrete design provides this benefit. Normal concrete is impervious and may contain entrained air up to 7.5 % as in our high performance concrete. The entrained air is discontinuous in normal concrete permeability is infinitesimal compared to the rate of flooding or ponding or run-off on the pavement surface. Pervious concrete is made up of gap-graded aggregate linked by cement paste, systematically placed to allow for contiguous voids or cavities that allow for free passage of water.

The reduction of pervious surfaces has been an issue of concern with the construction of bound pavement surfacing. Some Cities in the Metro area have been forced to improvise methods of minimizing storm water intrusion from developments that are in proximity to wetlands or some trout streams. Run-off from impervious surfaces has been known to distort the thermal balance of streams when extreme temperatures precede heavy rains. In solving this problem some communities they have made various attempts to encourage some infiltration by constructing pervious concrete on porous bases. While their understanding of the performance of pervious concrete in Northern climates is still rudimentary, MnDOT in collaboration with the Aggregate Ready mixed Association of Minnesota provides leadership in this technology. The partnership resulted in the construction of a pervious concrete pavement in a parking lot in MnROAD in 2005 and a pedestrian walkway in 2006. In 2008 three pervious test cells were constructed in MnROAD's mainline.

### ***1.2.1 Hypothesis***

Research objective is to validate these hypotheses.

- Pervious concrete improves surface drainage
- Minimizes Peak flow
- Under traffic condition and freeze thaw cycles it may perform sufficiently.
- Reduces noise through the slip stick and slap mechanism. Due to porosity and the structure, noise reduction is enhanced by the horn mechanism.
- Pervious concrete provides good wet weather friction and excellent anti-hydroplaning potential.
- EPA records filtration of pollutants. Studies conducted in Maryland indicate reduction of 80 to 90% total solids 65 to 80% in phosphorus and 60 to 60% of total nitrogen.
- The measured Effective flow Resistivity (EFR) values for porous pavements are lower than those of non-porous pavements.

### ***1.2.2 Research Matrix and Methods***

- Construct and instrument pervious concrete cells in the MnROAD low-volume roads.
- Create sub cells with different mix design types Based on the MnDOT 2005 initiative and the ISU 2005 report on Mix Design Development for Pervious Concrete in Cold Weather Climates.
- Provide an infiltration model for the pervious media. This includes characterizing the soils up to 20 ft deep and analyzing infiltration based on porosity of the various layers. Create a Hydrological model and validate.
- Determine actual freezing and thawing cycles as well conduct a surface condition survey.
- Monitor qualitatively and quantitatively for more than 5 years comparing performance of pavement on clay to performance of pavement over sand
- Observe and measure stress strain response, freeze-thaw degradation and cracking or heaving.

## 1.3 Synthesis

### 1.3.1 *Mechanical and Rheological Properties of Pervious Concrete Pavements*

Izevbekhai et al (1) wrote a construction report for the pervious concrete driveways in MnROAD observed that the surface characterization of a pervious concrete surface is not as easy as with the normal concrete. In their report titled Construction of a Pervious Concrete Parking Lot in MnROAD, a detailed instrumentation layout was discussed. Preliminary FWD tests accentuated some comparison between Pervious concrete and normal concrete. Their respective elastic moduli were back calculated as 10 and 25 GigaN/m<sup>2</sup> (.5 & 3.8 Kpa) respectively.

Izevbekhai and Eller (2), performed a 1 year performance report on the pervious concrete driveway. The report is comprised of petrographic analysis, surface rating, a schmidt hammer Survey as well as a chain drag. The petrographic analysis identified voids ranging from 10 to 23 percent in the test cores from top to bottom. The variation in porosity was observed only in test cores taken from adjacent test pads placed bas sacrificial sources for taking semi destructive samples. Uniform void content with respect to depth was observed in cores taken on the actual pad. A distress survey showed extensive raveling on the spot where concrete trucks were delayed and a cold joint could have otherwise been formed. Moderate raveling was observed in the tooled joints.

Since the completion of the above reports (1,2) more work has been done. Concerns about the structure clogging up with time birthed a research task in place to develop hydraulic conductivity monitoring. A “Perveammeter” has been improvised and calibrated for this purpose. The perveammeter measures and consequently monitors hydraulic conductivity, which is a quantitative indication of degree of clogging. Relevant equations for discharge from a varying head were developed. The Perveammeter was calibrated for discharge time in air as lower bound, in normal concrete as lower bound. Results for discharge time through the pervious concrete media would be expected to stay within this range otherwise equipment malfunction is suspected. The degree of clogging will be compared to the sound absorption and tire pavement interaction noise and other properties. Typical unit weight of pervious concrete ranged from 127 to 129 pcf.

In the report titled Interlocking Concrete Block Pavements (ICBP)At Howland Hook Marine Authors (3) described how ICBP was used to tackle the problem of Subgrade soils that would have otherwise caused instability in normal pavements. Sieglen-We; and Von-Langsdorff-H catalogued the performance of Interlocking Concrete block Pavements in Ports. In a report published by the American Society for Civil Engineers ASCE in 2004, The Port Authority of New York and New Jersey has constructed the first port pavement in North America that includes both impermeable and permeable interlocking concrete block pavements for container handling equipment. Located in the northwest corner of Staten Island in New York City, the Howland Hook Marine Terminal expanded the existing container yard by approximately 5 ha (12 acres) in an area with a subgrade that is subject to failure due the presence of gypsum. Interlocking concrete block pavement (ICBP) was selected for resistance to container loads, particularly damage at corner castings, and because of the potential subgrade problems. They are frequently used for overseas ports, and are now an established option for ports in North America.

(3) The pavement design was for a 20-year service life of the current grounded container yard that uses chassis (highway and off-road) to move container between the yard and the ship, and top picks and lift trucks at the 4-high container stacks.

According to authors (3) the container handling equipment resulted in dual wheel axle loads of 97,500 kg (215,000 lb) excluding dynamic forces. The stacked containers can result in point loads of up to 23,000 kg (50,000 lb) at each corner casting at the bottom container. A unique aspect of this project was the inclusion of an installation of 0.25 acres of permeable interlocking concrete block pavement (PICBP) that can be utilized to demonstrate the structural, hydraulic and water quality enhancement properties of PICBP. Permeable pavement is one of several strategies that will be considered for meeting water quality requirements that are anticipated for many future major expansions of existing facilities or for new port facilities. This paper presents information on the selection, design, and construction of the ICBP and PICBP and the experience during the initial container yard operations. Haselbach-Liv-M; Freeman-Robert-M (4) discussed some hydrological and structural properties of pervious concrete pavements in a report titled "Vertical Porosity Distributions in Pervious Concrete Pavement" The material was studied for its potential in solving environmental problems caused by urban runoff occurring in developed areas. This was part of a report published in ACI Materials Journal. 2006/11. Additionally this paper discusses the porosity, hydrological strength and properties of pervious concrete, an alternative paving material. Results of the research show significant top to bottom increases in porosity when slabs of approximately 15 cm (six inches) in height are placed with an approximately 10% surface compaction technique. This is modeled in a series of vertical porosity distribution equations that use both the compaction percentage and average cored porosities. This is similar to what was discussed by Izevbekhai and Eller. Uniform porosity with respect to depth is a needed property of pervious concrete and construction practices must strive to minimize this variability

The American Concrete Institute committee (5) also published a working document titled Pervious Concrete ACI 522 R06 in 2006. This document serves as a generic process that industry uses for construction and general source of fundamental practice related issues pertaining to pervious concrete. Tennis, Paul D. Leming, Michael L. Akers, David J. (8) published a document titled Portland Cement Association similar to the ACI document discussed already (5) . The publication titled Pervious concrete pavements 3<sup>rd</sup> edition was published by Portland Cement Association, Skokie in 2004.

A publication of the 2005-03 issue of Concrete international discussed the link between pervious pavements and hydrological problems and a stepwise approach to a pervious pavement solution to a storm water or hydrological problem. In one paper, Offenbergh-M (6) discussed the advantages of ground water infiltration and reduction of run-off. The article describes a low strength, dry porous concrete that has characteristics that may make pervious concrete a tricky material to work with, but that may also make it a developer's friend. One of the key features of pervious concrete is that it can be used to create structurally sound pavement that drains storm water, thus reducing runoff and replenishing groundwater supplies. The article points out that each party involved in the construction of a pervious concrete pavement must know their responsibility and identify the keys to their success. Finally, the paper focused on the concrete contractors' role in the success of the pervious pavement.

Many features of pervious concrete are similar to those of pervious asphalt. Many reports on pervious asphalt are in consequence germane to pervious concrete. In a study of the aggregate for the pervious asphalt concrete. Partl, M.N.; Momm, L; Filho B; Bernucci, L.L. (7) presented a paper titled Performance Testing and Evaluation of Bituminous Materials PTEBM'03 at the RILEM conference held in 2003. The paper is available in the Proceedings of the 6<sup>th</sup> International RILEM Symposium Held Zurich, Switzerland, 14-16 April 2003. 2003. pp237-43. The aggregate gradation of pervious asphalt concrete is studied to maximize the interconnected void contents and the permeability. The arrangement of the aggregate gradation was chosen from three aggregate maximum sizes and different gaps in the gradation. The binder contents have been getting with the aid of Marshall test, considering the functions: the void content, the interconnected void content and the Cantabro test. The interconnected void contents are defined from the Marshall specimens. Plates were made to evaluate rutting and permeability; three plates for each mixture, according to the French standard with the tire machine LPC. The test results showed that the optimum choice of the gap resulted in interconnected void higher than 25% and with speed of drainage higher than 7 cm/s in the permeability test. The values of the loss in the Cantabro test were less than 25% and the rutting values were smaller than 10%. The study showed that it is possible to obtain pervious asphalt concrete with interconnected void content close to 25% by controlling the gap in the aggregate gradation.

### ***1.3.2 Mix Design & Structural Design of Pervious Concrete Pavements***

Delatte NJ (9) presented a paper titled “Structural Design of Pervious Concrete Pavement” at the 2007 Transportation Research Board 86th Annual Meeting. It identified the challenges facing prospective designers of pervious concrete notably, the absence of a current rational process for design.

As the use of pervious concrete pavement broadens, it is inevitable that it will begin to be considered for medium and heavy duty pavements. According to authors, expansion into these applications is hampered by the fact that to date there is no rational method for structural design of pervious pavements. Structural design of pavements should be based on material properties, and those material properties should be measurable through standardized test methods. This paper reviewed the current state of the practice on structural design of pervious concrete pavements, and outlined a methodology for moving forward to develop a new, more appropriate structural design method. Design methods should identify the failure mechanisms for pervious concrete pavements, as well as the layer properties and thickness and joint detailing necessary to prevent failure. Structural design must also be integrated with hydraulic design. Design examples and charts developed using ACPA StreetPave software were presented.

Portland Cement Association and National Ready Mixed Concrete Association (10) also published a document titled “Pervious Concrete Hydrological Design and Resources”. Skokie, Ill.; Portland Cement Association.; Silver Spring, Md.; National Ready Mixed Concrete Association. The CD produced with the publication contains software to assist with hydrological design as well as related materials addressing the proportioning, production, and placement of pervious concrete.

Schaefer, Vernon R; Kevern, J.; Wang, K.; Suleinan, M.; (11) produced research report titled Mix Design Development for Pervious Concrete In Cold Weather Climates in 2005. The result

of the study developed a set of useful information leading to better pervious concrete design and construction practices. These include: optimal void content, Optimal aggregate content, best water/ cement ration to optimize durability and strength. The result recommended, 3/8 or 1/2 inch aggregate as the best size to optimize strength and durability while the optimum porosity was between 20 and 25 percent. The research also investigated basic rheological properties of pervious concrete. Some of these results will be used for the construction of a porous overlay in MnROAD in 2008.

Burk R.J. (12) in his paper titled “Permeable Interlocking Concrete Pavements - Selection, discussed hydrological evaluations in a design and selection process that can be applied to pervious concrete. According to author, urbanization brings an increasing concentration of pavements, buildings, and other impervious surfaces. They generate additional runoff and pollutants during rainstorms, causing stream-bank erosion as well as degenerating lakes and polluting sources of drinking water. Increased runoff also deprives groundwater from being recharged, decreasing the amount of available drinking water in many communities. Many jurisdictions are now requiring best management practices (BMP’s) to control non-point source water pollution. Structural Bumps capture runoff and rely on gravitational settling and/or the infiltration through a porous medium for pollutant reduction and peak discharge control. They include detention dry ponds, wet retention ponds, infiltration trenches, sand filtration systems, and permeable pavements. This paper discussed the use of permeable interlocking concrete pavements as a structural BMP under infiltration and partial treatment of storm water pollution. It will cover the selection of the pavement cross-section based upon the municipal storm water management objective, and the criteria for design, construction and maintenance.

Another publication by ACI (13) titled *Guide For Selecting Proportions For No-Slump Concrete* is also a typical reference document for pervious concrete. This document is intended as a supplement to the document titled "Standard Practice for Selecting Proportions for Normal, Heavyweight, and Mass Concrete." This publication describes a procedure for proportioning concretes having slumps in the range of zero to one inch and consistencies below this range, for aggregates up to three inch maximum size. Suitable equipment for measuring such consistencies are described in the document. Tables similar to those in ACI 211.1-91 are provided which, along with laboratory tests on physical properties of fine and course aggregate, yield information for obtaining concrete proportions for a trial mixture. The new edition also includes chapters on proportioning mixes for roller-compacted concrete, concrete roof tile, concrete masonry units and pervious concrete for drainage purposes. Document provided as an aid to calculating proportions for these specialty applications.

### ***1.3.3 Performance of Pervious Concrete***

Fowler, D.W. (14) in a paper titled *Aggregates For Pervious Concrete* discussed the aggregate properties required for good performance of pervious concrete. He reaffirmed the need for single graded aggregate but was not definite on the optimal size desired. Author discussed the feasibility of pervious concrete for parking lots Pervious concrete, although used for over a hundred years, is receiving increased interest as a permeable material for parking lots. It uses a single size aggregate without fines. It generally has low strength and very good permeability. Author outlines 4 noteworthy points in relation to construction process, base, thermal advantages and need for further research. The paper concludes:

- Pervious concrete utilizes a coarse aggregate base for storing water.
- Limited research has shown that little clogging occurs over time, but that the initial surface finishing is very important in order to have a permeable surface.
- Permeable concrete can reduce or eliminate the need for detention ponds, and reduces the surface heat. There have been numerous applications, particularly in the Southeast.
- In order for pervious concrete to succeed, research is required and actions by building officials and owners are needed.

In his article titled Voids Add Value to Pervious Concrete, Kuennen-T (15) outlined succinctly the importance of void content and determination of optimal void structure for good performance of pervious Concrete. The article also describes installations at specific sites and new techniques for designing and building pervious concrete pavement, which is gaining popularity in the Sunbelt and Pacific Coast. Author (13) outlined the following performance issues:

- It can help local communities meet EPA Phase II storm water pollution regulations.
- It also reduces hydroplaning and tire spray.
- The optimum structure has voids in 20-25%. Anything higher tends to compromise compressive strength. In addition to parking lots, pervious concrete can be used in recreation trails, plazas and other paved pedestrian areas.
- It also cuts down in stored heat in the summer,
- Effective passive water treatment media, which catches non-point pollutants and transfers them to soils where microbes can convert them into harmless materials. While pervious concrete costs more to install, it does eliminate the need for gutters, curbs and storm drains.

Shackel, B.; Pearson, A. (16) (University of New South Wales and Concrete Masonry Association of Australia respectively) presented a paper titled “Permeable Concrete Eco-Paving As Best Management Practice In Australian Urban Road Engineering”. Research into the structural and hydraulic properties of permeable concrete segmental eco-paving has now been active in Australia for almost 10 years. Over the last six years a significant number of projects in Australia have successfully utilized this new form of construction. Their paper (16), summarized the progress that has been made in the testing, evaluation, design and construction of permeable eco-paving and critically reviewed the state of the art. Author outlined the role and potential of permeable concrete segmental paving in best management practice in Australian Urban Road Engineering, providing case histories to accentuate the state of the art.

Wanielista, Martin P. Chopra, Manoj Bhopinder (17) wrote a research report on extensive pervious concrete research performed in Florida. The report titled Performance Assessment of Portland Cement Pervious Pavement and Cement Pervious Pavement and published by the University of Central Florida, Storm water Management Academy, is in 4 parts.

- Summary of final report, BD521-02
- Report 1. Hydraulic performance assessment of pervious concrete pavements for storm water management credit
- Report 2. Construction and maintenance assessment of pervious concrete pavements
- Report 3. Compressive strength of pervious concrete pavements

- Report 4. Performance assessment of a pervious concrete pavement used as a shoulder for an interstate rest area parking lot.

Smith-DR (18) was author of another paper on Permeable Interlocking Concrete Pavement in the magazine: *Public Works*. Post-construction Best Management Practices (BMPs) should be guided by regulations that are based on sound watershed planning and hydrology and pollutant planning. Phase II of the national regulations calls for municipalities below 100,000 in population with municipal separate storm sewer systems to devise programs to control storm water runoff from new and redeveloped projects. The article described links to Environmental Protection Agency (EPA) fact sheets and menus of acceptable BMPs. Emerging BMPs for runoff control include permeable interlocking concrete pavement. Typically, they are built on open-graded, crushed stone base. Used extensively in Europe, they are especially appropriate where impervious cover is restricted by regulations, the storm drain capacity is limited, and there is limited space for retention ponds. They work best when the total catchment area is not greater than five acres and the level of the water table is at least two feet below the bottom of the pavement base. Included is an extensive list of possible sites where the paving would be appropriate.

Waagberg-L-G (19) provided the Swedish state of the art with permeable asphalt in a report titled *Draining Asphalt Concrete*. Permeable Asphalt has been used extensively in Sweden but as noise reducing surfaces as well as BMPs for Storm water Management. Pervious asphalt concrete is a relatively new type of wearing course on Swedish roads. Preliminary specifications were published prior to the surfacing season in 1980. The main reason for the introduction of pervious asphalt concrete in Sweden was that it promised to alleviate the risk of aquaplaning. It has however been found that this type of surfacing also has other favorable properties which primarily enhance traffic safety but also have a favorable effect on the environment along the road. The principal favorable effects are:

- less risk of aquaplaning;
- better friction in wet conditions; (3)
- better reflection characteristics; (4)
- traffic noise is reduced by up to 8 db(a) in relation to close textured asphalt concrete.
- its resistance to wear by studded tires is about the same as that of close textured asphalt concrete.

There were some reports from Denmark and Holland that this surfacing is prone to icing under certain conditions. No such problems have been experienced in Sweden, due mainly to the fact that the road authority has been made aware of this possibility and at times applied more intensive anti-skid treatment. Winter maintenance on this surfacing has not, however, been more expensive than on other surfacing.

#### ***1.3.4 Tire-Pavement Acoustics of Pervious Concrete***

Cackler, Harrington, and Ferragut (20) of Iowa State University wrote a report evaluating Pavement practices in US and Europe after a European scan Tour. The report titled “Evaluation of U.S. and European Concrete Pavement Noise Reduction Methods” was part of a larger Surface characteristics Study led by the CP Tech Center, ISU. The document contained the

results of Part 1, Task 2 of the ISU-FHWA project entitled "Concrete Pavement Surface Characteristics Project." It addresses the noise issue by evaluating conventional and innovative concrete pavement noise reduction methods. The first objective of this task was to determine what if any concrete surface textures currently constructed in the United States or Europe were considered quiet, had long-term friction characteristics, could be consistently built, and were cost effective. Any specifications of such concrete textures would be included in this report. The second objective was to determine whether any promising new concrete pavement surfaces to control tire-pavement noise and friction were in the development stage and, if so, what further research was necessary. The final objective was to identify measurement techniques used in the evaluation. The Part 1, Task 2 evaluation reported herein included (1) examination of conventional concrete pavement noise reduction methods used in the United States; (2) identification of promising new concrete pavement surfaces to control tire-pavement noise and friction in Europe; and (3) initial consistent field measurements of tire-pavement noise and friction with respect to texture. The evaluation concludes that (a) careful construction practices in the United States for artificial turf and burlap drag, longitudinal tining, and diamond grinding can be used to initially control noise (99/100-104/105 dBA) and provide adequate initial friction; (b) the noisiest pavements (>104/105 dBA) should be rehabilitated immediately, with no new noisy pavements constructed; (c) to achieve the quietest concrete pavements (<99/100 dBA), innovative solutions such as exposed aggregate and pervious concrete, need to be advanced; and (d) more study is necessary to understand the change of noise and texture characteristics over time and to increase consistency.

Lefebvre, J-P (GTM); Marzin-M (Ciments Lafarge) presented a paper titled Strides In Highway Engineering. In France - Pervious Cement Concrete Wearing Course Offering Less Than 75 Db(A) Noise Level. The Authors (21) present an experimental draining cement concrete site for which the management of the Roads and company signed in 1994. The objectives were to confirm the feasibility of the placement of concrete draining in 16 cm thickness by observing conditions of plain equivalents has on the national network. Performance indicators in this project were outlined as follows:

- Draining concrete present 25% of communicating vacuums with a minimum of 22%.
- The measurement of noise in LPmax according to the standard S 31-119 with the passage of a light vehicle at 90Km/h 7,50m from microphones will have to tend towards 72 dBA and not exceed 75 dBA.

### ***1.3.5 Construction Issues Benefit-Over-Cost of Pervious Concrete***

Howe-J (Interpave) (22) in an article titled Comparing Paving Costs published in the 2006/09 issue of Concrete Journal discussed research conducted by Scott Wilson on the costs of different pavement types, including concrete block permeable pavements (CBPP), used in different applications and ground conditions. In the first part of the research, pavement and drainage construction requirements and initial costs were compared. Author considered more than 200 different cases including car parks, estate roads for housing and industrial developments, parking for warehouses, and airport pavements. The second stage of the research involved whole life cost (WLC) analysis. The principles of WLC analysis for pavements are outlined. Factors influencing the long-term performance of pavements are considered: vehicle weight, axle loadings, vehicle

suspension, tire pressure and tire type. The authors considered relationships between CBPP type, costs and application

Tatsushita, F; Abe-H; Inoue, T; Yagi, Y (23) presented a paper titled Test Application Of Pervious Asphalt Concrete Surface Layer In Maintenance Project: Aiming Noise Reduction And Driving Safety. This paper (21) is contained in the proceedings of the Sixth Conference, Road Engineering Association of Asia and Australasia, Kuala Lumpur; The first trial of pervious asphalt concrete resurfacing was applied to a conventional milling and overlay project on a Tokyo Metropolitan arterial road in 1987 to confirm the noise reduction effect. This paper introduced the mix design of fiber-reinforced mixtures, their physical properties in the laboratory, and the result of noise measurement after overlay comparing with the result after 9 months at the site. It also stated the details of acoustic noise analysis and water permeability of the mixture, which was measured on the overlaid surface.

Stidger, RW (24) discussed the factors affecting pavement life in an article titled How To Manage Concrete Road Life Cycles in the 2002/02 edition of *Better Roads*. 2002/04. 72(4) pp 44-48. According to experts, the life of concrete pavement can be extended up to nine times their original design life. One of the factors affecting pavement life is finding the right mix of Portland or blended cement and supplementary materials. Heavy traffic can impact the life of rigid (concrete) and flexible pavements. Quick reconstruction of damaged concrete pavement is feasible, thus disproving popular belief that concrete materials are slow curing. Another method of increasing the life cycle of roads that are subject to heavy rains is by using pervious concrete. Other elements needed to achieve a porous paving system include an appropriate base soil and evaluation, proper preparation of a compacted, well-drainable sub base, an appropriate mix design, and correct mixing, placement, finishing, and curing.

Kuennen, T (25) in his article "Voids Add Value to Pervious Concrete" In *Better Roads Better Roads*. 2003/08 discusses other Benefits of pervious concrete and suggests an optimal void content. They (25) described new techniques for designing and building pervious or permeable Portland cement concrete pavement, which is gaining popularity in the Sunbelt and pacific coast. It Can Help Local Communities meet EPA Phase II storm water pollution regulations. It also reduces hydroplaning and tire spray. The final structure has voids in 20-25%. Anything higher tends to compromise compressive strength. In addition to parking lots, pervious concrete can be used in recreation trails, plazas and other paved pedestrian areas. It also cuts down in stored heat in the summer, but its greatest benefit is its effective passive water treatment, which catches non-point pollutants and transfers them to soils where microbes can convert them into harmless materials. While pervious concrete costs more to install, it does eliminate the need for gutters, curbs and storm drains. The article also describes installations at specific sites.

Lefebvre, J-P, Marzin, M (26) In Their Paper "Strides In Highway Engineering. The Year 1995 In France - Pervious Cement Concrete Wearing Course Offering Less Than 75 Db(A) Noise Level" Studied and successfully demonstrated the placement of that met one performance requirements including pervious concrete present 25% porosity providing good acoustical properties. According to authors (99) the measurement of noise in LPmax according to the standard S 31-119 with the passage of a light vehicle at 90Km/h 7,50m from microphones ranged from 72 dB(A) to 75 dB(A).

Pervious asphalt concrete is a relatively new type of wearing course on Swedish roads. Preliminary specifications were published prior to the surfacing season in 1980. The main reason for the introduction of pervious asphalt concrete in Sweden was that it promised to alleviate the risk of aquaplaning. It has however been found that this type of surfacing also has other favorable properties which primarily enhance traffic safety but also have a favorable effect on the environment along the road. The principal favorable effects are: (1) less risk of aquaplaning; (2) better friction in wet conditions; (3) better reflection characteristics; (4) traffic noise is reduced by up to 8 db(a) in relation to close textured asphalt concrete. Its resistance to wear by studded tires is about the same as that of close textured asphalt concrete. There were some reports from Denmark and Holland that this surfacing is prone to icing under certain conditions. No such problems have been experienced in Sweden, due mainly to the fact that the road authority has been made aware of this possibility and at times applied more intensive anti-skid treatment. Winter maintenance on this surfacing has not, however, been more expensive than on other surfacing.

Welleman, T (27) studied some factors affecting friction in porous surfaces. They showed that the frictional forces that can be transmitted between the tire and road surface are greatly reduced by the presence of water-layers only a few millimeters in depth. The water layer thickness at any point of a road surface depends on the cross fall and longitudinal slope, the surface texture, the length of the drainage path and the presence of ruts. These factors are discussed in the report together with a number of measures to reduce the water nuisance. They recommended solutions included : the construction of transverse drainage channels or grooves on the road surface, a high-quality surface dressing based on synthetic resins, and the use of highly pervious asphaltic concrete for the wearing course. Lawther-JM (29) Pavement Effects In Tire/Pavement Interaction Noise Transportation Research Board Unpublished Report. 1979/03. (10) pp88-94 (10 Fig., 25 Ref.).

Bendtsen, H (28) compared dense to porous asphalt. Using textured asphalt concrete as reference. Porous surfacing achieved 4 dB(A) noise reduction. Traffic volume would have to be reduced by 60% to achieve same effect. The porous surfacing has 8-12 mm max aggregate size and 20-25% voids. It must be at least 4 cm thick. The cost is about 20% higher since polymer modified bitumen is used. No Danish experience is as yet available concerning durability. Apart from noise reduction, porous surfacing have good friction, no aquaplaning, reduced spray. Authors (28) concluded that though free-draining effect may complicate winter maintenance. This type of surfacing can be used to reduce noise in towns.

Crocker, MJ; Hanson, D; Li, Z; Karjatkar, R; Vissamraju, KS (29) (Measurement Of Acoustical And Mechanical Properties Of Porous Road Surfaces) outlined the procedure for laboratory determination of sound absorption properties of porous pavements. The absorption coefficients of dense and porous road surfaces have been measured in the laboratory with core samples with 4- and 6-in.-diameter impedance tubes and with an impedance tube mounted vertically in situ on the pavement surfaces. The 6-in. tube allows the absorption of a large core sample surface to be determined, but only up to a frequency of about 1,250 Hz. The 4-in. tube allows the absorption coefficient to be determined up to a frequency of about 1,950 Hz. The two different-diameter impedance tubes also were mounted vertically on some of the same pavement types, and the absorption coefficients of these pavement types were measured in this way too. The measured peak sound absorption coefficients of the fine- and coarse-mix aggregate porous surfaces suggest

that the first peak frequency and peak absorption coefficient magnitude are only slightly different for the two types of porous surfaces. Because the fine-mix aggregate porous surface is smoother, it is preferred because it should result in less tire-tread impact noise and thus lower overall tire noise than the coarse aggregate surface. A porous surface between 1.5 and 2.0 in. thick is recommended for the type of porous surface examined, if a peak absorption frequency of about 1,000 Hz is desired, so as to be most effective at reducing the Interstate highway noise of automobiles.

Neithalath, et al (30) discussed effects of porosity on Pavement surface Characteristics (103). Their report statistically analyzed the effect of porosity enhancement on performance of concrete. To facilitate the study, the researchers (103) carefully introduced priority enhancers through the use of “soft inclusions”. The freeze thaw durability of the enhanced product was maximum when the ‘macronodule’(Aggregate like 2 – 8 mm size) fibers were used. Neithalath, et al discussed the mechanism of noise generation originally discussed by Sandberg et al (8). The mechanism attributes the main noise source in the tire-pavement interaction to the knocking action of the thread-blocks on the surface. According to Neithalath, et al, the impact causes radial excitation on the tire walls. In consequence, air borne noise as well as structure & pavement) borne noise are generated. The resulting mechanisms occur and are associated with less than the critical IKHZ frequency. Another impact phenomenon that results in tangential strain in the thread block is dominant above IKHZ. Neithalath, also identified the place of porosity in the mechanism of sound propagation and generation. Porosity destroys the horn amplification and causes attenuation of sound through the cavities.

The November 1999 edition of *Surveyor* C Pratt (31). Discusses the benefits of pervious pavements in an article titled *Clear Benefits*. Storm water can flush large amounts of toxic pollutants into rivers and watercourses. Storm water source control, using a permeable surface and detention subsystem, was introduced into the UK around 1995, and it is rapidly becoming the preferred method of handling run-off, especially where there are environmental or capacity limitations. I laid trial areas, using his design, over ten years ago, but generated little enthusiasm from engineers. Outside the UK, it was found that about 90% of surface pollution was washed off by the first 20% of heavy rain; if this first 'flush' could be contained at source, flooding and pollution would become much less likely. The Forth River Purification Board (FRPB) conducted its own research, and led a new approach to the problem in the UK. Formpave worked with the FRPB and later with Pratt to produce a permeable concrete paver, from which the Formpave storm water source control system evolved. Pratt's sub-base design acts like a detention pond, and contains about 30% voids, which hold the water before releasing it to infiltration or in a controlled way into sewers or streams. Discharge rates below 2.5 liter /Ha/s can easily be achieved, and the discharge water is clean, due to the combined effects of a geotextile membrane and micro-organisms in the sub-base.

## **CHAPTER 2 CONCEPT DESIGN, MIX DESIGN, AND GEOTECHNICAL EXPLORATION**

### **2.1 Introduction and Initiative**

The Minnesota Department of Transportation (MnDOT) constructed the Minnesota Road Research Project (MnROAD) between 1990 and 1994. MnROAD is located along Interstate 94 forty miles northwest of Minneapolis/St. Paul and is an extensive pavement research facility consisting of two separate roadway segments containing 55 distinct test cells. Each MnROAD test cell is approximately 500 feet long. Subgrade, aggregate base and surface materials, as well as, roadbed structure and drainage methods vary from cell to cell. All data presented herein, as well as historical sampling, testing, and construction information, can be found in the MnROAD database and in various publications. Layout and designs used for the Mainline and low-volume road can also be found on its web site at <http://mnroad.dot.state.mn.us/research/mnresearch.asp>.

Parallel and adjacent to Interstate 94 Mainline (ML) is the low-volume road (LVR). The LVR is a two-lane, 2½-mile closed loop that contains 20 test cells. Traffic on the LVR is restricted to a MnROAD operated vehicle, which is an 18-wheel, 5-axle, tractor/trailer with two different loading configurations. The "heavy" load configuration results in a gross vehicle weight of 102 kips (102K configuration). The "legal" load configuration has a gross vehicle weight of 80 kips (80K configuration). On Wednesdays, the tractor/trailer operates in the 102K configuration and travels in the outside lane of the LVR loop. The tractor/trailer travels on the inside lane of the LVR loop in the 80K configuration on all of the other weekdays. This results in a similar number of ESALs (equivalent single axle loads) being delivered to both lanes. ESALs on the LVR are determined by the number of laps (80 per day on average) for each day and are entered into the MnROAD database. These are adjusted for down times during construction as well as unusual traffic events. The mainline consists of a 3.5-mile, two-lane interstate roadway carrying "live" traffic. The Mainline consists of both 5-year and 10-year pavement designs. The 5-year cells were completed in 1992 and the 10-year cells were completed in 1993. Originally, a total of 23 cells were constructed consisting of 14 Hot Mixed Asphalt (HMA) cells and 9 Portland Cement Concrete (PCC) test cells. Traffic on the mainline comes from the traveling public on westbound I-94. Typically the mainline traffic is switched to the old I-94 westbound lanes once a month for three days to allow MnROAD researchers to safely collect data. The mainline ESALs are determined from an IRD hydraulic load scale, which was installed in 1989, and a Kistler Quartz sensor, which was installed in 2000. The mainline has received roughly 6.5 million flexible Equivalent Single Axle Loads (ESALs) and 9.0 million Rigid ESALs as of December 31, 2007.

#### ***2.1.1 MnROAD Instrumentation and Surface Data Collection***

Strength shrinkage, deflection and temperature data collection at MnROAD is accomplished with a variety of methods to help describe the layers, the pavement response to loads and the environment, and actual pavement performance. Layer data is collected from a number of different types of sensors located throughout the pavement surface and sub-layers, which initially numbered 4,572. Since then, there have been many added to this total with additional installations and sensors types. Data travels from these sensors to several roadside cabinets,

which are connected by a fiber optic network that is feed into the MnROAD database for storage and analysis. Data can be requested from the MnROAD database for each sensor along with the performance data that is collected throughout the year. This includes ride, distress, rutting, faulting, friction, forensic trenches, material laboratory testing and the sensors measurable variables such as temperature, moisture, strain, deflection, and frost depth in the pavement along with so much more.

Noise, texture, ride and friction measurements are conducted seasonally. Data obtained from surface characteristics are stored in temporary files from which they are subsequently transcribed to the MnROAD database. Such data is not yet directly fed to the database and thus it is more expensive to collect, reformat and export. Texture measurements are done with the ASTM E-2157 Texture Meter as well as the ASTM E-956 Sand Volumetric technique. Ride measurements are done seasonally with the MnDOT pathways van that records an International Roughness Index (IRI) value. The vehicle makes one sweep through each of the 4 lanes. The lanes include the low-volume road's inside and outside loop and the Mainline's driving and passing lane. For each run, a unique file of IRI is recorded and an ERD file is preserved for further analysis. Friction measurements are done according to ASTM E-274 for smooth and ribbed tire measurement. Sound intensity measurements are conducted with a MnDOT set up that records the tire pavement sound intensity without the bias of aerodynamic noise or stack noise. In the future, OBSI data from MnROAD can be obtained from the database as they are currently being loaded.

## **2.2 Research Matrix**

This section accentuates the test sections and the sensor layouts for the full-depth porous pavements as well as the porous overlay.

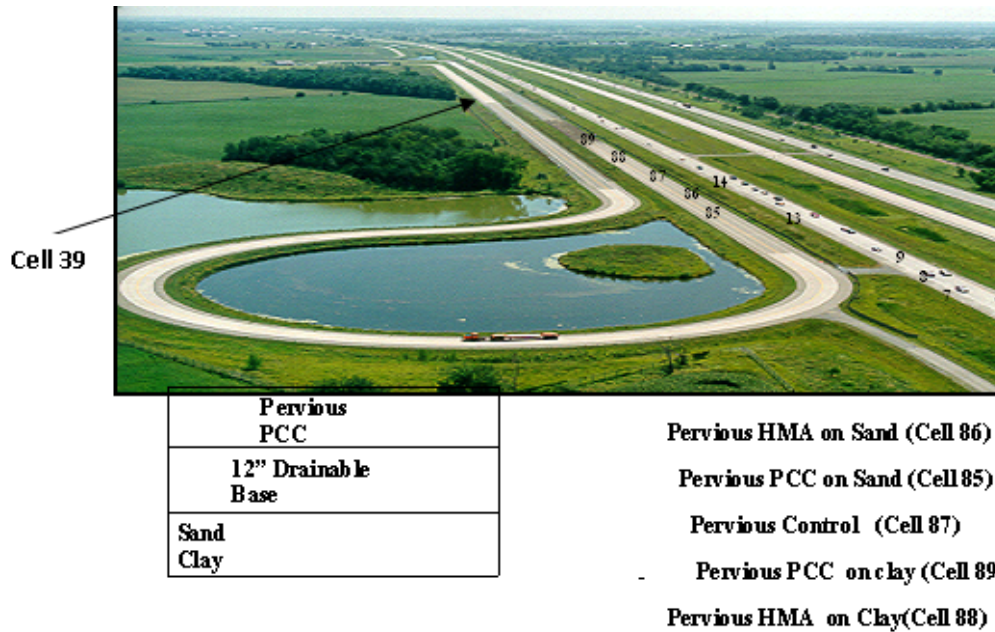


**Figure 2.1: Aerial View of MnROAD, Showing the Pervious Cells 39, 85 and 89 the LVR**

Cells 85 to 89 were designed with a full infiltration scenario in cell 85 and a retention system in cell 89. Each of these cells, as well as cells 86 and 88 (porous asphalt on sand and clay respectively), were built on a base made up of 12-inches of CA 15 aggregate. It was determined that in the concrete cells, there would be a 12 inch layer CA 15 crushed rock to accommodate the detention storage nominal sized aggregate. In the bituminous sections, the 14 inches of CA 15 was determined as required base detention storage. The total storage volume was uniform across test sections. As the total porous storage depth was the same for both the concrete and bituminous sections down to the top of grading grade. In addition to a 5-inch bituminous pavement and a 7-inch concrete pavement were built in their respective cells. A porosity benefit was hypothetically anticipated from the base and subgrade in cells 85 and 86 because the subgrade is granular. Although the joints were cut to match the existing ones, it is believed that the overlay system joints should be cut through the overlay to the substrate. The mix designs for cell 85 and 87 consisted of a water and cement ratio of 0.3.

This research scenario allows the comparison of sound absorption of porous asphalt to pervious concrete, pervious concrete on clay subgrade to pervious concrete on sand subgrade, and pervious concrete to porous overlay at the inception of service. Subsequently, research will establish a quietness survival metric for each of these designs.

**Table 2.1: Location Allocation and Design Matrix for New Pervious Pavements**

<b>PSC CODE</b>	<b>FINISHING</b>	<b>Cell/ Location Allocation</b>	<b>Performance Specification</b>
Perv B	Pervious Asphalt	86,87,88	The oil content, VMA unit weight and porosity shall meet the industry standard prevailing at the time of paving or as designed and specified by others.
Perv C	Pervious Concrete	85,87,89	Porosity shall be 15 to 18 % and the void ratio shall be 18 to 21%. The surface shall be void of laitance or slurry and should guarantee uniform porosity through the depth of the concrete. The matrix should be resistant to undesirable raveling and weathering. This shall be established during the trial mixing process. Unit weight may not exceed 135 pcf unless it is improved by practice or otherwise, contractor achieves desired porosity while attaining 7-day flexural strength of 300psi.
PERV OL	Pervious Concrete Overlay	37	Specified by Iowa State University. Unique porous mix contains fibers and 6% sand which is self consolidating and slip formable.
PERV BC	Pervious Control cell	87	Non- Porous HMA
Perv C	Pervious Concrete Driveway	64 (2005)	Construction and performance reports are located at: <a href="http://www.lrrb.org/detail.aspx?productid=2139">http://www.lrrb.org/detail.aspx?productid=2139</a> <a href="http://www.mrr.dot.state.mn.us/research/pdf/2006MRRD-OC007.pdf">http://www.mrr.dot.state.mn.us/research/pdf/2006MRRD-OC007.pdf</a>
Perv D	Pervious Concrete Sidewalk	(2006)	Construction report is located at : <a href="http://www.mrr.dot.state.mn.us/research/pdf/2006MRRD-OC012.pdf">http://www.mrr.dot.state.mn.us/research/pdf/2006MRRD-OC012.pdf</a>

## 2.3 Design of Pervious Concrete

### 2.3.1 Design Process

The study undertook an unconventional pavement design approach to the pavement. The traffic loads were computed from the new loading configuration recently announced for MnROAD Phase 2. Previously and up to the reconstruction of the LVR, the inside lane was and will be loaded with 80kips 5-axle semi, making 80 laps a day 4 days a week and the outside lane by a

102 Kips semi-trailer traversing the loop one day a week. The proposed configuration retains the 5 axle semi trailer but in the inside lane only. The inside lane will be loaded by the 80 kips semi trailer, making 80 laps a day, 5 days a week through the loop. The outside lane will be subject to environmental loading only. Consequently any distress disparity between directions of the LVR will be attributed to fatigue although fatigue and environmental load may be synergistic and cause distress patterns that exceed the algebraic sum of each (traffic + environmental) loading.

Tables 2.11a and b and c compute the design ESALs based on single and multiple laps of the semi in the previous loading sequence as well as the proposed sequence. Following the identification of design ESALs, the pervious concrete cell whose thickness was determined originally by storage requirements was analyzed by the following design tools: Mechanistic Empirical design Guide MEPDG and I-SLAB.

The Mechanistic Empirical design process, utilized Mechanical properties obtained from MnROAD Cell 64. This included Unit weight of  $127\text{lb/ft}^3$  as well as flexural strength of 450 psi as well as compressive strength of 2000 to 3000psi in 28 days. The Poisson's ratio was assumed to be same until research in this area proves otherwise. In the ISLAB analysis stresses in two pavements of similar design were compared. The stress and deflections occurring at critical locations in the pervious slab were compared with a slab of normal concrete built over the 12 base.

The Design Guide showed that a 90 percent reliability was obtained for the pavement in 3 critical criteria including ride quality faulting and cracking. ISLAB showed similar deflection trends with normal and pervious concrete. It however showed that the stresses were higher in the pervious concrete than in the normal concrete, to one order of magnitude.

Failure patterns observed in 64 include, raveling and differential icing. These patterns are not taken into account in either of the design tools used. Obviously, the use of a normal concrete design process for pervious concrete design without some unique material performance or features is only mechanistic and lacks the empirical component for a reliable design. The development of empirical data for the design of pervious concrete is one of the intents of this project.

Section I also covers the mix design process. Section 2 discusses the environmental/hydrological models for pervious concrete. Models are predicated on the expectation that vertical flow fall outside of the flow regimes for laboratory permeameters or infiltrometers. The models do perveammeter model does not therefore ignore the velocity head in the energy equations. Chapter 3 covers the Baseline Environmental Sampling report and Chapter 4 discusses the Geotechnical Report from 8 borings and 4 Probes.

**Table 2.2: Design ESALS for Current and Proposed LVR Cells**

		(Given)	Load Eqv Factor	ESAL	Load Eqv Factor	ESAL
<b>Single Axle</b>						
5000-6999	6	9	0.015	0.135	0.01	0.09
7000-8999	8	10	0.046	0.46	0.032	0.32
9000-10999	10	62	0.11	6.82	0.085	5.27
11000-12999	12	156	0.221	34.476	0.176	27.456
13000-14999	14	54	0.395	21.33	0.341	18.414
15000-16999	16	65	0.646	41.99	0.604	39.26
17000-18999	18	4	1	4	1	4
<b>Tandem Axle</b>						
14000-17999	16	4	0.065	0.26	0.082	0.328
18000-21999	18	12	0.151	1.812	0.206	2.472
22000-25999	20	68	0.302	20.536	0.444	30.192
26000-29999	22	97	0.541	52.477	0.85	82.45
30000-33999	24	108	0.888	95.904	1.49	160.92
34000-37999	26	32	1.38	44.16	2.43	77.76
38000-41999	28	12	2.045	24.54	3.75	45
TOTAL ESALs			348.9			493.932
RUCK FACTOR			1.54			2.19

**Table 2.3: Present Load Configurations**

	Lane	Inside	Outside	New Config
	LVR CONFIG	80	102	80
	# Axles	5	5	5
	Daily Repetitions	80	80	80
	Inside Lane Days Weekly	4	1	5
Repetitions/ Year	84/day Weekly	16697	4174	20871
	Cumulative 10 years	166971	41743	208714
	Load Range lb/axle		18	
	Avg Load (Kips)	21000	18888	21000
	Repetition (Given)	166971	41743	208714
Flexible Pavement SN=3.5	Load Eqv	2.3	7.6	2.3
	ESAL	384034	317246	480043
Rigid Pavement	Load Eqv	3.73	11.65	3.73
	ESAL	622803	486304	778504

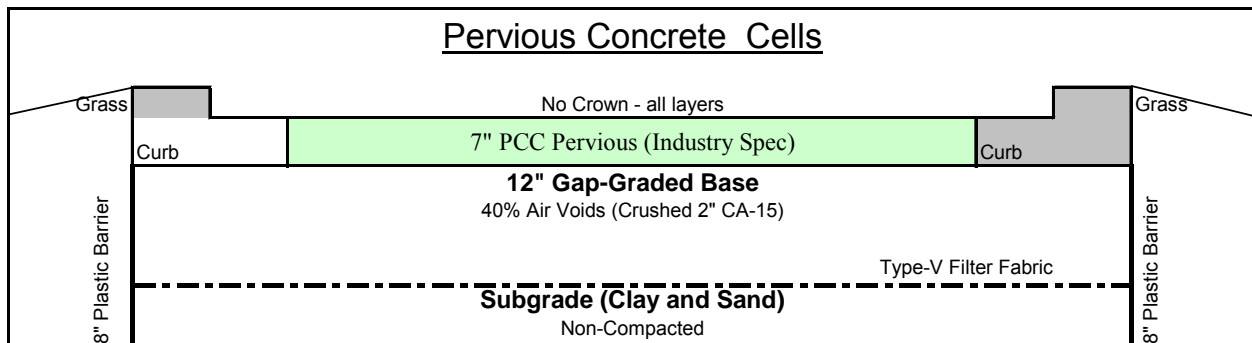


**Figure 2.2: Pavement Design Layout**

**Table 2.4: Mix Design Process**

Reference	Process	Recommendation
Table 10.7 MYD	<p><u>Cement Type</u></p> <p>Exposure to Sulfates/ Chlorides/ deicers</p>	Type 5 Cement
ACI 318	Less than 0.2 for normal exposure but due to cavities use Type 5 cement	
Table 9.2, 9.3 MYD	<p><u>Slump and Air</u></p> <p>Slump range 0 to 1</p>	Choose lower Range of zero Slump
Table 10.1 MYD	No available tables.( air is not in paste but in cavities)	Required Water = 0.48
ACI 211.1	<p>Nominal aggregate size = ½ inches</p> <p>Modification for 18 percent cavities</p>	Use 0.40 and allow for HRWRA
Tables 9.8, 10.2 MYD	<p><u>Estimation of Mixing Water</u></p> <p>Exposed to freezing and thawing, w/c is .45</p> <p>Mixing water = 190kg/m<sup>3</sup></p> <p>This amounts to 340lb of water</p> <p><u>Required Cement</u></p> <p>At 0.4 w/c ratio Cement content is 300/.4 = 750lb</p>	<p>Max Sized aggregate is ½ inch</p> <p>Retain 0.4 w/c ratio</p> <p>Use 230lb of water for zero slump</p> <p>This is too high</p>

Reference	Process	Recommendation
<p>Table 10.3 ACI 211.1</p> <p>Table 10.8MYD waived</p>	<p><u>Coarse Aggregate Content</u></p> <p>Given BSG= 2.7</p> <p>Assume absorption =1.5% and surface moisture =1.0%</p> <p>Dry Rodded unit weight is 100pcf,</p> <p>At SSD weight = (1-A/100)(Z)</p> <p>Oven Dry Unit Weight of Aggregate= 0.63 x 100(lb/ft<sup>3</sup>) X 27 (ft<sup>3</sup>/lb)</p> <p>Considering Absorption,</p> <p>Weight at SSD= (1+ [1.5/100])(2309)= 2426</p>	<p><b>CA content is 2309 lb/yd<sup>3</sup></b></p> <p>CA content due to moisture is 2343 lb/yd<sup>3</sup></p>
<p>Table 10.8 MYD</p>	<p><u>Estimation Of Concrete Unit Weight</u></p> <p>Assuming no pozzolan substitution, Concrete unit weight is</p> <p><math>U = 16.8 G_a (100-A) + C (1-G_a/G_s) - w (G_a - 1)</math></p> <p>assumed <math>G_a = 2.7</math> <math>G_p = 2.8</math> if used</p> <p><math>G_c = 3.15</math></p> <p><math>W = 300</math> <math>A=18</math></p>	

Reference	Process	Recommendation
	<p><u>Estimated Batch Weights (1<sup>st</sup> Iteration)</u></p> <p>Estimated concrete weight =  <math>16.85 \times 2.7 (100-18) + 3.15 (1 - [2.7/3.15]) - 300(2.7-1)</math>  <math>= 3320 \text{ kg/yd}^3</math></p> <p><u>By Volume method</u></p> <p>Cement = <math>700 \text{ lb} / 3.15 \times 62.4 (\text{lb}/\text{ft}^3) = 3.56 \text{ cu ft}</math>  Water = <math>300 \text{ lb} / 62.4 (\text{lb}/\text{ft}^3) = 4.80 \text{ cu ft}</math>  Aggregate = <math>2309 \text{ lb} / 2.7 \times 62.4 (\text{lb}/\text{ft}^3) = 13.7 \text{ cu ft}</math>  Total = 22.06</p> <p>Air cavity required = <math>27 - 22.06 = 4.94 \text{ cu ft} = \text{cavity vol}</math></p> <p><u>Mix Proportion</u></p> <p>Pozzolan: 15 % Substitution 100 LB  Cement: 600lb  Coarse: MnDOT 3137 CA 15 Aggregate 2000-2100 lb  Fine Aggregate: Zero  Water/Cementitious Ratio: 0.35 to 0.4  Viscosity Modifier: Manufacturer's Spec  Required Slump: 0-0.5"</p>	<p>Unit weight of concrete is  <math>3320 \text{ lb/yd}^3</math></p> <p>Entrained air = 6%  + cavity 18%</p> <p>Adjust Aggregate by 252 Lb  Aggregate batch = 2057lb</p>

Reference	Process	Recommendation
	Mid Range WRA: 4lb/yd <sup>3</sup>	

### 2.3.2 *Desired Performance Requirements*

- Pervious Concrete > 200 in/hr
- Granular base CA 15 > 200 in/hr
- Sand Subgrade > 50in/hr
- Clay Subgrade: No Minimum (Aquiclude should not be distorted since perched aquifers are charged by infiltration in this project)
- Strength and Gradation
  - Flexural Strength @28days >480Psi
  - Compressive strength@28days >3000psi
  - Choker Course is not required
  - Max Aggregate ½ inch
  - Porosity End Spec 20-24%
  - 1.21 Unless otherwise stated, relevant Concrete construction and Materials items in the MnDOT Specification for construction and materials 2005 or relevant special provision clause shall apply.

### 2.3.3 *Trial Mixing Requirements*

The Contractor or Ready Mix Concrete producer shall supply to an accredited laboratory, materials for trial mixing of 2 mix designs. Prior to this, the Supplier or contractor shall submit a mix design request to MnDOT (Bernard Izevbekhai, phone 651-366-5454) for review and acceptance. The trial mixes shall target the performance requirements in section 6 (Mix Proportions). The trial mixing shall determine the following parameters:

- Modified Slump (ASTM C 172) One lift tapped with a mallet 4 blows at mid height
- Unit weight (ASTM C 138)
- Compressive strength (ASTM C- 139) at 7, 14 21, and 28 days

- Flexural strength (ASTM C- 78) at 7, 14, 21, and 28 days
- Freeze Thaw Durability (ASTM C-666) 300 cycles

### 2.3.4 Strength and Gradation Requirements

Mix shall be proportioned with durable materials to achieve a 28-day compressive strength of 3000 psi and a 7 day and 28 day flexural strength of 300 and 500 psi respectively.

Aggregate for concrete shall be crushed dolostone meeting MnDOT Spec 3137 and shall be single graded (1/2” or 3/8”). Optionally, a granite aggregate (crushed) may be used. Gravels shall not be used for the concrete mixture. Recycled pavement aggregate shall not be used. Fine aggregate is not required.

Aggregate for base course shall consist of CA-50 gradation and shall be either crushed or rounded virgin aggregate. Fine aggregate component is not required. Crushed recycled pavement aggregate shall not be used. A choker course shall not be used.

### 2.3.5 Permeability and Porosity Performance Requirements

**Table 2.5: Permeability and Porosity Performance Range**

LAYER	Porosity (Void Content)	Void Ratio	Permeability (inch/hr)
* Pervious Concrete layer	15-18%	20-22%	>200
Base Layer	25%	30%	>200
Fine Granular Aggregate Subgrade	25%	30%	>50/In Situ
Fine Cohesive Aggregate Subgrade	NA	NA	No Minimum/In Situ

The above permeability and porosity requirements are not prescriptive but suggestive. Achievement of the permeability and durability optimum will not preclude a reasonable change in this value

### 2.3.6 Mix Proportions

For this research project, the Contractor or Supplier shall provide specific mix design approval by MnDOT prior to trial mixing. Performance of trial mixes shall inform the Engineer of the preferred choice of mixes. General variations will occur in unit weight, but mix proportions shall be within the range stipulated in Table 2.5.

**Table 2.6: Mix Proportioning**

<b>Component</b>	<b>Specified Range per yd<sup>3</sup> Concrete</b>	<b>Note</b>
Cement ASTM C150 Type I	500 – 600 lb	From a source recently tested for Blaine fineness, SO <sub>3</sub> , etc.
Fly Ash ASTM C618 Type F	90 –120 lb	Coal Creek / Similar Type F source
Coarse Aggregate	2300-2500 lb	MnDOT 3137
Fine Aggregate	0	Not allowed
Water Cement ratio	0.4	
Water content	250 –305 lb	Adjust with absorption to SSD
Mid range Water Reducing Admixture	4 oz	
Viscosity Modifier	Manufacturer’s spec	MnDOT Approved List
Air Entraining Agent	4 oz	MnDOT Approved List
Air Content	15-18% Volume	

**2.3.7 Sampling**

Modified Slump: 2 in first 2 trucks and thereafter every 3<sup>rd</sup> truck per truckload

*2.3.7.1 Prisms: Hand Roller Compacted, 24 ASTM C666*

Compressive Strength, Poisson’s Ratio and Elastic Modulus: 3” x 6” Cylinders (20)

6” x 12” Cylinders (12). Hand roller compacted.

Flexural Strength Beams: 12 total

**Table 2.7: Mix Designs for Cell 64**

Cement C150/Type I	467 lb
Fly Ash ASTM C618/Class F	83 lb
3/8" Dolostone MnDOT 3137/CA-80	719 lb SSD
1/2" Gravel ASTM C33/#7	1438 lb SSD
Water	149 lb 17.9 gal
Air	33%
MRWRA ASTM C494	22 oz
W/C Ratio	0.27
Slump	0.00 inch
Anticipated Unit Weight	127 pcf

**Table 2.8: Final Mix Designs for Cell 64**

<b>Material</b>	<b>Mixture 1</b>	<b>Mixture 2</b>	<b>Mixture 3</b>
Cement (ASTM C150/Type I)	495	467	456
Fly Ash (ASTM C618/Class F)	87	83	80
3/8" Dolomite, Falkstone, Northwood Iowa (MnDOT 3137/CA-80) Source 80 171041	2379	719	0
1/2" Gravel Dolomite, Northwood Iowa (MnDOT 3137/CA-80) Source 70 182001	0	0	2189
3/8" Gravel (MnDOT 3137 - Aggregate Industries)	0	1438	0
Water	157	149	145
Mid Range Water Reducer Agent (ASTM C494/Type A) (oz/lbm Cementitious material)	4	4	4
AEA (ASTM C260 (oz/cubic yard)	4	4	4
Viscosity Modifying Admixture (oz/100 lbm Cementitious material)	3	3	3
Set Retarding Admixture (oz/cubic yard)			
Water/Cementitious Ratio	0.27	0.27	0.27
Cemstone ID	KAM3096	KAM3376	KAM3276

## 2.4 Design Guide Output of Pervious Cells

### Project: MnROAD Pervious

#### General Information

Design Life 10 years  
Pavement construction: May, 2008  
Traffic open: October, 2008  
  
Type of design JPCP

Description:

#### Analysis Parameters

#### Performance Criteria

	Limit	Reliability
Initial IRI (in/mi)	63	
Terminal IRI (in/mi)	130	90
Transverse Cracking (% slabs cracked)	15	90
Mean Joint Faulting (in)	0.12	90

Location: Albertville MnROAD Low Volume Road  
Project ID: Bernard LRRB Pervious  
Section ID: Cells 24 25,26

Date: 11/20/2007

Station/milepost format:  
Station/milepost begin:  
Station/milepost end:  
Traffic direction: West bound

#### Default Input Level

Default input level Level 3, Default and historical agency values.

#### Traffic

Initial two-way AADTT: 168  
Number of lanes in design direction: 1  
Percent of trucks in design direction (%): 50  
Percent of trucks in design lane (%): 50  
Operational speed (mph): 50

2.4.1 Design Guide Output Summary Pervious on Sand

Table 2.9: MnROAD Pervious Reliability Summary

<b>Project: MnROAD Pervious Reliability Summary</b>					
<b>Performance Criteria</b>	<b>Distress Target</b>	<b>Reliability Target</b>	<b>Distress Predicted</b>	<b>Reliability Predicted</b>	<b>Acceptable</b>
Terminal IRI (in/mi)	130	90	70.9	99.34	Pass
Transverse Cracking (% slabs cracked)	15	90	0	99.999	Pass
Mean Joint Faulting (in)	0.12	90	0.008	99.999	Pass

**Distress Model Calibration Settings - Rigid (new)**

**Faulting**

**Faulting Coefficients**

C1	1.0184
C2	0.91656
C3	0.002185
C4	0.000884
C5	250
C6	0.4
C7	1.83312
C8	400

**Reliability (FAULT)**

Std. Dev.  $\text{POWER}(0.0097*\text{FAULT},0.5178)+0.014$

**Cracking**

**Fatigue Coefficients**

C1	2
C2	1.22

**Cracking Coefficients**

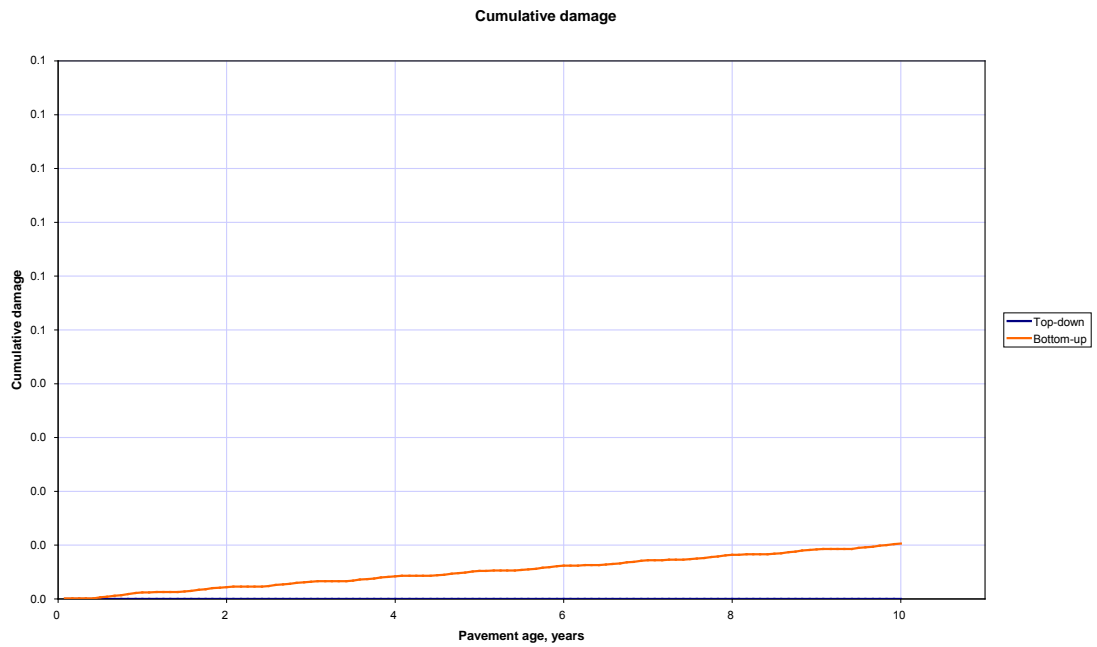
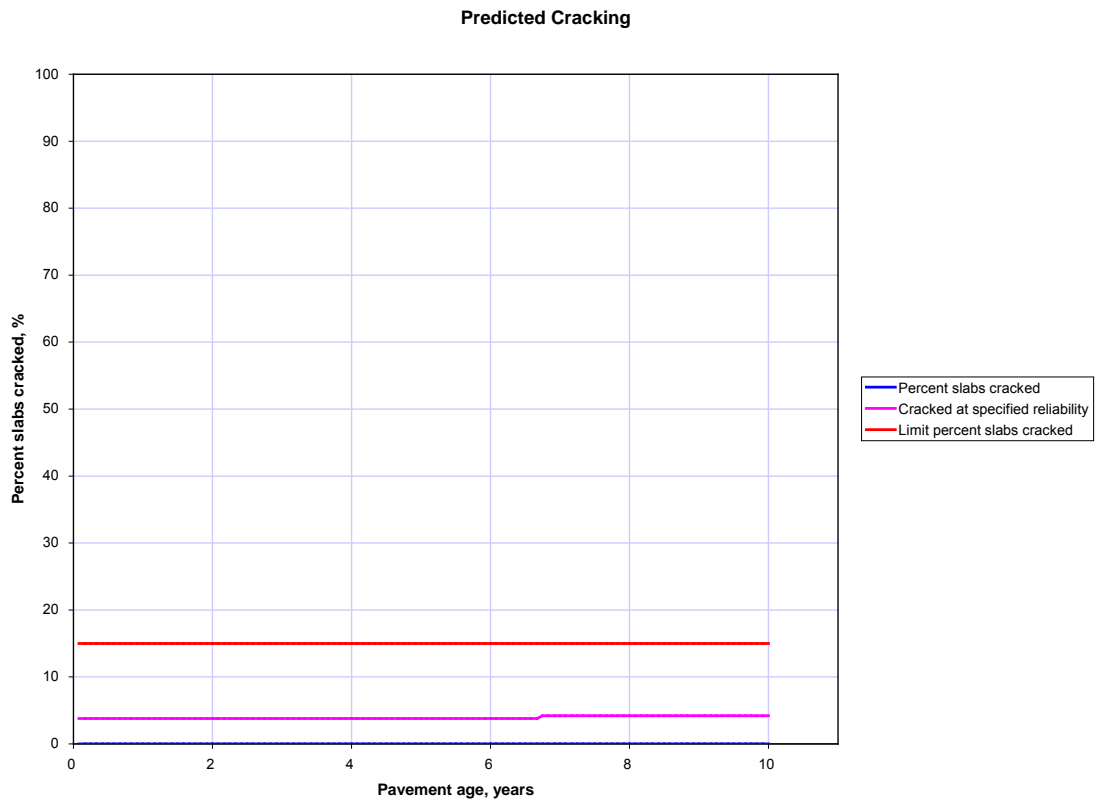
C4	1
C5	-1.98

**Reliability (CRACK)**

Std. Dev.  $\text{POWER}(5.3116*\text{CRACK},0.3903) + 2.99$

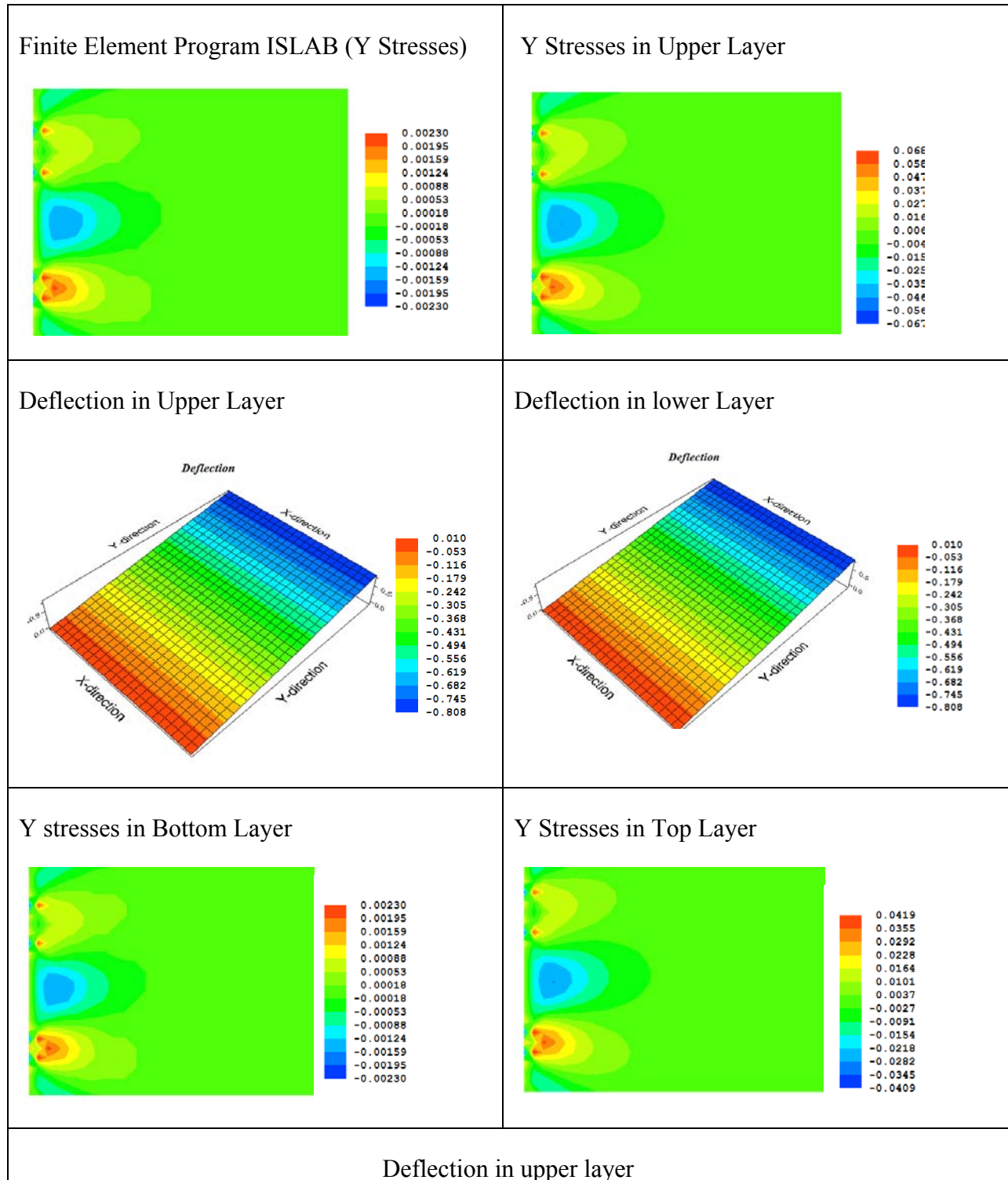
**IRI(jpcp)**

C1	0.8203
C2	0.4417
C3	20.37
C4	1.4929
C5	25.24
Standard deviation in initial IRI (in/mile):	5.4



**Figure 2.3: Crack Prediction for Pervious Pavement on Clay**

## 2.5 Structural Analysis of Pervious Versus Normal Concrete Using I-Slab



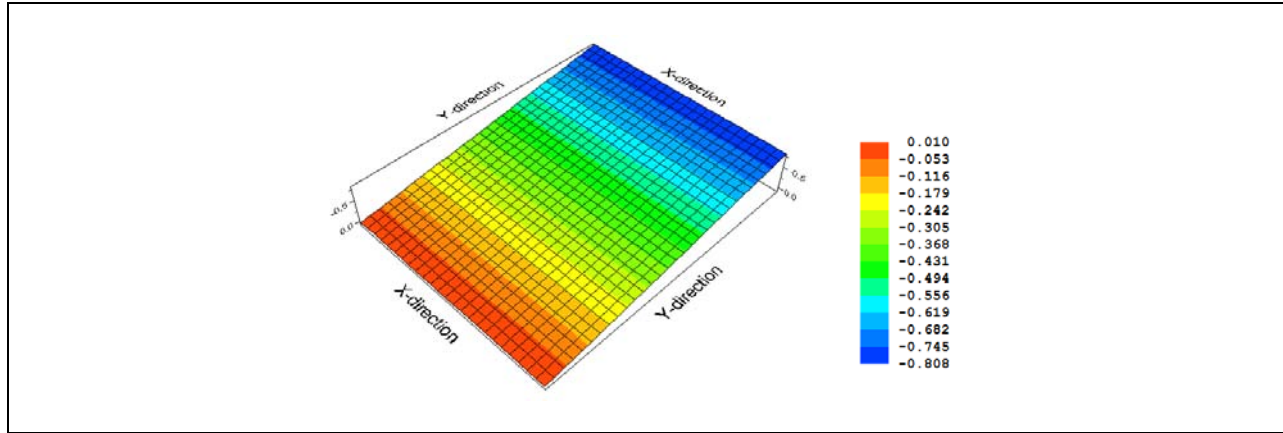


**Figure 2.4: Structural Analysis of Pervious Versus Normal Using ISlab**

**2.6 Hydrological Infiltration Model for Pervious Concrete**

**2.6.1 Vertical Pipe and Block Model (Bernard's Tortuosity Model)**

Arrange the Aggregate and paste assumed to be spheroidal and the remaining pores serve as the vertical hydraulic conductivity path

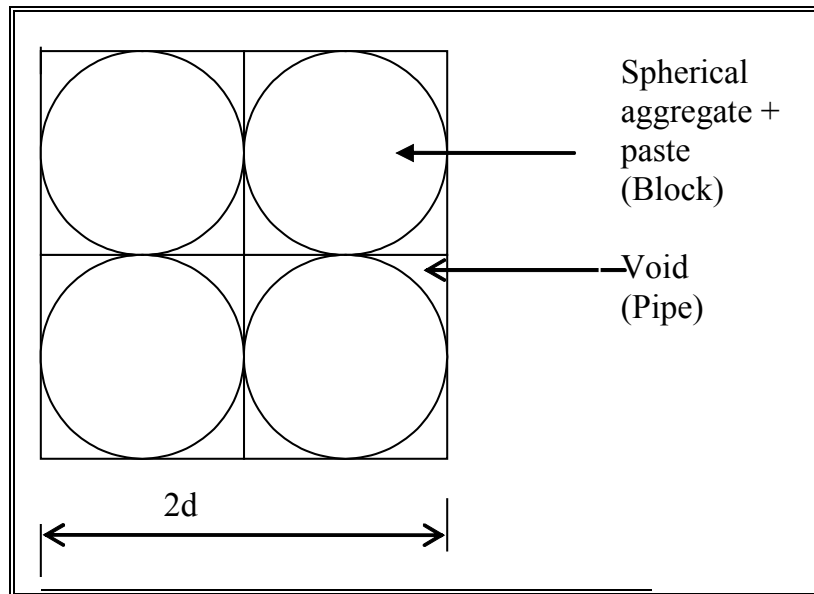


**Figure 2.5: Bernard's Block and Pipe Hydraulic Model**

Bernard's Block/ Pipe model

Paste factor (Pa) =

Pipe length =

Block length =

t =

$$\eta = 1 - \left[ \frac{4}{3} [1+Pa] (\pi d^3/8)/d^3 \right]$$

$$\left[ \frac{W_w}{\gamma_w} + \frac{W_{Cem}}{\gamma_{cem}} \right] / \frac{W_{agg}}{G_{agg} \gamma_w}$$

$$\pi t / 2$$

Pavement thickness

thickness of the pavement layer.

Start with the flow of a viscous fluid in a channel. The channel has a width in the  $y$ -direction of  $a$ , a length in the  $z$ -direction of  $l_z$ , and a length in the  $x$ -direction, the direction of flow. There is a pressure drop along the length of the channel, so that the constant pressure gradient is (such a pressure gradient could be supplied by gravity, for instance). Assuming the flow to be steady,  $\mathbf{v}/\delta t = \mathbf{0}$ . Also, we'll assume that the flow is of the form.

The no-slip boundary condition at the top and bottom edges of the channel reads.  
 $v_x(y = \pm a/2) = 0$ ;

The Navier-Stokes equation then becomes  $\eta \frac{\delta^2 v_x}{\delta y^2} + \frac{\Delta p}{l_x} = 0$ .

Integrating twice, we obtain  $v_x(y) = -\frac{1}{2\eta} \frac{\Delta p}{l_x} y^2 + C_1 y + C_2$

where  $C_1$  and  $C_2$  are integration constants. To determine these, we impose the boundary conditions to obtain

$$v_x(y) = \frac{1}{2\eta} \frac{\Delta p}{l_x} \left[ \left(\frac{a}{2}\right)^2 - y^2 \right]$$

We see that the velocity profile is a parabola, with the fluid in the center of the channel having the greatest speed. Once we know the velocity profile we can determine the flow rate  $Q$ , defined as the volume of fluid which passes a cross section of the channel per unit time. This is obtained by integrating the velocity profile over the cross sectional area of the channel:

$$Q = \int_0^{l_x} dx \int_{-a/2}^{a/2} dy v_x(y) = \frac{l_x a^3}{12\eta l_x} \frac{\Delta p}{l_x}$$

The analogous result for flow through a pipe of radius  $a$  and length  $l$  in the presence of a uniform pressure gradient  $\Delta p/l$  is  $Q = \frac{d^4}{128\eta l} \frac{\Delta p}{l}$ ,  $Q$  = Discharge and  $\eta$  is kinematic viscosity of water.

Layer 2 is modeled as not having the Pa component. Additionally it assumes that the reservoir includes the pond depth + thickness (actual) of surface.

### 2.6.2 Reversed Draw Down Model (Bernard's Concept of Reversed Drawdown)

The model assumes a homogenous, confined aquifer, with radial flow to the pumping well. The drawdown can be estimated from the Theis Well equation:

$$h_0 - h(r, t) = \frac{Q}{4\pi T} \int_u^\infty \frac{e^{-u}}{u} du = \frac{Q}{4\pi T} W(u)$$

$h_0 =$	The initial elevation of the piezometric surface (m)
$r =$	distance from the pumping well (m)
$t =$	time since pumping began (d)
$h(r,t) =$	the elevation of the piezometric surface at distance r and time t (m)
$Q =$	the pumping rate (m <sup>3</sup> /day)
$T =$	Aquifer transmissivity
$U =$	Well Function
$S =$	Aquifer storativity
$h_0-h(r,t) =$	drawdown (m).
$W(u) =$	Well function, defined as the integral in the first equation. This function is tabulated in most ground water hydrology textbooks. It can also be predicted based on a polynomial equation.

### 2.6.3 Hantush Mounding Model

According to Hantush 1967 (32) the following equations for predicting the maximum height of the water table beneath a circular recharge area:

$$h_m^2 - h_i^2 = (V/2\Pi K)[w(u_0) + (1-\exp(-u_0))/u_0] \quad \dots \quad 1$$

$$V = w\Pi R^2$$

$$\Pi = Kb/\varepsilon$$

$$b = 0.5[h_i(0) + h(t)]$$

$$u_0 = R^2/4vt$$

where  $h_m$  is maximum height of mound above aquifer base (i.e., maximum saturated thickness of aquifer beneath recharge area);  $h_i$  is initial height of water table above aquifer base (i.e, initial saturated thickness of aquifer);  $K$  and  $\varepsilon$  are hydraulic conductivity and storativity (specific yield) of the aquifer, respectively;  $w(u)$  is Theis (3) well function for non-leaky aquifers;  $w$  is constant rate of percolation from circular recharge area of radius  $R$ ; and  $b$  is a constant of linearization. The aquifer is unconfined and assumed to have infinite extent. Equation 1 is nonlinear owing to the definition of  $b$ ; however, the solution is readily obtained using successive iteration.

**Table 2.10: Prediction of Mounding for a Sustained 1in/hr Rain Using a VBA Model for the above Equation**

<b>Results of Groundwater Mounding Calculation</b>				
<b>Solution by Successive Approximation</b>			<b>K [L/T]</b>	1
<b>Iteration</b>	<b><math>h_m^*</math></b>	<b>% Change</b>	<b>e</b>	0.5
1	11.13	11.35	<b><math>h_i</math> [L]</b>	10
2	11.196	0.56	<b>R [L]</b>	24
3	11.2	2.91E-02	<b>w [L/T]</b>	0.6
4	11.2	1.55E-03	<b>t [T]</b>	1
5	11.2	8.34E-05	<b><math>h_m</math> [L]</b>	11.2
<b>maximum water-table rise (<math>h_m - h_i</math>) = 1.199</b>				

*2.6.3.1 Mounding Effects*

Results shows that a sustained 1in/hr rainfall for 24 hours will mound by 3ft over the original phreatic surface. This head above the top of grading grade (the bottom of the base) must be transformed into actual height of water.

Example: Elevation of phreatic surface = 900

Elevation of Top of grading subgrade = 902.5

Height of water in Base theoretically is ½ ft but the accommodation is done by 40% void. Whence effective height of water is  $10/4 * 0.5 = 1.25$  ft but the Storage is only a foot thick. The water appears on the surface since the pavement has 20% voids and the Base 40%

Another quick application is the effective void which is  $(0.4*1 + 0.2*.5)/1.5 = 0.33$ .

Actual rise of water in the base and pavement will be  $1/ 0.333$  or 3 times the volumetric height.

Clue: The actual storage volume is the void content.

## 2.6.4 Dynamic Hydraulic Conductivity Model

### 2.6.4.1 Model 1 Constant Volume Constant Time, Variable Spread

Case 1: Pour a 5 gallon bucket in a defined time ((30 sec) on a defined 8inch diameter circle and measure the spread area.

Advantage

- Easy

Disadvantages

- Surface tension
- Surface unevenness and local slopes
- Very qualitative
- Very surficial (Surface may define the spread before the interior cavities kick in)

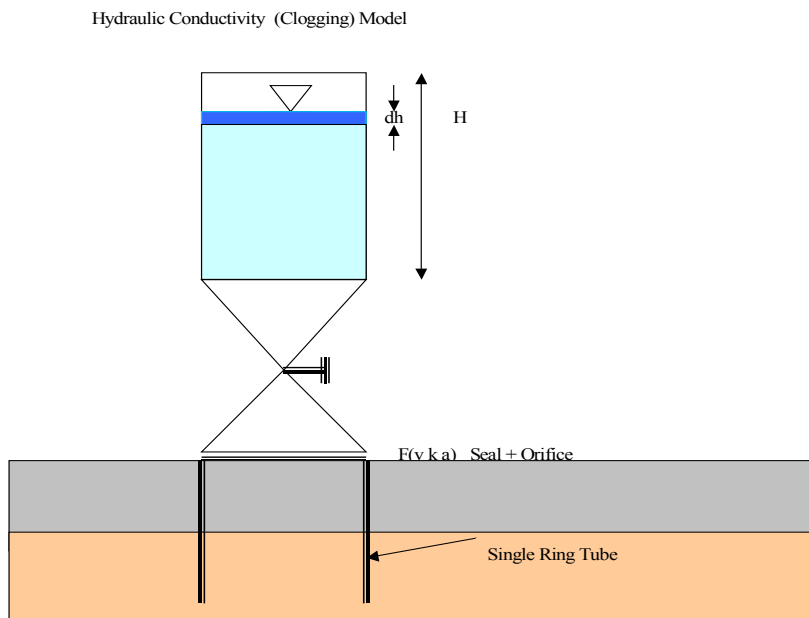


**Figure 2.6: Hydraulic Conductivity Model (Perveammeter Design)**

### 2.6.4.2 Model 2: Perveammeter Analysis from Discharge through a Varying Head

Flow equations through the perveammeter

Construction: A Thin walled vessel with non-corrugated interior a conical base

Control valve and rubber seal-rimmed

Belled exterior coincides with single ringed tube vessel

*By Continuity Equation*

$$\Pi d^2/4 dh = V_o A_o dt \quad (1)$$

*Bernoulli Equation*

$$P_1/\rho_1 g + V_1^2/2g + Z_1 + \text{Losses} = (P_2/\rho_2 g + V_2^2/2g + Z_2) \quad (2a)$$

$$V_o = K \sqrt{2gh} \quad (2b)$$

*Substituting eqn 2 in 1*

$$\Pi d^2/4 dh \sqrt{2g} [A_o K (h)^{-1/2}] dh = dt \quad (3)$$

*Integrating both sides,*

$$T = -\Pi d^2/8 \sqrt{2g} [A_o K (h^{1/2} + C)] \quad (4)$$

*Boundary Conditions, When T=0 h=H Equation 4 becomes*

$$T = -\Pi d^2/8 \sqrt{2g} [A_o K (h^{1/2} - H^{1/2})] \quad (5)$$

At empty  $h=h_e$ , Generic equation  $T = \lambda (h_e^{1/2} - H^{1/2})$  from where  $\lambda$  can be deduced, where  $\lambda$  is the porosity function for the measured location.

**The constant K will change with the clogging Of the pervious layer and that will affect the Time function.**

$T_{air} =$  will be an important calibration function.

**Any change in this will indicate a change in the Perveammeter**

**To is the Time of Discharge through the porous media after construction**

**T is the Conductivity dependent variable** Monthly readings of T will be taken.

It must be noted that this discharge equation does not neglect the velocity head as would be done in the Static/ dynamic head permeammeter. In the permeammeter, fluid motion is essentially due to suction or infiltration and would not include high infiltration rates as is prevalent in adequately functioning pervious pavements.

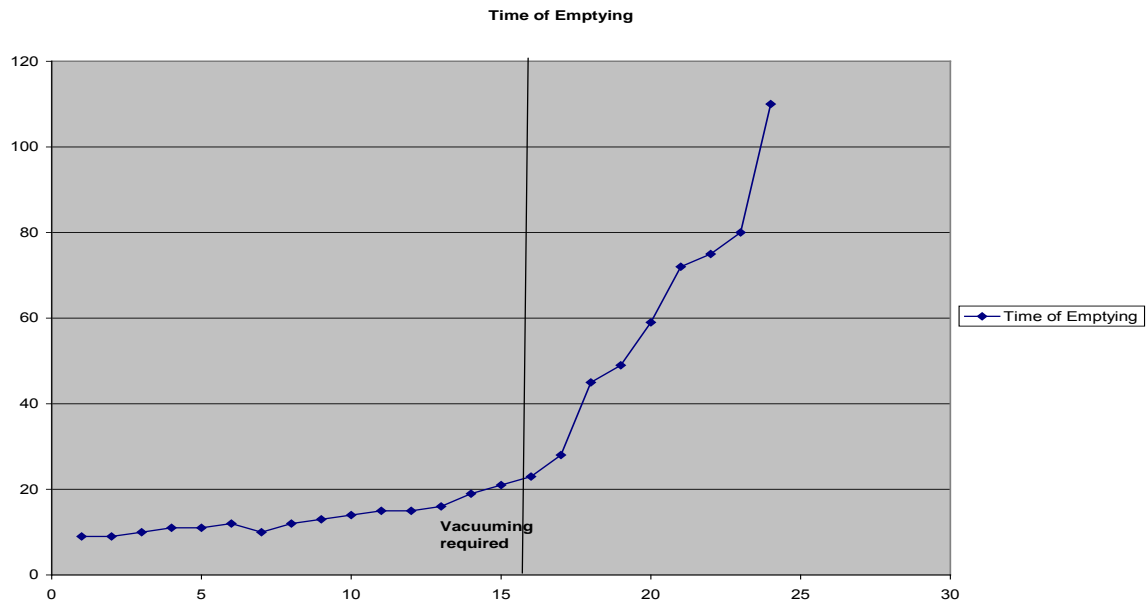


**Figure 2.7: Predicted Hydraulic Conductivity Model**

Importance of a Single Ringed Tube + Perveammeter Assembly

- One Dimensional flow
- Constrained (Non-Splashing) Measurement
- Simulates actual infiltration
- Not affected by surface tension
- Simple analysis of unsteady flow.

### 2.6.5 Conventional Green Ampt Infiltration Model

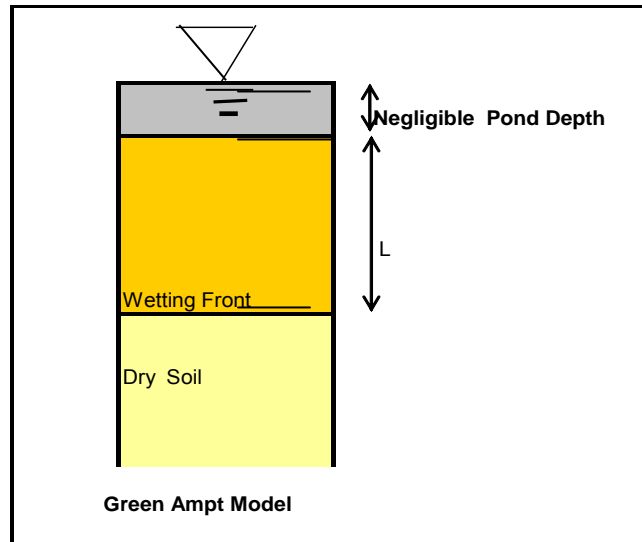


**Figure 2.8: A Green-Ampt Model**

$$f = K(L + S_c)/L \quad (3)$$

Where  $f$  is infiltration rate in inches/ hour

$S_c$  is capillary suction at wetting point

$L$  is Distance of Water table to wetting Point

$K$  is hydraulic Conductivity of wetted Zone at Saturation

If  $\eta$  is available porosity which is soil porosity minus initial water content (assume 0 water content of base and surface before a rain event).

If  $F$  is accumulated infiltration,

$$F = K(1 + \eta S_c/F)$$

## 2.7 Baseline Environmental Contamination and Conditions

### 2.7.1 Introduction

As we continue to add impervious surfaces to our land more and more stormwater is added to our already stressed receiving waters causing excessive erosion, damage to the environment, and costly repairs. Stone Jr. (2003) cites studies that a 30% or more impervious cover severely impacts the watershed. The need to provide solutions to reduce post development runoff to pre development numbers is necessary if we want to keep the waters of the state in Minnesota clean and our environment intact. The EPA and MPCA has identified that reduction in stormwater

runoff is necessary and future trends will require projects to retain as much as the first 1 inch of rainfall. Some watershed districts in Minnesota have already adopted this as rule for meeting their permit requirements. Pervious pavements will be one of several tools to help meet these needs in urban areas. Research in other countries, such as Sweden, by Magnus Backstrom (1999), has shown promising results. Adding this research by incorporating low-volume roads will provide more data to the benefits of porous pavement roads in cold climates both for structural and water quality purposes.

The MnRoad facility provides excellent opportunities to meet these goals. The Backstrom (1999) report will be used to help quantify the results. Existing environmental conditions at the MnRoad facility will provide baseline information to compare results of the porous pavement test sections for runoff reduction and water quality.

Instrument Setup and measurement plan will comprise of measuring runoff from the three porous asphalt test sections. This runoff may occur from the surface or from flows captured by drain tile under the pavement sections. The results will provide us with information when the porous sections begin to clog and require maintenance. This also provides us with infiltration rates of the underlying soils and the capacity of the chamber under the pavement.

## ***2.7.2 Baseline Environmental***

### *2.7.2.1 Historic Rainfall*

The rainfall data for this area has been monitored for the past 10 years. The average annual rain fall has been 29.7 inches and the average monthly rainfall (May thru August) is 7.5 inches. The maximum recorded single daily event was 4.98 inches.

### *2.7.2.2 Groundwater*

Piezometers use will be primarily to periodically test the groundwater and monitor ground water flow and elevations. Ground water elevations were measured on 3/04/08 in two wells on the site. Well number 1 measured 9.55 below the surface and well number 2 measured 21.45 feet below the surface. A survey of the site to determine the ground elevations at each well will be completed so that ground water elevations can be computed and added to the report. Samples of the groundwater were taken directly from the piezometers and sent to the Minnesota Department of Health to test for PH, chlorides, nutrients, suspended solids, and various heavy metals. Attached are the results from the tests in Appendix c.

### *2.7.2.3 Overland Flow*

Drainage areas of each section will be the pavement only with no other overland flow occurring from adjacent areas. Runoff volumes will be measured from the surface of each test sections, including a base section which is our standard non-porous bituminous surface. The runoff volumes will be compared and recorded to determine the effectiveness of the porous surface to reduce runoff rates and help to develop a maintenance schedule.

### ***2.7.3 Baseline Contamination Levels***

The samples taken of the ground water prior to construction and underlying soil samples taken during construction will be used to develop baseline contamination levels. The test results of these samples are needed to determine what is in the water and soils before the research testing begins. Surface runoff samples from the base section will be taken during the research period and incorporated as baseline data. This data will be compared to runoff and ground water sampling of the test sections to measure the effectiveness of the pervious surface system, and underlying soils.

#### ***2.7.3.1 Testing Parameters***

The surface runoff of the non-porous section and groundwater will be tested for PH, suspended solids, chlorides, Nitrogen, Phosphorous, cadmium, chromium, copper, iron, lead, mercury, nickel, and zinc.

#### ***2.7.3.2 Groundwater Test Results***

The ground water testing results will be used to monitor if the surface water runoff contains any of the tested parameters, how the porous pavement system filters out these contaminants and if, or how, they impact the groundwater levels.

### ***2.7.4 Planned Water Quality Testing***

The testing parameters that will be done throughout the research period will be consistent with those taken for the baseline information. Storm water retention, infiltration, and runoff rates will be monitored monthly and after major rain events, and the water quality will be documented. Temperature of the stormwater will be recorded as it flows through the filter layers and at the outfall. For comparison, the adjacent impermeable pavement control section will have the same water testing and monitoring protocol. Water samples will be measured and samples taken during rainfall events for each test section. These samples will be tested for PH, suspended solids, chlorides, Nitrogen, Phosphorous, cadmium, chromium, copper, iron, lead, mercury, nickel, and zinc.

Testing will be conducted throughout the research period and samples taken to the department of health for testing. The sampling and testing will take place when automatic sampling devices have captured enough rainfall events to develop valid comparisons. The testing will be monitored and adjusted to keep within budget and provide enough data to adequately develop conclusions to the treatment quality of the porous pavements.

#### ***2.7.4.1 Sampling Methods***

Rainfall data and Storm water retention, infiltration, and runoff rates will be monitored monthly and after major rain events. Temperature of the stormwater will be recorded as it flows through the filter layers and at the outfall. For comparison, the adjacent impermeable pavement control section will have the same water testing and monitoring protocol. These samples will be taken from the automatic sampling equipment.

#### *2.7.4.2 Groundwater Testing*

Groundwater testing is planned to be taken annually and in accordance to the baseline testing procedures.

#### *2.7.4.3 Surface Water Testing*

Tentatively the sampling will be taken from each section when a rain event of 1 inch or greater occurs. The anticipation is to have at least 6 samples in a two year period. This procedure may be adjusted during the research period to provide for these samples. These samples will be taken to the Department of health to test for the above as mentioned parameters.

### **2.8 Geotechnical Report**

#### ***2.8.1 Introduction***

The recommendation by industry to construct the Pervious concrete in over a granular subgrade in a subcell and over a cohesive subgrade on the other subcell necessitated the choice of cells 24 25 and 26 as the destination cells for this project. One half of Cell 24 is a bituminous cell with 6 inches of flexible pavement built over 18 inches of aggregate base. The second half consists of a 7 inch concrete pavement built over 12 inches of aggregate base. The Subgrade material was initially believed to be granular. Cell 25 is separated from cell 25 by a transition area of approximately 50 ft long. Cell 25 is believed to be built on granular material while cell 26 was recorded as a 6 inch bituminous pavement built over 8 inches of base. This layer is underlain by cohesive soils.

#### ***2.8.2 Sub-Surface Exploration Strategies***

MnROAD Operations borrowed a drilling equipment from the MnDOT Materials Office in Bemidji. This equipment facilitates construction of shallow borings of small diameters. The crew drilled Pervious Borings 1 2 3 and 4 in their respective locations on cell 24. Each boring was equipped with screens with slots meeting the hydro geological characteristics of the water bearing strata. Drilling was done on the 5<sup>th</sup> and 6<sup>th</sup> of November 2007

To adequately characterize the soils and drill below the thick layer of cohesive material two other arrangements were made:

- MnDOT Foundations Section to obtain Geotechnical borings from the project and install piezometers
- Plan for Foundations section to use the Cone Penetrometer equipment to ascertain descriptive hydrogeological features such as extent of granular / cohesive layers, true phreatic surface and soil characterization
- Foundations section to provide 4 piezometer-equipped borings in the low-volume road

The CPT exploration was scheduled for the week of November 12 and was performed on 11/13 07

### **2.8.3 Subsurface Description**

#### **2.8.3.1 MnROAD Piezometer Borings**

The locations for these borings are shown in the layout below.

- Well 1 was taken in the vicinity of the existing pond. This boring encountered clays up to 3 ft at the surface. This may represent the lining of the pond when it was constructed 14 years ago. The lateral and areal extent of this lining will be ascertained during construction. It is anticipated that the clay layer does not extend below the top of grading subgrade. If that happens, it should be removed in the subcells that are to be constructed over sand subgrade. The clay lining was not a fat clay but it formed 2 inch ribbons before breakage.
- The clay soils were underlain by a layer of wet to saturated clay extending to 10 feet below the surface. This layer was underlain by a layer of saturated clean sand extending to a depth of 32 ft below the surface. It is not historically obvious that this was a borrowed fill or not but the layer was underlain by a layer of stiff cohesive dark gray Clays. For the purpose of this exercise, the layers encountered from 10 to 32 ft below the surface are in an aquitard. The extent of the containing (not confining) clay layer was not immediately known though it extended to the 36 ft depth at which the drilling was concluded.
- Well 2 encountered wet to saturated sands from surface to 10 ft depth. This was underlain by a layer of saturated sand to a depth of 32 ft and similar to well 1, the aquitard (from a hydrological perspective) which is a perched aquifer (from a historical perspective) was underlain by stiff gray clays extending below the depth of drilling.
- Wells 3 and 4 encountered wet to saturated sands from top surface to 10 ft depth. This was underlain by gray stiff clays extending to and predictably below the extent of drilling.

The drilling strategy was confined to the limitations of auger borings. Retrieval of the borings resulted in a visual observation of the soils encountered. The granular saturated soils were not easily retrieved in the auger but the stiff clays were tenaciously adhered to the auger even after the latter were retrieved and slammed on the pavement to dislodge adhering soils. The permeability of the clay is negligible and will provide a bottom containment for the perched aquifer. However when saturated sands are encountered 3 ft below the surface, this leaves only a reduced storativity of the entire perched aquifer to accommodate additional infiltration coming through the pavement.

Piezometers were installed at depths shown in the layout. The screens were suited to the hydrogeological characteristics of the aquifer layers in the vicinity of the screens. The casings were gravel packed and grouted with bentonite slurry mix and then extended 2 ft above the ground and capped.

#### **2.8.4 MnDOT Cone Penetrometer Test Probes**

MnDOT Foundations Section performed cone penetrometer test probing in the test cells on the 13<sup>th</sup> of December 2007. The 4 probe logs are shown as Figures 2.16 to 2.19. Each probe provided detailed information on each layer encountered. The Cone penetrometer probes do not retrieve samples nor characterize soils. They however quantify the resistance of soils to the tip

and sleeve and in comparing them, an inference of the cohesiveness can be deduced. The following guidelines were used in the interpretation of the CPT Probes

- A sleeve stress/ tip stress ratio less than 2 to 4 psi is indicative of a granular soil.
- A Sleeve Stress/ Tip Stress exceeding 4 psi is indicative of Cohesive soils
- Pore pressure is a dynamic measure. Saturation at any depth will be determined by relief tests that will indicate static pressures. Hydrodynamic influence of the aquifer transmissivity may affect these results.

Logs showed that the friction ratios ranged from 2 to 4. This indicates that the sands encountered are not clean but may include some silt. This may be prevalent in the vicinity of the clay layers.

Based on these observations it was conclusive that soils encountered were generally granular between 10 ft and 32 ft depth. The suggested piezometer level was 20ft. The perched aquifer encountered in cell 24 is believed to slope westward towards the NW end of MnROAD. Ground water sampling should therefore be done with the understanding that contaminants may travel longitudinally across the cell subgrade with the upstream side being east and the downstream westward.

### **2.8.5 *Foundation Borings***

Foundation borings will be taken to 45 ft in the test cells. They are arranged such that each of the Subcells where pervious pavements are placed over granular subgrades have at least one Foundation boring /piezometer. The location of the proposed foundation borings are shown in Figure 2.9.

SUBSURFACE EXPLORATION LOGS MnROAD Piezometer Borings  
11/13/07

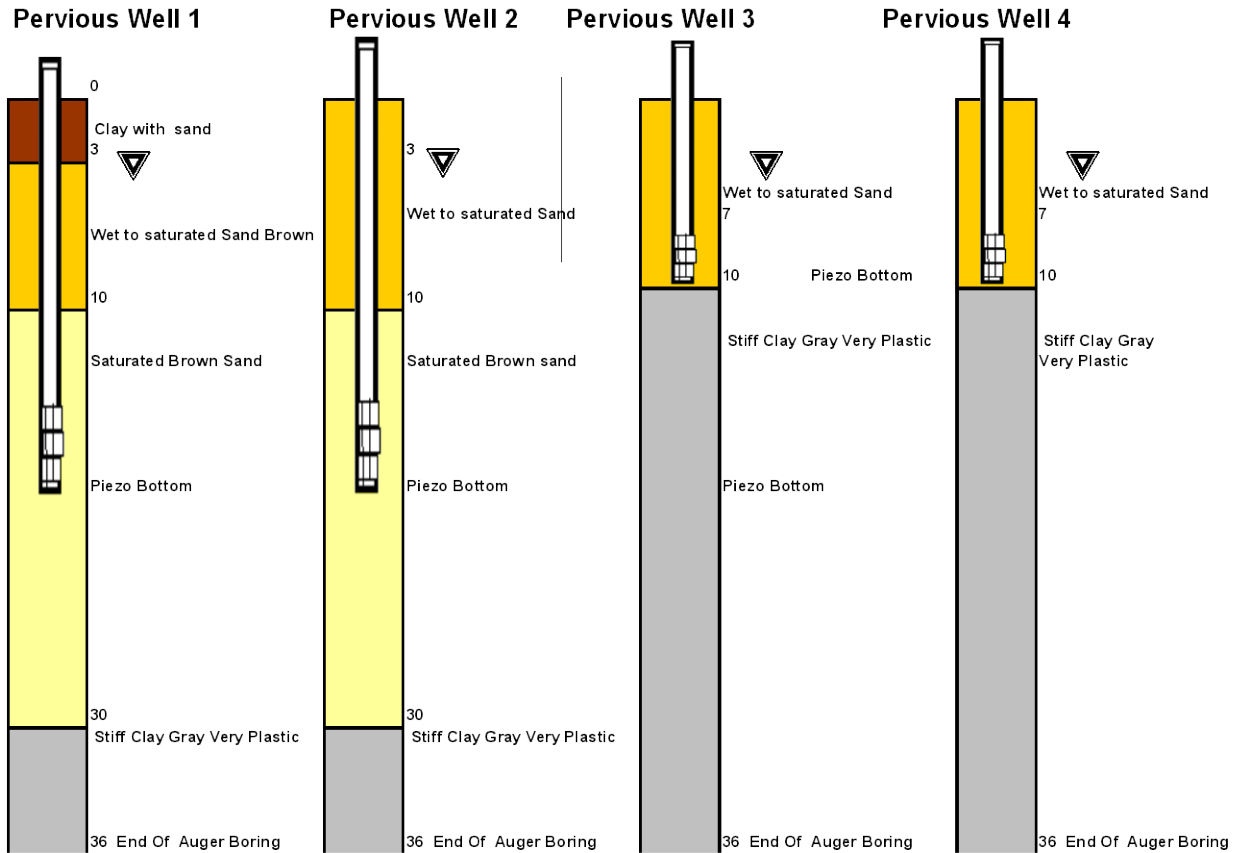


**Figure 2.9: Borings for MW 1 2 3 & 4 Showing Soils Encountered**

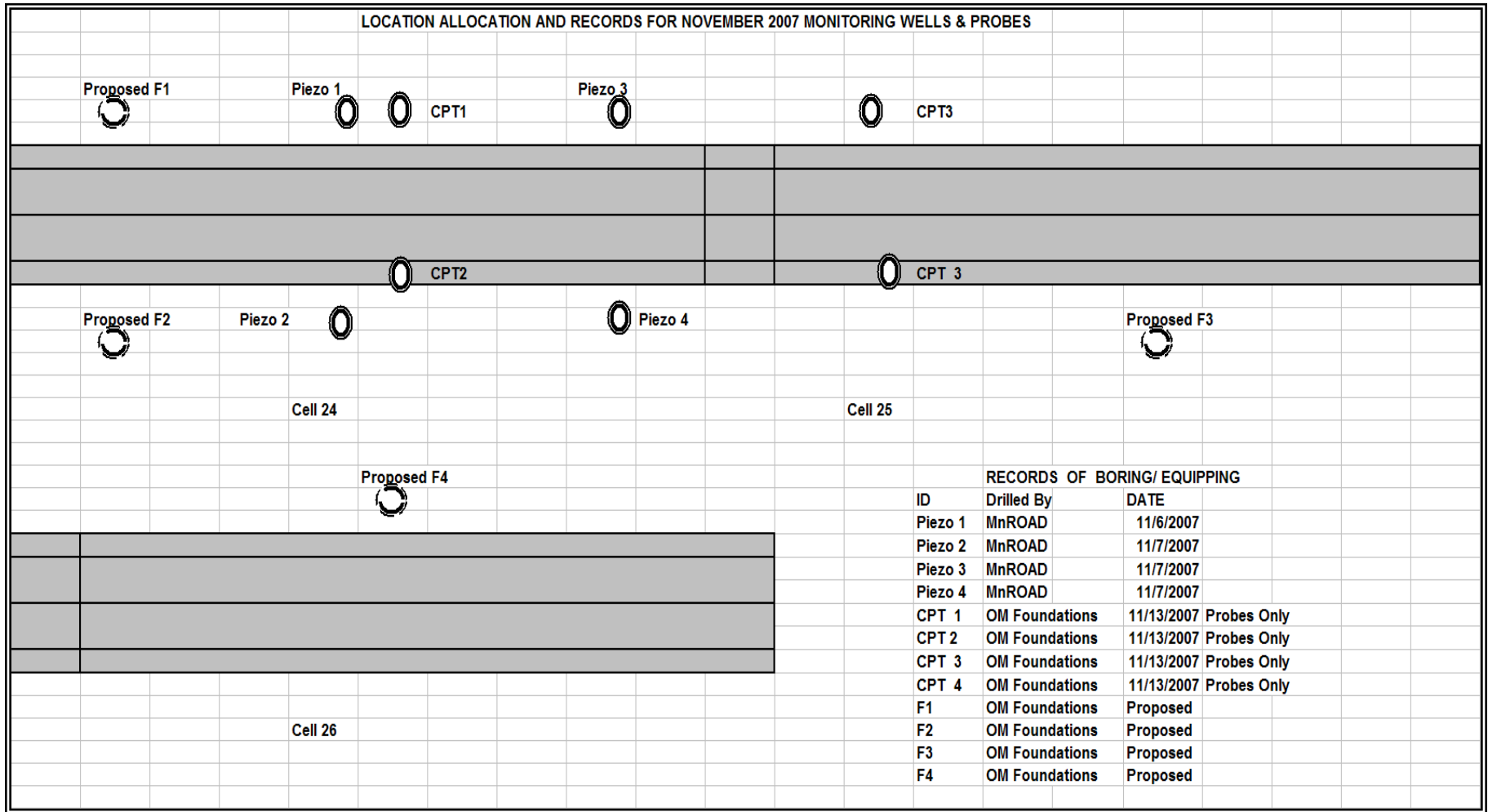


**Figure 2.10: Layout of November 2007 Borings**



**Figure 2.11: Pervious Well 1 Completed Sand-and-Gravel-Packed, Bentonite-Slurried Cased and Capped**



**Figure 2.12: Saturated Sands Encountered**



**Figure 2.13: Well 2 Encountered Saturated Sands Up to 30 Ft Depth below Surface**



**Figure 2.14: Stiff Gray Clays Encountered at 32 to 36 ft Well 2**

This Westward sloping Aquiclude was made up of this material encountered at 10 ft in wells 3 and 4 and at 30ft in wells 1 and 2.



**Figure 2.15: Doug Lindenfelser, Chavonne Hopson and Jack Herndon Drilling Well #4**



**Figure 2.16: In the Water Bearing/Saturated Layers, Auger Sample-Retention Was Minimal**

MINNESOTA DEPARTMENT OF TRANSPORTATION - GEOTECHNICAL SECTION  
**CONE PENETRATION TEST RESULTS**  
**UNIQUE NUMBER 69249**  
 U.S. Customary Units

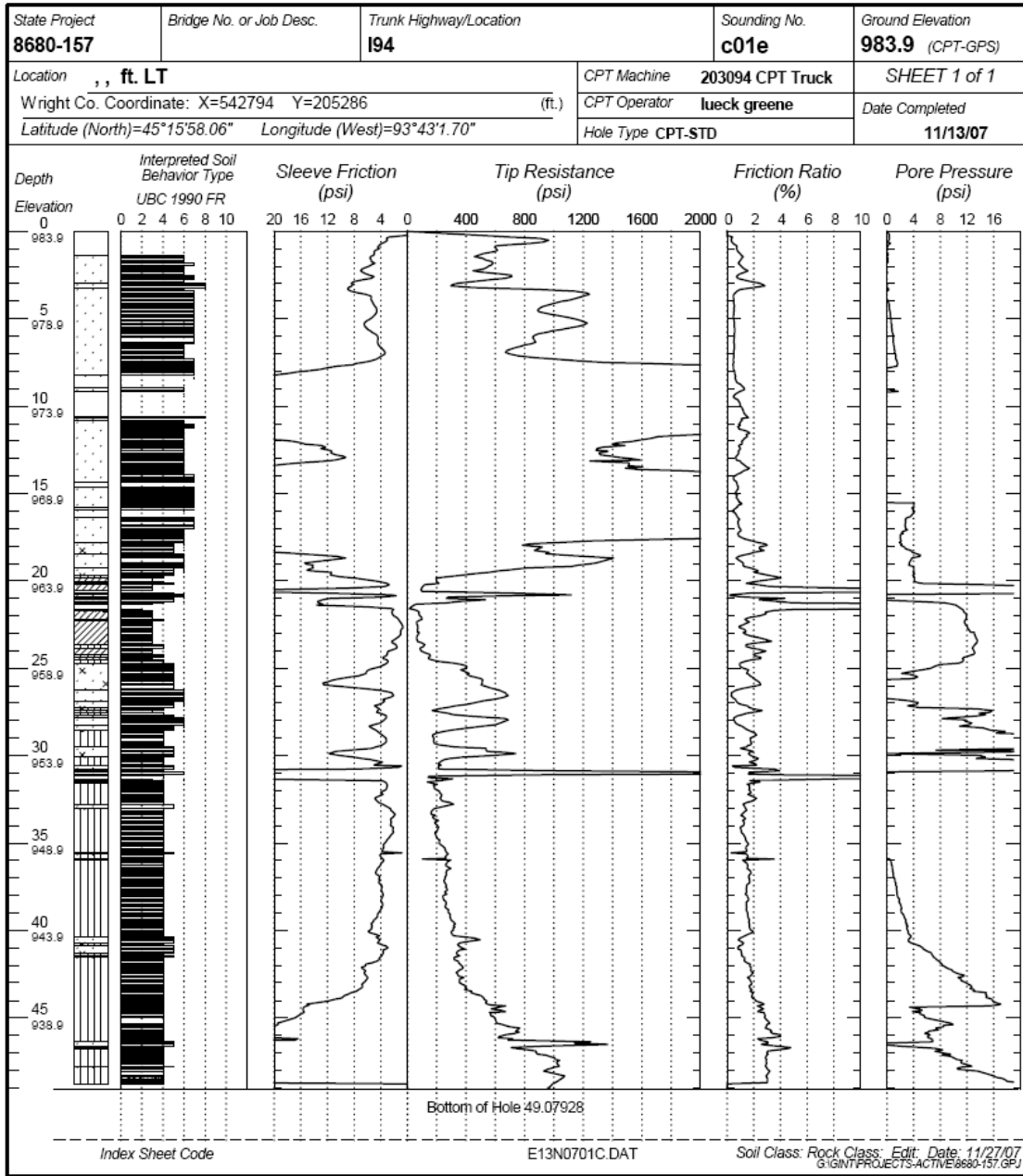


**Figure 2.17: CPT PROBE 1**

MINNESOTA DEPARTMENT OF TRANSPORTATION - GEOTECHNICAL SECTION

**CONE PENETRATION TEST RESULTS**  
**UNIQUE NUMBER 69250**

U.S. Customary Units

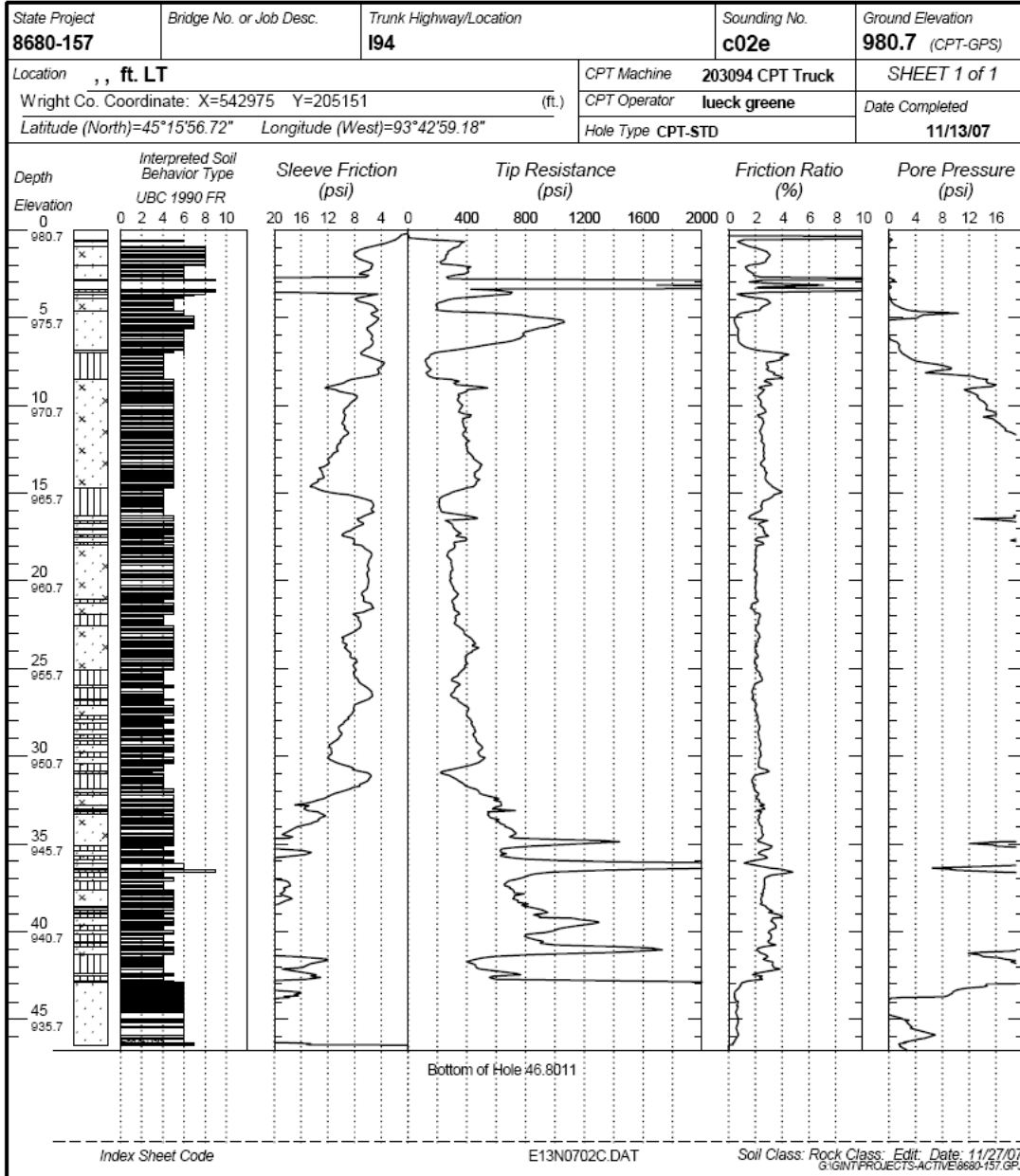


**Figure 2.18: CPT Probe 2**

MINNESOTA DEPARTMENT OF TRANSPORTATION - GEOTECHNICAL SECTION

**CONE PENETRATION TEST RESULTS**  
**UNIQUE NUMBER 69251**

U.S. Customary Units

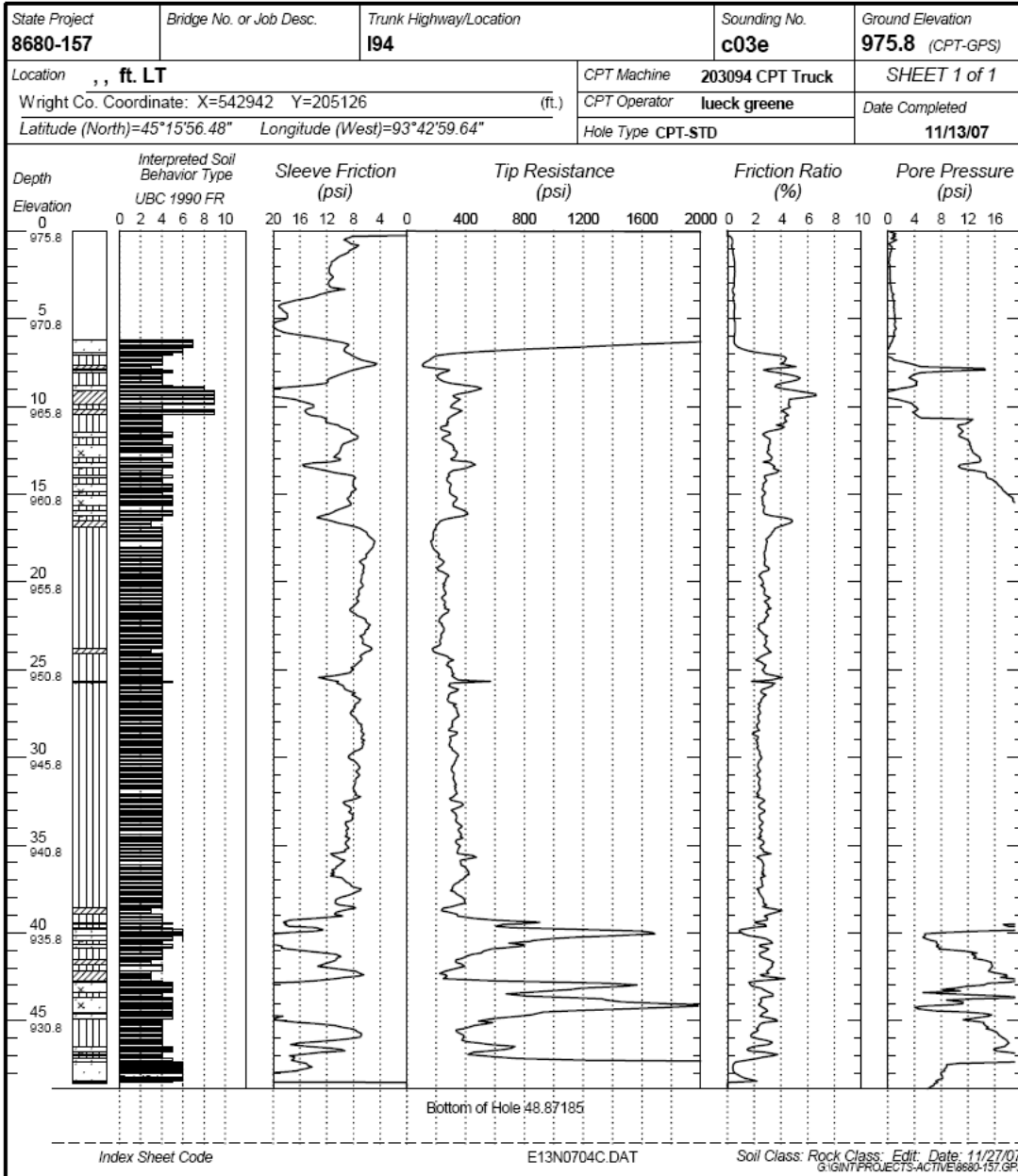


**Figure 2.19: CPT Probe 3**

MINNESOTA DEPARTMENT OF TRANSPORTATION - GEOTECHNICAL SECTION

CONE PENETRATION TEST RESULTS  
**UNIQUE NUMBER 69252**

U.S. Customary Units

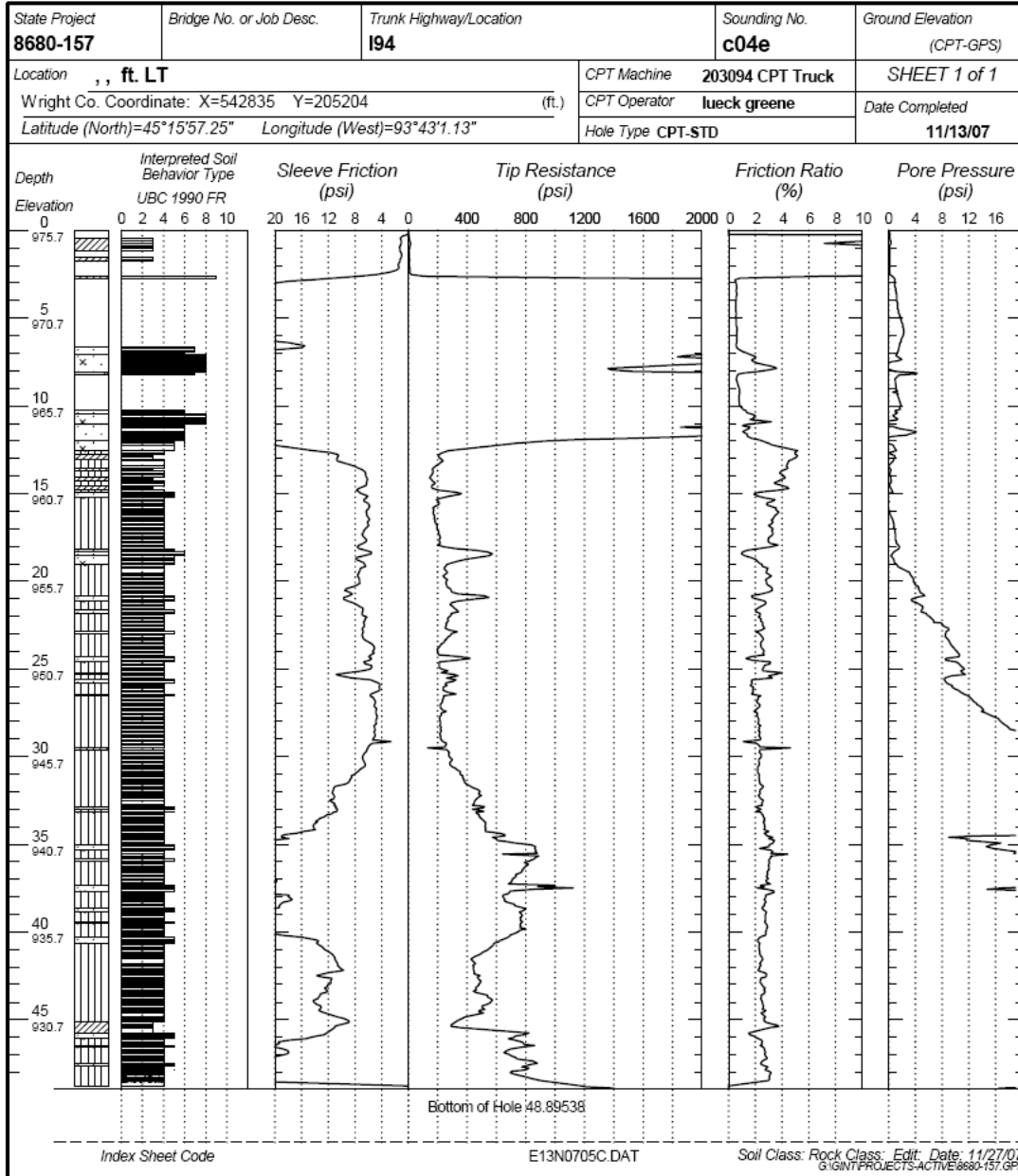


**Figure 2.20: CPT Probe 4**

## CHAPTER 3 CONSTRUCTION OF CELL 39, 85 AND 89

Two full-depth pervious concrete pavements and one porous overlay were constructed in 2008. The porous overlay was placed over a skew-jointed 20 ft panel concrete pavement built in 1994. The joints were in various degrees of disrepair but were averagely in fair condition prior to the overlay. The overlay was performed on the 1<sup>st</sup> of October 2008. It was made of a unique self-consolidating slip formable porous mix developed by the CP tech center in Iowa State University. Remarkable items in the mix included, fiber reinforcement and high workability but it also used a low water cement ration of 0.3. MnDOT researchers instrumented the section with vibrating wire strain gauges, water blocks and thermocouples.

This chapter primarily discusses the construction sequence.

Cell 37 consisted of 4-inch porous concrete placed on 8 inches of existing concrete substrate, previously the riding surface for cell 39 from 1994 to 2008. One of the requirements for this was that it needed a 20 to 25 percent void content and single sized aggregate gradation and the porous overlay met this requirement. It maintained a water and cementitious ratio of 0.3 and was designed to be self-consolidating and slip formable. Placement was achieved by direct discharge from the concrete truck and by fixed forming. The concrete was roller compacted with a set of three drums rolling in the longitudinal axis (1-ft diameter and 13 ft long) and they were powered by a gasoline engine that imparted the vibratory motion onto the drums for effective consolidation without loss of design porosity.

The drums were closely followed by the curing compound applicator that discharged enough con-film to cover the surface. This was closely followed by the placement of the two layers of polyethylene sheeting spread over the pavement and anchored from wind and other elements with a series of steel rods. The transverse joints were cut through the polyethylene sheeting to a thickness of one-third of the overall overlay thickness. To facilitate drainage from the porous pavement, French drains consisting of CA 15 aggregate were place along the shoulder and against the pavement. Within the French drains, drainage routes were constructed across the aggregate shoulder at 50 ft interval to expel the water from the pavement

The concrete surface was allowed to cure for 28 days before traffic was placed on it. Unique features of this pavement include the dispersion of polyolefin fibers and other non-fibrous polymers in the matrix and the addition of 6% sand (by volume) to enhance bonding with the substrate. Initial sound absorption test showed this pavement to be comparable to cell 85 where the pavement is 7 inches thick and built on 12 inches of rail road ballast. The porous overlay maximized the advantages of lesser tortuosity, more absorbent materials (fibers) and efficient placement. Figures 3.5, 3.6 and 3.7 show construction pictures and the resulting surface.

**11/6/07:** MnROAD crew drill and equip monitoring wells in the vicinity of proposed porous pavements and commence monitoring of ground water.

**11/13/07:** MnDOT Foundations perform cone penetrometer tests probing at four locations to a depth of 40 ft.

**12/13/07:** MnDOT Foundations drill and equip 4 monitoring wells in the vicinity of Cells 85 to 89 and subsequently render geotechnical report. The report is included in task 2 of The LRRB Pervious Concrete Research Project.

**6/30 2008: Trial Placement of Sensors:** Researchers tried 2 methods of topical sensor placement. One of which involved the stamping of a Plexiglas underlain loosely with the sensor unto the pavement. Glass was vibrated until the sensor and cables were embedded in the top ½ inch of concrete. The other method entailed the use of a lumbar in lieu of the Plexiglas to achieve the same purpose. Test slab was distressed and a relief joint was subsequently provided to minimize the distress on the test slab. The process improved the level of proficiency of the two placement methods to some degree.

**7/30/08 Trial Mixing Process:** A trial mixing was performed at American Engineering Testing in the months of June and July of 2008. The Producer and the Concrete Testing Consultant as well as Iowa State University (designer representative) set the machinery in motion and conducted three trials. The result of the trial mix is shown in Appendix E Trial Mix Results. For a distinction, the porous overlay mix is referenced in the trial mix report as “porous” while the pervious mixes are referred to as “pervious”.

**9/10/08-9/15/08: Base material for Cells 85 and 89:** Initial requirement for CA 15 was revised because the surface formed with CA15 was not capable of supporting construction traffic. Many alternatives considered were:

- Pumping the concrete: Jettisoned because that was a new dimension to a sufficiently new product
- Belt placement of the concrete from trucks docked on the other side of the low-volume loop.
- Fortify the 12-inch base with a 4-inch undercut and replace with 4 inches of railroad ballast nominal size 2-3 inches and compact. This compaction would be evaluated by a quality compaction.

The third option was chosen and a design correction was made immediately.

**Nov- 2007- March 2008: Soils Investigation.**

**9/20/08: Trial placement of porous overlay:** A concrete truck with a load arrived at 2:00 pm to place a 6' X 6' X 4" porous slab on the concrete substrate. The concrete was covered with a layer of polythene and allowed to cure. Cores were taken on the second day and unit weight values were measured using the vacuum bag method in the MnDOT Bituminous Laboratory (the concrete laboratory did not have the artifice to seal bags hermetically and perform gravimetric test and measurements on pervious concrete at the time of measurement). The results were 124 PCF and 129 pcf for the two samples tested.

**9/28/08: Preparation of surface for porous overlay:** Contractor destroys and removes 50 ft of notch at ends of the cell to allow an inlay in transition area.

**9/29/08:** The surface of cell 39 was sand blasted and forms were placed for still-formed construction.

**9/30/08: Placement of Sensors:** Vertical dowels were placed in predrilled holes and trimmed to prescribed height within 4 inches to allow for a slight cover to the upper sensors. Sensors were covered with concrete and poker vibrated prior to the approach of the screed drum rollers

**9/30/08: Instrumentation of the pervious Cell:** The instrumentation layout plan are shown below. Summarily, instrumentation included a sensor tree of thermocouples, water blocks arranged to a depth of 6 ft and a concentration of vibrating wire strain gauges on the concrete substrate. These were held down with wooden dowels encased in the concrete substrate. A 6-ft hole was drilled through the concrete and augured into the existing base and subgrade. A sensor tree comprising of thermocouples and water blocks were installed in the drilled hole. A schematic layout of the sensor trees is shown in the sensor layout shown above.

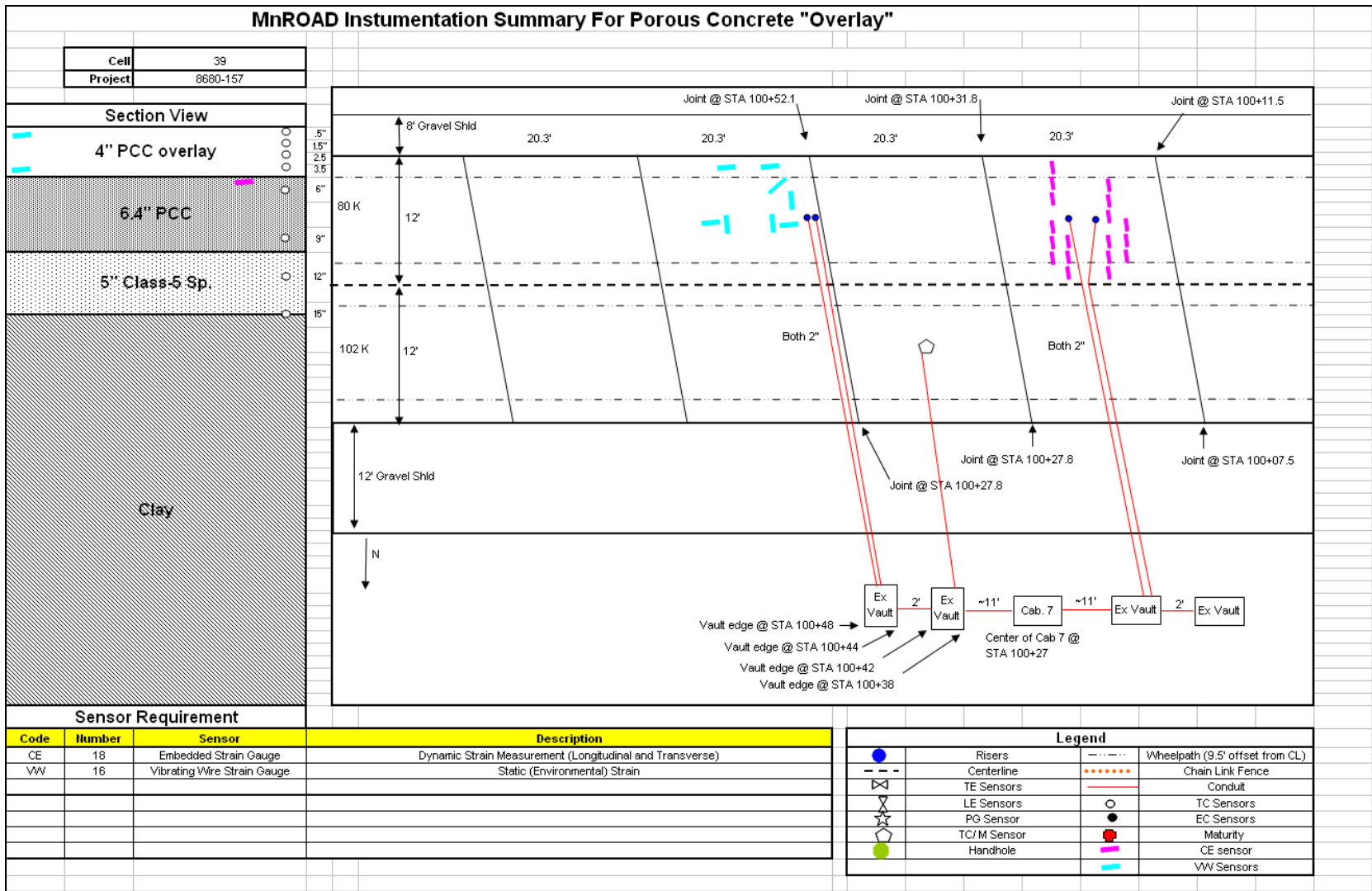
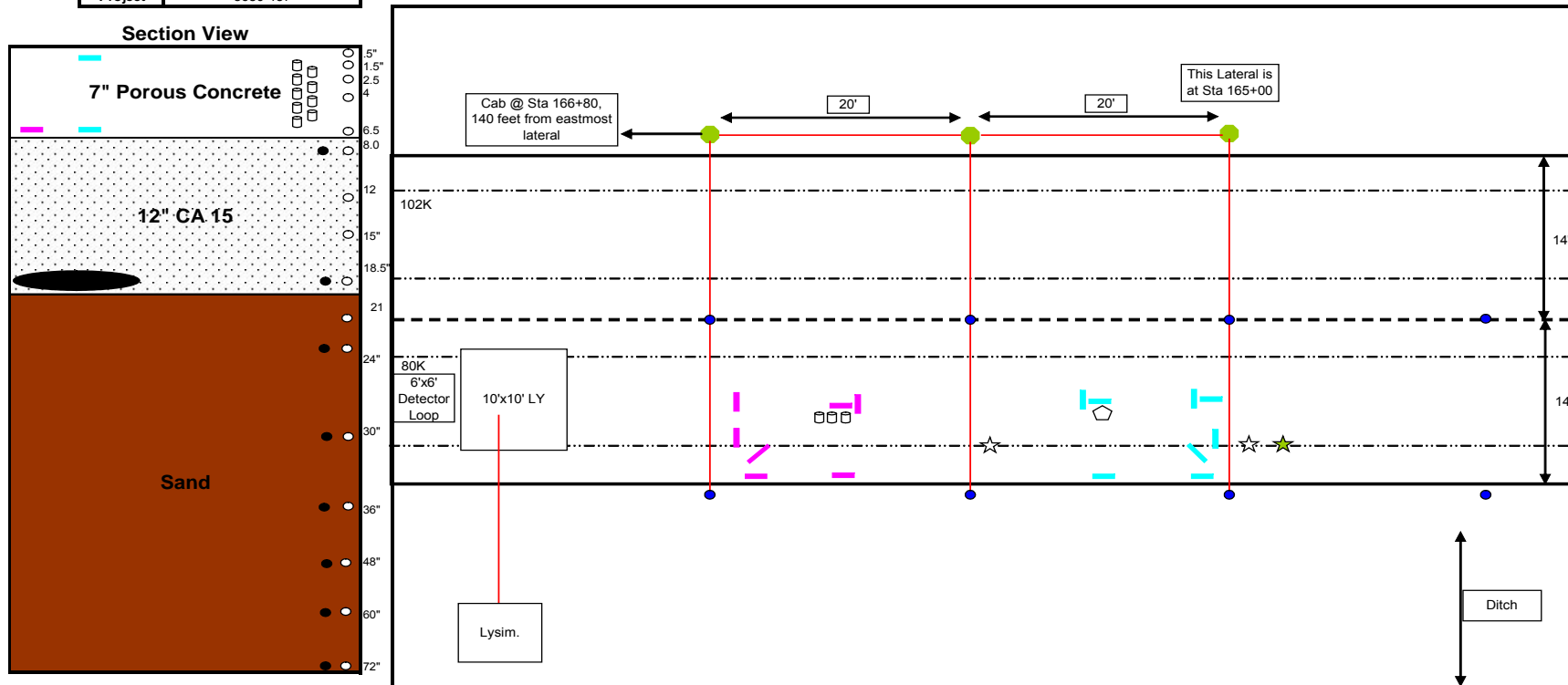


**Figure 3.1: Cell 39 Sensor Layout**

### MnROAD Instrumentation Summary

Cell	85
Project	8680-157



Sensor Requirement		
Code	Number	Sensor
TC	16	ThermoCouple (Temperature)
EC	8	Dedcagon ECH <sub>2</sub> O-TE (Moisture)
TE	6	CTL Strain Gauge, TE
LE	6	CTL Strain Gauge, LE
PG	3	Geokon Pressure Cell, PG
IK	9	Maturity
CE	8	Concrete Embedded Strain Gauge
VW	16	Vibrating Wire Strain Gauge

Description	
Measures Temperature - Installed in a Thermal Couple Tree to a depth of 6' from the surface	
Measures volumetric moisture content, temperature, electric conductivity	
Embedded transverse (TE) strain gauge-measures transverse strain at the bottom of bound layers	
Embedded longitudinal (LE) strain gauge-measures longitudinal strain at the bottom of bound layers	
Measures normal stress at base/subgrade interface	
Wireless Maturity Sticks	
Dynamic Strain Measurement (Longitudinal and Transverse)	
Static (Environmental) Strain	

Legend			
●	Risers	---	Wheelpath (9.5' offset from CL)
---	Centerline	---	Conduit
⊗	TE Sensors	○	Thermocouples
⊗	LE Sensors	●	Moisture Sensor
☆	PG Sensor	□□□	Maturity
☆	TC/ M Sensor	■	CE sensor
●	Handhole	■	VW Sensors

**Figure 3.2: Sensor Layout in Cell 85**

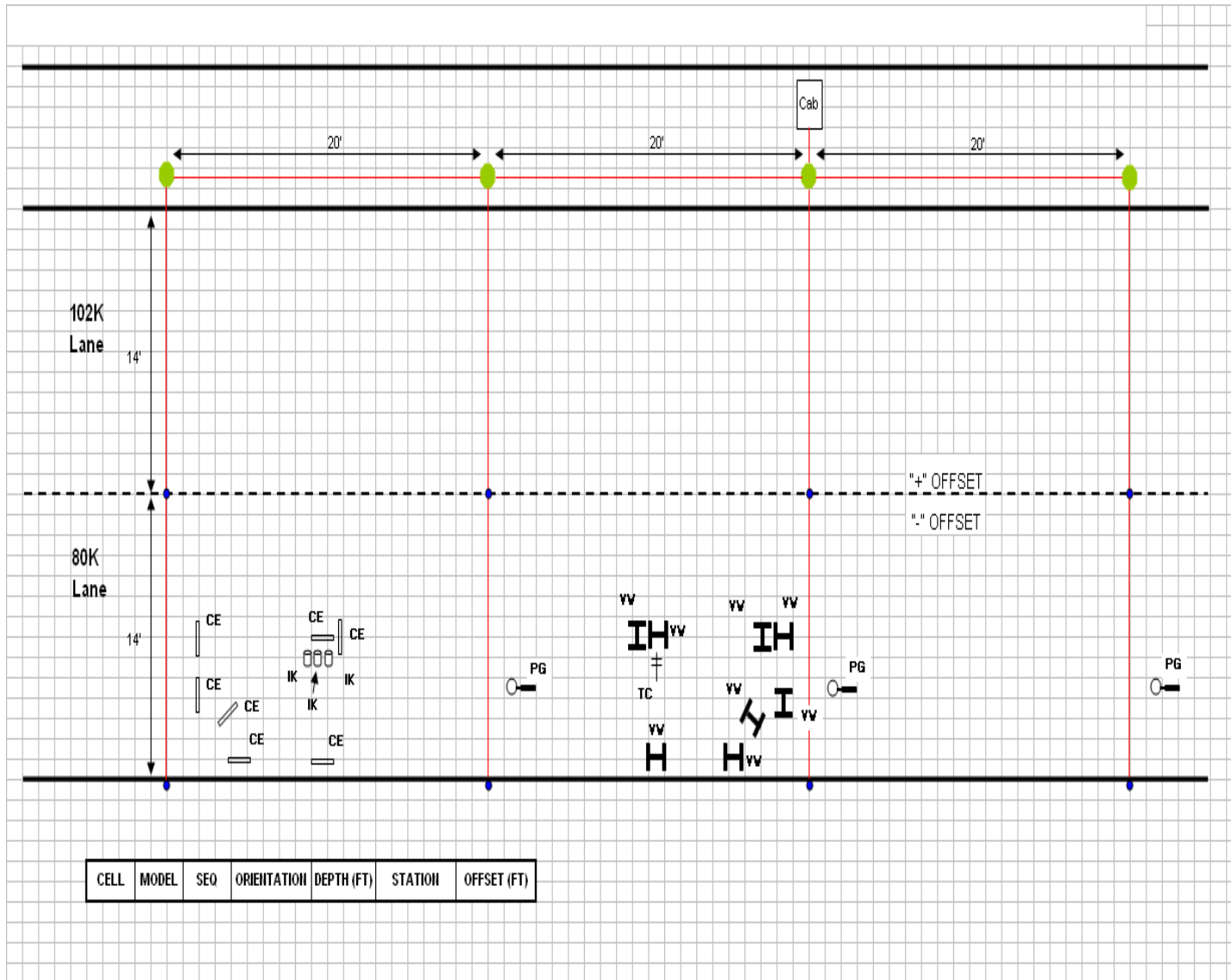
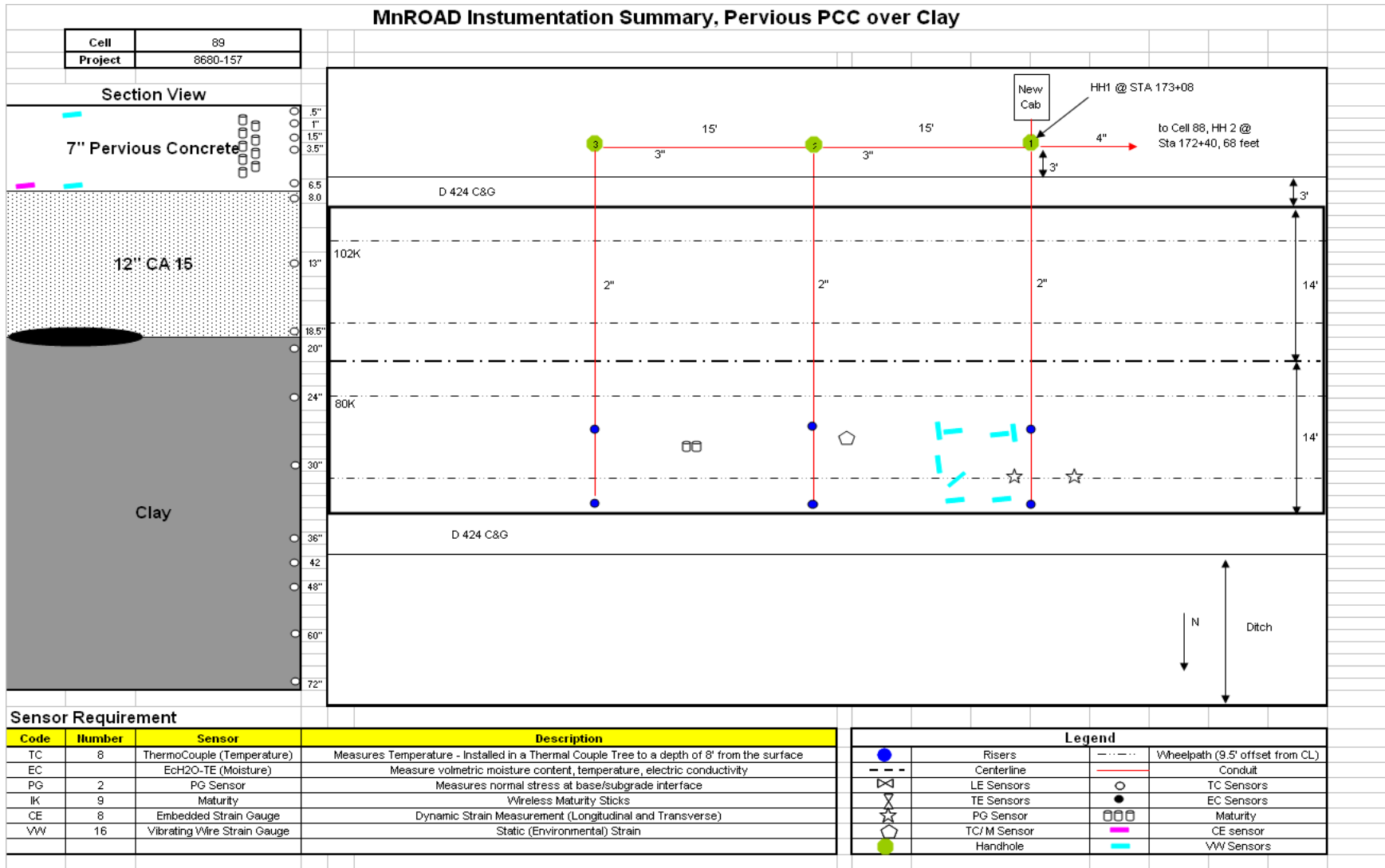


Figure 3.3: Sensor Layout



**Figure 3.4: Layout of Sensors in Cell 89**

**9/30/08: Curbs and Gutters:** Customized curbs were placed on both sides of cells 85 to 89 with the aid of a slipform concrete curb and gutter paver. This was the first curb and gutter system installed since the inception of the MnROAD Facility.

**10/02/08: Placement of Environmental Lane Concrete Cell 39:** Paving of the environmental (outside) lane commenced at 7:00 am. The paving process consisted of direct delivery from the truck chute. The concrete was maintained at a delivery temperature of 60 degrees and was subjected to the gravimetric tests on site for unit weight. The initial tests yielded a compacted unit weight of 123-130 lb per cubic ft while the uncompacted unit weight was at 115 lb per cubic ft. Compaction was achieved by the industry standard by allowing loosely placed concrete in the air meter cylinder to drop 30 times from a height of two inches. By gravimetric analysis, the unit weights and porosity were determined. Maturity data loggers were inserted during the placement and were anchored on the substrate and wedged for a mid-depth location. The wires were not retrieved after shoulder construction and thus the maturity data for the porous overlay was unavailable.

**10/17/08: Paving of Traffic Lane (Cell 85 and 89):** Placement of concrete commenced at 7:00 am with the paving of the traffic (inside) lane. The paving process used a direct delivery truck chute. The concrete was maintained at a delivery temperature of 61 degrees and was subjected to the gravimetric tests on site for unit weight. The initial tests yielded a compacted unit weight of 126-130 lb per cubic ft while the uncompacted unit weight was at 115 lb per cubic ft. Maturity data loggers were inserted during the placement and anchored on the substrate and wedged for a mid-depth location. Researchers placed a mound of concrete in the vicinity of sensors and carefully poked vibrated around the sensors to minimize bumping, displacement and floatation of the sensors by the screed drum rollers. A con-film curing compound was generously applied to the surface and then was covered immediately with two layers of polyethylene. The concrete was allowed to cure for 28 days. Approximately, 150 cubic yards of concrete were placed to pave this lane. The joints were established every 10 ft to match the curb joints. Subsequently, the aggregate shoulder and the transition asphalt pavements were built.

**10/20/08: Placement of environmental and cells 85 and 89:** Placement of concrete commenced at 7:00 am with the paving of the traffic (inside) lane. The paving process used a direct delivery from the truck chute. The concrete was maintained at a delivery temperature of 60 degrees and was subjected to the gravimetric tests on site for unit weight. The initial tests yielded compacted unit weight of 123-130 lb per cubic ft while the uncompacted unit weight was at 115 lb per cubic ft. Maturity data loggers were inserted during the placement and anchored on the substrate and wedged for a mid-depth location. The wires were not retrieved after shoulder construction and thus the maturity data for the porous overlay was lost. Researchers placed a mound of concrete in the vicinity of the sensors and carefully poked vibrated around the sensors to minimize bumping, displacement and floatation of the sensors by the screed drum rollers. A con-film curing compound was generously applied to the surface and was covered immediately after with two layers of polyethylene sheeting. The concrete was allowed to cure for 28 days. Approximately, 150 cubic yards of concrete were placed to pave this lane.

**10/25/08: Placement of traffic lane concrete:** Placement of concrete commenced at 7:00 am with the paving of the traffic (inside) lane. The paving process used a direct delivery from the truck chute. The concrete was maintained at a delivery temperature of 60 degrees and was

subjected to the gravimetric tests on site for unit weight. The initial tests yielded compacted unit weight of 123-130 lb per cubic ft while the uncompacted unit weight was at 120 lb per cubic ft. Maturity Data loggers were inserted during the placement and anchored on the substrate and wedged for a mid-depth location. Researchers placed a mound of concrete in the vicinity of sensors and carefully poker-vibrated around the sensors to minimize bumping, displacement and floatation of the sensors by the screed drum rollers. A con-film curing compound was generously applied to the surface and was covered immediately after with two layers of polyethylene. The concrete was allowed to cure for 28 days. Approximately, 150 cubic yards of concrete were placed to pave this lane. Con-film was applied for the following reasons

Alpha-methyl styrene bonds effectively with the curing surface and may compromise communicating voids. Attenuation of communicating voids is detrimental to the concrete in cold weather.

Con-film is mainly an organic compound that is biodegradable and will not have measurable effect on surface run off or ground water.

Con-film provides a layer that minimizes evaporation during curing yet it does not volumetrically diminish communicating voids but effectively.

**11/12/08: Cross-Drains: Cells 85, 87 and 89 (None in the Porous Overlay Cell):** Four of the six cross drains were placed. Locations for the other two were temporarily filled with concrete to allow continuous traffic flow. They are scheduled for removal and placement of the permanent structure in spring of 2009. Subsequently, the collection system of the cross-drains was intricately designed to allow low depth abstraction.

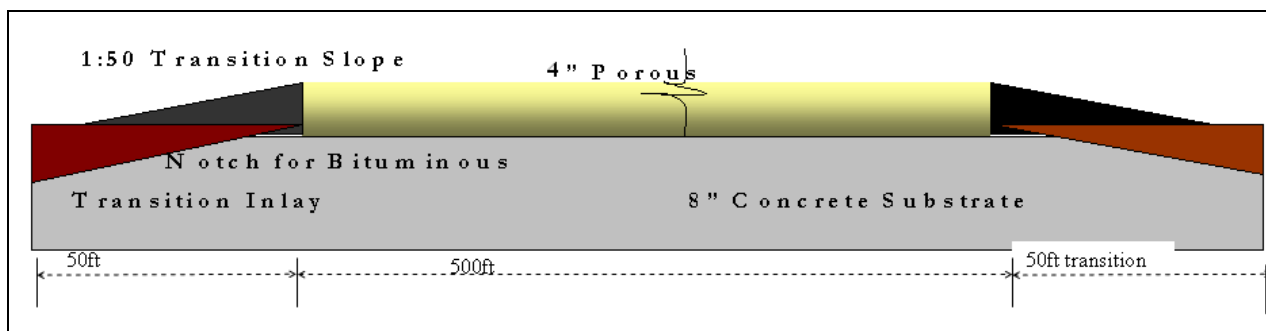


**Figure 3.5: Schematic Longitudinal Section through the Porous Overlay Cell**



**Figure 3.6: Porous Overlay Compaction**



**Figure 3.7: Porous Overlay Multi-Drum Screed Compactor**



**Figure 3.8: Porous Overlay Surface**



**Figure 3.9: Cell 89 Pervious Concrete on Clay and Cell 88 Porous Asphalt on Clay**

A separating drainage structure was constructed between the cells.



**Figure 3.10: Establishing 10 Ft Joints in Cells 85 and 89**



**Figure 3.11: Cell 39 Looking NW Showing Porous Concrete Overlay, Bituminous Transition and French Drain Shouldering Aggregate**



**Figure 3.12: Cross Drain Construction between Porous Cell 86 and Control Cell 87**

Cell 39 showed no evidence of distress apart from a transverse crack that radiated from a previously installed sensor conduit. From the proceeding chapter, there is evidence that the ride quality was very bad. Initial analysis of the ERD files lead to a suggestion that the effect of the roller screed may have imparted some local mega profiles unto the pavement. The sound absorption factors for cell 39, 85 (sand) and 89 were within 0.22 and 0.25. Details of these and other test results are discussed in the next chapter.

## CHAPTER 4 INITIAL TESTING

Basic surface characteristics testing performed on the new cells include the following:

- Texture Measurement ASTM E-2157 using the Circular Track Meter method
- In-Situ Sound Absorption Measurement using the prescribed ISO standard (NCAT Device)
- In-Situ (Dynamic) OBSI measurements using the provisional AASHTO standard
- Ride measurement using the MnDOT LISA Light Weight Profiler
- Friction Measurement using MnDOT Dynatest Friction Lock Wheel Skid trailer ASTM E-274
- Friction Measurement using FHWA Grip Tester from the FHWA Loans Program
- Indirect Hydraulic Conductivity tests

### 4.1 Texture Measurements

For convenience, texture was recorded in millimeters in order to enable a quick comparison to the one millimeter threshold for acceptable textures for adequate friction. The Circular Texture Meter (CTM) ASTM E-2157-04 was used with the main objective of monitoring the changes in configuration due to ravelling of the surface. Figure 4.1a shows initial screen shots of designated spots that will be monitored over time. The texture values ranged from 1.75 to 2.6 mm but there was evidence for deep laser texture.

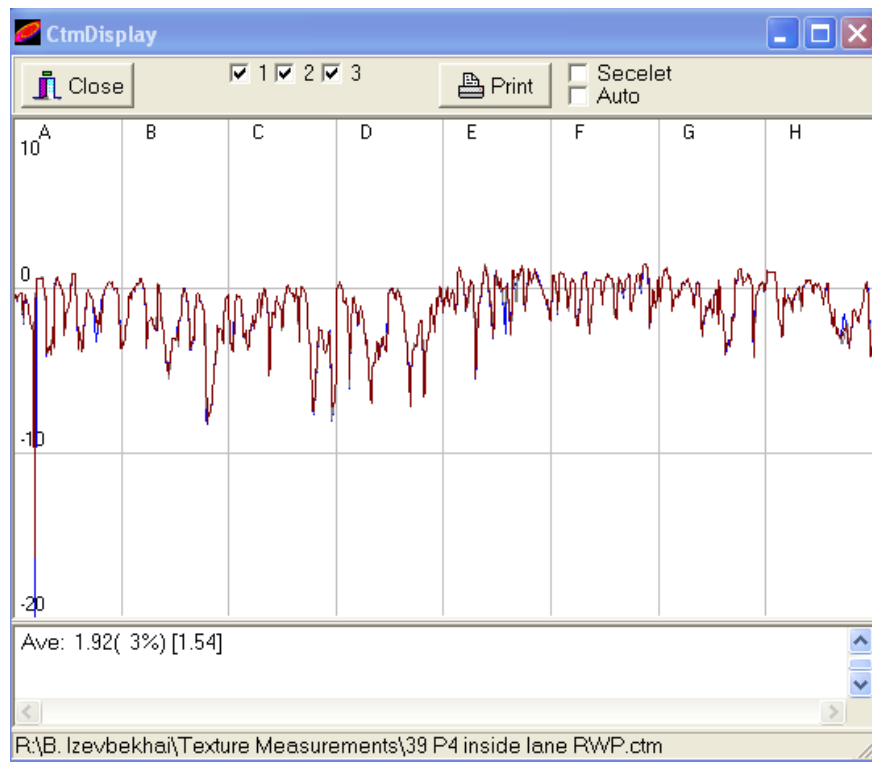


**Figure 4.1: CTM Display of a RWP Inside Lane Spot after 800 Cycles**

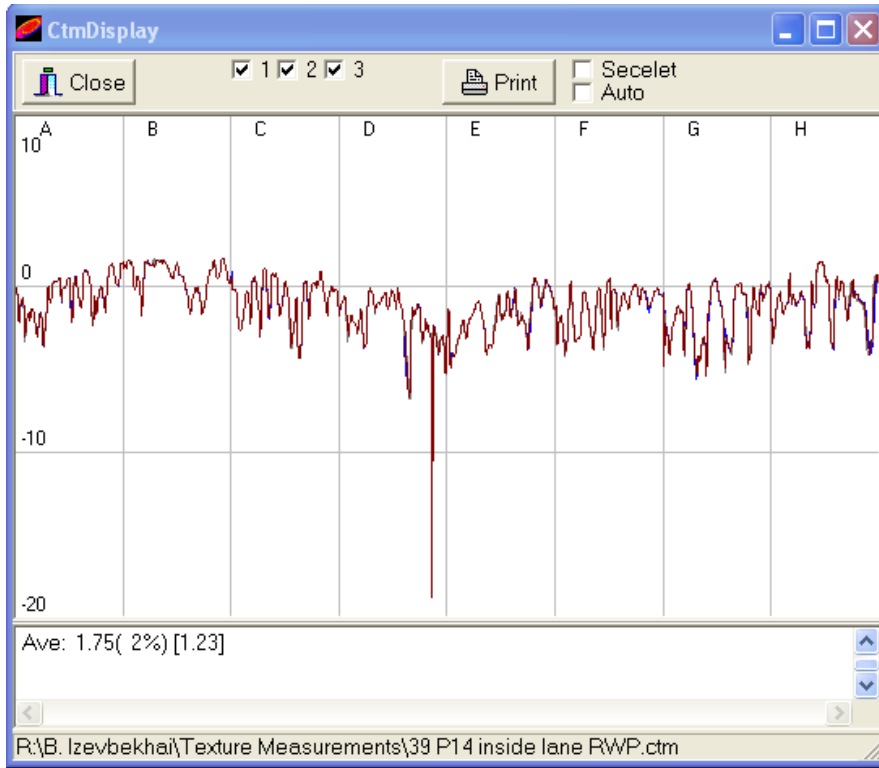


**Figure 4.2: CTM Display of a RWP Inside Lane Spot after 800 Cycles**

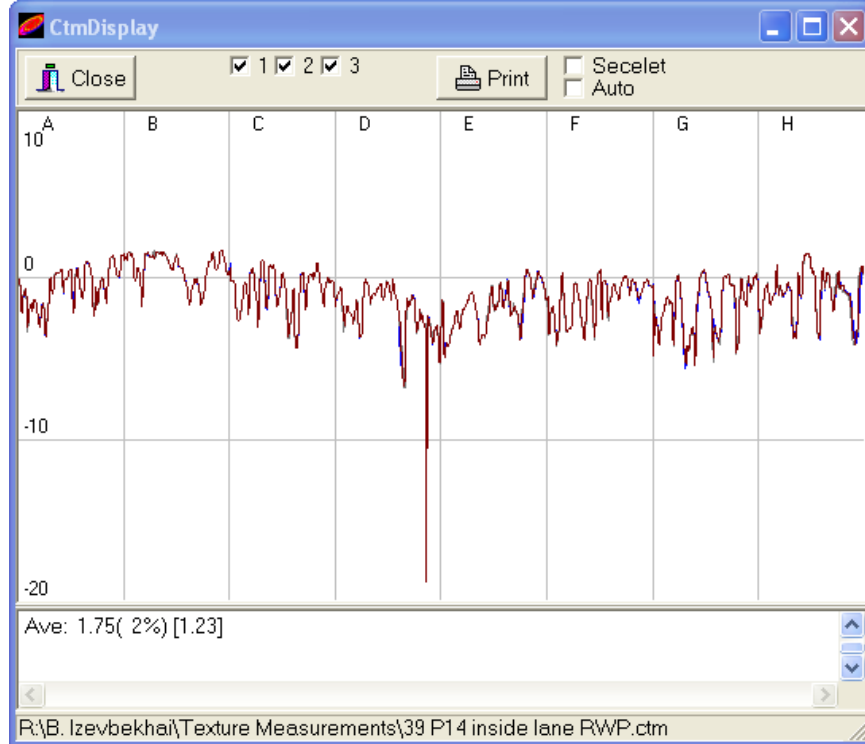


**Figure 4.3: CTM Display of a RWP Outside Lane Spot**

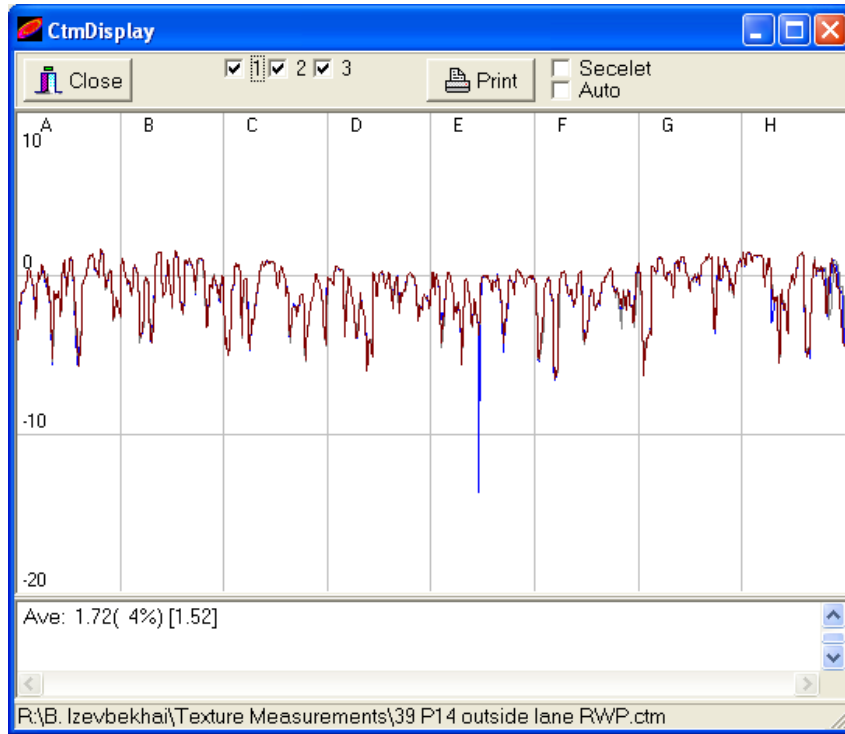


**Figure 4.4: CTM Display of a RWP Outside Lane Spot**

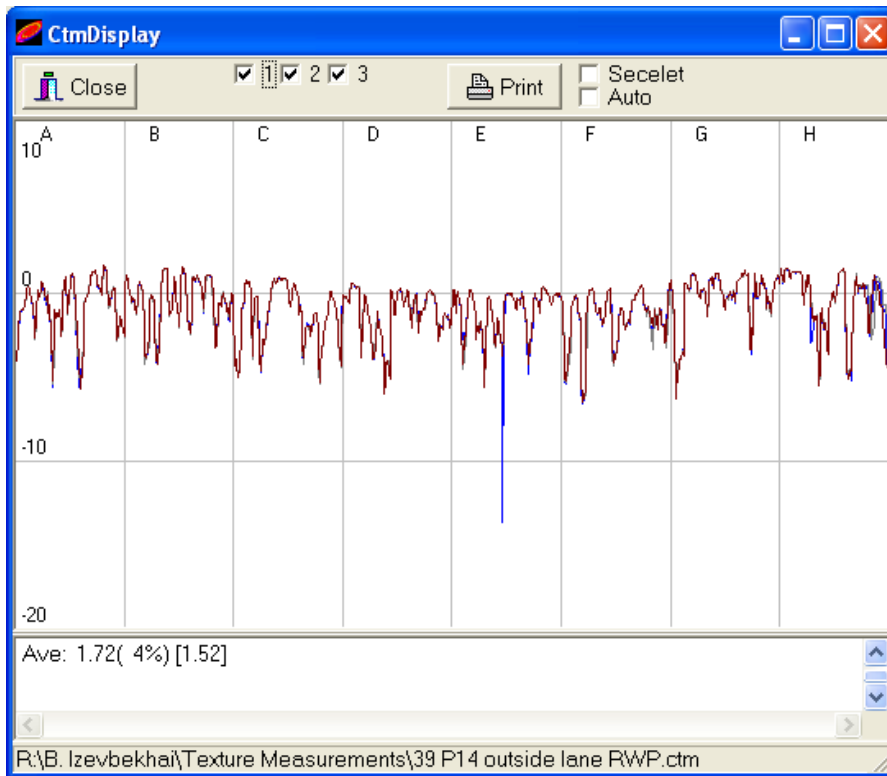


**Figure 4.5: CTM Display of a RWP Outside Lane Spot**

## 4.2 Friction Testing

Friction measurements were performed with the MnDOT Dynatest Skid truck on the 17<sup>th</sup> of October 2008.

Later in the month, the Federal Highway Loans Program lent a grip tester to MnDOT. A more comprehensive friction measurement was performed on all the cells with the grip tester. Some of the collected results are shown in appendix. While the grip tester measures in International Friction Index, it also provides a grip number that is easily correlated to the skid number. Although thresholds were not established for the friction numbers, sufficient friction in cell 5 led to the grinding of that surface. The grip tester results for cell 5 are for the ground surface, however at the behest of FHWA, the 1" ft fog line of ungrounded but longitudinally tined strip was also measured with the grip tester. The results for these tests are shown in appendix. The grip tester provided initial friction numbers for cell 37 but could not test cells 85 and 89 because the cross drains were under construction. The series of tests in the spring of 2009 included the porous overlay but data is still being extracted and processed.



**Figure 4.6: Grip Tester**

The Tests were performed in large continua of multiple cells and ultimately cropped into the individual cell readings. Three runs of various levels of wetting were performed. The initial run was performed with a low rate of flow resembling a semi-dry pavement when the wetting of the surface is lower than the saturation level, the second run had a condition similar to the wetness at incipient hydroplaning and the last run was when the flooding exceeds the hydroplaning threshold of wetness. The results of the grip test are stored in the database. Table 4.1 is a relevant excerpt of the grip numbers and shows the friction test results using the grip tester. It also compares that data with a diamond grinding cell and an astro turf drag cell.

**Table 4.1: Initial friction Test (GRIP NUMBER)**

Descriptive Statistic	GNAverage for Cell 39 Porous Overlay	GNAverage cell 11 Transverse Tine	GNAverage Cell 5 Diamond Grind	GNAverage Cell 53 Turf Drag
<b>Mean</b>	<b>0.711</b>	0.455	0.779	0.558
<b>Standard Error</b>	<b>0.006</b>	0.005	0.008	0.012
<b>Median</b>	<b>0.750</b>	0.460	0.816	0.569
<b>Mode</b>	<b>0.520</b>	0.440	0.970	0.000
<b>Standard Deviation</b>	<b>0.132</b>	0.060	0.187	0.084
<b>Sample Variance</b>	<b>0.017</b>	0.004	0.035	0.007
<b>Kurtosis</b>	<b>-0.964</b>	-0.542	-1.038	43.300
<b>Skewness</b>	<b>-0.626</b>	-0.16	-0.464	-6.397
<b>Range</b>	<b>0.598</b>	0.28	0.700	0.604
<b>Minimum</b>	<b>0.367</b>	0.31	0.350	0.000
<b>Maximum</b>	<b>0.965</b>	0.59	1.050	0.604
<b>Sum</b>	<b>331.237</b>	74.14	434.650	27.366
<b>Count</b>	<b>466.000</b>	163	558.000	49.000
<b>Largest(1)</b>	<b>0.965</b>	1.06	1.050	0.604
<b>Smallest(1)</b>	<b>0.367</b>	.89	0.350	0.000
<b>Confidence Level(95.0%)</b>	<b>0.012</b>	0.005	0.016	0.024

### 4.3 Sound Absorption Characteristics of the Test Cells

A sound absorption measurement was conducted in the new cells in MnROAD. The sound absorption test is a static test in the sense that the white noise is not generated by the interaction of the rolling tire with pavement surface but by a specific source. A white noise is a random audio signal with a flat power spectral density that contains noise at the same level for all of the frequencies. The signal's spectral density has equal power in all of the bands and at the various frequencies. The noise is transmitted to the pavement surface through a projection distance and is reflected to a set of microphones that are located at a certain distance from the source. The reflected noise is received by a set of microphones and then transferred to an analyzer that identifies the actual reflection or absorption of each frequency. The frequencies range from zero to 2000 Hz. The absorption ratios for 315, 400 500, 750, 1000, 1250 and 1650 hertz were isolated and analyzed.

To calculate absorption for the entire spectrum, the weighted value of each recorded measurement was calculated and subsequently divided by 1650-315 Hz. Then, this number is plotted against the corresponding frequency. In addition, the absorption ratio for each frequency is plotted against the pavement type. The results show evidence of higher absorption ratio in the pervious cells. Ordinarily, the reflectance of a concrete surface is higher than that of an aggregate base and it was expected that absorption ratios would be higher in cell 85 than in cell 39 but the converse happened.

Viscoelastic and gravimetric properties of pervious asphalt are most likely responsible for the high sound absorption level of the pavement. Uncharacteristically, the absorption ranged from 0.35 (315 Hz) to 0.57 (1600 Hz) in cell 89. Cell 85's values ranged from 0.18 (400 Hz) to 0.26 (1200Hz). The porous overlay cell 39's values ranged from 0.32 (315 Hz) to 0.22 (800 Hz). Bituminous cells were generally more absorbent than concrete of the same thickness design and void content. Absorption ratios for the bituminous cells ranged from 0.01 to 0.12. Figure 4.3a shows the S.A. spectra for all of the cells that were tested.

From figure 4.3a, the spectral for the measured cells are fairly obvious. The spectral trend for cell 89 is higher but similar in shape to cell 85. In addition, the similarity of absorption in each mix design/pavement type is reasonably obvious

A spectral area factor known as an absorption function was developed and computed. This value was called the unit absorption function. The concrete pavements were within 0.05 and 0.15. The concrete pavements were within 0.01 and 0.03.

**Absorption Spectrum for MnROAD Cells**

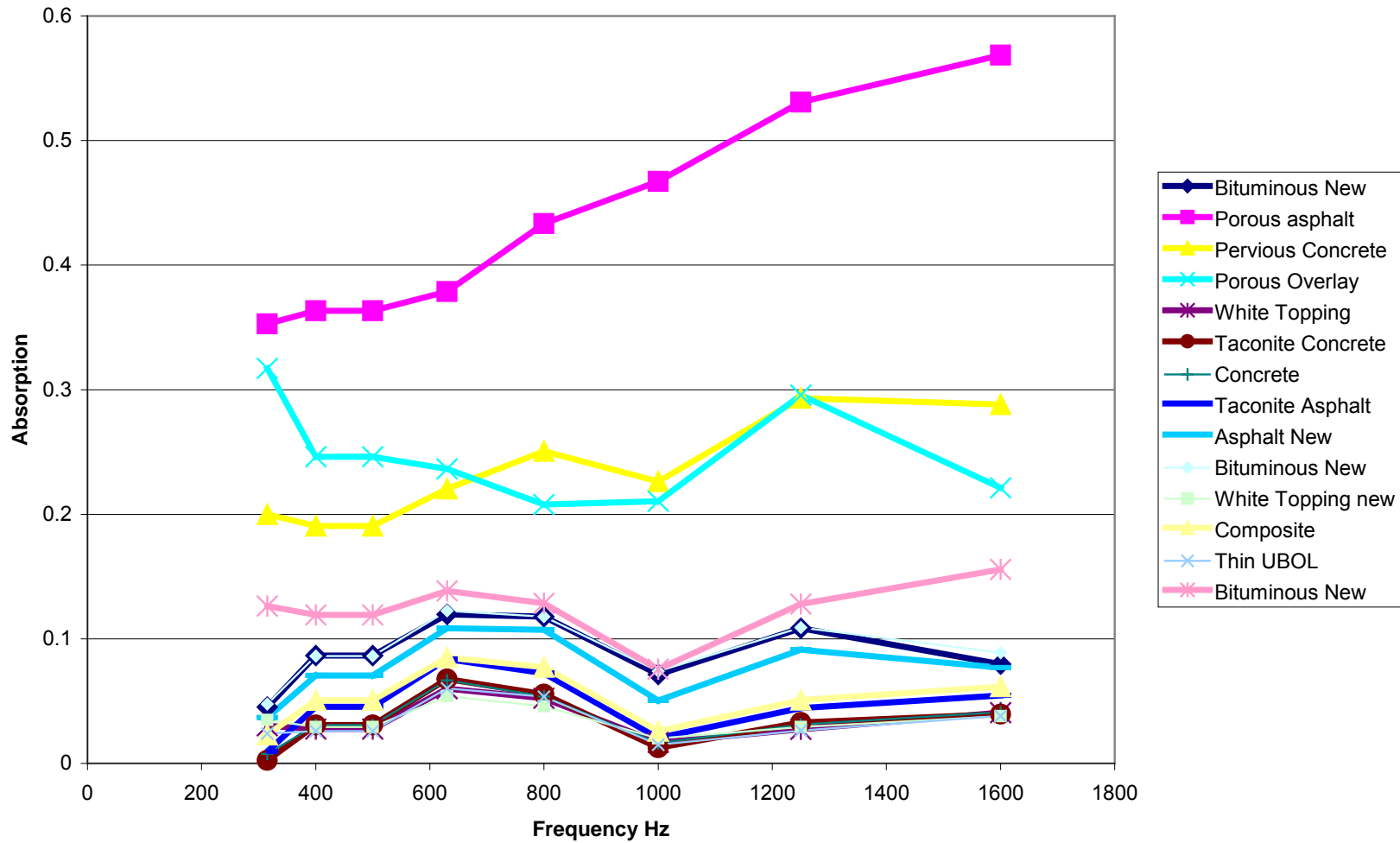


**Figure 4.7: Initial Sound Absorption Test Results**

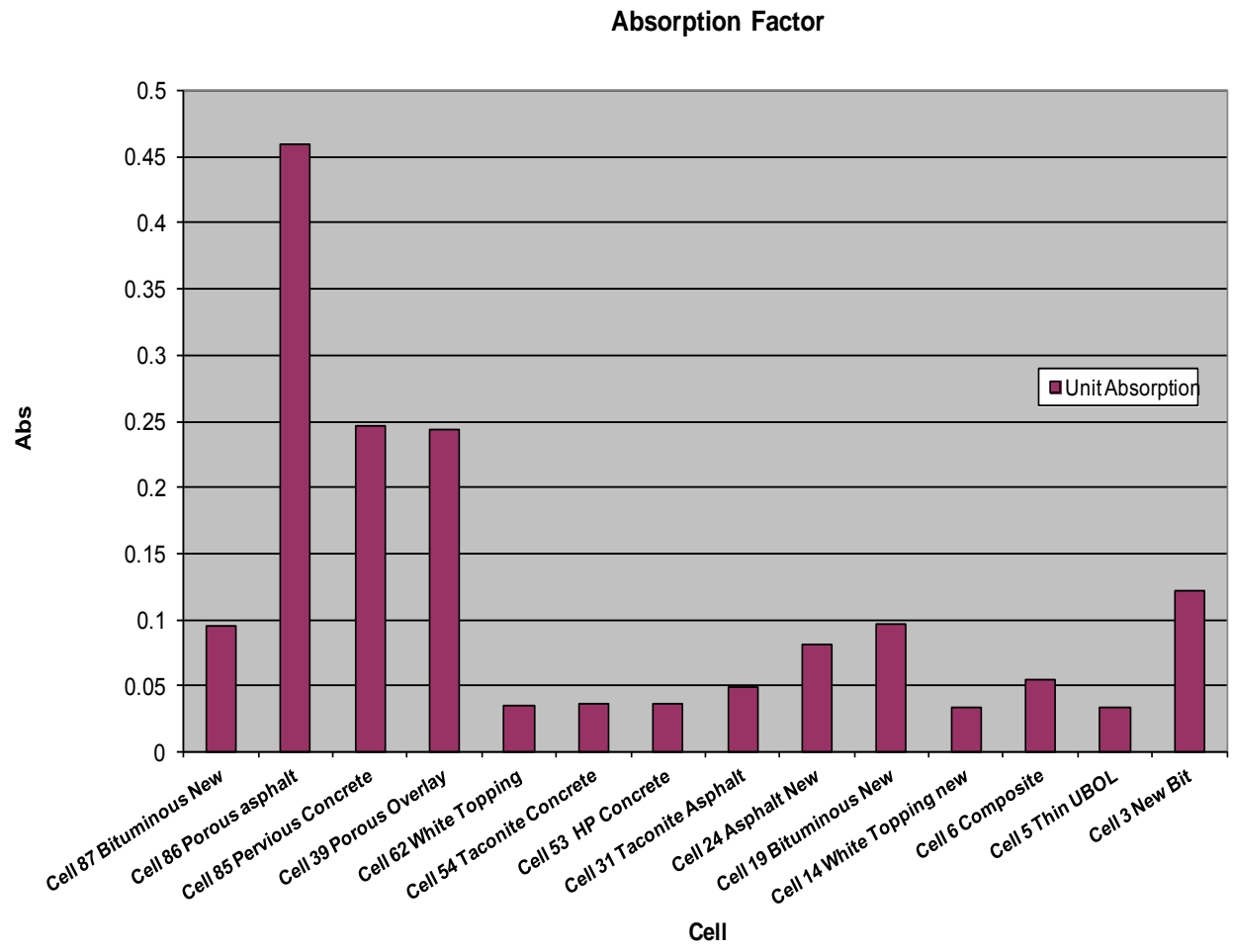


**Figure 4.8: Sound Absorption Factor for Each Cell**

**Table 4.2: Summary Data for Sound Absorption on MnROAD Pavements**

	<i>FREQUENCY</i>							
				Critical Low Speed Frequency		Critical Freeways Frequency		
TEST CELL	315	400	500	630	800	1000	1250	1600
Cell 87 Bituminous New	0.045265211	0.08665789	0.086658	0.119654	0.117885	0.071458	0.108418	0.079646
Cell 86 Porous asphalt	0.352771033	0.36329661	0.363297	0.37877	0.433311	0.467237	0.530949	0.568603
Cell 85 Pervious Concrete	0.199884789	0.19060511	0.190605	0.22037	0.250629	0.226229	0.293302	0.288177
Cell 39 Porous Overlay	0.317119944	0.24607648	0.246076	0.236405	0.207753	0.210514	0.295545	0.221276
Cell 62 White Topping	0.030313556	0.02760622	0.027606	0.059931	0.052263	0.016778	0.027413	0.040717
Cell 54 Taconite Concrete	0.002391333	0.03083192	0.030832	0.067684	0.055532	0.012484	0.032809	0.039628
Cell 53 HP Concrete	0.0077238	0.03072589	0.030726	0.066639	0.053806	0.016199	0.031247	0.04125
Cell 31 Taconite Asphalt	0.009608121	0.04546438	0.045464	0.083801	0.072431	0.020489	0.044369	0.054533
Cell 24 Asphalt New	0.036627233	0.07046403	0.070464	0.108579	0.107325	0.050575	0.09126	0.076923
Cell 19 Bituminous New	0.047690322	0.08622999	0.08623	0.122525	0.117802	0.074027	0.109175	0.088811
Cell 14 White Topping new	0.034834788	0.02916005	0.02916	0.053975	0.045902	0.020103	0.029208	0.037945
Cell 6 Composite	0.022915812	0.05061057	0.050611	0.084946	0.077338	0.025919	0.050816	0.061701
Cell 5 Thin UBOL	0.023943333	0.02593469	0.025935	0.060127	0.053516	0.014973	0.026284	0.038075
Cell 3 New Bit	0.1263604	0.11927564	0.119276	0.138553	0.12865	0.075566	0.128008	0.155754

#### 4.4 On Board Sound Interaction (OBSI) Collection Process

The MnDOT OBSI equipment consists of a Chevrolet Impala, eight intensity meters, connected via four communication cables to a Bruel and Kjaer Front-End Collector which is connected to a dell laptop computer. The intensity meters are mounted on a rig system attached to a standard reference test tire that is installed at the rear left side of the vehicle and maintained at a temperature of 30 degrees Celsius. After recording the temperature, the four intensity meters are plugged in to the B &K Front-End Unit, as well as 12 volt power supply and an ethernet (computer) cable. With this arrangement, the unit is capable of measuring repeatable tire pavement interaction noise at a speed of 60 miles an hour, thus measuring approximately 440 ft within six seconds. Mounting the rig on a non-dedicated vehicle and calibration of the microphones as well as durometer evaluation of the tire prior to measurement are mandatory operational procedure, prior to data collection. Subsequent data analysis is simplified by the existing Excel programs and Fourier transforms programs that facilitate analysis of the noise measured. Implicit in the transforms are the window functions that facilitate the program. According to Rasmussen et al, the filter used is the Hanning Window Function. The MnDOT collection template is saved in the collection laptop's desktop for use in collection of the OBSI. Pulse software program is used to collect the data. In the MnROAD texture experiment, a texture noise degradation algorithm is being validated. It is believed that texture degradation results in a reduction in Tire Pavement Interaction Noise in concrete pavements while ageing of flexible pavements result in increase of tire pavement interaction noise. While texture degradation of rigid pavements causes a redistribution of friction into its constituents: hysteresis and adhesion the effect of the tire pavement noise suction component is attenuated by averaging the reception of two sets of microphone four each on the trailing edge and the leading edge of the contact patch. Figure 4.4 shows the graph that is produced from this testing.

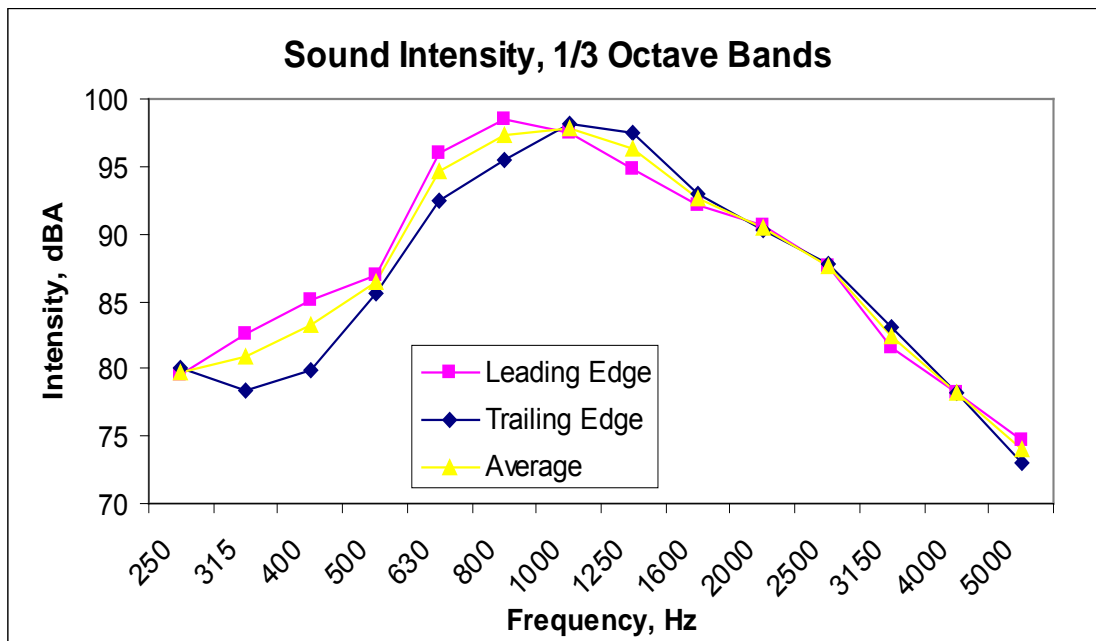
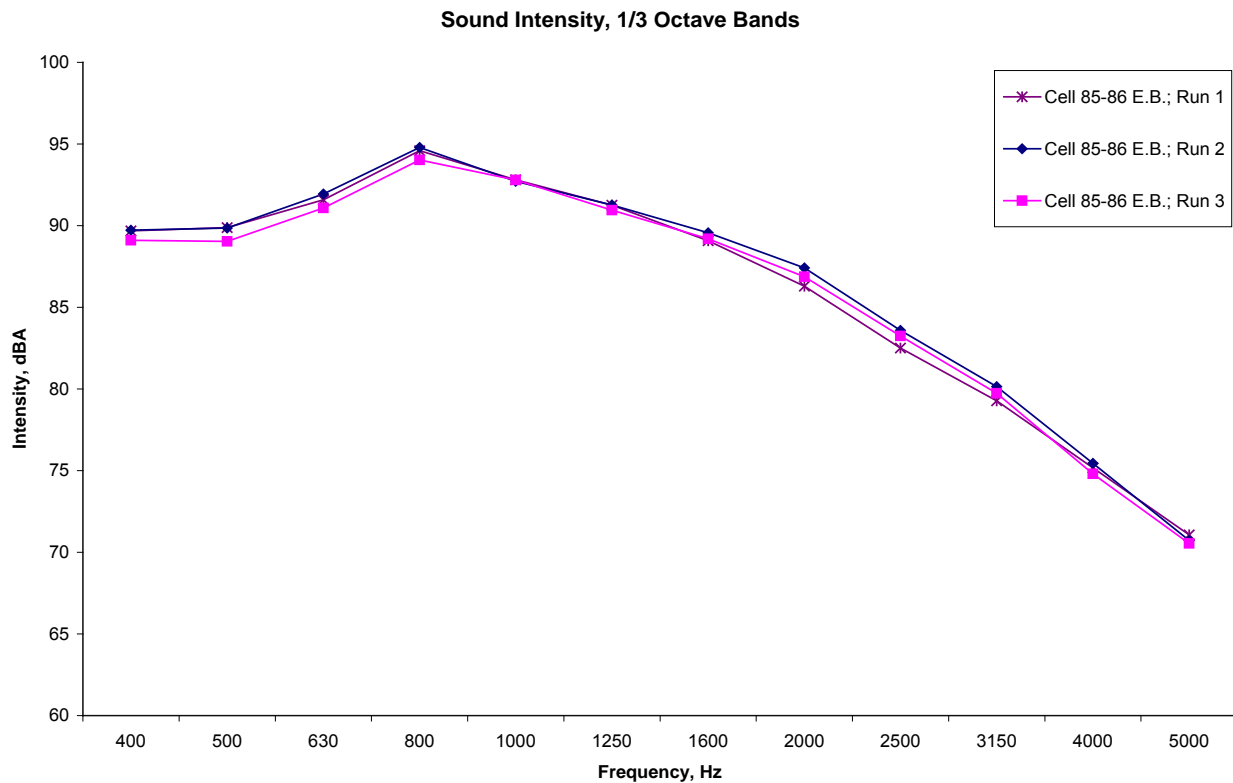


Figure 4.9: One Third Octave Frequency Response of 2 Sets of Microphones

The new MnROAD cells were measured except the transitional curves between the loops and the straight courses at the LVR cells. It was not practicable to safely attain 60 mph measuring speed in these transitional curves and so it was not possible to measure cells 54, 53, 52 and 40 in the LVR during the fall of 2007. In the spring of 2008 and in the summer of 2008, testing of the grinding cells resulted in a joint rodeo with the CP Tech center and fall of 2008 the new cells including the new cell 9 grind were tested and the results of the new OBSI test results for the new cells are shown in table 4.3.

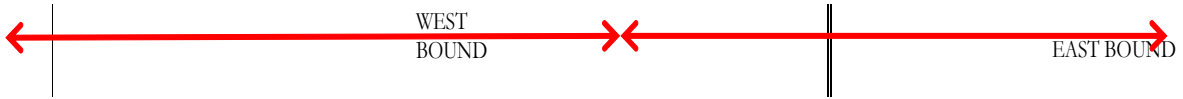
**Table 4.3: OBSI of South Side of LVR**

CELL NUMBER	54-52	32	31	79-78.5	78.5-77	28	27	89-88	86-85	24	24	85-86	88-89	27	28	77-78.5	78.5-79	31	32	52-54
RUN #1	104.05	103.91	101.59	100.71	100.73	100.99	100.38	100.14	99.41	100.71	98.99	100.03	99.50	101.51	100.66	99.76	99.54	101.15	102.46	105.29
RUN #2	103.11	103.19	100.71	100.10	100.13	101.85	100.82	100.06	99.42	100.45	99.36	100.25	98.64	102.03	100.94	99.27	99.85	101.51	102.63	105.28
RUN #3	103.43	103.33	100.88	99.91	99.76	101.57	100.29	100.09	99.08	100.86	99.09	99.74	99.03	100.95	100.59	99.11	99.60	101.34	102.35	105.19
A-wtd AVG:	103.5	103.5	101.1	100.2	100.2	101.5	100.5	100.1	99.3	100.7	99.1	100.0	99.1	101.5	100.7	99.4	99.7	101.3	102.5	105.3



**Figure 4.10: Cells 85 and 86 Spectral Properties**

**Table 4.4: OBSI Summary OBSI on North Side of LVR**



CELL NUMBER	40 TT	39 Porous Overlay	38 TT	37* Unground tine	36 TT	35 BIT	34 BIT	33BIT	33BIT	34BIT	35BIT	36BIT	37	38	39	40
RUN #1	104.29	98.05	104.87	104.45	104.40	99.60	99.84	99.27	99.04	99.14	99.50	103.61	103.93	104.49	100.52	104.89
RUN #2	104.37	98.01	104.58	104.42	104.47	99.60	99.76	99.37	99.29	99.21	99.49	104.07	103.64	104.74	100.40	104.60
RUN #3	104.14	97.84	104.54	104.37	104.34	99.54	99.81	99.15	99.68	99.39	99.77	103.92	103.92	104.34	100.22	104.97
A-wtd AVG:	104.3	98.0	104.7	104.4	104.4	99.6	99.8	99.3	99.3	99.2	99.6	103.9	103.8	104.5	100.4	104.8

OBSI SP09 SUMMARY North Side of LVR Loop

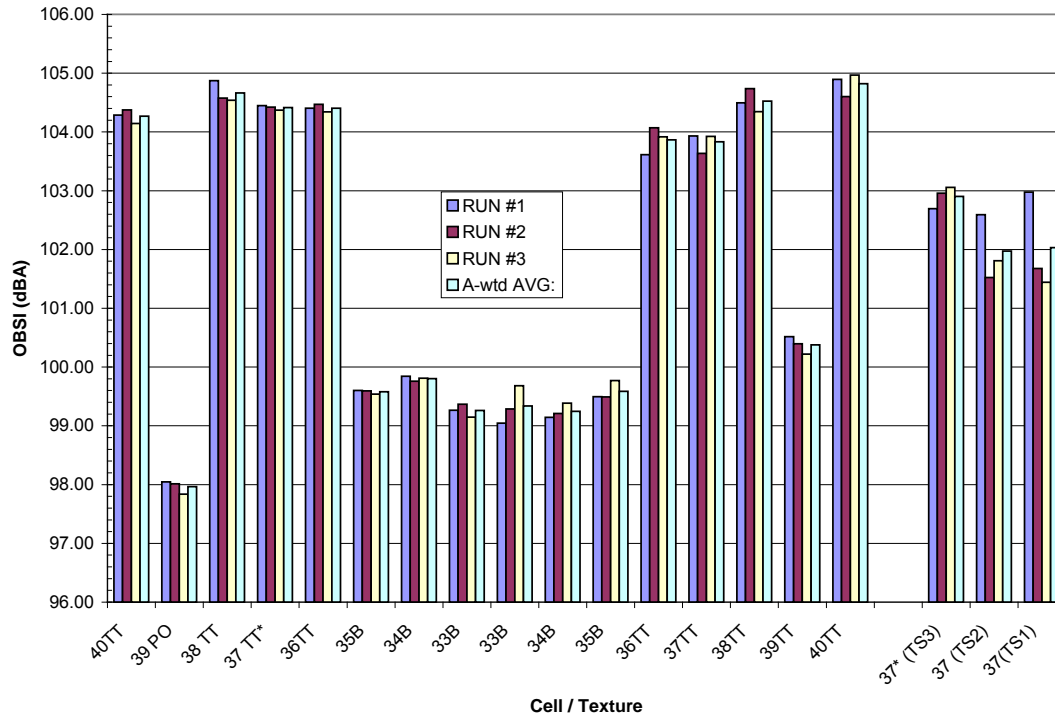
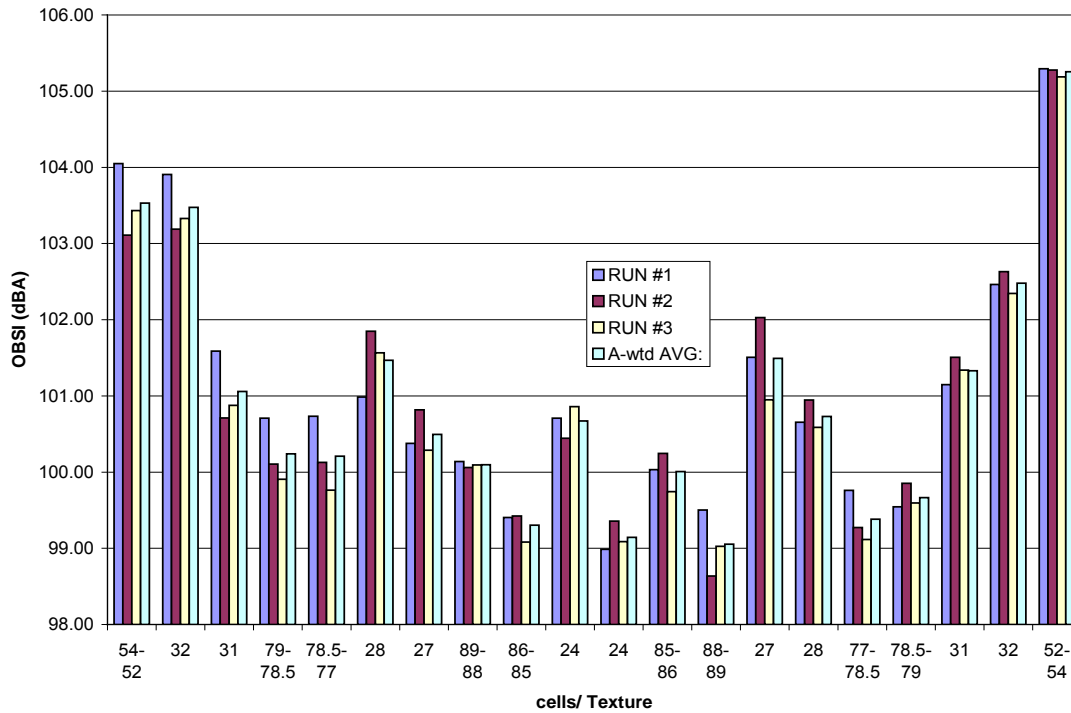


Figure 4.11: LVR North Side OBSI

### OBSI Summary South Side



**Figure 4.12: 2009 Spring OBSI Data**

Pervious Cells are the Quietest followed By Concrete cells . Further information is in the publication <http://www.lrrb.org/pdf/200845.pdf> (12) and <http://www.dot.state.mn.us/materials/researchdocs/ReportDiamondGrinding.pdf> (13)

#### 4.5 Initial Ride Measurement

Ride measurements were conducted on the new cells during the last week of November using the AMES Light Weight Profiler. A continuous run was made on the right wheel path and the left wheel path of the passing lane. The results were separated into cells by cropping the start and end stations of each cell of the cells. The new construction built cells in contiguity maintaining start and end points that were coincident with adjoining cells instead of transition areas. Results of Ride measurements are shown in tables 4.4 and 4.5.

**Table 4.5: IRI of Test Cells Measured with the LWP Fall 2008**

<b>Cell</b>	<b>Date</b>	<b>Lane</b>	<b>Wheel Path</b>	<b>IRI Run1</b>	<b>IRI Run2</b>	<b>Average IRI</b>	<b>IRI Run1</b>	<b>IRI Run2</b>	<b>Average IRI</b>
10	11/19/08	Driving	RWP	89.3	89.5	89.4	1.41	1.41	1.41
11	11/19/08	Driving	RWP	121.8	122.8	122.3	1.92	1.94	1.93
12	11/19/08	Driving	RWP	104.1	98.6	101.35	1.64	1.56	1.6
13	11/19/08	Driving	RWP	78.9	78.5	78.7	1.25	1.24	1.24
14	11/19/08	Driving	RWP	56.9	58.8	57.85	0.9	0.93	0.91
15	11/19/08	Driving	RWP	62.9	40.5	51.7	0.99	0.64	0.82
16	11/19/08	Driving	RWP	62.9	63.4	63.15	0.99	1	1
17	11/19/08	Driving	RWP	65.9	63.7	64.8	1.04	1.01	1.02
18	11/19/08	Driving	RWP	55	55.3	55.15	0.87	0.87	0.87
19	11/19/08	Driving	RWP	73.7	72.2	72.95	1.16	1.14	1.15
1	11/19/08	Driving	RWP	99.1	103.8	101.45	1.56	1.64	1.6
20	11/19/08	Driving	RWP	40.7	40.1	40.4	0.64	0.63	0.64
21	11/19/08	Driving	RWP	41.7	40.8	41.25	0.66	0.64	0.65
22	11/19/08	Driving	RWP	51.8	52.7	52.25	0.82	0.83	0.82
23	11/19/08	Driving	RWP	69.4	69.9	69.65	1.1	1.1	1.1
2	11/19/08	Driving	RWP	44.4	45.9	45.15	0.7	0.72	0.71
3	11/19/08	Driving	RWP	57.8	50.5	54.15	0.91	0.8	0.85
4	11/19/08	Driving	RWP	83.9	83.3	83.6	1.32	1.31	1.32
5	11/19/08	Driving	RWP	54	54.5	54.25	0.85	0.86	0.86
60	11/19/08	Driving	RWP	100.3	103.9	102.1	1.58	1.64	1.61
61	11/19/08	Driving	RWP	60.3	60.7	60.5	0.95	0.96	0.95
62	11/19/08	Driving	RWP	62.5	61.6	62.05	0.99	0.97	0.98
63	11/19/08	Driving	RWP	86.3	83.5	84.9	1.36	1.32	1.34
6	11/19/08	Driving	RWP	86.3	84.2	85.25	1.36	1.33	1.35
7	11/19/08	Driving	RWP	70.8	60.9	65.85	1.12	0.96	1.04
8	11/19/08	Driving	RWP	70.4	70.7	70.55	1.11	1.12	1.11
92	11/19/08	Driving	RWP	96.4	91.5	93.95	1.52	1.44	1.48
96	11/19/08	Driving	RWP	184.9	187.4	186.15	2.92	2.96	2.94
97	11/19/08	Driving	RWP	234.1	236.8	235.45	3.69	3.74	3.72
9	11/19/08	Driving	RWP	114.3	102.8	108.55	1.8	1.62	1.71
10	11/19/08	Driving	LWP	82.7	85.1	83.9	1.31	1.34	1.32
11	11/19/08	Driving	LWP	116.3	117.1	116.7	1.84	1.85	1.84
12	11/19/08	Driving	LWP	94.1	94.4	94.25	1.49	1.49	1.49

<b>Cell</b>	<b>Date</b>	<b>Lane</b>	<b>Wheel Path</b>	<b>IRI Run1</b>	<b>IRI Run2</b>	<b>Average IRI</b>	<b>IRI Run1</b>	<b>IRI Run2</b>	<b>Average IRI</b>
13	11/19/08	Driving	LWP	64.2	61.7	62.95	1.01	0.97	0.99
14	11/19/08	Driving	LWP	54.7	56	55.35	0.86	0.88	0.87
15	11/19/08	Driving	LWP	43.8	44.3	44.05	0.69	0.7	0.7
16	11/19/08	Driving	LWP	51.9	52.1	52	0.82	0.82	0.82
17	11/19/08	Driving	LWP	55.2	55.6	55.4	0.87	0.88	0.87
18	11/19/08	Driving	LWP	51.1	50.4	50.75	0.81	0.8	0.8
19	11/19/08	Driving	LWP	54.6	54.4	54.5	0.86	0.86	0.86
1	11/19/08	Driving	LWP	75.7		75.7	1.19		1.19
20	11/19/08	Driving	LWP	46.4	44.6	45.5	0.73	0.7	0.72
21	11/19/08	Driving	LWP	41.1	40.8	40.95	0.65	0.64	0.65
22	11/19/08	Driving	LWP	56.8	56.9	56.85	0.9	0.9	0.9
23	11/19/08	Driving	LWP	87	86.6	86.8	1.37	1.37	1.37
2	11/19/08	Driving	LWP	38.4		38.4	0.61		0.61
3	11/19/08	Driving	LWP	34.1		34.1	0.54		0.54
4	11/19/08	Driving	LWP	65.6		65.6	1.04		1.04
5	11/19/08	Driving	LWP	50.7		50.7	0.8		0.8
60	11/19/08	Driving	LWP	82.7	81.3	82	1.31	1.28	1.29
61	11/19/08	Driving	LWP	56.5	56.5	56.5	0.89	0.89	0.89
62	11/19/08	Driving	LWP	51.6	50.4	51	0.81	0.8	0.8
63	11/19/08	Driving	LWP	78.9	77.3	78.1	1.25	1.22	1.23
6	11/19/08	Driving	LWP	75.7	96.3	86	1.19	1.52	1.36
7	11/19/08	Driving	LWP	65.6	69.8	67.7	1.04	1.1	1.07
8	11/19/08	Driving	LWP	70.6	70.7	70.65	1.11	1.12	1.12
92	11/19/08	Driving	LWP	91.7	89.6	90.65	1.45	1.41	1.43
96	11/19/08	Driving	LWP	182.5	177.3	179.9	2.88	2.8	2.84
97	11/19/08	Driving	LWP	234.1	229.3	231.7	3.69	3.62	3.66
9	11/19/08	Driving	LWP	116.4	122.7	119.55	1.84	1.94	1.89
10	11/19/08	Passing	RWP	78.2	78.5	78.35	1.23	1.24	1.24
11	11/19/08	Passing	RWP	100.8	102.5	101.65	1.59	1.62	1.6
12	11/19/08	Passing	RWP	95.3	95	95.15	1.5	1.5	1.5
13	11/19/08	Passing	RWP	43.6	44.5	44.05	0.69	0.7	0.7
14	11/19/08	Passing	RWP	40.4	40.5	40.45	0.64	0.64	0.64
15	11/19/08	Passing	RWP	60.7	59.7	60.2	0.96	0.94	0.95
16	11/19/08	Passing	RWP	54.7	54.8	54.75	0.86	0.86	0.86

<b>Cell</b>	<b>Date</b>	<b>Lane</b>	<b>Wheel Path</b>	<b>IRI Run1</b>	<b>IRI Run2</b>	<b>Average IRI</b>	<b>IRI Run1</b>	<b>IRI Run2</b>	<b>Average IRI</b>
1	11/19/08	Passing	LWP	90.1	90.9	90.5	1.42	1.43	1.43
21	11/19/08	Passing	LWP	42.5	42.7	42.6	0.67	0.67	0.67
22	11/19/08	Passing	LWP	47.8	47.7	47.75	0.75	0.75	0.75
23	11/19/08	Passing	LWP	93.2	95.4	94.3	1.47	1.51	1.49
2	11/19/08	Passing	LWP	53.6	53.9	53.75	0.85	0.85	0.85
3	11/19/08	Passing	LWP	57.1	55.4	56.25	0.9	0.87	0.89
4	11/19/08	Passing	LWP	77.9	78.5	78.2	1.23	1.24	1.23
5	11/19/08	Passing	LWP	46.1	47	46.55	0.73	0.74	0.73
60	11/19/08	Passing	LWP	83.3	89.4	86.35	1.31	1.41	1.36
61	11/19/08	Passing	LWP	65.2	63.3	64.25	1.03	1	1.01
62	11/19/08	Passing	LWP	37.8	40.9	39.35	0.6	0.65	0.62
63	11/19/08	Passing	LWP	53.4	51.7	52.55	0.84	0.82	0.83
6	11/19/08	Passing	LWP	56	56.1	56.05	0.88	0.89	0.88
7	11/19/08	Passing	LWP	70.4	66.2	68.3	1.11	1.04	1.08
8	11/19/08	Passing	LWP	69.8	72.9	71.35	1.1	1.15	1.13
92	11/19/08	Passing	LWP	79.5	79.6	79.55	1.25	1.26	1.26
96	11/19/08	Passing	LWP	170.6	175.7	173.15	2.69	2.77	2.73
97	11/19/08	Passing	LWP	195.2	201.3	198.25	3.08	3.18	3.13
9	11/19/08	Passing	LWP	142.8	124.4	133.6	2.25	1.96	2.11
5	11/19/08	Driving	SHLDR	212.7	217.8	215.25	3.36	3.44	3.4
6	11/19/08	Driving	SHLDR	143	142	142.5	2.26	2.24	2.25
8	11/19/08	Passing	SHLDR	74.2	77.3	75.75	1.17	1.22	1.2
9	11/19/08	Passing	SHLDR	74.7	77.1	75.9	1.18	1.22	1.2
16	11/19/08	Driving	SHLDR	51.4	51.7	51.55	0.81	0.82	0.81
17	11/19/08	Driving	SHLDR	64.5	64.5	64.5	1.02	1.02	1.02
20	11/19/08	Passing	SHLDR	78.4	79.7	79.05	1.24	1.26	1.25

**Table 4.6: IRI of Test Cells Measured in Pervious Cells April 2009**

<b>CELL WP AVG DIRECTION</b>	<b>RUN1</b>	<b>RUN2</b>	<b>RUN 3</b>	<b>Aver</b>
39 9-APR EB LWP	211.8	214.4	213.1	212.7
39 9-APR EB RWP	208.5	216.1		212.3
39 9-APR WB LWP	227.5	227.9	227.7	233.3
39 9-APR WB RWP	240.2	237.6		238.9
85 9-APR EB LWP	184.3	202.1	193.2	213.9
85 9-APR EB RWP	235.4	233.6		234.5
85 9-APR WB LWP	253.6	255	254.3	254.3
85 9-APR WB RWP	265.6	270.9		268.3
86 9-APR EB LWP	134.2	131.1	128	129
86 9-APR EB RWP	127.9	125.9		126.9
86 9-APR WB LWP	213.8	202.7	172.8	208.3
86 9-APR WB RWP	139.4	135.1		137.3
87 9-APR EB LWP	144.8	147.9	146.4	145
87 9-APR EB RWP	146.1	141.2		143.7
87 9-APR WB LWP	163	162.9	162.7	147.4
87 9-APR WB RWP	135.1	128.8		132
<b>88 9-APR EB LWP</b>	<b>198</b>	<b>206.6</b>	<b>202.3</b>	<b>168.8</b>
<b>88 9-APR EB RWP</b>	<b>134.4</b>	<b>136.3</b>		<b>135.4</b>
<b>88 9-APR WB LWP</b>	<b>194.6</b>	<b>188</b>	<b>191.3</b>	<b>177</b>
<b>88 9-APR WB RWP</b>	<b>168</b>	<b>157.2</b>		<b>162.6</b>
<b>89 9-APR EB LWP</b>	<b>181.7</b>	<b>182.2</b>	<b>182</b>	<b>200.5</b>
<b>89 9-APR EB RWP</b>	<b>215.7</b>	<b>222.4</b>		<b>219.1</b>
<b>89 9-APR WB LWP</b>	<b>241.7</b>	<b>235</b>	<b>238.4</b>	<b>282.5</b>
<b>89 9-APR WB RWP</b>	<b>328.8</b>	<b>326.6</b>		<b>324.4</b>

#### **4.6 Hydraulic Conductivity Measurements in Pervious Concrete**

The device developed by MnDOT was an inverted Humboldt H-4245 sand cone as shown in figure 4.8. Duct seal compound created a seal between the pervious concrete and the bottom cone flanged opening. The permeability was measured by recording the time it took for water to drop between two lines along the straight portion of the 1-gal plastic jar. Measurements were taken at several locations on the pervious test cells. Measurements will periodically be repeated at these same locations in order to determine changes in permeability.

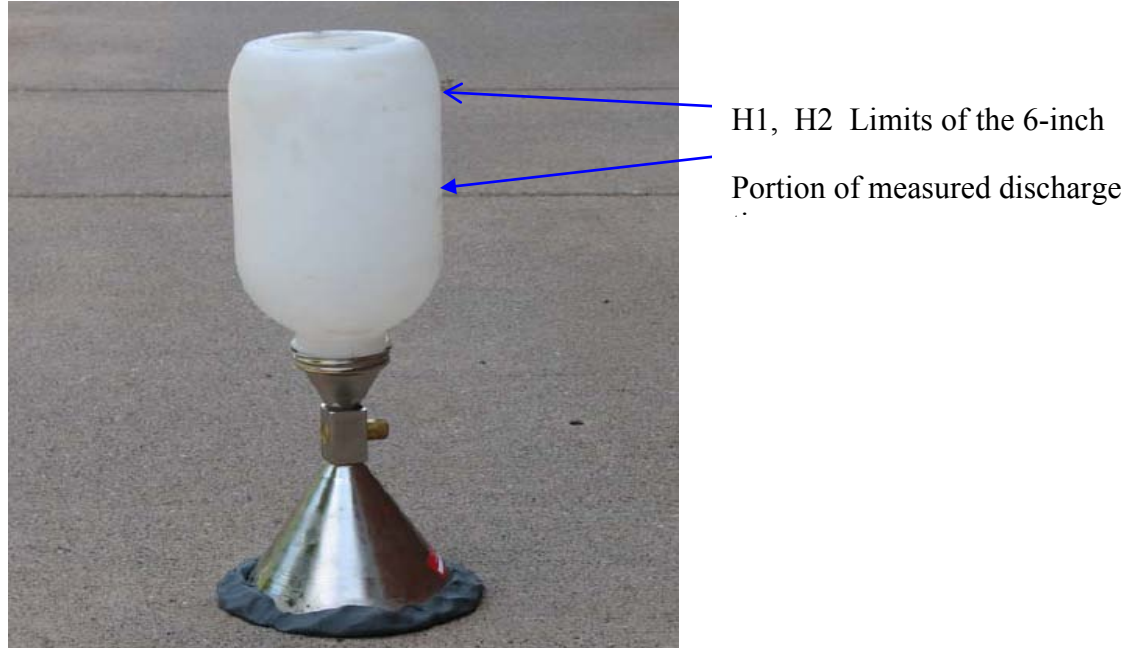


**Figure 4.13: In-Situ Hydraulic Conductivity Measurement Device (Crude Perveammeter)**

The permeability was determined as follows. From continuity, the flow rate of the water in the plastic jar must equal the flow rate exiting the sand cone, Equation 1.

$$\frac{\pi d^2}{4} dh = v_0 A_0 dt \quad (1)$$

Then Bernoulli gives Equation 2.

$$\frac{P_1}{\rho_1 g} + \frac{v_1^2}{2g} + z_1 + losses = \frac{P_2}{\rho_2 g} + \frac{v_2^2}{2g} + z_2 \quad (2a)$$

$$v_0 = \lambda \sqrt{2gh} \quad (2b)$$

Where  $\lambda$  is a constant that accounts for piezometric head loss. Combining equations 1 and 2, reorganizing, and integrating both sides gives:

$$-\frac{\pi d^2 \sqrt{h}}{2\lambda \sqrt{2g} A_0} + C = T \quad (3)$$

The substituting the boundary conditions of  $h = H$  when  $T = 0$  gives:

$$-\frac{\pi d^2}{2\lambda \sqrt{2g} A_0} (\sqrt{h} - \sqrt{H}) = T \quad (4)$$

To compensate for the losses due to the reduction in cross-sectional area at the valve, the time it takes for the permeameter to empty in air,  $T_{\text{air}} = 10$  s, is introduced. When  $T = 10$  s,  $H = 18.25$  in.,  $h = 12.0$  in., and  $\lambda'$  is  $1/\lambda$  substituting into Equation 4 gives:

$$\lambda' 10 = T \quad (5)$$

Equation 5 relates the hydraulic conductivity of the concrete as a multiple of the time it takes for the permeameter to empty in air. Equation 5 is similar to:

$$Q = KiA \quad (6a)$$

$$V = KiAt \quad (6b)$$

Where  $Q$  is discharge,  $K$  is hydraulic conductivity,  $A$  is area,  $i$  is the hydraulic gradient,  $V$  is volume, and  $t$  is the time of discharge. Assuming a tortuous path around a rounded aggregate, the hydraulic gradient is equal to

$$i = 2r/\pi r = 0.64. \quad (6c)$$

$$\text{Tortuosity in assumption of a 2 dimensional flow is } 1/0.64 \approx 1.56 \quad (6d)$$

$$\text{Tortuosity assuming a 3 dimensional path } 1.56 \sqrt{2} \approx 2.2 \quad (6e)$$

The effective porosity of the pavement system for a 7 in. thick pervious concrete with 20% porosity and 12 in. thick drainable base with 40% porosity is 33% therefore the effective volume available to store water is  $V = 0.33 \cdot 19 \cdot A$ .

**Table 4.7: Fall 2009 Flow Time for Porous Cells**

Cell	Type	Base	Location		Lane	Head Drop (in)	Time (s)
88	HMA	Clay	104.7' from East end	30" from South Curb	Environmental	8 to 0	3.49
88	HMA	Clay	104.7' from East end	30" from South Curb	Environmental	8 to 0	3.18
88	HMA	Clay	104.7' from East end	7 ft. from South Curb	Environmental	8 to 0	3.31
88	HMA	Clay	104.7' from East end	7 ft. from South Curb	Environmental	8 to 0	3.47
88	HMA	Clay	104.7' from East end	30" from North Curb	Traffic	8 to 0	3.76
88	HMA	Clay	104.7' from East end	30" from North Curb	Traffic	8 to 0	4.09
88	HMA	Clay	29.6' from West end	30" from South Curb	Environmental	8 to 0	3.54
88	HMA	Clay	29.6' from West end	30" from South Curb	Environmental	8 to 0	4.19
88	HMA	Clay	29.6' from West end	7 ft. from South Curb	Environmental	8 to 0	2.46
88	HMA	Clay	29.6' from West end	7 ft. from South Curb	Environmental	8 to 0	2.75
88	HMA	Clay	29.6' from West end	30" from North Curb	Traffic	8 to 0	3.57
88	HMA	Clay	29.6' from West end	30" from North Curb	Traffic	8 to 0	3.94
86	HMA	Sand	117.7' from West end	30" from South Curb	Environmental	8 to 0	2.12
86	HMA	Sand	117.7' from West end	30" from South Curb	Environmental	8 to 0	2.49
86	HMA	Sand	117.7' from West end	7 ft. from South Curb	Environmental	8 to 0	4.7
86	HMA	Sand	117.7' from West end	7 ft. from South Curb	Environmental	8 to 0	4.82
86	HMA	Sand	117.7' from West end	30" from North Curb	Traffic	8 to 0	1.94
89	Concrete	Clay	35.5' from East end	30" from South Curb	Environmental	8 to 0	8.64
89	Concrete	Clay	35.5' from East end	30" from South Curb	Environmental	8 to 0	8.4
89	Concrete	Clay	35.5' from East end	6 ft. from North Curb	Traffic	8 to 0	8.08
89	Concrete	Clay	35.5' from East end	6 ft. from North Curb	Traffic	8 to 0	8.02
89	Concrete	Clay	35.5' from East end	30" from North Curb	Traffic	8 to 0	5.21
89	Concrete	Clay	35.5' from East end	30" from North Curb	Traffic	8 to 0	5.92
89	Concrete	Clay	87.5' from East end	30" from South Curb	Environmental	8 to 0	11.05
89	Concrete	Clay	87.5' from East end	30" from South Curb	Environmental	8 to 0	10.88
89	Concrete	Clay	87.5' from East end	6 ft. from North Curb	Traffic	9 to 0	7.03
89	Concrete	Clay	87.5' from East end	6 ft. from North Curb	Traffic	9 to 0	6.99
89	Concrete	Clay	87.5' from East end	30" from North Curb	Traffic	8 to 0	5.21
89	Concrete	Clay	87.5' from East end	30" from North Curb	Traffic	8 to 0	5.5
85	Concrete	Sand	34' from East end	30" from South Curb	Environmental	8 to 0	7.69
85	Concrete	Sand	34' from East end	30" from South Curb	Environmental	8 to 0	7.61
85	Concrete	Sand	34' from East end	6 ft. from North Curb	Traffic	8 to 0	3.63
85	Concrete	Sand	34' from East end	6 ft. from North Curb	Traffic	8 to 0	3.61
85	Concrete	Sand	34' from East end	30" from North Curb	Traffic	8 to 0	2.27
85	Concrete	Sand	34' from East end	30" from North Curb	Traffic	8 to 0	2.46
85	Concrete	Sand	34' from East end	30" from North Curb	Traffic	8 to 0	2.1
85	Concrete	Sand	94.2' from West end	30" from South Curb	Environmental	8 to 0	5.02
85	Concrete	Sand	94.2' from West end	30" from South Curb	Environmental	8 to 0	5.08
85	Concrete	Sand	94.2' from West end	6 ft. from North Curb	Traffic	8 to 0	3.87
85	Concrete	Sand	94.2' from West end	6 ft. from North Curb	Traffic	8 to 0	4.09
85	Concrete	Sand	94.2' from West end	30" from North Curb	Traffic	8 to 0	7.86
85	Concrete	Sand	94.2' from West end	30" from North Curb	Traffic	8 to 0	7.59

## 4.7 Conclusion

This report focused on the pervious concrete cells that were built in the fall of 2008. The three cells are:

Cell 39 (Low-volume Loop) Porous Concrete Overlay, Cell 85 (Low-volume Loop) Pervious Concrete on Granular Subgrade, Cell 85 (Low-volume Loop) Pervious Concrete on Cohesive Subgrade.

Researchers measured tire pavement interaction noise sound absorption factor for most of these surfaces and the Tire Pavement Interaction Noise (TPIN) for all the surfaces in these cells. This report discussed the construction process for the establishment of the various textures, describes the testing process and discussed briefly the result obtained in the six broadly defined chapters.

The monitoring included friction measured by ASTM E274 smooth and ribbed tire, ride quality ASTM E-950 and friction (ASTM E-2157) and ASTM E-965 and on-board sound intensity (AASHTO Interim protocol as well as the ISO Sound Absorption process). The initial round of testing was performed immediately after construction in October and November of 2008. Rheological and strength data were conducted on all cells including the pervious cells that are germane to this construction report. These are reported in detail in the construction report for the pervious concrete cells.

Pervious concrete seems to exhibit high sound absorption and low OBSI compared to normal concrete. The IRI appears to be high. The High IRI is attributed to the fixed form construction and the influence of the screed. Friction appears to be comparable to normal pavement.

The cells will be monitored continuously. A separate task report on hydrologic evaluation goes into details about the hydraulics of the pervious pavements cells.

## CHAPTER 5 HYDROLOGIC EVALUATION

### 5.1 Introduction

This report analyzed the hydrological features of the pervious concrete cells built in the MnROAD facility in 2008.

Pervious concrete allows direct infiltration through the concrete and porous base with groundwater associated with the hydrological phenomena are:

- Infiltration
- Mounding
- Mass balance
- Aquifer transmissivity

These hydrological phenomena will analyze the adequacy of the pervious concrete cells. Piezometers, flush meters, and water marks facilitate analysis.

#### 5.1.1 *State of the Art*

A comprehensive literature survey has been done in this project (Reference task 1 of this project). Additionally some effort made on hydrological investigations are identified and addressed in this report. Izevbekhai, and Rohne (1) devised “perveammeter” for the evaluation of flow through a porous media in developing relevant equations, they considered mass balance (continuity) and energy balance (Bernoulli). The derived equations for head loss in a vessel from which water discharges at a varying head through the porous media. The time of discharge is an indicator of the porosity or hydraulic conductivity of the porous media and the porous base. Izevbekhai and Rohne developed relevant equations relative the time of discharge indicative of hydraulic conductivity properties of the porous media.

Hydraulic conductivity in terms of flow through the porous media is a dynamic parameter. Wanielista and Chopra (2) developed mass balance equations balancing infiltration, surface flow, evaporation, and storage in a mass balance equation. Based on a typical reservoir routine equation, it did not include porosity and permeability parameters to account for dynamic storage. That omission is overcome by this work. In the 3<sup>rd</sup> year report of the performance of cell 64, Izevbekhai and Rohne itemized the flow properties of the cell, concluding that after 3 years of zero vacuuming, the driveway at the MnROAD site cell 64 was considered clogged. That was based on the criterion and definition of clogging stipulated in a 2009 the paper (Izevbekhai & Rohne) (1).

Reference documents –preceding this task report are relevant. They include:

- The State of the Art Literature survey Task 1
- Mix design, Soil Investigation, Pavement Design (Task 2)
  - Geotechnical report
  - Pavement Design
  - Mix Design

- Infiltration models
- Perveammeter Concept

### 5.1.2 Objectives

This report evaluates the hydrological features of the pervious concrete cells at MnROAD. It computes the critical flood situation for hydrologic chaos using the mass balance, due to transmissivity and storage.

The mounding computations are performed to ascertain correlation to rainfall or other factors. For a start, the effectiveness of isolation of the test cells achieved by building a 4- ft hydraulic cut off is studied.

## 5.2 General Layout and Hydrologic Instrumentation

To effectively study the hydrologic features of the pervious cells, some instrumentation of the cells are considered. These include transverse drains, float meters, water marks, and thermocouple. Weather station for precipitation mounting wells, abstraction points for water above the top of grading sub grade. The top of grading subgrade is defined as the bottom of the base layer, which is the interface of CA, is sub base and sand subgrade in cell 85 and the interface of CA 15 sub base and clay subgrade in cell 89.

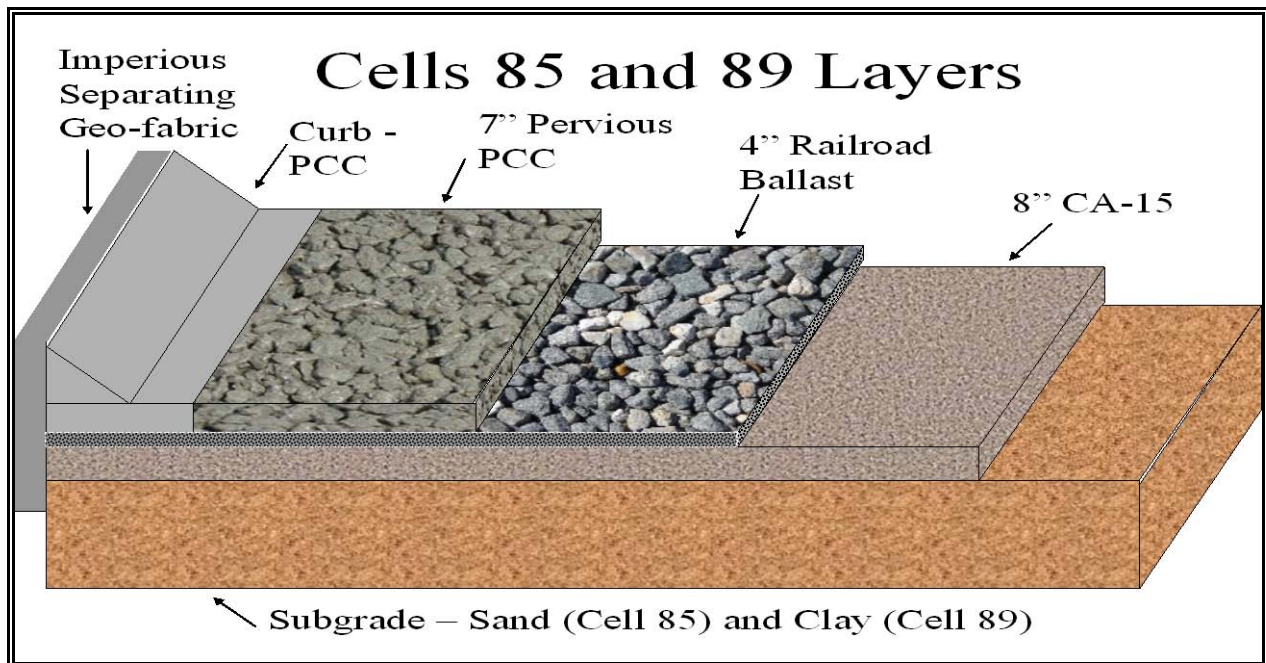


**Figure 5.1: Enhanced X-Section through the Pavement**

### **5.2.1 General Layout**

The control volume for analysis is the set of cells 85 to 89. Cell 85 was built with inches concrete underlain by 4-inches of Railroad ballast and 8 inches of Crushed rock meeting the MnDOT characterization of CA 15. The subgrade material was a well graded sand meeting the classification of granular material This design is similar to cell 89 with the exception that the subgrade material in cell 89 is stiff clay. Cell 85 was built with 5-inches of porous asphalt (20% porosity) underlain by 4-inches of Railroad ballast and 10 inches of crushed rock meeting the MnDOT Characterization of CA 15. The subgrade, material was a well graded sand meeting the classification of granular material. This design is similar to cell 88 with the exception that the subgrade material in cell 89 is stiff clay.

Cell 87 the non porous control cell was built with 7 inches impervious asphalt pavement underlain by 4-inches of Railroad ballast and 8 inches of Crushed rock meeting the MnDOT Characterization of CA 15. The subgrade material is within the transitional area of well graded sand on the west half and stiff clay on the right half. This design is similar to cell 89 with the exception that the subgrade material in cell 89 is stiff clay.

The hydrologic features include the transverse drains, abstraction wells, monitoring wells, and thermocouple and watermark trees. These are discussed in details. The parameters analyzed include top water level in water bearing granular subgrade, mounding, depression, freezing and thawing and transmissivity. There is a 24 X6 Concrete curb and gutter; They are laid flat and at the same elevation with the pavement so that they do not supply the pavement with runoff. The upper level of the curb is backfilled with organic soil and turf so that the gutters are not supplied with runoff from the back fill.

### **5.2.2 Transverse Drains**

An urban section design was adopted for cells 85 and 89. This consists of a 6 – 24 curb and gutter designed to forestall inflow from outside the pervious cells. These are linked by cross drains at cell boundaries. The cross drains are built to compare what does not infiltrate or evaporate. The extremities of the drains are equipped with modified tipping buckets that measure the "unevaporated" "uninfiltrated" volume.



**Figure 5.2: Transverse Drains in Cells 85-89**

### **5.2.3 *Piezometers***

Eight piezometers were established between November 2007 and January 2007. These piezometers were constructed from borings that ended at the impervious clay layer. This layer was encountered 7 ft below the surface in the Upstream end of the control volume and 32 ft below the surface at the downstream end of the study area. Between the topsoil and the aquiclude, sand and loam was encountered in wet to saturated conditions.

### **5.2.4 *Abstraction Wells***

Abstraction wells are 4 inch shafts built in the transverse drains to capture retention above the top of grading subgrade. They are also used for sampling water quality.

Four abstraction wells were established on the cross drains. The cross drains are connected to flow out meters. The flow-out meters are self-flushing and when filled to a certain volume. The total volume is therefore an indication of unfiltered unevaporated volume.



**Figure 5.3: Transverse Drain and Flow-Out Meters**



**Figure 5.4: Flow-Out Meter Partial Assembly**

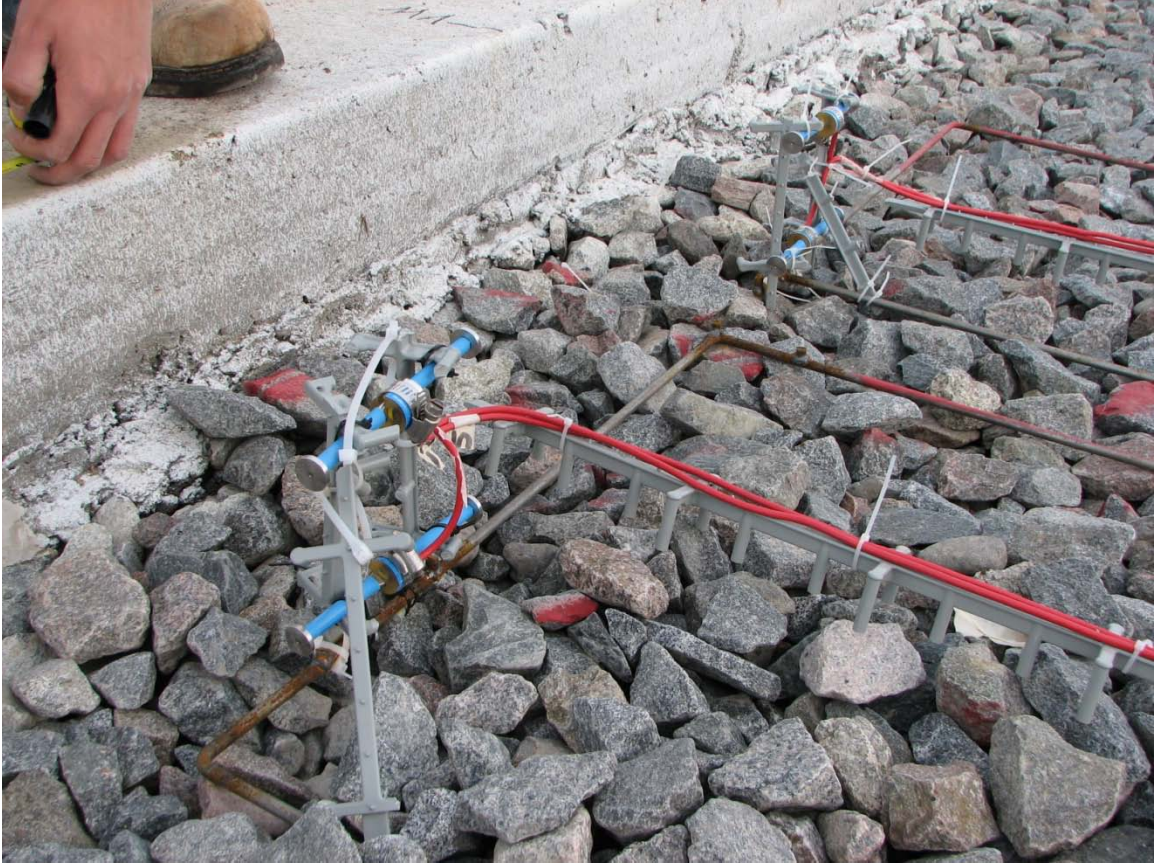


**Figure 5.5: Drainable Railroad Ballast and Improved Sensor Cage**

### 5.2.5 Water Marks and Thermocouples

Watermark and thermocouple tree was placed in the cell 85 during the grading and base construction. The sensors are placed at specific strategic depths to determine temperature, change of state (liquid – solid – liquid) as well as freeze thaw cycles. Thermo couples are arranged as branches of a 6 ft tree with those branches placed at strategic depths such as top, middle, and bottom of each layer. This has facilitated comparison of freeze thaw cycles of the porous surface, porous base and subgrade. It has also facilitated determination of true frost depth of porous pavements in comparison to normal concrete of similar design concrete thickness, base thickness, and subgrade material. R Similar freezing and thawing amplitudes were observed in the porous pavements at depths 2 ft lower than observed in normal concrete. Details of these are contained in an annual report due at the end of the year. Results thus indicate transmission of geothermal energy through the cavities facilitates a frost depth savings of 2-ft in cell 85.



**Figure 5.6: Water Mark on Cell 85, Installed to 6 Ft below the Surface**

### 5.3 Rainfall and Infiltration

Weather station at MnROAD captures rainfall, humidity, temperature sunshine continuously. This provides supporting data to the other instrumentation in the research facility and to researchers in general. It is important to know the hydraulic conductivity of the porous pavement as this relevant in general to infiltration and flooding or flood mitigation or reservoir routing with porous pavements

### 5.3.1 Rainfall Data

Monthly rainfall data was collected to match the well observation days and months. Summer is shown in table 5.1. Table 5.1 also shows an ensemble of monthly rainfall difference between 2008 and 2009. It will be noted that that construction occurred in October 2008. October 2008 and December 2008 value are thus compared in a “Before –Versus After” comparison.

**Table 5.1: Rainfall Data Summary**

Month	Total Precip, inches	Sigma Delta					
		3/19/2008	6/18/2008	10/24/2008	12/27/2008	4/28/2009	6/16/2009
Jan-08	0.08						
Feb-08	0.26						
Mar-08	1.11	0	8.04	8.34	3.49	4.41	2.73
Apr-08	2.93						
May-08	4.00						
Jun-08	3.30						
Jul-08	1.59						
Aug-08	1.88						
		Ensemble Delta					
Sep-08	3.29	Const Pre post	April	June			
Oct-08	1.58	-0.78	-0.18	-1.11			
Nov-08	1.01						
Dec-08	0.80						
Jan-09	0.22						
Feb-09	0.87						
Mar-09	2.39						
Apr-09	0.93						
May-09	0.54						
Jun-09	2.19						

### 5.3.2 Infiltration Measurements from Perveameter

Routine infiltration measurements are performed on the cells to determine the degree of clogging. The initial testing was performed with a crude perveameter, which is a modified Humboldt sand cone, subsequently.

**Table 5.2: Comparison of Average Time of Discharge through a Porous Pavement**

Cell	Average Time (s)	
	11.13.08	1.23.09
39	-	55.10
85	4.84	22.53
86	3.21	4.37
88	3.48	5.19
89	7.58	7.00

The device was modified into a 6 inch cylindrical shaft without a control valve. The time of discharge measured for both devices are similar but the latter is not with concomitant valve leaks and other problems associated with the sand cone. Moreover, the Iowa State university pervious concrete research team adopted the open cylindrical shaft for this purpose. National Center for Asphalt Technology (NCAT) uses a device with stepped height and diameter cascade of the open

shaft. This is reduced to 1½-inch diameter at the fourth step above, to allow for very low infiltration. Most agencies use only the base portion that is equivalent to the cylindrical shaft in diameter. Should flow transition from one segment to the next, the hydraulic equations will be too complex to assign porosity and gravimetric values. To solve this problem, Izevbekhai and Rohne (1) determined that at 50 seconds of flow time through the head loss of 8 inches, the media is described as clogged.

They also used a sand cone with a compressible malleable seal as the measuring device instead of the modified NCAT device. This improvisation was equipped with a valve that rendered the flow measurement more uniform than the NCAT device where filling and discharging occurs before measurement.

### ***5.3.3 Freeze Thaw Characteristics***

Figures 5.7 to 5.12 show the thermocouple and watermark data for Cell 85. The watermark is indicative of change of state from freezing to thawing and freezing in a time domain. The data compares December data to June data to ascertain that the aquifer did not experience any freezing during the winter months. Each figure shows a 24-hour snapshot. The cluster and constancy of temperature during the day below 20 inches indicates that the subgrade was likely liquid throughout the year. There were temperature fluctuations and a diurnal range of 12 degrees Fahrenheit in December within the concrete. In June, the diurnal range was 50 degrees Fahrenheit and resistivity was below 1000 kilo Ohms (KΩ). Transitional resistivity

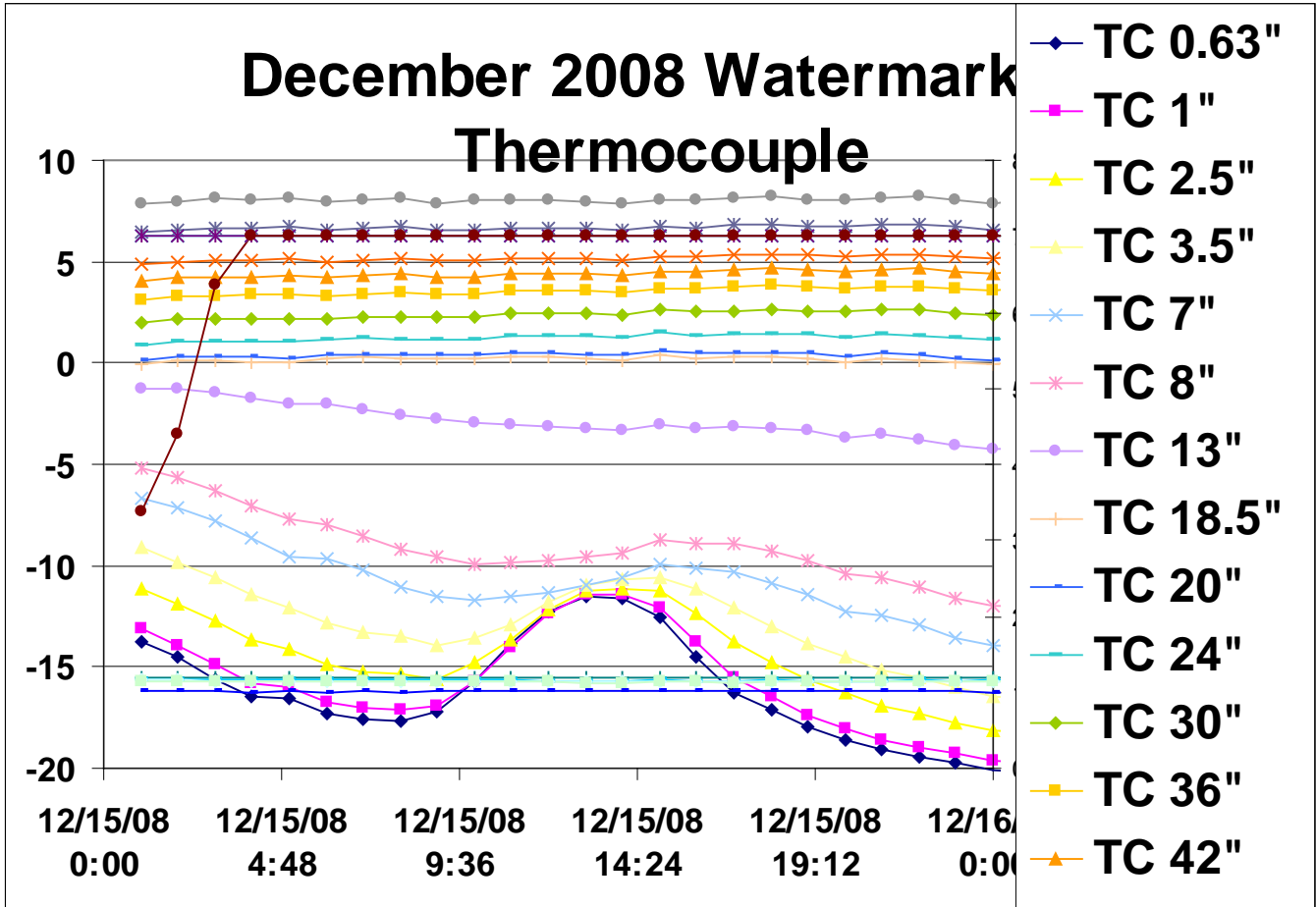


Figure 5.7: December 2008 Watermark and Thermocouple Data for Cell 85

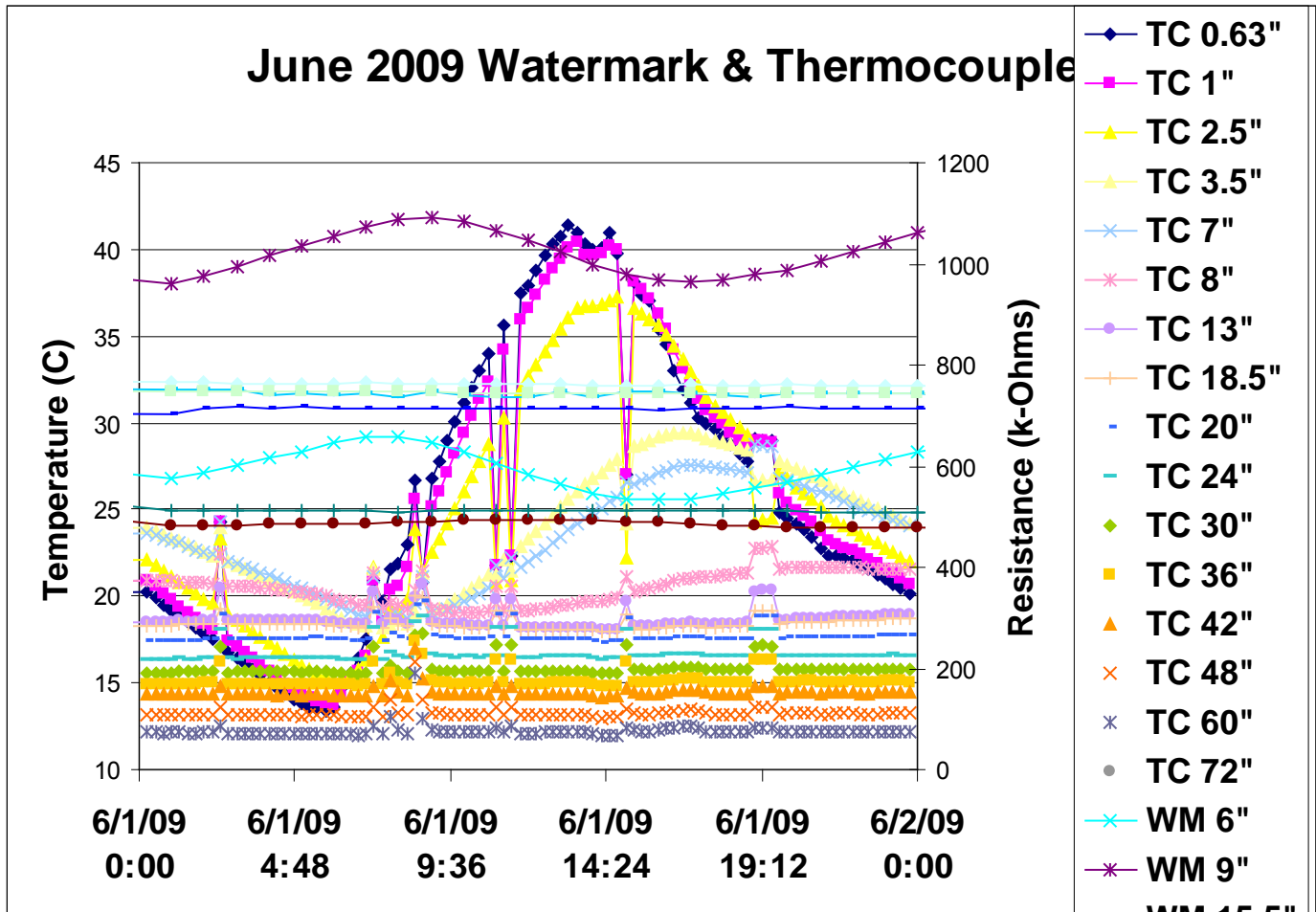


Figure 5.8: June 2009 Watermark and Thermocouple Data for Cell 85

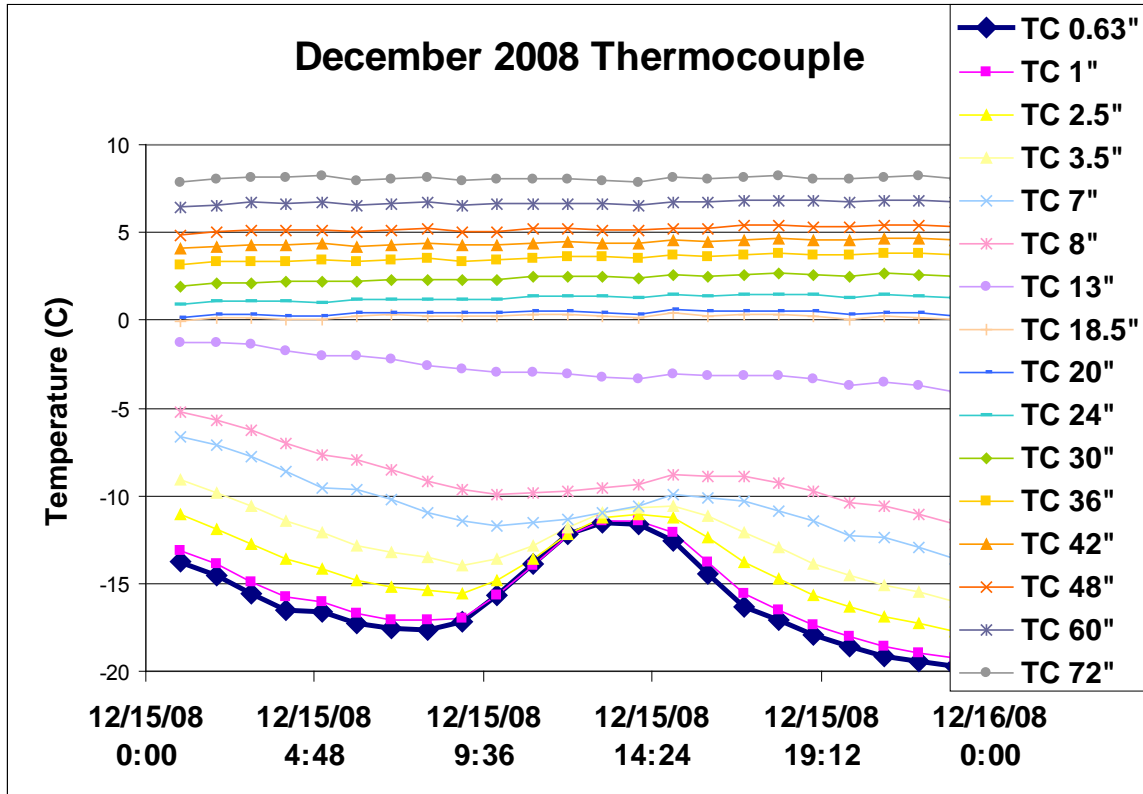


Figure 5.9: December 2008 Thermocouple Data for Cell 85

According to Berndt Bulesa in his review titled “A Critical Review of the Low-frequency Electrical

*“Properties of Ice Sheets and Glaciers, the activation energy in cold ice and firn is constant at  $\sim 0.25$  eV but poorly constrained in temperate ice and snow. The bulk resistivity of cold ice ranges from  $\sim 0.4 \times 10^5 \Omega\text{m}$  at  $-2^\circ\text{C}$  to  $4 \times 10^5 \Omega\text{m}$  at  $-58^\circ\text{C}$ , and is much higher in temperate ice (up to  $>1,000 \times 10^5 \Omega\text{m}$ ). The effects of impurity characteristics, temperature, and density on complex conductivity are poorly understood, although selected real conductivity components apparently increase with frequency, impurity concentration, or temperature.”*

The MnROAD watermarks measure resistance in Kilo-Ohms indicating that the resistivity has been converted to resistance by the geometric dimensions of the Ice are and length of influence. The actual multipliers will be determined in the laboratory in a research project that will commence soon.

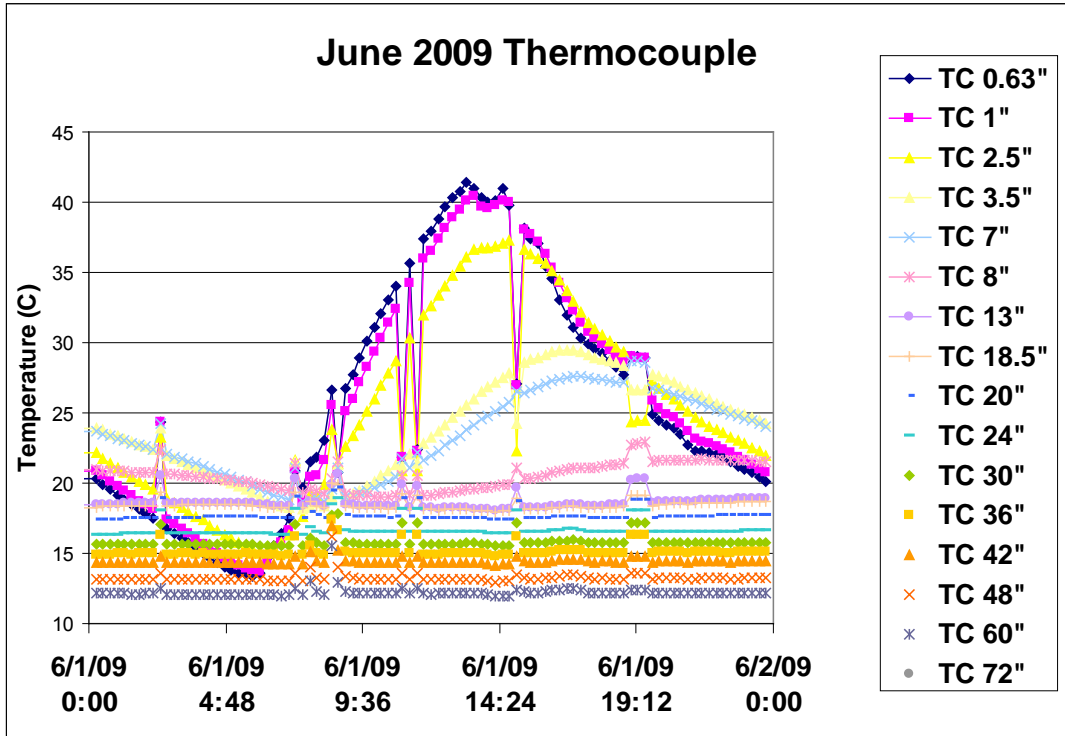


Figure 5.10: June 2009 Thermocouple Data for Cell 85

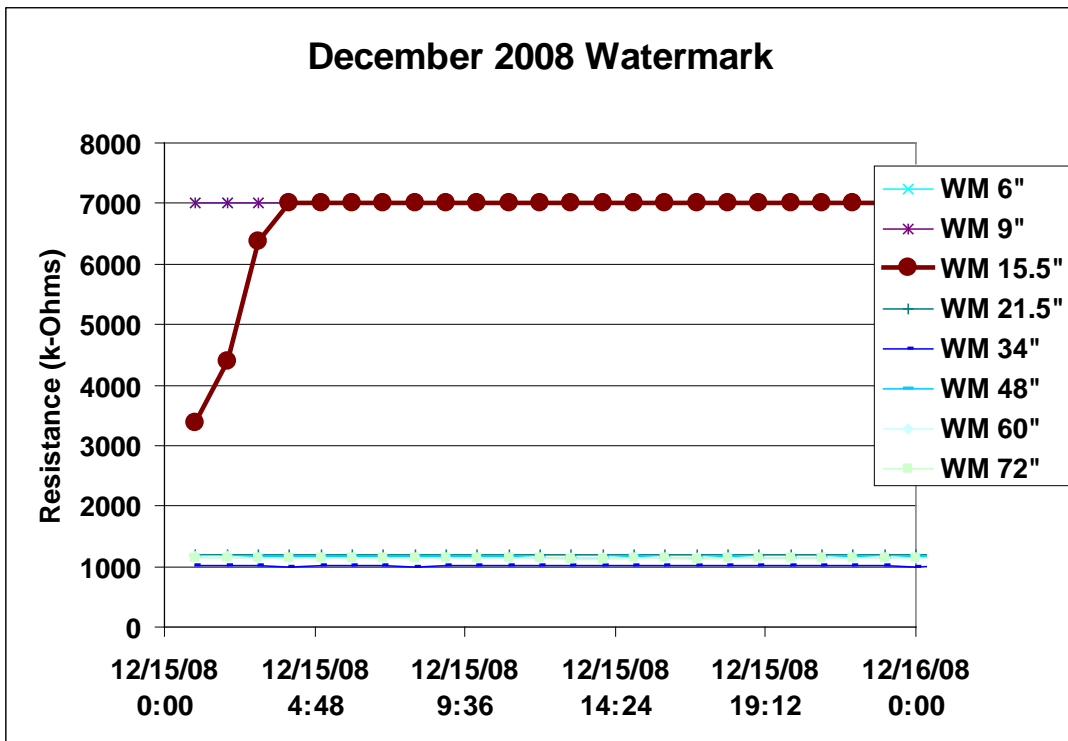


Figure 5.11: December 2008 Watermark Data for Cell 85

## June 2009 Watermark

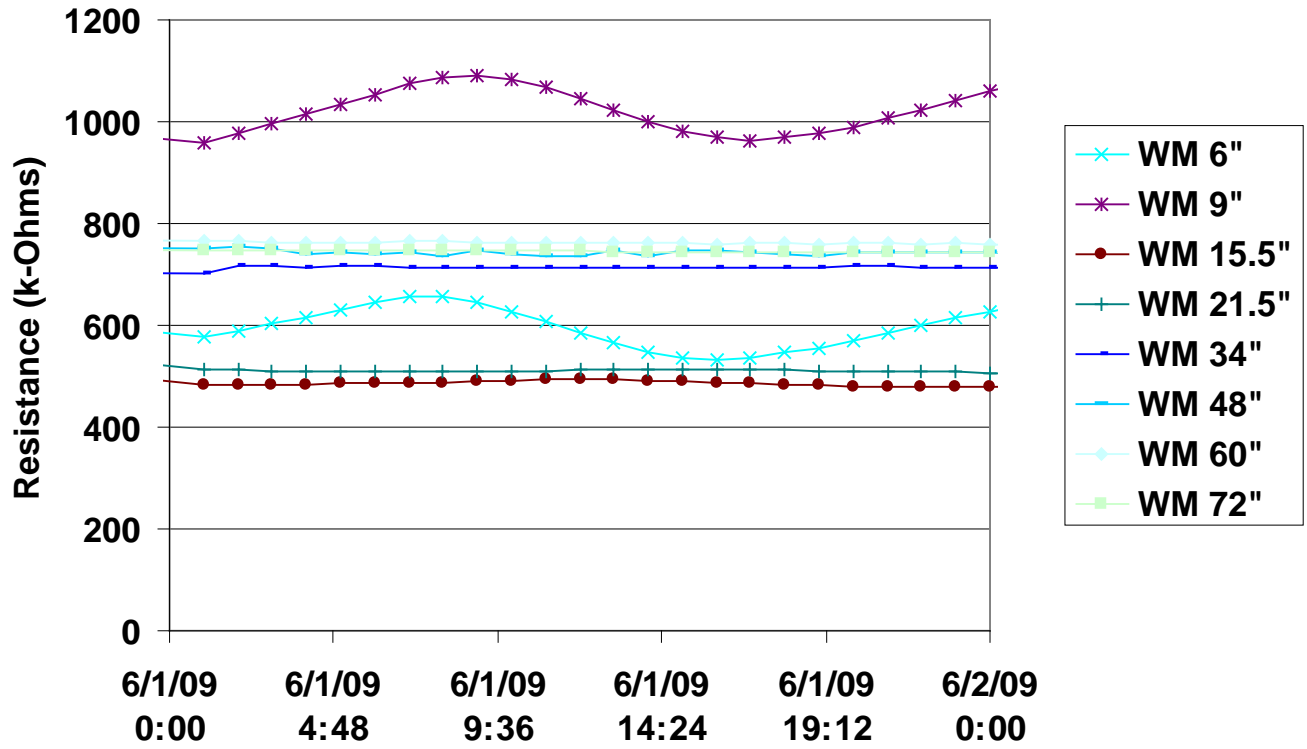


Figure 5.12: June 2009 Watermark Data for Cell 85

**Table 5.3: Flow Measurements Concrete 1/23/09**

Cell	Type	Base	Location		Lane	Initial Head (cm)	Head Drop (cm)	Thickness of Pavement (cm)	Cross Sectional Area (cm <sup>2</sup> )	Time (s)
85	Concrete	Sand	34' from East end	30" from South Curb	Environmental	8	0	18	167.53	7.69
85	Concrete	Sand	34' from East end	30" from South Curb	Environmental	8	0	18	167.53	7.61
85	Concrete	Sand	34' from East end	6 ft. from North Curb	Traffic	8	0	18	167.53	3.63
85	Concrete	Sand	34' from East end	6 ft. from North Curb	Traffic	8	0	18	167.53	3.61
85	Concrete	Sand	34' from East end	30" from North Curb	Traffic	8	0	18	167.53	2.27
85	Concrete	Sand	34' from East end	30" from North Curb	Traffic	8	0	18	167.53	2.46
85	Concrete	Sand	34' from East end	30" from North Curb	Traffic	8	0	18	167.53	2.1
85	Concrete	Sand	94.2' from West end	30" from South Curb	Environmental	8	0	18	167.53	5.02
85	Concrete	Sand	94.2' from West end	30" from South Curb	Environmental	8	0	18	167.53	5.08
85	Concrete	Sand	94.2' from West end	6 ft. from North Curb	Traffic	8	0	18	167.53	3.87
85	Concrete	Sand	94.2' from West end	6 ft. from North Curb	Traffic	8	0	18	167.53	4.09
85	Concrete	Sand	94.2' from West end	30" from North Curb	Traffic	8	0	18	167.53	7.86
85	Concrete	Sand	94.2' from West end	30" from North Curb	Traffic	8	0	18	167.53	7.59
86	HMA	Sand	117.7' from West end	30" from South Curb	Environmental	8	0	13	167.53	2.12
86	HMA	Sand	117.7' from West end	30" from South Curb	Environmental	8	0	13	167.53	2.49
86	HMA	Sand	117.7' from West end	7 ft. from South Curb	Environmental	8	0	13	167.53	4.7
86	HMA	Sand	117.7' from West end	7 ft. from South Curb	Environmental	8	0	13	167.53	4.82
86	HMA	Sand	117.7' from West end	30" from North Curb	Traffic	8	0	13	167.53	1.94
88	HMA	Clay	104.7' from East end	30" from South Curb	Environmental	8	0	13	167.53	3.49
88	HMA	Clay	104.7' from East end	30" from South Curb	Environmental	8	0	13	167.53	3.18
88	HMA	Clay	104.7' from East end	7 ft. from South Curb	Environmental	8	0	13	167.53	3.31
88	HMA	Clay	104.7' from East end	7 ft. from South Curb	Environmental	8	0	13	167.53	3.47
88	HMA	Clay	104.7' from East end	30" from North Curb	Traffic	8	0	13	167.53	3.76
88	HMA	Clay	104.7' from East end	30" from North Curb	Traffic	8	0	13	167.53	4.09
88	HMA	Clay	29.6' from West end	30" from South Curb	Environmental	8	0	13	167.53	3.54
88	HMA	Clay	29.6' from West end	30" from South Curb	Environmental	8	0	13	167.53	4.19
88	HMA	Clay	29.6' from West end	7 ft. from South Curb	Environmental	8	0	13	167.53	2.46
88	HMA	Clay	29.6' from West end	7 ft. from South Curb	Environmental	8	0	13	167.53	2.75
88	HMA	Clay	29.6' from West end	30" from North Curb	Traffic	8	0	13	167.53	3.57
88	HMA	Clay	29.6' from West end	30" from North Curb	Traffic	8	0	13	167.53	3.94
89	Concrete	Clay	35.5' from East end	30" from South Curb	Environmental	8	0	18	167.53	8.64
89	Concrete	Clay	35.5' from East end	30" from South Curb	Environmental	8	0	18	167.53	8.4
89	Concrete	Clay	35.5' from East end	6 ft. from North Curb	Traffic	8	0	18	167.53	8.08
89	Concrete	Clay	35.5' from East end	6 ft. from North Curb	Traffic	8	0	18	167.53	8.02
89	Concrete	Clay	35.5' from East end	30" from North Curb	Traffic	8	0	18	167.53	5.21
89	Concrete	Clay	35.5' from East end	30" from North Curb	Traffic	8	0	18	167.53	5.92
89	Concrete	Clay	87.5' from East end	30" from South Curb	Environmental	8	0	18	167.53	11.05
89	Concrete	Clay	87.5' from East end	30" from South Curb	Environmental	8	0	18	167.53	10.88
89	Concrete	Clay	87.5' from East end	6 ft. from North Curb	Traffic	9	0	18	167.53	7.03
89	Concrete	Clay	87.5' from East end	6 ft. from North Curb	Traffic	9	0	18	167.53	6.99
89	Concrete	Clay	87.5' from East end	30" from North Curb	Traffic	8	0	18	167.53	5.21
89	Concrete	Clay	87.5' from East end	30" from North Curb	Traffic	8	0	18	167.53	5.5

**Table 5.4: Sample Flow Measurement on 1/23/09**

Cell	Type	Base	Location	Lane	Initial Head (cm)	Head Drop (cm)	Thickness of Pavement (cm)	Cross Sectional Area (cm <sup>2</sup> )	Time (s)	Hydraulic Conductivity (cm/s)	Hydraulic Conductivity (in/s)
39	Concrete	Concrete	119.2' from west end 7.8' from Centerline	Traffic	10	5	10	167.52	55.1	0.10	0.04
85	Concrete	Sand	94.2' from West end 6' from North Curb	Traffic	8	0	18	167.53	22.53	1.27	0.50
89	HMA	Sand	117.7' from West end 30' from South Curb	Environmental	8	0	13	167.53	4.37	4.68	1.84
88	HMA	Clay	29.6' from West End 7' from South Curb	Environmental	8	0	13	167.53	5.19	3.94	1.55
89	Concrete	Clay	87.5' from East end 6' from North Curb	Traffic	8	0	18	167.53	7	4.09	1.61

## 5.4 Mounding Analysis

Mounding is the phenomenon where a phreatic surface suddenly rises due to infiltration. Seepage forces govern ground water flow. It therefore takes time for the effect of infiltration to be dissipated. The dissipation is contingent on aquifer transmissivity.

Mounding also affects storage component of the mass balance equation since the latter is a time dependent function. Any potentiometric height above the grading subgrade is viewed as storage albeit falsely.

The importance of mounding is easily accentuated by the need to ensure that unhindered infiltration does not cause flooding. Such a phenomenon will jeopardize neighboring foundations and cause severe pollution. To guard against such events, the mounding of the current pervious concrete cells are analyzed and discussed in detail.

### 5.4.1 Estimation of Aquifer Transmissivity (Not Based in Pumping)

As a necessary procedure in ground water hydraulics, pumping tests are conducted to determine the transmissivity of an aquifer. The transmissivity  $T$  is defined as

$$T = KQ/SW$$

$T$  is in US gall/day/ft where

$SW$  is the drawdown observed from 24 hours of pumping at a rate of gal/min

$Q$  is the rate of pumping in gal/min.

No pumping tests were conducted but based on the stratigraphy of the project location, the ground water elevation and porosity of the perched aquifer sands, an estimation of  $T$  was performed.

Using equation (1), (3) it is assumed that the following values to develop approximate formulas for estimating transmissivity from specific capacity in confined and unconfined aquifers. Given these assumed values, Driscoll (3) estimates transmissivity given the specific capacity of a well as follows:

$$T = 2000(Q/s_w) \quad \text{confined aquifer} \quad 4.1 \text{ a}$$

$$T = 1500(Q/s_w) \quad \text{unconfined aquifer} \quad 4.1 \text{ b}$$

where  $T$  is transmissivity [US gal/day/ft],  $Q$  is constant discharge rate [US gal/min] and  $s_w$  is drawdown in the pumped well after 1 day [ft].

If we express  $Q$  in  $m^3/day$  and  $s_w$  in  $m$ , the equations for computing  $T$  in  $m^2/day$  are (10)

$$T = 1.385(Q/s_w) \quad \text{confined aquifer}$$

$$T = 1.042(Q/s_w) \quad \text{unconfined aquifer}$$

#### 5.4.2 Monitoring Well Observation

The monitoring wells were observed at certain days of remarkable hydrologic events. (Post, precip or routine). A slope-indicator water-probe when inserted into the open well indicates the depth with a medium horning sound. Depth below the shaft was recorded in each case. The piezometers are located upstream or downstream of the control volume and are labeled as DS or US as necessary.

##### 5.4.2.1 Analysis of Ground Water Level Fluctuation

Various analysis conducted on the well observed include, impulsive mounding, ensemble mounding and the raw elevations. The ensemble mounding allowed a computation of the Groundwater Elevation (GWE) after each 2009 record to the corresponding 2008 record. It showed remarkable variability and some degree of unpredictability. The MnROAD wells and the spatially coincident MDH wells did not indicate equal elevations or moundings.

Table 5.5 shows actual well observations made in the eight wells. This is accentuated in figure 5.13, impulsive mounding values were observed in April 2008 and June 2008. The trend in April 2008 was followed by equally high 2009 value. The wells the showed the same time series in figure 6 with the upstream wells exhibiting more sensitivity and fluctuation than the downstream wells. The mounding values are much higher than the rainfall events if the catchment area is analytically restricted to the control volume. Evidently, the aquifer is receiving flow from other sources from where \_run-off from other sources get into the common subsurface water. That is the only reason a mounding of 40 inches may be observed in cell 86.

In figure 5.13, the mounding time series is plotted with respect to time. Figure 5.14 shows the change in TWL in each season. In Figure 5.15 ensemble mounding compares the TWL in each month in 2009 with the corresponding 2008 observation. From above it is evident that most of the downstream wells DS1 DS2 and DSL experienced TWL increase. The decrease in TWL of DS3 was minor.

**Table 5.5: Monitoring Well Observation with Respect to Time**

	<b>3/19/2008</b>	<b>6/18/2008</b>	<b>10/24/2008</b>	<b>12/27/2008</b>	<b>4/28/2009</b>	<b>6/16/2009</b>
MDH Well No. 577314 DS1	93.3	90.6	99	96	89.7	96
<b>MnROAD Well A DS2</b>	62.5	45.5	64	62.4	52.9	69.36
MDH Well No. 577321 DS3	97.5	97.2	99	97.2	92.7	94.1
<b>MnROAD Well B DS4</b>	77.5	48.5	72.5	64.8	61.2	69.36
MDH Well No. 577322 US 1	102.5	96	88	80.6	115.5	85.2
<b>MnROAD Well C US2</b>	86.5	57.6	70	76.8	52.5	56.52
<b>MnROAD Well D US4</b>	86.8	37.8	81	91.2	74.4	76.08
MDH Well No. 577322 US3	177.7	145.2	134	145.2	144	135.8

Table 5.6: Mounding Analysis

	<b>Mounding</b>					
	March 19, 2008	June 18, 2008	October 24, 2008	December 27, 2008	April 28, 2009	June 16, 2009
MDH Well No. 577314 DS1	0	2.7	-8.4	3	6.3	-6.3
MnROAD Well A DS2	0	17	-18.5	1.6	9.5	-16.46
MDH Well No. 577321 DS3	0	0.3	-1.8	1.8	4.5	-1.4
MnROAD Well B DS4	0	29	-24	7.7	3.6	-8.16
MDH Well No. 577322 US 1	0	6.5	8	7.4	-34.9	30.3
MnROAD Well C US2	0	28.9	-12.4	-6.8	24.3	-4.02
MnROAD Well D US4	0	49	-43.2	-10.2	16.8	-1.68
MDH Well No. 577322 US3	0	32.5	11.2	-11.2	1.2	8.2

Example:  $\Delta 2 = h_{(6/18/08)} - h_{(3/19/08)}$

$$\Delta 4 = h_{(Prior\ to\ Construction)} - h_{(before\ previous\ construction)}$$

## Mounding (Elevation) Time Series

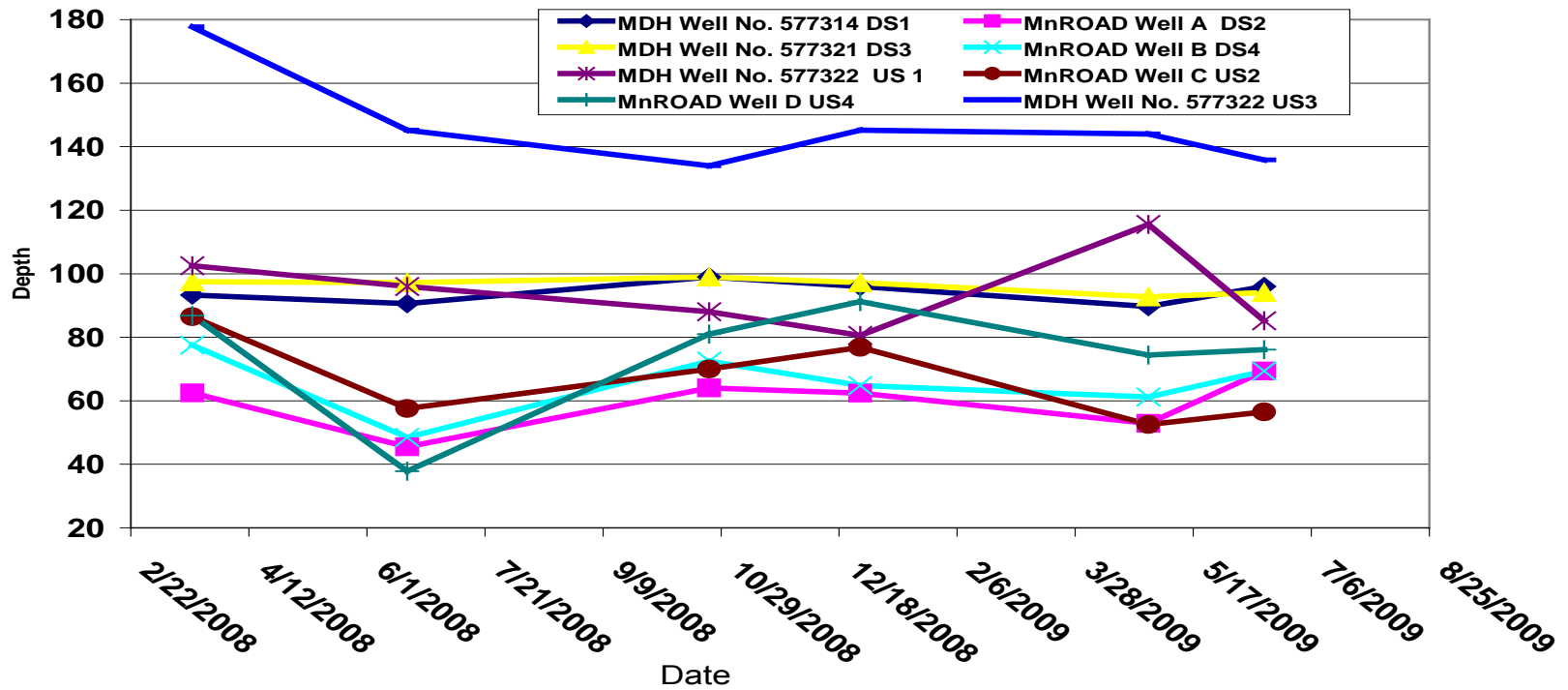


Figure 5.13: Fluctuation of Top Water Level in the Observational Wells

## Ensemble Mounding

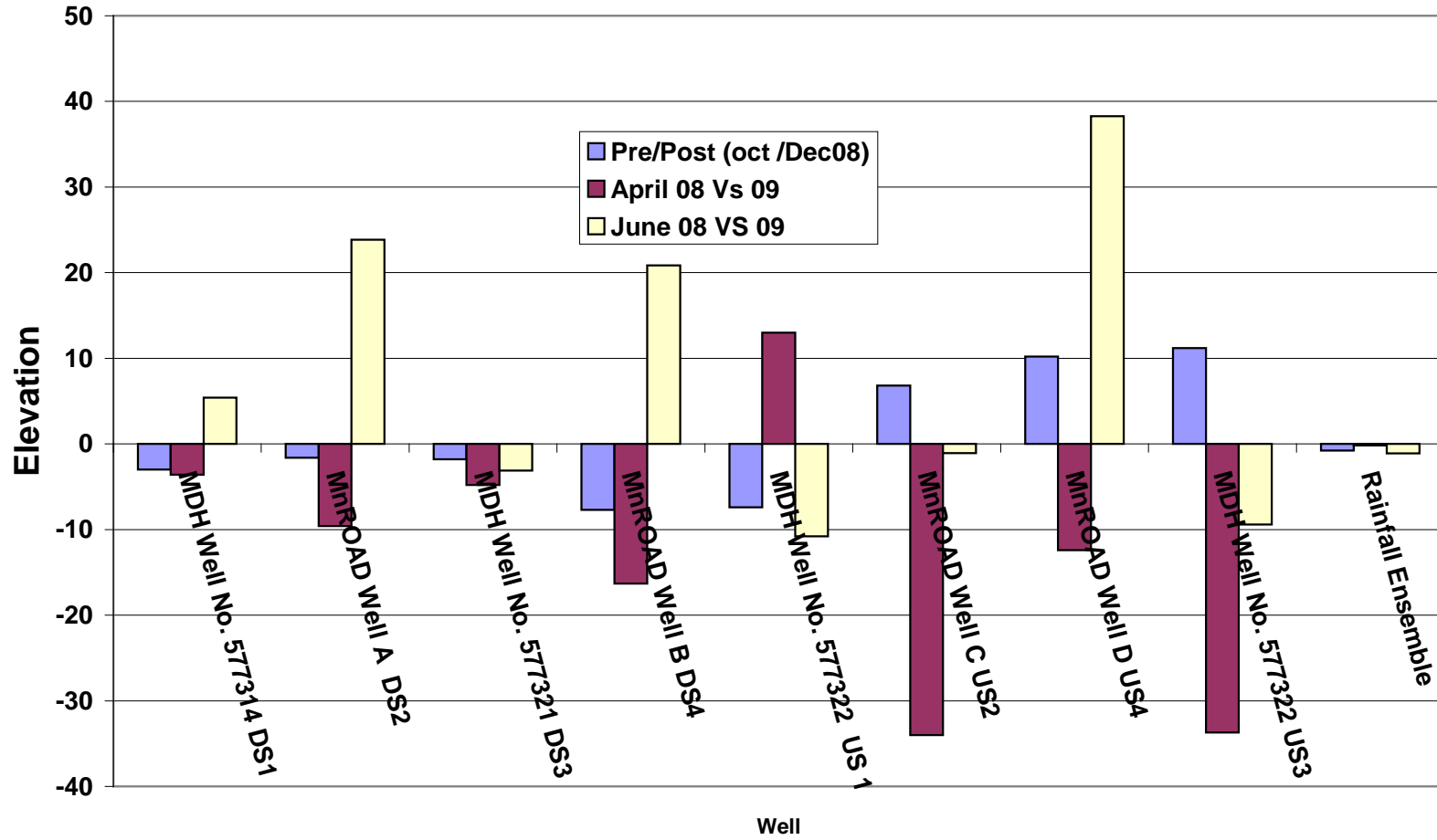


Figure 5.14: Ensemble Mounding Analysis

In Figure 5.14, ensemble mounding compares the TWL in each month in 2009 with the corresponding 2008 observation. From

Figure 5.14: above it is evident that most of the downstream wells DS1 DS2 and DS4 experienced TWL increase. The decrease in TWL of DS3 was minor.

**Table 5.7: Comparison of 2008 to 2009 Well Observation Considering Rainfall Difference**

<b>Ensemble Mounding Analysis</b>			
	<b>Pre/Post (Oct /Dec 08)</b>	<b>April 08 Vs 09</b>	<b>June 08 VS 09</b>
<b>MDH Well No. 577314 DS1</b>	-3	-3.6	5.4
<b>MnROAD Well A DS2</b>	-1.6	-9.6	23.86
<b>MDH Well No. 577321 DS3</b>	-1.8	-4.8	-3.1
<b>MnROAD Well B DS4</b>	-7.7	-16.3	20.86
<b>MDH Well No. 577322 US 1</b>	-7.4	13	-10.8
<b>MnROAD Well C US2</b>	6.8	-34	-1.08
<b>MnROAD Well D US4</b>	10.2	-12.4	38.28
<b>MDH Well No. 577322 US3</b>	11.2	-33.7	-9.4
<b>Rainfall Ensemble</b>	-0.78	-0.18	-1.11

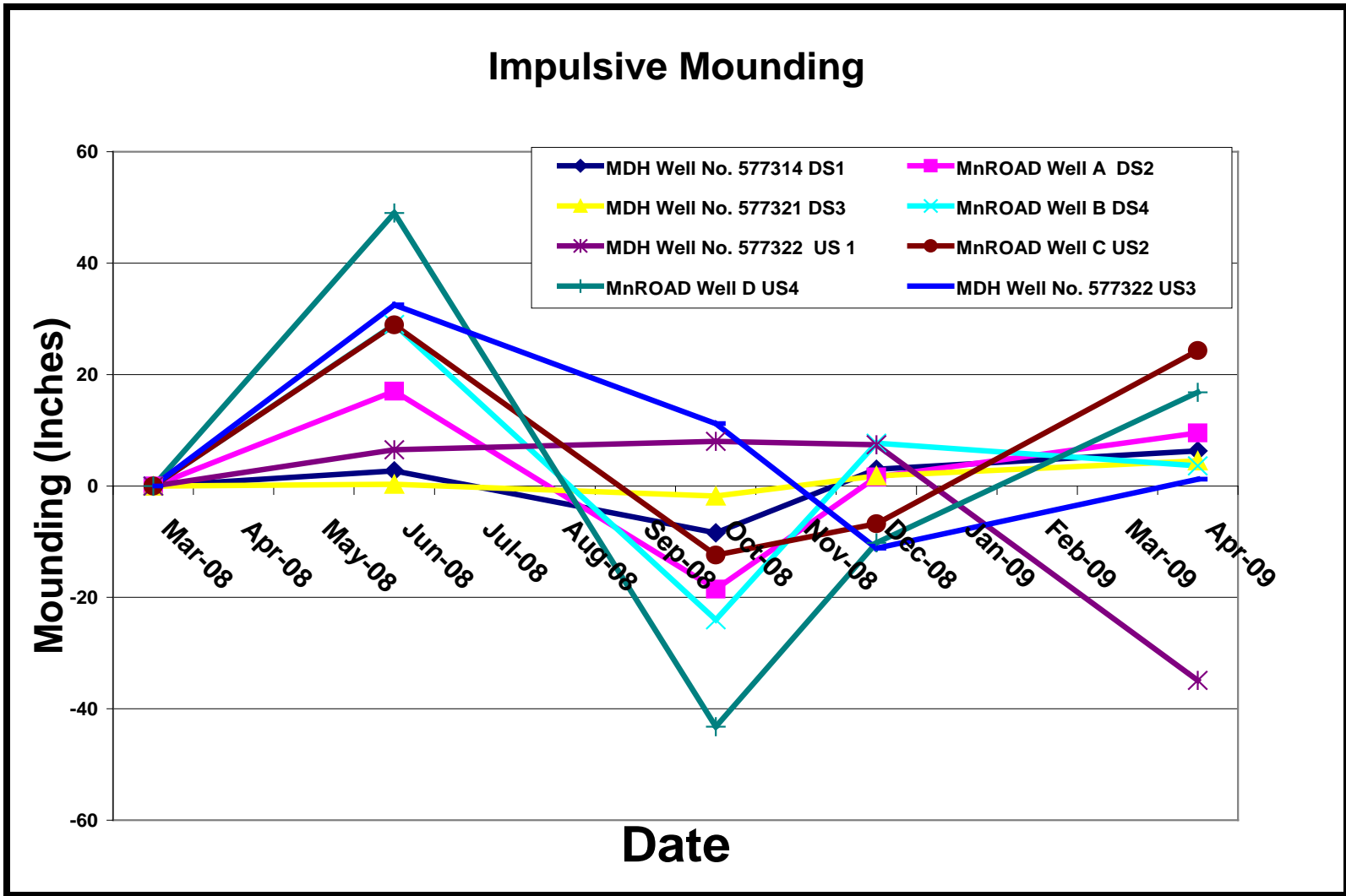


Figure 5.15: Impulsive Mounding

The impulsive mounding is the change in TWL between the current and last measurement

5.4.2.2 Dynamic Mass Balance and Computation and Reservoir Routing

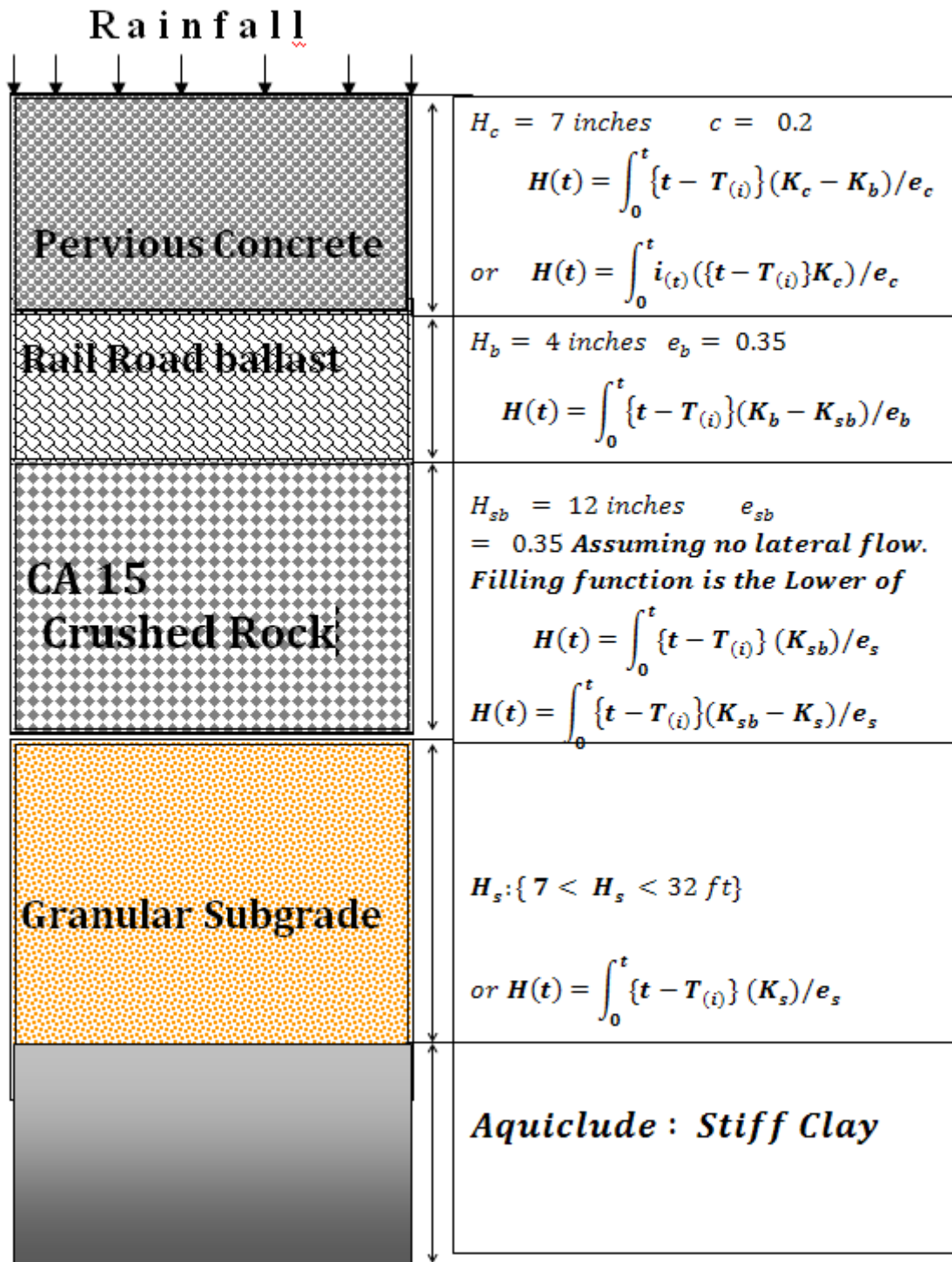


Figure 5.16: Reservoir Routing Algorithm Derived for Each Layer

The Aquiclude is made up of stiff clay and is thus impermeable. The impermeability of the Aquiclude permits the rise in water level in the subgrade.

***Rise in water elevation of the granular subgrade:***

$$H_s: \{7 < H_s < 32 \text{ ft}\}$$

Assuming no lateral flow

Filling function is the lower of

$$H(t_1) = \int_0^t i_{(t)} (K_b) / e_s$$

$$\text{Or } H(t) = \int_0^t i_{(t)} (K_s) / e_s$$

***Rise in water elevation of the porous subbase:***

$$H_{sb} = 12 \text{ inches}, \quad e_{sb} = 0.3$$

Filling function

$$H(t) = \int_0^t \{t - T_{(i)}\} (K_{sb} - K_s) / e_s$$

***Rise in water elevation of the porous base:***

$$H_b = 4 \text{ inches}, \quad e_b = 0.35$$

$$H(t) = \int_0^t \{t - T_{(i)}\} (K_b - K_s) / e_b$$

***Rise in water elevation of the concrete pavement:***

$$H_c = 7 \text{ inches}, \quad c = 0.20$$

$$H(t) = \int_0^t \{t - T_{(i)}\} (K_b - K_s) / e_c$$

$$\text{Or } H(t) = \int_0^t (\{t - T_{(i)}\} - K_s) / e_c$$

### 5.4.3 Critical Flood Analysis

$$H(t) = \int_0^{t1} t_{(i)}(K_s) e_s = (TLW - 19)t1$$

$$\int_0^{t2} \{t - T_{(i)}\}(K_{sb})/e_{sb} = H_{sb}$$

$$\int_0^{t3} \{t - T_{(i)}\}(K_b)/e_b = H_b$$

$$\int_0^{t4} \{t - T_{(i)}\}(K_c)/e_c = H_c$$

For rainfall of 1 inch per hour

$$17 \times 0.2 + 12 \times 0.35 - F \text{ (Transmissivity in subgrade)}/1 \text{ inch per hour}$$

Assuming (FT) = 0.15 inch/hour

$$7.7 + 0.15t = t$$

$$t = 7.7/0.85 \approx 9 \text{ hours in cells 85 and 86}$$

Assuming zero transmissivity, it will take 7 hours to fill up in cells 88 and 89 because their subgrade is clay.

**Table 5.8: Approximate Transmissivity Deductions (6)**

$K$ (cm/s)	$10^2$	$10^1$	$10^0=1$	$10^{-1}$	$10^{-2}$	$10^{-3}$	$10^{-4}$	$10^{-5}$	$10^{-6}$	$10^{-7}$	$10^{-8}$	$10^{-9}$	$10^{-10}$
$K$ (Ft/day)	$10^5$	10,000	1,000	100	10	1	0.1	0.01	0.001	0.0001	$10^{-5}$	$10^{-6}$	$10^{-7}$
Relative Permeability	Pervious				Semi-Pervious				Impervious				
AQUIFER	Good				Poor				None				
UnconsolidatSand & Gravel	Well Sorted Gravel	Well Sorted Sand or Sand & Gravel			Very Fine Sand, Silt, Loess/ Loam								
Unconsolidated Clay & Organic					Peat	Layered Clay			Fat / Unweathered Clay				
Consolidated Rocks	Highly Fractured Rocks		Rocks	Fresh Sand Stone		Fresh Limestone/ Dolo		Fresh Granite					

$$7.7 - f(T)t = ict$$

But  $ft$  is zero in cells 88 and 89

$$7.7 - 0.15t < ict$$

Thus  $ict + 0.15t < 7.7$

For  $t = 1 \text{ hr}$ ,  $1c < 7.7$

For  $T = 12 \text{ hrs}$ ,  $1c \approx 0.4 \text{ inches per hour}$

#### 5.4.4 Future Hydrologic Monitoring

MnROAD cells are monitored every month but routine porous cell monitoring is scheduled for every 3 months. Data from the flow out meter, abstraction wells, and sensors will be examined.

Monitoring wells will be examined once a month subsequently. The watermarks will be examined for the depth of freezing in each of the cells. This will guide provide an added indication of actual water depth when freezing temperatures are prevalent.

## 5.5 Conclusion

Hydrologic evaluation of porous cells in MnROAD has been conducted. Fluctuation in the phreatic surface has been examined. In the examination the pre-construction and post construction TWL were compared in corresponding months. There was evidence of increase in the TWL of the downstream monitoring wells. One year of monitoring is however insufficient to ascribe the spike or mounding to the presence of the porous cells that were designed for direct infiltration.

The absence pumping of the wells did not facilitate estimation of transmissivity that would enhance a more tenable dynamic mass balance. However, some equations were developed that would facilitate future analysis.

This research predicts a rainfall of 0.4 inches per hour sustained for 123 hours as the critical flood level. This level is contingent on the continuity of the base beneath the cross drains and takes advantage of the sloping aquifer that will force trapped water above the clay subgrade to migrate westward through the porous subgrade of the downstream cells.

Unusually high TWL increases point to the suggestion that the geo-fabrics had not cordoned the test cells as intended and migration of subsurface water into the test cells occurred.

Aggressive monitoring of the test cells will continue at a more frequent pace (once a month).

## **CHAPTER 6 EARLY PERFORMANCE OF PERVIOUS CELLS**

### **6.1 Introduction**

This chapter will discuss the approach used to measure the performance of the test cells and will describe the particular test methods and equipment used to make the performance assessments. Next, it will include the results of the tests and monitoring obtained over the past two years. Finally, analysis and data regression of the results collected will be given to form meaningful, valuable insight on the performance of pervious concrete pavements.

The following performance criteria were measured on cells 39, 85 and 89 over the past two years:

#### **Ride Characteristics**

- International Roughness Index (IRI)
- Surface Rating (SR)

#### **Surface Properties**

- Surface Texture
- Friction Number (FN)

#### **Noise Characteristics**

- On Board Sound Intensity (OBSI)
- Sound Absorption (SA)

#### **Physical Properties**

- Nuclear Density
- Dissipated Volumetric Rate
- Clogging Characteristics
- Pavement Surface Deflection from FWD
- Temperature and Moisture

Analysis of the data collected from this comprehensive set of tests will provide a better understanding on the performance of pervious concrete pavements and their potential for use.

### **6.2 Test Descriptions**

The last chapter gave a summary of the design and construction of the three pervious test cells at MnROAD. This chapter will review the approach that was used for assessing the performance of cells 39, 85 and 86 described in chapter 1. All of these properties are influenced by the difference in air void structure of pervious concrete. Pervious concrete has an increased percentage of air, typically over 15% of the volume. In contrast to the microscopic entrained air voids in conventional PCC, the air in pervious concrete is held in large voids outside of the concrete

paste. This air void structure influences durability, creates a unique surface texture, alters sound absorption and drainability, and influences other physical properties. To evaluate the resulting performance of pervious concrete, tests were performed to measure ride, noise, surface properties and other physical characteristics. These tests will help determine what benefit pervious concrete would have in pavement and also provide data that could help develop a mechanistic-empirical design process for pervious pavement.

### **6.2.1 Ride Characteristics**

The MnDOT uses the following three tests to evaluate how the surface characteristics of pervious concrete influence how a user would define the pavement performance.

#### *6.2.1.1 International Roughness Index*

The International Ride Index (IRI) is measured using two different pieces of equipment: a Lightweight Inertial Surface Analyzer (LISA) and the Pathway Services, Inc. Digital Inspection Vehicle (DIV). The LISA shown in Figure 6.1 below is a profile device used to measure the amount of vertical rise over a horizontal distance. This is done with two separate laser sources on the side of the vehicle, one which takes continuous profile measurements over a four inch path and one which measures three discrete profiles across the four inch path. The Minnesota Department of Transportation's pavement management section measures IRI using the Digital Inspection Vehicle (DIV) shown in Figure 6.2 below. As the van moves along a section of roadway at highway speeds, a laser mounted to the front bumper captures the profile of the pavement surface at approximately once every 1/8 inches. This raw data is then used to calculate the IRI value. This is done with a mathematical simulation that estimates the amount of vertical movement a vehicle would experience while driving. The simulation uses a higher IRI to correspond to a rougher pavement. It is important to note that the calculated IRI can be highly dependent on the section length; a single rough spot would have a larger negative influence on a shorter segment than it would on a longer one.

#### *6.2.1.2 Surface Rating*

Pavement distress is measured by the Surface Rating (SR). The Surface Rating depends on the amount of observed defects on a pavement surface, and is a good indicator for determining the specific type or cause of deterioration the pavement is experiencing. As with IRI, SR is measured using the DIV. Besides lasers, the DIV is equipped with four digital cameras. The two front view and two side view cameras take images of the pavement as it travels down the roadway. These images are transferred to a workstation to be viewed and analyzed by operators. The actual calculation of the Surface Rating is done with the assistance of software, and is dependent on the amount of observed cracks and distress the pavement surface is experiencing. A pavement in better condition will have a higher surface rating. The maximum SR a pavement can achieve is 4.0. The disadvantage of this method is that it only allows for two dimensional analysis, making it easy to overlook certain types of distress which are typical to pervious pavements, such as raveling and weathering.



**Figure 6.1: Lightweight Inertial Surface Analyzer**



**Figure 6.2: Digital Inspection Vehicle**

### **6.2.2 *Surface Characteristics***

The unique surface texture of pervious pavements can have a large impact on the friction and skid resistance. Because driver safety is always a major concern in pavement design, the following two tests will provide very important insight on the performance of pervious concrete pavements.

### 6.2.2.1 Texture Meter

To analyze the surface of the pervious test cells, a Circular Texture Meter (CTM) is used to measure the profile of the pavement surface. The CTM shown in figure 6.3(a) below is used in accordance with ASTM E2157. The texture meter uses a laser to measure the profile depth throughout an 11.2 inch diameter circle. This profile is segmented into eight sections, and the average of the mean profile depth for each segment is calculated. The test is performed three times at each location, and the root mean square of all tests is taken as the final mean profile depth.

### 6.2.2.2 Friction Number

The pervious cells 39, 85 and 89 were tested for friction with the standard method used at MnROAD. This method utilizes the KJ Law Friction Trailer show in Figure 6.3(b) to perform skid testing of the pavement surface. This test is usually performed twice annually on all cells at MnROAD. Friction testing is done in accordance with the following three ASTM standards for skid resistance of paved surfaces: ASTM E274 using a full-scale tire, ASTM E501 using a standard ribbed tire, and ASTM E524 using a smooth tire. The friction trailer is pulled at 40 mph speed. Once the trailer mists the pavement surface with water, a break activates locking the wheel in place. This applies both horizontal drag forces and vertical load forces to the pavement. Sensors located at the wheel assembly take the friction measurements. The test is performed on both wheel paths and in both lanes. The average of the four measurements is used to calculate the friction number for the test cell. The test generates friction numbers between 0 and 100. A pavement with a friction number from a smooth tire of 25 is considered a safe pavement with adequate skid resistance. A friction number less than 15, however, would describe a pavement needing rehabilitation to achieve sufficient skid resistance [1].



(a) Circular Texture Meter



(b) KJ Law Friction Trailer

**Figure 6.3: (a) Circular Texture Meter and (b) Friction Trailer**

### 6.2.3 Noise Characteristics

As with ride characteristics, pavement noise also has a large impact on the user's perception of pavement performance. Pervious pavements have shown the ability to reduce the amount of undesirable traffic noise. The following tests help determine if noise generation is affected by the change in surface conditions of pervious pavements, and whether or not the air void structure leads to increased sound absorption compared to typical pavement.

#### 6.2.3.1 On Board Sound Intensity

The On Board Sound Intensity (OBSI) test measures the noise generated from the tire interaction with the pavement surface. MnDOT became one of only five states to utilize OBSI when it began testing in 2007. The test is performed while driving at freeway speeds, when the dominant noise generation source becomes that from the tire-pavement interaction. One benefit of OBSI testing is that it allows noise generated from the pavement-tire interaction to be isolated from other sources, such as engine noise. OBSI is also not subject to influence from other landscape and surrounding environmental factors, making it favored to the traditional Statistical Pass By Method. The tire-pavement interaction noise is measured using four intensity meters mounted on the tire near the pavement surface. This setup is shown in Figure 6.4(a) below. The sound intensity captured from these meters is then used to calculate OBSI using following logarithmically scaled, A-weighted equation to closely relate it to the human hearing spectrum.

$$OBSI = 10 \log_{10} \left[ \sum_{i=1}^n 10^{(SI_i/10)} \right] \quad (1)$$

*i = Third – Octave Frequency*

*SI<sub>i</sub> = Measured Sound Intensity at frequency "i"*

The OBSI is determined by averaging the sound intensity measurements from each of the following 12 third-octave frequencies: 400, 500, 630, 800, 1000, 1250, 1600, 2000, 2500, 3150, 4000, and 5000 hertz. These frequencies are determined using the algorithm below.

$$\text{For the } n^{\text{th}} \text{ octave: } \frac{F_{n+1}}{F_n} = 2^{\left(\frac{1}{n}\right)} \quad (2)$$

*Such that if  $n = 3$  and  $F_1 = 400$  Hz:*

$$F_2 = 400 * 2^{\left(\frac{1}{3}\right)} = 500 \text{ Hz,} \quad F_3 = 500 * 2^{\left(\frac{1}{3}\right)} = 630, \quad \text{Hz } F_4 = 630 * 2^{\left(\frac{1}{3}\right)} \dots$$

### 6.2.3.2 Sound Absorption

MnDOT takes in field measurements of Sound Absorption (SA) using the BSWA 435 device shown in Figure 6(b) below. This device uses a capped impedance tube equipped with a white noise source that is sent to the pavement surface. The base/tube combination provides a barrier from outside noise sources. Inside the tube are two microphones. When the noise source sends incident waves to the surface, some are absorbed by the pavement. Those that are not are reflected back and captured by the microphones. The microphones are previously connected to an analyzer software which uses the data to calculate sound absorption coefficients at each of the third octave frequencies. The calculated coefficients are between one and zero, with zero being the condition where no sound is absorbed. The data in this report is presented at the following third octave narrow band frequencies: 315, 400, 500, 750, 1000, 1250 and 1650 Hertz. The narrow band is chosen to minimize the amount of data presented.



(a) OBSI Intensity Meters

(b) Sound Absorption Tube

**Figure 6.4: (a) OBSI Intensity Meters and (b) Sound Absorption Tube**

### 6.2.4 Physical Properties

The following tests were performed to assess other properties which are expected to have a large divergence in pervious pavement from typical PCC. Results from the tests may illuminate other possible benefits beyond just reduced pavement noise or increased tire traction. The first two tests described will help evaluate the pavement density and permeability, and the last test will

evaluate if these properties are affected by clogging agents. The results obtained will provide insight on whether the pavements can perform as an effective, drainable material.

#### 6.2.4.1 Nuclear Density

The density of the pervious pavements was measured using the Seaman C-200 Nuclear Density Test device in figure 6.5(a). This device allows for very fast, non-destructive, in field measurements of densities ranging from 70 to 170 pounds per cubic foot. The Nuclear Density Gauge has an internal radioactive source that emits a known amount of gamma radiation to the pavement surface. Some radiation is absorbed into the pavement, while the radiation that gets reflected is measured by a Geiger-Muller detector tube. The detector measures the electrical pulses from the ionized gasses created from the reflected radiation. This meter count is then used to calculate the density of the pavement.

#### 6.2.4.2 Dissipated Volumetric Rate

MnDOT uses the falling head permeability device to evaluate the drainability of pavement. This device consists of a 90 centimeter long, six inch diameter clear tube contented to a water source tank with a hose. The tube is placed vertically on the pavement surface and sealed using a duct seal compound. The tube is filled fully with the connected hose from the water tank. Before testing begins, the water is allowed to drain into the pavement until a smooth, steady flow is developed. Once it reaches a constant flow, the time it takes for the water to drain from the 37 cm mark to the 11 cm mark is recorded. This recording was then used in the following equation to calculate the dissipated volumetric rate.

$$\text{dissipated volumetric rate} = \frac{(\text{initial head} - \text{final head}) \times \text{cross sectional area}}{\text{measured flow time}} \quad (3)$$

The dissipated volumetric rate is not a direct measurement of the permeability of the concrete, but is a good indicator that enables accurate estimates to be made.



(a) Nuclear Density Meter



(b) Falling Head Permeability Device

**Figure 6.5: (a) Nuclear Density Meter and (b) Falling Head Permeability Device**

#### 6.2.4.3 Clogging Effects

Clogging agents are considered any form of debris that is allowed to fill the pores of the concrete and alter the air void structure. A Relikor Vacuum Truck shown in the figure 6.6a below was used on cells 39, 85 and 89 to assess how clogging agents can affect the properties of permeable pavements. The brush on the vacuum truck was not used to avoid further distress and clogging of the pavements. The first vacuuming was done in 2009 on only cells 85 and 89, where the difference in flow time was taken at one location in each cell. The second vacuum in 2010 was done on all three test cells. Measurements for the dissipated volumetric flow rate and sound absorption were taken before and after this vacuuming at multiple locations throughout the cells.

#### 6.2.4.4 Surface Deflection from Falling Weight Deflectometer

MnDOT uses Dynatest Falling Weight Deflectometer equipment to measure the surface deflection of pavement as a result of an impulse load. The van/trailer setup shown in figure 6.6(b) below applies impulse loads using a load bearing pad directly over strain gauges embedded in the pavement. The load drops are applied at 6000 lbs, 9000 lbs and 15000 lbs, with three impulses drops each. The resulting deflections at the center sensor location, along with those from sensors at varying distance from the load location, are collected and used to plot deflection basins. These deflection basins can be used to gauge pavement performance and evaluate material behavior of pavement layers.



(a) Relikor Vacuum Truck Assembly



(b) Dynatest FWD

**Figure 6.6: (a) Relikor Vacuum Truck Assembly and (b) Dynatest FWD**

#### 6.2.4.5 Temperature and Moisture Sensors

As stated before, all cells were equipped with temperature and moisture sensors to monitor the pavement response to environmental change. The MnROAD thermocouple tree design was used to place Omega Thermocouples at varying depths throughout the pavement. The temperature was measured in the pavement, pavement base, and pavement subgrade to evaluate the temperature gradient. Irrrometer Water Mark Sensors are solid-state electrical resistance sensors that measure tension produced from moisture. [1] Fluctuating moisture content in the pavement results in a change in water tension and resistance. A transition from solid to liquid water during freeze-thaw cycles can be detected by a sharp change in the measured resistance. The thermocouple and watermark data can be compared to other non-porous cells to evaluate the difference in temperature transmissivity between the two pavement types.

The previously described tests in this chapter were conducted at MnROAD on pervious cells 39, 85 and 89. The tests were performed periodically from the time of construction in 2008. The results obtained up until 2010 will be discussed in the following section.

### 6.3 Results

The previous section describes the methods for the eight different tests which will be discussed in this report. This chapter will provide the data collected from construction in 2008 up through October 2010. The notable observations from each different test will be listed as bullets after the data has been presented.

All data used for the plots in this section will be included in the appendix of this report for further reference.

### 6.3.1 Ride Results

#### 6.3.1.1 IRI Results

The following abbreviations are made in the legend below: Inside Lane (IL), Outside Lane (OL), Left Wheel Path (LWP), and Right Wheel Path (RWP).

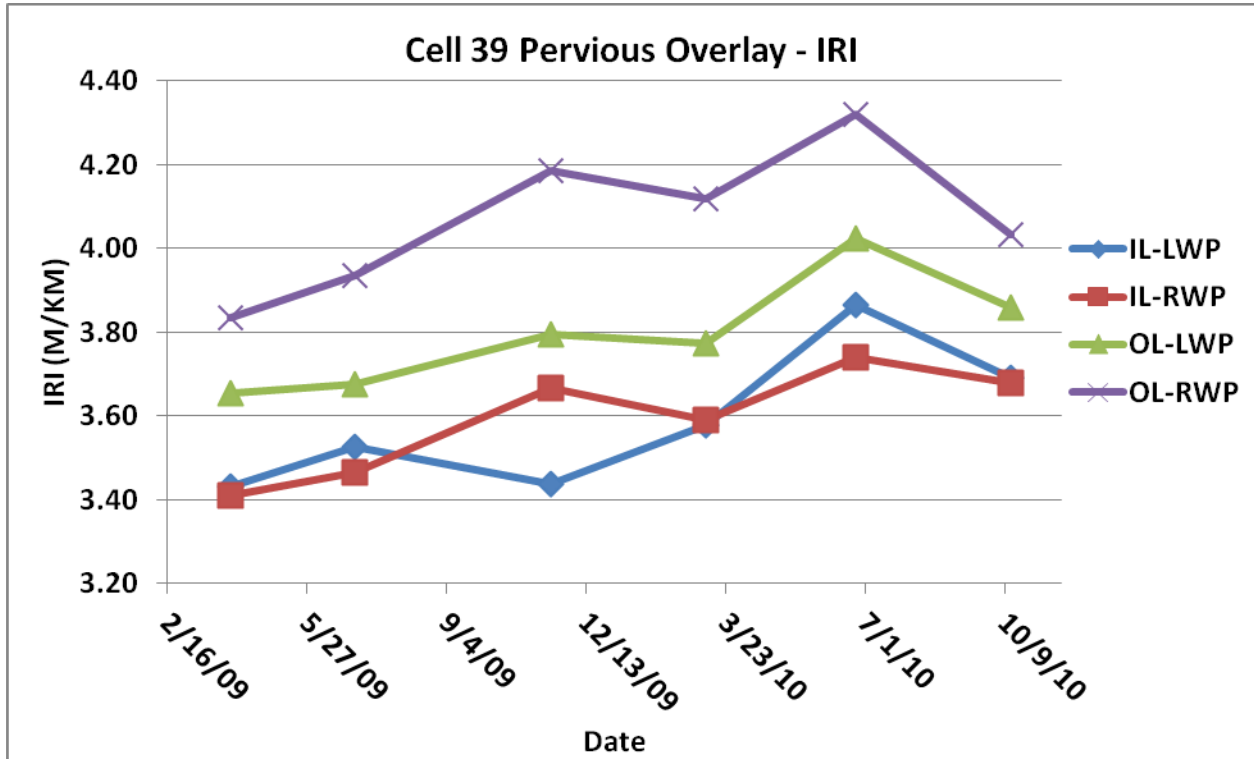


Figure 6.7: Cell 39 IRI

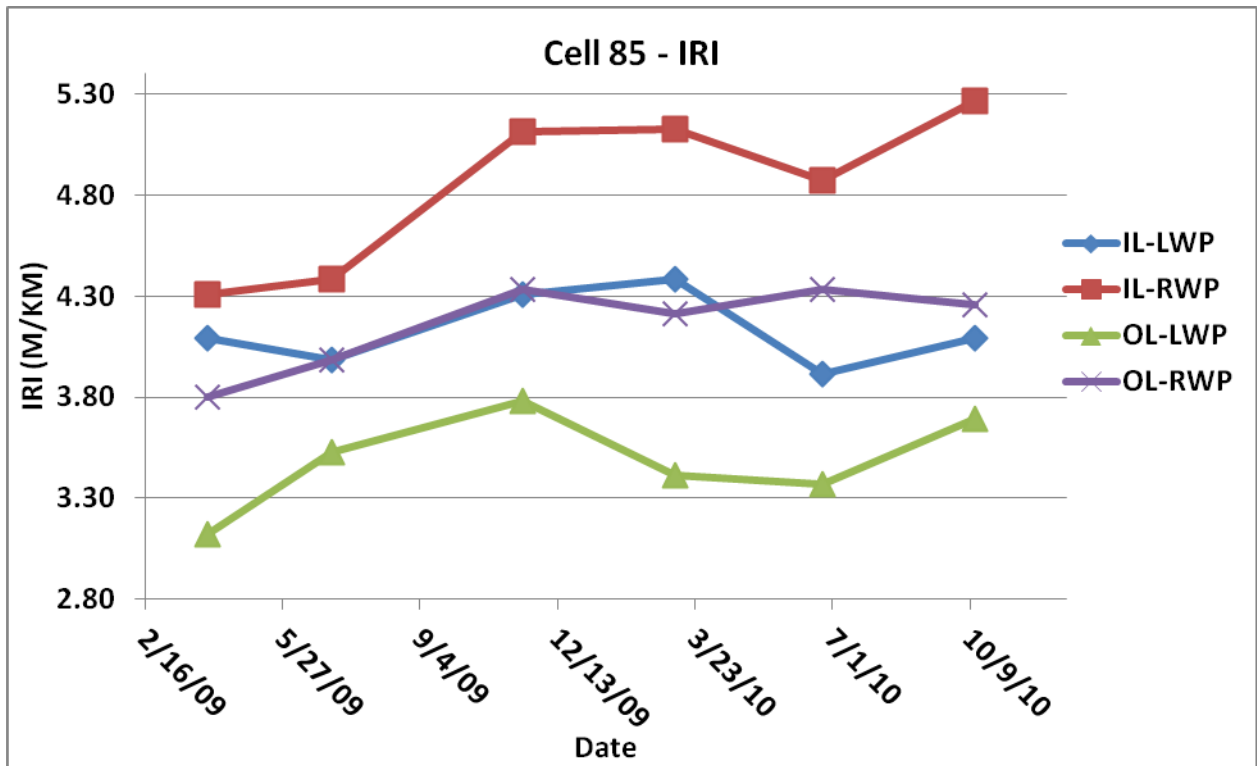


Figure 6.8: Cell 85 IRI

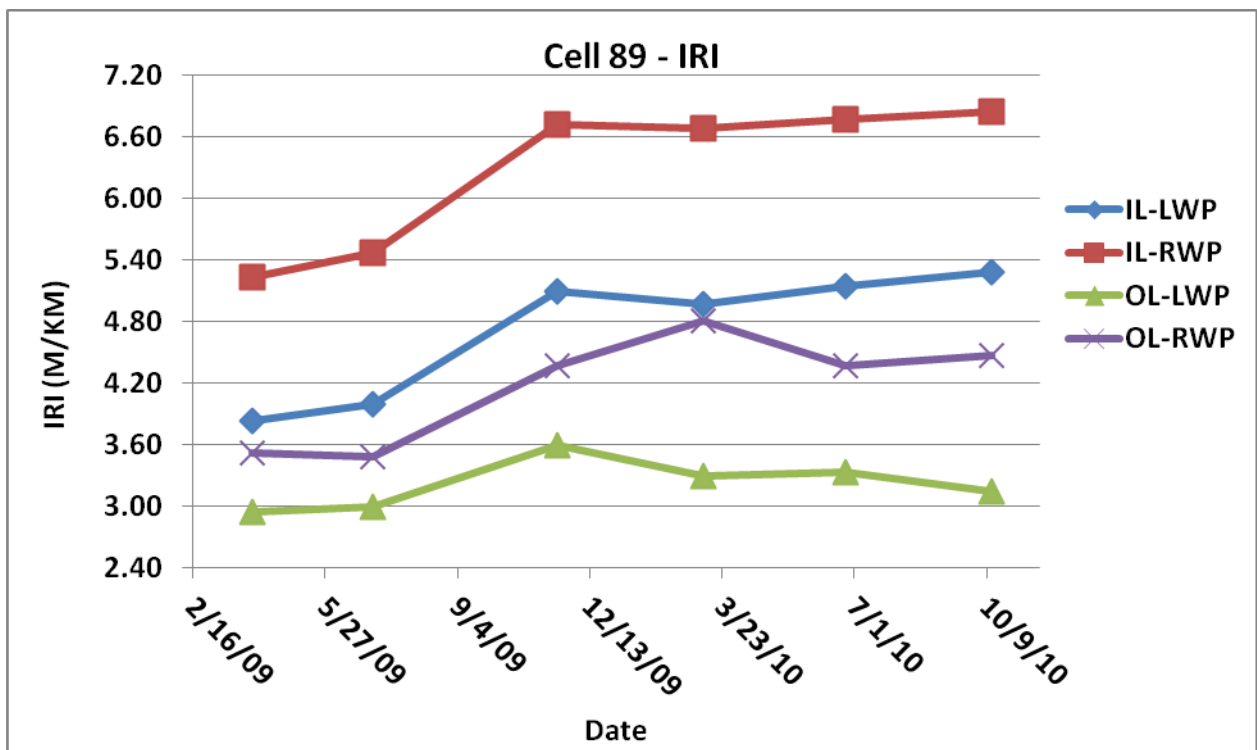


Figure 6.9: Cell 89 IRI

- IRI Cell 89 > IRI Cell 85 > IRI Cell 39
- IRI is lowest in the first two tests for all cells, suggesting some raveling and weathering occurred making the pavement rougher as time went on.
- No clear or distinct seasonal variation.

6.3.1.2 SR Results

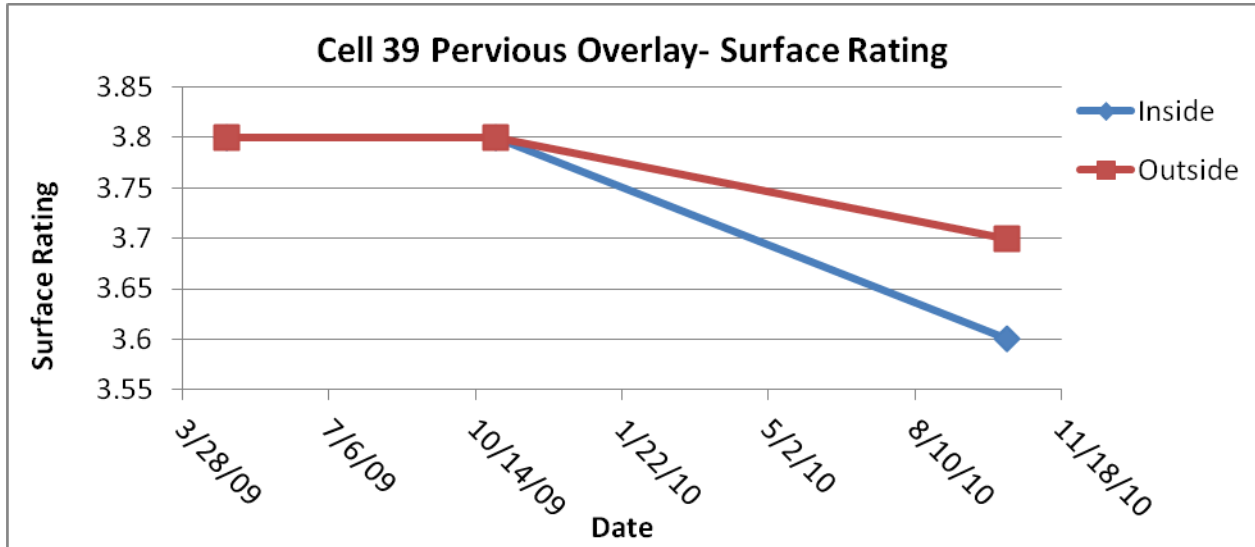


Figure 6.10: Cell 39 SR

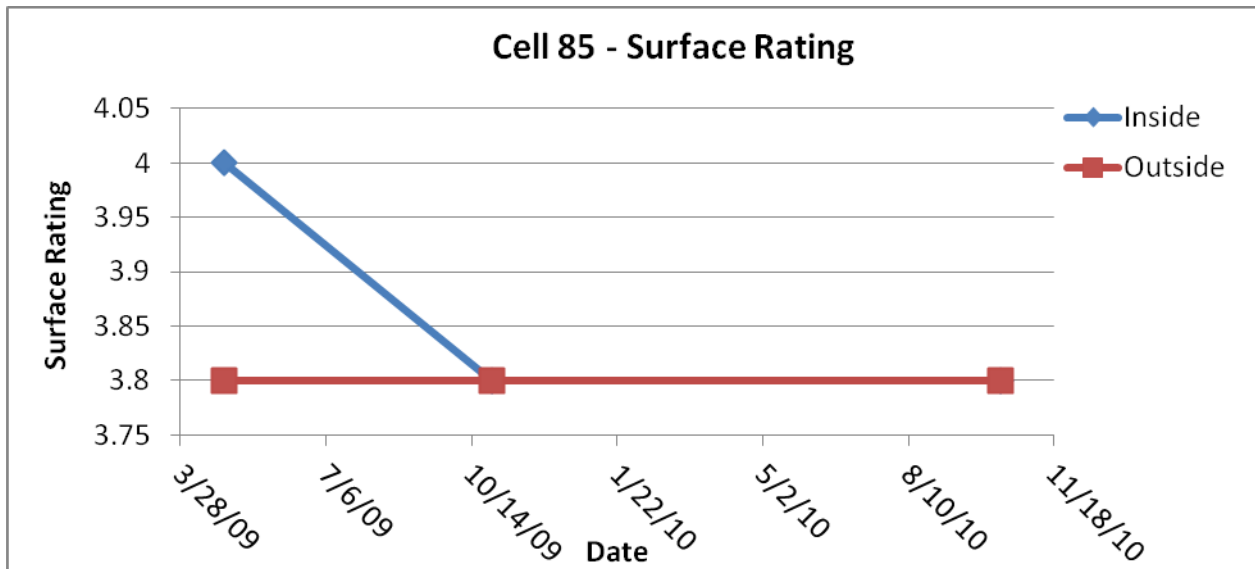
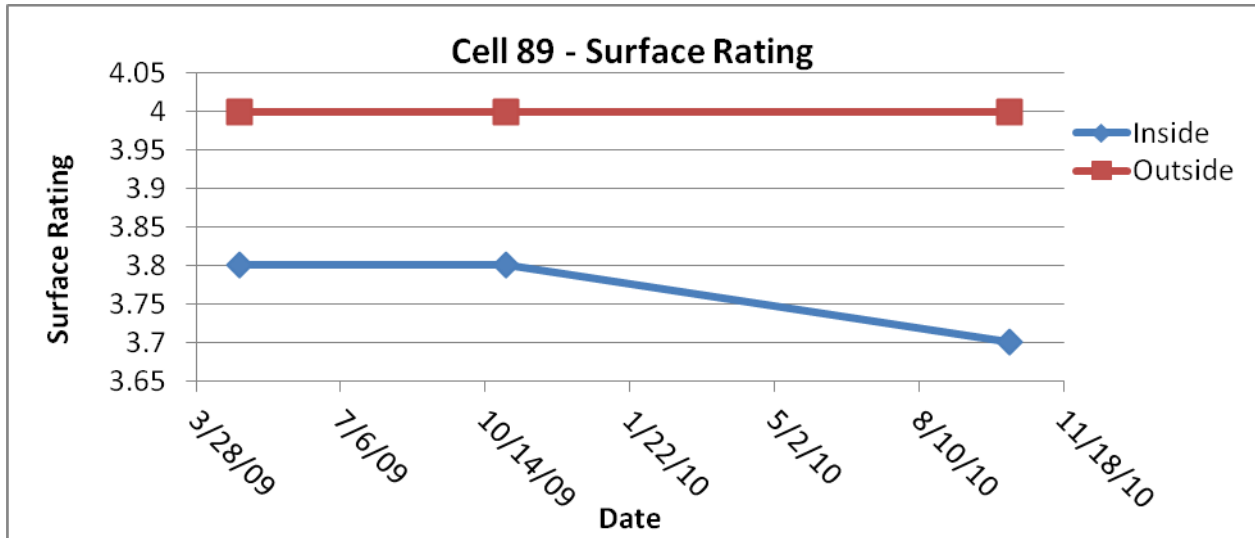


Figure 6.11: Cell 85 SR



**Figure 6.12: Cell 89 SR**

- SR measurements for all three cells are very high, close to 4 for the first measurement.
- All SR measurements decrease at the third test in September 2009. The decrease is expected due to probable raveling and weathering.
- Cell 39 porous overlay dropped the most to a minimum value of 3.6

### 6.3.2 Surface Results

#### 6.3.2.1 CTM Results

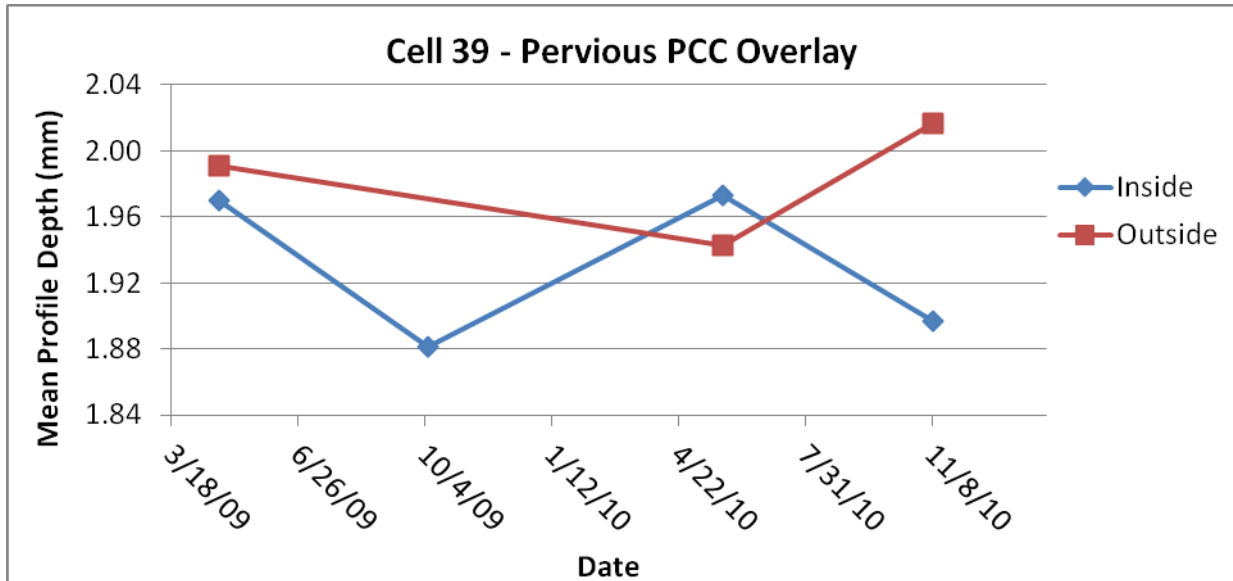


**Figure 6.13: Cell 39 CTM**

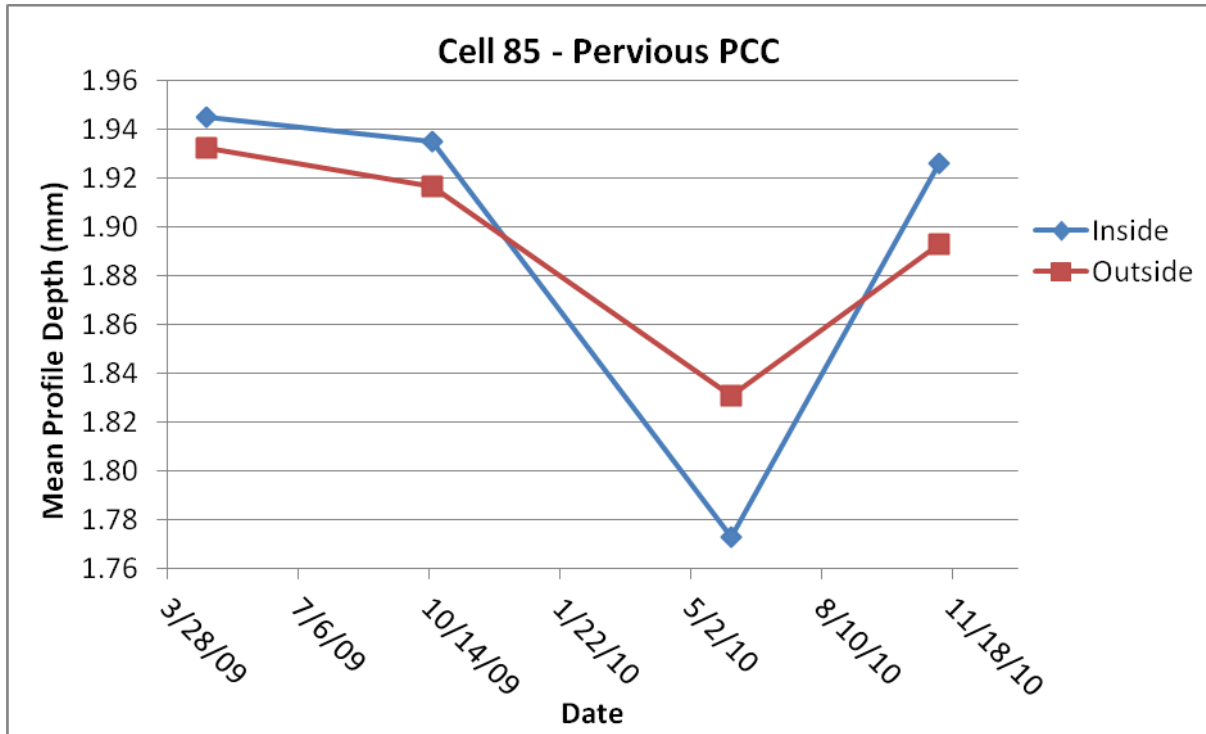


Figure 6.14: Cell 85 CTM

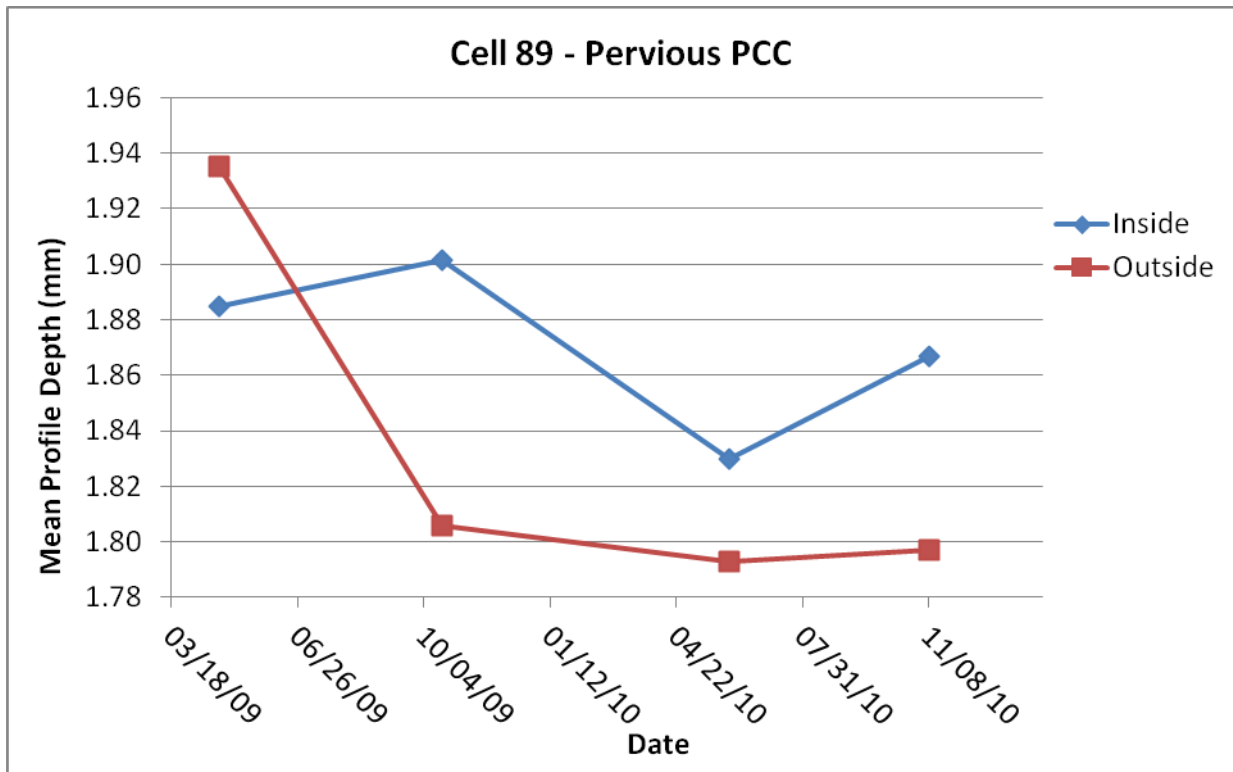


Figure 6.15: Cell 89 CTM

- Cell 85 and 89 show lowest at May 2<sup>nd</sup> 2010.
- Cell 39 seems to have a generally higher mean profile depth
- Cells 85 and 89 do not have the same seasonal variation as cell 39.
  - Cell 39 shows a drop in winter months and an increase in summer months
  - Cells 85 and 89 have the opposite pattern of Cell 39.

### 6.3.2.2 Friction Number Results

In the following plots, RB stands for Ribbed Tire and SM stands for Smooth Tire.

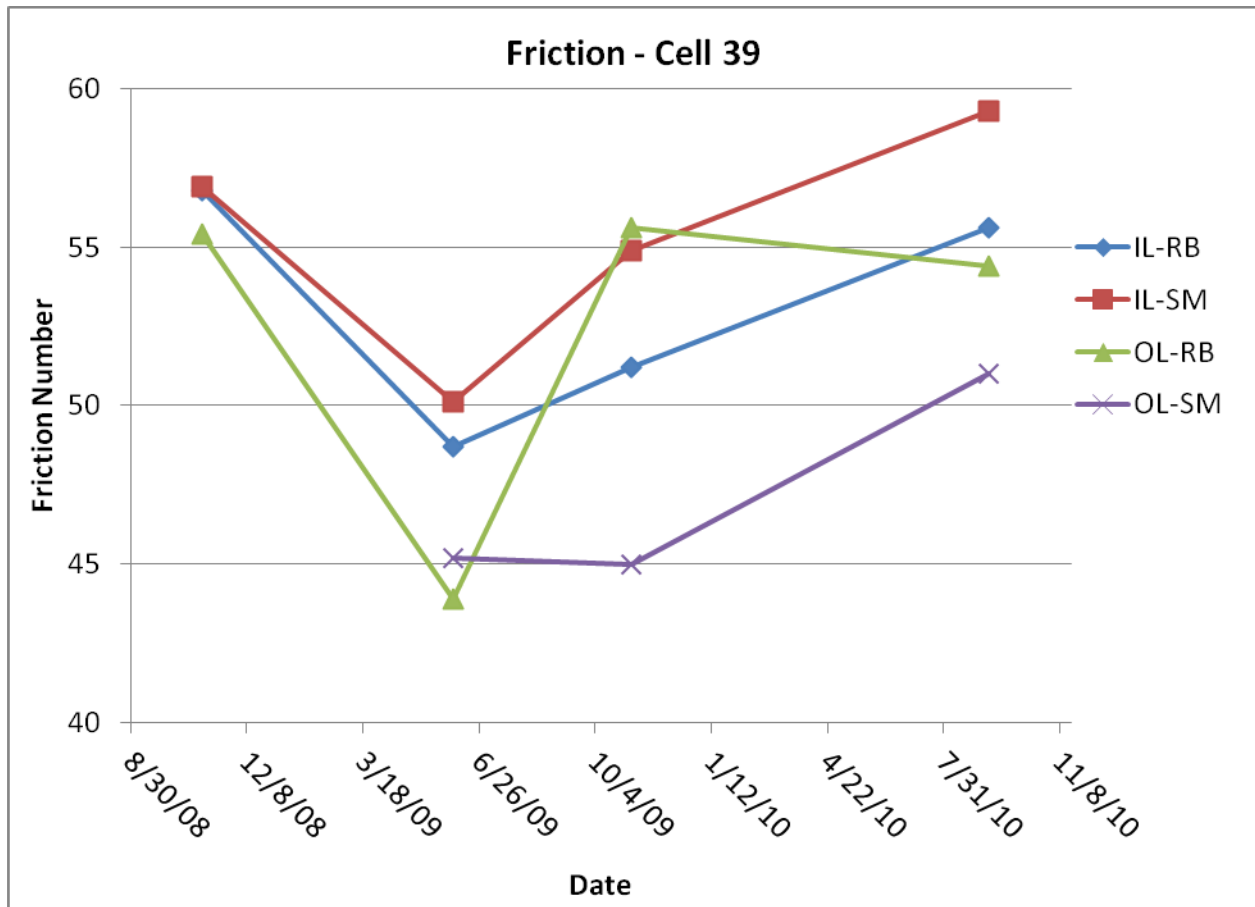


Figure 6.16: Cell 39 FN

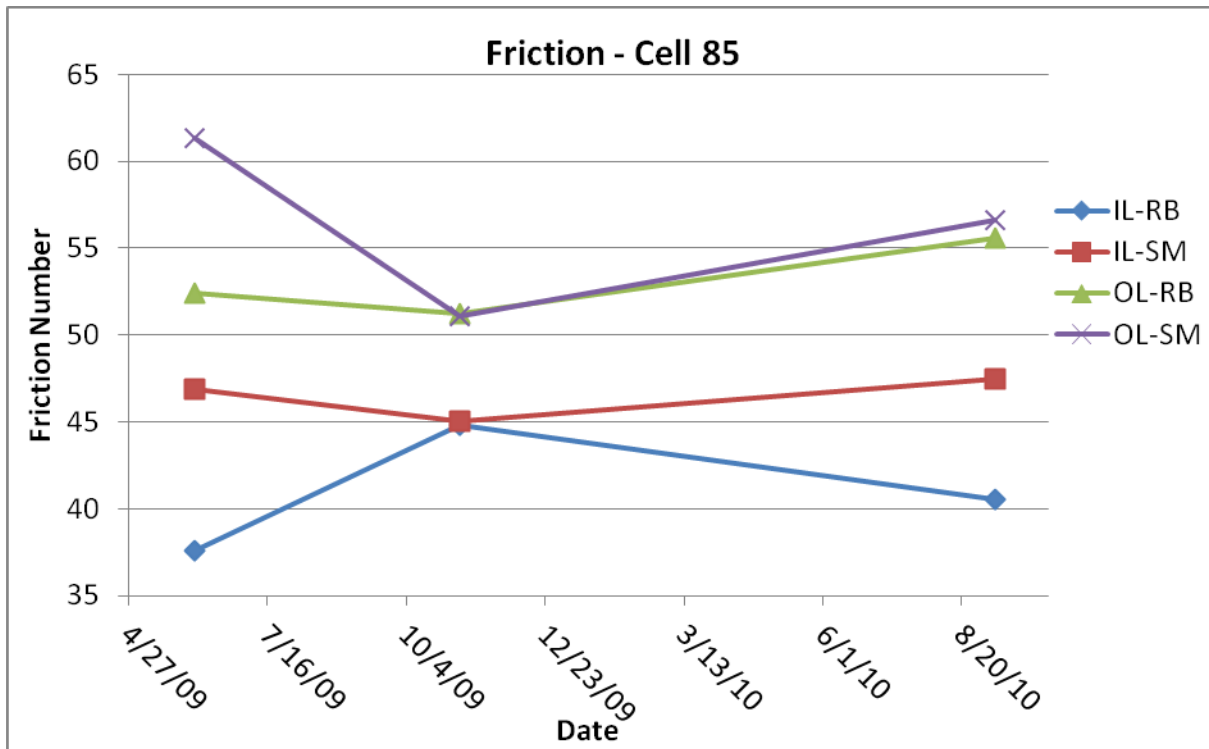


Figure 6.17: Cell 85 FN

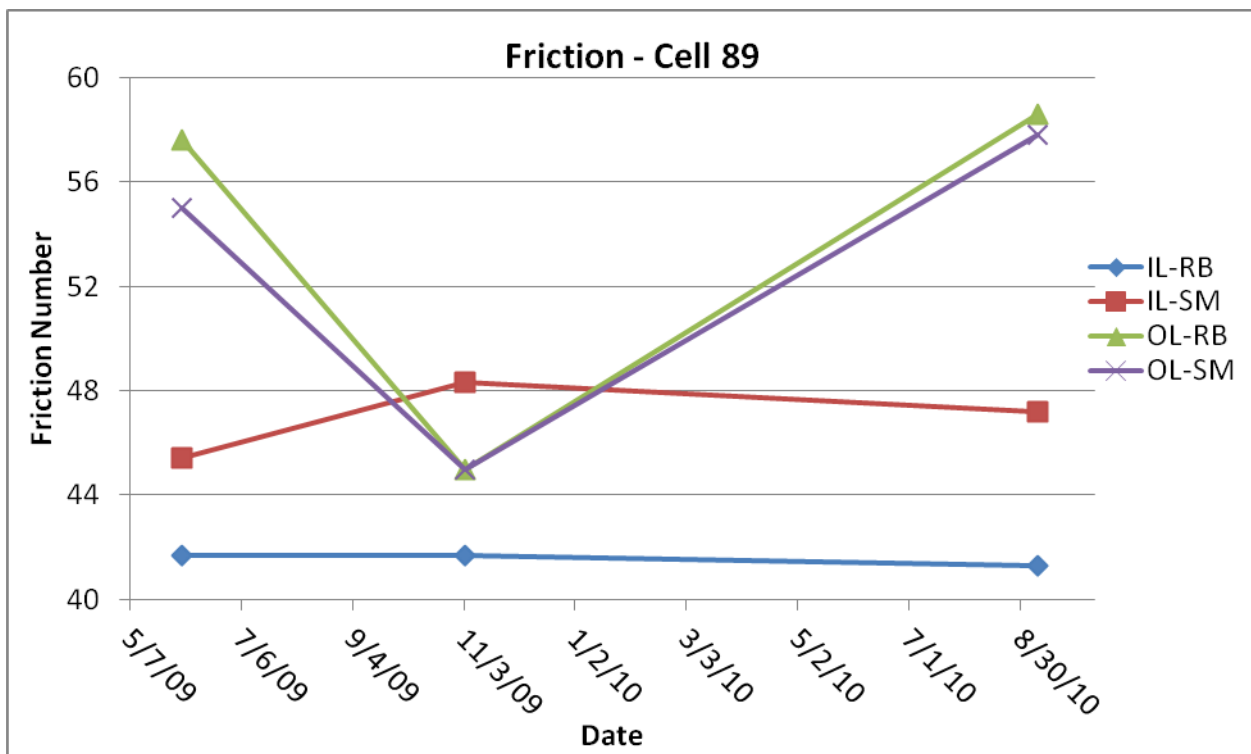


Figure 6.18: Cell 89 FN

- Cell 85 has the widest range of FN from 65 to 35 in different lanes
- No real seasonal fluctuation in measured FN in Cell 85 and 89 over the 2009 and 2010.
- Cell 39 shows the most distinct variation with a decrease in friction from the time of construction to May 2009, followed by a slow increase until 2010.

### 6.3.3 Noise Results

#### 6.3.3.1 OBSI Results

The OBSI for cells 85 and 89 also include adjacent cells 86 and 88. These two cells are pervious hot mix asphalt following similar base and subgrade design as their adjacent cells: Cell 86 with a granular subgrade and cell 88 with cohesive subgrade. This was done because the OBSI test must be done over a 500 ft section. Because OBSI was monitored frequently over the last two years a clear fluctuation in sound intensity can be illustrated in the plots below.

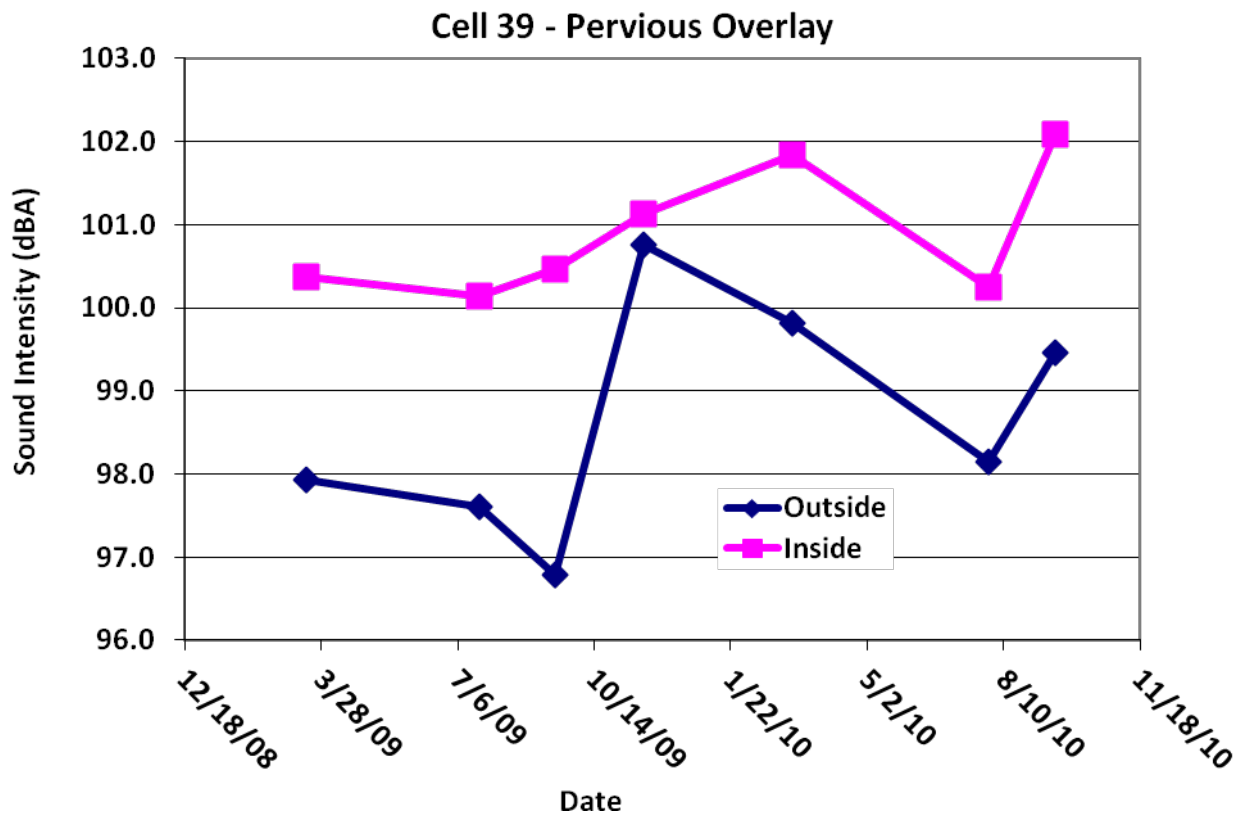


Figure 6.19: Cell 39 OBSI

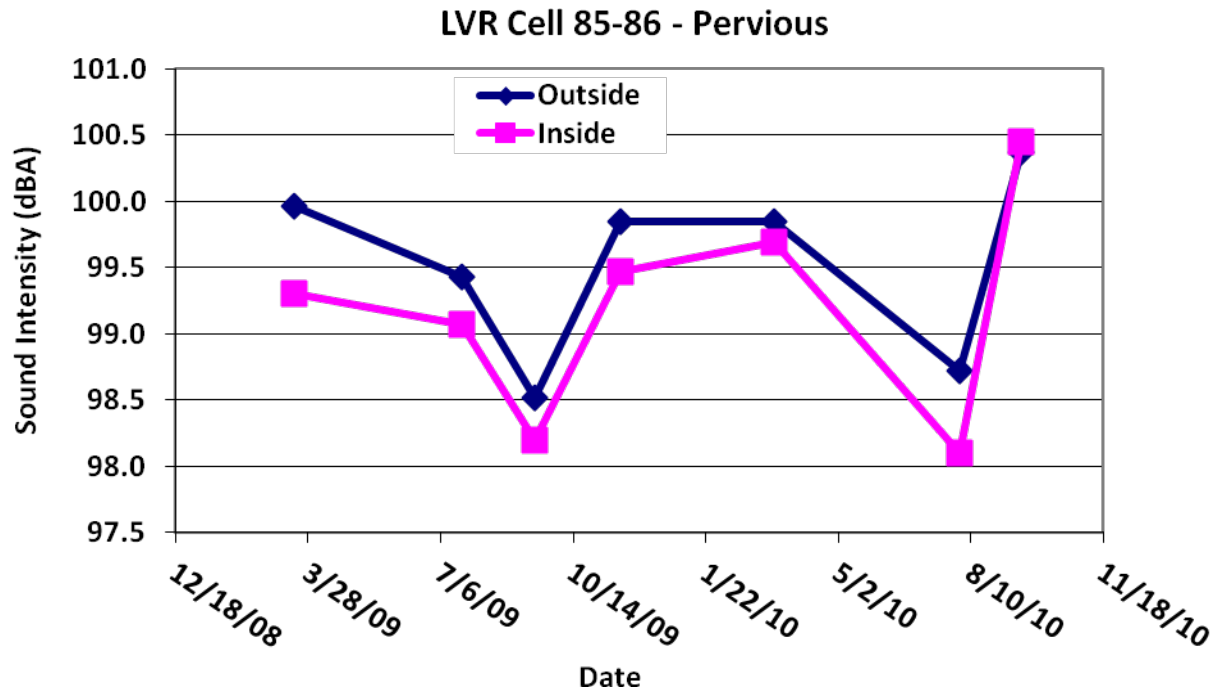


Figure 6.20: Cell 85-86 OBSI

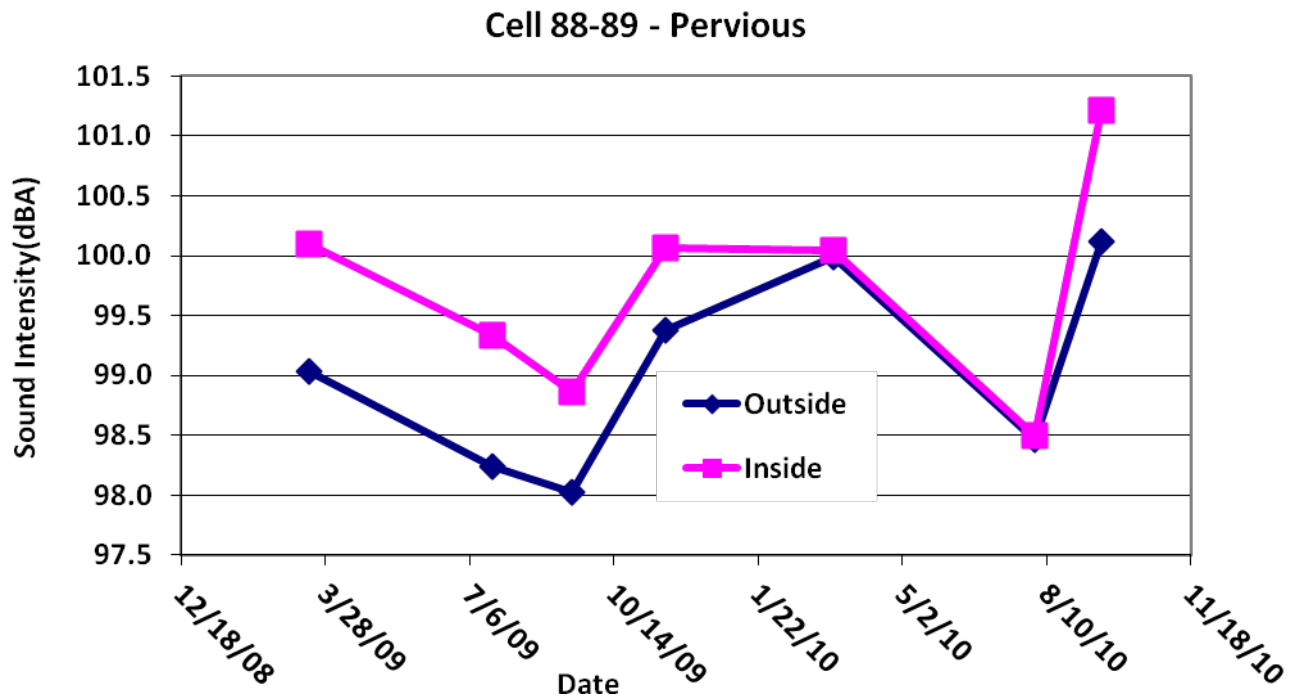


Figure 6.21: Cell 88-89 OBSI

- All three test sections experienced a large decrease in OBSI during the summer months, particularly in August of both years.

- The highest OBSI value for all three test cells was recorded during the last series of tests, in October 2010.

The following plots and tables show the Sound Intensity Spectrum for a single run from the last OBSI measurements taken in September 2010. The Leading Edge and Trailing Edge refer to the position of the two intensity meters on the tire.

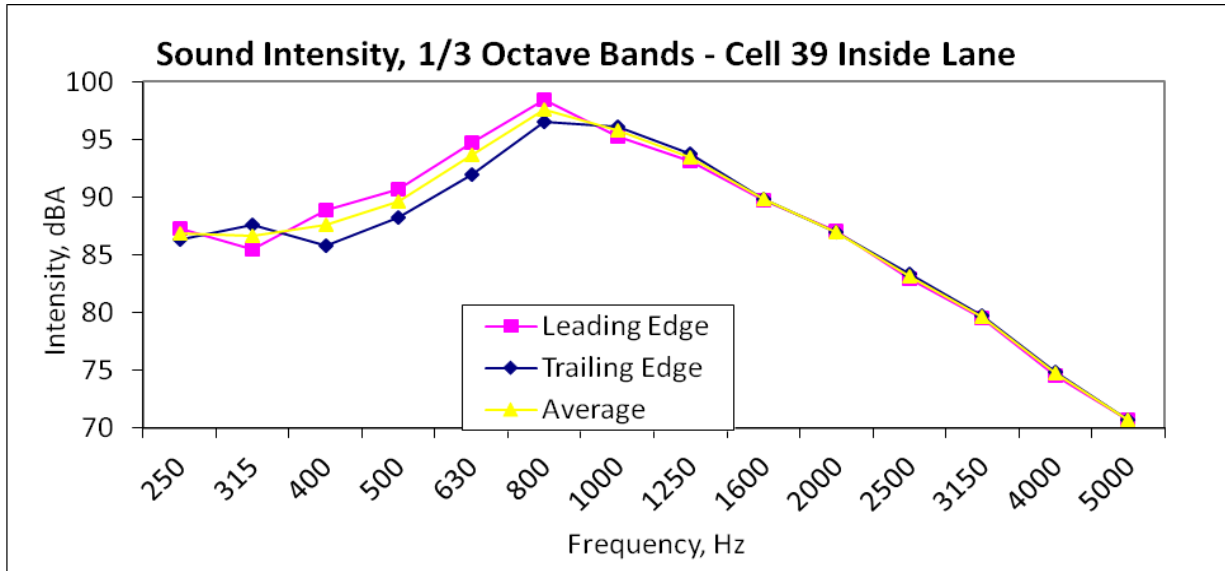


Figure 6.22: OBSI Spectrum – Cell 39 IL

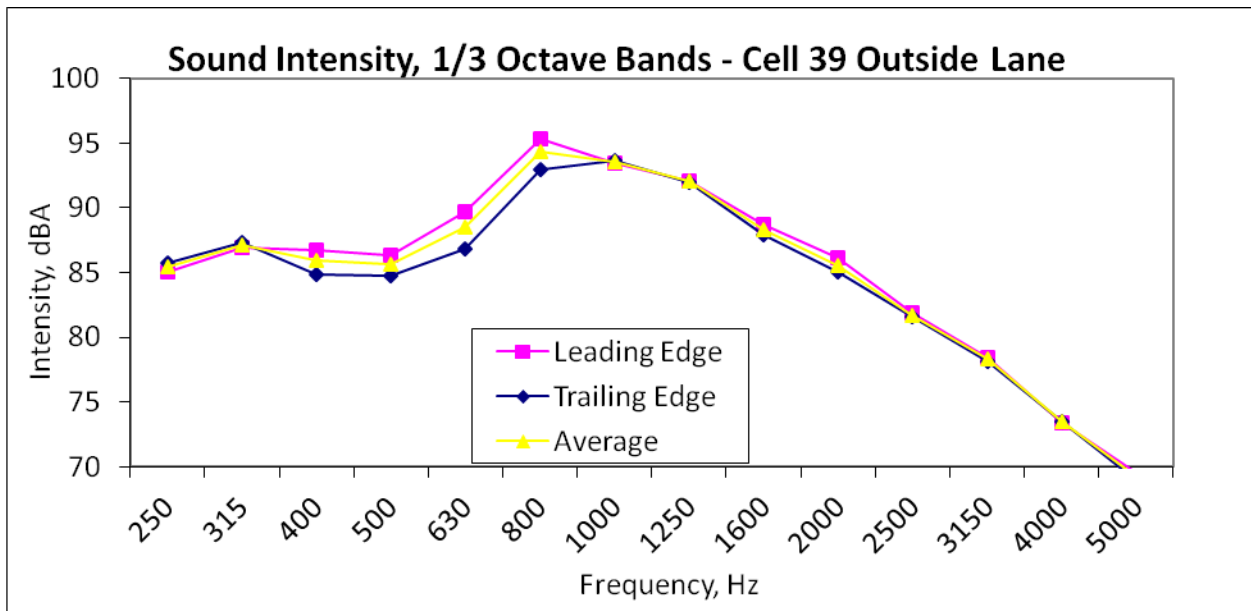


Figure 6.23: OBSI Spectrum – Cell 39 OL

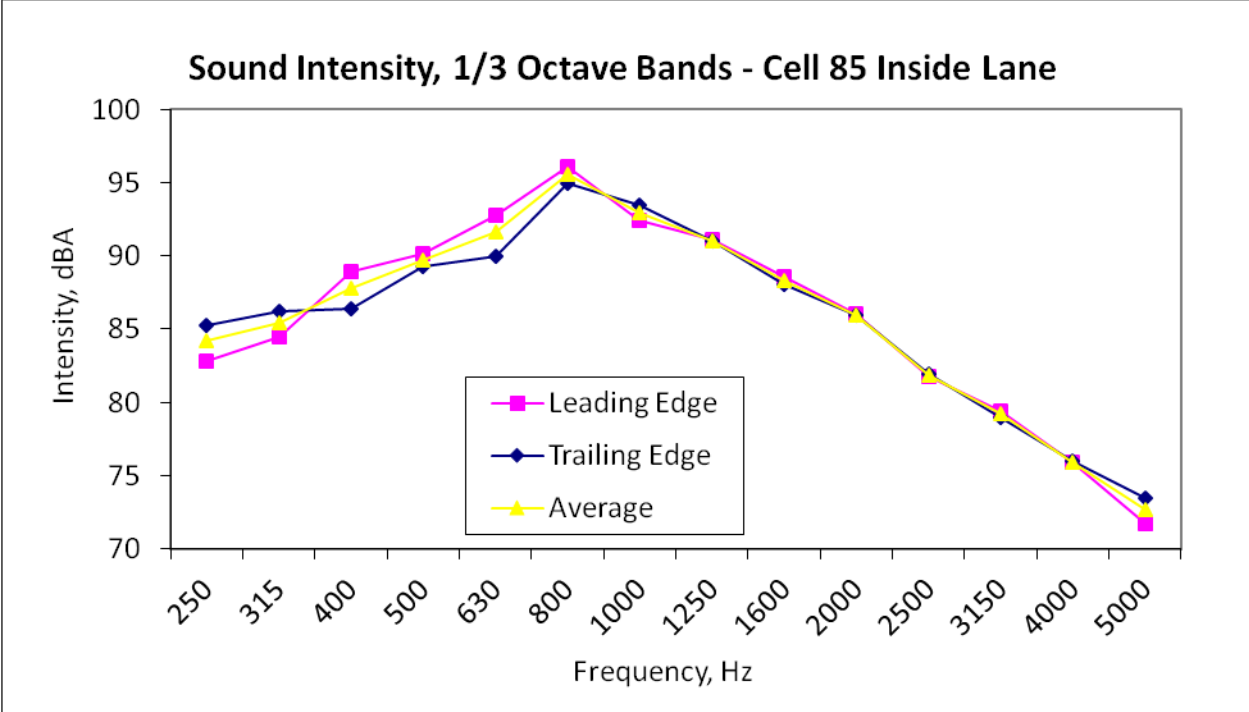


Figure 6.24: OBSI Spectrum – Cell 85 IL

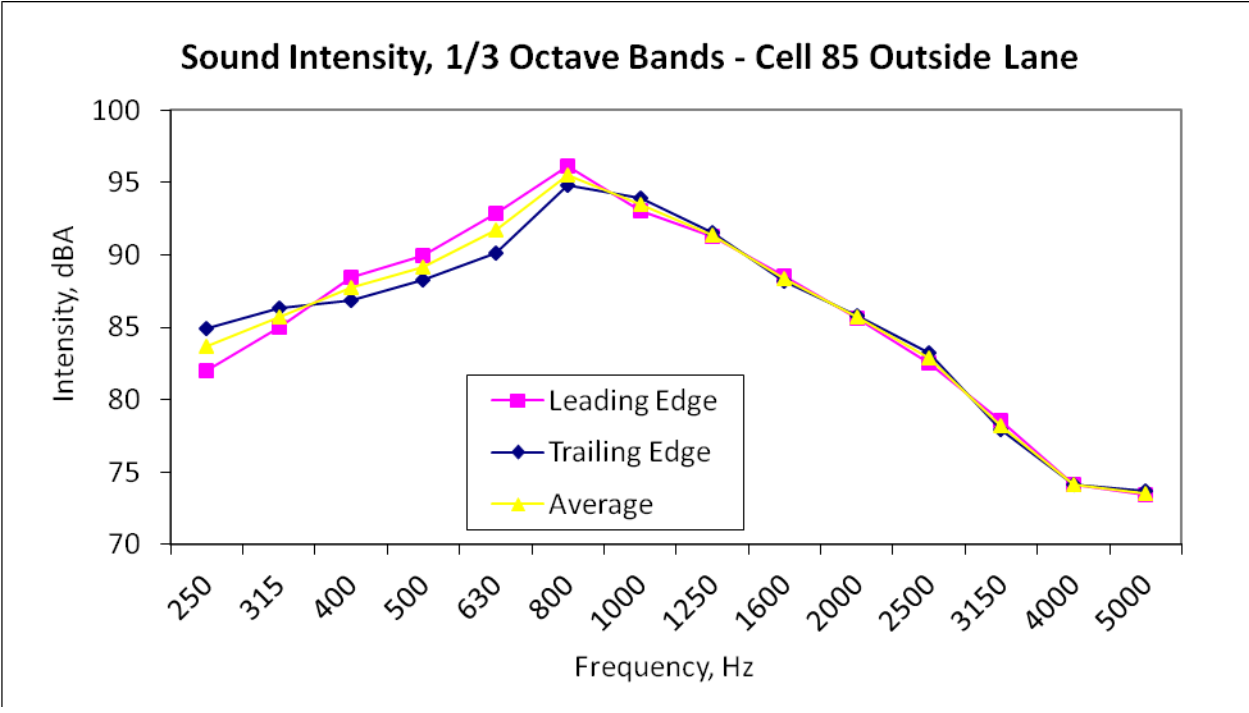


Figure 6.25: OBSI Spectrum – Cell 85 OL

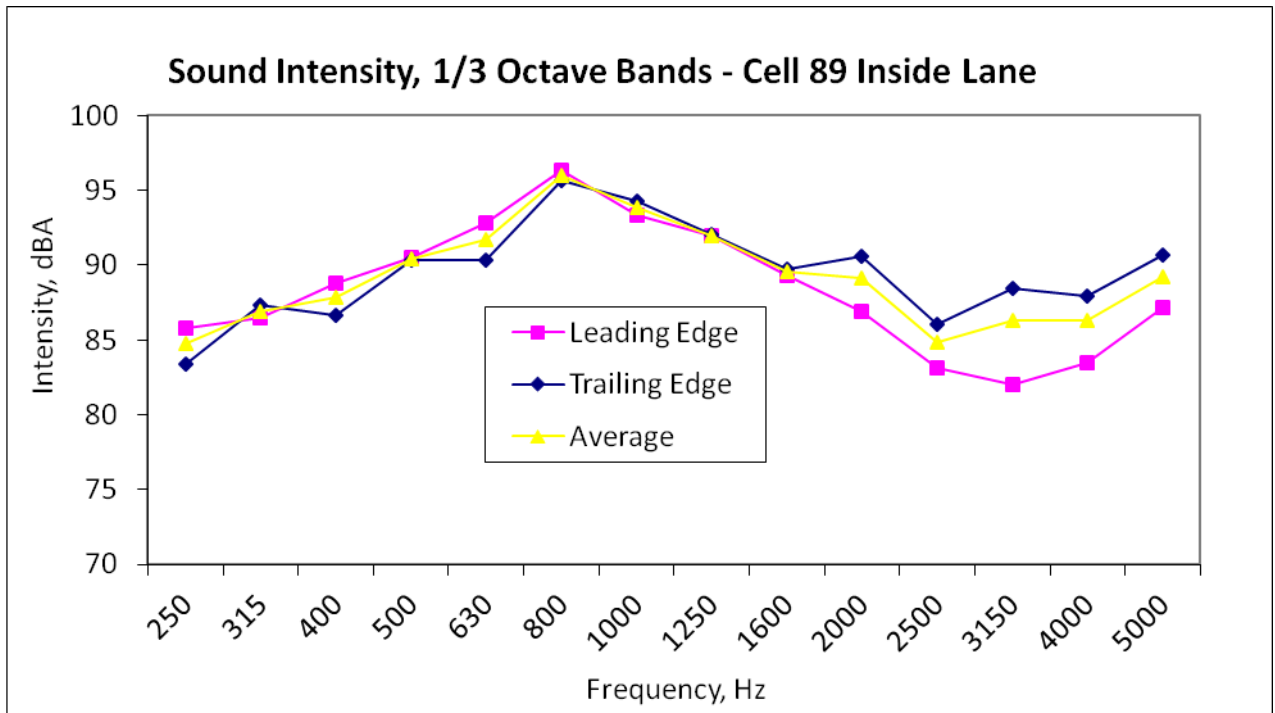


Figure 6.26: OBSI Spectrum – Cell 89 IL

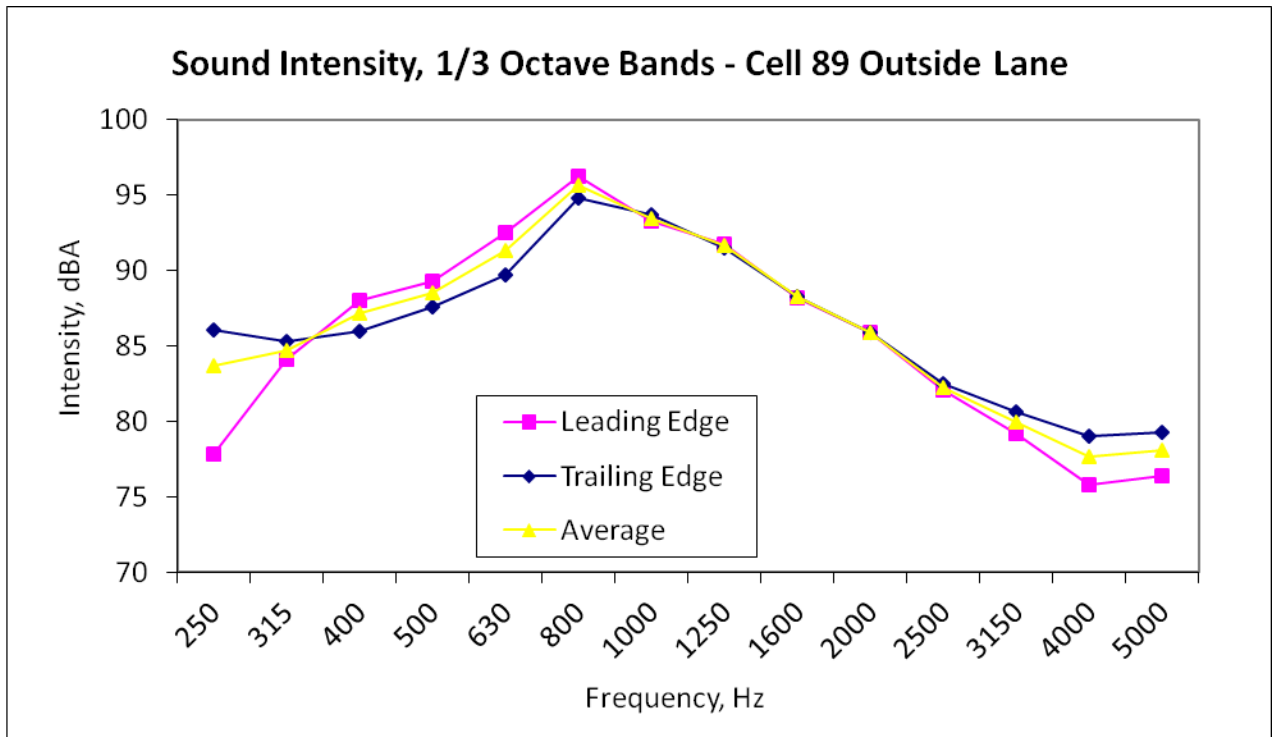


Figure 6.27: OBSI Spectrum – Cell 89 OL

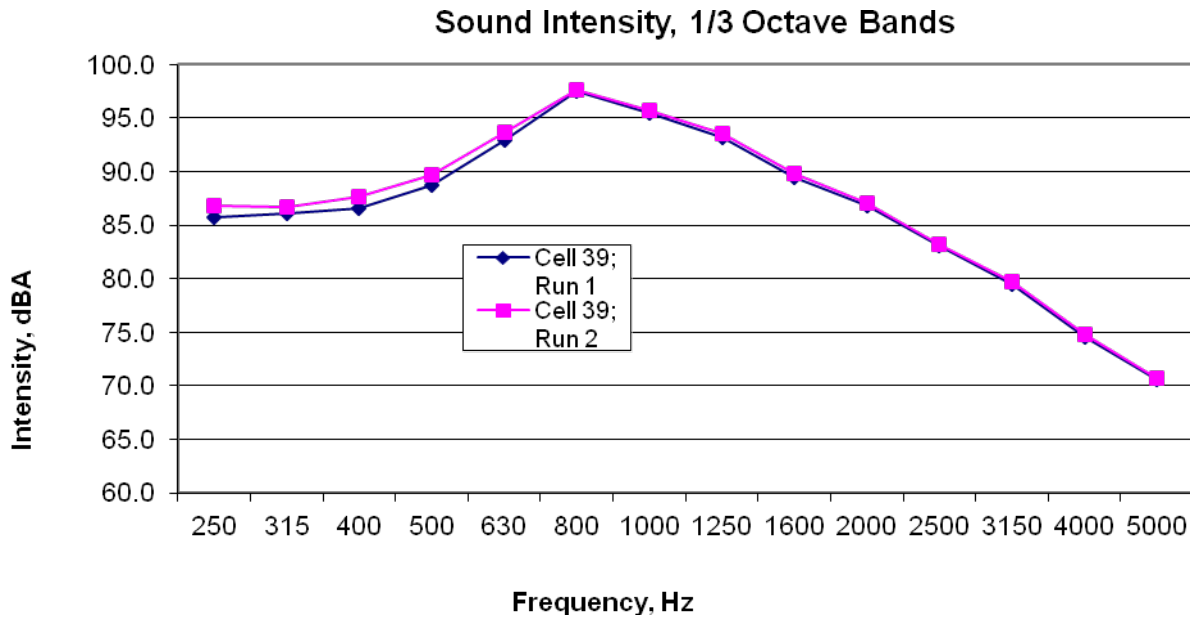


Figure 6.28: Difference in OBSI Octave Bands Between Runs – Cell 39

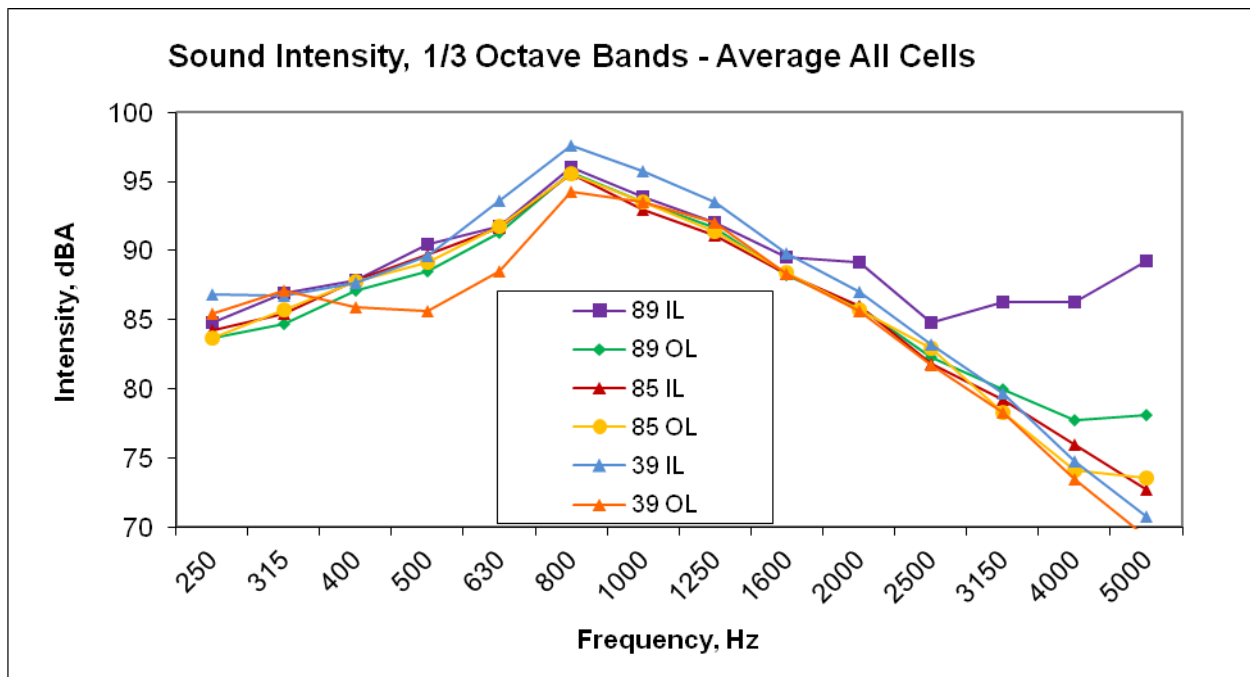


Figure 6.29: OBSI Spectrum – All Cells Average

The plots above show that there is very little difference between measured OBSI 1/3 Octave Bands between test runs on a given cell. Figure 6.29 also shows that the average 1/3 Octave Band of each lane of the three cells generally are very similar. However, figure 6.29 does illustrate the large divergence cell 89 experiences past 2000 Hz. The cell which seems to experience the most difference between runs is cell 39, where at times the inside lane and outside

lane are respectively the maximum and minimum of all cells. The following tables provide the data used in these plots.

**Table 6.1: OBSI Spectrum Cell 39**

Cell 39 Inside Lane – Intensity (dBA)				Cell 39 Outside Lane – Intensity (dBA)			
Frequency	Leading Edge	Trailing Edge	Average	Frequency	Leading Edge	Trailing Edge	Average
250	87.3	86.4	86.8	250	85.1	85.8	85.43
315	85.5	87.6	86.7	315	86.9	87.3	87.10
400	88.9	85.8	87.6	400	86.7	84.8	85.89
500	90.7	88.2	89.6	500	86.4	84.7	85.62
630	94.8	92.0	93.6	630	89.7	86.8	88.49
800	98.5	96.5	97.6	800	95.3	93.0	94.30
1000	95.3	96.2	95.8	1000	93.4	93.6	93.53
1250	93.1	93.8	93.5	1250	92.1	91.9	92.01
1600	89.7	89.9	89.8	1600	88.7	87.9	88.30
2000	87.1	87.0	87.0	2000	86.1	85.0	85.58
2500	82.9	83.4	83.2	2500	81.9	81.6	81.74
3150	79.5	79.8	79.7	3150	78.5	78.1	78.31
4000	74.5	74.9	74.7	4000	73.4	73.5	73.47
5000	70.7	70.7	70.7	5000	69.5	69.0	69.26
A-wtd	102.7	101.8	102.3	A-wtd	100.0	98.9	102.3

**Table 6.2: OBSI Spectrum Cell 85**

Cell 85 Inside Lane - Intensity (dBA)				Cell 85 Outside Lane – Intensity (dBA)			
Frequency	Leading Edge	Trailing Edge	Average	Frequency	Leading Edge	Trailing Edge	Average
250	82.8	85.3	84.2	250	82.0	84.9	82.8
315	84.5	86.2	85.4	315	85.0	86.4	84.5
400	88.9	86.4	87.8	400	88.4	86.9	88.9
500	90.1	89.3	89.7	500	89.9	88.3	90.1
630	92.8	90.0	91.6	630	92.9	90.2	92.8
800	96.1	95.0	95.6	800	96.2	94.8	96.1
1000	92.4	93.5	93.0	1000	93.0	93.9	92.4
1250	91.1	91.0	91.1	1250	91.3	91.5	91.1
1600	88.6	88.0	88.3	1600	88.5	88.2	88.6
2000	86.0	85.9	86.0	2000	85.6	85.8	86.0
2500	81.7	81.9	81.8	2500	82.5	83.3	81.7
3150	79.4	78.9	79.2	3150	78.5	77.9	79.4
4000	75.9	76.0	75.9	4000	74.1	74.1	75.9
5000	71.7	73.5	72.7	5000	73.4	73.7	71.7
A-wtd	100.6	99.9	100.3	A-wtd	100.7	100.0	100.6

**Table 6.3: OBSI Spectrum Cell 89**

Cell 89 Inside Lane - Intensity (dBA)				Cell 89 Outside Lane - Intensity (dBA)			
Frequency	Leading Edge	Trailing Edge	Average	Frequency	Leading Edge	Trailing Edge	Average
250	85.8	83.4	84.8	250	77.8	86.1	83.7
315	86.5	87.3	86.9	315	84.1	85.3	84.7
400	88.8	86.7	87.9	400	88.0	86.0	87.1
500	90.5	90.3	90.4	500	89.3	87.6	88.5
630	92.8	90.3	91.7	630	92.5	89.7	91.3
800	96.4	95.6	96.0	800	96.3	94.8	95.6
1000	93.3	94.3	93.9	1000	93.3	93.7	93.5
1250	91.9	92.1	92.0	1250	91.7	91.5	91.6
1600	89.3	89.7	89.5	1600	88.2	88.3	88.2
2000	86.9	90.6	89.1	2000	85.9	85.9	85.9
2500	83.1	86.0	84.8	2500	82.1	82.5	82.3
3150	82.0	88.4	86.3	3150	79.2	80.7	80.0
4000	83.5	88.0	86.3	4000	75.8	79.0	77.7
5000	87.1	90.7	89.3	5000	76.4	79.2	78.1
A-wtd	101.3	101.8	101.6	A-wtd	100.7	99.9	100.4

*6.3.3.2 Sound Absorption Results*

Sound absorption tests were run on the three previous test cells three times over the last two years using consistent equipment. The SA measurements taken in 2008 with different equipment showed large discrepancies between the old equipment and the new equipment. This is illustrated in the three plots shown in Appendix I. Because SA measurements are taken to show the entire deflection basin, it is difficult to plot a meaningful time series where seasonal variation can be easily depicted. The time series showing this data will be included in Appendix H of the report for reference. The following three plots show that sound absorption has very minimal fluctuation at different times of the year.

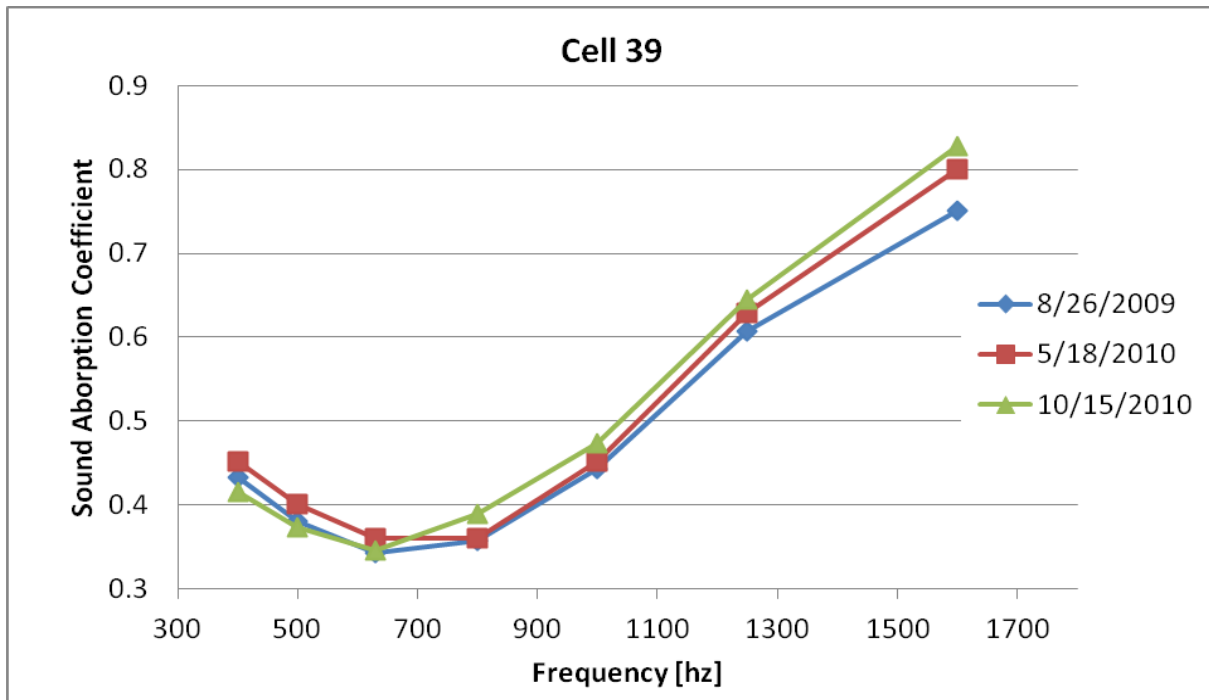


**Figure 6.30: Cell 39 SA**

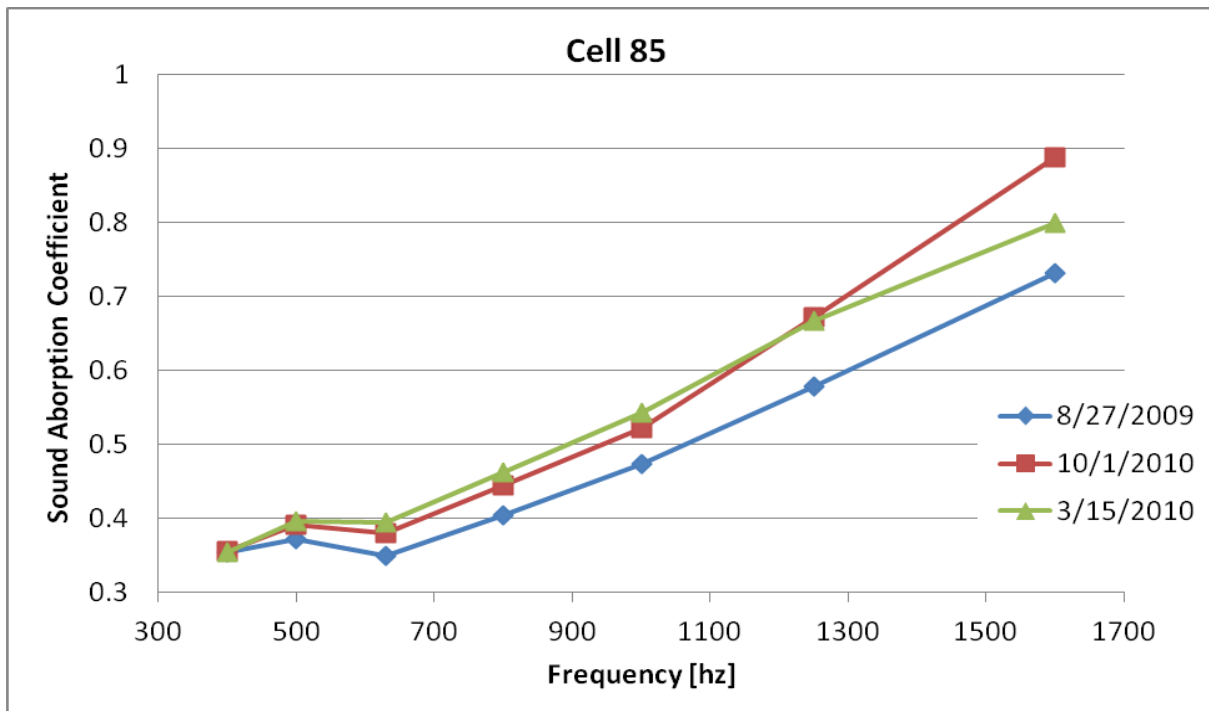


**Figure 6.31: Cell 85 SA**

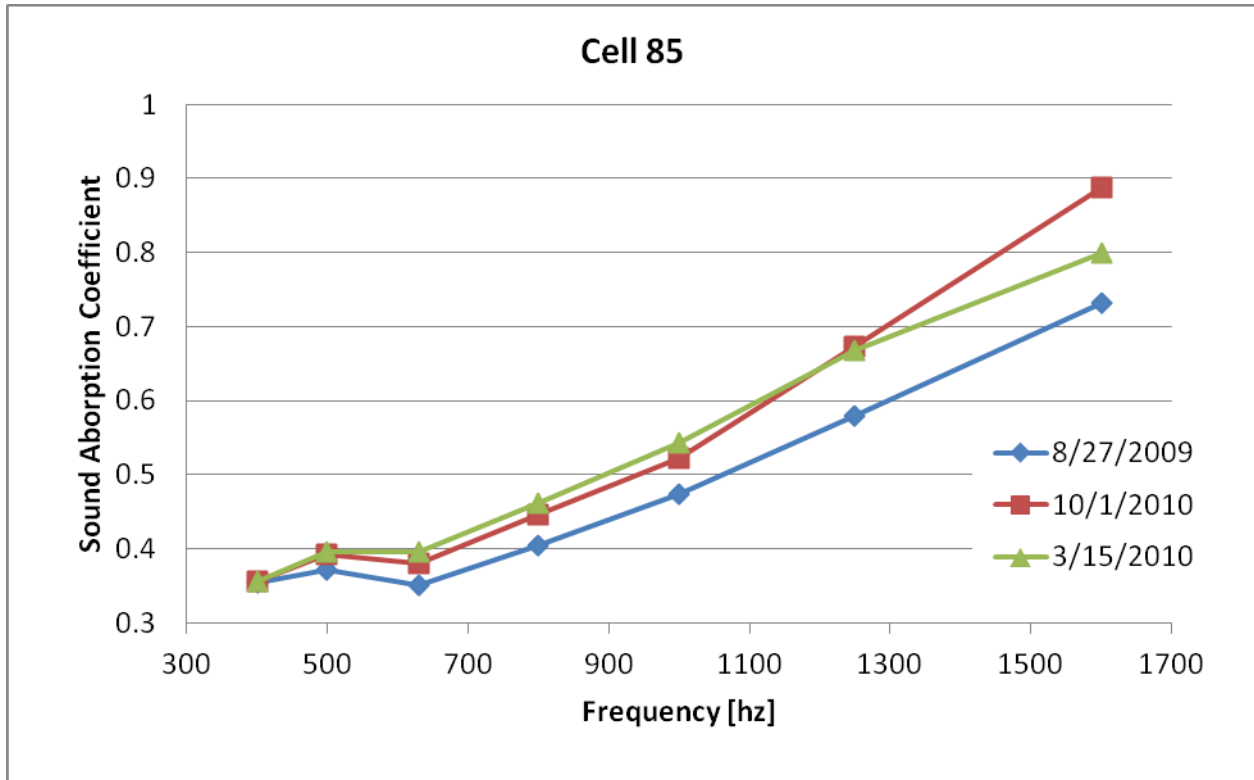


**Figure 6.32: Cell 89 SA**

- All Cells show a sound absorption coefficient range between 0.3 and 0.9.
- Cell 39 shows a larger decrease in sound absorption at the 600 and 800 frequencies.
- In cells 85 and 89 the sound absorption was the lowest in August of 2009 and has increased in the measurements in 2010.

### 6.3.4 Physical Property Results

#### 6.3.4.1 Density Results

The nuclear density was measured in multiple locations across each test cell, with multiple test runs at each location. This test produced somewhat variable results for the different locations within a test cell at each of the three days test. The plot below shows the mean for the entire cell at the three days tested over the last two years.

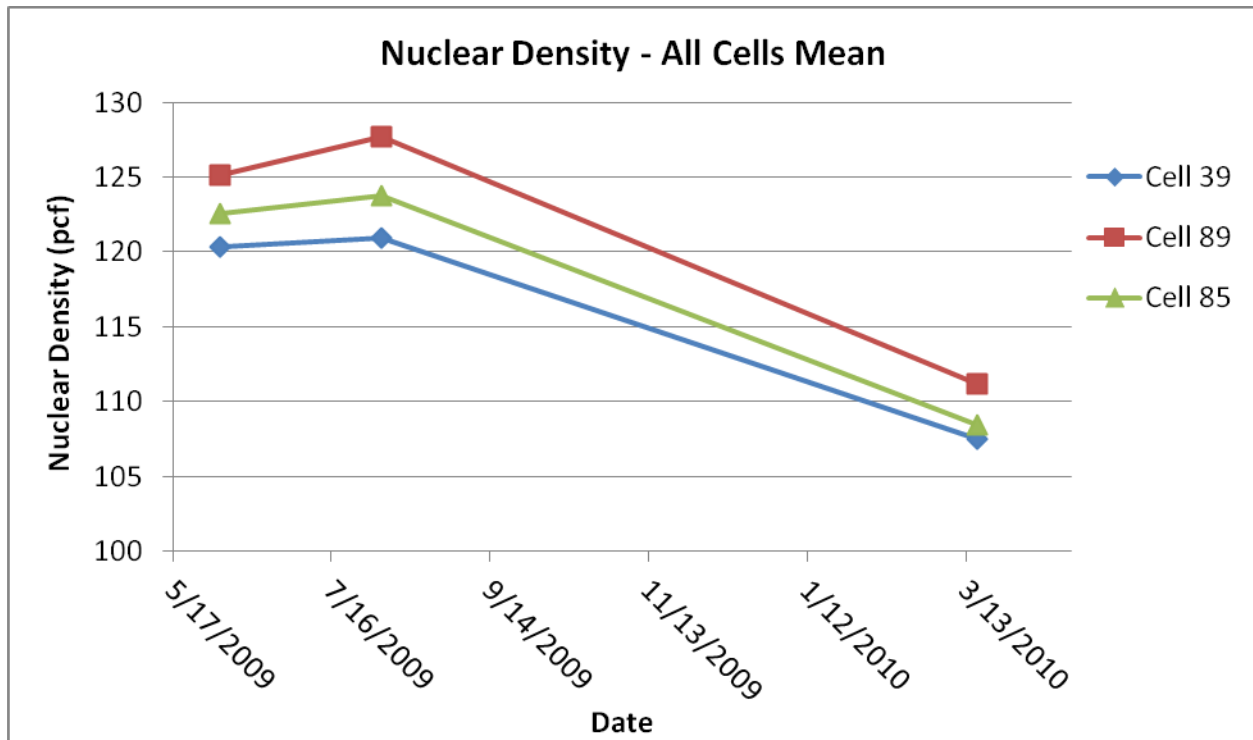


**Figure 6.33: Nuclear Density Results - All Cells**

- This plot shows that the porous overlay in cell 39 is consistently less dense than the two pervious full-depth cells.
- The plot shows a slight increase in measured density from May 09 to August 09, but very sharp decrease thereafter in May 2010.

#### 6.3.4.2 Dissipated Volumetric Rate Results

The Mean Dissipated Volumetric Rate is measured in multiple locations across each test cell, with multiple test runs at each location. The results show a very large variation in the calculated rate, suggesting that the air void composition varies throughout the cell. Further discussion of this observation can be found in the following analysis chapter.

Figure 6.34 illustrates the average of all measurements taken on a particular test day for each cell. This plot shows that cell 39 is consistently lower than cells 85 and 89, which is expected because it is not a full-depth pervious pavement.

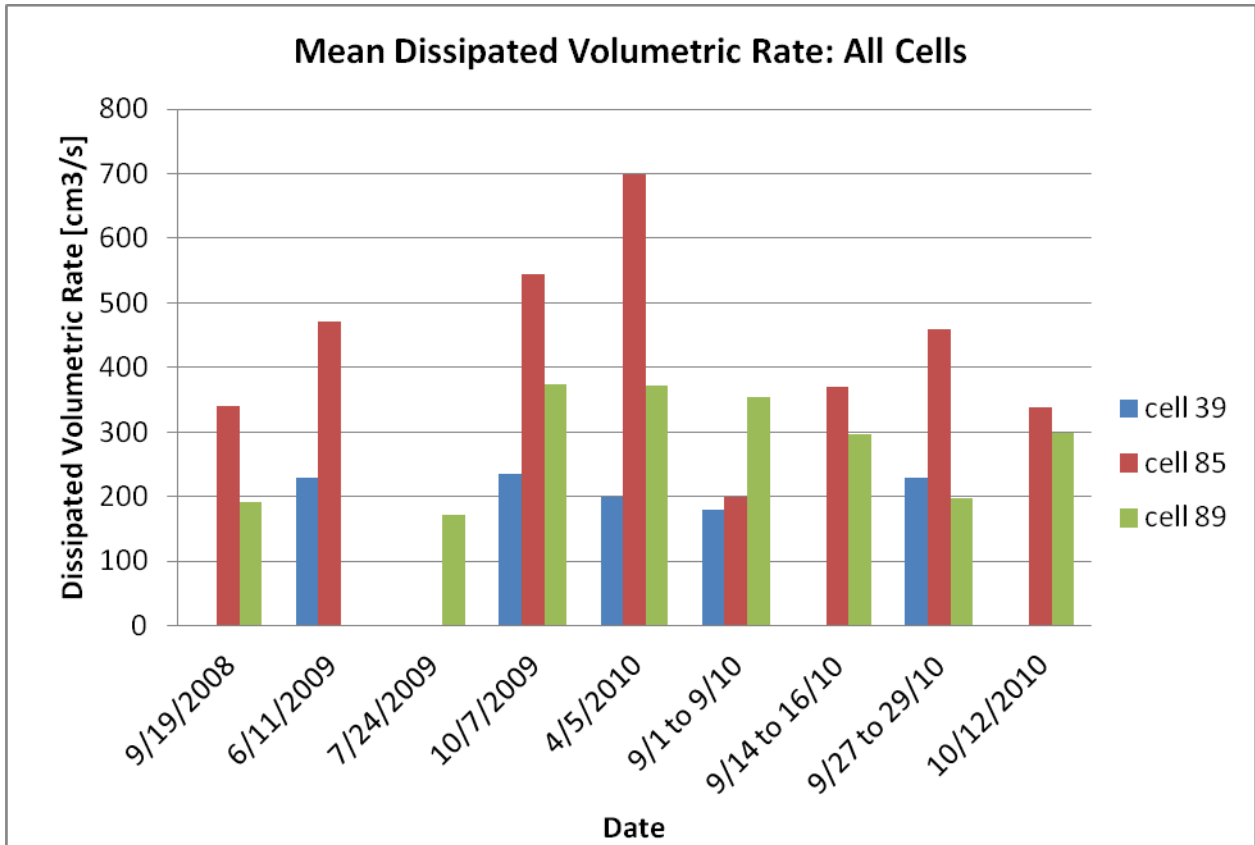


**Figure 6.34: Mean Dissipated Volumetric Rate - All Cells**

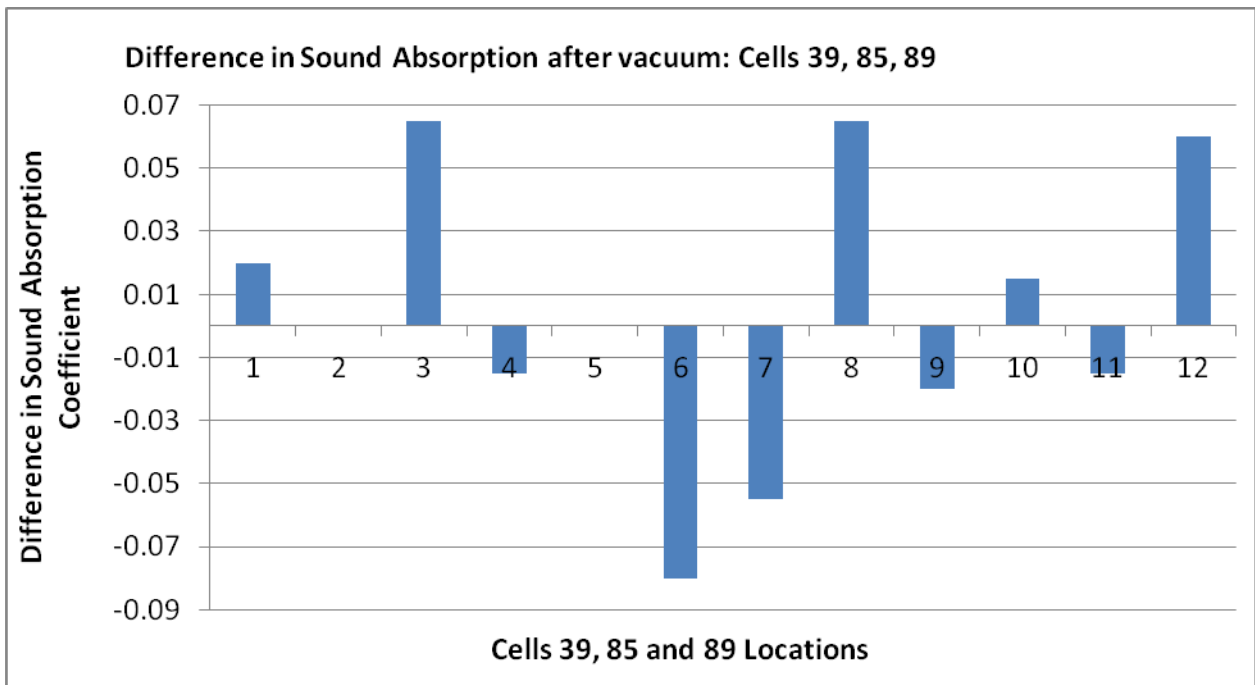


**Figure 6.35: Difference in Sound Absorption after 2<sup>nd</sup> Vacuum: Cells 39, 85 and 89**

6.3.4.3 Clogging Effects: Sound Absorption and Dissipated Volumetric Rate Before and After

The first vacuuming was only done on cells 85 and 89 on November 4<sup>th</sup> 2009. The table below shows the difference in time it took for the water to fall from the 37 cm mark to the 11 cm mark in the falling head permeability tube.

**Table 6.4: Difference in Flow Time after 1<sup>st</sup> Vacuum**

Cell	Time Before (s)	Time After (s)	Percent Change (%)
85	6	6	0
89	17	15.5	9

The second vacuuming was done on November 13<sup>th</sup> 2010. The following two plots show the difference in sound absorption and dissipated volumetric rate before and after the second vacuuming at 12 different locations throughout cells 39, 85 and 89.

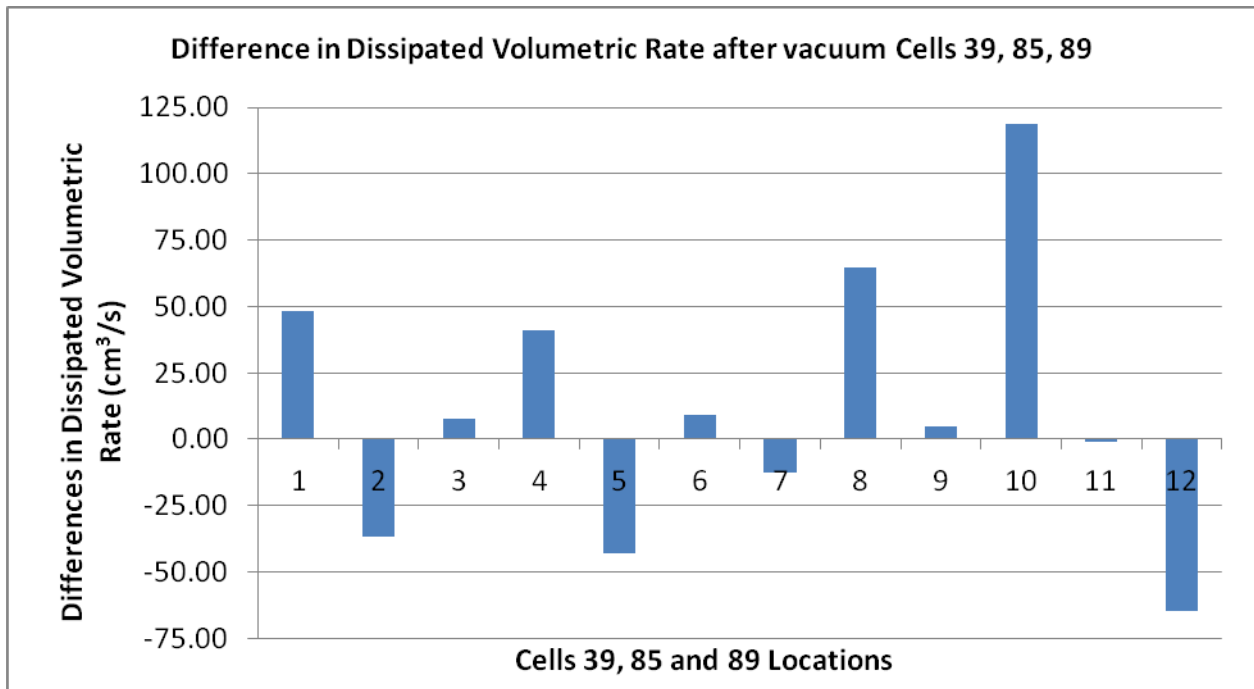


**Figure 6.36: Difference in Dissipated Volumetric Rate after 2<sup>nd</sup> Vacuum: Cells 39, 85 and 89**

As shown in the plots above, there is not a clear benefit in sound absorption or dissipated volumetric rate from vacuuming the pavement. Both properties show increases and decreases at different test locations throughout the three cells.

#### *6.3.4.4 FWD Results*

In the six groups of plots below, the deflections basins for each lane of cells 39, 85 and 89 are given from FWD tests performed throughout 2009. All tests were done in the center of the slab.

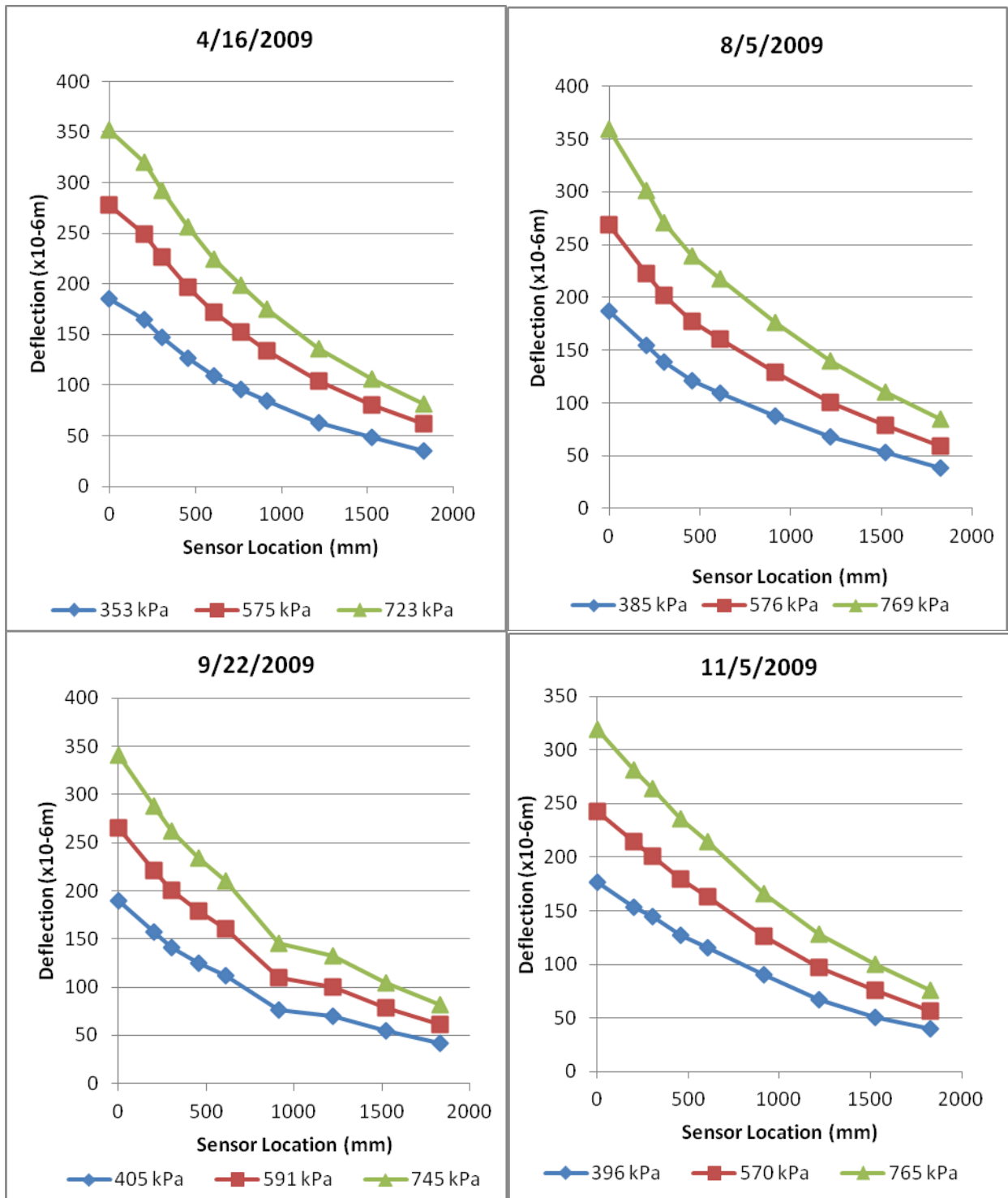


Figure 6.37: 2009 FWD Results – Cell 39 IL Slab 2 Center

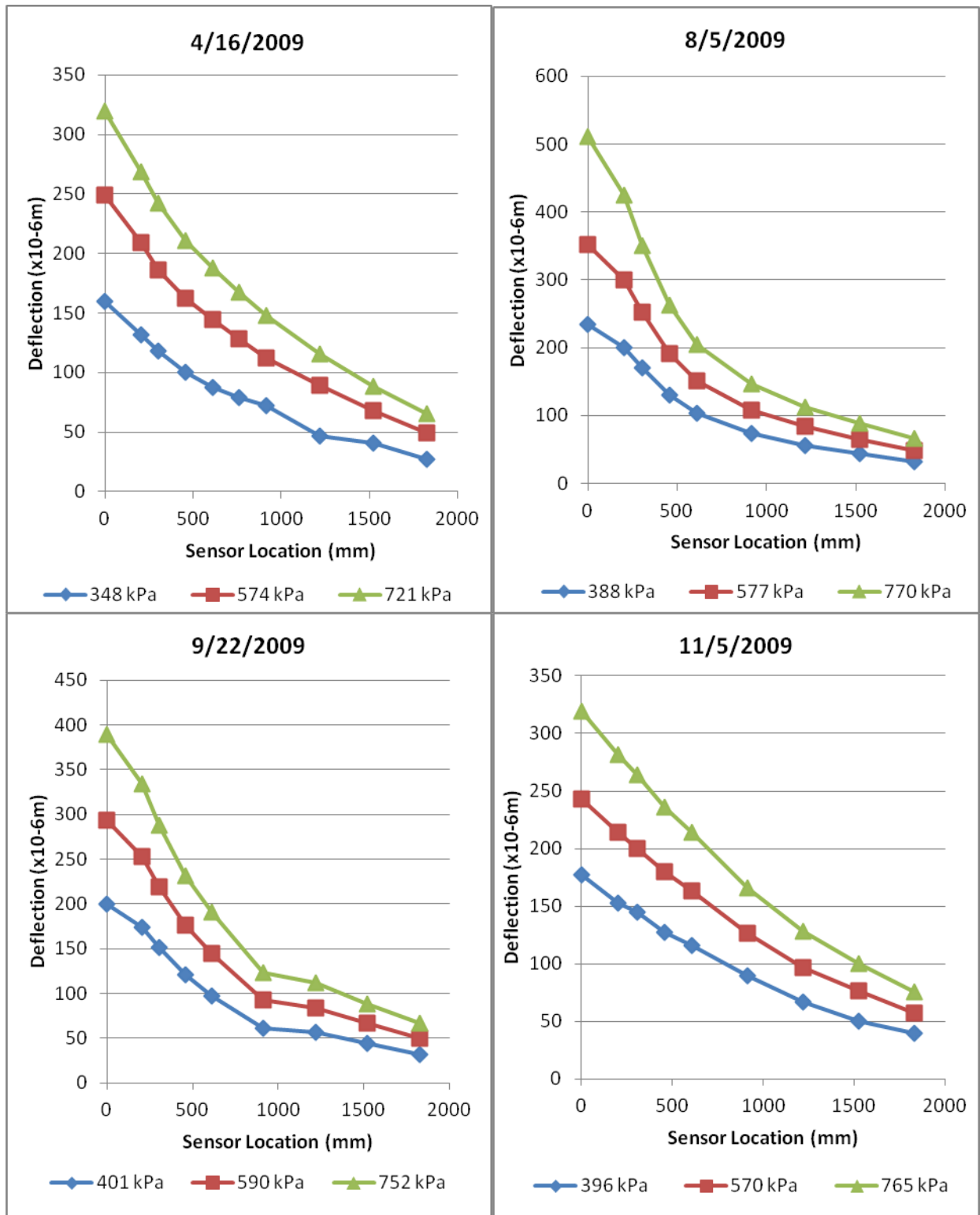


Figure 6.38: 2009 FWD Results – Cell 39 OL Slab 2 Center

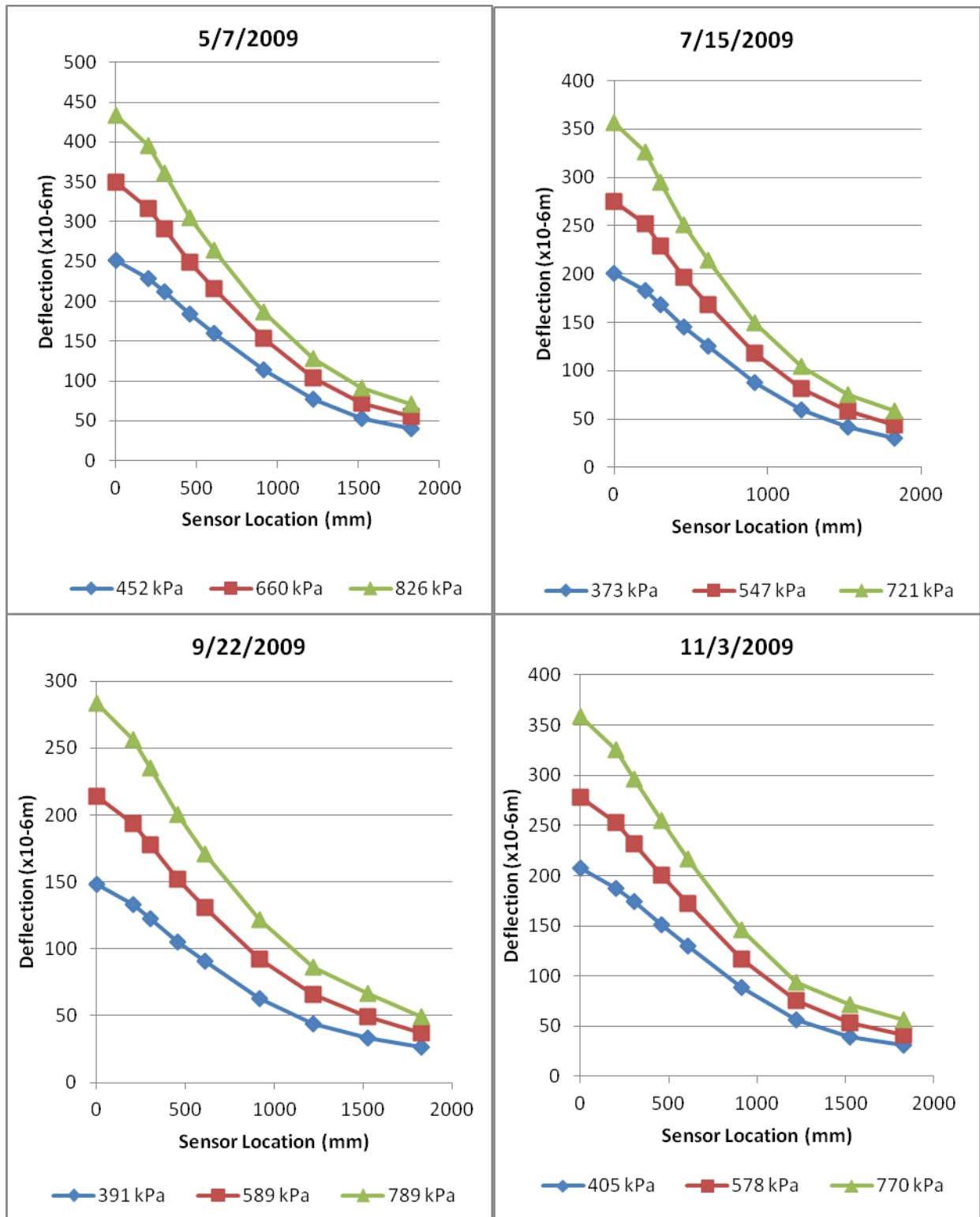


Figure 6.39: 2009 FWD Results – Cell 85 IL Slab 8 Center

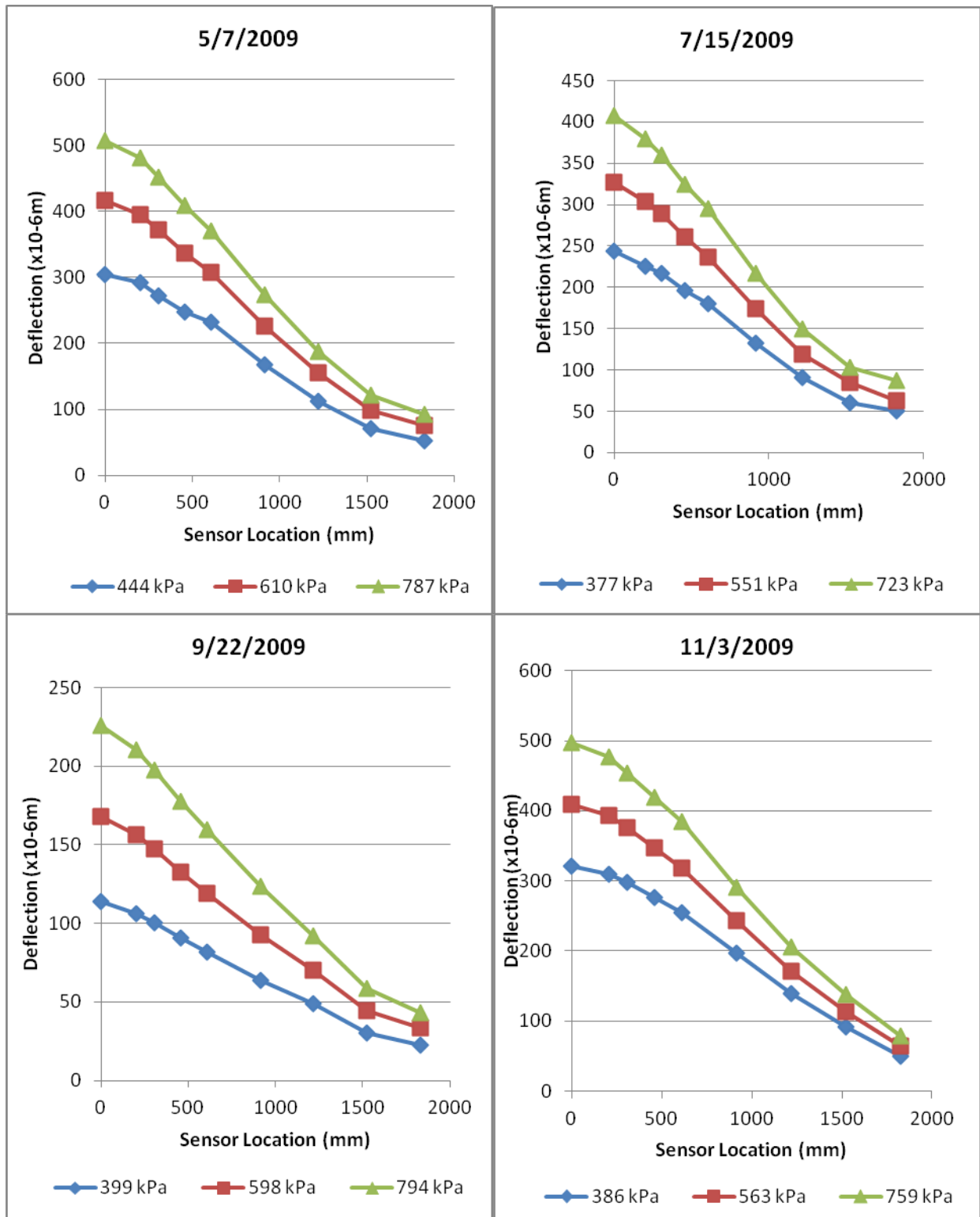


Figure 6.40: 2009 FWD Results – Cell 85 OL Slab 8 Center

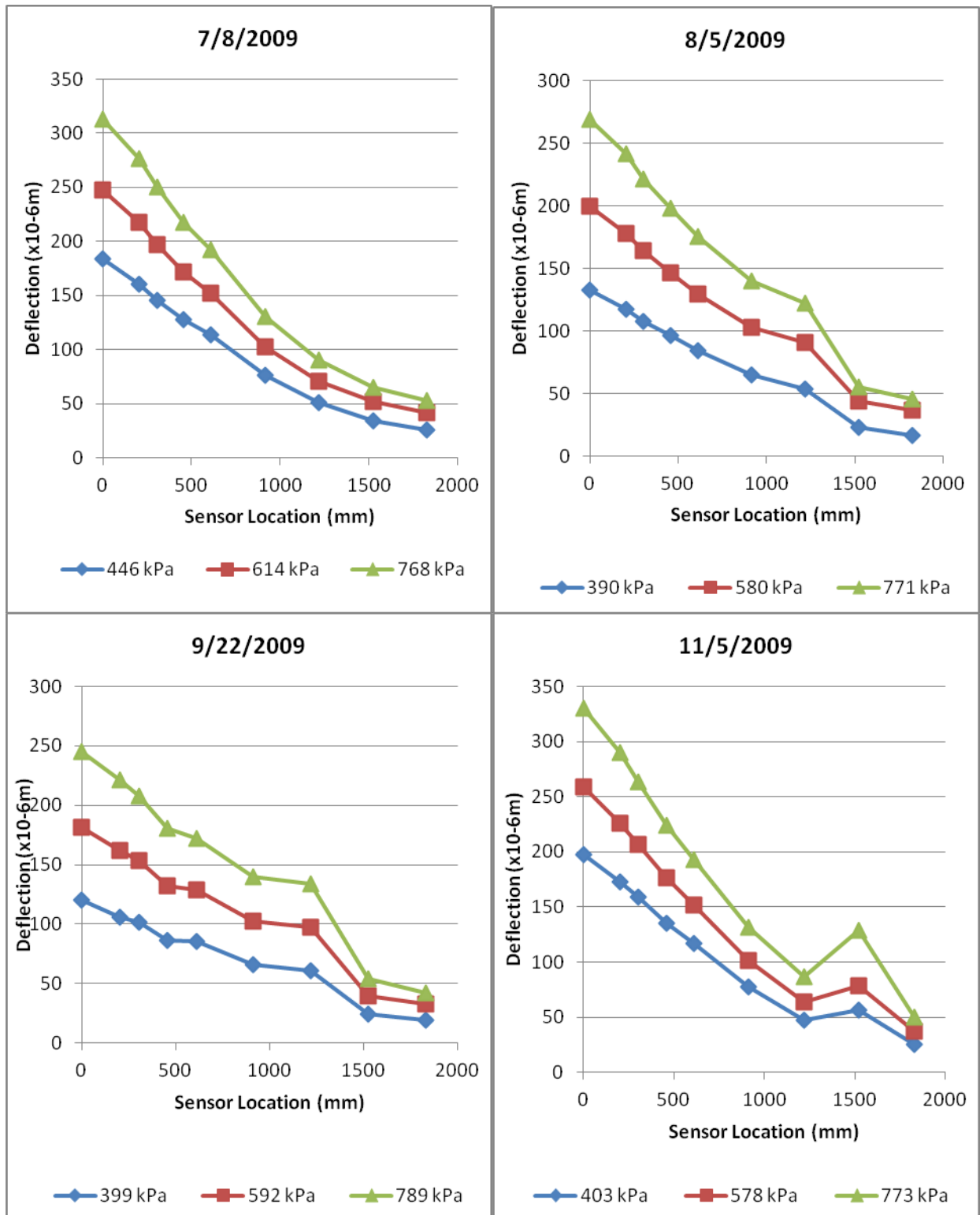


Figure 6.41: 2009 FWD Results – Cell 89 IL Slab 16 Center

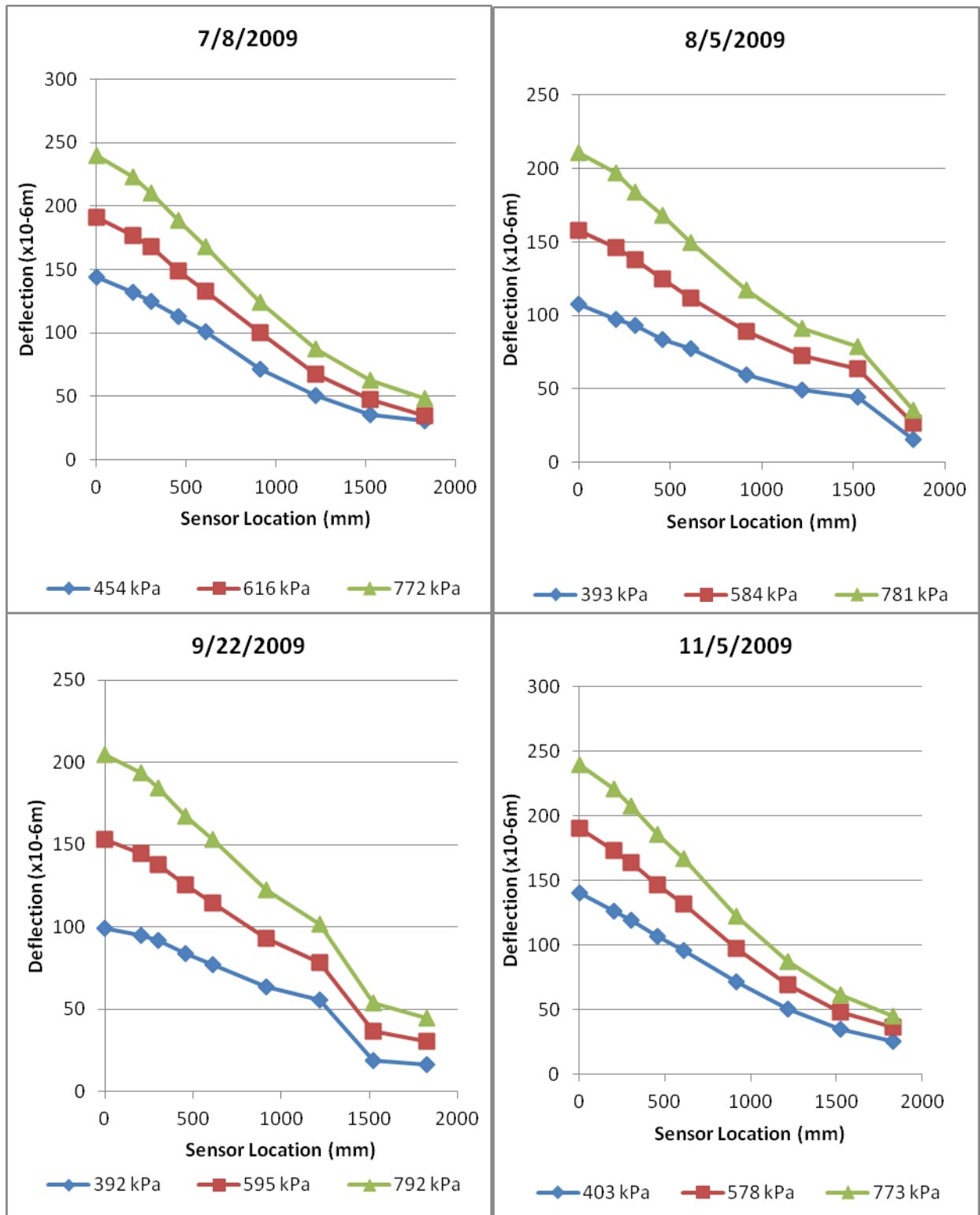
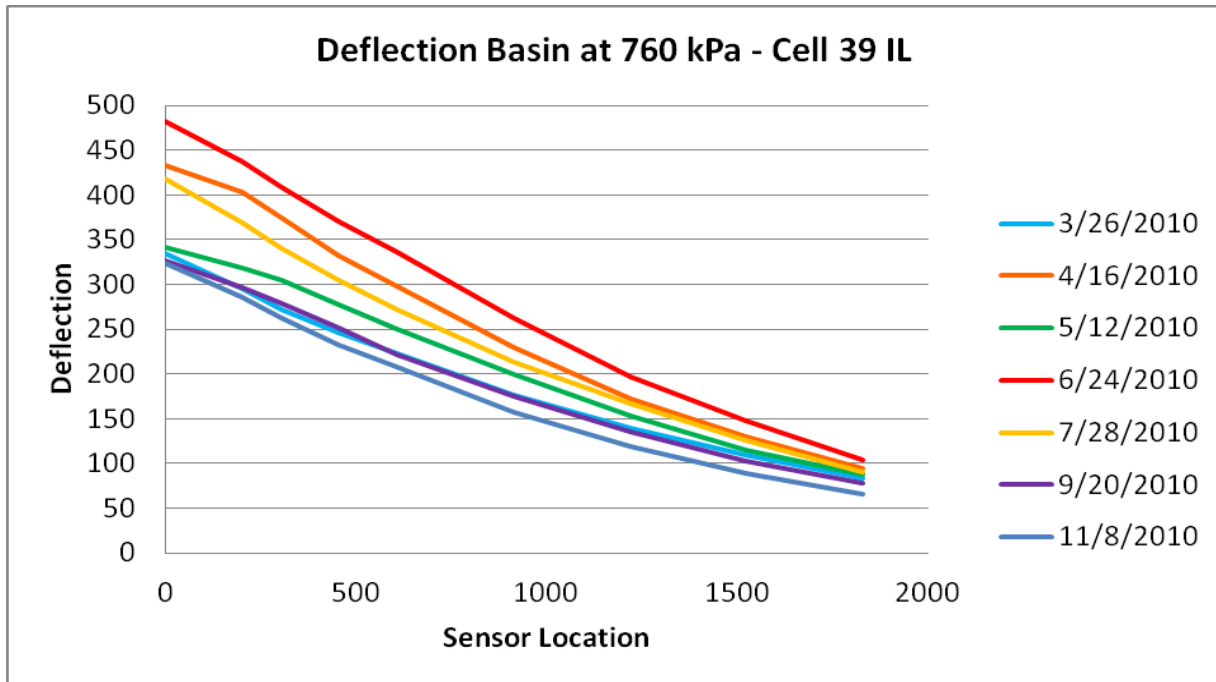
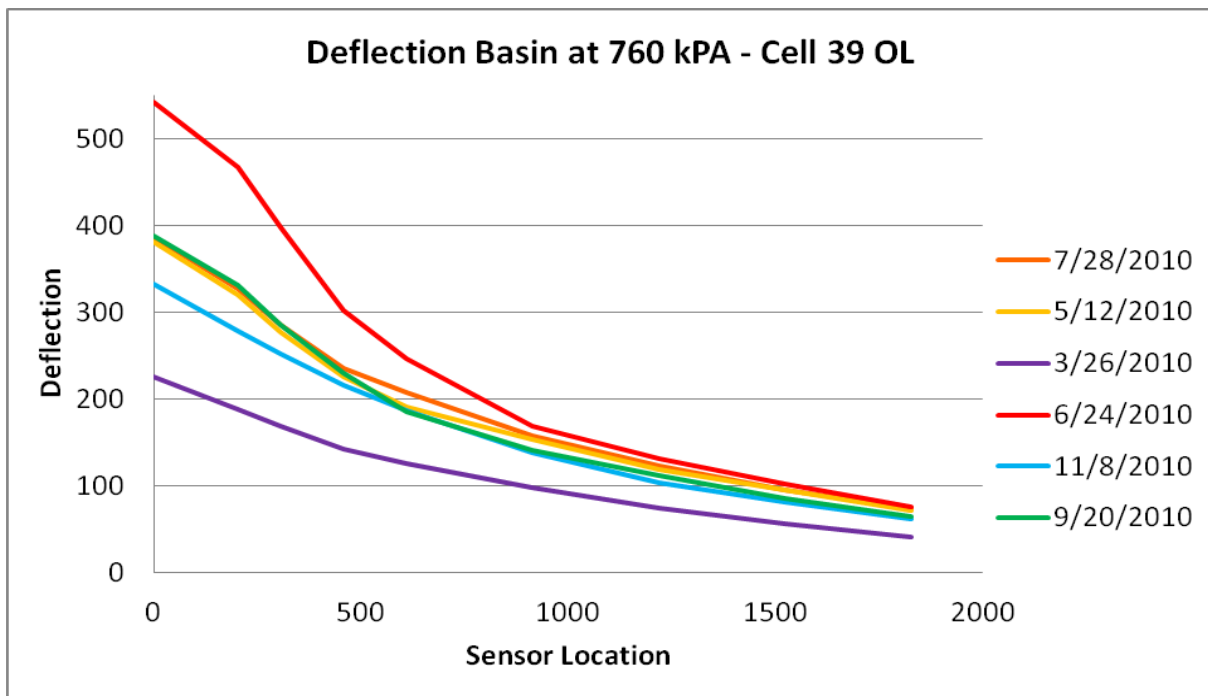


Figure 6.42: 2009 FWD Results – Cell 89 OL Slab 16 Center

The following plots show FWD results from 2010 at the load level near 760 kPa to illustrate the fluctuation over different seasons.



**Figure 6.43: 2010 FWD Results – Cell 39 IL**



**Figure 6.44: 2010 FWD Results – Cell 39 OL**

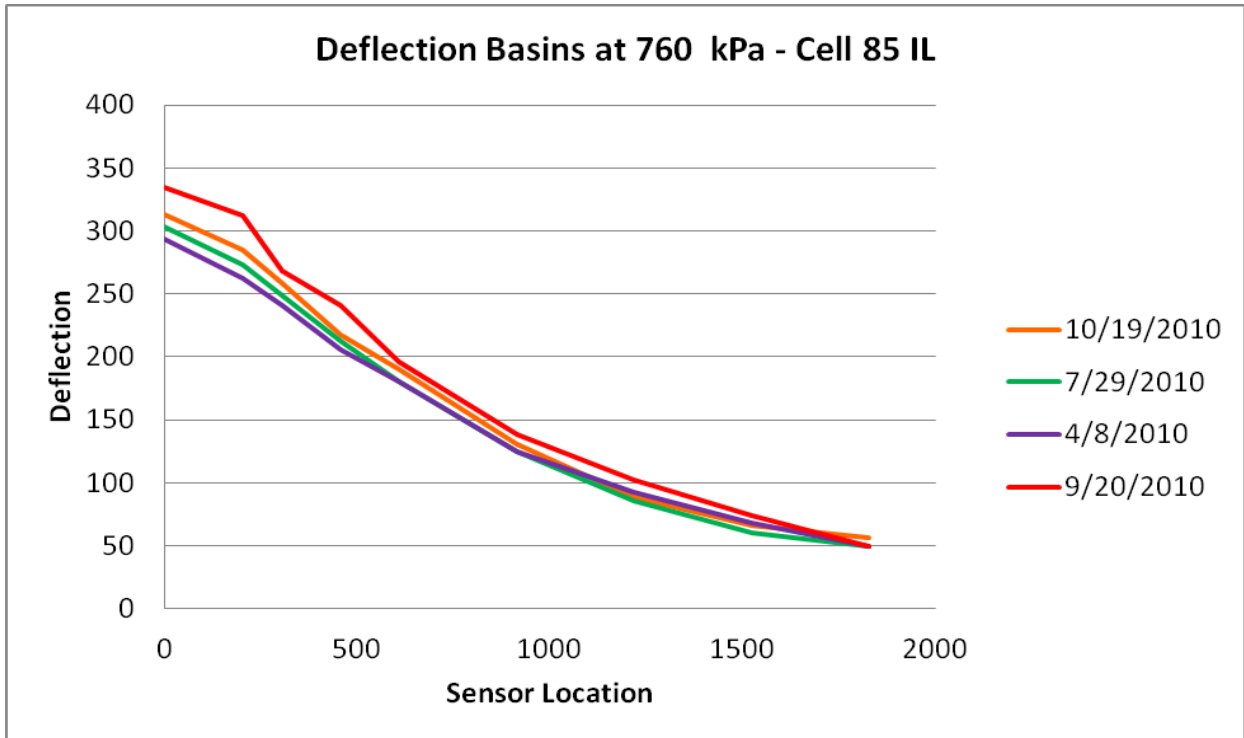


**Figure 6.45: 2010 FWD Results – Cell 85 IL**

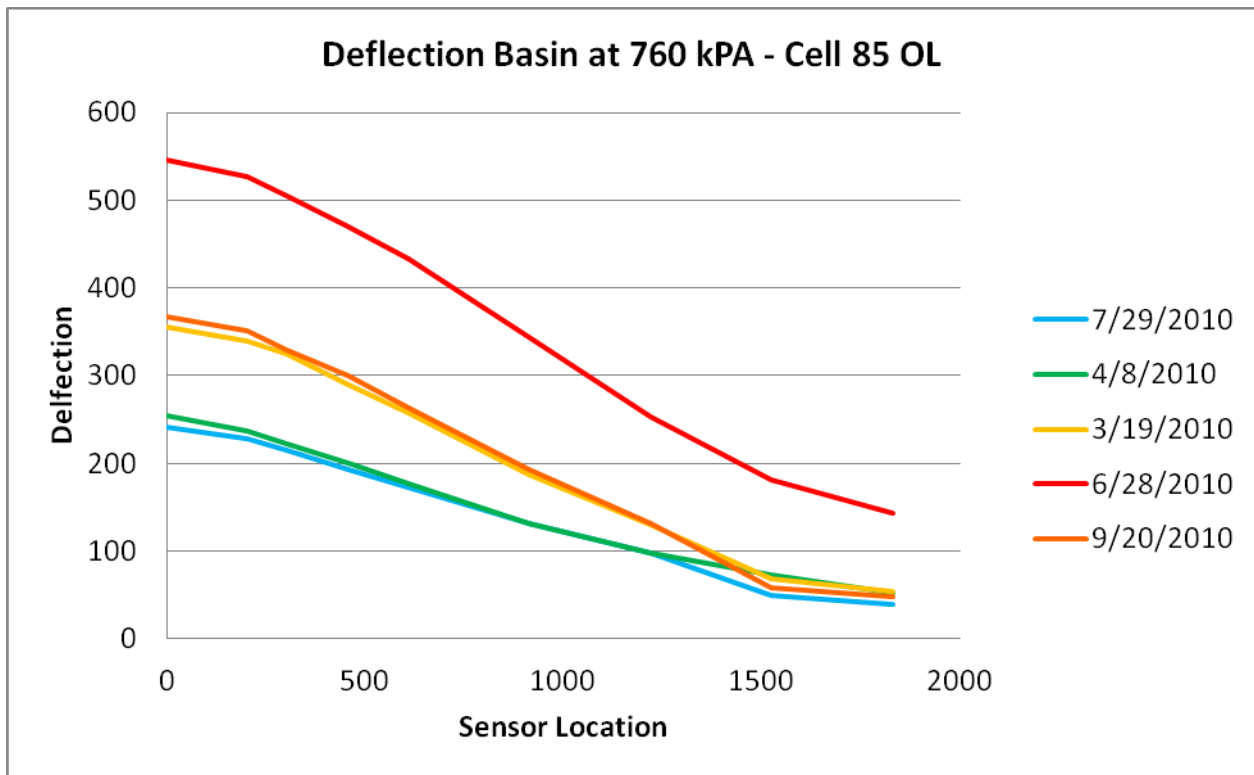


**Figure 6.46: 2010 FWD Results – Cell 85 OL**

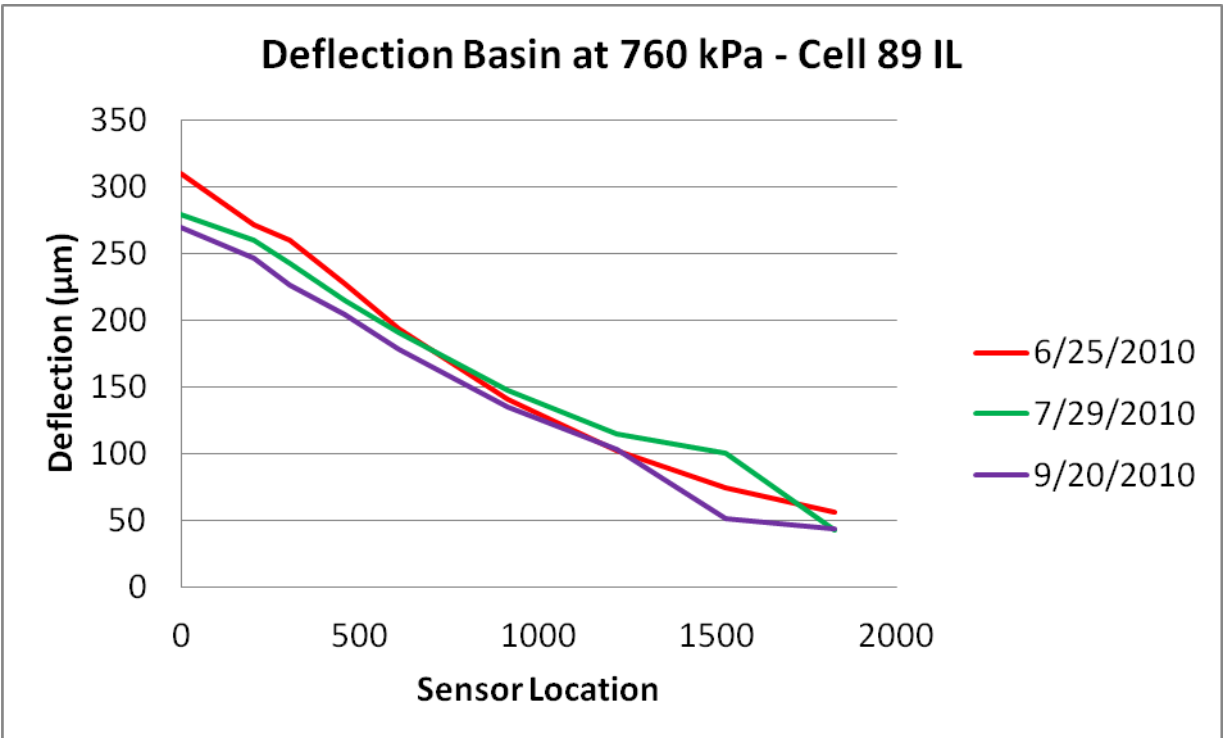


**Figure 6.47: 2010 FWD Results – Cell 89 IL**

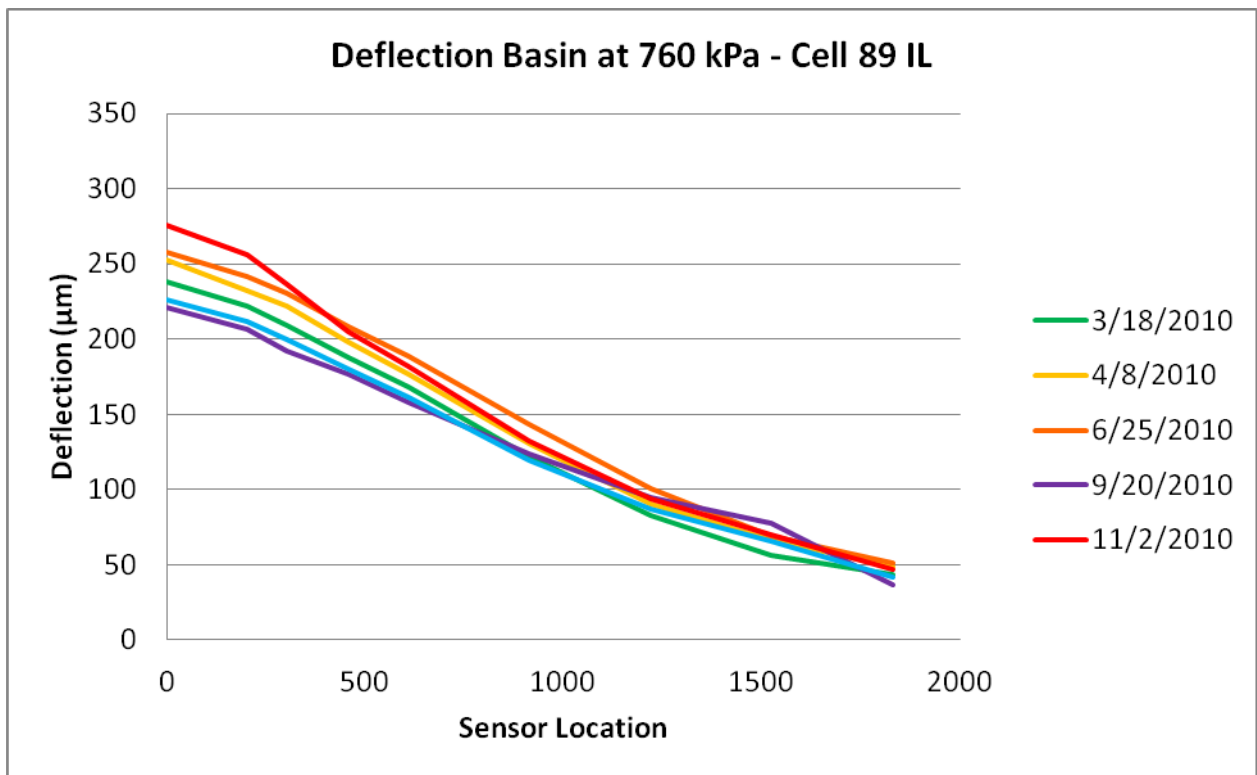


**Figure 6.48: 2010 FWD Results – Cell 89 OL**

### 6.3.4.5 Temperature and Moisture Results

The thermocouple and watermark plots for cells 39, 85 and 89 are given for summer 2009 to summer 2010 to illustrate the variation at different seasons. Cell 87 was constructed as a control non-pervious test cell to be compared to the pervious test cells at MnROAD. The thermocouple data for cell 87 shows the larger difference in temperature between the first few inches of pavement and the clay subgrade than in the pervious test cells. For comparison purposes of the watermark data, Cell 39 can be considered a non-pervious test cell when examining the watermark data in the base and subgrade.

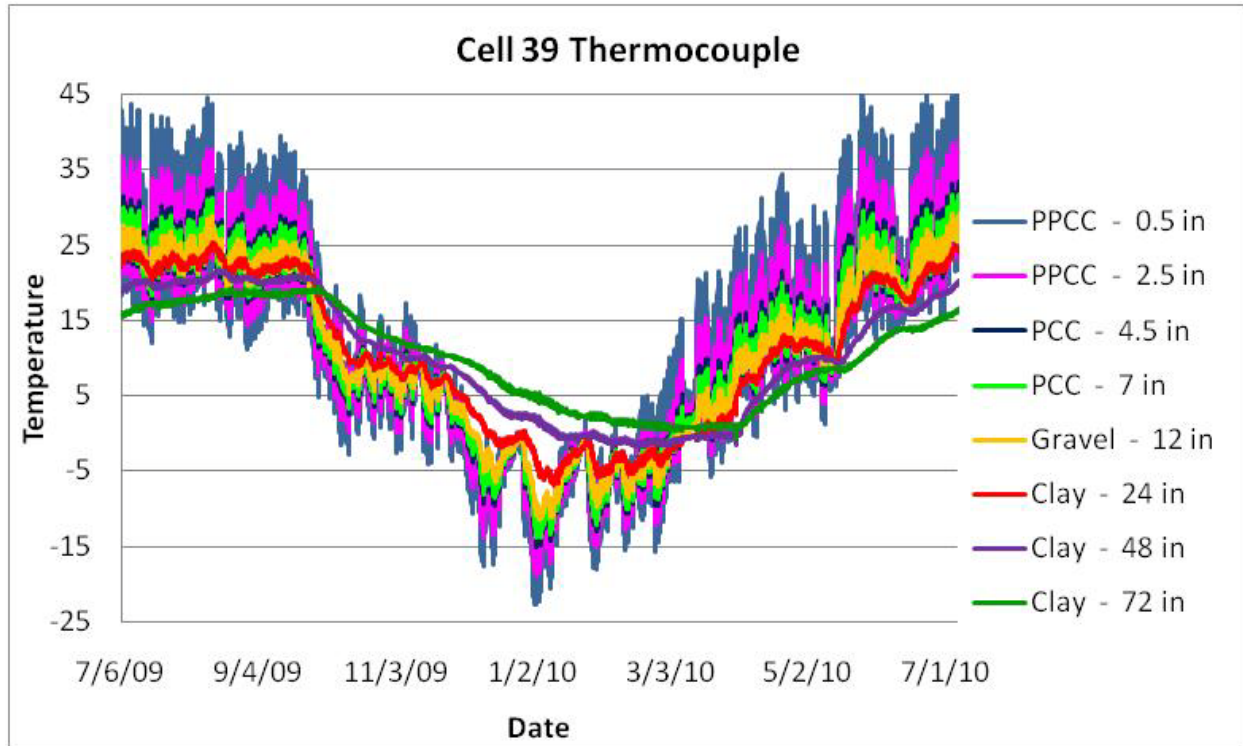
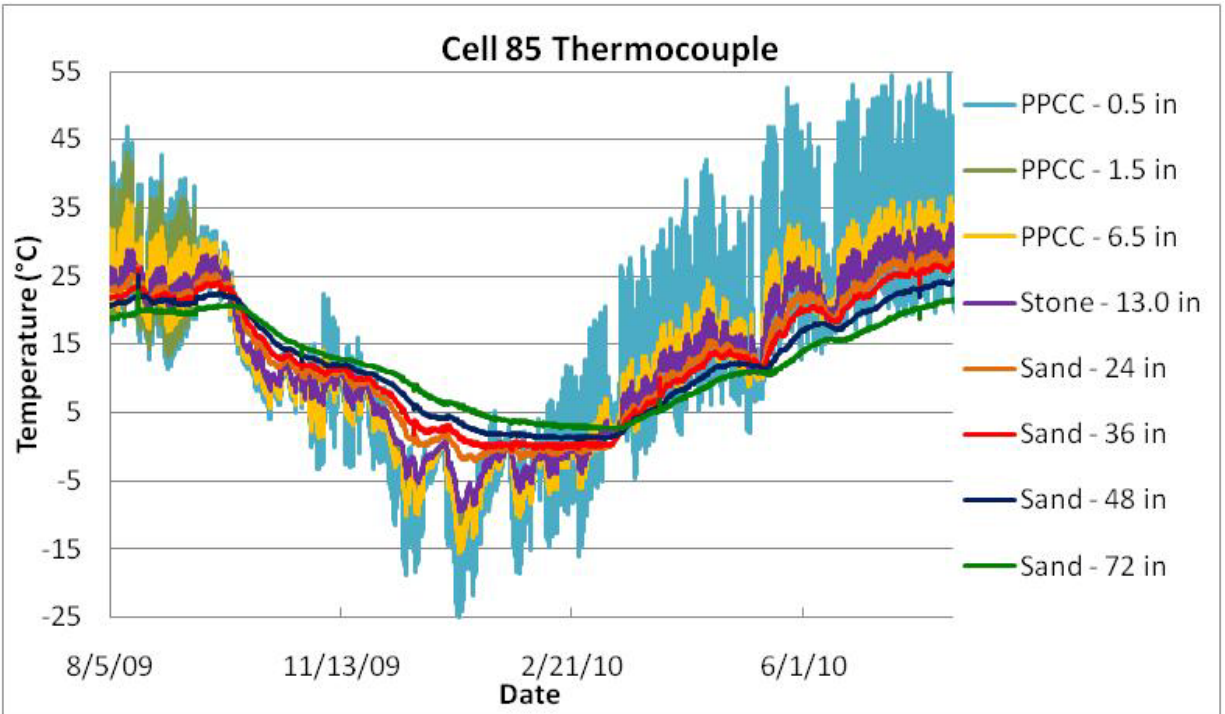
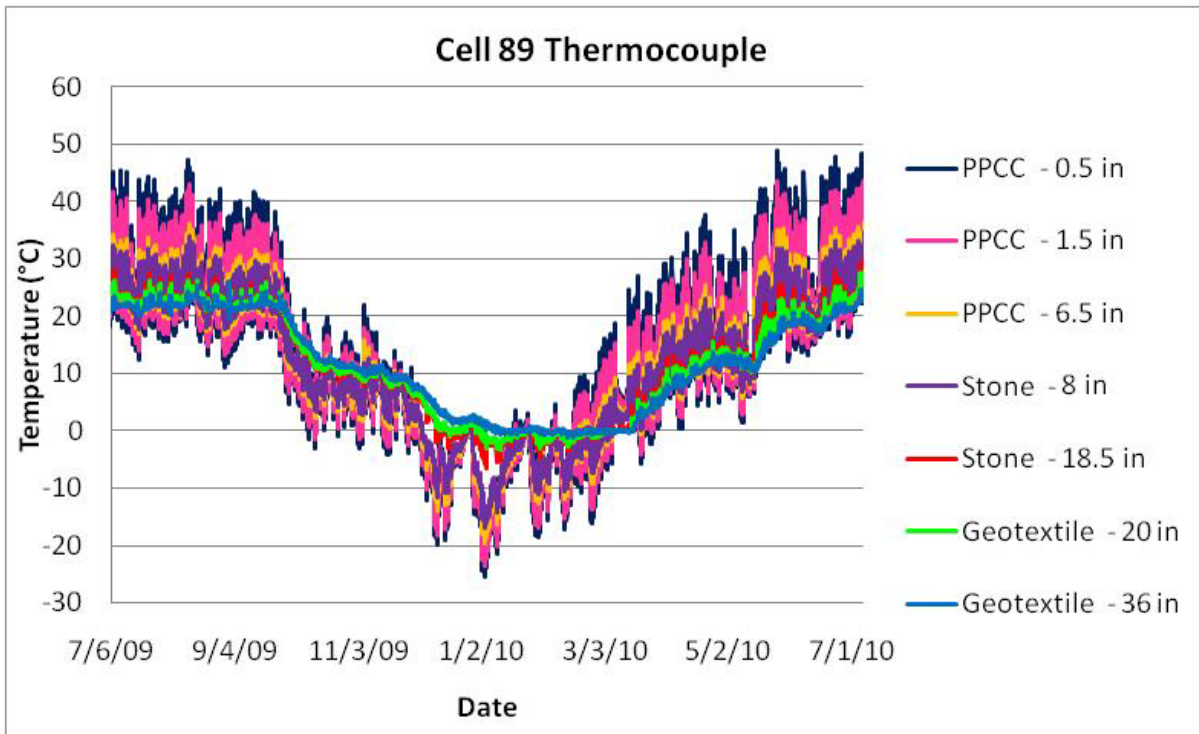


Figure 6.49: Cell 39 Thermocouple



**Figure 6.50: Cell 85 Thermocouple**



**Figure 6.51: Cell 89 Thermocouple**

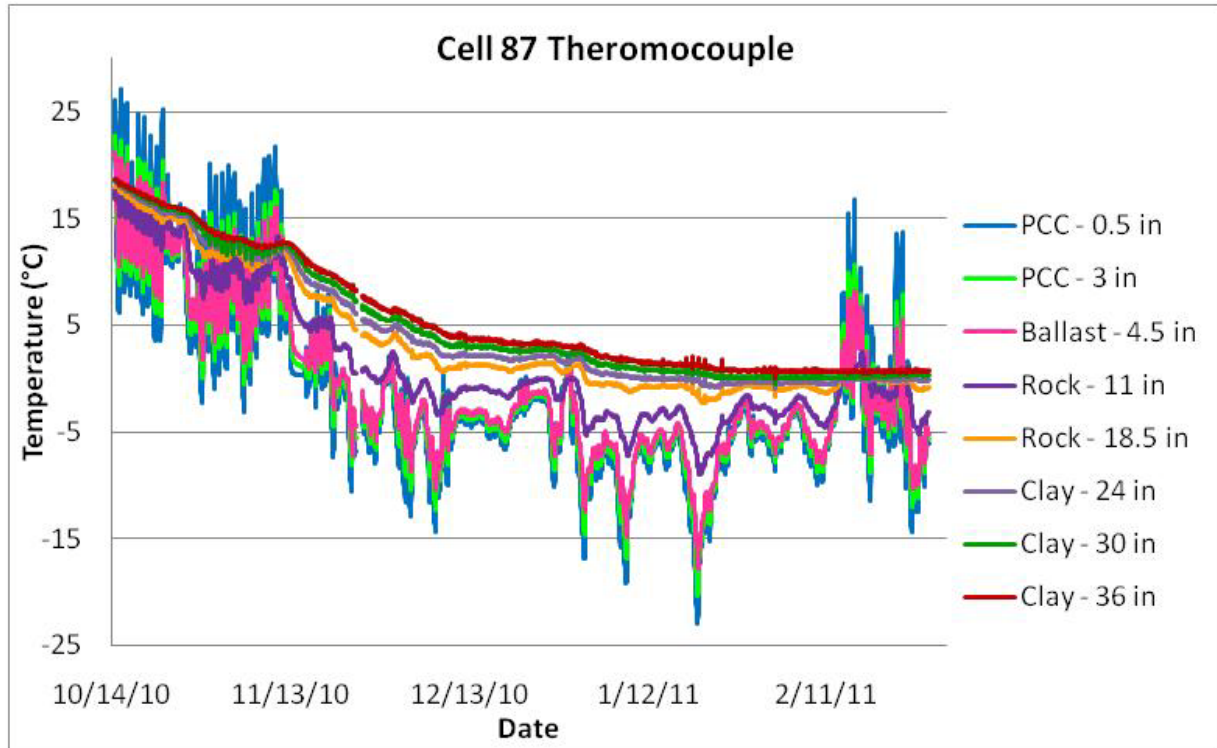


**Figure 6.52: Cell 87 Thermocouple**

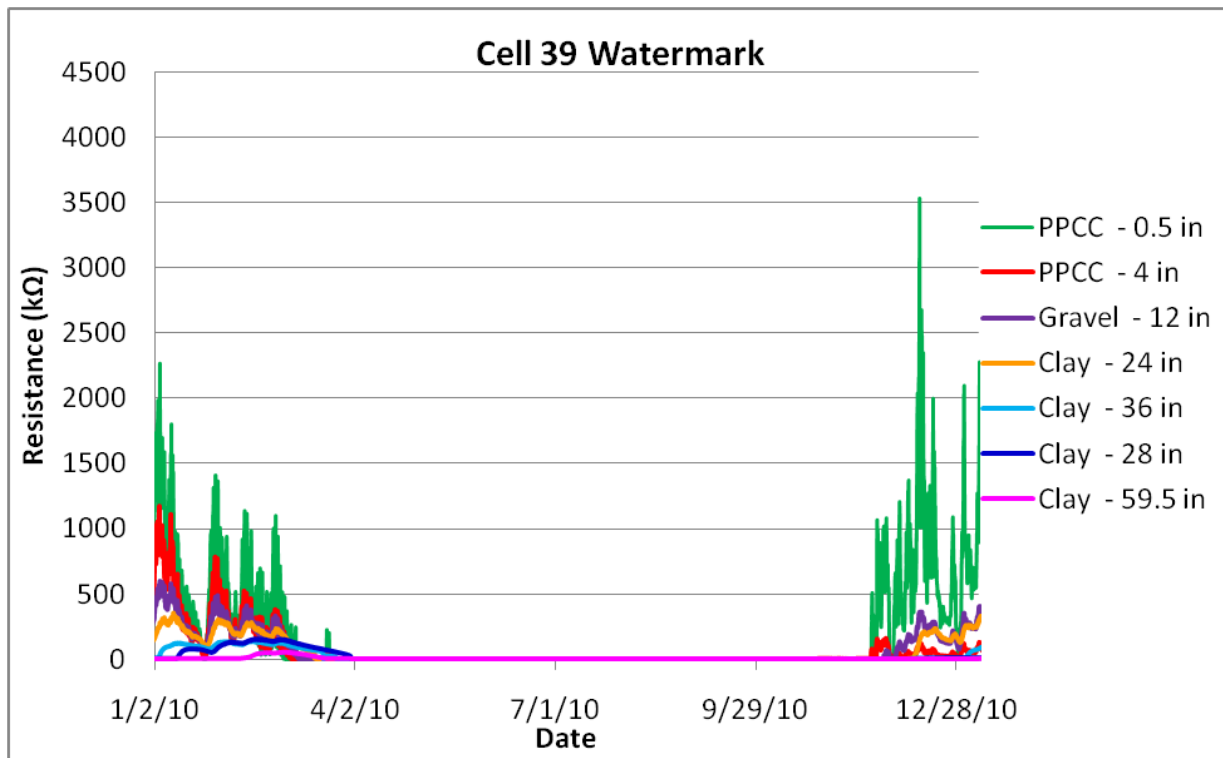


**Figure 6.53: Cell 39 Watermark**

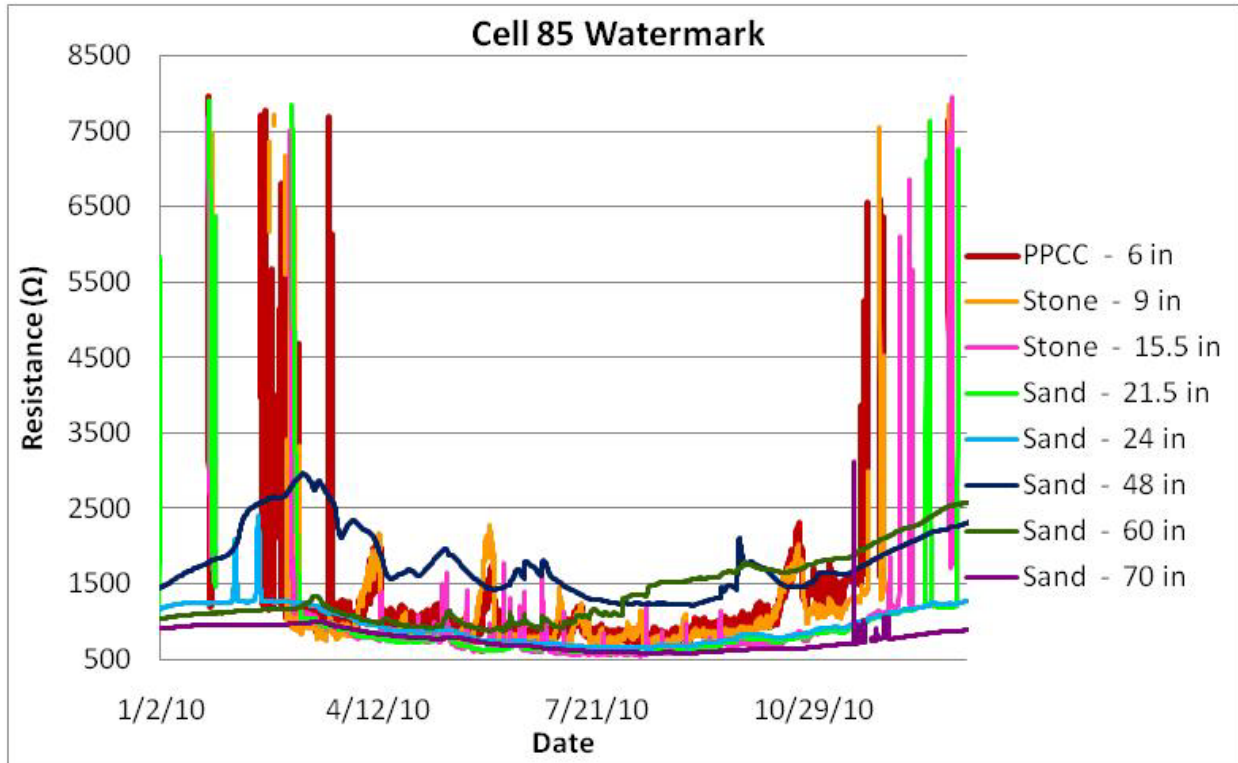


**Figure 6.54: Cell 85 Watermark**

This section provided the data measurements for ride, surface, noise and other physical properties taken from cells 39, 85 and 89 over the first two years of service life. The next section will discuss and analyze this data to help develop a deeper understanding of pervious concrete pavement performance.

#### **6.4 Analysis and Interpretation of Results**

The last section presented the raw data collected for the first two years of service life of pervious cells 39, 85 and 89 at MnROAD, and stated any major trends or observations. This section will discuss the implication of these results and further analyze the data to draw more significant conclusions.

##### **6.4.1 Roughness Index and Surface Rating Discussion**

The Surface Rating is used to measure pavement condition. MnDOT considers a SR below 2 poor condition and in need of repair. A SR of 4.0 is given for pavement in perfect condition. The measured Surface Ratings for the pervious cells fell above 3.5 for all dates measured. Pavements with a SR below 2.0 are considered poor and in need of repair. A SR of 4.0 is for pavement in perfect condition. The average surface rating for all concrete pavements in Minnesota is 3.3, suggesting that the pervious test cells have better than average surface quality. The high SR found in the previous tests cells would be interpreted to a good pavement rating.

The average IRI in Minnesota is 1.4 m/km on interstates, and 1.7 m/km on non-interstates [4]. In 2007, only 8% of Minnesota state highways had an IRI greater than 2.7. The FHWA roughness categories place pavements with IRI values less than 1.5 as in good condition. Pavements must have an IRI less than 2.6 to even be considered acceptable. However, most of the IRI values from the pervious cells were between 3 and 5, with the maximum over 6.5. These IRI ratings are well above the FHWA standards for acceptable, and could be due to the different paving practices used.

The International Roughness Index is used by MnDOT’s Pavement Management Section to calculate the Ride Quality Index, which is then used to gauge whether or not the pavement is in need of repair or rehabilitation. However, this calculation is done with a formula which was previously developed for typical PCC pavements. When this relationship was used with the IRI values for the pervious test cells, all resulting Ride Quality Indices showed that the pavements were in severe need of repair according the MnDOT’s rating scale. The high Surface Ratings do not correlate to the very poor ratings which were found with the RQI scale. These discrepancies suggest that the unique surface texture of pervious pavements may produce a profile that does not directly relate to the amount of vertical movement a vehicle will actually experience, and therefore is not an accurate measure of pavement ride condition. Still, IRI provides some insight on the magnitude of texture of different pervious pavements and therefore is a valuable test in assessing the performance.

**6.4.2 Texture and Friction Discussion**

Because the measured Friction Number and Mean Profile Depth of the three test cells do not follow a very clear seasonal variation, a comparison of the overall mean and range of each cell was done to draw more general conclusions.

Statistical analysis of the surface texture data collected from 2008 to 2010 show there is a significant difference in the mean profile depth of the MnDOT standard Astroturf drag used in cell 32 and the pervious cells 39, 85 and 89. This is summarized in Table 6.5 below.

**Table 6.5: Mean Profile Depth Summary**

<b>Mean Profile Depth (mm)</b>				
<b>Cell</b>	<b>32</b>	<b>39</b>	<b>85</b>	<b>89</b>
Mean	0.35	1.95	1.89	1.85
Range	0.13	0.14	0.17	0.14
Minimum	0.28	1.88	1.77	1.79
Maximum	0.41	2.02	1.95	1.94
Upper 95% CL	0.41	2.00	1.94	1.90
Lower 95% CL	0.29	1.91	1.84	1.81

The mean profile depth of the roller compacted pervious cells is about 1.6 mm larger than the Astroturf drag cell. It is also important to note that the porous overlay in cell 32 has a large MPD than the full-depth pervious cells 85 and 89.

As stated in chapter 2, the friction number should be above 25 for a smooth tire to be considered a safe pavement with adequate skid resistance. Anything below 15 will not provide sufficient tire traction and would be in need of rehabilitation. Table 6.6 below compares the friction numbers for the three pervious cells 29, 85 and 89 to cell 32.

**Table 6.6: Friction Number Summary**

<b>Friction Number – Smooth Tire</b>				
<b>Cell</b>	<b>32</b>	<b>39</b>	<b>85</b>	<b>89</b>
Mean	32.1	52.7	47.0	47.7
Minimum	24.9	43.9	37.6	41.3
Maximum	53.8	56.8	55.6	58.6
Range	28.9	12.9	18.0	17.3
Upper 95% CL	38.1	56.4	54.5	56.3
Lower 95% CL	26.1	49.0	39.5	39.0

This table shows the mean, range, and the 95% confidence interval of all friction measurements using a smooth tire collected from up until 2010. The pervious cells have a slightly higher mean than the Astroturf drag cell. More significantly is the smaller range in friction numbers for the pervious cells and the much higher minimum values. Cell 32 reached a minimum friction number of 24.9, which is under the minimum to be considered a safe skid resistant pavement. The pervious cells, however, achieved a minimum friction number far above this limit, with the lowest being cell 85 at a FN of 37.6. This analysis suggests the porous overlay mix cell 39 and the pervious concrete in cells 85 and 89 can provide sufficient friction for skid resistance.

### **6.4.3 Sound Absorption Analysis**

To compare the difference in sound absorption between PCC pavements and pervious pavements at MnROAD, the ratio of sound absorption coefficients from the two at each frequency are plotted, and the frequency most influenced by the porosity of the pavement can be determined.

This comparison was also done using the non-pervious HMA control cell 87 at MnROAD. The results are shown in the figure below from Izevbehai [3].

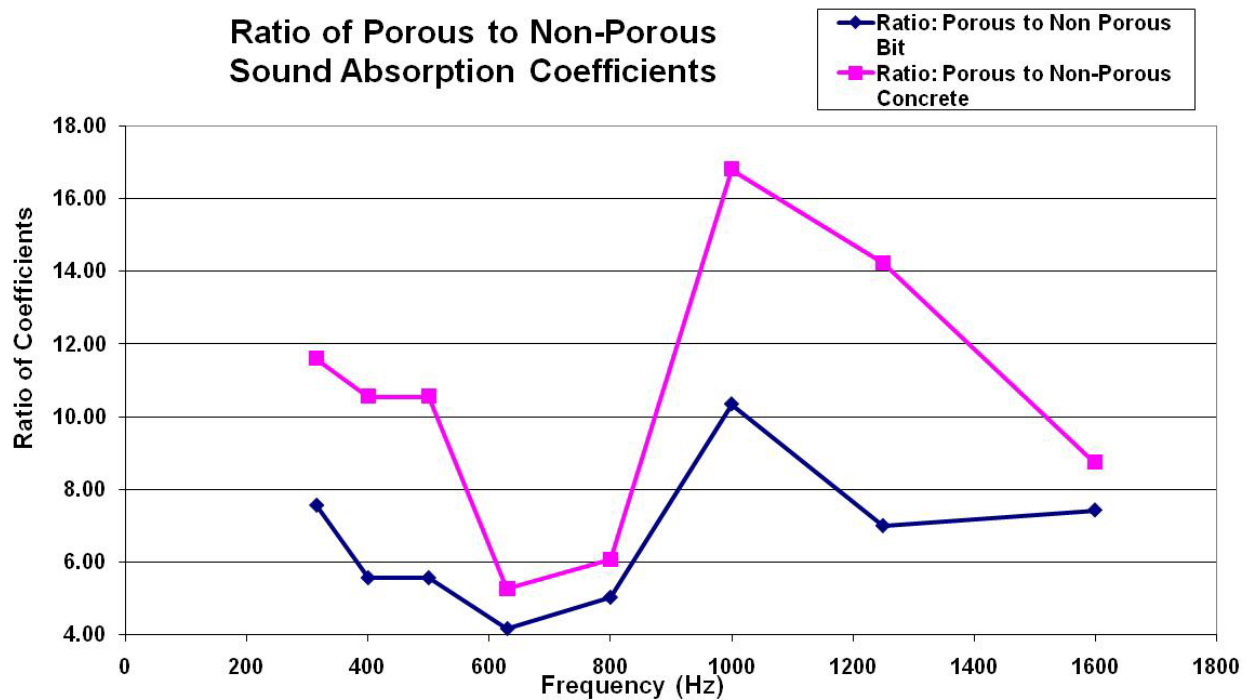


**Figure 6.55: Ratio of Porous Versus Non-Porous SA – Bit and PCC**

This plot shows that the ratio of sound absorption between non-porous and porous pavements is highly dependent on the sound frequency. When the ratios of both bituminous and concrete are compared, the most advantage is found at 1000 Hz.

#### **6.4.4 Variation in Nuclear Density**

Because of the wide range of measured densities found throughout the test cells using the nuclear density gauge, statistical analysis was done to determine a range around the mean value which could be considered highly probable for other such pervious pavements. A confidence level of 95% proves that if a test was repeated on that particular day, the measured density would fall within the given range 95% of the time. The results from this analysis are shown in figures 6.58 to 6.59 below for each of the pervious concrete cells at MnROAD.

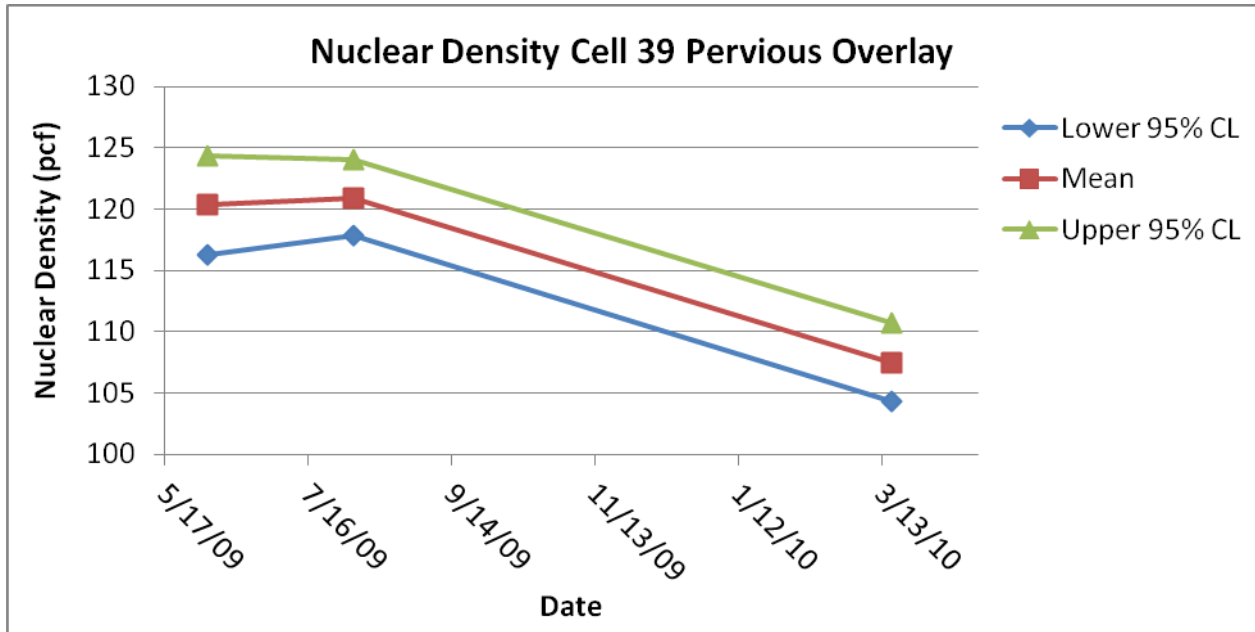


**Figure 6.56: Density 95% Confidence Interval – Cell 39**

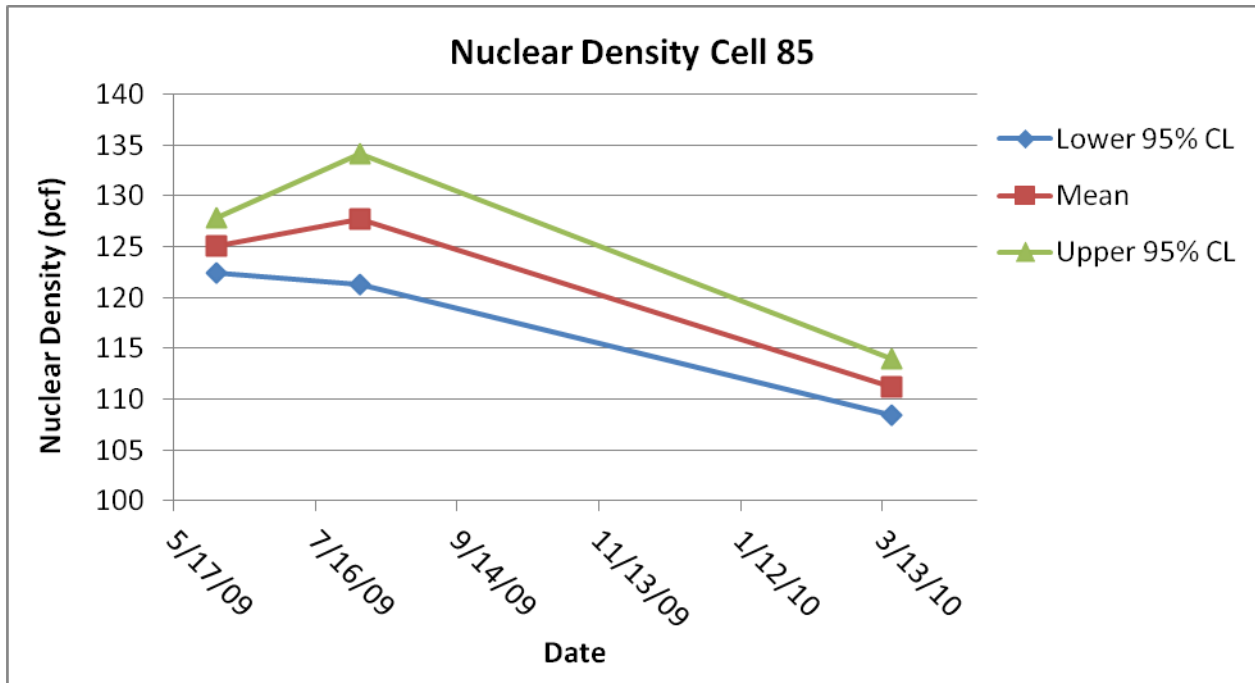


**Figure 6.57: Density 95% Confidence Interval – Cell 85**

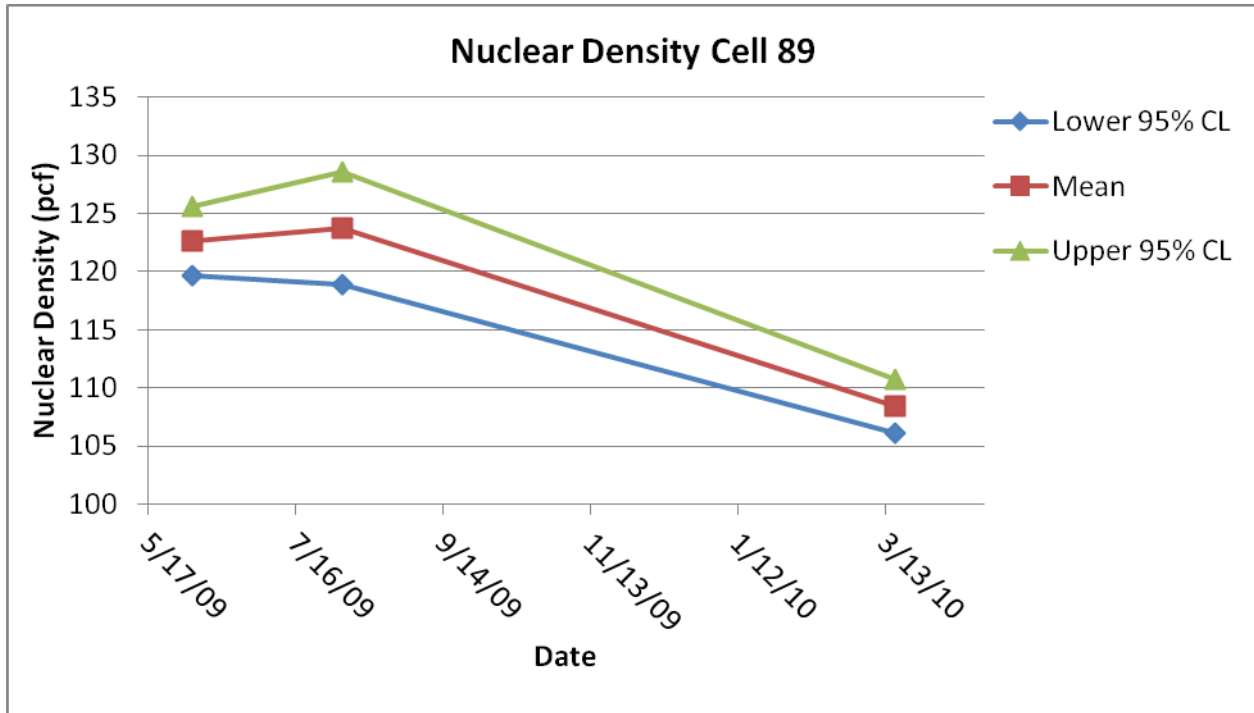


**Figure 6.58: Density 95% Confidence Interval – Cell 89**

The analysis found a maximum confidence interval of 12.9 pcf from August 09 on cell 85, and a minimum confidence interval of 4.6 pcf from March 10 on cell 89. Most intervals were in the range of 5 to 8 pcf. The analysis of the most recent density tests performed suggest the porous overlay in cell 39 is more likely to be less dense (at 112 to 104 pcf) than the pervious full-depth concrete in cells 85 and 89 (at 114 to 106 pcf). However, it's important to note that this difference is marginal. Future testing will be done to determine if the drop in density at shown in the last round of tests can be attributed to seasonal and environmental effects.

Nuclear density measurements from the inside lane and outside lane were compared to evaluate the effect traffic loading can have. A set of density measurements was taken on June 4<sup>th</sup>, 2009 for both the inside and outside lane of the three pervious test cells. By limiting the data to only day of testing, environmental and seasonal effects are eliminated. The following plot illustrates the difference in the mean density between the cells and two lanes on this date.

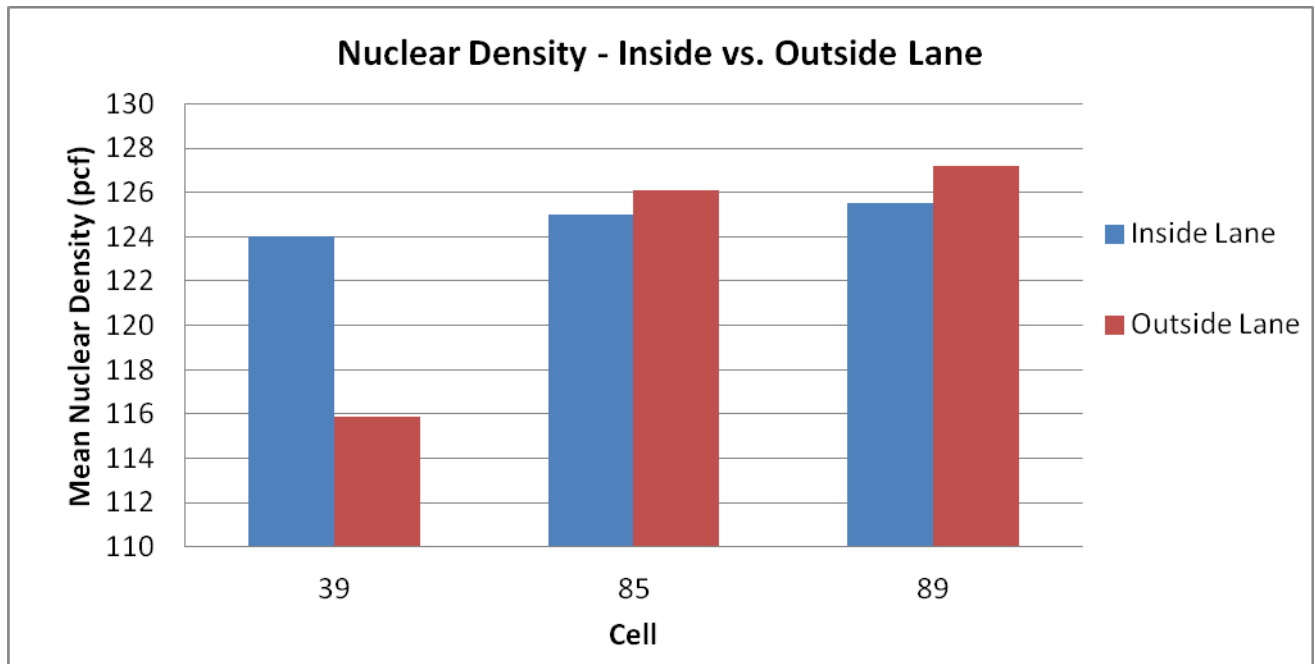


**Figure 6.59: Density – Inside Versus Outside Lane All Cells**

The bar chart above illustrates the opposite pattern between the porous overlay in cell 39 and the full-depth pervious concrete in cells 85 and 89. In Cell 39 there is a drastic difference in density, with the inside lane much higher than the outside lane. However, in cells 85 and 89 there is actually a slight reduction in density in the inside lane. To further analyze these results, the Mann Whitney Z-Test was performed. This test allows you to determine the confidence level at which the two lanes experience significantly different results. The null hypothesis is that the density data collected from the inside lane is similar to the density from the outside lane. The alternative hypothesis is that the two data sets are different.

To test these hypotheses, the data from the each data set (inside and outside lane) are combined and ranked in order from greatest to smallest. The ranks from each data set are then summed separately. Next, the following formula is used to calculate the U statistic for each data set where subscripts 1 and 2 refer to the two separate data sets.

$$U_1 = n_1 \times n_2 + \frac{n_1(n_1 + 1)}{2} - R_1 \quad (4)$$

$$U_2 = n_2 \times n_1 + \frac{n_2(n_2 + 1)}{2} - R_2 \quad (5)$$

*R = Sum of Ranks for data set*

*n = number of measured densities in data set*

Using a normal approximation, the smaller of the two U values is converted to the Z statistic using the following equations.

$$\mu = \frac{n_1 n_2}{2} \quad (6)$$

$$\sigma = \sqrt{\frac{n_1 n_2 (n_1 + n_2 + 1)}{12}} \quad (7)$$

$$Z = \frac{U - \mu}{\sigma} \quad (8)$$

A Standard normal distribution table is used to find the required  $Z_0$  values for different probabilities (or confidence levels). If the calculated  $Z$  is larger than  $Z_0$ , the null hypothesis that both lanes have similar densities is accepted. If the calculated  $Z$  is less than  $Z_0$ , then the null hypothesis is rejected and the alternative hypothesis that the lanes have significantly different densities can be accepted at the corresponding confidence level. Table 6.7 below summarizes the test results for each of the three cells.

**Table 6.7: Mann Whitney Z-Test Density Results**

Confidence Level	99%	95%	90%	80%	75%
Cell 39	Accept Null → IL = OL	Accept Null → IL = OL	Reject Null → <b>IL ≠ OL</b>	Reject Null → <b>IL ≠ OL</b>	Reject Null → <b>IL ≠ OL</b>
Cell 85	Accept Null → IL = OL	Accept Null → IL = OL	Accept Null → IL = OL	Accept Null → IL = OL	Accept Null → IL = OL
Cell 89	Accept Null → IL = OL	Accept Null → IL = OL	Accept Null → IL = OL	Accept Null → IL = OL	Accept Null → IL = OL

The test proves that the outside lane and inside lane of cell 39 have different densities with 90% confidence. However, the test shows that even at the 75% confidence level, the data for the inside lane and outside lane for both cells 85 and 89 cannot be said to be significantly different. In summary, the traffic loading only seemed to influence the density of the porous overlay in cell 39, but did not have a major effect on the full-depth pervious concrete in cells 85 and 89.

#### 6.4.5 Variation in Dissipated Volumetric Rate

The dissipated volumetric rate displayed an even wider range of measurements within a test cell, and followed a very sporadic pattern from season to season. The results from each test were analyzed using the same method for determining the 95% confidence level which was used for nuclear density. The results are shown in Figures 6.60 to 6.62.

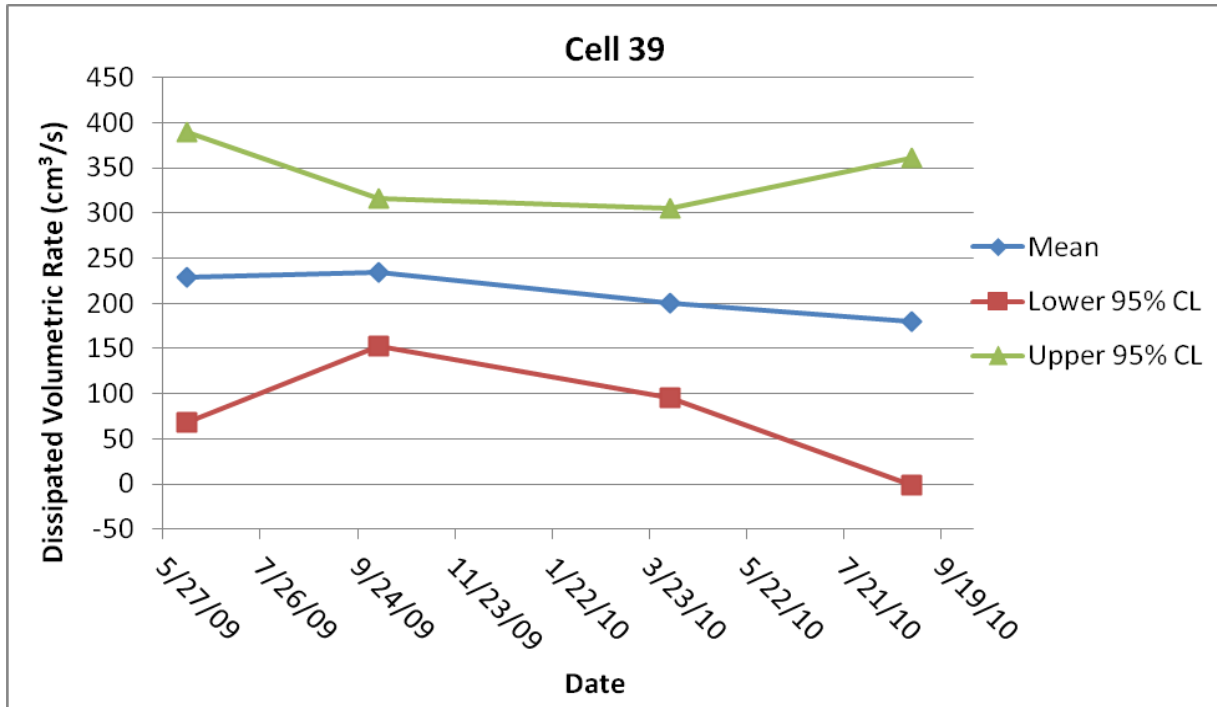


**Figure 6.60: Dissipated Volumetric Rate 95% CL – Cell 39**

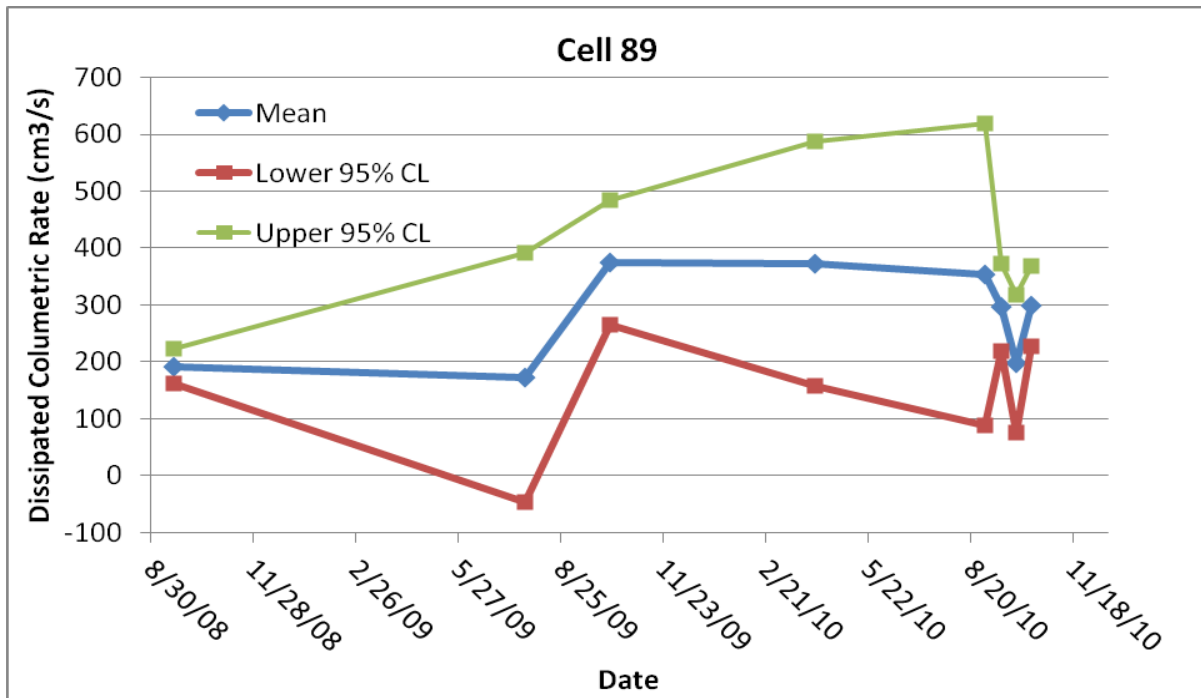


**Figure 6.61: Dissipated Volumetric Rate 95% CL – Cell 89**

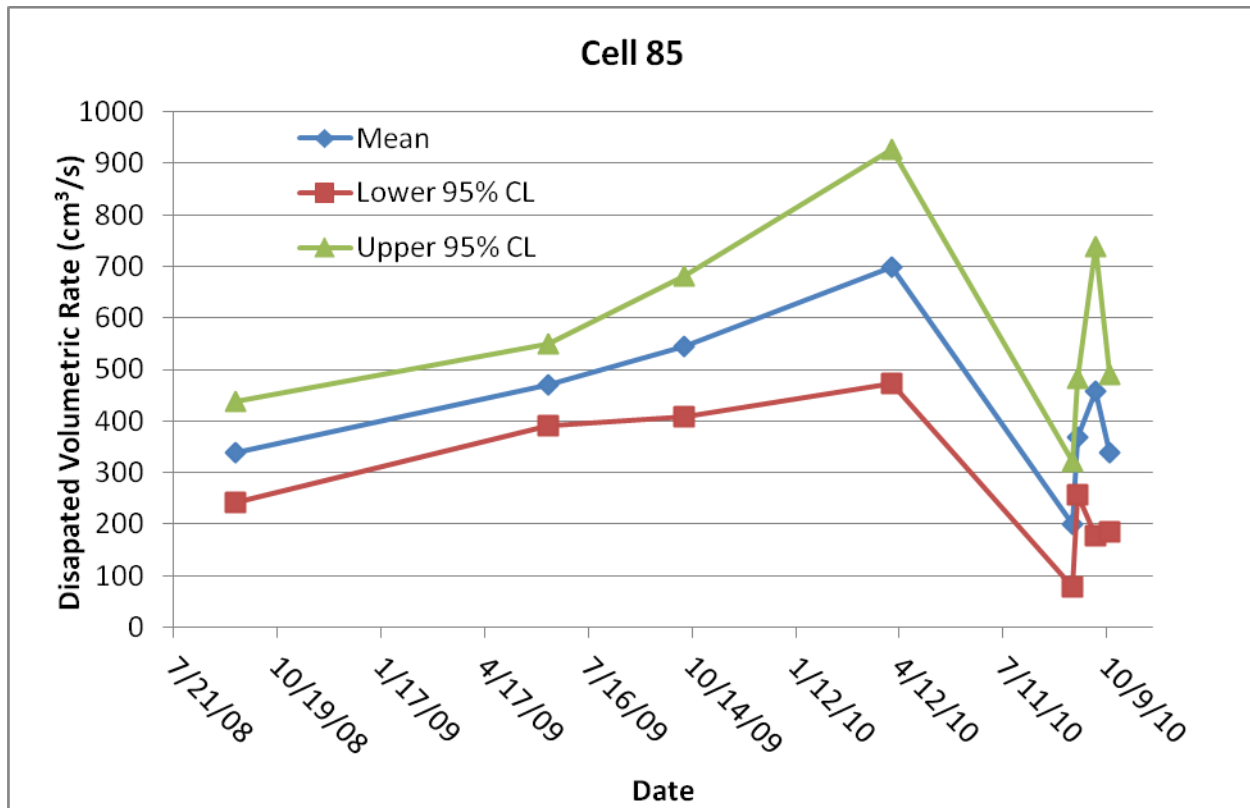


**Figure 6.62: Dissipated Volumetric Rate 95% CL – Cell 85**

This analysis shows how the porosity of the cells largely differs from location to location. Despite the number of tests done for each cell, confidence intervals were found to reach up to 450 cm<sup>3</sup>/s in cell 85 in April 2010. In both Cells 39 and 89 the lower confidence level falls into negative values. This analysis suggests that the porous overlay and pervious concrete mixes used in cells 39, 85 and 89 at MnROAD are a highly variable mix, with uneven consistency throughout the test cells. The typical methods for measuring permeability may not be accurate for pervious pavements because there is significant velocity head that cannot be ignored, unlike in soil systems where the velocity head is so small it is neglected. Neglecting the velocity head converts the Bernoulli Equation to a mere continuity equation, or Darcy's Equation. Instead, the in situ permeameter is therefore a valid device for pervious concrete. Falling head permeability testing may not be an exact or accurate method to relate to the permeability of the pavement. The data collected does not support the theory that removal of clogging agents by vacuuming will increase the sound absorption and drainability of the pavements.

#### 6.4.6 FWD Trend Discussion

The deflection basin plots for the three pervious cells show that there is a strong fluctuation in deflection between test months in 2009. Almost always, however, the deflection reached a minimum in September months. The deflection results for 2010 do not show any very clear trends, although the maximum deflection was most usually measured in April.

More importantly, there doesn't seem to be a trend of either the inside or outside lane showing higher deflections. For cell 39, most of the deflection measurements were fairly similar between lanes for corresponding months. For cell 85, however, the outside lane tended to achieve higher deflections. Finally, for cell 89 the inside lane almost always showed higher deflection. This suggests that the surface deflection of pavements is not necessarily dependent on traffic loading conditions. The section 6.4.8 will look further into the difference in performance between the outside and inside lanes.

#### ***6.4.7 Temperature and Moisture Trends and Comparison***

A large temperature gradient throughout the pavement, base, and subgrade can cause unwanted tensile stresses that are a common cause of pavement warping [5]. Pervious pavement may have the ability to reduce these stresses by promoting better temperature transmissivity. The thermocouple data from cells 39, 85 and 89 were compared to the control PCC cell 87. Cell 87 is a 4 inch PCC pavement with a similar base and subgrade as cells 85 and 89. All three pervious cells have more uniform temperature throughout the pavement, base and subgrade than cell 87.

Also important for cold weather climates like Minnesota is the amount of freeze thaw cycles the pavement experiences. Although there is not an exact procedure to determine freeze thaw cycles in the field, many methods have been developed to approximate their occurrence. A procedure developed in 2006 by MnDOT counted a freeze thaw cycle each time the daily maximum rose above 0°C and the daily minimum fell below 0°C, taking into account the time it takes for change between solid and liquid state [6]. However, the thermocouple plots can be used for a more simple comparison between the pervious and non pervious test cells. Thermocouple plots for Cells 85 and 89 are much more dense with less drastic peaks and drops than cell 87, suggesting the pervious cells experience fewer freeze-thaw cycles.

Watermark sensors can also provide useful data for evaluating freeze-thaw cycles. A phase change from liquid to solid moisture is reflected by a large spike in resistance. When comparing watermark data from the pervious overlay in cell 39 to the full-depth pervious concrete in cell 85, it is clear that moisture freezes at further depths below pervious concrete. Major freeze thaw spikes are only mainly visible in pervious overlay in cell 39, but are seen frequently in the base and subgrade in cell 85. By reducing the moisture gradient, pervious pavement may experience less pavement curling.

#### ***6.4.8 Environmental Versus Traffic Loading***

The following plot shows the how results varied between the inside lane (IL) which was subjected to a traffic load, and the outside lane (OL) which only experienced environmental effects. The shaded cells refer to the inside lane, and the bold cells with larger font represent a significant difference in results between outside and inside lanes.

**Table 6.8: Environmental Versus Traffic Loading**

	Cell 39	Cell 85	Cell 89
Lower IRI	IL	<b>OL</b>	<b>OL</b>
Higher SR	OL	IL	<b>OL</b>
Larger Mean Profile Depth	OL	IL	IL
Higher Friction Number	IL	<b>OL</b>	<b>OL</b>
Less Generated Noise	<b>OL</b>	IL	OL

Although it may be expected that the outside lane show more distress, and consequently higher IRI and lower surface ratings, from the traffic loading, the above table illustrates that this is not necessarily true. In fact, the outside lane gave better results more times than the inside lane. The variability in results suggests that the pavement distress and performance in the pervious test cells can generally be contributed to environmental effects over traffic loading.

The next chapter will use the OBSI measurements to conduct a time series analysis. This analysis will give insight into the long term performance of the three different pervious cells at MnROAD.

## 6.5 Auto-Regression Integrated Moving Average Modeling

### 6.5.1 Time Series Analysis

The last section was concerned with analyzing the data collected over the years to evaluate how the test cells have performed with time in relation to themselves, each other, and other non-pervious cells. However, one of the main goals of this study is to assess the long term performance of pervious pavements. In this chapter, time series analysis will be used to predict the future performance of the test cells based on the observed trends in results obtained thus far. The Auto-Regression Integrating Moving Average (ARIMA) method was used in hope of developing a forecasting model for On Board Sound Intensity levels. The complexity of ARIMA models can take into account the large seasonal fluctuation that the measured OBSI values experienced. If successful, the derived model will display seasonality while still following the general rate of increase (or decrease).

ARIMA models are characterized by three parameters using the notation ARIMA(p,d,q) for each type. In this notation, p is designated as the number of autoregressive terms in the model, d is the number of non seasonal differences used, and q is the number of lagged forecast errors included in the model equation. [7] After testing multiple different ARIMA models, it was concluded that the ARIMA(2,1,0) was most able to fit the measured data and produce reasonable forecasted values that followed the expected trend. The equation below was used to generate the forecasted OBSI.

$$\hat{Y}(t) = \mu + Y_{t-1} + \sigma_1 (Y_{t-1} - Y_{t-2}) + \sigma_2 (Y_{t-2} - Y_{t-2}) \quad (9)$$

$$\hat{Y}(t) = \text{predicted OBSI at test number } t$$

$$Y_t = \text{measured OBSI at test } t$$

$$\mu = \text{average difference in measured OBSI}$$

$$\phi_1 \text{ and } \phi_2 = \text{auto - regressive coefficients 1 and 2}$$

The equation above includes two lags of the measured OBSI data and, consequently, two autoregressive coefficients. To utilize the ARIMA model, it was assumed that the OBSI measurements were taken at equal time intervals, and therefore the dependent variable became the test number,  $t$ . The Solver function in excel was used to determine the autoregressive coefficients which minimized the sum of squared error between the measured and predicted values at test number  $t$ . Different auto-regressive coefficients were calculated for each lane or each cell to create a model that is specific for that location.

Next OBSI predictions for future tests were made from the model using the predetermined coefficients, calculated average difference in the measured OBSI values, and the previous OBSI test values predicted in the optimization step above. For example, for a series of OBSI data that included seven test measurements, the eighth test measurement would be predicted using the OBSI values for tests 5 and 6 that were generated from the model, and not the actual measurements taken.

The following plots show the measured and predicted OBSI values for the inside and outside lanes for cells 39, 85 and 89.

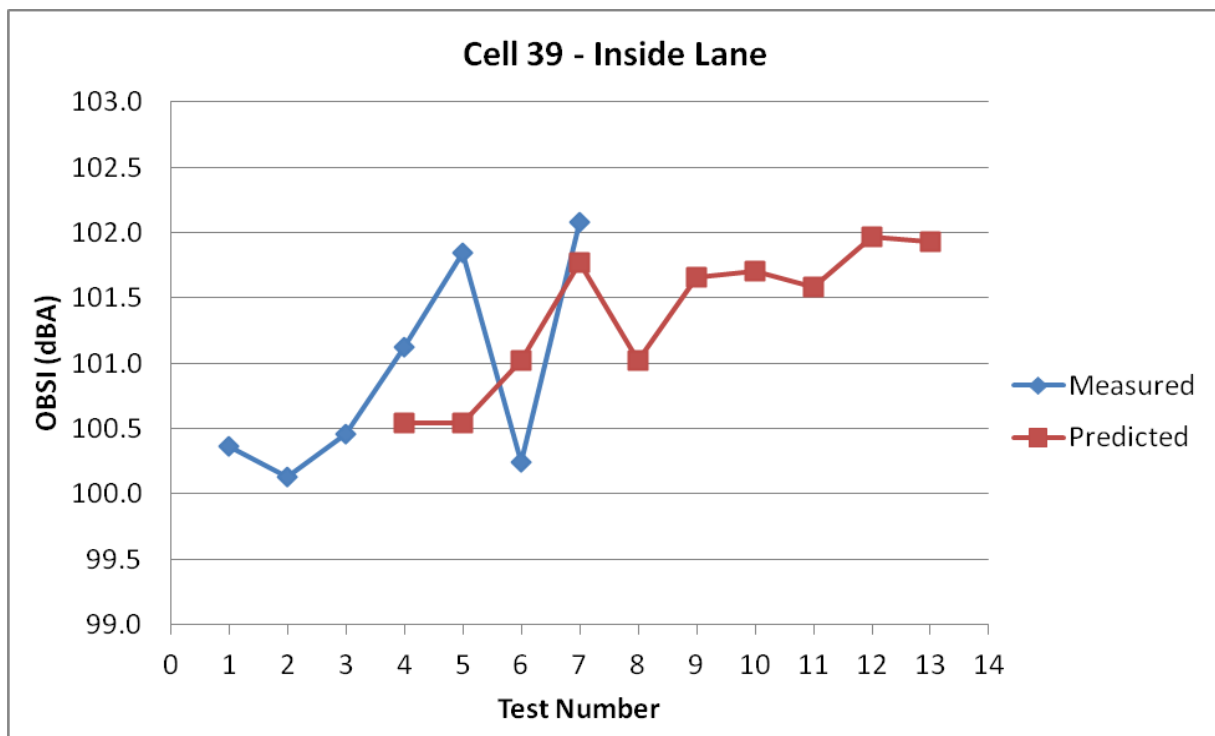


**Figure 6.63: Cell 39 IL Predictions**

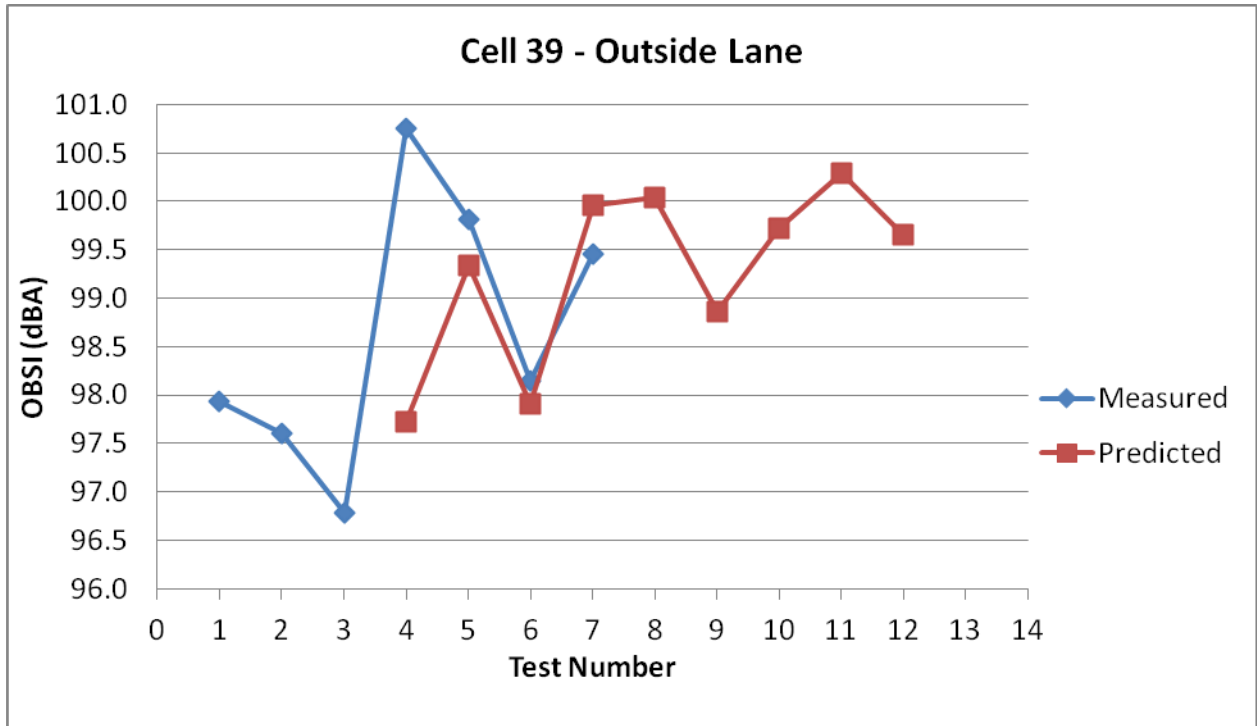


**Figure 6.64: Cell 39 OL Predictions**

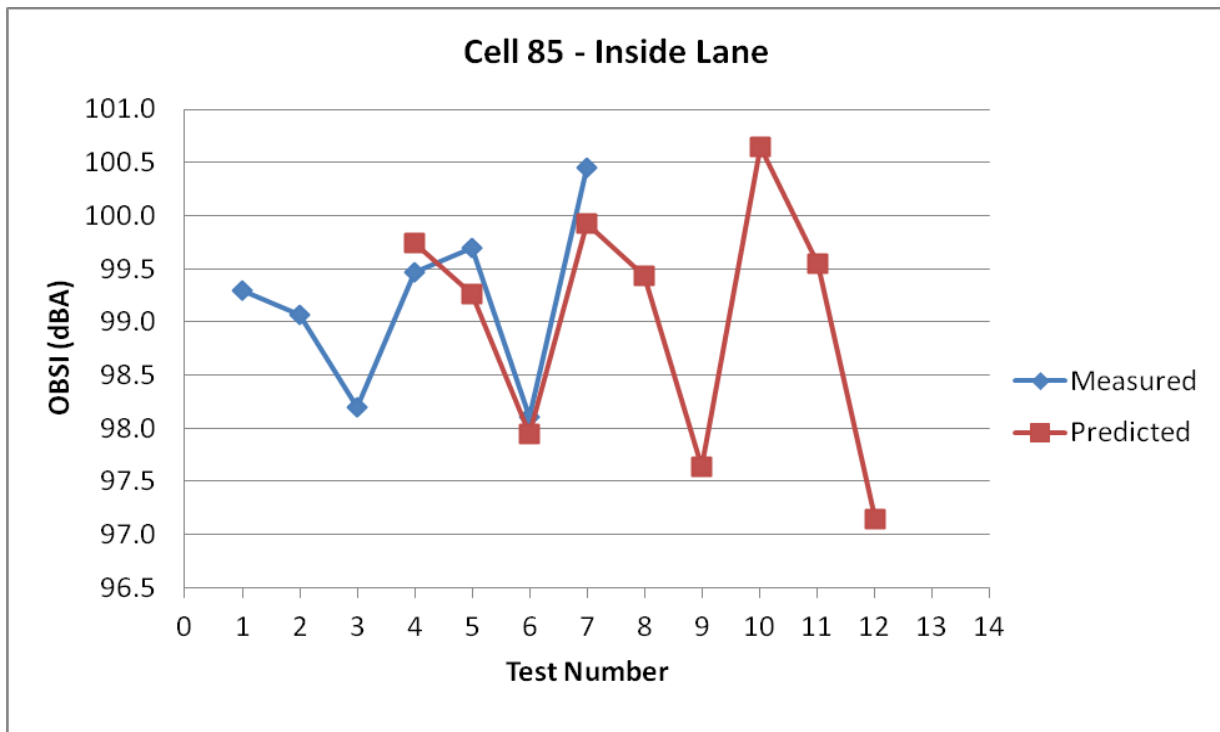


**Figure 6.65: Cell 85 IL Predictions**

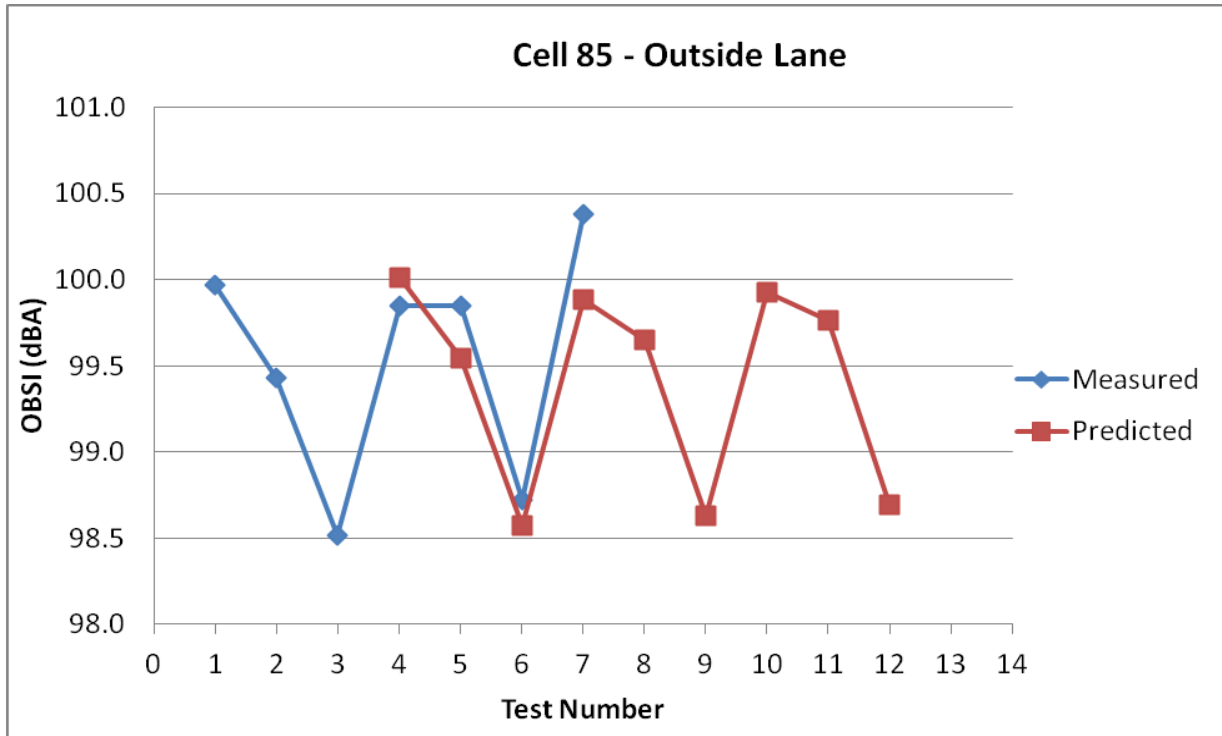


**Figure 6.66: Cell 85 OL Predictions**

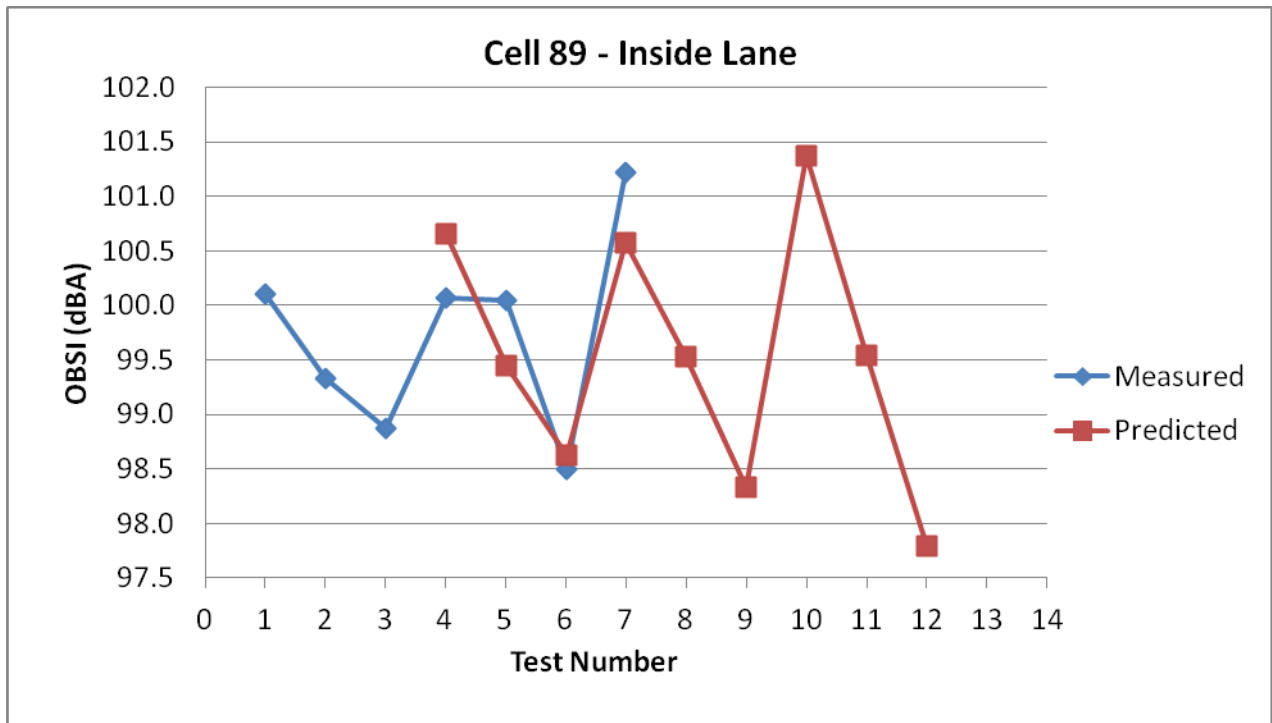


**Figure 6.67: Cell 89 IL Predictions**

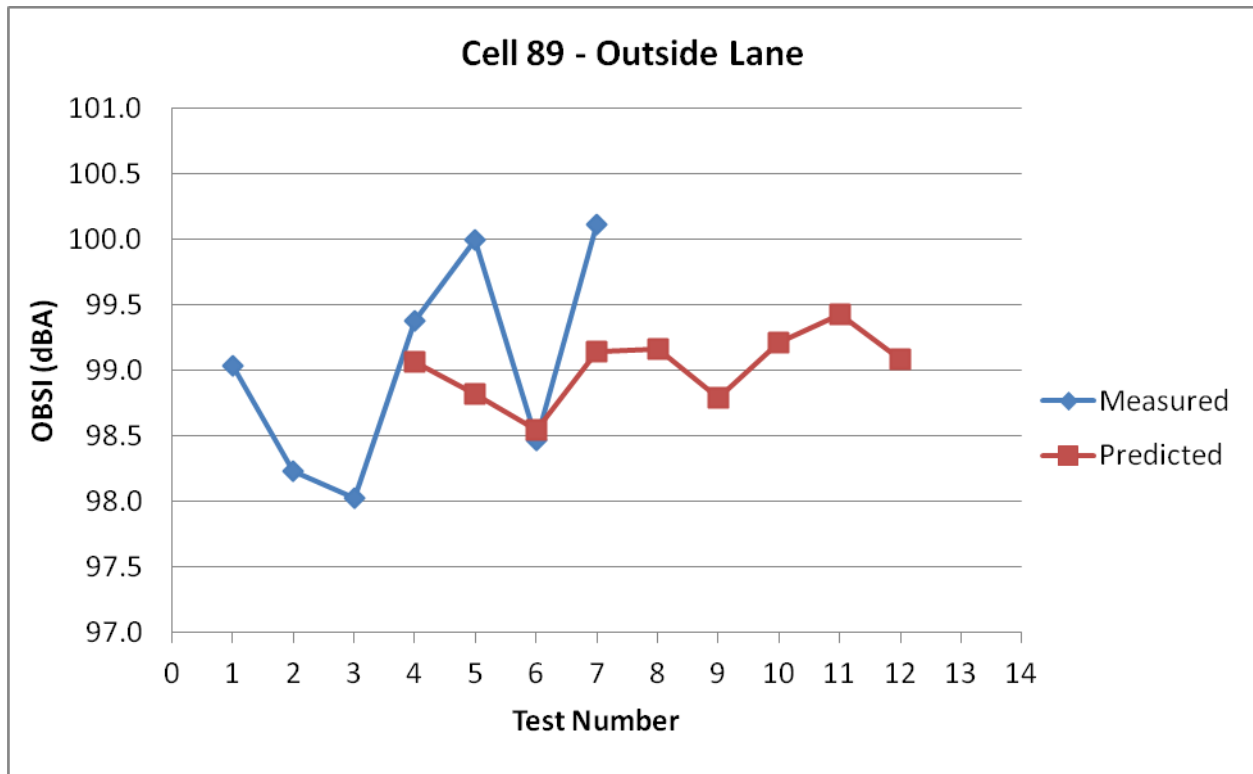


**Figure 6.68: Cell 89 OL Predictions**

The limited number of data points collected thus far gave little information to help fit an accurate model. As seen in the inside lane of both 85 and 89, the model projects an increased fluctuation between tests with time. However, all other models show an increase in OBSI over time, while still following a reasonable seasonal variation.

To better gauge how accurately the data may be represented by the above ARIMA models, the autocorrelation coefficient was determined for each data set. The autocorrelation coefficient is used as a measure of the correlation of time series with its own past and future values. [8] It refers to the tendency of an OBSI values to depend on previous measurements. Equation (5) below was used to calculate the autocorrelation coefficient ( $r$ ) for each data set taken from , using the same notation as equation (4) [8].

$$r = \frac{\sum_{t=1}^{N-k} (y_t - \bar{y})(y_{t+k} - \bar{y})}{\sum_{t=1}^N (y_t - \bar{y})^2} \quad (10)$$

$k$  = number of lags

$\bar{y}$  = mean of all OBSI measurements

$N$  = number of OBSI measurements

As stated above,  $k$  refers to two lags for all of the data series. The autocorrelation coefficients for both the inside and outside lane of the three pervious cells are given in table 6.8 below.

**Table 6.9: OBSI Autocorrelation Coefficients**

Cell	39	85	89
Inside Lane $r$	0.163	-0.076	-0.135
Outside Lane $r$	-0.268	-0.280	-0.096

These autocorrelation coefficients are compared to the two-sided 95% confidence limits to determine if using two lags of data in the prediction equation will give probable results, or if more lags may be necessary. The upper and lower confidence limits (CL) were calculated using equation (11) below taken from Salas [9].

$$CL = \frac{-1 \pm 1.96\sqrt{N - k - 1}}{N - k} \quad (11)$$

Using the same notation as equations (5) and (6) above with  $N=7$  for all data series, the upper and lower confidence limits were calculated as 0.586 and -0.984 respectively. Because all of the calculated autocorrelation coefficients were between these limits, it is assumed that two lags is an appropriate number for the prediction equations

In summary, the ARIMA models developed for the porous overlay in cell 39, and the pervious full-depth concrete in cells 85 and 89, all show a general increase in OBSI overtime. Once more data has been collected, the analysis will be revisited and the models will be updated to develop more accurate predictions.

## 6.6 Chapter Summary

This report gives a technical performance summary of the three pervious concrete test cells at MnROAD: the porous overlay in cell 39, and the full-depth concrete cells 85 and 89. The construction and cell overview was given in the introduction and chapter one of this report. Ride characteristics, surface properties, noise characteristics, temperature, moisture and other physical properties of the three test cells were measured periodically to evaluate the performance of the pervious pavement. The data collected from the time of construction in 2008 until 2010 was presented in chapter 3. The notable trends from analysis of the results are given in the list below.

### 6.6.1 Surface Characteristics

- There was only a very slight increase in IRI and decrease in SR over the two years.
- The IRI values were much higher than typical pavements in Minnesota, and did not meet the FHWA standards for acceptable pavement. This may be due to the fixed-form paving method used.

- The surface ratings of all cells continue to meet MnDOT requirements for “good” pavement.
- All friction values were well above the minimum required for adequate skid resistance and driver safety.

### **6.6.2 Noise Characteristics**

- OBSI experienced a general increase during summer months, with a slight overall increase over the two years monitored. The 1/3 Octave Bands were not significantly affected by test location throughout all three cells, or between the test runs at a single location.
- Sound absorption did not experience any major variation during the first two years. However, results showed that the ratio of porous to non-porous sound absorption coefficients is highly dependent on sound frequency. Sound absorption was improved in pervious test cells when compared to other non-porous concrete at MnROAD,

### **6.6.3 Physical Properties**

- Analysis shows that the Dissipated Volumetric Rate varied between cells. Between the two full-depth pervious cells (85 and 89), the granular base achieved higher flow rates than the clay base. As expected, the porous overlay continually achieved the lowest flow rate.
- Dissipated volumetric rate varied significantly between locations within a cell, suggesting uneven pavement consistency and void structure.
- Vacuuming of the pervious concrete did not provide a distinguishable improvement in dissipated volumetric rate and sound absorption.
- Results from FWD testing suggest the surface deflection is highly variable between seasons, with the minimum deflection usually during fall and winter months.
- Thermocouple and watermark sensors show that pervious pavements can reduce temperature and moisture gradients, helping to prevent unwanted warping and curling.

When considering all performance tests, neither the outside traffic lane nor inside environmental lane showed superior performance. Results support the theory that traffic load is no longer the major contributing factor in pavement distress, as most issues and reduced pavement performance and service life are a result of environmental effects.

Time series analysis was done on all OBSI data collected from 2008 through 2010. Autoregressive integrated moving average modeling was used to forecast OBSI measurements for each lane of each cell. These models showed a general increase in OBSI with time. However, the limited amount of data available makes these models very rudimentary predictions. Once more data has been collected, the models should be modified for more accurate forecasts. As monitoring of the pervious concrete test cells at MnROAD continues, time series analysis may also be done on other properties to further understand the long term performance.

## CHAPTER 7 IMPLEMENTATION

Since the construction of the MnROAD pervious test cells, a few implementation projects using pervious concrete have been completed in the region. Pervious concrete has been used in both Shoreview and Detroit Lakes. *Please note that in this chapter, dissipated volumetric rate measured from the falling head permeameter is referred to as permeability. The dissipated volumetric rate is not actually equivalent to permeability, but is simply a measure that can generally correlate to permeability.*

### 7.1 Detroit Lakes

Pervious concrete was used to construct a driveway for a boat entrance. The figures below show the finished driveway and pavement surface.



**Figure 7.1: Detroit Lakes Pervious Concrete**



**Figure 7.2: Detroit Lakes Pervious Concrete Surface**

Permeability was tested with the falling head permeameter described in section 6.2.4. The device was used following the same method and measured the dissipated volumetric rate at 19 different location on the driveway. The results are shown in figure 7.3 below. As is illustrated in this figure, the flow rate was highly variable throughout the driveway. Some areas showed negligible permeability, whereas others had a measured flow rate of almost 700 cm<sup>3</sup>/s.

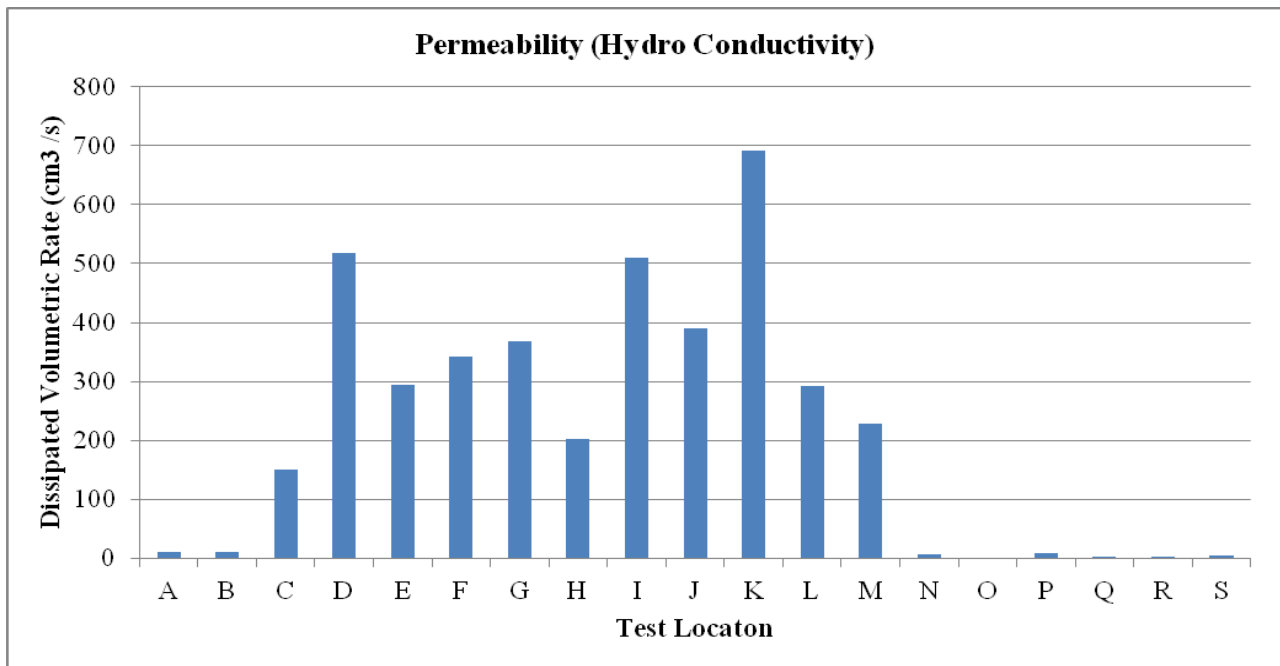


**Figure 7.3: Detroit Lakes Pervious Concrete Permeability**

Sound absorption was also monitored using the impedance tube described in section 6.2.3. The sound absorption coefficient for 18 different locations corresponding to those tested for permeability. The graph below in figure 7.4 shows the third octave narrow band sound absorption coefficients for each location. There is a visible spike in the sound absorption at multiple locations at 800 hz. This may suggest that pervious pavements can reduce tire-pavement interaction noise at frequencies close to those most easily heard by the human ear (easiest is 1000 hz).

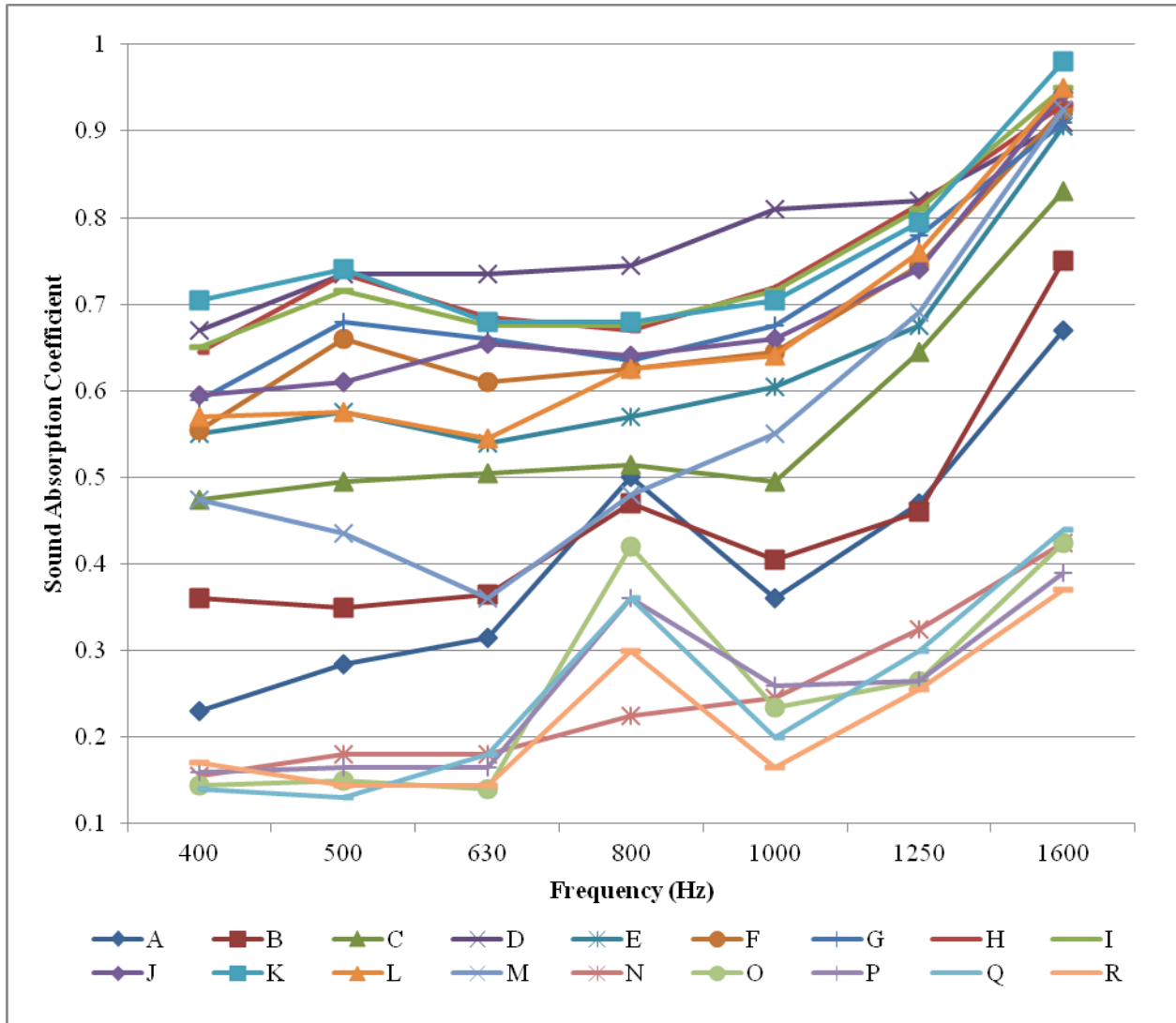


**Figure 7.4: Detroit Lakes Pervious Concrete Sound Absorption**

## 7.2 Shoreview

Another implementation of pervious concrete can be found in Shoreview, MN. Pictures of this neighborhood roadway and pavement surface can be seen in figures 7.5 and 7.6 below.



**Figure 7.5: Pervious Concrete in Shoreview**

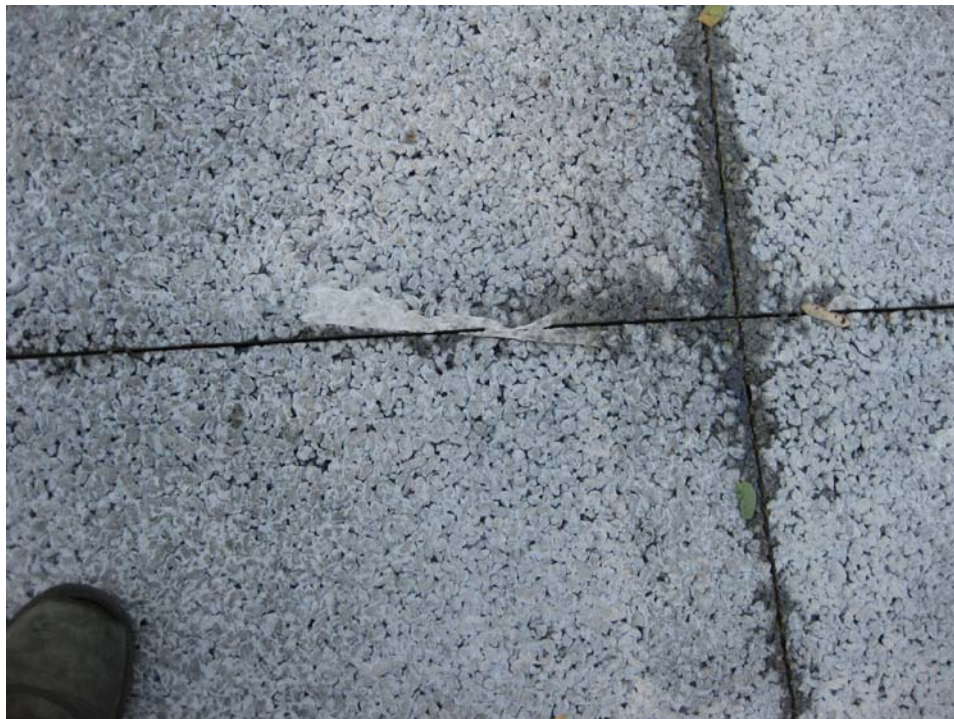


**Figure 7.6: Pervious Concrete Surface in Shoreview**

Sound absorption and permeability were measured by the same methods described in sections 6.2.3. and 6.2.4 of this report. These properties were measured in both 2010 and 2011 for comparison. The results from this testing is shown in figures 7.7. and 7.8 below.

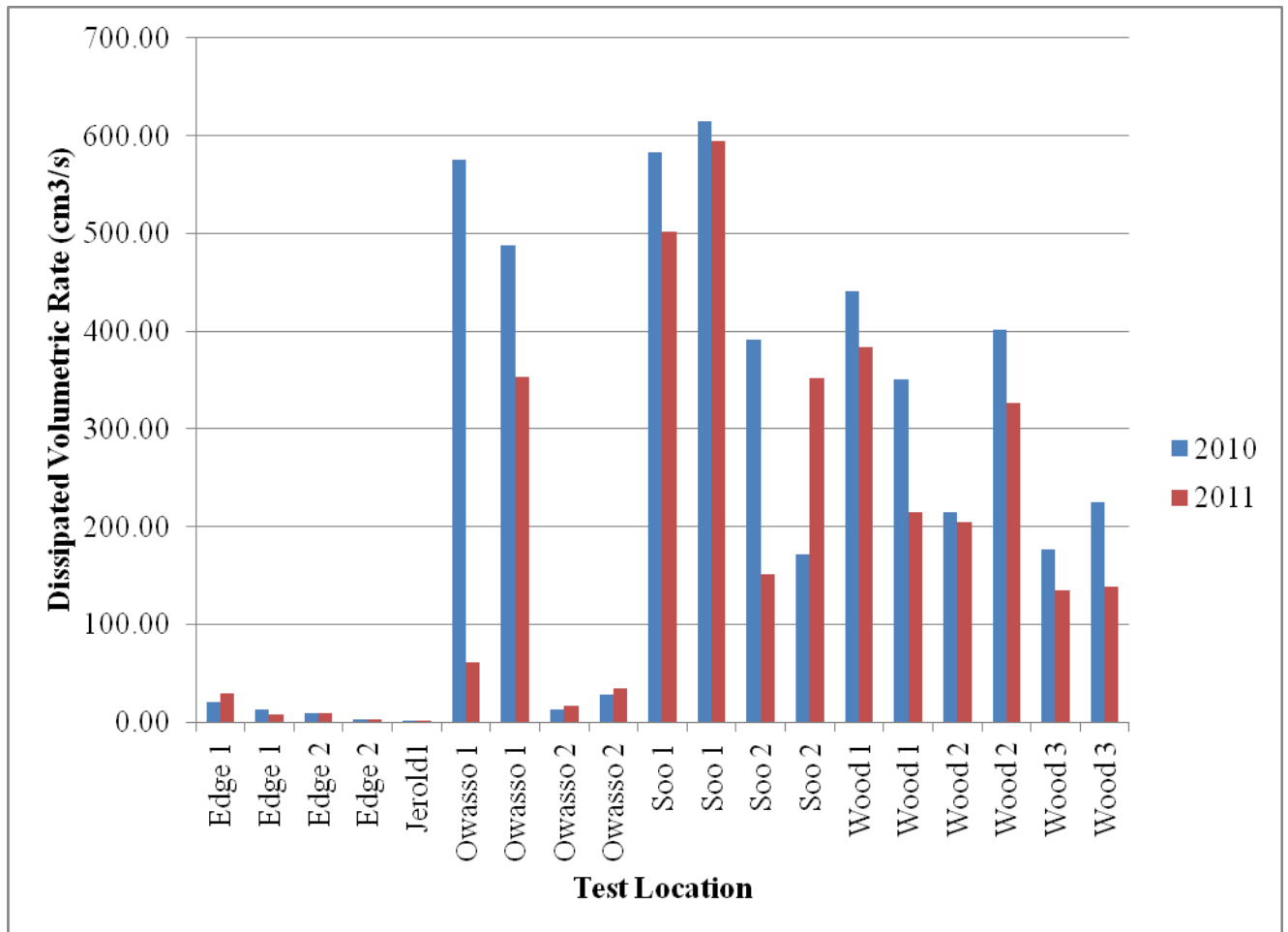
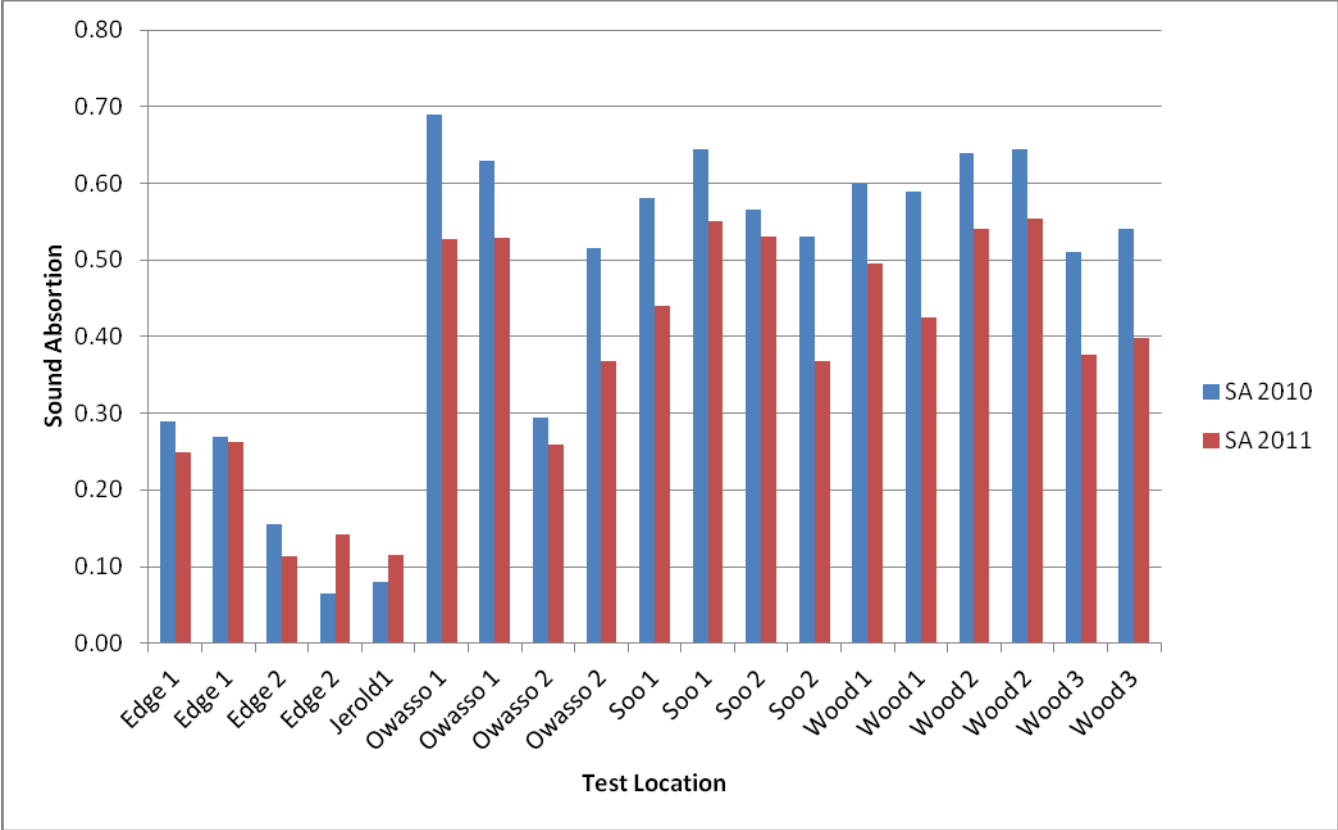


Figure 7.7: Shoreview Pervious Concrete Permeability

**Table 7.1: Shore Test Location Description and Permeability**

Test Location	Name	Lane	Dissipated Volumetric Rate (cm <sup>3</sup> /s)		Change in Dissipated Volumetric Rate (cm <sup>3</sup> /s)
			2010	2011	
Jerold Avenue near corner of Soo	Jerrold 1	Centerline	1.34	48.03	46.69 increase
Edgewater Avenue near # 175	Edge 2	Eastbound	8.93	8.84	25.74 increase
	Edge 2	Westbound	3.29	2.51	12.99 increase
Edgewater Avenue near corner of Woodbridge	Edge 1	Eastbound	21.11	29.55	332.64 increase
	Edge 1	Westbound	13.23	7.45	47.53 increase
Owasso Lane near #196	Owasso 2	Southbound	12.9	34.68	125.89 increase
	Owasso 2	Northbound	28.09	16.29	106.87 increase
Woodbridge Street on curve	Wood 3	Southbound	177.2	138.79	37.39 increase
	Wood 3	Northbound	225.05	134.96	159.10 increase
Soo Street near corner of Jerold	Soo 2	Northbound	390.9	151.14	239.76 decrease
	Soo 2	Southbound	171.57	352.19	180.62 increase
Woodbridge Street near #3232	Wood 2	Southbound	214.84	326.62	206.00 decrease
	Wood 2	Northbound	400.95	204.41	398.43 decrease
Woodbridge Street near #3257	Wood 1	Southbound	440.3	214.59	410.75 decrease
	Wood 1	Northbound	351.13	384.16	343.69 decrease
Owasso Lane near #224	Owasso 1	Southbound	574.72	353.74	248.10 decrease
	Owasso 1	Northbound	488.17	60.77	283.76 decrease
Soo Street near corner of Edgewater	Soo 1	Northbound	583.12	501.73	81.39 decrease
	Soo 1	Southbound	614.79	594.41	20.38 decrease



**Figure 7.8: Shoreview Sound Absorption at 1000 Hz**

It is evident that the Shoreview pervious pavement, like the pervious concrete driveway in Detroit Lakes, has highly variable permeability and sound absorption. Figures 7.9 and 7.10 illustrate how sound absorption and permeability typically dropped from 2010 to 2011. This implies that there was clogging of the pore structure which may have been caused by raveling at the surface or other debris entering the pavement, consequently hindering flow through the pavement and reducing the sound absorption capability. A detailed report on how clogging of pervious concrete can affect the performance and noise characteristics is included in Appendix N. This report also describes important maintenance activities for pervious concrete, such as vacuuming, and how these activities affect the performance relative to ride, noise and flow properties.

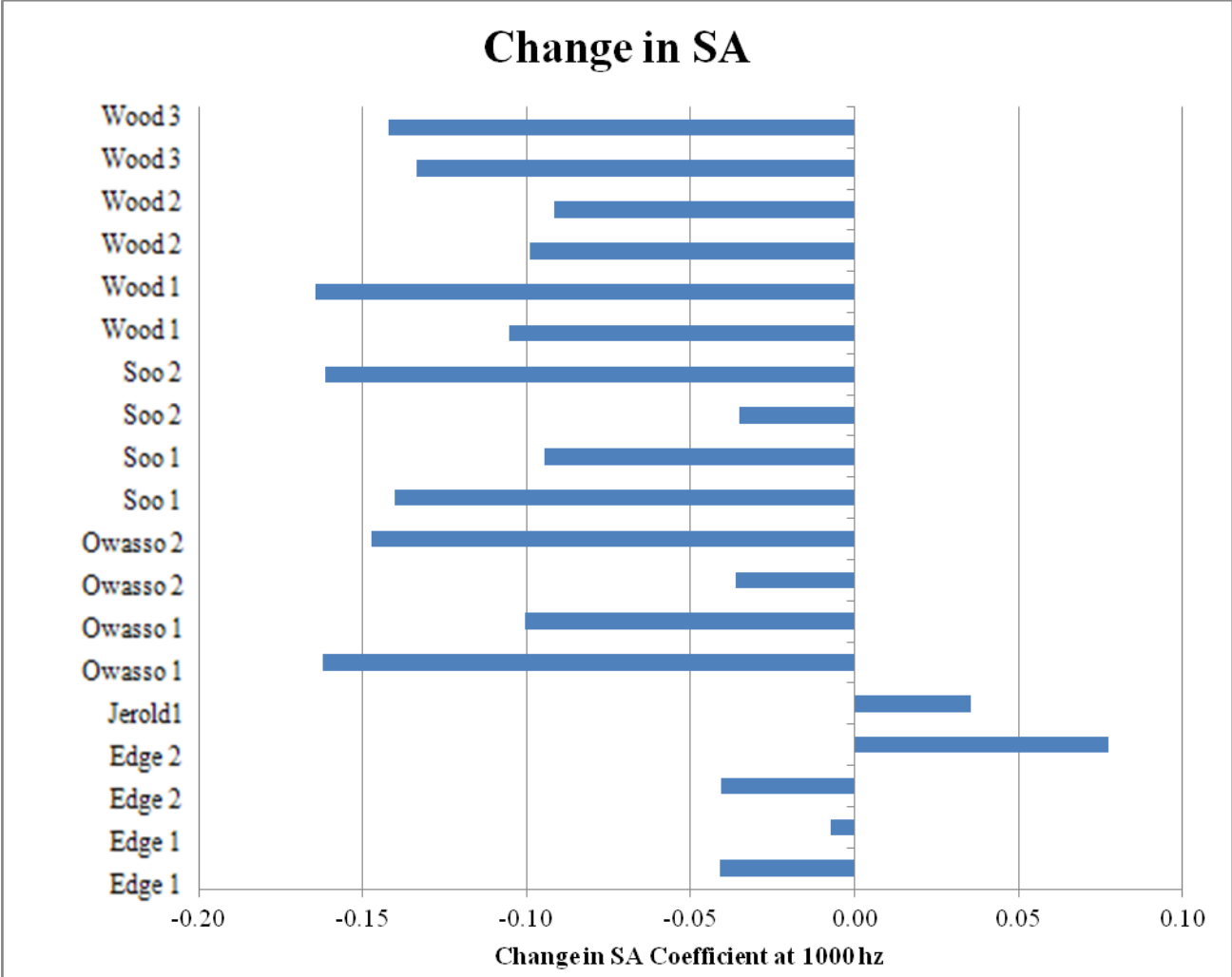


**Figure 7.9: Change in Shoreview SA from 2010 to 2011**

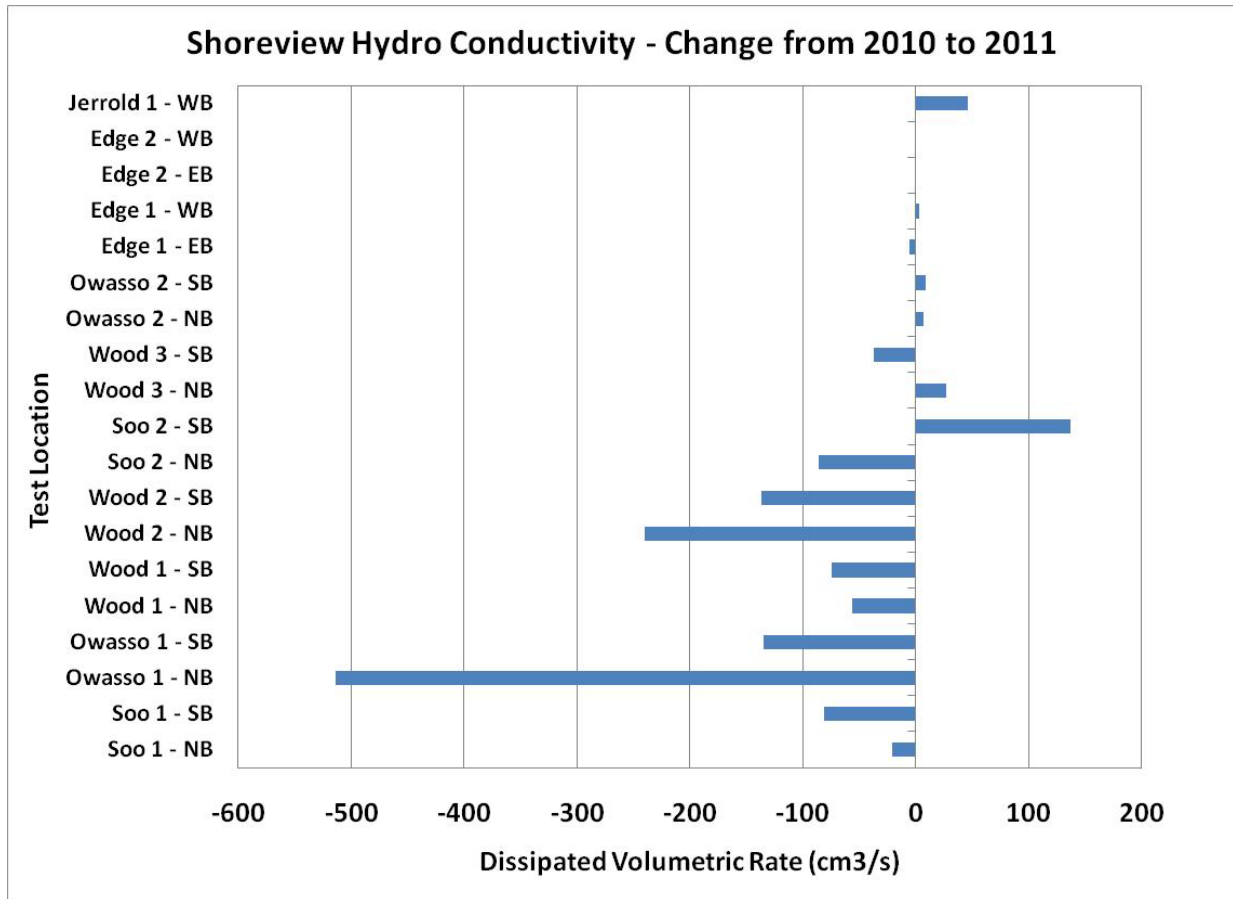


**Figure 7.10: Change in Permeability from 2010 to 2011**

### 7.3 Relation of Sound Absorption to Permeability of Pervious Pavements

Figure 7.11 illustrates how sound absorption of pervious pavements correlates to permeability of pervious pavements. It investigates whether the pore structure which influences flow through the pavement has a similar effect on how well the pavement can absorb sound. Through many trials it was found that the two properties are most closely related through a logarithmic equation. The plot shows four data sets for sound absorption-DVR measurements: Shoreview in 2010, Shoreview in 2011, Detroit Lakes in 2010, and all of the data combined.

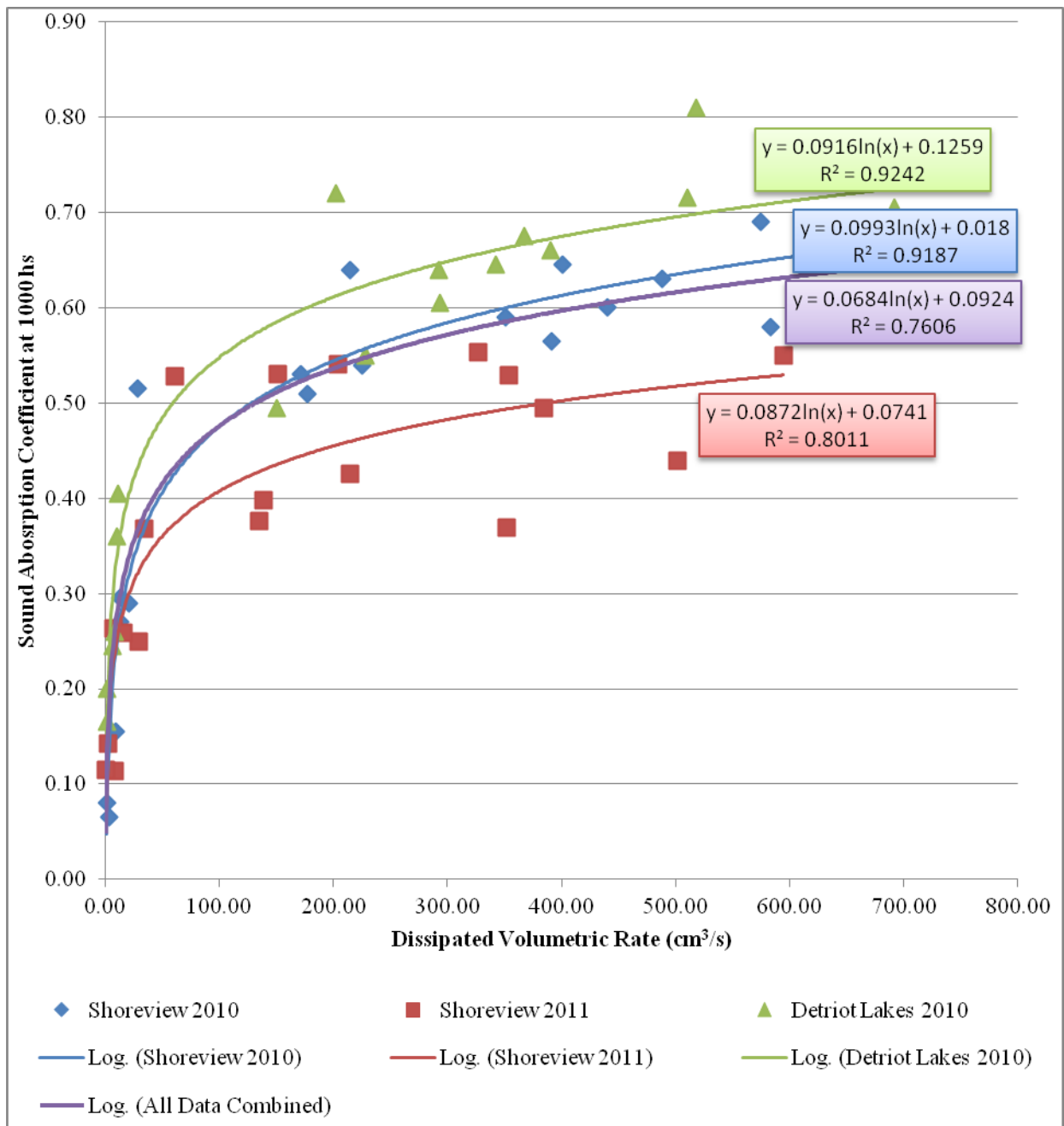


**Figure 7.11: Sound Absorption Versus Dissipated Volumetric Rate**

Although each data set produced a different logarithmic equation, the  $R^2$  values which gauge the accuracy of the model (more accurate close to 1) and the coefficients of each equation are fairly similar. This suggests that there may be a direct relationship between these two important properties of pervious concrete. Further evaluation of different pavements should be done to help determine if more accurate models can be developed.

## CHAPTER 8 EFFECT OF SOUND ABSORPTION COEFFICIENT ON TIRE PAVEMENT INTERACTION NOISE

### 8.1 Introduction

Tire pavement interaction generates noise from one of many mechanisms that occur at the tire pavement interface. These mechanisms are either noise generating or noise amplifying. Noise generating mechanisms are the Stick-slip phenomena, the snap-stick phenomena, the thread-block acceleration, and the thread-block-impact mechanism (1). Amplification mechanisms include the horn effect and resonant-frequency-induced tire-carcass vibration. The known sound-generation mechanisms are predominantly dependent on thread-block impact sliding rolling or suction at the tire pavement interface. They are therefore associated with the forces presenting at the tire pavement interface. These mechanisms are briefly discussed.

Izevbekhai (2) observed the reduction of trailing edge microphone sound intensity when pavements are porous. This advantage is attributed to relief of air compression. It was not clear if sound absorption was partly responsible for the noise reduction.

The thread block phenomenon is generated by the impact of the tire asperities on the pavement surface similar to the impact of a mallet on a surface (Sandberg et al 1). By randomization and disorientation of tire thread-block array the tire industry has minimized thread block impact phenomena. The tire thread block acceleration is a unique noise generated similar to a body that is vectorially accelerating when moving. In tire-pavement interaction, slip-snap and stick snap generation mechanism are associated with hysteresis phenomena and with the characteristics of rubber friction. A rolling tire experiences localized instantaneous collapse at the contact patch but this interfacial contact is released more rapidly than the tire would allow, thus causing negative pressures and suction. This phenomenon, which is generally associated with hysteresis friction (3), where it has extensively been analyzed, is responsible for the noise generating stick snap slip stick snap phenomena (1).

Sound absorption coefficient varies with the frequency and the angle of incidence. A diffusive surface splits the reflected sound wave in many directions. In acoustics design, diffusivity of the surface is enhanced by using various textures and curved surfaces. This knowledge has not been utilized in pavement design but current research showed that corrugation of some porous surfaces did enhance their sound absorption coefficient (4). Many experiments have been performed to examine the trend of peak absorption of porous pavements with respect to frequency. These include the work of Sandberg et al (1), Kuemmel et al (5) Nelson et al (6) and Crocker et al (7) who measured acoustical absorption coefficients of more than 140 pavement cores.

Nelson et al obtained acoustic impedance data with the impedance tube method with two microphones and cross-spectral analyses. They further examined the effectiveness of the impedance tube in predicting noise reduction for different mixes by comparing the correlations between onboard sound intensity levels and absorption. Theoretical predictions of acoustical absorption due to friction between air and porous matrix and thermal relaxation were compared with measured results for an idealized porous structure. The model was used to determine

porosity, tortuosity, and pore size from measured acoustical absorption spectra for porous asphalt. Crocker et al (7) studied the absorption coefficients of dense and porous road surfaces through cores tested in the laboratory using 4-in and 6-in.-diameter impedance tubes and with the impedance tube mounted vertically in-situ on the pavement surfaces. The diameter of the tube determined the range of frequencies that the absorption test may examine. The 6-in. tube allows the absorption of a large core sample surface to be determined, but only up to a frequency of about 1,250 Hz. The 4-in. tube allows the absorption coefficient to be determined up to a frequency of about 1,950 Hz. They mounted the two different diameter impedance tubes on each pavement type to determine absorption coefficients of these pavement types. The measured peak sound absorption coefficients suggested that the first peak frequency and peak absorption coefficient were slightly different for fine- and coarse-mix aggregate porous surfaces. Because the fine-mix aggregate porous surface is smoother, it is preferred because it should result in less tire-tread impact noise and thus lower overall tire noise than the coarse aggregate surface. The results thus recommended an optimum porous surface between 1.5 and 2.0 in. thick for the type of porous surface examined particularly for a peak absorption frequency of about 1,000 Hz to be most effective at reducing the Interstate highway noise of automobiles.

Sandberg (8) discussed the tendency of a cluster of optima of tire pavement noise phenomena around 1000-Hz (700-1300-Hz) as a “multi-coincidence peak”. Their research indicated this as the characteristic frequency range for most tire pavement interaction features at freeway speeds. This is particularly important in the evaluation of porous pavements. A change of the peak frequency due to a porous surface or any surface treatment is one mechanism of effectiveness. Occasionally in pavement treatments, there is no change in resonant frequency but there is still a quiet pavement advantage. The paper also identified and examined this peak, analyzes its causes and suggested some noise reduction possibilities. They attributed the concentration of noise emission on that frequency range to a number of coinciding factors, which are described in the paper. They include: Tread pattern pitch, pipe resonances, tangential block resonances, belt resonances, and the horn effect and road texture geometry. The elimination or modification of these frequency-coincident factors, aimed at a mismatching the parameters, will be the key issue in order to effectively reduce tire/road noise generation. (8) Moreover, recent developments in tire design, dictated by concerns other than exterior noise, have tended to increase the concentration. This a challenge facing both tire and road engineers in the near future. (8)

Although Crocker et al and Nelson et al indicated that the more porous pavements were quieter in terms of OBSI; they did not develop correlative curves for OBSI and sound absorption. This research and analysis provided the unique advantage of addressing that deficiency. There has are various types of absorption (8) that are broadly categorized into porous and non-porous absorption. Non-porous absorption is associated with resonant absorption, as the latter does not depend on the properties of the material but on prevalent frequencies. The two types of resonant absorption are Cavity (HelmHoltz Resonators and membrane resonators.

Kohler et al (7) showed that porous pavements attenuate sound by the friction between the air mass and the cavities when the surface is acoustically open and the core has air filled pores. Porous pavements suppress noise of various frequencies with the porous sound absorption mechanism. (7) On the contrary, sound absorption by the cavity resonator phenomenon maximizes absorption at a determinable resonant frequency. A resonator consists of a narrow air

opening connected to a larger air volume. According to a publication by Isover (8), and Horoshenkov, K.V et al, (10) an open narrow necked bottle may be regarded as a cavity resonator. The porous pavement surface is a combination of side-by-side arrangement of resonator openings if the matrix air voids are interconnected. Reasonable estimate idealizes the surface openings as connected to one large volume of partially enclosed air.

## 8.2 Porous Pavement Sound Absorption Theory

When the tire rides over a porous pavement, there is initial compression of the air at the orifice of the cavities, this causes a displacement in the volume and the resonant frequency at which absorption is maximized is given by the following equation (9).

$$f_o \approx \frac{c}{2\pi} \sqrt{\frac{S}{V(l + \pi b / 2)}} \dots\dots\dots 1.1$$

$f_o$  = resonant frequency

$c$  = Speed of Sound

$S$  = Surface area of each cavity

$V$  = Volume of void

$l$  = Aggregate diameter

$b$  = average surface void radius

If  $C = 340$  m/s and the diameter of aggregate is  $\frac{1}{2}$  inch,  $l$  is approximately  $\frac{1}{2}$  inch and  $b$  is approximately  $\frac{1}{4}$  inch.  $F_o$  is ranges from 700 to 1350-Hz based on variation of aggregate size and void size combinations. This equation provides an indication for any design modification for quiet pavements. Important parameters in this direction include  $S/V$  and  $l + \pi b$ . Such design adjustments would shift the resonant frequency from the multi coincidence peak.

The peaks of acoustic absorption occur at frequencies that can be calculated according to the relationship

$$F_{\text{peak}} = nc/4l$$

where  $f_{\text{peak}}$  is the frequency at peak absorption,  $n$  is an odd integer number corresponding to the peak (1 for 1st peak, 3 for 2nd peak and so on),  $c$  is the effective speed of wave in the medium (343 m/s for air at 20oC), and  $l$  is the thickness of the sample.

Horoshenkov, K.V (10) also showed that up to 25% surface perforation the absorption of an absorber increases with degree of perforation. Subsequently they observed that the absorption curve almost coincides with the absorption curve of the mineral wool that filled the perforation. When extended to a pavement at 25 % porosity that was typical of the porous pavements tested at MnROAD, an optimum sound-absorption performance is expected. This 25 % porosity also

coincides with the maximum porosity that does not compromise mechanical properties of the pavement.

Based on the work of many authors (1,2,3,4,5,6,7,8,9, 10) Sound absorption coefficients in a frequency domain are relevant to design of quiet pavements particularly if the noise generation and amplification mechanisms are understood.

### 8.3 In-Situ Data Collection

#### 8.3.1 Objective

This chapter discusses in-situ sound absorption tests conducted on some pavements in the MnROAD test Facility and the accompanying analysis performed. It identifies component parameters of sound absorption for non-porous and porous pavements while examining the place of porosity in sound absorption. Finally, it discusses the implication of sound absorption on On-Board-Sound-Intensity

The main parameters, sound absorption coefficient and On-board sound intensity are hereby defined. The data collection process for in situ Sound Absorption (sub section 2.2) and On-Board Sound Intensity (sub section 2.3) are discussed in this section.

#### 8.3.2 Definitions

##### 8.3.2.1 Sound Absorption Coefficient

Sound Absorption Coefficient ( $\alpha$ ) is the ratio of the absorbed sound energy to the transmitted sound energy when a white noise of frequency ranging from 315 to 1800 Hz is projected into the pavement within an impedance tube placed normal to the pavement surface.

##### 8.3.2.2 On Board Sound Intensity (OBSI)

On-Board-Sound-Intensity (OBSI) test is a dynamic test that records the pavement-tire interaction noise from the contact patch alone at 60 miles per hour. A set of sophisticated microphones installed near the contact patch facilitates this unique property. The leading edge microphone captures the leading edge while the trailing microphone captures the trailing edge.

The AASHTO TP 76-08 interim procedure (11) describes the OBSI protocol used in this experiment. The OBSI parameter is the logarithmic sum of sound intensity at each of the designated frequencies of 250, 315, 400, 500, 630, 800, 1000, 1250, 1600, 2000, 2500, 3150, 4000 and 5000 Hz.

$$\text{OBSI} = 10 * \log [10^{\{SI_1/10\}} + 10^{\{SI_2/10\}} + \dots + 10^{\{SI_{14}/10\}}] \dots \dots \dots 1.1$$

Where  $SI_i$  ( $i=1, 2, 3, 14$ ) are sound intensities in dB at each the frequencies.

It is important to consider existing tire pavement interaction correlations including OBSI, sound absorption and MTD.

#### **8.4 Results of Sound Absorption Testing**

Initial sound absorption testing of the porous and non porous cells was performed in November 2008. Results are shown in table 8.2. Subsequent sound absorption and OBSI testing were conducted in the spring summer and fall of 2009. The summary statistics for the porous pavements as well as the non porous pavements are shown in table 8.2. A mean OBSI of 98.9-dBA observed in porous pavements is 3.8 dBA lower than the mean of 102.73-dBA observed in non porous pavements. The quietest test data in the porous pavements (97.1-dBA) is 2-dBA lower than the quietest non porous OBSI of 99.1dBA. Conversely, the mean sound absorption coefficient of porous pavements (0.456 dBA) is 20 times as high as the sound absorption coefficient of 0.029 observed in non-porous pavements. The lowest porous sound absorption observed was 0.21 and 0 respectively for porous and non-porous cells and the maximum observed were 0.75 and 0.17 (table 8.1) respectively. Consequently there was no overlap in the range of observed sound absorption between porous and non porous pavements , whereas there was a significant overlap of the OBSI values.

**Table 8.1: Descriptive Statistics Comparing Porous to Non-Porous Sound Absorption and OBSI**

	OBSI		SOUND ABSORPTION	
	Porous	Non Porous	Porous	Non Porous
<b>Mean</b>	98.947	102.727	0.456	0.029
<b>Standard Error</b>	0.082	0.114	0.007	0.003
<b>Median</b>	99	103	0.46	0.03
<b>Standard Deviation</b>	1.173	1.134	0.101	0.027
<b>Sample Variance</b>	1.377	1.285	0.010	0.001
<b>Kurtosis</b>	-1.092	1.373	0.269	7.556
<b>Skewness</b>	0.082	-0.918	0.122	2.067
<b>Range</b>	3.8	5.8	0.54	0.17
<b>Minimum</b>	97.1	99.1	0.21	0
<b>Maximum</b>	100.9	104.9	0.75	0.17
<b>Count</b>	207	99	207	99
<b>Confidence Level (95.0%)</b>	0.161	0.226	0.014	0.005

### 8.5 OBSI – Sound Absorption Correlation

OBSI and corresponding SA were measured at MnROAD. To investigate the effect of porous pavements in noise reduction, the ratio of porous to non porous sound absorption coefficient were analyzed. The results are shown in table 8.1 and Figure 8.3. Evidently the ratio was at a peak at the 1000-Hz frequency. This is significant because the resonant frequency of the tire carcass is 1000-Hz. Furthermore, there is a multi-coincidence phenomenon between 750-Hz and 120-Hz (8). If the effect of porosity peaks at 1000-Hz, this lends credence to the validity of porous pavements as a traffic noise attenuation or abatement strategy.

Factors other than that noise optimum thus governed the test sections built at MnROAD test track. The three porous cells were constructed in the same month and on different days with

varying temperature and humidity. There were slight variations in surface appearance in spite of similar quality control. (Figure 8.1)

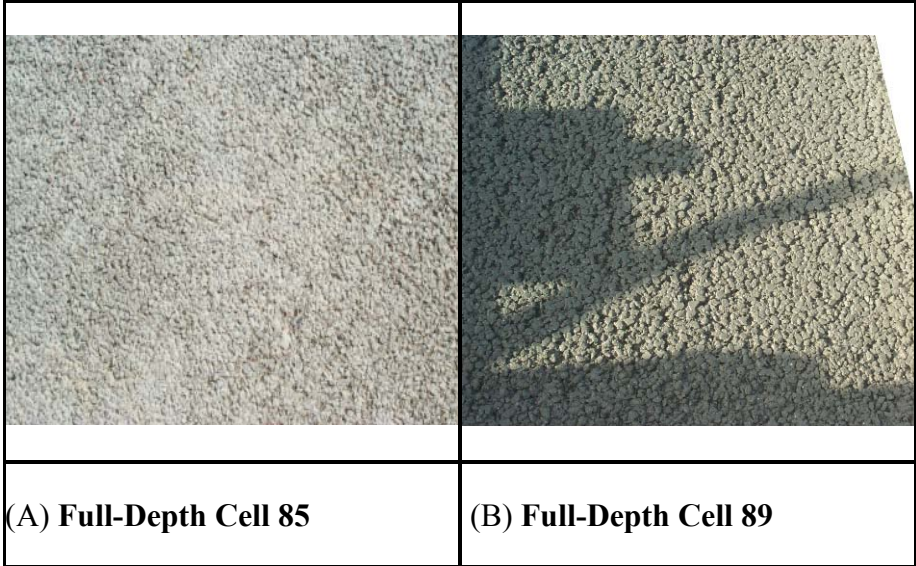


**Figure 8.1: Porous Concrete Cells**

**Table 8.2: Sound Absorption Ratios for Various Pavements**

	<b>Fall 2008 Sound Absorption Coefficient <math>\alpha</math> at Various Frequencies (Hz)</b>							
	<b>315 Hz</b>	<b>400 Hz</b>	<b>500 Hz</b>	<b>630 Hz</b>	<b>800 Hz</b>	<b>1000 Hz</b>	<b>1250 Hz</b>	<b>1600 Hz</b>
<b>Porous asphalt, Cell 86</b>	<b>0.3528</b>	<b>0.3633</b>	<b>0.3633</b>	<b>0.3788</b>	<b>0.4333</b>	<b>0.4672</b>	<b>0.5309</b>	<b>0.5686</b>
Bituminous Cell 87	0.0453	1.3945	0.0867	0.1197	0.1179	0.0715	0.1084	0.0796
Cell 24	0.0366	0.0705	0.0705	0.1086	0.1073	0.0506	0.0913	0.0769
Cell 19	0.0477	0.0862	0.0862	0.1225	0.1178	0.074	0.1092	0.0888
Cell 3	0.1264	0.1193	0.1193	0.1386	0.1287	0.0756	0.128	0.1558
<b>Mean Non-Porous Bituminous Cells</b>	<b>0.0467</b>	<b>0.0653</b>	<b>0.0653</b>	<b>0.0909</b>	<b>0.0862</b>	<b>0.0452</b>	<b>0.0759</b>	<b>0.0766</b>
<b>Ratio: Porous to Non Porous Bit</b>	<b>7.55</b>	<b>5.56</b>	<b>5.56</b>	<b>4.17</b>	<b>5.03</b>	<b>10.34</b>	<b>6.99</b>	<b>7.42</b>
Porous Concrete Overlay Cell 39	0.3171	0.2461	0.2461	0.2364	0.2078	0.2105	0.2955	0.2213
Pervious Concrete Pavement Cell 85	0.1999	0.1906	0.1906	0.2204	0.2506	0.2262	0.2933	0.2882
<b>Mean Pervious Concrete</b>	<b>0.2585</b>	<b>0.2183</b>	<b>0.2183</b>	<b>0.2284</b>	<b>0.2292</b>	<b>0.2184</b>	<b>0.2944</b>	<b>0.2547</b>
White Topping Cell 60	0.0303	0.0276	0.0276	0.0599	0.0523	0.0168	0.0274	0.0407
White Topping Cell 14	0.0348	0.0292	0.0292	0.054	0.0459	0.0201	0.0292	0.0379
Thin Concrete Unbonded Overlay, Cell 5	0.0239	0.0259	0.0259	0.0601	0.0535	0.015	0.0263	0.0381
<b>Mean Non-Porous Concrete Cells</b>	<b>0.0223</b>	<b>0.0207</b>	<b>0.0207</b>	<b>0.0435</b>	<b>0.0379</b>	<b>0.013</b>	<b>0.0207</b>	<b>0.0292</b>
<b>Ratio: Porous to Non-Porous Concrete</b>	<b>11.59</b>	<b>10.55</b>	<b>10.55</b>	<b>5.25</b>	<b>6.05</b>	<b>16.80</b>	<b>14.22</b>	<b>8.72</b>

**Ratio of Porous to Non-Porous Sound Absorption Coefficients**

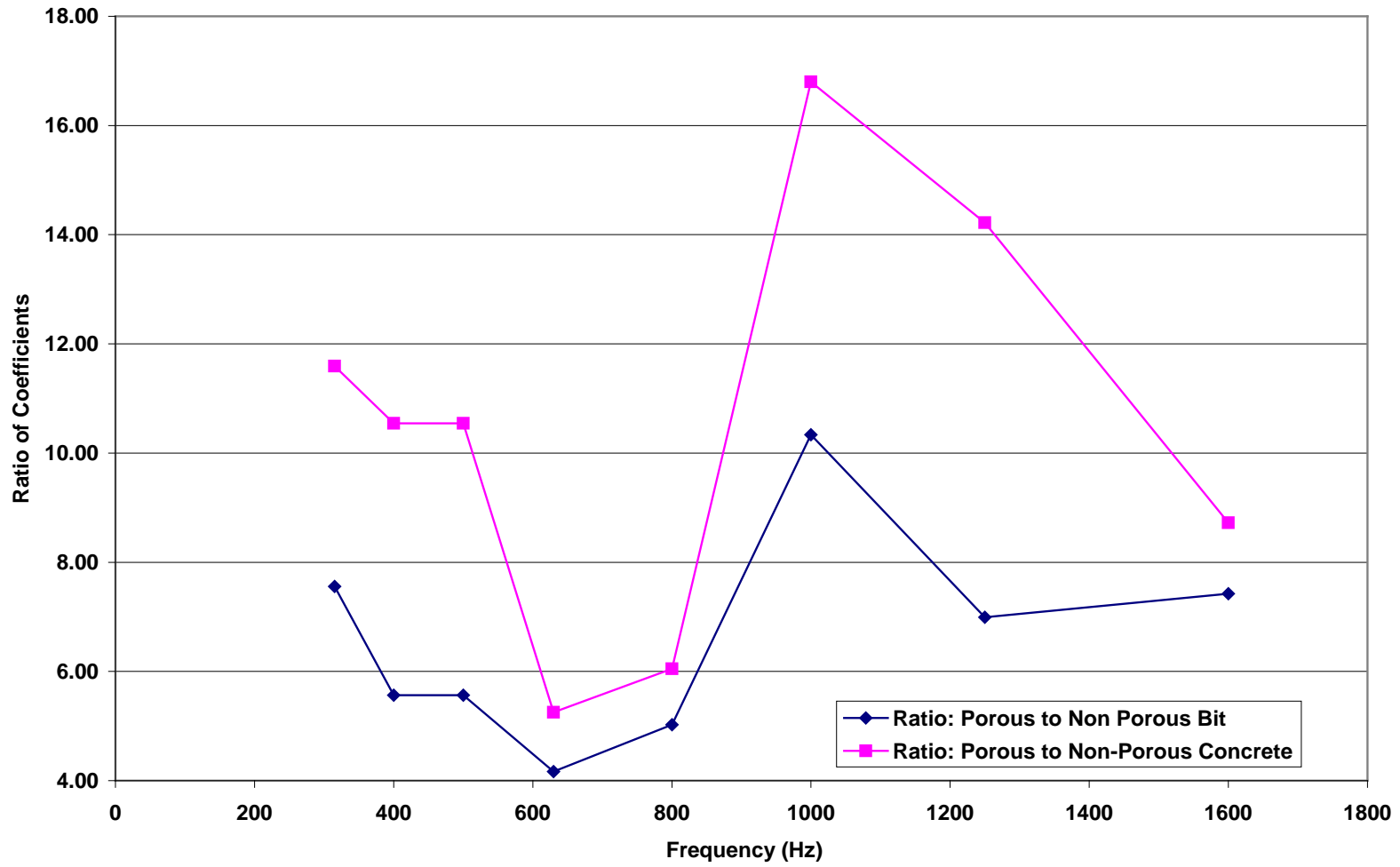


**Figure 8.2: Comparison of Sound Absorption Coefficients of Porous and Non Porous Pavements**

The existence of other quiet pavement strategies in non porous pavements diminishes the comparative effect of porosity on OBSI.

To ascertain the actual effect of porous pavements on OBSI, data obtained from measurement of the 2 variables was analyzed further. A of all 306 data points yielded a least squares regression of

$$\text{OBSI} = 0.52 \text{ Log (SA+1) } - 4.3820 * \text{Porosity} + 102.47.$$

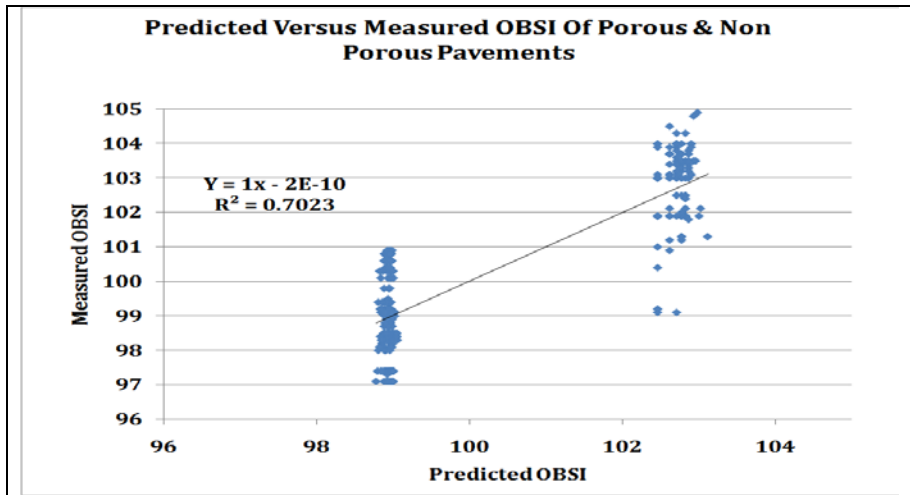
Coefficient of determination is 0.70

Where SA is Sound absorption (%)

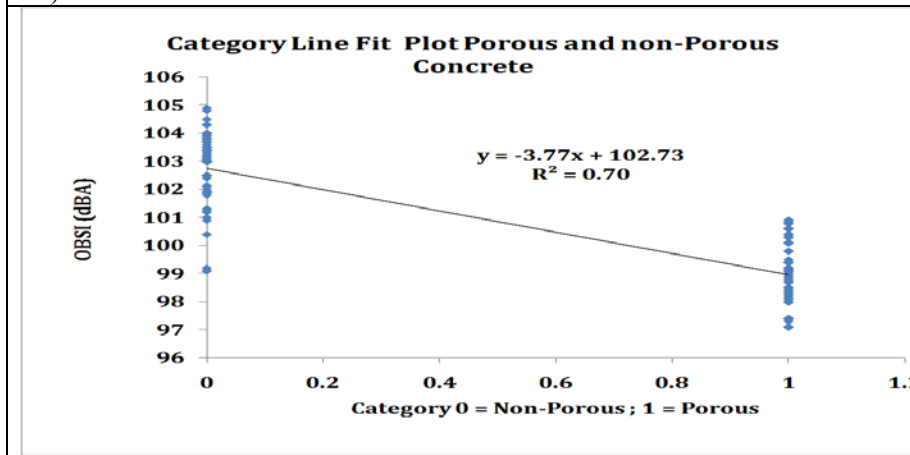
Porosity is a categorical variable where 1 is porous pavement and 0 is non porous pavement.

The P-value of the porosity function and the Log (SA +1) were 1.036E-20 and 0.1449 respectively. To a 95 % confidence limit, the sound absorption function is not correlated to OBSI. However if  $\alpha$  is 0.15 based on the 85 percent confidence limit, then the correlation can be validated. The p-value of the categorical variable indicates that for all intents and purposes, porosity has an influence on OBSI. Other attempts were made to ascertain the extent to which the 2 parameters are correlated.

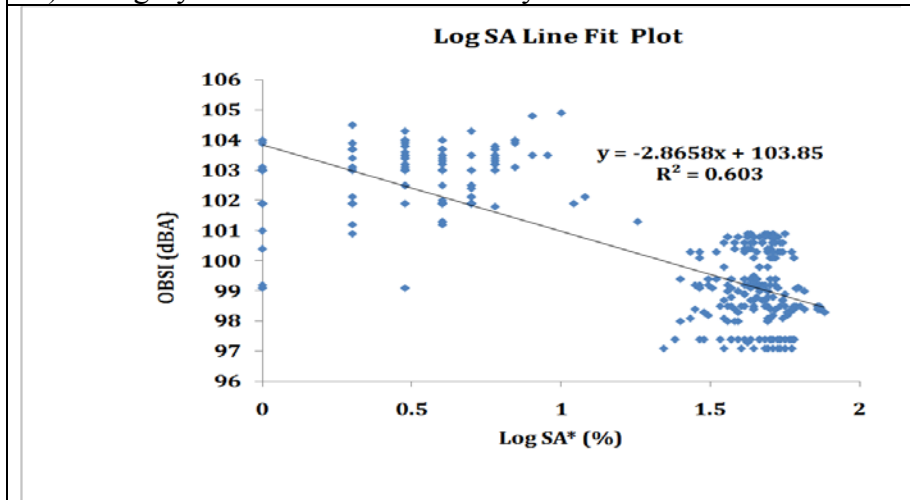
The porous concrete data was isolated and a separate regression analysis was performed. In the Porous pavements, alone, a coefficient of determination of 0.0018 showed that sound absorption was not correlated to OBSI in the porous pavements. However, when porous pavements are placed among non-porous pavements, there is some evidence of some correlation based on the use of categorical variables. It follows that the sound absorption property of porous pavements may not be the actual mechanism by which porous pavements reduce tire pavement interaction noise. Vary likely the air compression relief mechanism (4) may be the actual mechanism by which porous PCC pavements reduce noise. However, all the analysis done so far was in the spatial domain. Before a thorough conclusion is made it is expedient to look into the frequency domain if better correlations can thereby be obtained.



A) Predicted Versus Measured OBSI



B) Category Line Fit Plot For Porosity



c) Log SA –OBSI Line Fit Plot

**Figure 8.3: Line-Fit Plots for Porous and Non-Porous OBSI Versus Sound Absorption**

**Table 8.3: Summary Output for OBSI of Porous and Non-Porous Pavements**

<b>Regression Statistics</b>						
Multiple R	0.8380367		Adjusted R Square	0.700		
R Square	0.7023056		Standard Error	1.1586		
			Observations	306		
<b>Analysis of Variance</b>						
	<i>df</i>	<i>SS</i>	<i>MS</i>	<i>F</i>	<i>Significance F</i>	
Regression	2	959.583	479.792	357.411	1.8891E-80	
Residual	303	406.749	1.34241			
Total	305	1366.339				
	<b>Coefficients</b>	<b>Standard Error</b>	<b>t Stat</b>	<b>P-value</b>	<b>Lower 95%</b>	<b>Upper 95%</b>
Intercept	102.466	0.21283	481.448	0	102.0479	102.885
Log SA	0.520	0.35610	1.4614	0.1449	-0.18031	1.22121
Porosity	-4.3820	0.4358	-10.054	1E-20	-5.239	-3.524

The factors that affect the OBSI of porous types were discussed. Porosity of the pervious cells was identified as the primary factor that enhanced the sound absorption characteristics of porous pavements. Factors related to porosity included tortuosity and gravimetric properties of the pavement. The pavements were categorized broadly into porous concrete and non-porous concrete. Two levels of analysis were performed. In the first level, a ratio of the porous to non-porous sound absorption at each frequency was calculated and plotted as shown in figure 8.2. It was evident that the maximum ratio in both pavement types occurred at 1000-Hz. This underscores the advantage of porous pavements in the multi-coincidence peaks encountered in tire pavement interaction

### 8.6 Investigation of OBSI SA Correlation in 3<sup>rd</sup> Octave Frequency Domain

It is noted that OBSI has been defined as the logarithmic sum of the Sound intensity of 14 frequencies. Similarly, the Sound Absorption analysis, reference is made to only 7 frequencies in the third octave band. These frequencies are 400, 500, 630, 800 1000 1250 and 1600 Hertz. These 7 frequencies are coincident with 7 of the 14 OBSI frequencies. This implies that some of the relation if any may be concealed in the frequencies that are addressed by neither SA nor OBSI or may be concealed in the OBSI frequencies that are not considered for sound absorption.

This section analyzes the Sound absorption results in a 2-step strategy. It successfully determines the effect of porosity, flexibility and hardened content on sound absorption. The 2 steps include:

Step 1: Fragmentation of the Sound absorption coefficient into component factors: This entailed the separation of the sound absorption component into the aggregate and paste component and the porosity component.

Step 2: Comparison of the sound absorption value to the corresponding OBSI at the same frequency and development of model parameters.

### 8.7 Components of the Sound Absorption Coefficient

It was hypothesized that the sound absorption of the non-porous concrete was made up of the sound absorption of the aggregate  $X_{agg}$  as well as the sound absorption of the mortar phase  $X_{cem}$ . Similarly, the sound absorption in the porous pavements, the porosity phase was introduced as the third component in the pervious concrete.

It was elucidated from previous data that the SA ratio was composed of the sound absorption ratios of the constituents of the surface type, whence the sound absorption ratio is ramified into components and idealized as aggregate constituent, cement constituent, flexible component, and the porosity component. The model development ascribed to pervious asphalt all the above-mentioned components while pervious concrete lacked. Normal concrete provides only the aggregate and cement component while normal bituminous presents the aggregate, cement and viscoelastic constituents. The model successfully identified developed and validated the above constituents of the sound absorption ratio (SA).

Thus  $\alpha_{Concrete} \approx \alpha_0 + K_1 \alpha_{cem} + K_2 \alpha_{agg} - \dots$

$$\alpha \text{ Porous Concrete} \approx \alpha_0 + K_6 X_{\text{cem}} + K_7 X_{\text{agg}} + K_8 X_{\text{por}}$$

- The analytical process to determine the correlation tabulated the sound intensity values corresponding to the sound absorption frequencies and sound absorption along different wavelengths for various cells using data from noise and sound absorption test results. A logarithmic sum of 14 specified Sound intensity values is the OBSI used following cells and grouped similar ones together.
  - Cells 5, 14, 53, 54, 62 – Concrete
  - Cells 39, 85, 89– Pervious Concrete
- Used following equation to calculate the model OBSI values (except for the porous asphalt and pervious concrete):
  - $SI = \alpha_{0(f)} + K_1 \alpha_{\text{solid}(f)} + K_2 \alpha_{\text{Cement}(f)} + k_3 \alpha_{\text{porosity}(f)}^n$
  - For the pavements that involved concrete, the flex wasn't used in the equation
- The three alphas ( $\alpha$ ) correspond to the coefficients that were found in the Sound ABS Component Model (shown in table 8.4) and the constants model parameters to be obtained by minimizing summation of square residuals.
- Sum of squared errors were calculated from the model OBSI and the measured OBSI values
- Minimized sum of squared errors to find constants
- Graphed calculated OBSI values versus the measured OBSI values
- Produced a least-squares regression line those points and found corresponding coefficient of determination (r-squared)
- Table 8.4 (below) shows the results for the different groups of surface characteristics and the corresponding  $R^2$  value.

**Table 8.4: Component Absorption Coefficients  $\alpha$  (f) Obtained from all MnROAD Pavements**

Frequency (Hz))	400	500	630	800	1000	1250	1600
$\alpha_{\text{χεμεντιτιουσ}}$	-0.0558	-0.0583	-0.0156	-0.0022	0.1247	-0.0327	0.0028
$\alpha_{\text{αγγρεγατε}}$	-0.0640	-0.0649	0.0207	-0.0522	0.0683	-0.0444	-0.0121
$\alpha_{\text{Ποροσιτη.}}$	0.4003	0.3945	0.3622	0.3960	0.4598	0.4807	0.4888
$\alpha_{\text{χονσταυτ}}$	0.1008	0.1042	-0.0069	0.0495	-0.2106	0.1133	0.1036

		<b>Pervious Concrete</b>	<b>Non Pervious Concrete</b>
<b>Agg</b>	k1	-37.3296	-5.5160
<b>Cem</b>	k2	99.5340	165.9029
<b>Porosity</b>	K3	75.0153	87.1419
<b>Exponent</b>	n	-0.1862	0.0000
<b>Constant</b>	Beta	19.9421	55.6068

The Porous Concrete model was:

$$\text{Sound Intensity}(f) = 99.5 X_{\text{cement}(f)} - 37.32X_{\text{-aggregate}(f)} + 75.3 X_{\text{-porosity}(f)}^{-0.186} + 1.994$$

$$(R^2 = 0.47)$$

For non-porous Concrete, regression yielded:

$$\text{Sound Intensity}(f) = 165.9029 X_{\text{cement}(f)} - 5.516 X_{\text{-aggregate}(f)} + 6.56$$

$$(R^2 = 0.49)$$

The coefficient of determination for each pavement group and corresponding model are shown in table 8.4. It is also probable that with more data, the models will be validated. This model predicts the sound intensity at corresponding frequencies from the component sound absorption factors at that frequency.

Better correlation between Sound Intensity and OBSI is obtained in a frequency domain analysis but the coefficient of determination is not still high enough to suggest a strong correlation between OBSI and sound absorption. The initial conclusions that sound absorption may not be the major process by which porous concrete reduces noise is thus validated in the spectral domain.

## 8.8 Conclusions

Sound absorption factors and corresponding OBSI of many cells in the MnROAD facility were examined.

- Sound absorption factors of non-porous pavements ranges from 0.02 to 0.09 but the porous pavement sound absorption ranged from 0.27 to 0.78. The OBSI of porous pavements ranged from 97.6 dBA to 101dBA while OBSI of non porous pavements ranged from 98.5-dBA to 107-dBA. The Innovative diamond grinding with OBSI ranging from 98.1 to 101 dBA is generally as quiet as the porous pavements although its sound absorption factor is low.
- When all the cells (porous and non porous were considered together, and the pavement types were assigned categorical variables (0 for non-porous and I for porous). The porosity proved to be the most important parameter influencing the model. However, an examination of the OBSI versus SA for porous pavements showed no correlation. It was then concluded that in the spatial domain SA had no direct correlation to OBSI ( $r^2 = 0.0018$ )
- A spectral domain analysis showed improved correlation of SA to OBSI ( $R^2 = 0.47$ ). This was not sufficient however to conclude that SA is well correlated to OBSI.
- The ratio of porous to non porous sound absorption factor was maximum at 1000-Hz, which is the resonant frequency for the tire carcass and thus the peak frequency for the tire vibration. Porous pavements thus provide relief for the tire carcass vibration noise.
- With the exception of the innovative grinding, OBSI of porous pavements were generally lower than OBSI of non-porous pavements that exhibited much less Sound absorption

than the porous pavements. Consequently, the quietness property of porous pavements is not necessarily driven by the mechanism of sound absorption. Possibly, the relief of air compression, which is the same mechanism employed in the innovative grinding noise reduction is the favored mechanism by which porous concrete pavements reduce noise.

- Since porous pavements are positive texture, it is not clear if they provide relief for the treadblock impact mechanism.

# CHAPTER 9 ACOUSTIC PROPERTIES OF CLOGGED PERVIOUS CONCRETE PAVEMENTS

## 9.1 Introduction

A pervious concrete driveway project in 2005 was the earliest in Minnesota. Eller and Izevbekhai (1) described the pervious concrete initiative that constructed a pervious concrete driveway at the MnROAD research facility in 2005. The pervious concrete driveway was subsequently monitored and according to Rohne and Izevbekhai (2) most of the driveway was clogged after 4 years of no vacuuming. Clogging resulted in early raveling as well as loss of mechanical strength properties as observed from Schmidt Hammer spot tests.

The 64 ft X 24 ft (19.2m X 7.2m) driveway was designed for 20 percent porosity. According to Sandberg and Ejsmont (3) pervious pavements can be categorized into pervious, semi pervious or non pervious according to ranges of porosity. Pervious pavements have porosity of 15% or greater. Semi-Pervious pavements are characterized 12-15% porosity and non pervious pavements have less than 12% porosity. A sustainability of porosity of pervious pavements is pivotal to their durability. In addition to compromising drainage and sound absorption, pores or cavities of pervious pavements tend to retain ice lenses during the freezing cycles but these do not thaw uniformly as would a uniform interconnected (communicating) void system when they harbor clogging agents. The non uniform freezing and thawing pressures result in early degradation of pervious pavements. Therefore clogging is regarded as one of the most undesirable that pervious pavement phenomena.

Monitoring and maintenance strategies are therefore designed to ascertain degree of clogging and restore the void system of pervious pavements. Clogging of pervious pavements is defined as the reduction of communicating voids due to the ingress and accumulation of certain agents in the cavities. Observations made in the pervious pavements at this location indicated that most of the clogging agents resided in the upper 2 inches of the driveway pavement. A pavement is clogged when there is such an accumulation of clogging agents at the surface that it no longer conducts water or absorbs sound as expected even if cavities in the core of the structure is still open.

Quantitatively, Rohne and Izevbekhai (2, 4) showed that if the time to empty an 8 inch head of water through a dynamic head infiltrometer exceeded 2 minutes, the pavement was considered clogged. That exemplified suggested institutional limits required to trigger maintenance repair or rehabilitation activities. A report of pervious concrete for cold climate (5) optimizes porosity with respect to performance (5) at 20-25 % void content. In a closely packed aggregate system if the gravel and surrounding mortar are idealized as spherical and of a single radius  $r$ , it can be shown that the packing efficiency amounts to  $\frac{\pi\sqrt{2}}{6} \cong 0.74$ .

The maximum porosity is thus  $1 - \frac{\pi\sqrt{2}}{6}$  which is approximately 25 %. It was also shown by

Horeskenov (6), that when an acoustic surface is indented, there is a progressive increase in sound absorption of that surface up to 25 percent surface area. Thereafter, the sound absorption of the surface was equal to that of mineral wool that was used as filler for the indentation as

though the entire surface was made of mineral wool. Optimum sound absorption characteristics may therefore be achieved at maximum void content but it is doubtful if above 25% void system, there is any further improvement. Additionally, Nethaliath (7) showed that beyond that optimum void content there may be a reduction in strength.

Institute for Safe Quiet and Durable (7) Highways in Purdue University recommends that for optimum noise attenuation performance, the aggregate should contain a blend of 3/8 inch or 1/2 inch (9.5mm or 12.5mm) aggregate. Use of this aggregate size has resulted in less segregation and better void distribution in subsequent pervious concrete projects.

Unfortunately, irrespective of best design practices, pervious pavements tend to experience an accumulation of material in the voids with time. This accumulation, called clogging, forestalls the free drainage properties of the pavement thus rendering it susceptible to freeze thaw degradation.

## **9.2 Research Significance**

Pervious pavements are primarily designed to facilitate storm water infiltration and noise reduction. However, these benefits are constrained by clogging of the pores. It is easy to perform in-situ hydraulic conductivity and acoustic measurements to ascertain the hydrologic and acoustic health of pervious concrete. Consequently this research evaluates the effect of clogging and the efficacy of simple maintenance practices to mitigate clogging.

This paper discusses and evaluates the prevailing pervious pavements maintenance practices in Minnesota. It also discusses the impacts of clogging on hydraulic conductivity and acoustic properties. Finally it simulates by an accelerated clogging test the effect of certain clogging agents on acoustic and hydraulic conductivity properties. It also examines some intricacies of tortuosity to accentuate how the convoluted paths caused by clogging agents may reduce fluid flow rate and inhibit sound absorption.

## **9.3 Description of Test Sections**

Many pervious pavement construction projects have been executed in MnDOT. Their design and monitoring strategies are shown in table 9.1. Cell64 measuring (64-ft X-24 ft (19.2m x 7.2m) Driveway-Full-depth) was constructed in fall 2005 with 8 inch concrete on a 12 inch (200mm) base made up of 1 inch (25.4mm ) sized aggregate. Subsequently in 2006 a sidewalk measuring 5-ft X 100-ft (1.5m X30m) was constructed with 8 inch concrete on a 12 inch (200mm) base made up of 1 inch (25.4mm ) sized aggregate. In late summer 2008, MnDOT constructed a pervious concrete boat landing in Detroit Lakes Minnesota as a filtration system. It was built of eight-inch pervious concrete underlain by 2-ft (600mm) of 2-inch (50.8mm) nominal rock base on a sloped impervious geo-fabric that conducts the water to a collection point for partial treatment before release to Detroit Lakes (FIGURE 9.1).

Experience from the earlier initiatives helped to provide new and improved designs for 3 cells (39, 85 and 89) (FIGURE 9.2) that were built at MnROAD in fall of 2008. Cell 39 was designed as a 4-inch (100-mm) pervious overlay on a concrete substrate primarily for noise reduction. Poly propylene and cellulosic fibers enhanced bond with substrate. Cell 85 was designed as a full-depth-7-inch (175-mm) concrete on 4-inch (100-mm) railroad ballast above 8-inch (200-

mm) of single grade one-inch rock base built on a sand subgrade. The layer of railroad ballast stabilized the rock base for construction traffic. Cell 89 was of a similar design to cell 85 except the former was built on a clay subgrade.

Separate projects initiated by the Cities of Minneapolis and Shoreview followed best design practices although the former was built in 2006. City of Minneapolis Cul-de-Sac consisted of a pervious concrete pavement built in 2006 at Lake Street and 12<sup>th</sup> street in Minneapolis. It consists of an 8-in (200mm) pavement built on one ft (300mm) of base over granular subgrade.

Owasso Community Streets in the City of Shoreview is the single largest pervious concrete project in Minnesota. This consists of 0.6 miles (0.96km) of city streets pavement with 8-inch (200mm) pervious concrete on 12-inch (300mm) CA 50/ rail road ballast as base course. The subgrade is made up of granular material.

#### **9.4 Municipal Maintenance Strategies**

Table 9.1 shows the maintenance strategies used by the municipalities and agencies. Ferguson (8) recommended that sanding and salting operations may clog pervious pavements and should then be excluded from snow and ice operations in pervious pavements. This section discusses the existing maintenance strategies.

All communities and agencies in Minnesota exclude sanding and salting from their winter maintenance of pervious pavements. They either plow for removal or groom the snow and ice for snowmobile recreation. The strategy of snow and ice operation in the MnROAD pervious test cells are no different from the operation conducted on other test cells at MnROAD low-volume road. Activities consist of the application of salt very sparingly on the test cells in extreme cases in addition to snow plowing. When salting is performed, the MnDOT powdery salt is applied lightly on the surface and the melted solution or suspension flows to the shoulders. Regular snow and ice operation uses the snow plow to remove snow or ice from the surface. Due to very low testing activities at MnROAD low-volume road, concern for skid resistance in the winter months is determined solely by the need for the 5 axle 80 kilo pound vehicle to safely make 80 trips a day 5 days a week. The boat ramp at Detroit Lakes provides winter recreation for the residents. The snow and ice is groomed and used as a snowmobile trail in the winter. During the spring thaw, the groomed snow and ice is allowed to melt into the pavement. At that time of the year, larger agents such as leaves and other debris are swept off the surface and with broom-vacuum equipment, the surface is cleaned. In the non winter seasons, a monthly sweeping and vacuuming is done.

In addition to monthly vacuuming City of Shoreview performs snowplowing of their pervious streets. They also perform monthly sweeping of larger debris such as leaves and a regenerative air vacuuming of the 3000-ft (900m) of pervious pavements. This City performs continuous education of the residents so that sodding and seeding and such activities that cause clogging are minimized in the vicinity of the pervious pavements.

Most Agencies have adopted pervious pavement cleaning techniques which are discussed below: They include vacuum sweepers and regenerative air sweepers.

According to Kuehl et al (9) regenerative air street sweepers move debris from the curb into the path of the sweeper head. The regenerative air process blows air into one end of the sweeper head and onto the pavement dislodging materials. The other end of the sweeper head has a suction hose that vacuums up the materials and deposits it into a hopper. The air is then re-circulated back through the system to the sweeper head, and water must be used to “knock“ the dust and small particles out of the air and into the hopper or they will be pulled through the fan and cause wear on the impeller. The ability of regenerative air sweepers to improve air quality, and pick limited size of debris is a great advantage. However they are not suited for collection of wet organic debris such as leaves. They also spread residue onto the surface.

Vacuum sweepers use gutter brooms to move debris into the path of a vacuum nozzle. There vacuum sweeper in FIGURE 9.3 has the vacuum nozzle located near the tire along the curb line. This allows the curb to be dry-vacuumed. Most vacuum sweepers utilize a fan that exhausts its air directly to the atmosphere. These sweepers must use water for dust suppression to forestall the obvious environmental hazard and minimize fan wear. Vacuum sweepers are known to remove fine sand and silt, but surface must be dry. The adaptation of this process to picking up entrained material within cavities under vacuum head facilitates an efficient operation. However, the tortuosity of pervious pavements poses a challenge to the efficacy of these vacuums. They are also restricted to temperatures above freezing.

## **9.5 Field Evaluation of Maintenance Strategy**

Maintenance strategies are evaluated by the degrees to which acoustic, hydraulic and volumetric properties are restored after a chosen maintenance practice is applied. The volumetric properties are detected with the nuclear density backscatter method, the hydraulic properties are evaluated with the infiltrometer and the acoustic properties are evaluated with the sound absorption equipment ASTM E1050, preferably measured in-situ. Core sound absorption tests are also possible but for evaluation of clogging, it is almost impossible to harvest a representative core. A maintenance strategy must improve or maintain, drainability, sound absorption and /or pore structure. Tools for evaluation are now described.

### **9.5.1 Infiltrometer**

The Pervious concrete cells were monitored for flow time as an index of hydraulic conductivity. The infiltrometer is a device that facilitates measurement of the hydraulic conductivity of a pervious pavement. It is a falling head device with the water level maintained at atmospheric pressure. Its cylindrical housing accomodates a clear 8-inch (200mm) discharge head difference marked “upper” and “lower”. It differs from conventional permeameters in the sense that the velocity head is a significant part of the energy (Bernoulli) equations and is not ignored unlike the standard falling head permeameters used for infiltration of soils. The MnDOT infiltrometer is a modification of the ASTM (10) vessel.

FIGURE 9.4 shows the open ended single ring infiltrometer 24 in (600mm)long and 4 inch (100mm)diameter flanked by supporting dead-weights to enhance a hydraulic seal at the flange-pavement interface. During testing, the flow device is simply placed on the pavement and filled continuously until water is at least 2-inches above an upper mark. The discharge time from the upper to the lower mark is noted as an indication of the hydraulic conductivity of the pavement.

Some clogged portions of the driveway did not allow any vertical flow. In consequence, anything beyond 100 seconds is regarded as clogged. In clogged spots, a record of the head difference and time taken was occasionally recorded for reference. Waiting till the 8-inch head loss is obtained in a clogged pavement is not expedient. Initially a sand cone device was used but this was replaced by a uniform cross section, varying head device. The equations for discharge were developed for the sand cone but were retained for the uniform cross section device (3) under atmospheric pressure,

$$\frac{\pi d^2}{4} dh = v_0 A_0 dt \quad (\text{Equation 1})$$

Where h is small change in height of water

A<sub>0</sub> is the area at the discharge orifice, d is diameter of infiltrometer; v<sub>0</sub> is discharge velocity at orifice. Substituting the boundary conditions of h = H when T = 0 it can be shown that

$$T = \frac{\pi d^2}{2\lambda\sqrt{2g}A_0} (\sqrt{h} - \sqrt{H}) \quad (\text{Equation 2})$$

Here, T is discharge time, λ is a system calibration constant, g is acceleration due to gravity, A is top open end area, H is maximum head loss, h is head loss d is diameter at orifice so derived to accommodate different open end areas else A<sub>0</sub> = πd<sup>2</sup> in uniform area infiltrometers. The test is conducted in impervious surfaces and air during calibration. Locations on the test cells were monitored in 2008, spring 2009 and Summer 2009. Some of these locations were coincident with test spots for Nuclear density and sound absorption.

### 9.5.2 In-Situ Density Evaluation

Seamans Nuclear density gauge is a device that measures density of a pavement surface or layer by emitting radioactive rays into that layer. Response of the media is dependent on the absorptive property of the pavement. This pulse is calibrated to known densities that facilitate true measurements. The principle and process of use of this device at the test cells is called the “back scatter” method.

If γ is the bulk density of a pervious layer and γ<sub>np</sub> is density of a non-pervious layer, it can be shown that

$$\gamma V = \gamma_{np} (V - V_v) \quad (\text{Equation. 3})$$

Where V is total volume of a pervious concrete and V<sub>v</sub> is volume of voids. (V<sub>v</sub>/V) is porosity. It is therefore evident that

$$(\gamma_{np} / \gamma)(1-n) = 1 \quad \text{where } n \text{ is porosity} \quad (\text{Equation. 4})$$

$$\text{Therefore, Porosity (n) = } 1 - (\gamma / \gamma_{np}) \quad (\text{Equation. 5})$$

For example cell 40 a non pervious cell averaged 146 pcf and the outside lane of pervious cell 39 averaged 120 pcf. The average porosity from equation 5 is  $1 - 119/148 = 0.19$

### 9.5.3 In-Situ Sound Absorption Measurements

The sound absorption test is a process that measures the sound absorptiveness of a pavement surface. In the sound absorption test, the sound analyzed is not generated by the interaction of the rolling tire with pavement surface but by noise source above the impedance tube (FIGURE 9.5). Occasionally a white noise source is used. This is a random audio signal with a flat power spectral density that contains noise at the same power at all frequencies. During the test an

impedance tube is placed on the pavement surface and a set of sensitive microphones are attached to the pre-installed housing at the lower end of the tube. Microphones are connected to an analyzer. The noise source sends the incident sound energy to the surface and the incident and reflected waves are captured by the two microphones. Software windows the reflected waves and converts the data to the 3<sup>rd</sup> octave sound absorption coefficient at 315, 400, 500, 750, 1000, 1250 and 1650 hertz. Berengier et al (7) discussed sound absorption coefficient ( $R_p$ ) is expressed as a function of frequency ( $R_p(f)$ ):

$$|R_p(f)|^2 = 1 - \frac{1}{K_r^2} \left| \frac{P_r(f)}{P_d(f)} \right|^2 \quad (\text{Equation 6})$$

$K_r$  is the spreading factor,  $P_r$  and  $P_d$  are the reflected sound energy and the incident sound energy respectively as defined. The output of a sound absorption factor is typically in the form of the sound absorption at the eight frequencies defined above. Hence, the factor is therefore expressed as a function of frequency (equation 6).

### 9.6 Performance Evaluation of Clogged Test Cells

In the clogged cell 64 the SA at 400-Hz was 0.12 and 0.08 in the left lane and right lane respectively. An unusual local peak at 800-Hertz characterized the SA frequency plot with a spike to 0.32 and 0.14 respectively in the left and right lane. At 1000-Hz, SA was 0.12 and 0.18 respectively and at 1600-Hz the SA was at a maximum of 0.48 and 0.33 respectively.

In comparison, Cell 89 SA ranges gradually and uniformly from 0.3 at 400-Hz to 0.5 at 1600-Hz (FIGURE 9.6a). Cell 89 being new in service shows no signs of raveling and clogging, unlike cell 64.

If cell 64 was evaluated by the infiltrometer method alone, it would be regarded as clogged but that would be from a hydraulic conductivity perspective. Most of the spots were found to be clogged as there was either no vertical movement of water into the pavement or the rate of discharge was so low that after 100 seconds the standard 8 inch head loss was not achieved. In this cell, sound absorption was lower than the new cells but was significantly higher than what was observed in the non-pervious cells.

The surface of cell 64 is in very poor condition with significant raveling and cracking. These distresses have released a high quantity of clogging agents on the pavement. The surface is

loaded with the 5 axle semi trailer 2 times a day 5 days a week. After 4 years, this pavement has not been vacuumed once and it is in the path of run-off from the 100-ft X 140-ft (30m X 42m) driveway/parking lot. This contributed to its clogging. The difference in sound absorption coefficient between cell 64 and cell 85 is a reflection of the degradation and clogging of cell 64. Nevertheless, the clogged pavement exhibits significantly higher sound absorption than non-pervious pavements. General hydraulic conductivity measurements have shown with the example of a pervious pavement left unmaintained for 4 years that clogging leads to accelerated pavement degradation as freeze thaw capitalizes on the trapped lenses of ice to damage the pavement. Before and after measurements of hydraulic conductivity of pervious pavements indicates that there is a noticeable improvement of this variable, when vacuuming is performed but when left undone for a long time, the pervious pavement falls apart and the original void content.

The rate of degradation of an unclogged pavement may be dependent on the traffic load, weather severity including freezing and thawing, mix design and level of construction proficiency. However when a pavement is clogged, the voids are not necessarily communicating and are thus more likely to be susceptible to freeze thaw forces. These in turn accelerate raveling and subsequent degradation. It is therefore not surprising that the rate of degradation of the driveway has increased exponentially with each additional year. From the driveway, it is evident that vacuuming of pervious pavements must be performed if they are to achieve a cost effective service life.

Various test locations in the city of Shoreview indicated differing sound absorption spectra due to the varying degrees of clogging. For instance a fairly clogged location near the curb line exhibited SA ranging from 0.15 to 0.25 between 400 and 1000Hz. Proximate unclogged location resulted in higher SA ranging from 0.3 to 0.53 between 400 and 1000-Hz (FIGURE 9.6b). Consequently, the clogged MnROAD cell and the Shoreview City Street portrayed that clogging reduces sound absorption coefficient.

## **9.7 A Quantitative Evaluation of Maintenance Strategy**

MnDOT demonstrated a pervious pavement vacuuming process using equipment owned and operated by a Minnesota based company at MnROAD in November 2009. Pervious concrete test cells 85 and 89 and pervious asphalt cells 86 and 88 were vacuumed. The test cells were approximately one year old at the time of the demonstration and were in good condition. The pervious concrete test cells had no surface raveling or joint distress and very few fine cracks. The pervious asphalt test cells had isolated areas of surface raveling and light rutting. The voids in the pervious concrete and pervious asphalt test cells appeared to be clean and free of debris. It is important to note that the brush on the vacuum was not used. The contents of the vacuum were collected after vacuuming each test cell. While the test sections did not have visible debris in the voids, there was some surface material, likely from the shoulders and neighboring test cells. Flow measurements were made the day before and immediately after vacuuming. The change in time of discharge was indicated by the MnDOT falling head infiltrometer which has been described. The setup is shown in FIGURE 9.8. A test was performed in each test cell at the wheel path. It was apparent that the pervious concrete test cells (85 and 89) were very clean with no surface distress there was very little change in flow time. This improvement is likely

attributable to the removal of the raveled surface aggregate. Two vacuuming activities per year were therefore recommended.

## **9.8 Field Evaluation and Analysis**

The most common clogging agents encountered in the MnROAD Cells are the “ravelings” from the pavements. Aggregate and cements and asphalt in various degrees of fragmentation were visible in the receptacle of the vacuuming equipment used in the MnDOT Cells. The three cities had encountered more organic as well as colloidal clogging agents than were observed at MnROAD. These organic and colloidal materials undergo volume changes in the voids, depending on their moisture content. Fwa et al (11) observed that most of the clogging agents in Singapore came from automobile tires that had picked up silty particles from other sources and transferred it to the pervious pavements. That may be applicable to city streets in which turf was established by sod application, leaving clay and silt debris that tires may pick up and disperse in the pavement surface. Additionally, during the fall, a large quantity of leaves was deposited on the pavement surface. These were pulverized by traffic and washed into the pores. The city streets were more susceptible to clogging than the MnROAD cells. In the Detroit lakes boat ramp, sand is occasionally encountered. In 2 years of service the pavement still exhibits good drainability.

To ascertain the relative long term effect of various agents, an accelerated clogging study was conducted. In this study, clogging agents are idealized into three representative groups.

Group 1: Cohesive/ colloidal agents: Simulated and represented by clay

Group 2: Clean granular material: Represented by Ottawa Sand

Group 3: Granular but finer gradation than Ottawa Sand: Represented by glass beads

Pervious concrete blocks measuring 20 inches by 20 inches and 6 inches thick were all were examined to ensure that the clogging agents were retained within the test wedge. These blocks were placed on an elevated stand so that the underside of the pavement was visible. Using the BSWA impedance tube, sound absorption was measured. 100-milliliters of Ottawa sand was poured on the surface and spread uniformly with a brush on the surface. The block was tamped with a mallet until all the sand had disappeared into the pervious pavement. The sound absorption coefficient of the surface was then measured. The test was repeated with increments of 100-milliliters until the pervious pavement could no longer absorb the Ottawa sand. The test wedge facilitated the assurance that there was no loss of clogging falling through the wedge. Fwa et al (11) had flushed the agent through the matrix in their experiment. That method was not used in this experiment as it would lead to segregation and haphazard retention of the larger fractions.

The actual clogging tests were then repeated on 3 different spots on cell 89 as shown (FIGURE 9.7) below.

The results of sound absorption at 1000-Hz versus volume of clogging agent was then plotted.

There is a remarkable decrease in sound absorption factor due to the clogging agents. The three clogging agents exhibited different rates of decrease in SA with respect to volume applied. In all cases, the sound absorption coefficient decreased with respect to volume in a nonlinear trend best fitted to an exponential decay (FIGURE 9.8). Initial sound absorption was not the same but the incremental volumes were 100-ml in all cases. The relationship was then normalized by determining the percentage decrease in sound absorption with respect to the volume of clogging. (FIGURE 9.8).

## 9.9 Discussion

The three agents all exhibit reduction in acoustic absorption due to increase in the volume of clogging agent. The rate of loss of sound absorption is however different in the 3 agents and plausible reasons have been advanced for this. Total volume of agent to clog the pervious concrete was the same in each of the agents. This was not originally designed but it turned out to be 400-ml. This removed the variability of the quantity of clogging agent including the fact that core porosity values ranged from 18% to 20% which is reasonable uniformity for field evaluation.

**Loss of Sound Absorption Due to Clogging:** Loss of SA factor at full clogging of approximately 30% was observed in the Ottawa sand and clay agents. However in the glass beads a loss of 20 percent was observed. The above losses are not expressed in terms of the ratio of initial sound absorption but as actual losses in values subtracted from the original.

In terms of the actual factors, the clay lost the highest percentage of initial sound absorption as at full clogging (75%). This was followed by glass beads (52%) and by Ottawa sand (48%). The trend suggests the gravity of clogging when clogging agents are colloidal or cohesive in comparison to granular or flocculated agents. It is therefore more hazardous to subject the pervious concrete pavement to a clay environment than to a granular environment. It is suggested that various factors influence the impact of the clogging agents. They include particle size distribution, cohesion and adhesion, effective porosity and effective tortuosity. The effect of a clogging agent depends on the particle size distribution, moisture content, mineralogy and effective tortuosity. It is therefore advisable to prevent ingress of cohesive agents as much as possible.

When clogging occurs, there is a reduction in the efficiency of the void system but by volumetric reduction of the void system or by a loss of communication of voids. It can therefore be shown that the effect of clogging depends on the gravimetric properties, the particle size distribution, adhesiveness or cohesiveness of the clogging agent.

**Particle Size Distribution of Clogging Agents:** Clay particles are <2  $\mu\text{m}$  size fraction in size while the glass beads range from 150 microns to 300 microns. The size distribution between is supposedly uniformly graded. Ottawa sand fractions range from 150  $\mu\text{m}$  to 2-mm. This may explain why the percentage loss of sound absorptiveness of the clay clogged matrix was more than those of other agents.

**Adhesion and cohesion:** Clay particles cohere or are more closely packed irrespective of their moisture content. They also adhere to the tortuous cavities in the pervious matrix more than would the glass beads and Ottawa sand.

**Effective Porosity:** When clogging occurs there is a loss of volume of cavities. This volume is occupied by the clogging agent that theoretically introduces its void content.

Consider a fully clogged matrix of total volume  $V$  and pore / cavity system  $V_p$

The clogging agent introduces a void system  $V_a$  into the cavities

The natural porosity of the agent =  $V_a/V_p$  Equation 7

Porosity before clogging =  $V_p/V$  Equation 8

Porosity after clogging =  $V_a/V = (V_a/V_p) (V_p/V)$  Equation 9

**Porosity after Clogging = Natural porosity of clogging agent X Porosity before clogging.**

The assumptions for the above to be valid are that the pervious cavities are completely clogged and neither the clogging agent nor the pervious media is segregated.

**Effective Tortuosity:** Tortuosity is defined as a measure of the difficulty of fluid flow through a pervious media. The path through the pores of a densely packed fine graded agent is more labyrinthine than that of a granular agent if the total thickness of the pervious media is similar. The effective tortuosity is a combination of the tortuosity of the pervious media and the clogging agent. Consequently, in the same pervious media, the clay agent is expected to produce a higher effective tortuosity than a more granular agent. In simplified form, tortuosity is the ratio of the straight path between two points in a pervious

FIGURE 9.8 shows the effect of gradual filling of voids with the 3 agents. Evidently clay shows a more damaging effect than the other agents.

From FIGURE 9.9 it can be shown that the chord length for a fluid travelling vertically unaffected by lateral transmissivity is  $L = 2\sqrt{2} R$ . The travel length is

$$S = 2\sqrt{2} R - 2R + \pi R \quad \text{Equation 10}$$

Simple tortuosity of unclogged matrix is

$$= \frac{(2\sqrt{2} R - 2R + \pi R)}{2\sqrt{2} R} \cong 1.4 \quad \text{Equation 11}$$

If the void is clogged by stacking  $n$  layers of clogging agent of radius  $r$ , additional path due to clogging agent is  $nr(\pi-2)$  which is always positive.

Tortuosity of clogged matrix

$$S/L \text{ (clogged)} = \frac{(2\sqrt{2} R - 2R + \pi R + nr(\pi - 2))}{2\sqrt{2} R} = 1.4 + \frac{nr(\pi - 2)}{2\sqrt{2} R} \quad \text{Equation 12}$$

Comparing equation 11 to 12, there is an increase in tortuosity when the pavement is clogged. In practice, aggregates are not rounded and they may not be consolidated to the maximum packing. Nevertheless, a clogged matrix will be more tortuous than an unclogged matrix. This validates the reduction in hydraulic conductivity and sound absorption when pervious concrete is clogged.

Due to the complexity of diffusion paths, some other methods that are less direct than (arc length / chord length) have been proposed. Enrico et al (12) proposed another method that divides the curved path into several (N) parts where the chord length is S and the arc length is L. Thus the arc-chord ratio for each part is found and the tortuosity  $\tau$  is estimated by:

$$\tau = \frac{N-1}{L} \cdot \sum_{i=1}^N \left( \frac{L_i}{S_i} - 1 \right) \quad \text{Equation 13}$$

When clogging occurs, N increases tremendously, summation  $L_i/S_i$  increases rapidly and the path becomes more tortuous. Another method by Mächler (13) proposed an analogy that considers the tortuosity of navigating a changing curvature in lieu of a smooth curve implying that roughness (or tortuosity) could be measured by relative change of curvature. In this case the "local" measure of curvature is:

$$\frac{d}{dx} \log(k) = \frac{K'}{K} \quad \text{Equation 14}$$

Here, k is curvature. More changes in curvature k occur with clogging agents of various sizes and would depend on degree of clogging when these agents are lodged in the pores. This method is relevant to measurement of hydraulic conductivity through time of discharge of a falling head infiltrometer. It was proposed to measure tortuosity in time domain by an integral of square of the product of derivative of curvature and time divided by the curve length.

$$\tau = \frac{\int_{t_1}^{t_2} (K'(t))^2 dt}{L} \quad \text{Equation 15}$$

Here again k is curvature t is time and L is the arc length as already defined. Irrespective of which of the above equations (13, 14, or 15) of tortuosity is employed, the fluid path within the already convoluted porous media is rendered even more tortuous by the presence of clogging agents. The accelerated clogging experiment with Ottawa sand, glass beads and clay reveals that the level of loss of sound absorption coefficient is thus related to the gravimetric, physical and natural properties of the clogging agent.

## 9.10 Conclusion and Recommendation

Municipalities in Minnesota adhere to best practices for maintenance of pervious pavements as they commonly vacuum their pavements once every month. MnROAD test cells are not in the path of a wide range of clogging agents and are vacuumed 2 or 3 times a year. Maintenance of

the French drains of the pervious overlay has provided stable hydraulic conductivity to the pervious Overlay.

The accelerated clogging experiment accentuates that fact that clogging reduces the acoustic properties of pervious pavements. It also shows that the colloidal or plastic clogging agents such as clay have the worst clogging effects. The effective void content of a clogged pavement can be deduced from the original porosity of the pavement and the natural porosity of the clogging agent.

Clogging increases the tortuosity of pervious concrete. Clogging decreases sound absorption of pervious concrete and the original SA coefficient can be restored if effective vacuuming can be done.

General hydraulic conductivity measurements have shown with the example of a pervious pavement left unmaintained for 4 years that clogging leads to accelerated pavement degradation as freeze thaw capitalizes on the trapped lenses of ice to damage the pavement. Before and after measurements of hydraulic conductivity of pervious pavements indicates that there is a noticeable improvement of this variable, when vacuuming is performed but when left undone for a long time, the pervious pavement falls apart and the original void content cannot be restored.

It is recommended that communities adopt best practices methods for maintenance of pervious pavements and adopt the continuing education strategy of City of Shoreview so that influent clogging agents can be minimized.

**Table 9.1: MnDOT and Municipal Pervious Concrete Projects and Test Sections**

CITY OR AGENCY	PERVIOUS PROJECT	MAINTENANCE			MONITORING		
		SNOW AND ICE	VACUUM	OTHERS	FLOW TIME	POROSITY	ACOUSTIC
DETROIT LAKES	Boat Landing & Treatment System	None	Once a month	Snow and Ice Groomed for Snowmobile Trail	Qualitative (Empty 5 gallon Bucket)	Proposed By DOT	Sound Absorption ASTM E-1050
MINNEAPOLIS	Cul-de-sac at 10 <sup>th</sup> street & Lake Street	Plow as needed	Once a month		Sand Cone Apparatus for Discharge Time	Qualitative Indicated by Discharge Time	None
SHOREVIEW	3000ft (900m) Of City Streets Near Lake Owasso	Plow as needed	Once a month	Educational Campaign to Residents	(Empty 5 gallon Bucket) & measure spread	Qualitative Indicated by Discharge Time	Sound Absorption ASTM E 1050
MINNESOTA DOT	Pervious Concrete Driveway Cell 64	Plow as needed	None	Example of Unmaintained System	MnDOT's Infiltrometer	Nuclear Density	Sound Absorption ASTM E-1050
MINNESOTA DOT	Pervious Concrete Full-depth Cells 85 and 89	Plow as needed	2/3 times a year	Inspect and maintain Flouts	MnDOT's Infiltrometer	Nuclear Density	OBSI AASHTO TP 7609 and Sound Absorption ASTM E-1050
MINNESOTA DOT	Pervious Concrete Overlay Cell 39 on Concrete substrate	Plow as needed	2/3 times a year	Inspect and Repair French Drains	MnDOT's Infiltrometer	Nuclear Density	OBSI and Sound Absorption ASTM E 1050
Minnesota DOT	Sidewalk at MnROAD	Plow as needed	2/3 times a year	Replace portion destroyed by freeze thaw	MnDOT's Infiltrometer	Nuclear Density	Sound Absorption ASTM E-1050
Minnesota DOT	Driveway at MnROAD	Plow as needed	2/3 times a year	Inspect and maintain flow at outlet of subsurface pervious pipe	MnDOT's Infiltrometer	Nuclear Density	Sound Absorption ASTM E 1050

**Table 9.2: Flow Times Before and After Vacuuming**

<b>Cell #</b>	<b>Before Time (s)</b>	<b>Time After (s)</b>	<b>% Change</b>
<b>85</b>	<b>6.0</b>	<b>6.0</b>	<b>0</b>
<b>89</b>	<b>17.0</b>	<b>15.5</b>	<b>-9</b>

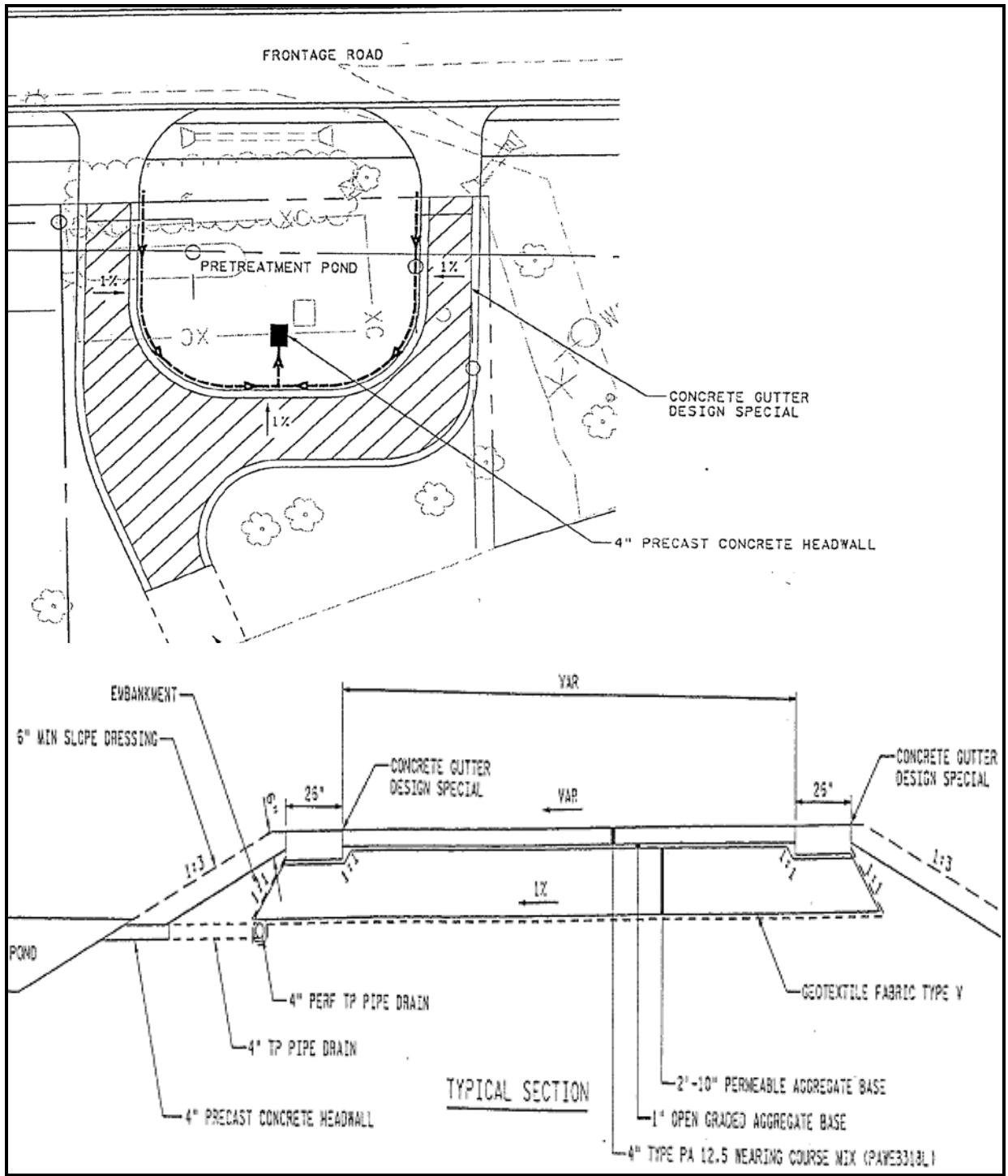
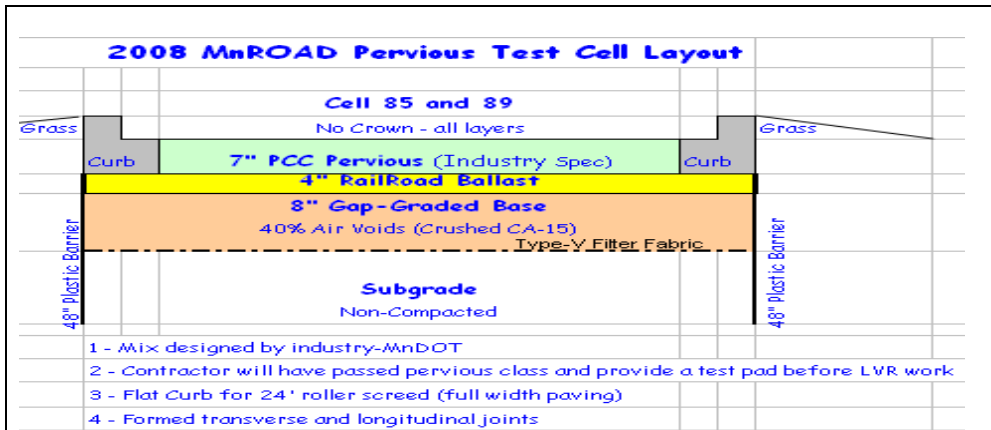
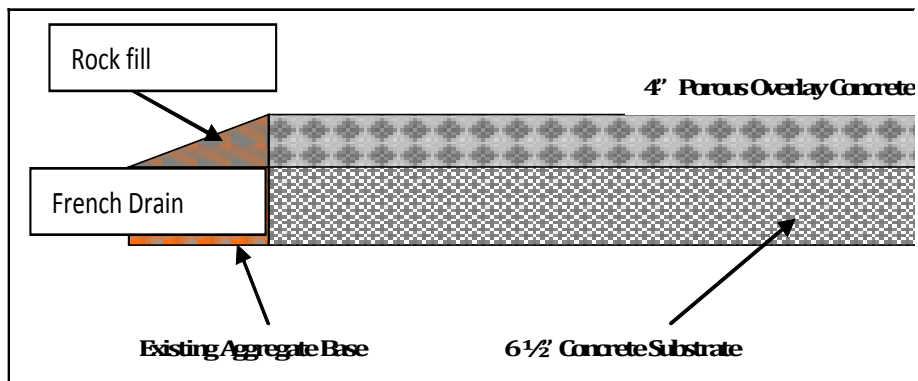


**Figure 9.1: Boat Ramp Pervious Filtration System Detroit Lakes Minnesota**



**Pervious cells 85 Sand Subgrade ; 89 (Clay Subgrade)**



**Schematic Section Through the Pervious Concrete Overlay Cell 39.  
(French Drains at 100-ft Intervals)**

**Figure 9.2: General Structure of MnROAD Pervious Pavement**



a) Regenerative Air Vacuum



b) Agents Vacuumed from MnROAD Pervious Pavements

**Figure 9.3: Vacuum Used on MnDOT Test Cells and Agents Collected at the Receptacle**



**MnDOT Infiltrometer Test**



**a) Infiltrometer**

**Figure 9.4: MnDOT's Pervious Pavement Hydraulic Conductivity/ Infiltrometer Device**

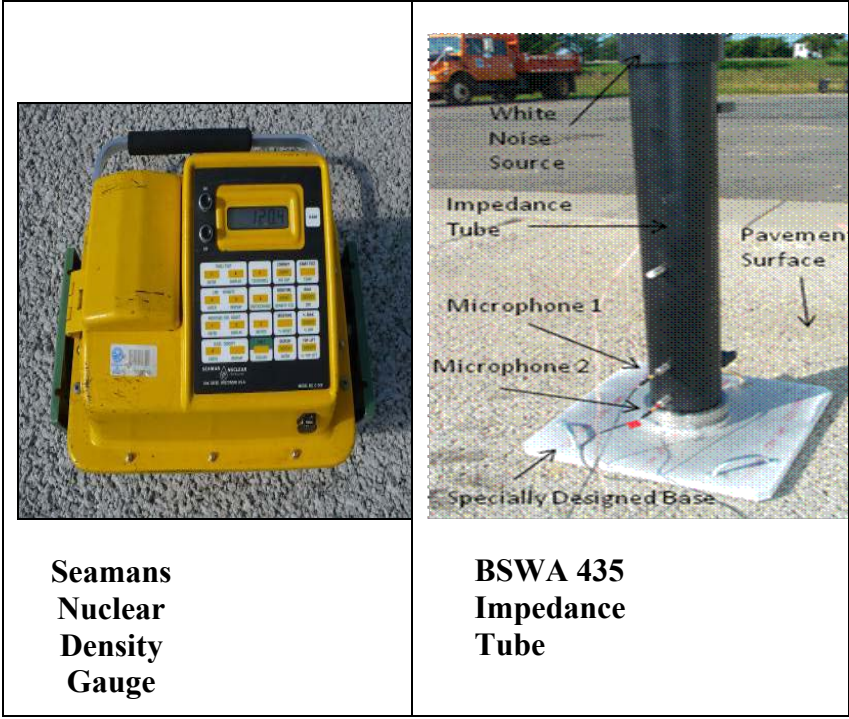


**Figure 9.5: Nuclear Gage and BSWA 435 Sound Absorption Impedance Tube**

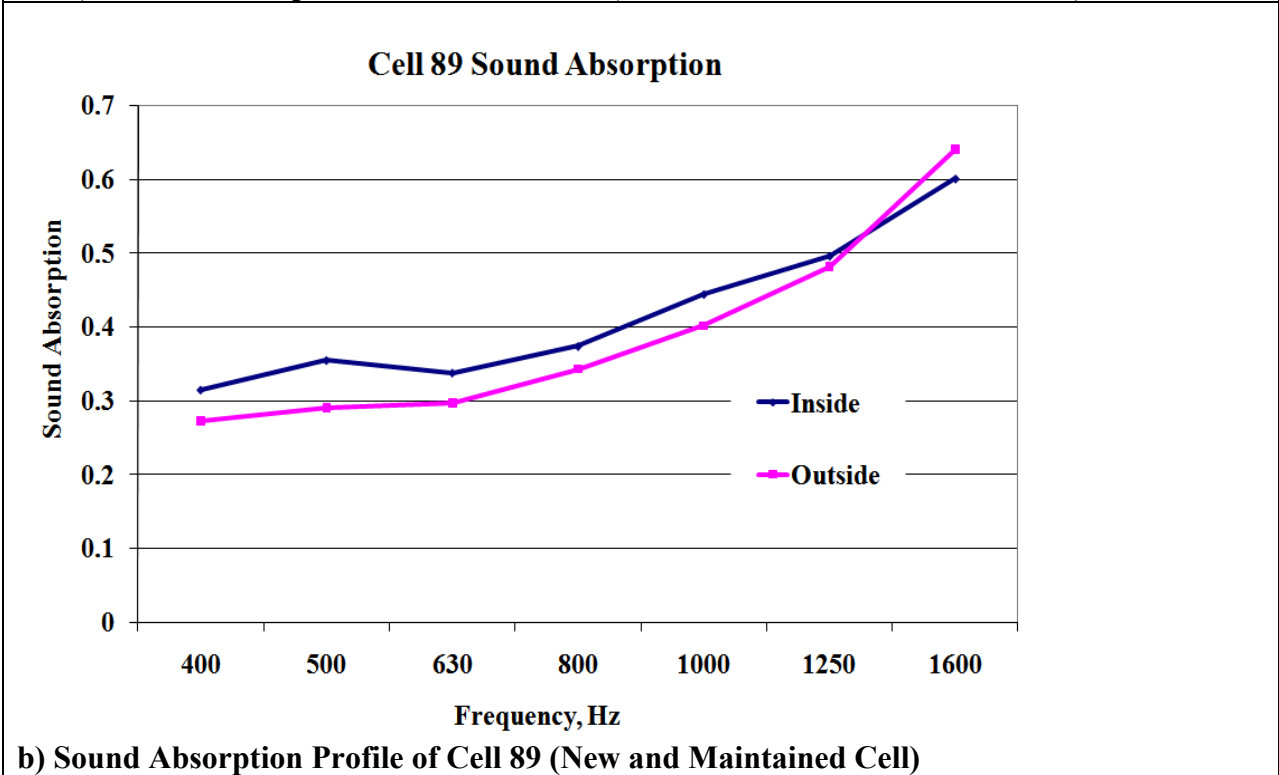
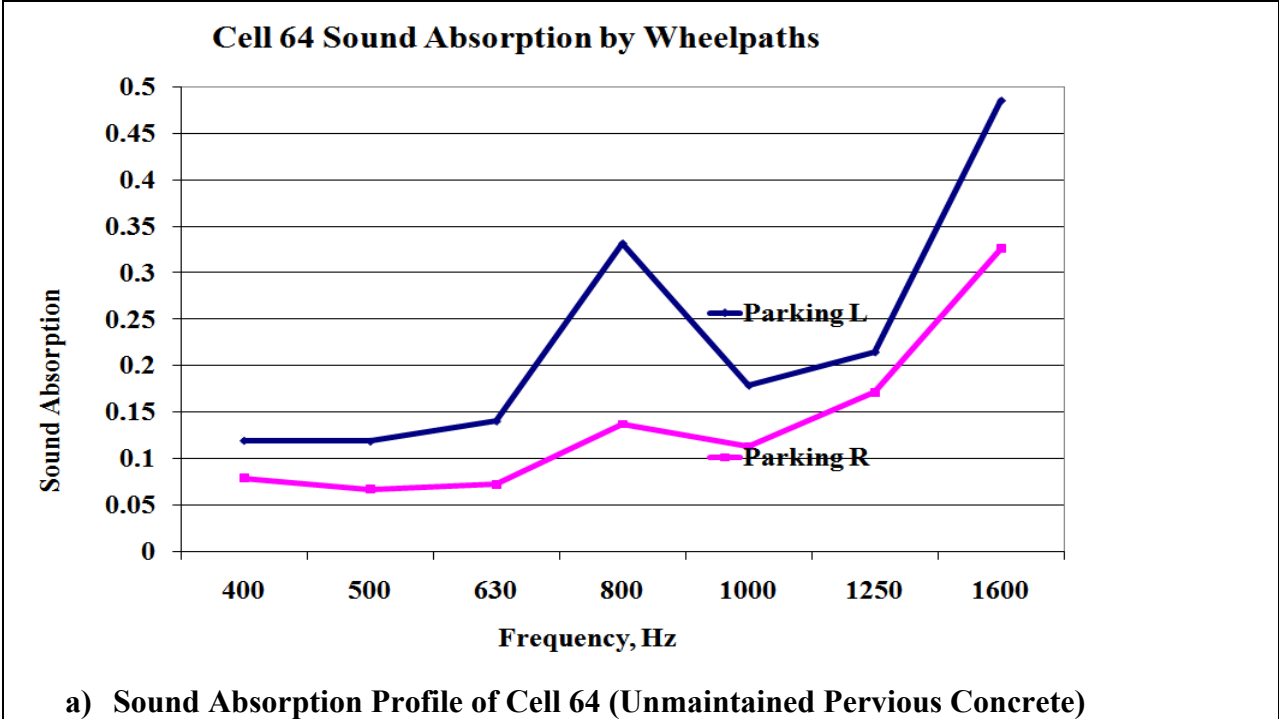
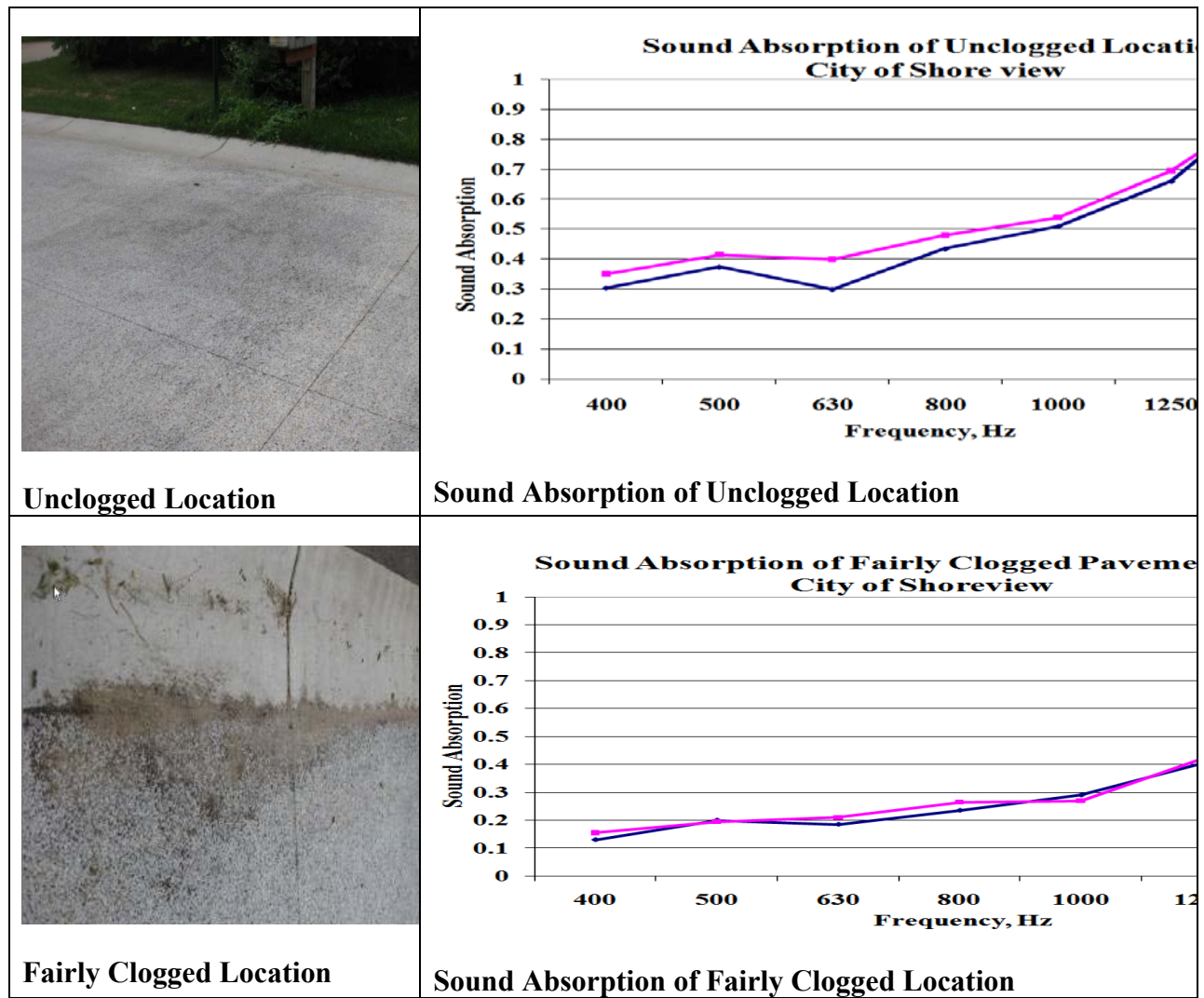


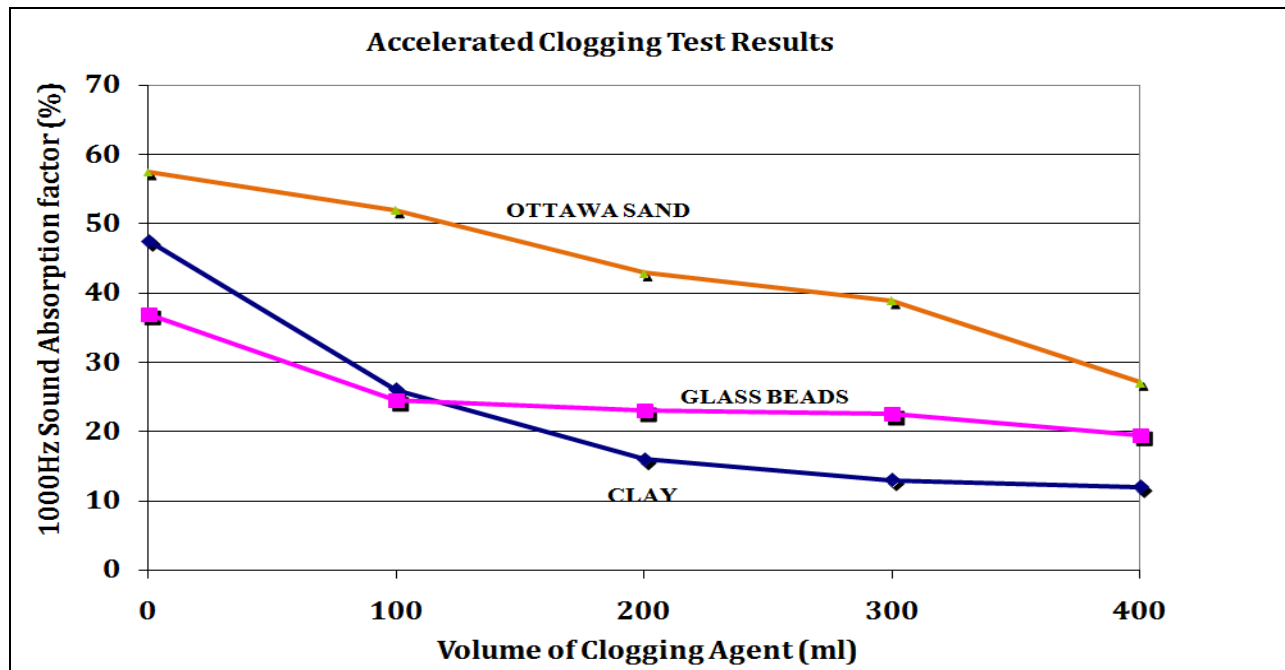
Figure 9.6: Maintained Versus Unmaintained SA Trends



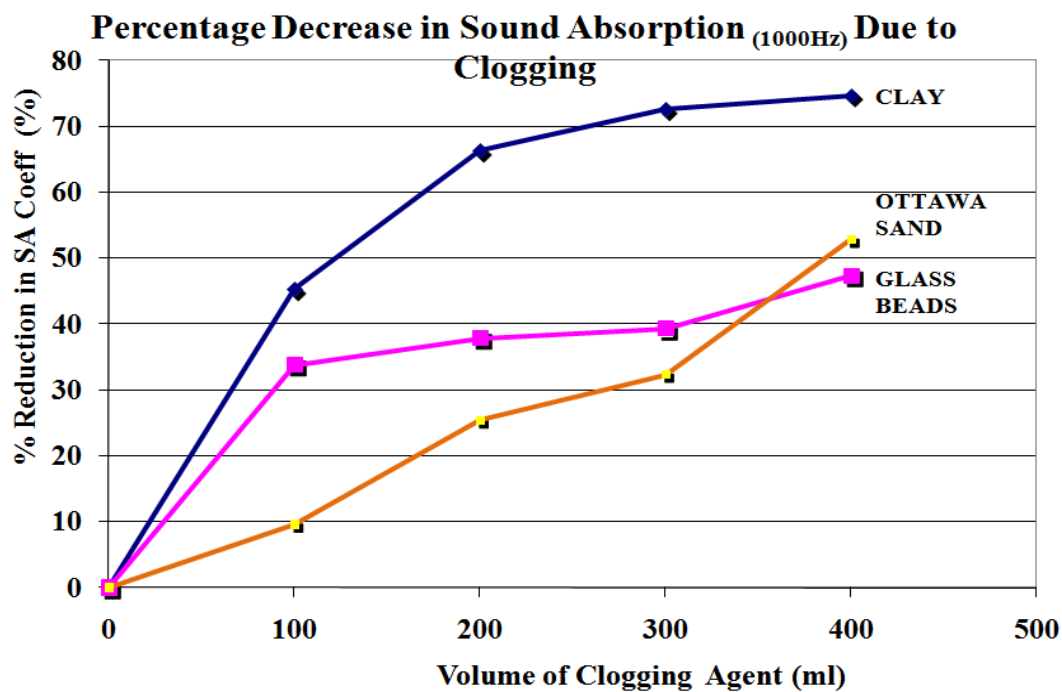
**Figure 9.7: Sound Absorption of Clogged and Unclogged Locations in City of Shoreview**



**Figure 9.8: Accelerated Clogging Test**



(A) Sound Absorption Versus Clogging Agent Volume



(B) Percentage Reduction in Sound Absorption Versus Clogging Volume

Figure 9.9: Results of Clogging Experiment

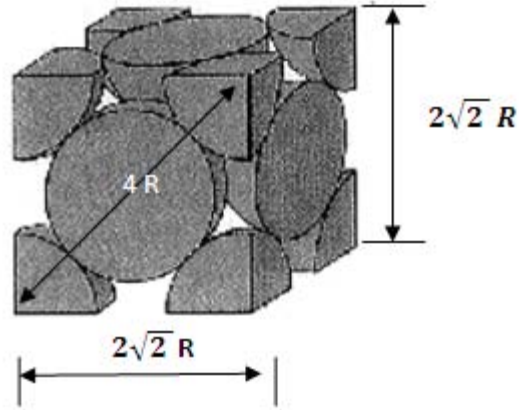


**Figure 9.10: Section through Idealized Closely Packed Pervious Matrix**

## CHAPTER 10 FINAL CONCLUSIONS

This report includes the design, construction, and early performance of three pervious concrete test cells construction at MnROAD in 2008. These cells were constructed to evaluate the performance of pervious concrete pavements on a low-volume road in a cold weather climate. The three cells discussed in this report are as follows: Cell 39 Porous Concrete Overlay, Cell Pervious Concrete On Granular Subgrade, Cell 85 Pervious Concrete On Cohesive Subgrade. This report has the following seven chapters which uniquely discuss each phase of this project: research synthesis; mix design, pavement design, and geotechnical evaluation; construction sequence, initial testing, hydrologic evaluation, early two ear performance, and implementation. After over two years of monitoring and evaluation, the following conclusions can be made of pervious concrete.

- Results show IRI measurements significantly higher than FHWA standards for acceptable pavements. However, all three cells maintained excellent surface ratings.
- The pervious test cells show improved sound absorption compared to typical PCC pavement, with the degree of improvement dependent on the sound frequency being tested.
- Dissipated volumetric rate varied significantly throughout cells, suggesting uneven material consistency. This flow rate was generally higher in cell 85 (granular base) than cell 89 (clay base).
- Temperature and moisture sensors show a reduced temperature gradient throughout the pavement, base, and subgrade, and possibly a reduced amount of freeze thaw cycles for full-depth pervious concrete.
- Vacuuming more than two times a year has shown promising results and improved performance compared to the original lighter maintenance schedule. Pervious pavements can be maintained over time with this amount of effort.
- The frequent raveling the pervious cells experienced is expected to be from freeze thaw distress. Keeping the pavement unclogged can likely lessen the chances for this freeze thaw damage to happen, and therefore reduce raveling.
- Predicting OBSI from sound absorption does not seem feasible at this point. This is likely because sound relief in pervious pavements come from air compression instead of the conventional methods found in normal concrete. A relation between the two is also difficult to establish due to the difference between the sound spectrums measured in OBSI and sound absorption. However, it is evident the sound absorption is related to the porosity of pervious pavements.
- Pervious concrete pavements can be designed with traditional methods such as the AASHTO 1993 method or the MEPDG. The design processes discussed in chapter 2 of this report produced pervious concrete pavement which met performance expectations.
- ISLAB and similar programs can be used to accurately analyze and predict stresses in pervious concrete.
- The infiltration methods used in the pervious concrete cells can be maintained over time if proper maintenance activities are performed.
- Evaluation of the pervious test cells over the years has shown FWD deflection results higher than other typical concrete pavements. It is unsure how this can translate into

durability. However, a relationship between the two is very likely and this matter should be a subject of further study.

# REFERENCES

## Chapter 1 References

- 1) Izevbekhai, B.I., Burnham, T., Worel, B., Frentress, D., Macdonald, K. "Construction Report for Cell 64 Pervious Concrete." St. Paul, MN: Minnesota Department of Transportation, Aggregate Ready Mix Association of Minnesota.  
<http://www.mrr.dot.state.mn.us/reports/onlinereports>. Accessed 3/15/2008.
- 2) Izevbekhai, B.I., Eller, A.J. "1st Year Performance Report for Cell 64 Pervious Concrete." Minnesota Department of Transportation, Aggregate Ready Mix Association of Minnesota.  
<http://www.mrr.dot.state.mn.us/reports/onlinereports>. Accessed 3/15/2008.
- 3) Sieglen, W.E., Von-Langsdorff, H. "Interlocking Concrete Block Pavements at Howland Hook Marine Terminal." *Proceedings of Port Development in the Changing World*, 2004/05/23-2004/05/26. Houston, TX. 2004. pp. 10.
- 4) Haselbach, L.M., Freeman, R.M. "Vertical Porosity Distributions in Pervious Concrete Pavement." *ACI Materials Journal*. 2006. 103(6), pp. 452.
- 5) ACI Committee 522. *Pervious concrete*. Report #522R-06. Farmington Hills, MI: American Concrete Institute. 2006.
- 6) Offenberg, M. "Producing Pervious Pavements." *Concrete International*. 2005. 27(3), pp. 50-54.
- 7) Partl, M.N., Momm, F., Bariani, B. "Study of the Aggregate for the Pervious Asphalt Concrete Performance Testing and Evaluation of Bituminous Materials." *Proceedings of the 6th International RILEM Symposium*, 2003/04/14-2003/04/16. Zurich, Switzerland. 2003. pp. 237-43.
- 8) Tennis, P.D., Leming, M.L., Akers, D.J. *Pervious concrete pavements*. Skokie, IL: Portland Cement Association. 2004.
- 9) Delatte, N.J. "Structural Design of Pervious Concrete Pavement." *Proceedings of Transportation Research Board 86th Annual Meeting*. Washington, D.C. 2007. pp. 16.
- 10) Portland Cement Association. *Pervious Concrete Hydrological Design and Resources*. Skokie, IL: Portland Cement Association. 2006.
- 11) Schaefer, V. *Remix design development for pervious concrete in cold weather climates*. Ames, IA: Iowa Department of Transportation. 2006.

- 12) Burk, R.J. "Permeable Interlocking Concrete Pavements - Selection, Design, Construction and Maintenance." *Proceedings of the 2004 Annual Conference and Exhibition of the Transportation Association of Canada*. 2004. pp. 17.
- 13) American Concrete Institute. *Guide For Selecting Proportions For No-Slump Concrete*. Report #ACI 211.3R-97. 2002. pp. 26.
- 14) Fowler, D.W. "Aggregates for Pervious Concrete." *Proceedings of the International Center for Aggregate Research 11th Annual Symposium*. Austin, TX. 2003. pp. 9.
- 15) Kuennen, T. "Voids Add Value To Pervious Concrete." *Better Roads*. 2003. 73(8), pp. 6, 22-29.
- 16) Shackel, B., Pearson, A. "Permeable Concrete Eco-Paving as Best Management Practice on Australian Urban Road Engineering." *Proceedings of the 21<sup>st</sup> ARRB Transport Research Conference*. Cairns, Queensland, Australia. 2003. pp. 11.
- 17) Wanielista, M.P., Chopra, M.B. *Performance assessment of Portland cement pervious pavement and cement pervious pavement*. Report # FDOT BD 521-02. Orlando, FL: Storm Water Management Academy, University of Central Florida. 2007.
- 18) Smith, D.R. "Storm Water Runoff: Permeable Interlocking." *Public Works*. 2003. pp. 28-30.
- 19) Waagberg, L.G. "Draining Asphalt Concrete." (Statens Vaeg- och Trafikins titut, Sweden) *Nordiska Vaegtekniska Foerbundets XIV Kongress*, 1984/06/04-1984/06/06. Stockholm, Sweden. pp. 126-9.
- 20) Cackler, E.T., Harrington, D.S., Ferragut, T. "Evaluation of U.S. and European Concrete Pavement Noise Reduction Methods." Ames, IA: Center for Transportation Research and Education. pp. 101.
- 21) Lefebvre, J.P., Marzin, M. "Strides In Highway Engineering." *The Year 1995 In France - Pervious Cement Concrete Wearing Course Offering Less Than 75 Db(A) Noise Level*. 1995. (735), pp. 33.
- 22) Howe, J. "Comparing paving costs." (*Interpave*) *Concrete*. 2006. 40(8), pp. 37-9.
- 23) Tatsushita, F., Abe, H., Inoue, T., Yagi, Y. "Test Application of Pervious Asphalt Concrete Surface Layer in Maintenance Project: Aiming Noise Reduction and Driving Safety." *Proceedings of the Sixth Conference Road Engineering Association of Asia and Australasia*. 1990/03/04-1990/03/10. Kuala Lumpur, Malaysia. 1990. pp. 16.

- 24) Stidger, R. "How To Manage Concrete Road Life Cycles." *Better Roads*. 2002. 72(4), pp. 44-48.
- 25) Kuennen, T. "Voids Add Value To Pervious Concrete." *Better Roads*. 2003. pp. 22-29.
- 26) Lefebvre, J.P., Marzin, M. "Strides in Highway Engineering." *The Year 1995 In France - Pervious Cement Concrete Wearing Course Offering Less Than 75 Db(A) Noise Level*. 1995. (735), pp 33-35.
- 27) Welleman, T. "Crossfall Transitions and Rainfall." Berkshire, England: Transport and Road Research Laboratory. 1976. pp.143-55.
- 28) Bendtsen, H. "Road Surfacing and Noise Reduction." *Pavement Technique and Pavement Surface*. 1992/10/05-1992/10/06. Finland. 1993.
- 29) Crocker, M.J., Hanson, D., Li, Z., Karjatkar, R., Vissamraj, K.S. "Measurement of Acoustical and Mechanical Properties of Porous Road Surfaces and Tire and Road Noise." *Transportation Research Record*, 1891. 2004. pp. 16-22.
- 30) Neithalath, N., Weiss, W.J., Olek, J. "Reducing the Noise Generated in Concrete through Modifications of Surface Characteristics." *Research and Development Information*, PCA R&D Serial No. 2878.
- 31) Pratt, C. "Clear Benefits" *The Surveyor*. November 1999.

### Chapter 3 and 4 References

- 1) Izevbekhai, B.I. "Optimization of Texture and Ride Quality in Pavement Infrastructure." Minneapolis, MN: University of Minnesota Institute of Technology. December 2004.
- 2) Kuemmel, A.A., Sonntag, R.C., Jackel, J.R., Satanovsky, A. *Noise and Texture on PCC Pavements*. Report # WI/ SPR 08 -093. Wisconsin Department of Transportation. 2000.
- 3) Hanson, D.I., Waller, B. *Evaluation of the Noise Characteristics of Minnesota Pavements*. St. Paul, MN: Minnesota Department of Transportation. 2005.  
<http://www.mrr.dot.state.mn.us/pavement/PvmtDesign/noise/MNCPXnoiseresultsfinalreport.pdf>. Accessed 2/29/08.
- 4) Hanson, D.I., James, R.S. *Noise Evaluation of Colorado Pavements*. Report No. CDOT-DTD-R-2004-5. Colorado Department of Transportation. 2004.
- 5) Wu, C., Nagi, M.A. "Optimizing Surface Texture of Concrete Pavement." *Research and Development Bulletin*. RD111T. Skokie, IL: Portland Cement Association. 1995.

- 6) Sandberg, U., Ejsmont, J. *Tyre/Road Noise Reference Manual*. Kisa, Sweden: Informex Ejsmont & Sandberg. 2002.
- 7) Izevbekhai, B.I. *Innovative Diamond Grinding Research Summary*. St. Paul, MN: Minnesota Department of Transportation. February 2008.  
<http://www.dot.state.mn.us/materials/research.html>. Accessed 3/13/08.
- 8) Izevbekhai, B.I. *New generation Diamond grinding*.  
[http://www.concretepavements.org/Membership/Newsletter/ISCP\\_enewsletter\\_Vol4\\_No6.htm](http://www.concretepavements.org/Membership/Newsletter/ISCP_enewsletter_Vol4_No6.htm). Accessed 2/28/08.
- 9) McNERNEY, M.T., LANSBERGER, B.J., PANDELINDES, A. *Field Measurement of Time/Pavement Noise of Selected Texas Pavements*. Report # 7-2957-2. Texas Department of Transportation. 2000.
- 10) US Department of Transportation Federal Highway Administration. *Technical Advisory on Pavement Texture*. Report # T 5040-36. 2005.  
<http://www.fhwa.dot.gov/legregs/directives/techadvs/t504036.htm>. Accessed 7/ 21/2008.
- 11) Izevbekhai, B.I. *MnROAD OBSI Mini Rodeo*. 2008. <http://www.lrrb.org/pdf/200845.pdf>. Accessed 12/1/08.
- 12) Izevbekhai, B.I. *Report on Diamond Grinding of Cells 7 and 8*. St. Paul, MN: Minnesota Department of Transportation.  
<http://www.dot.state.mn.us/materials/researchdocs/ReportDiamondGrinding.pdf>. Accessed 12/1/08.
- 13) Izevbekhai, B.I., Eller, A. “MnROAD Cell 64 Pervious Concrete – First Year Performance Report.” St. Paul, MN: Minnesota Department of Transportation. 2007.
- 14) Izevbekhai, B., Burnham, T., Worel, B., MacDonald, K., Burke, B., Frentress, D. *2005 MnROAD – Pervious Concrete Project: Cell – 64 Driveway Construction Report*. St. Paul, MN: Minnesota Department of Transportation. 2006.
- 15) Worel, B., Frentrss, D., Clendenen, J. *2006 MnROAD – Pervious Concrete Project Pervious Concrete Sidewalk Project*. St. Paul, MN: Minnesota Department of Transportation. 2007.

## Chapter 5 References

- 1) Izevbekhai, B.I., Rohne, R. “Pervious Concrete in MnROAD Low-volume Road.” *Transportation Research Board Annual General Meeting*. 2009.
- 2) Wanielista, M., Chopra, M. *Performance Assessment of Portland Cement Pervious Concrete*. Report # FDOT Project BD521-02. Orlando, FL: Stormwater Management Academy, University of Central Florida.
- 3) Driscoll, F.G., *Groundwater and Wells*. St. Paul, MN: Johnson Filtration Systems, Inc. (2nd ed.). 1986. pp. 1089.

## Chapter 6 References

- 1) Eller, A. *Drainable Pavements at MnROAD: Pervious Concrete and Porous Concrete Overlay Cells 39, 85, and 89*. St. Paul, MN: Minnesota Department of Transportation. 2010.
- 2) The Irrometer Company, Inc. "Watermark Solid Moisture Sensor – Model 200SS." <http://www.irrometer.com/sensors.html#wm>. Accessed 2/2/2011.
- 3) Izevbekhai, B., Maloney, M. "Maintenance and Evaluation of Porous Pavement Infrastructure in Minnesota." *Annual Transportation Research Board Conference*. 2011/01/25.
- 4) MnDOT. "Introduction to the International Roughness Index." Bituminous Smoothness Training Workshops. Minnesota Department of Transportation. 2007/04/11. St. Paul, MN. 2011.
- 5) Mohamed, R.A., Hansen, W. "Effect of Nonlinear Temperature Gradient on Curling Stress in Concrete Pavements." *Transportation Research Record*, 1568. 1997. Pp. 65-71.
- 6) Rohne, R., Izevbekhai, B. *MnROAD Cell 64 Pervious Concrete: Third Year Performance Report*. Minnesota Department of Transportation. 2009.
- 7) Nau, B. "Introduction to ARIMA: nonseasonal models." *Decision 411 Forecasting*. Durham, NC: Duke University, Fuqua School of Business. 2011. <http://www.duke.edu/~rnau/411arim.htm>. Accessed 2/10/2011.
- 8) Meko, D.M. "Autocorrelation." *Applied Time Series Analysis*. University of Arizona. 2011. [http://www.ltrr.arizona.edu/~dmeko/notes\\_3.pdf](http://www.ltrr.arizona.edu/~dmeko/notes_3.pdf).
- 9) Salas, J.D., Delleur, J.W., Yevjevich, V.M., Lane, W.L. *Applied modeling of hydrologic time series*. Littleton, CO: Water Resources Publications. 1980. pp. 484.

## Chapter 8 References

- 1) Sandberg, U., Ejsmont, J., Tyre. *Road Noise Reference Manual*. Kisa, Sweden: Informex Ejsmont & Sandberg. 2002.
- 2) Izevbekhai, B.I. *Construction report of Cells 7 and 8 MnROAD Diamond Grinding*. St. Paul, MN: Minnesota Department of Transportation. 2008.
- 3) Wu, C., Nagi, M.A. "Optimizing Surface Texture of Concrete Pavement." *Research and Development Bulletin*. RD111T. Skokie, IL: Portland Cement Association. 1995.
- 4) Simon, F., Roderiguez, M.R., Pfretzschner, J. "On the Absorption Coefficient of Porous Corrugated Surfaces." *Journal of Vibration and Acoustics*. 2002. 124, pp. 329-335.

- 5) Kuemmel, A.A., Sonntag, R.C., Jackel, J.R., Satanovsky, A. *Noise and Texture on PCC Pavements Report of a Multi-State Pooled Fund Study*. Report # WI/ SPR 08 –09. Wisconsin Department of Transportation.
- 6) Nelson, J.T., Kohler, E., Öngel, A., Rymer, B. “Acoustical Absorption of Porous Pavement.” *Transportation Research Record*, 2058. 2008. pp. 125-132.
- 7) Crocker, M.J., Hanson, D., Li, Z., Karjatkar, Vissamraju, K.S. “Measurement of Acoustical and Mechanical Properties of Porous Road Surfaces and Tire and Road Noise.” *Transportation Research Record*, 1891. 2004. pp. 16-22.
- 8) Sandberg, U. *The Multi-Coincidence Peak around 1000 Hz in Tyre/Road Noise Spectra. Proceeding of Euronoise Conference*. Paper Id 498. Staples, Italy. 2003.
- 9) Kuehl, R., Marti, M., Schilling, J. *Resource for Implementing a Street Sweeping Best Practice*. St. Paul, MN: Minnesota Department of Transportation. 2008.
- 10) Horoshenkov, K.V., Hothersall, D.C., Attenborough, K. “Porous Materials for Scale Model Experiments in Outdoor Sound Propagation.” *Journal of Sound and Vibration*. 1996. 194(5), pp. 685-708.
- 11) Bérengier, M., Garai, M. *In Situ Sound Absorption Coefficient Measurement of Various Surfaces*. Cedex, France: Laboratoire Central des Ponts et Chaussées. Bouguenais.
- 12) Hanson, D.I., Waller, B. *Evaluation of the Noise Characteristics of Minnesota Pavements*. St. Paul, MN: Minnesota Department of Transportation. 2005.  
<http://www.mrr.dot.state.mn.us/pavement/PvmtDesign/noise/MNCPXnoiseresultsfinalreport.pdf>. Accessed 8/29/09.
- 13) Hanson, D.I., James, R.S. *Noise Evaluation of Colorado Pavements*. Report # CDOT- DTD-R-2004-5. Colorado Department of Transportation. 2004.
- 14) ASTM E-1050. *Sound Absorption measurement with the Impedance Tube*. ASTM. 2007.
- 15) Beranek, L.L. *Noise and Vibration Control*. New York: McGraw Hill. 1971.

## Chapter 9 References

- 1) Eller, A.J., Izevbekhai, B.I. *MnROAD Cell 64 Pervious Concrete First Year Performance Report*. Report # MN/RC – 2007-17. St. Paul, MN: Minnesota Department of Transportation, Office of Materials. 2007.
- 2) Sandberg, U., Ejsmont, J. *Tyre Road Noise Reference Manual*. Kisa, Sweden: Informex Ejsmont & Sandberg. 2002.
- 3) Rohne, R., Izevbekhai, B.I. “Early Performance of a Pervious Concrete Cell.” *Transportation Research Board Annual Meeting*. 2009.

- 4) Rohne, R., Izevbekhai, B. *MnROAD Cell 64 Pervious Concrete: Third Year Performance Report*. Report # 2009-19. St. Paul, MN: Minnesota Department of Transportation. 2009.
- 5) Schaefer, V.R., Wang, K., Suleiman, M.T., Kevern, J.T. *Mix Design Development for Pervious Concrete in Cold Weather Climates*. Ames, IA: Center for Transportation Research and Education. 2006.
- 6) Neithalath, N. "Properties of Enhanced porosity (Pervious) concrete." *Proceedings of the Indian Concrete Institute – Innovative World of Concrete (ICI-IWC) conference*. New Delhi, India. 2008. pp. 14.
- 7) Garai, M., Berengier, M., Guidorzi, P., L'Hermite, P. "Procedure for measuring the sound absorption of road surfaces in-situ from spectra." *Proceedings of Euro Noise '98 Conference*. 1998/10/04-1998/10/07. Munich, Germany.
- 8) Ferguson, B.K. "Integrative studies in Stormwater Management and Land Development. Pervious Pavements." *Best Management Practice*. Boca Raton, FL: Taylor & Francis Group. 2005.
- 9) Kuehl, R., Marti, M., Schilling, J. "Resource for Implementing a Street Sweeping Best Practice." Report # 008RIC06. Minnesota Department of Transportation. <http://lrrb.org/PDF/2008RIC06.pdf>. Accessed 7/7/2010.
- 10) ASTM Standard C1701. *Standard Test Method for Infiltration Rate of In Place Pervious Concrete*. West Conshohocken, PA: ASTM International. 2003.
- 11) Fwa, T.F., Tana, S.A., Chuaia, C.T., Guwea, Y.K. "Expedient Permeability Measurement for Pervious Pavement Surface." *International Journal of Pavement Engineering*. 2001. 2(4), pp. 259-270.
- 12) Grisan, E., Foracchia, M., Ruggeri, A. "A novel method for automatic evaluation of retinal vessel tortuosity." *Proceedings of the 25th Annual International Conference of the IEEE EMBS*. Cancun, Mexico. 2003.
- 13) Mächler, M. *Very smooth nonparametric curve estimation by penalizing change of curvature*. Report #71. Zurich: Eidgenossische Technische Hochschule. 1993.
- 14) Patasius, M., Marozas, V., Lukosevicius, A., Jegelevicius, D. "Evaluation of tortuosity of eye blood vessels using the integral of square of derivative of curvature." *EMBE'05: Proceedings of the 3rd IFMBE European Medical and Biological Engineering Conference*, 2005/11/20-2005/11/25. Prague, Czech Republic. pp. 1-4.

**APPENDIX A: GEOTECH REPORT FROM FOUNDATIONS  
UNIT**



**Minnesota Department of Transportation**

---

**Office of Materials**  
Geotechnical Engineering Section  
1400 Gervais Ave - Mailstop 645  
Maplewood, MN 55109

**Date:** March 18, 2008

**To:** Bernard Inerbekhai, Research Operations Engineer  
MnROAD

**From:** Gary Person, Foundations Engineer  
Foundations Unit

 Digitally  
signed  
by Gary  
Person

**Phone:** (651)366-5598

**Concur:** Rich Lamb, Foundations Projects Engineer  
Foundations Unit



**Subject:** S.P. 8680-157  
MnROAD Test Facility Interstate 94  
Foundation Investigation and Monitoring Well Installation

---

**Project Description**

This letter is in response to your request to install four monitoring wells at the MnROAD Test Facility. Prior to installing the monitoring wells, four CPT soundings were taken to verify anticipated soil type and determine an approximate depth for the monitoring wells.

**Field Investigation and Foundation Conditions**

Four CPT soundings were advanced November 2007. Four SPT borings were drilled February 2008. The monitoring wells were installed in the SPT borings.

The foundation soils encountered at T1MW and T2MW consist primarily of sand and loamy sand with some gravel.

The foundation soils encountered at T3MW and T4MW consist of 12' of sandy soils followed by 10' of sandy clay loam. Below the sandy clay loam is plastic sandy loam or sandy clay loam to the bottom of the borings.

Water was encountered while sampling and drilling between elevation 949.9 and 953.1.

Please see the attached borings and CPT soundings for a more detailed description of the foundation soils.

Please notify the Foundations Unit when the monitoring wells are no longer in use, so they can be removed and sealed.

**Attachments:**

Boring Layout

SPT Index sheet

SPT Boring: T1MW, T2MW, T3MW, and T4MW ((Unique Numbers 70089, 70090, 70091, and 70092)

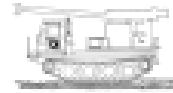
CPT Index Sheet

CPT Sounding

cc: Glenn Engstrom, Dave VanDeusen, File



Boring Log Descriptive Terminology (English Units)



**USER NOTES, ABBREVIATIONS AND DEFINITIONS - Additional information available in Geotechnical Manual.**

This boring was made by ordinary and conventional methods and with care deemed adequate for the Department's design purposes. Since this boring was not taken to gain information relating to the construction of the project, the data noted in the field and recorded may not necessarily be the same as that which a contractor would desire. While the Department believes that the information as to the conditions and materials reported is accurate, it does not warrant that the information is necessarily complete. This information has been edited or abridged and may not reveal all the information which might be useful or of interest to the contractor. Consequently, the Department will make available at its offices, the field logs relating to this boring.

Since subsurface conditions outside each borehole are unknown, and soil, rock and water conditions cannot be relied upon to be consistent or uniform, no warrant is made that conditions adjacent to this boring will necessarily be the same as or similar to those shown on this log. Furthermore, the Department will not be responsible for any interpretations, assumptions, projections or inferences made by contractors, or other users of this log.

Water levels recorded on this log should be used with discretion since the use of drilling fluids in borings may seriously distort the true field conditions. Also, water levels in cohesive soils often take extended periods of time to reach equilibrium and thus reflect their true field level. Water levels can be expected to vary both seasonally and yearly. The absence of notations on this log regarding water does not necessarily mean that this boring was dry or that the contractor will not encounter subsurface water during the course of construction.

- WH ..... Weight of Hammer
- WR ..... Weight of Rod
- Blsd ..... Drilling Fluids in Sample
- CS ..... Confusion Sample

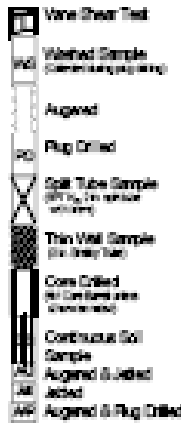
**SOIL-CORE TESTS**

- SPT  $N_{60}$  ..... ASTM D1586 Modified (Blows per foot with 140 lb. hammer and a standard energy of 210 ft-lbs. This energy represents 60% of the potential energy of the system and is the average energy provided by a Rope & Catch system.)
- MC ..... Moisture Content
- CC ..... Cohesion
- $\gamma$  ..... Sample Density
- LL ..... Liquid Limit
- PI ..... Plasticity Index
- $\phi$  ..... Phi Angle
- RCC ..... Percent Core Recovered
- RQD ..... Rock Quality Description (Percent of total core interval consisting of unbroken pieces 4 inches or longer)
- ACL ..... Average Core Length (Average length of core that is greater than 4 inches long)
- CB ..... Core Breaks ..... Number of natural core breaks per 3-foot interval.

**DISCONTINUITY SPACING**

- |                  |                              |                  |
|------------------|------------------------------|------------------|
| <b>Fractures</b> | <b>Discontinuity Spacing</b> | <b>Condition</b> |
| Very Close       | < 2 inches                   | Very Thin        |
| Close            | 2-12 inches                  | Thin             |
| Mod. Close       | 12-36 inches                 | Medium           |
| Wide             | > 36 inches                  | Thick            |

**DRILLING SYMBOLS**



**RELATIVE DENSITY**

- Conspicuous ..... Consensus Soils
- SEC

- very loose ..... 0-4
- loose ..... 5-10
- medium dense ..... 11-34
- dense ..... 35-50
- very dense ..... >50

**Consensus ..... Consensus Soils**

- SEC
- very soft ..... 0-1
- soft ..... 2-4
- firm ..... 5-9
- stiff ..... 9-15
- very stiff ..... 16-30
- hard ..... 31-60
- very hard ..... > 60

**COLOR**

- |     |                    |     |        |
|-----|--------------------|-----|--------|
| bl  | Black              | wh  | White  |
| gn  | Green              | brn | Brown  |
| org | Orange             | yel | Yellow |
| dk  | Dark               | lt  | Light  |
| IOB | Iron Oxide Stained |     |        |

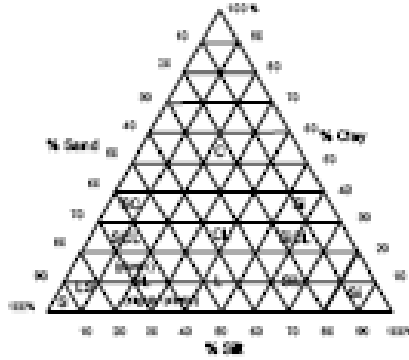
**GRAIN SIZE ELASTICITY**

- VF ..... Very Fine
- F ..... Fine
- CF ..... Coarse
- pl ..... Plastic
- slpt ..... Slightly Plastic
- Ps ..... Plastic

**SOIL-ROCK TERMS**

- |     |  |     |           |
|-----|--|-----|-----------|
| C   | Clay   | Lm  | Limestone |
| L   | Loam   | Sst | Sandstone |
| S   | Sand   | Dsk | Dolomite  |
| Sl  | Silt   | wt  | weathered |
| G   | Gravel (No. 10 Sieve to 3 inches)                |     |           |
| Bdr | Boulder (over 3 inches)                          |     |           |
| T   | Tuff (unsorted, non stratified glacial deposits) |     |           |

**Mn/DOT Triangular Textural Soil Classification System**



**WATER MEASUREMENT**

- AB ..... After Bailing
- AC ..... After Completion
- AF ..... After Flushing
- w/c ..... with Casag
- w/bl ..... with Blsd
- WSD ..... With Sampling/Drilling
- w/WG ..... with Hollow Stem Auger

**MISCELLANEOUS**

- NA ..... Not Applicable
- wt ..... with
- w/o ..... with out
- wt ..... retained

**DRILLING OPERATIONS**

- AG ..... Augered
- CD ..... Core Drilled
- DD ..... Disturbed by Drilling
- DDJ ..... Disturbed by Jetting
- PD ..... Plug Drilled
- ST ..... Split Tube (SPT test)
- TH ..... Thinwall ( Shelby Tube)
- WS ..... Wash Sample
- WSS ..... Wash Sample (No. 20 Sieve)

MINNESOTA DEPARTMENT OF TRANSPORTATION - GEOTECHNICAL SECTION  
 LABORATORY LOG & TEST RESULTS - SUBSURFACE EXPLORATION



**UNIQUE NUMBER 70089**

U.S. Customary Units

State Project <b>8680-157</b>		Bridge No. or Job Desc. <b>Interstate Highway I94</b>		Boring No. <b>T1MW</b>		Ground Elevation <b>960.1</b> (survey)			
Location <b>ft. LT</b> Wright Co. Coordinate: X=642570 Y=205391 (ft.) Latitude (North)=45°15'59.10" Longitude (West)=93°43'04.83"				Drill Machine <b>205120 CME(LC55) Track</b>		SHEET 1 of 1			
				Hammer <b>CME Automatic Calibrated</b>		Drilling Completed <b>2/13/08</b>			
DEPTH	Depth	Lithology	Classification	Drilling Operation	SPT	MC	COH	γ	Other Tests Or Remarks
	Elev.				No	(%)	(pcf)	(pcf)	
					RES (%)	RQD (%)	ACL (ft)	Cone Breaks	Formation or Member
	4.0 956.1	slightly plastic Sandy Loam with a few pebbles, dark gray-brown and moist				15			
	5.0 954.1	plastic Loam, grays and moist			8	23			
	10.0	Loamy Sand with some Gravel and a few pockets of plastic Sandy Loam, brown to gray-brown, moist to wet			48	10			
	12.0				12	15			
	15.0				9	16			
	22.0 938.1	Loamy Sand and Gravel, brown and saturated			6	15			
	25.5 934.6				18	20			
	25.5 934.6				43	16			
Bottom of Hole - 25.5' Water measured at 9.6' while sampling and/or drilling with augers									
Index Sheet Code 3.0				Soil Class:DSB Rock Class: Edit: Date: 3/18/08 G:\CNT\PROJECTS-ACTIVE\8680-157.GPJ					

MINNESOTA DEPARTMENT OF TRANSPORTATION - GEOTECHNICAL SECTION  
 LABORATORY LOG & TEST RESULTS - SUBSURFACE EXPLORATION



**UNIQUE NUMBER 70089**  
 U.S. Customary Units

State Project <b>8680-157</b>		Bridge No. or Job Desc.		Trunk Highway/Location <b>Interstate Highway I94</b>		Boring No. <b>T1MW</b>		Ground Elevation <b>960.1 (survey)</b>	
Location <b>,, ft. LT</b> Wright Co. Coordinate: X=542570 Y=205391 (ft.) Latitude (North)=45°15'59.10" Longitude (West)=93°43'04.83"						Drill Machine <b>205120 CME(LC55) Track</b>		SHEET 1 of 1	
						Hammer <b>CME Automatic Calibrated</b>		Drilling Completed <b>2/13/08</b>	
DEPTH	Depth	Lithology	Classification	Drilling Operation	SPT	MC	COH	Y	Other Tests Or Remarks
	Elev.				No	(%)	(pcf)	(pcf)	
					RES (%)	RQD (%)	ACT. (ft)	Cone Breaks	Formation or Member
	4.0 956.1	slightly plastic Sandy Loam with a few pebbles, dark gray-brown and moist				15			
	5.0 954.1	plastic Loam, grays and moist			8	23			
	6.0 954.1	Loamy Sand with some Gravel and a few pockets of plastic Sandy Loam, brown to gray-brown, moist to wet			48	10			
	10.0				12	15			
	15.0				9	16			
	22.0 938.1				6	15			
	25.0 934.6	Loamy Sand and Gravel, brown and saturated			18	20			
	25.5 934.6				43	16			
Bottom of Hole - 25.5' Water measured at 9.6' while sampling and/or drilling with augers									
Index Sheet Code 3.0						Soil Class:DSB Rock Class: Edit: Date: 3/18/08 G:\AN7\FPROJECTS-ACTIVE\8680-157.GPJ			

MINNESOTA DEPARTMENT OF TRANSPORTATION - GEOTECHNICAL SECTION  
**PIEZOMETER LOG & WATER LEVEL READINGS**

**UNIQUE NUMBER 70089**

**MDH Number 577314**

Boring Log Addendum

State Project <b>8680-157</b>	Bridge No. or Job Desc.	Trunk Highway/Location <b>194</b>	Boring No. <b>T1MW</b>
Location Wright Co. Coordinate: X=542570 Y=205391 Latitude (North)=45°15'59.10" Longitude (West)=93°43'04.83"		Drill Machine <b>205120 CME(LC55) Track</b>	Ground Elevation <b>960.1</b> ( )
		Supervisor <b>J. Hasselquist</b>	Install Date <b>2/13/2008</b>
		Operator <b>D. Zerwas</b>	Seal Date
		Sealed by	Seal Licensee
If sealing details are blank, well has not been sealed as of time of printing (bottom right).			
<p>The diagram shows a vertical piezometer casing and riser pipe. Key elevations are: Top of Protective Casing (962.7 ft), Top of Riser Pipe (962.4 ft), Ground Surface (960.1 ft), Water Elevation (950.5 ft), Top of Seal (949.1 ft), Top of Sand (948.1 ft), Top of Screen (937.0 ft), Bottom of Screen (937.0 ft), and Bottom of Borehole (934.6 ft). The riser pipe is 15 feet long, and the screen is 10.4 feet long. The casing is 7 feet long. The seal is made of bentonite/cement, and the annular space is filled with native material. The screen is made of PVC with a 2-inch diameter and 0.01 slot size. The sand pack is washed sand from mother earth.</p>			
<b>Interior Casing / Riser Pipe Details</b>			
Type of Riser Pipe	2" PVC		
Diameter of Riser Pipe	2 inch		
Top of Riser Pipe	2.3 feet		
Total Length of Riser Pipe	15		
<b>Screen Details</b>			
Type of Screen	PVC		
Diameter of Screen	2 inch		
Screen Slot Size	0.01 slot		
Depth to Top of Screen	12.7 feet		
Screen Length	10.4 feet		
Depth to Bottom of Screen	23.1 feet		
<b>Protective Casing Details</b>			
Type of Casing	Steel		
Diameter of Casing	8 inch		
Height of Top of Casing	2.6 feet		
Total Casing Length	7 feet		
Lock Type & Number	2108		
Diameter of Borehole	8 inch		
<b>Annular Space and Seal Details</b>			
Type of Surface Seal	Bentonite/Cement		
Type of Annular Seal	Native material		
Type of Screen Seal	Bentonite		
Type of Sand Pack	Washed Sand		
Source of Sand	Mother Earth		
Amount of Sand (pounds)	150		
Type of Bottom Seal	Native material		
Soil Class: DSB Rock Class: Edit: Date: 3/18/08			

MINNESOTA DEPARTMENT OF TRANSPORTATION - GEOTECHNICAL SECTION  
 LABORATORY LOG & TEST RESULTS - SUBSURFACE EXPLORATION



**UNIQUE NUMBER 70090**

U.S. Customary Units

State Project <b>8680-157</b>		Bridge No. or Job Desc. <b>Interstate Highway 194</b>		Boring No. <b>T2MW</b>		Ground Elevation <b>960.7</b> (survey)			
Location <b>1.1 ft. LT</b> Wright Co. Coordinate: X=642603 Y=205440 (ft.) Latitude (North)=45°15'59.58" Longitude (West)=93°43'04.37"				Drill Machine <b>205120 CME(LC55) Track</b>		SHEET 1 of 1			
				Hammer <b>CME Automatic Calibrated</b>		Drilling Completed <b>2/13/08</b>			
DEPTH	Depth	Lithology	Classification	Drilling Operation	SPT	MC	COH	γ	Other Tests Or Remarks
	Elev.				Neo	(%)	(pcf)	(pcf)	
					REG (%)	RQD (%)	ACL (ft)	Cone Breaks	Formation or Member
	4.0 966.7		Loamy Sand with some Fine Gravel, dark brown and moist			8			
	5					7	19		
	8.5 962.2		Sand with a little Gravel and a layer of Clay Loam, brown with gray, moist to wet			9	18		
	10					8	18		
	12.0 948.7		Loamy Sand and Gravel, brown and saturated			15	18		
	15					22	14		
	20		Loamy Sand with a little Gravel and a seam of plastic Sandy Loam, gray-brown and saturated			W/R	14		
	25 935.2								
Bottom of Hole - 25.5' Water measured at 7.6' while sampling and/or drilling									
Index Sheet Code 3.0				Soil Class:DSB Rock Class: Edit: Date: 3/18/08 G:\DATA\PROJECTS-AC\T2M090-157.GPJ					

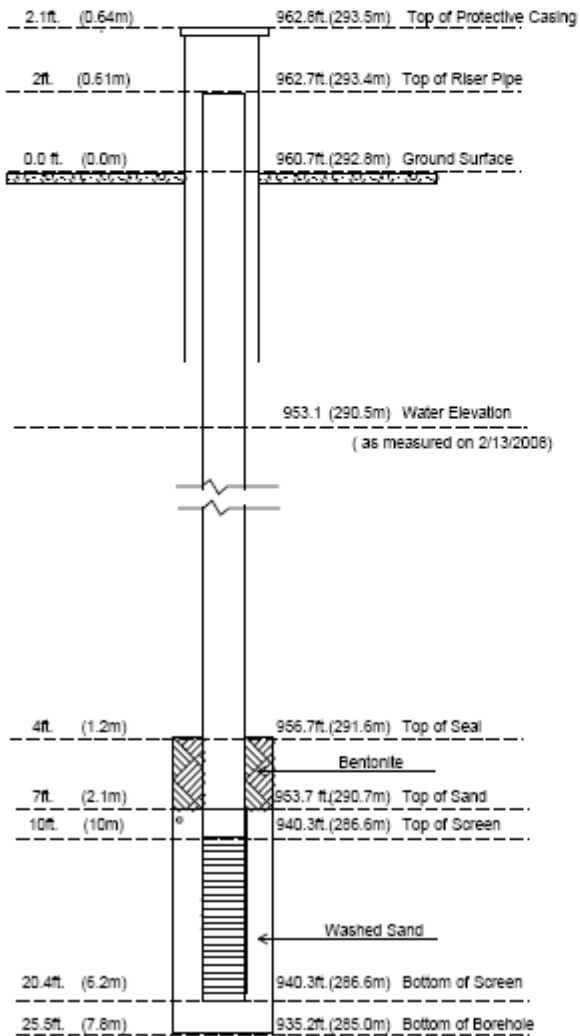
MINNESOTA DEPARTMENT OF TRANSPORTATION - GEOTECHNICAL SECTION  
**PIEZOMETER LOG & WATER LEVEL READINGS**

**UNIQUE NUMBER 70090**

**MDH Number 577321**

Boring Log Addendum

State Project <b>8680-157</b>	Bridge No. or Job Desc.	Trunk Highway/Location <b>194</b>	Boring No. <b>T2MW</b>
Location Wright Co. Coordinate: X=542603 Y=205440 Latitude (North)=45°15'50.58" Longitude (West)=93°43'04.37"		Drill Machine <b>205120 CME(LC55) Track</b>	Ground Elevation <b>960.7</b>
		Supervisor <b>J. Hasselquist</b>	Install Date <b>2/13/2008</b>
		Operator <b>D. Zerwas</b>	Seal Date
		Sealed by	Seal Licensee
If sealing details are blank, well has not been sealed as of time of printing (bottom right).			
<b>Interior Casing / Riser Pipe Details</b>			
Type of Riser Pipe		2" PVC	
Diameter of Riser Pipe		2 inch	
Top of Riser Pipe		2 feet	
Total Length of Riser Pipe		12	
<b>Screen Details</b>			
Type of Screen		PVC	
Diameter of Screen		2 inch	
Screen Slot Size		0.01 slot	
Depth to Top of Screen		10 feet	
Screen Length		10.4 feet	
Depth to Bottom of Screen		20.4 feet	
<b>Protective Casing Details</b>			
Type of Casing		Steel	
Diameter of Casing		8 inch	
Height of Top of Casing		2.1 feet	
Total Casing Length		7 feet	
Lock Type & Number		2108	
Diameter of Borehole		8 inch	
<b>Annular Space and Seal Details</b>			
Type of Surface Seal		Bentonite/Cement	
Type of Annular Seal		Bentonite	
Type of Screen Seal		Bentonite	
Type of Sand Pack		Washed Sand	
Source of Sand		Mother Earth	
Amount of Sand (pounds)		150	
Type of Bottom Seal		Native material	



Soil Class: D56 Rock Class: E01 Date: 3/18/08

MINNESOTA DEPARTMENT OF TRANSPORTATION - GEOTECHNICAL SECTION  
 LABORATORY LOG & TEST RESULTS - SUBSURFACE EXPLORATION



**UNIQUE NUMBER 70091**

U.S. Customary Units

State Project <b>8680-157</b>		Bridge No. or Job Desc.		Trunk Highway/Location <b>Interstate Highway 194</b>		Boring No. <b>T3MW</b>		Ground Elevation <b>960.9</b> (survey)	
Location <b>,, ft. LT</b>						Drill Machine <b>205120 CME(LC55) Track</b>		SHEET 1 of 1	
Wright Co. Coordinate: X=642934 Y=206116 (ft.)						Hammer <b>CME Automatic Calibrated</b>		Drilling Completed <b>2/14/08</b>	
Latitude (North)=45°15'56.37" Longitude (West)=93°42'59.75"									
DEPTH	Depth	Lithology	Classification	Drilling Operation	SPT	MC	COH	γ	Other Tests Or Remarks
	Elev.				No	(%)	(psf)	(pcf)	
					REG (%)	RQD (%)	ACT. (t)	Core Breaks	Formation or Member
	4.0 956.9	organic plastic Loam, black and moist				20			
5	7.0 953.9	slightly plastic Fine Sandy Loam, marbled light brown and light gray, moist			16	20			
10	12.0 948.9	slightly plastic Sandy Loam with a few pebbles, light gray-brown and moist			16	19			
15	22.0 938.9	Sandy Clay Loam with a few pebbles, gray-brown to gray, moist			13	18			
20	27.0 933.9	plastic Sandy Loam with some pebbles, gray and damp			15	17			
25	30.5 930.4	Sandy Clay Loam with a few pebbles, gray and moist			27	15			
30					21	17			
Bottom of Hole - 30.5' Water measured at 11.5' with auger									
Index Sheet Code 3.0						Soil Class: Rock Class: Edit: Date: 3/18/08 G:\INT\PROJECTS\ACT\70091-157.GPJ			

MINNESOTA DEPARTMENT OF TRANSPORTATION - GEOTECHNICAL SECTION  
**PIEZOMETER LOG & WATER LEVEL READINGS**

**UNIQUE NUMBER 70091**

**MDH Number 577322**

Boring Log Addendum

State Project <b>8680-157</b>	Bridge No. or Job Desc.	Trunk Highway/Location <b>194</b>	Boring No. <b>T3MW</b>
Location Wright Co. Coordinate: X=542934 Y=205116 Latitude (North)=45°15'56.37" Longitude (West)=93°42'59.75"		Drill Machine <b>205120 CME(LC55) Tracker</b>	Ground Elevation <b>960.9</b> ( )
		Supervisor <b>J. Hasselquist</b>	Install Date <b>2/14/2008</b>
		Operator <b>D. Zerwas</b>	Seal Date
		Sealed by	Seal Licensee
If sealing details are blank, well has not been sealed as of time of printing (bottom right).			
<b>Interior Casing / Riser Pipe Details</b>			
Type of Riser Pipe		2" PVC	
Diameter of Riser Pipe		2 inch	
Top of Riser Pipe		2 feet	
Total Length of Riser Pipe		18	
<b>Screen Details</b>			
Type of Screen		PVC	
Diameter of Screen		2 inch	
Screen Slot Size		0.01 slot	
Depth to Top of Screen		14 feet	
Screen Length		15.4 feet	
Depth to Bottom of Screen		29.4 feet	
<b>Protective Casing Details</b>			
Type of Casing		Steel	
Diameter of Casing		8 inch	
Height of Top of Casing		2.2 feet	
Total Casing Length		7 feet	
Lock Type & Number		2106	
Diameter of Borehole		8 inch	
<b>Annular Space and Seal Details</b>			
Type of Surface Seal		Bentonite/Cement	
Type of Annular Seal		Bentonite	
Type of Screen Seal		Bentonite	
Type of Sand Pack		Washed Sand	
Source of Sand		Mother Earth	
Amount of Sand (pounds)		500	
Type of Bottom Seal		Native material	

The diagram shows a vertical piezometer log with the following key features and elevations:

- Top of Protective Casing:** 963.1 ft (293.6 m)
- Top of Riser Pipe:** 962.9 ft (293.5 m)
- Ground Surface:** 960.9 ft (292.9 m)
- Water Elevation:** 949.4 ft (289.4 m) (as measured on 2/14/2008)
- Top of Seal:** 957.9 ft (292.0 m)
- Top of Sand:** 952.9 ft (290.4 m)
- Top of Screen:** 931.5 ft (283.9 m)
- Bottom of Screen:** 931.5 ft (283.9 m)
- Bottom of Borehole:** 930.4 ft (283.6 m)

Additional details from the diagram:

- Seal:** Bentonite, 3 ft (0.9 m) high.
- Screen:** 14 ft (4.3 m) long, 29.4 ft (9.0 m) depth to bottom.
- Bottom Seal:** Native material, 30.5 ft (9.3 m) from top of casing.
- Washed Sand:** Located between the screen and the bottom seal.

Soil Class: Rock Class: Eolt: Date: 3/18/08

MINNESOTA DEPARTMENT OF TRANSPORTATION - GEOTECHNICAL SECTION  
 LABORATORY LOG & TEST RESULTS - SUBSURFACE EXPLORATION



**UNIQUE NUMBER 70092**

U.S. Customary Units

State Project <b>8680-157</b>		Bridge No. or Job Desc.		Trunk Highway/Location <b>Interstate Highway 194</b>		Boring No. <b>T4MW</b>		Ground Elevation <b>961.6</b> (survey)	
Location <b>,, ft. LT</b> Wright Co. Coordinate: X=542968 Y=205158 (ft.) Latitude (North)=45°15'56.79" Longitude (West)=93°42'59.27"						Drill Machine <b>205120 CME(LC55) Track</b>		SHEET 1 of 1	
						Hammer <b>CME Automatic Calibrated</b>		Drilling Completed <b>2/14/08</b>	
DEPTH	Depth	Lithology	Classification	Drilling Operation	SPT No	MC (%)	COH (psf)	γ (pcf)	Other Tests Or Remarks
	Elev.				REC (%)	RQD (%)	ACL (ft)	Cone Breaks	
	4.5 957.1	plastic Sandy Loam, gray, moist to wet			18				
	5 954.6	Sand with a little Gravel, brown and saturated			16	26 14			
	7.0 949.6	plastic Sandy Loam with a few pebbles, brown and moist			17	19			
	12.0 949.6	Sandy Clay Loam with some pebbles, gray and moist			15	17			
	22.0 939.6	plastic Sandy Loam with a few pebbles, gray and damp			19	16			
	30.5 931.1				26	16			
Bottom of Hole - 30.5' Water measured at 8.5' while sampling and/or drilling									
Index Sheet Code 3.0						Soil Class: Rock Class: Edit: Date: 3/18/08 G:\DATA\PROJECTS\ACT\MN680-157\GJV			

MINNESOTA DEPARTMENT OF TRANSPORTATION - GEOTECHNICAL SECTION  
**PIEZOMETER LOG & WATER LEVEL READINGS**

**UNIQUE NUMBER 70092**

**MDH Number 577323**

Boring Log Addendum

State Project <b>8680-157</b>	Bridge No. or Job Desc.	Trunk Highway/Location <b>194</b>	Boring No. <b>T4MW</b>
Location Wright Co. Coordinate: X=542958 Y=205158 Latitude (North)=45°15'56.70" Longitude (West)=93°42'50.27"		Drill Machine <b>205120 CME(LC55) Track</b>	Ground Elevation <b>961.6</b> ( )
		Supervisor <b>J. Hasselquist</b>	Install Date <b>2/14/2008</b>
		Operator <b>D. Zerwas</b>	Seal Date
		Sealed by	Seal Licensee
If sealing details are blank, well has not been sealed as of time of printing (bottom right).			
<b>Interior Casing / Riser Pipe Details</b>			
Type of Riser Pipe		2" PVC	
Diameter of Riser Pipe		2 inch	
Top of Riser Pipe		1.6 feet	
Total Length of Riser Pipe		10	
<b>Screen Details</b>			
Type of Screen		PVC	
Diameter of Screen		2 inch	
Screen Slot Size		0.01 slot	
Depth to Top of Screen		3 feet	
Screen Length		20.4 feet	
Depth to Bottom of Screen		28.8 feet	
<b>Protective Casing Details</b>			
Type of Casing		Steel	
Diameter of Casing		6 inch	
Height of Top of Casing		1.8 feet	
Total Casing Length		7 feet	
Lock Type & Number		2108	
Diameter of Borehole		8 inch	
<b>Annular Space and Seal Details</b>			
Type of Surface Seal		Neat cement	
Type of Annular Seal		Bentonite	
Type of Screen Seal		Bentonite	
Type of Sand Pack		Washed Sand	
Source of Sand		Mother Earth	
Amount of Sand (pounds)		500	
Type of Bottom Seal		Native material	

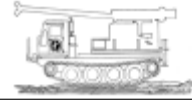
  

The diagram shows a vertical piezometer log. Key features include:  
 - Top of Protective Casing: 1.8 ft (0.55m) above 963.4 ft (293.6m).  
 - Top of Riser Pipe: 1.6 ft (0.49m) above 963.2 ft (293.6m).  
 - Ground Surface: 0.0 ft (0.0m) at 961.6 ft (293.1m).  
 - Water Elevation: 953.1 (290.5m) (as measured on 2/14/2008).  
 - Top of Seal: 3 ft (0.9m) above 958.6 ft (292.2m).  
 - Bentonite seal zone between 958.6 ft and 953.6 ft.  
 - Top of Sand: 8 ft (2.4m) above 953.6 ft (290.7m).  
 - Top of Screen: 3 ft (3m) above 932.8 ft (284.3m).  
 - Washed Sand zone between 932.8 ft and 931.1 ft.  
 - Bottom of Screen: 28.8 ft (8.8m) above 932.8 ft (284.3m).  
 - Bottom of Borehole: 30.5 ft (9.3m) above 931.1 ft (283.8m).

Soil Class: Rock Class: Edit: Date: 3/18/08



# Minnesota Department of Transportation Geotechnical Section Cone Penetration Test Index Sheet 1.0 (CPT 1.0)



## USER NOTES, ABBREVIATIONS AND DEFINITIONS

This Index sheet accompanies Cone Penetration Test Data. Please refer to the Boring Log Descriptive Terminology Sheet for information relevant to conventional boring logs.

This Cone Penetration Test (CPT) Sounding follows ASTM D 5778 and was made by ordinary and conventional methods and with care deemed adequate for the Department's design purposes. Since this sounding was not taken to gather information relating to the construction of the project, the data noted in the field and recorded may not necessarily be the same as that which a contractor would desire. While the Department believes that the information as to the conditions and materials reported is accurate, it does not warrant that the information is necessarily complete. This information has been edited or abridged and may not reveal all the information which might be useful or of interest to the contractor. Consequently, the Department will make available at its offices, the field logs relating to this sounding.

Since subsurface conditions outside each CPT Sounding are unknown, and soil, rock and water conditions cannot be relied upon to be consistent or uniform, no warrant is made that conditions adjacent to this sounding will necessarily be the same as or similar to those shown on this log. Furthermore, the Department will not be responsible for any interpretations, assumptions, projections or interpolations made by contractor, or other users of this log.

Water pressure measurements and subsequent interpreted water levels shown on this log should be used with discretion since they represent dynamic conditions. Dynamic Pore water pressure measurements may deviate substantially from hydrostatic conditions, especially in cohesive soils. In cohesive soils, water pressures often take extended periods of time to reach equilibrium and thus reflect their true field level. Water levels can be expected to vary both seasonally and yearly. The absence of notations on this log regarding water does not necessarily mean that this boring was dry or that the contractor will not encounter subsurface water during the course of construction.

### CPT Terminology

CPT.....Cone Penetration Test  
CPTU.....Cone Penetration Test with Pore Pressure measurements  
SCPTU.....Cone Penetration Test with Pore Pressure and Seismic measurements  
Piezocone...Common name for CPTU test

(Note: This test is not related to the Dynamic Cone Penetrometer DCP)

### qt TIP RESISTANCE

The resistance at the cone corrected for water pressure. Data is from cone with 60 degree apex angle and a 10 cm<sup>2</sup> end area.

### fs SLEEVE FRICTION RESISTANCE

The resistance along the sleeve of the penetrometer.

### FR Friction Ratio

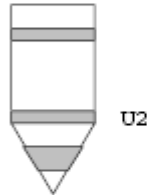
Ratio of sleeve friction over corrected tip resistance.  
 $FR = fs/qt$

### Vs Shear Wave Velocity

A measure of the speed at which a seismic wave travels through soil/rock.

### PORE WATER MEASUREMENTS

Pore water measurements reported on CPT Log are representative of water pressures measured at the U2 location, just behind the cone tip, prior to the sleeve, as shown in the figure below. These measurements are considered to be dynamic water pressures due to the local disturbance caused by the cone tip. Dynamic water pressure decay and Static water pressure measurements are reported on a Pore Water Pressure Dissipation Graph.



### SBT SOIL BEHAVIOR TYPE

Soil Classification methods for the Cone Penetration Test are based on correlation charts developed from observations of CPT data and conventional borings. Please note that these classification charts are meant to provide a guide to Soil Behavior Type and should not be used to infer a soil classification based on grain size distribution.

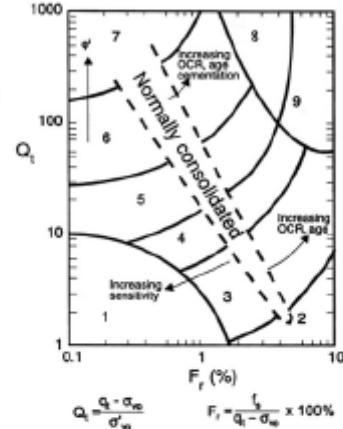
The numbers corresponding to different regions on the charts represent the following soil behavior types:

1. Sensitive, Fine Grained
2. Organic Soils - Peats
3. Clays - Clay to Silty Clay
4. Silt Mixtures - Clayey Silt to Silty Clay
5. Sand Mixtures - Silty Sand to Sandy Silt
6. Sands - Clean Sand to Silty Sand
7. Gravelly Sand to Sand
8. Very Stiff Sand to Clayey Sand
9. Very Stiff, Fine Grained

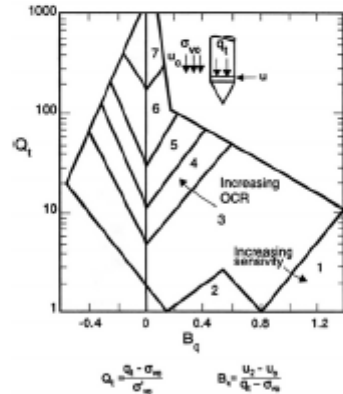
Note that engineering judgment, and comparison with conventional borings is especially important in the proper interpretation of CPT data in certain ge-materials.

The following charts are used to provide a Soil Behavior Type for the CPT Data.

Robertson CPT 1990  
Soil Behavior type based on friction ratio



Robertson CPTU 1990  
Soil Behavior type based on pore pressure



where ...  
Qt.....normalized cone resistance  
Bq.....pore pressure ratio  
Ft.....Normalized friction ratio  
sigma'vo.....overburden pressure  
sigma'vo.....effective over burden pressure  
u2.....measured pore pressure  
u0.....equilibrium pore pressure

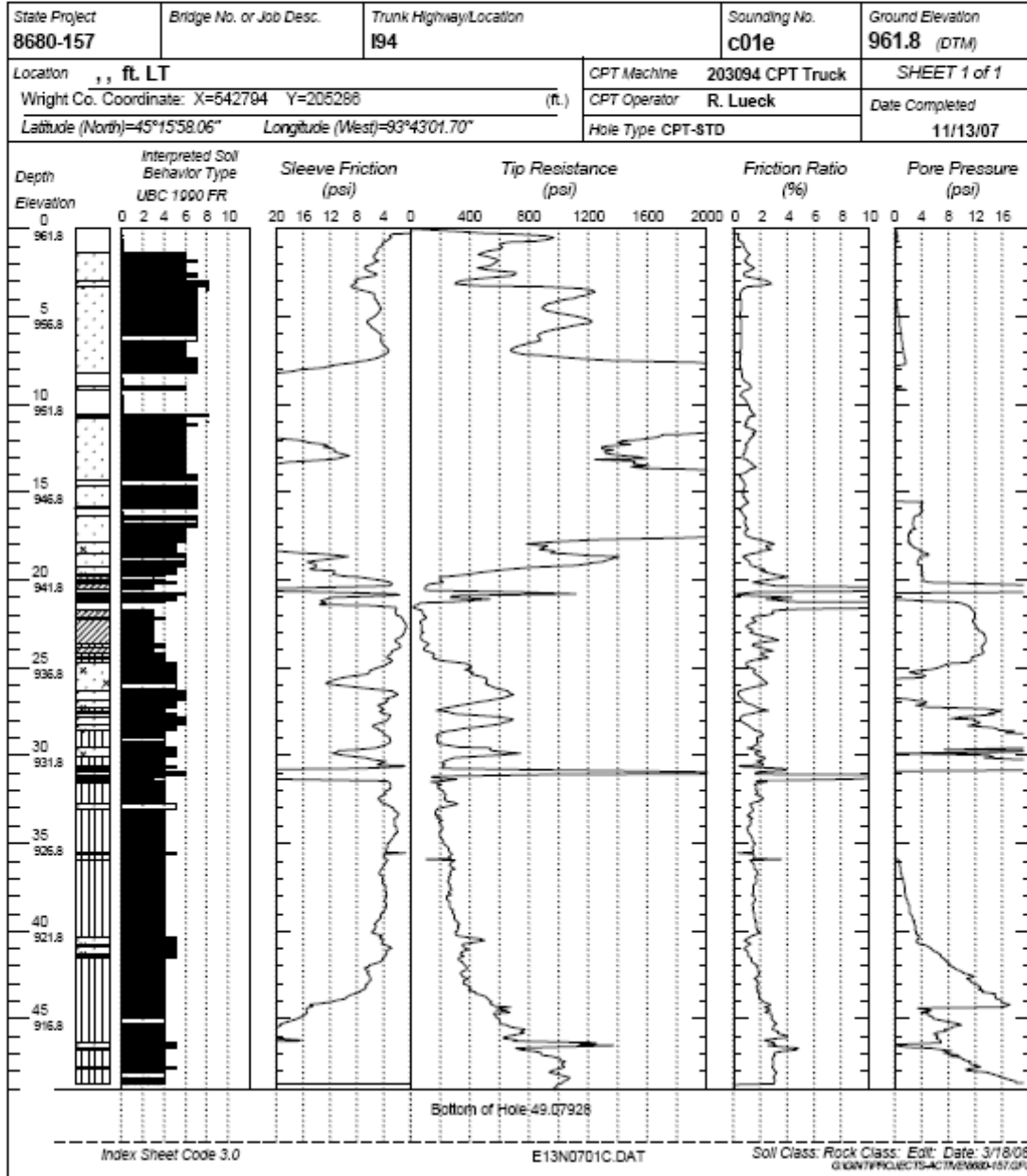
GA\GEOTECH\FM\BUC\FORMS\CPTINDS.DOC, January 30, 2002

MINNESOTA DEPARTMENT OF TRANSPORTATION - GEOTECHNICAL SECTION

CONE PENETRATION TEST RESULTS

UNIQUE NUMBER 69249

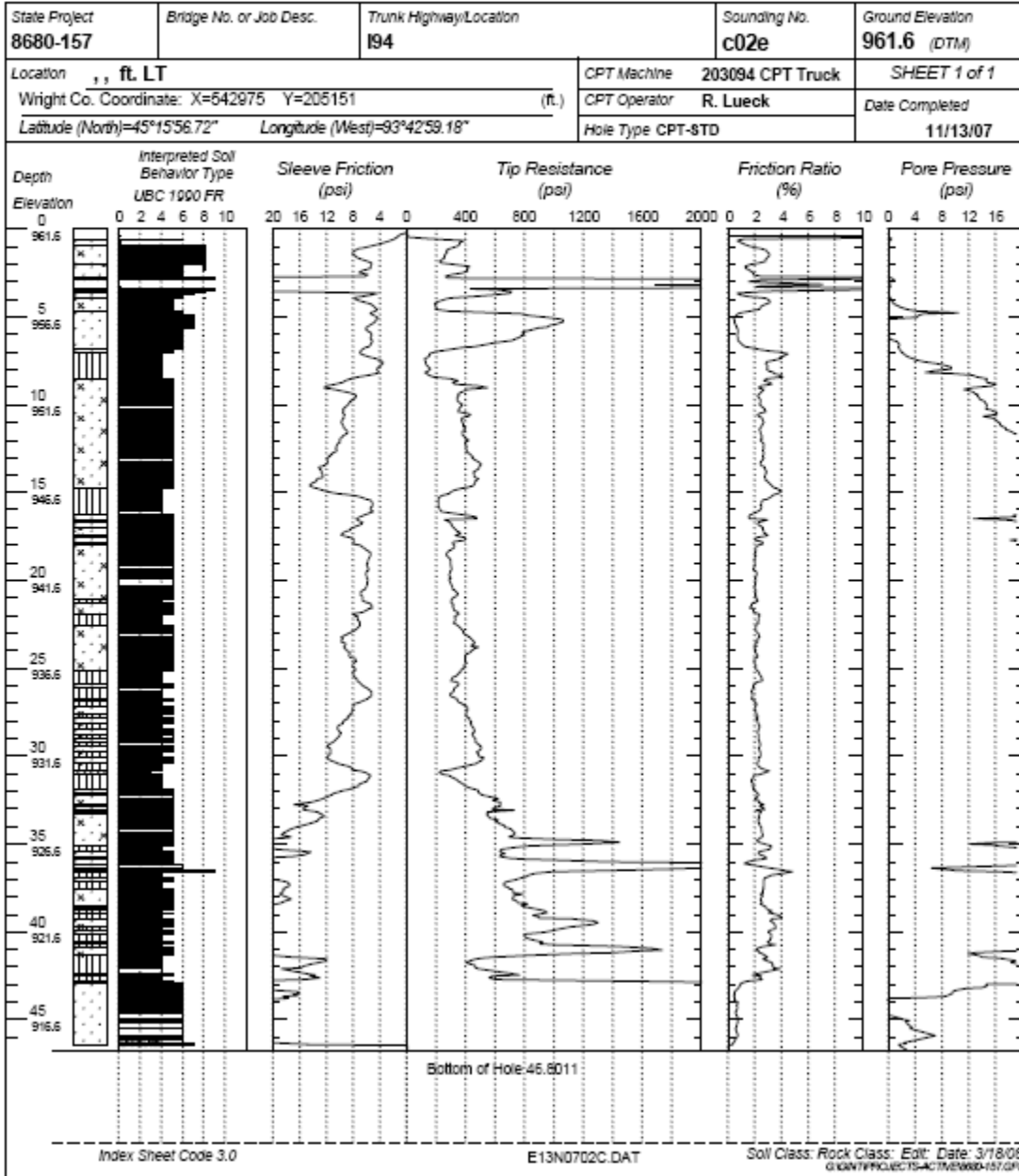
U.S. Customary Units



MINNESOTA DEPARTMENT OF TRANSPORTATION - GEOTECHNICAL SECTION

CONE PENETRATION TEST RESULTS  
**UNIQUE NUMBER 69250**

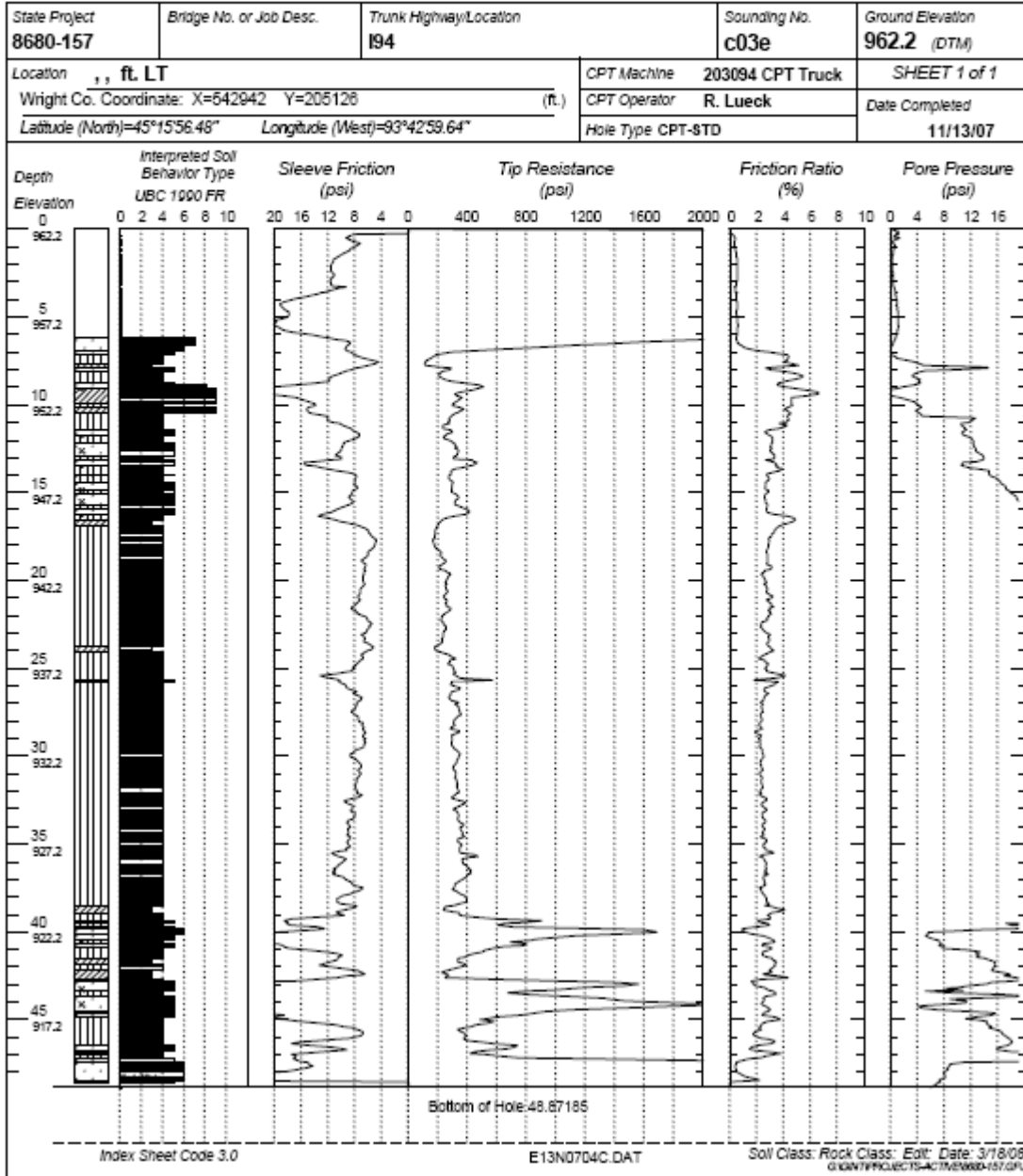
U.S. Customary Units



MINNESOTA DEPARTMENT OF TRANSPORTATION - GEOTECHNICAL SECTION

CONE PENETRATION TEST RESULTS  
**UNIQUE NUMBER 69251**

U.S. Customary Units





## **APPENDIX B: GLOSSARY**

**Diffusivity ( $\alpha$ )**

The ratio of **Transmissivity (T)** to **Storativity (S)** ,  $\alpha=T/S$ . [ $L^2/T$ ]

**Hydraulic Conductivity (K)**

Constant of proportionality defining the specific Discharge of a porous medium under a unit hydraulic gradient  $q=K*i$ . [ $L/T$ ]

**Hydraulic Gradient (i)**

Hydraulic head loss per distance,  $i=dh/dl$ . [dimensionless]

**Porosity (n)**

Ratio of void volume ( $V_v$ ) to total volume ( $V_T$ ) in a rock or porous media,  $n=V_v/V_T$ . [dimensionless]

**Specific Discharge (q)**

Flow rate per unit cross-sectional area of aquifer  $q=Q/A$ . Also known as Darcy velocity or Darcy flux given by the product of hydraulic conductivity and Hydraulic gradient  $=K*i$ . [ $L/T$ ]

**Specific Storage ( $S_s$ )**

Volume of water released from storage from a unit volume of aquifer per unit decline in hydraulic head. [ $1/L$ ]

**Specific Yield ( $S_y$ )**

Volume of water released from storage by an unconfined aquifer per unit surface area of aquifer per unit decline of the water table. [dimensionless]

**Storativity (S)**

Volume of water released from storage by a confined aquifer per unit surface area of aquifer per unit decline in hydraulic head normal to surface,  $S=S_s*b$ . [dimensionless]

**Transmissivity (T)**

The product of hydraulic conductivity and saturated thickness,  $T=K*b$ . [ $L^2/T$ ]

## **APPENDIX C: ENVIRONMENTAL SAMPLING**

<b>Porous Pavement Study (Purge Volume)</b>	<b>Well 1 T3MW</b>	<b>Well 2 T4MW</b>
	Date: 3/4/08 Time:	Date: 3/4/08 Time:
Depth to water measurement-pre-sample (ft.)	9.55	21.45
<b>HYDROLAB READINGS</b>		
Temperature (degrees Celsius)	8.35	10.47
Turbidity (NTU)	78.0	100.3
DO (% Sat)	n/a	n/a
DO (mg/L)	n/a	n/a
pH (Units)	6.67	6.08
Specific conductance (micro siemens)	0.695	1.035

**Field notes/Observations:** \_\_\_\_\_

**APPENDIX D: TEST WELL MEASUREMENTS AS OF 6/18/08**

Well Station	ID	Water level from Cap	
160+94	Piezo 1	3.45 feet	+ (South)
160+78	Piezo 2	3.78 feet	- (North)
162+23	Piezo 3	4.98 feet	- (North)
163+09	Piezo 4	3.5 feet	+ (South)
165+50	Piezo *	2.26 feet	- (North).
MDH Well 1	F1	ND	
MDH Well 2	F2	ND	
MDH Well 3	F3	ND	
MDH Well 4	F4	ND	

## **APPENDIX E: EXCERPTS OF TESTING REPORT**



**Table E1: Coefficient of Thermal  
Expansion**

Specimen	CTE (10 <sup>-6</sup> in/in/F)	Data sheet number		
MNRD-05-CT-005	5.4	4		
MNRD-05-CT-006	5.3	1		
MNRD-05-CT-007	5.3	4		
MNRD-05-CT-008	5.3	12	Ave.	Stan. Dev.
MNRD-05-CT-009	5.5	11	5.4	0.09
MNRD-06-CT-010	5.3	3		
MNRD-06-CT-011	5.3	1		
MNRD-06-CT-012	5.4	7		
MNRD-06-CT-013	5.3	7	Ave.	Stan. Dev.
MNRD-06-CT-014	5.3	4	5.3	0.04
MNRD-13-CT-015	5.3	7		
MNRD-13-CT-016	5.3	12		
MNRD-13-CT-017	5.2	9		
MNRD-13-CT-018	5.3	2	Ave.	Stan. Dev.
MNRD-13-CT-019	5.3	11	5.3	0.04
MNRD-39-CT-003	5	3		
MNRD-39-CT-004	5	9		
MNRD-39-CT-020	4.8	13		
MNRD-39-CT-021	4.7	5		
MNRD-39-CT-022	4.6	6	Ave.	Stan. Dev.
MNRD-39-CT-024	4.8	2	4.8	0.16
MNRD-53-CT-001	5.3	13	Ave.	Stan. Dev.
MNRD-53-CT-002	5.3	12	5.3	0.00
MNRD-85-CT-028	4.8	6		
MNRD-85-CT-029	4.8	11		
MNRD-85-CT-030	4.8	9		
MNRD-85-CT-031*	4.8	1		
MNRD-85-CT-032*	4.9	8		
MNRD-85-CT-033*	4.8	10		
MNRD-85-CT-034*	4.8	5	Ave.	Stan. Dev.
MNRD-85-CT-035*	5	10	4.8	0.07
MNRD-89-CT-026	4.8	6		
MNRD-89-CT-025	4.9	8		
MNRD-89-CT-027	5	8		
MNRD-89-CT-036	5.1	2		
MNRD-89-CT-037	4.8	13		
MNRD-89-CT-038	4.9	5	Ave.	Stan. Dev.
MNRD-89-CT-039	4.8	3	4.9	0.12

**Table E2: Coefficient of Thermal Expansion Specimen**

Specimen	1
ID	MNRD-39-CT-003
Cast Time	10/1/2008
Height	12"1/8"
Diameter	6"
CTE (10 <sup>-6</sup> /F)	5
Weight (lbs)	25.4
Description	Fiber reinforced Concrete specimen; very porous; Intact; No visible cracks
Pictures	

**Table E3: Coefficient of Thermal Expansion (More Data)**

Specimen	4
ID	MNRD-39-CT-004
Cast Time	10/1/2008
Height	12"1/8"
Diameter	6"
CTE (10 <sup>-6</sup> /F)	5
Weight (lbs)	25.4
Description	Fiber reinforced Concrete specimen; very porous; Intact; No visible cracks
Pictures	

**Table E4: Coefficient of Thermal Expansion (More Data)**

Specimen	10
ID	MNRD-39-CT-024
Cast Time	10/17/2008
Height	12"
Diameter	6"
CTE (10 <sup>-6</sup> /F)	4.8
Description	Good shape; 90% wet; porous
Pictures	

## Plate E1: Report of Freeze Thaw Durability ASTM C-666



CONSULTANTS  
• ENVIRONMENTAL  
• GEOTECHNICAL  
• MATERIALS  
• FORENSICS

### REPORT OF RAPID FREEZING AND THAWING OF CONCRETE

**PROJECT:**

MN/ROAD  
PERVIOUS CONCRETE

**REPORTED TO:**

MINNESOTA DEPT. OF TRANSPORTATION  
1400 GERVAIS AVENUE  
MAIL STOP 645  
MAPLEWOOD, MN 55109-2044

**ATTN:** RICH LAMB

**AET PROJECT NO:** 01-04293

**DATE:** FEBRUARY 20, 2009

---

### INTRODUCTION

This report presents the results of recent freeze-thaw testing. This testing was performed from October 29, 2008 through January 29, 2009. The scope of our work was limited to performing freeze-thaw testing of three concrete prisms.

### TEST PROCEDURES

The concrete prisms were cast at MN/Road on October 1, 2008. The prisms were brought back to our laboratory the next working day. The prisms were identified and placed in our 100% moist curing room until they reached an age of 28 days.

The prisms were then tested in accordance with Procedure A of ASTM:C666, "Standard Test

**RESULTS**

Cycles Completed	Test Criteria	Sample Identification			Average
		Cell #39			
		4	5	6	
34	Weight, loss %	.06	.05	.10	.07
	Length, Exp. %	.006	.004	.009	.006
	RDME, %	99.0	97.0	97.0	98
70	Weight, loss %	1.1	1.8	1.5	1.5
	Length, Exp. %	.05	.07	.06	.06
	RDME, %	84.0	78.0	80.0	81
100	Weight, loss %	4.3	5.3	4.8	4.8
	Length, Exp. %	.09	.16	.14	.13
	RDME, %	64.0	50.0	53.0	56.0
	Weight, loss %	FAILED			
	Length, Exp. %				
	RDME, %				
Durability Factor		21	17	18	19

**REMARKS**

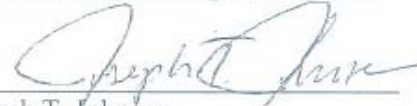
The samples tested will be saved until May 30, 2009. Should you have any questions regarding this report or if we can be of further assistance, please contact us.

Report Prepared by:  
American Engineering Testing, Inc.



Daniel M. Vruno, P.E.  
Senior Concrete Engineer  
MN Lic. No. 42037  
Phone: 651-659-1334  
Fax: 651-647-2744  
[dvruno@amengtest.com](mailto:dvruno@amengtest.com)

Report Reviewed by:  
American Engineering Testing, Inc.



Joseph T. Johnson  
Engineering Technician II

## Plate E2: Report on Freeze-Thaw Durability Test (ASTM C-666)



CONSULTANTS  
• ENVIRONMENTAL  
• GEOTECHNICAL  
• MATERIALS  
• FORENSICS

### REPORT OF RAPID FREEZING AND THAWING OF CONCRETE

**PROJECT:**

MN/ROAD  
PERVIOUS CONCRETE

**REPORTED TO:**

MINNESOTA DEPT. OF TRANSPORTATION  
1400 GERVAIS AVENUE  
MAIL STOP 645  
MAPLEWOOD, MN 55109-2044

**ATTN:** RICH LAMB

**AET PROJECT NO:** 01-04293

**DATE:** FEBRUARY 20, 2009

---

### INTRODUCTION

This report presents the results of recent freeze-thaw testing. This testing was performed from November 14, 2008 through February 3, 2009. The scope of our work was limited to performing freeze-thaw testing of three concrete prisms.

### TEST PROCEDURES

The concrete prisms were cast at MN/Road on October 17, 2008. The prisms were brought back to our laboratory the next working day. The prisms were identified and placed in our 100% moist curing room until they reached an age of 28 days.

The prisms were then tested in accordance with Procedure A of ASTM:C666, "Standard Test Method for Resistance of Concrete to Rapid Freezing and Thawing."

### SAMPLE IDENTIFICATION

Cell #39      Cast October 17, 2008      Samples 20, 21 and 22



**Plate E3: Report on Compressive Strength Test**

**MnRoad 2008 Reconstruction  
Concrete Compressive Strength Summary**

**Cell 39**

**Sample Location:** Cell 39, Outside Lane  
**Mix Type:** Pervious Overlay  
**Specimen Type:** 6" X 12" Cylinder  
**Date Cast:** 10/1/2008

Sample #'s:	<u>MNRD-39-CC-09</u>	<u>MNRD-39-CC-10</u>	
Date Broken:	10/4/2008	10/4/2008	
Age @ Testing (Days):	3	3	
Load @ Failure (lbs.):	36,890	39,790	
Strength @ Failure (psi):	1,300	1,410	
<b>Average Compressive Strength @ 3 Days(psi):</b>			<b>1,355</b>

Sample #'s:	<u>MNRD-39-CC-11</u>	<u>MNRD-39-CC-12</u>	
Date Broken:	10/8/2008	10/8/2008	
Age @ Testing (Days):	7	7	
Load @ Failure (lbs.):	67,890	67,440	
Strength @ Failure (psi):	2,400	2,390	
<b>Average Compressive Strength @ 7 Days(psi):</b>			<b>2,395</b>

Sample #'s:	<u>MNRD-39-CC-13</u>	<u>MNRD-39-CC-14</u>	
Date Broken:	10/22/2008	10/22/2008	
Age @ Testing (Days):	21	21	
Load @ Failure (lbs.):	88,310	82,670	
Strength @ Failure (psi):	3,120	2,920	
<b>Average Compressive Strength @ 21 Days(psi):</b>			<b>3,020</b>

Sample #'s:	<u>MNRD-39-CC-15</u>	<u>MNRD-39-CC-16</u>	
Date Broken:	10/29/2008	10/29/2008	
Age @ Testing (Days):	28	28	
Load @ Failure (lbs.):	112,630	114,910	
Strength @ Failure (psi):	3,980	4,080	
<b>Average Compressive Strength @ 28 Days(psi):</b>			<b>4,020</b>

**REPORT OF COMPRESSIVE STRENGTH OF CYLINDRICAL CONCRETE SPECIMENS - ASTM:C39**

**PROJECT:**  
MN/ROAD RECONSTR. MATERIAL TEST  
ST. PAUL, MINNESOTA

**REPORTED TO:**  
MINNESOTA DEPARTMENT OF TRANSPORTATION  
1400 GERVAIS AVENUE  
M.S. 645  
MAPLEWOOD, MN 55109-2044

**ATTN:** BERNARD IZEVBEKHAI

**CC:**

**AET PROJECT NO:** 01-04293

**DATE:** December 2, 2008

**Placement Information:**

**Set No:** CC 009 A  
**Date Cast:** 10/1/2008  
**Cast By:** Joe Clem  
**Date Received in Laboratory:** 10/2/2008

**Concrete Supplied By:** Aggregate Industries  
**Mix No:** Pervious  
**Truck No:** 147  
**Placement Method:** Truck Discharge

**Plastic Properties:** (ASTM:C143, ASTM:C231, ASTM:C1064)

**Slump, in:** .25

**Air Content, %:** 20.0

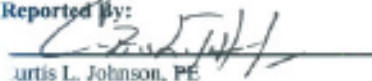
**Concrete Temp, F°:**

**Placement Location:** Cell 39, Outside Lane

<b><u>Cylinder No.</u></b>	CC 009 A
<b><u>Cylinder Information</u></b>	
Weight (lbs):	25.25
Height (in.):	12.00
Diameter (in.):	6.00
Cross-sectional area (sq. in.):	28.27
Cylinder condition/preparation:	
<b><u>Curing Information</u></b>	
Test date:	10/4/2008
Days on site:	1
Days in curing:	2
Age at testing(days):	3
<b><u>Test Information</u></b>	
Load at Failure (lbs.):	36,890
Strength at Failure (PSI):	1,300
Specified Strength (PSI):	
Type of Failure:	Shear

**Conformance:** The 3-day result is reported for informational use only.

**Reported By:**

  
Curtis L. Johnson, PE

Staff Engineer II

DR

# Plate E4: Report on Compressive Strength Test

## REPORT OF COMPRESSIVE STRENGTH OF CYLINDRICAL CONCRETE SPECIMENS - ASTM:C39

**PROJECT:**  
MN/ROAD RECONSTR. MATERIAL TEST  
ST. PAUL, MINNESOTA

**REPORTED TO:**  
MINNESOTA DEPARTMENT OF TRANSPORTATION  
1400 GERVAIS AVENUE  
M.S. 645  
MAPLEWOOD, MN 55109-2044

**ATTN:** BERNARD IZEVBEKHAI

**CC:**

**AET PROJECT NO:** 01-04293

**DATE:** December 2, 2008

**Placement Information:**

**Set No:** CC 010 A  
**Date Cast:** 10/1/2008  
**Cast By:** Joe Clem  
**Date Received in Laboratory:** 10/2/2008

**Concrete Supplied By:** Aggregate Industries  
**Mix No:** Pervious  
**Truck No:** 147  
**Placement Method:** Truck Discharge

**Plastic Properties:** (ASTM:C143, ASTM:C231, ASTM:C1064)

**Slump, in:** .25

**Air Content, %:** 20.0

**Concrete Temp, F°:**

**Placement Location:** Cell 39, Outside Lane

<b><u>Cylinder No.</u></b>	CC 010 A
<b><u>Cylinder Information</u></b>	
Weight (lbs):	25.30
Height (in.):	12.00
Diameter (in.):	6.00
Cross-sectional area (sq. in.):	28.27
Cylinder condition/preparation:	
<b><u>Curing Information</u></b>	
Test date:	10/4/2008
Days on site:	1
Days in curing:	2
Age at testing(days):	3
<b><u>Test Information</u></b>	
Load at Failure (lbs.):	39,790
Strength at Failure (PSI):	1,410
Specified Strength (PSI):	
Type of Failure:	Comp
<b>Conformance:</b> The 3-day result is reported for informational use only.	

**Reported By:**

  
Curtis L. Johnson, PE

Staff Engineer II

DR

## Plate E5: Report on Compressive Strength Test

### MnRoad 2008 Reconstruction Concrete Compressive Strength Summary

#### Cell 39

**Sample Location:** Cell 39, Inside Lane  
**Mix Type:** Pervious Overlay  
**Specimen Type:** 6" X 12" Cylinder  
**Date Cast:** 10/17/2008

Sample #s:	<u>MNRD-39-CC-41</u>	<u>MNRD-39-CC-42</u>	
Date Broken:	10/22/2008	10/22/2008	
Age @ Testing (Days):	5	5	
Load @ Failure (lbs.):	71,600	72,770	
Strength @ Failure (psi):	2,530	2,570	
<b>Average Compressive Strength @ 5 Days(psi):</b>			<b>2,550</b>

Sample #s:	<u>MNRD-39-CC-43</u>	<u>MNRD-39-CC-44</u>	
Date Broken:	10/24/2008	10/24/2008	
Age @ Testing (Days):	7	7	
Load @ Failure (lbs.):	80,250	84,470	
Strength @ Failure (psi):	2,840	2,990	
<b>Average Compressive Strength @ 7 Days(psi):</b>			<b>2,915</b>

Sample #s:	<u>MNRD-39-CC-45</u>	<u>MNRD-39-CC-46</u>	
Date Broken:	11/7/2008	11/7/2008	
Age @ Testing (Days):	21	21	
Load @ Failure (lbs.):	116,670	123,940	
Strength @ Failure (psi):	4,130	4,380	
<b>Average Compressive Strength @ 21 Days(psi):</b>			<b>4,255</b>

Sample #s:	<u>MNRD-39-CC-47</u>	<u>MNRD-39-CC-48</u>	
Date Broken:	11/14/2008	11/14/2008	
Age @ Testing (Days):	28	28	
Load @ Failure (lbs.):	133,460	135,140	
Strength @ Failure (psi):	4,720	4,780	
<b>Average Compressive Strength @ 28 Days(psi):</b>			<b>4,750</b>

## Plate E6: Report on Compressive Strength Test

REPORT OF COMPRESSIVE STRENGTH OF CYLINDRICAL CONCRETE SPECIMENS - ASTM:C39

**PROJECT:**  
MN/ROAD RECONSTR. MATERIAL TEST  
ST. PAUL, MINNESOTA

**REPORTED TO:**  
MINNESOTA DEPARTMENT OF TRANSPORTATION  
1400 GERVAIS AVENUE  
M.S. 645  
MAPLEWOOD, MN 55109-2044

ATTN: BERNARD IZEVBEKHAI

CC:

AET PROJECT NO: 01-04293

DATE: December 2, 2008

**Placement Information:**

Set No: CC 041 A  
Date Cast: 10/17/2008  
Cast By: Ben Hoefler  
Date Received in Laboratory: 10/20/2008

Concrete Supplied By: Aggregate Industries  
Mix No: Pervious  
Truck No:  
Placement Method: Truck Discharge

**Plastic Properties:** (ASTM:C143, ASTM:C231, ASTM:C1064)

Slump, in: .75

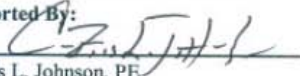
Air Content, %:

Concrete Temp, F°: 62

**Placement Location:** Cell 39, Inside lane

<b><u>Cylinder No.</u></b>	CC 041 A
<b><u>Cylinder Information</u></b>	
Weight (lbs):	
Height (in.):	12.00
Diameter (in.):	6.00
Cross-sectional area (sq. in.):	28.27
Cylinder condition/preparation:	
<b><u>Curing Information</u></b>	
Test date:	10/22/2008
Days on site:	3
Days in curing:	2
Age at testing(days):	5
<b><u>Test Information</u></b>	
Load at Failure (lbs.):	71,600
Strength at Failure (PSI):	2,530
Specified Strength (PSI):	
Type of Failure:	Shear
<b>Conformance:</b> The 5-day result is reported for informational use only.	

Reported By:

  
Curtis L. Johnson, PE  
Staff Engineer II

DR





**REPORT OF COMPRESSIVE STRENGTH OF CYLINDRICAL CONCRETE SPECIMENS - ASTM:C39**

**PROJECT:**  
MN/ROAD RECONSTR. MATERIAL TEST  
ST. PAUL, MINNESOTA

**REPORTED TO:**  
MINNESOTA DEPARTMENT OF TRANSPORTATION  
1400 GERVAIS AVENUE  
M.S. 645  
MAPLEWOOD, MN 55109-2044

**ATTN:** BERNARD IZEVBEKHAI

**CC:**

**AET PROJECT NO:** 01-04293

**DATE:** December 2, 2008

**Placement Information:**

**Set No:** CC 045 A  
**Date Cast:** 10/17/2008  
**Cast By:** Ben Hoefler  
**Date Received in Laboratory:** 10/20/2008

**Concrete Supplied By:** Aggregate Industries  
**Mix No:** Pervious  
**Truck No:**  
**Placement Method:** Truck Discharge

**Plastic Properties:** (ASTM:C143, ASTM:C231, ASTM:C1064)

**Slump, in:** .75

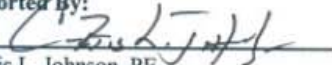
**Air Content, %:**

**Concrete Temp, F°:** 62

**Placement Location:** Cell 39, Inside lane

<b><u>Cylinder No.</u></b>	CC 045 A
<b><u>Cylinder Information</u></b>	
Weight (lbs):	
Height (in.):	12.00
Diameter (in.):	6.00
Cross-sectional area (sq. in.):	28.27
Cylinder condition/preparation:	
<b><u>Curing Information</u></b>	
Test date:	11/7/2008
Days on site:	3
Days in curing:	18
Age at testing(days):	21
<b><u>Test Information</u></b>	
Load at Failure (lbs.):	116,670
Strength at Failure (PSI):	4,130
Specified Strength (PSI):	
Type of Failure:	Shear
<b>Conformance:</b> The 21-day result is reported for informational use only.	

**Reported By:**

  
Curtis L. Johnson, PE  
Staff Engineer II

DR









## Plate E7: Report on Compressive Strength Test

### MnRoad 2008 Reconstruction Concrete Flexural Strength Summary

#### Cell 39

**Sample Location:** Cell 39, Outside Lane  
**Mix Type:** Pervious Overlay  
**Specimen Type:** 6" X 6" X 22" Beam  
**Date Cast:** 10/1/2008

Sample #'s: MNRD-53-CB-07  
Date Broken: 10/2/2008  
Age @ Testing (Days): 1  
Load @ Failure (lbs.): 1,120  
Strength @ Failure (psi): 90  
**Average Flexural Strength @ 1 Days(psi): 90**

Sample #'s: MNRD-53-CB-08  
Date Broken: 10/4/2008  
Age @ Testing (Days): 3  
Load @ Failure (lbs.): 4,350  
Strength @ Failure (psi): 360  
**Average Flexural Strength @ 3 Days(psi): 360**

Sample #'s:	<u>MNRD-53-CB-09</u>	<u>MNRD-53-CB-10</u>	
Date Broken:	10/8/2008	10/8/2008	
Age @ Testing (Days):	7	7	
Load @ Failure (lbs.):	5,320	4,730	
Strength @ Failure (psi):	410	390	
<b>Average Flexural Strength @ 7 Days(psi):</b>			<b>400</b>

Sample #'s:	<u>MNRD-53-CB-11</u>	<u>MNRD-53-CB-12</u>	
Date Broken:	10/29/2008	10/29/2008	
Age @ Testing (Days):	28	28	
Load @ Failure (lbs.):	5,430	5,840	
Strength @ Failure (psi):	460	470	
<b>Average Flexural Strength @ 28 Days(psi):</b>			<b>465</b>



**REPORT OF FLEXURAL STRENGTH OF CONCRETE BEAM SPECIMENS - THIRD POINT LOADING - ASTM:C78**

**PROJECT:**  
MN/ROAD RECONSTR. MATERIAL TEST  
ST. PAUL, MINNESOTA

**REPORTED TO:**  
MINNESOTA DEPARTMENT OF TRANSPORTATION  
1400 GERVAIS AVENUE  
M.S. 645  
MAPLEWOOD, MN 55109-2044

**ATTN:** BERNARD IZEVBEKHAI

**CC:**

**AET PROJECT NO:** 01-04293

**DATE:** December 2, 2008

**Placement Information:**

**Set No:** CB 008 A  
**Date Cast:** 10/1/2008  
**Cast By:** Joe Clem  
**Date Received in Laboratory:** 10/2/2008

**Concrete Supplied By:** Aggregate Industries  
**Mix No:** Pervious  
**Truck No:** 147  
**Placement Method:** Truck Discharge

**Plastic Properties:** (ASTM:C143, ASTM:C231, ASTM:C1064)

**Slump, in:** .25

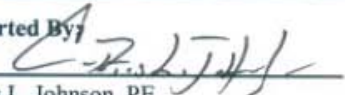
**Air Content, %:** 20.0

**Concrete Temp, F°:**

**Placement Location:** Cell 39, Outside Lane

<b><u>Beam No.</u></b>	CB 008 A
<b><u>Beam Information</u></b>	
Weight (lbs):	6.04
Width (in.):	6.03
Depth (in.):	18.00
Span (in.):	
<b><u>Curing Information</u></b>	
Test date:	10/4/2008
Days on site:	1
Days in curing:	2
Age at testing(days):	3
<b><u>Test Information</u></b>	
Load at Failure (lbs.):	4,350
Strength at Failure (PSI):	360
Specified Strength (PSI):	
Type of Failure:	

**Conformance:** The 3-day result is reported for informational use only.

**Reported By:**   
Curtis L. Johnson, PE  
Staff Engineer II

DR

**REPORT OF FLEXURAL STRENGTH OF CONCRETE BEAM SPECIMENS - THIRD POINT LOADING - ASTM:C78**

**PROJECT:**  
MN/ROAD RECONSTR. MATERIAL TEST  
ST. PAUL, MINNESOTA

**REPORTED TO:**  
MINNESOTA DEPARTMENT OF TRANSPORTATION  
1400 GERVAIS AVENUE  
M.S. 645  
MAPLEWOOD, MN 55109-2044

**ATTN:** BERNARD IZEVBEKHAI  
**CC:**

**AET PROJECT NO:** 01-04293

**DATE:** December 2, 2008

**Placement Information:**

**Set No:** CB 009 A  
**Date Cast:** 10/1/2008  
**Cast By:** Joe Clem  
**Date Received in Laboratory:** 10/2/2008

**Concrete Supplied By:** Aggregate Industries  
**Mix No:** Pervious  
**Truck No:** 147  
**Placement Method:** Truck Discharge

**Plastic Properties:** (ASTM:C143, ASTM:C231, ASTM:C1064)

**Slump, in:** .25

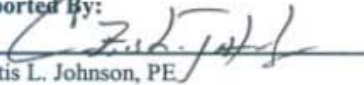
**Air Content, %:** 20.0

**Concrete Temp, F°:**

**Placement Location:** Cell 39, Outside Lane

<b>Beam No.</b>	CB 009 A
<b>Beam Information</b>	
Weight (lbs):	6.08
Width (in.):	6.18
Depth (in.):	18.00
Span (in.):	
<b>Curing Information</b>	
Test date:	10/8/2008
Days on site:	1
Days in curing:	6
Age at testing(days):	7
<b>Test Information</b>	
Load at Failure (lbs.):	5,320
Strength at Failure (PSI):	410
Specified Strength (PSI):	
Type of Failure:	

**Conformance:** The 7-day result is reported for informational use only.

**Reported By:**  
  
Curtis L. Johnson, PE  
Staff Engineer II

DR

**REPORT OF FLEXURAL STRENGTH OF CONCRETE BEAM SPECIMENS - THIRD POINT LOADING - ASTM:C78**

**PROJECT:**  
MN/ROAD RECONSTR. MATERIAL TEST  
ST. PAUL, MINNESOTA

**REPORTED TO:**  
MINNESOTA DEPARTMENT OF TRANSPORTATION  
1400 GERVAIS AVENUE  
M.S. 645  
MAPLEWOOD, MN 55109-2044

**ATTN:** BERNARD IZEVBEKHAI

**CC:**

**AET PROJECT NO:** 01-04293

**DATE:** December 2, 2008

**Placement Information:**

**Set No:** CB 010 A  
**Date Cast:** 10/1/2008  
**Cast By:** Joe Clem  
**Date Received in Laboratory:** 10/2/2008

**Concrete Supplied By:** Aggregate Industries  
**Mix No:** Pervious  
**Truck No:** 147  
**Placement Method:** Truck Discharge

**Plastic Properties:** (ASTM:C143, ASTM:C231, ASTM:C1064)

**Slump, in:** .25

**Air Content, %:** 20.0

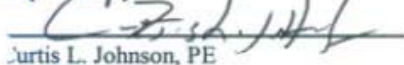
**Concrete Temp, F°:**

**Placement Location:** Cell 39, Outside Lane

<b>Beam No.</b>	CB 010 A
<b>Beam Information</b>	
Weight (lbs):	5.98
Width (in.):	6.02
Depth (in.):	18.00
Span (in.):	
<b>Curing Information</b>	
Test date:	10/8/2008
Days on site:	1
Days in curing:	6
Age at testing(days):	7
<b>Test Information</b>	
Load at Failure (lbs.):	4,730
Strength at Failure (PSI):	390
Specified Strength (PSI):	
Type of Failure:	

**Conformance:** The 7-day result is reported for informational use only.

**Reported By:**

  
Curtis L. Johnson, PE

Staff Engineer II

DR

**REPORT OF FLEXURAL STRENGTH OF CONCRETE BEAM SPECIMENS - THIRD POINT LOADING - ASTM:C78**

**PROJECT:**  
MN/ROAD RECONSTR. MATERIAL TEST  
ST. PAUL, MINNESOTA

**REPORTED TO:**  
MINNESOTA DEPARTMENT OF TRANSPORTATION  
1400 GERVAIS AVENUE  
M.S. 645  
MAPLEWOOD, MN 55109-2044

**ATTN:** BERNARD IZEVBEKHAI

**CC:**

**AET PROJECT NO:** 01-04293

**DATE:** December 2, 2008

**Placement Information:**

**Set No:** CB 011 A  
**Date Cast:** 10/1/2008  
**Cast By:** Joe Clem  
**Date Received in Laboratory:** 10/2/2008

**Concrete Supplied By:** Aggregate Industries  
**Mix No:** Pervious  
**Truck No:** 147  
**Placement Method:** Truck Discharge

**Plastic Properties:** (ASTM:C143, ASTM:C231, ASTM:C1064)

**Slump, in:** .25

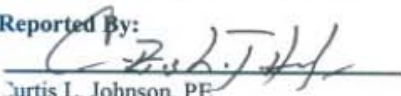
**Air Content, %:** 20.0

**Concrete Temp, F°:**

**Placement Location:** Cell 39, Outside Lane

<b>Beam No.</b>	CB 011 A
<b><u>Beam Information</u></b>	
Weight (lbs):	5.86
Width (in.):	6.04
Depth (in.):	18.00
Span (in.):	
<b><u>Curing Information</u></b>	
Test date:	10/29/2008
Days on site:	1
Days in curing:	27
Age at testing(days):	28
<b><u>Test Information</u></b>	
Load at Failure (lbs.):	5,430
Strength at Failure (PSI):	460
Specified Strength (PSI):	
Type of Failure:	
<b>Conformance:</b> The 28-day result is reported for informational use only.	

**Reported By:**

  
Curtis L. Johnson, PE

Staff Engineer II

DR

**REPORT OF FLEXURAL STRENGTH OF CONCRETE BEAM SPECIMENS - THIRD POINT LOADING - ASTM:C78**

**PROJECT:**

MN/ROAD RECONSTR. MATERIAL TEST  
ST. PAUL, MINNESOTA

**REPORTED TO:**

MINNESOTA DEPARTMENT OF TRANSPORTATION  
1400 GERVAIS AVENUE  
M.S. 645  
MAPLEWOOD, MN 55109-2044

ATTN: BERNARD IZEVBEKHAI

CC:

AET PROJECT NO: 01-04293

DATE: December 2, 2008

**Placement Information:**

Set No: CB 012 A  
Date Cast: 10/1/2008  
Cast By: Joe Clem  
Date Received in Laboratory: 10/2/2008

Concrete Supplied By: Aggregate Industries  
Mix No: Pervious  
Truck No: 147  
Placement Method: Truck Discharge

**Plastic Properties:** (ASTM:C143, ASTM:C231, ASTM:C1064)

Slump, in: .25

Air Content, %: 20.0

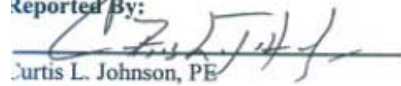
Concrete Temp, F°:

**Placement Location:** Cell 39, Outside Lane

<b><u>Beam No.</u></b>	CB 012 A
<b><u>Beam Information</u></b>	
Weight (lbs):	6.16
Width (in.):	6.00
Depth (in.):	18.00
Span (in.):	
<b><u>Curing Information</u></b>	
Test date:	10/29/2008
Days on site:	1
Days in curing:	27
Age at testing(days):	28
<b><u>Test Information</u></b>	
Load at Failure (lbs.):	5,840
Strength at Failure (PSI):	470
Specified Strength (PSI):	
Type of Failure:	

**Conformance:** The 28-day result is reported for informational use only.

Reported By:

  
Curtis L. Johnson, PE  
Staff Engineer II

DR

# MnRoad 2008 Reconstruction Concrete Flexural Strength Summary

## Cell 39

**Sample Location:** Cell 39, Inside Lane  
**Mix Type:** Pervious Overlay  
**Specimen Type:** 6" X 6" X 22" Beam  
**Date Cast:** 10/17/2008

Sample #'s:	<u>MNRD-53-CB-28</u>	<u>MNRD-53-CB-29</u>	
Date Broken:	10/21/2008	10/21/2008	
Age @ Testing (Days):	4	4	
Load @ Failure (lbs.):	4,660	4,680	
Strength @ Failure (psi):	390	370	
<b>Average Flexural Strength @ 4 Days(psi):</b>			<b>380</b>

Sample #'s:	<u>MNRD-53-CB-30</u>	<u>MNRD-53-CB-31</u>	
Date Broken:	10/24/2008	10/24/2008	
Age @ Testing (Days):	7	7	
Load @ Failure (lbs.):	7,160	6,870	
Strength @ Failure (psi):	590	560	
<b>Average Flexural Strength @ 7 Days(psi):</b>			<b>575</b>

Sample #'s:	<u>MNRD-53-CB-32</u>	<u>MNRD-53-CB-33</u>	
Date Broken:	11/14/2008	11/14/2008	
Age @ Testing (Days):	28	28	
Load @ Failure (lbs.):	9,840	10,660	
Strength @ Failure (psi):	820	890	
<b>Average Flexural Strength @ 28 Days(psi):</b>			<b>855</b>



**REPORT OF FLEXURAL STRENGTH OF CONCRETE BEAM SPECIMENS - THIRD POINT LOADING - ASTM:C78**

**PROJECT:**  
MN/ROAD RECONSTR. MATERIAL TEST  
ST. PAUL, MINNESOTA

**REPORTED TO:**  
MINNESOTA DEPARTMENT OF TRANSPORTATION  
1400 GERVAIS AVENUE  
M.S. 645  
MAPLEWOOD, MN 55109-2044

**ATTN:** BERNARD IZEVBEKHAI

**CC:**

**AET PROJECT NO:** 01-04293

**DATE:** December 2, 2008

**Placement Information:**

**Set No:** CB 028 A  
**Date Cast:** 10/17/2008  
**Cast By:** Joe Clem  
**Date Received in Laboratory:** 10/20/2008

**Concrete Supplied By:** Aggregate Industries  
**Mix No:** Pervious  
**Truck No:**  
**Placement Method:** Truck Discharge

**Plastic Properties:** (ASTM:C143, ASTM:C231, ASTM:C1064)

**Slump, in:** .75

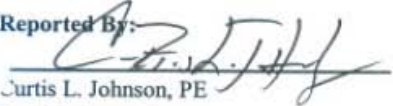
**Air Content, %:**

**Concrete Temp, F°:**

**Placement Location:** Cell 39, Inside Lane

<b><u>Beam No.</u></b>	CB 028 A
<b><u>Beam Information</u></b>	
Weight (lbs):	5.85
Width (in.):	6.09
Depth (in.):	18.00
Span (in.):	
<b><u>Curing Information</u></b>	
Test date:	10/21/2008
Days on site:	3
Days in curing:	1
Age at testing(days):	4
<b><u>Test Information</u></b>	
Load at Failure (lbs.):	4,660
Strength at Failure (PSI):	390
Specified Strength (PSI):	
Type of Failure:	
<b>Conformance:</b> The 4-day result is reported for informational use only.	

**Reported By:**

  
Curtis L. Johnson, PE

Staff Engineer II

DR

**REPORT OF FLEXURAL STRENGTH OF CONCRETE BEAM SPECIMENS - THIRD POINT LOADING - ASTM:C78**

**PROJECT:**

MN/ROAD RECONSTR. MATERIAL TEST  
ST. PAUL, MINNESOTA

**REPORTED TO:**

MINNESOTA DEPARTMENT OF TRANSPORTATION  
1400 GERVAIS AVENUE  
M.S. 645  
MAPLEWOOD, MN 55109-2044

**ATTN:** BERNARD IZEVBEKHAI

**CC:**

**AET PROJECT NO:** 01-04293

**DATE:** December 2, 2008

**Placement Information:**

**Set No:** CB 029 A  
**Date Cast:** 10/17/2008  
**Cast By:** Joe Clem  
**Date Received in Laboratory:** 10/20/2008

**Concrete Supplied By:** Aggregate Industries  
**Mix No:** Pervious  
**Truck No:**  
**Placement Method:** Truck Discharge

**Plastic Properties:** (ASTM:C143, ASTM:C231, ASTM:C1064)

**Slump, in:** .75

**Air Content, %:**

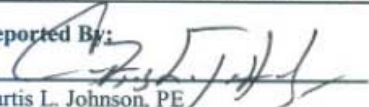
**Concrete Temp, F°:**

**Placement Location:** Cell 39, Inside lane

<b>Beam No.</b>	CB 029 A
<b>Beam Information</b>	
Weight (lbs):	6.01
Width (in.):	6.13
Depth (in.):	18.00
Span (in.):	
<b>Curing Information</b>	
Test date:	10/21/2008
Days on site:	3
Days in curing:	1
Age at testing(days):	4
<b>Test Information</b>	
Load at Failure (lbs.):	4,680
Strength at Failure (PSI):	370
Specified Strength (PSI):	
Type of Failure:	

**Conformance:** The 4-day result is reported for informational use only.

**Reported By:**

  
Curtis L. Johnson, PE

Staff Engineer II

DR



**REPORT OF FLEXURAL STRENGTH OF CONCRETE BEAM SPECIMENS - THIRD POINT LOADING - ASTM:C78**

**PROJECT:**  
MN/ROAD RECONSTR. MATERIAL TEST  
ST. PAUL, MINNESOTA

**REPORTED TO:**  
MINNESOTA DEPARTMENT OF TRANSPORTATION  
1400 GERVAIS AVENUE  
M.S. 645  
MAPLEWOOD, MN 55109-2044

**ATTN:** BERNARD IZEVBEKHAI

**CC:**

**AET PROJECT NO:** 01-04293

**DATE:** December 2, 2008

**Placement Information:**

**Set No:** CB 031 A  
**Date Cast:** 10/17/2008  
**Cast By:** Joe Clem  
**Date Received in Laboratory:** 10/20/2008

**Concrete Supplied By:** Aggregate Industries  
**Mix No:** Pervious  
**Truck No:**  
**Placement Method:** Truck Discharge

**Plastic Properties:** (ASTM:C143, ASTM:C231, ASTM:C1064)

**Slump, in:** .75

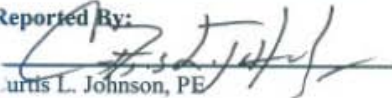
**Air Content, %:**

**Concrete Temp, F°:**

**Placement Location:** Cell 39, Inside lane

<b><u>Beam No.</u></b>	CB 031 A
<b><u>Beam Information</u></b>	
Weight (lbs):	6.09
Width (in.):	6.01
Depth (in.):	18.00
Span (in.):	
<b><u>Curing Information</u></b>	
Test date:	10/24/2008
Days on site:	3
Days in curing:	4
Age at testing(days):	7
<b><u>Test Information</u></b>	
Load at Failure (lbs.):	6,870
Strength at Failure (PSI):	560
Specified Strength (PSI):	
Type of Failure:	
<b>Conformance:</b> The 7-day result is reported for informational use only.	

**Reported By:**



Curtis L. Johnson, PE

Staff Engineer II

DR



**REPORT OF FLEXURAL STRENGTH OF CONCRETE BEAM SPECIMENS - THIRD POINT LOADING - ASTM:C78**

**PROJECT:**

MN/ROAD RECONSTR. MATERIAL TEST  
ST. PAUL, MINNESOTA

**REPORTED TO:**

MINNESOTA DEPARTMENT OF TRANSPORTATION  
1400 GERVAIS AVENUE  
M.S. 645  
MAPLEWOOD, MN 55109-2044

**ATTN:** BERNARD IZEVBEKHAI

**CC:**

**AET PROJECT NO:** 01-04293

**DATE:** December 2, 2008

**Placement Information:**

**Set No:** CB 033 A  
**Date Cast:** 10/17/2008  
**Cast By:** Joe Clem  
**Date Received in Laboratory:** 10/20/2008

**Concrete Supplied By:** Aggregate Industries  
**Mix No:** Pervious  
**Truck No:**  
**Placement Method:** Truck Discharge

**Plastic Properties:** (ASTM:C143, ASTM:C231, ASTM:C1064)

**Slump, in:** .75

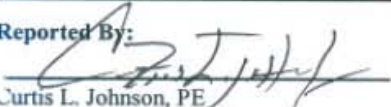
**Air Content, %:**

**Concrete Temp, F°:**

**Placement Location:** Cell 39, Inside lane

<b><u>Beam No.</u></b>	CB 033 A
<b><u>Beam Information</u></b>	
Weight (lbs):	6.00
Width (in.):	6.00
Depth (in.):	18.00
Span (in.):	
<b><u>Curing Information</u></b>	
Test date:	11/14/2008
Days on site:	3
Days in curing:	25
Age at testing(days):	28
<b><u>Test Information</u></b>	
Load at Failure (lbs.):	10,660
Strength at Failure (PSI):	890
Specified Strength (PSI):	
Type of Failure:	
<b>Conformance:</b> The 28-day result is reported for informational use only.	

**Reported By:**

  
Curtis L. Johnson, PE

Staff Engineer II

DR

## Plate E9: Site Report on Construction Activities

### 2008 MnROAD Reconstruction Engineer's Update For the Week of October 20, 2008

Things are starting to wind down at MnROAD, but you'd never know it by the looks of things. PCI grading crews spent the week adding Class 5 aggregate shouldering material to Cells 5, 6, 13, 14, 39, and 53. They were careful to keep construction traffic off of the pervious concrete overlay on Cell 39, as we as to minimize the amount of gravel that got onto the surface so as not to clog the pores. They added wick drains to Cell 5, which are designed to drain the water from the PASSRC layer to the shoulder.

The big news of the week was paving pervious concrete on Cells 85 and 89. PCI poured the outside lane of each cell on Monday, and they came back Friday to pour the inside lane. The trucks backed onto the underlying drainable base to deliver the concrete, and PCI had to re-compact the base layer to make it smooth again. The concrete was poured into forms and compacted with a rolling screed. Immediately behind the screed, a special curing compound was sprayed on the concrete. Transverse joints were toole every ten feet with a tool that resembled a large pizza cutter. The slab was immediately covered up with white plastic sheet to initiate curing. Everything about the pervious concrete paving went well, including the new unit weight tests that were run on the material in lieu of air pot tests. The challenge came the next day – as the Mn/DOT inspector tried to take the beams out of the molds, the first one crumbled to pieces. The other two beams were still soft to the touch, and even the in-place slab was so soft that you could poke a hole in it with your thumb. This was likely due to a combination of cold weather condition (overnight air temperature was 28°F), use of retarders, pozzolanic substitution, and flat work. However, Aggregate Industries advised everyone to be patient and wait for another day or two to let the concrete set up. Lo and behold, by Wednesday and later in the week, the concrete set up nicely and allowed us to pour the other lane on Friday. This pervious concrete is a different animal than what people are used to, but with a little education we learned how to work with it properly. PCI also paved the 3" concrete shoulders on Cell 53 on Tuesday with no problems or issues to work out.



MnROAD crews spent the week working busily on instrumentation. We installed vibrating wires, thermocouples, maturity meters, pressure cells, water marks, and other gauges in Cells 85 and 89. The instrumentation plans for these cells was much lighter than the Mainline concrete cells, but it still took time to complete. The bulk of the work took place on Cells 5, 6, 13, 14, and 53. This involved preparing the concrete slabs for LVDTs, which measure vertical deflection along the joints and at midpanel. First we saw cut along the edge of the slab to get a smooth, straight surface to work on. We drilled anchor bolts into the side of the slab that would hold the LVDT brackets and their protective boxes. Next we augured a hole at each location and installed a 6-foot PVC pipe, compacting around it. We will come back at a later date to install an invar rod in each pipe, which will provide a vertical reference for the LVDTs. Then we custom-drilled each mounting bracket and bolted the boxes onto the slab. The LVDT boxes were custom-made earlier this summer at a local machine shop. We put covers back on each box and connected several boxes in each cell with conduit, which will be used to rout the lead wires back to data collection terminals. We backfilled gravel along the boxes and conduits, preparing the shoulder for paving next week. There are 30 boxes in all to install, and on a good day we could install 8 per day with a 3-4 person team. We haven't even installed the LVDTs, their lead wires, and invar rods yet, but that's another project for another day...

**Plate E10:Excerpt of Testing Report**

**REPORT OF PAVEMENT MATERIALS  
TESTING**

Mn/ROAD Reconstruction - 2008  
Otsego, Minnesota

---

AET #01-04293

**Date:**

March 31, 2009

**Prepared for:**

Minnesota Department of Transportation  
Office of Materials and Road Research  
1400 Gervais Avenue  
Maplewood, MN 55109

Attn: Bernard Izevbekhai, P. E.



CONSULTANTS  
• ENVIRONMENTAL  
• GEOTECHNICAL  
• MATERIALS  
• FORENSICS

March 31, 2009

Minnesota Department of Transportation  
Office of Materials and Road Research  
1400 Gervais Avenue  
Maplewood, MN 55109

Attn: Bernard Izevbekhai, P. E.

RE: Pavement Materials Testing  
Mn/ROAD Reconstruction - 2008  
Otsego, MN  
AET Project # 01-04293

Dear Mr. Izevbekhai:

This report presents the results of a pavement materials testing project performed on the concrete materials placed during the reconstruction of several cells at the Mn/ROAD facility located in Otsego, Minnesota. A copy of all test reports is attached as Appendix A.

Please contact me if you have questions about the report.

Very truly yours,

**American Engineering Testing, Inc.**

David L. Rettner, PE  
Principal Engineer, Geotechnical Division  
Phone: (651) 755-5795  
Fax: (651) 659-1347  
[drettner@amengtest.com](mailto:drettner@amengtest.com)

## OFFICE OF MATERIALS AND ROAD RESEARCH

AET #01-04293

### INTRODUCTION

This report presents the results of the pavement materials testing performed on concrete placed at the Mn/ROAD facility located in Otsego, Minnesota between September 19, 2008 and October 24, 2008.

### Scope of Services

The scope of work for the project is outlined below:

- Fabricate concrete test specimens as directed by Office of Materials and Road Research staff, to include:
  - 40 Coefficient of Thermal Expansion Specimens – cast with vibrating wire strain gauges in the specimens.
  - 9 sets of 3 beams for ASTM C-666 (rapid freeze-thaw) testing.
  - 4 sets of 2 cylinders for ASTM C1202 (rapid chloride ion permeability) testing.
    - 1 set of cylinders from high performance concrete
    - 3 sets of cylinders from pervious concrete
  - 57 Flexural Beam Specimens (ASTM C 78)
  - 82 Compressive Strength Specimens (ASTM C39)
- Perform Concrete Materials Testing on the hardened concrete specimens at the ages directed by Office of Materials and Road Research staff.
- Summarize data in report, grouped by Mn/ROAD cell.

## **PROJECT INFORMATION**

Mn/ROAD Cells 5, 6, 13, 14, 39, 53, 85, and 89 were reconstructed or rehabilitated during the summer and fall of 2008. Several rehabilitation techniques were used including unbounded overlays, white-topping, and reconstruction. Several hundred pavement sensors were installed at part of the reconstruction. The concrete pavement was placed in September and October 2008 in several paving operations. The temperature during construction ranged from nighttime lows of 28 °F to daytime highs in the upper 70's °F. The mainline cells (5, 6, 13, and 14) were constructed using a slip-form paver in a single pass. The low-volume road cells (39, 53, 85, and 89) were constructed one lane at a time using forms and a screed. There were three (3) concrete mixes used in the reconstruction, one typical high-performance concrete mix (Cells 5, 6, 13, 14, and 53), and two pervious concrete mixes (Cells 39, 85, and 89).

## **HARDENED CONCRETE TEST RESULTS**

Concrete samples were transported from the Mn/ROAD facility to American Engineering Testing, Inc.'s laboratory in St. Paul, Minnesota for stripping, curing, and testing. The specimens were tested at ages determined by Office of Materials and Road Research personnel. Several of the freeze/thaw beam specimens cast in Cell 89 were damaged during stripping due to low strength at 24-40 hours of age. As a result there was one less set of tests performed for ASTM C-666 than was planned in Cell 89. Two of the Coefficient of Thermal Expansion specimens (23 and 40) were damaged during shipping and could not be tested. All of the test reports are contained in Appendix A of this report. Summaries of each test, by cell, are included below.

### **Coefficient of Thermal Expansion Test Results**

The coefficient of thermal expansion (CTE) is a critical input to the new AASHTO Mechanistic

Empirical Pavement Design Guide. At the time of this project the FHWA determined that there were some potential inconsistencies with the equipment being used to perform the test using the AASHTO TP-60 procedure. It was determined by Mn/DOT staff, AET, and the University of Pittsburgh, that the best method to use for this project would be to cast vibrating wire strain gauges vertically aligned into the center of 6" x 12" cylinders and measure the temperature induced strain from a constant temperature bath rather than to try and deal with the issues involving TP-60 (FHWA is currently conducting a round-robin study of different testing equipment to determine the accuracy and variability in equipment and operators). A total of 40 specimens were cast with Geokon 4200 vibrating wire strain gauges. The specimens were cured for 28 days and shipped to the University of Pittsburgh where the CTE testing was performed. The temperature conditioning of the specimens followed the requirements of TP-60, however rather than measuring the elongation with a comparator and LVDT and converting it to strain the embedded strain gauges were measured. This method provides better accuracy due to a lack of complications that can be developed from the thermal interactions of the test specimen, LVDT, and comparator stand. During shipping two of the specimens were damaged and could not be tested. A summary of the testing data is shown in Table 1 below. From the data it is apparent that there is a significant difference between the high performance concrete (HPC) used in Cells 5, 6, 13, 14, and 53 and the pervious concrete used in Cells 39, 85, and 89.

**Table 1 - Mn/ROAD Concrete Pavement Coefficient of Thermal Expansion**

<b>Cell</b>	<b>Average CTE (10<sup>-6</sup> in/in/°F)</b>	<b>Std. Dev.</b>
5	5.4	0.09
6	5.3	0.04
13	5.3	0.04
39	4.8	0.16
53	5.3	0.00
85	4.8	0.07
89	4.9	0.12

### **Rapid Chloride Ion Permeability**

Four sets of two 4" x 8" cylinder specimens were cast for the purposes of performing ASTM C 1202 "Rapid Determination of the Chloride Permeability of Concrete." One set of specimens was cast from the HPC concrete placed in Cell 5, the others from the pervious concrete placed in Cells 39, 85, and 89. The test results for Cell 5 are shown below. The pervious nature of the concrete in Cells 39, 85, and 89 did not allow the test to provide accurate results.

**Table 2 - Mn/ROAD Rapid Chloride Ion Permeability Test Results ASTM C 1202**

<b>Cell</b>	<b>Coulombs</b>	<b>Milliamps</b>
5	2040	116.1

### **Freeze/Thaw Durability Testing**

A total of nine (9) sets of freeze/thaw beams were cast for performing Procedure A of ASTM C 666 "Standard Test Method for Resistance of Concrete to Rapid Freezing and Thawing." Three (3) sets of beams were cast from the HPC concrete mixture (Cells 5, 6, and 53) and six (6) sets of beams were cast from the pervious concrete mixtures (Cells 39, 85, and 89). One set of beams from Cell 89 was damaged during removal from the forms due to a lack of strength in the first day after paving and therefore could not be tested. The results of the remaining test specimens are summarized in Table 3 below. It can be seen that the HPC mixture performed very well with an average durability factor of 94.7% at 300 cycles. The pervious pavement mixtures performed reasonably well for this type of mixture, surviving between 83 and 228 cycles before failure.

Cell	Dynamic Modulus (%)	Dilation (%)	Weight Loss %	Durability Factor
5	95	0.04	0.35	95
6	94	0.04	0.38	94
39	Failed at 83 Cycles			15
39	Failed at 100 Cycles			19
53	95	0.04	0.32	95
85	Failed at 228 Cycles			44
85	Failed at 127 Cycles			24
89	Failed at 117 Cycles			23

### **Concrete Compressive Strength Testing**

A total of 82 6" x 12" compressive strength specimens were cast at the direction of Office of Materials and Road Research staff. A summary of the test results is shown in Table 4 below. The majority of the cells had samples broken at 3, 7, 21 and 28 days, although there was some variation in this schedule due to weekends. It can be seen that there is a significant amount of variability in the strength of the HPC (cells 5, 6, 13, 14, and 53) where the 7-day compressive strength varies between 3760 psi and 4445 psi and the 28-day compressive strength varies between 5030 psi and 5895 psi. The pervious pavement (cells 39, 85, and 89) showed even greater variability with 7-day strengths ranging between 2395 psi and 4160 psi and the 28-day compressive strength ranging between 4020 psi and 5200 psi. It is possible that the high degree of variability in the pervious pavement cylinder strength could be due to differences in the consolidation method used when preparing the cylinders. It is recommended that cores be taken of the pavement in the Spring of 2009 to determine the actual pavement strength.

**Table 4 - Concrete Compressive Strength Summary**

<b>Average Compressive Strength @ 3 Days(psi):</b>					
Cell	Number of Specimens	Average Strength	Standard Deviation	High	Low
Trial Batch	1	2700	N/A		
5	4	2550	194	2830	2390
6	1	3750	N/A		
13-14	1	3210	N/A		
39 Inside Lane					
39 Outside Lane	2	1355	N/A	1410	1300
53 Inside Lane	2	3250	N/A	3270	3230
85 Inside Lane	2	3110	N/A	3190	3020
85 Outside Lane	2	3280	N/A	3470	3080
89 Inside Lane	2	3070	N/A	3210	2930
89 Outside Lane	2	2270	N/A	2370	2160
<b>Average Compressive Strength @ 5 Days(psi):</b>					
Cell	Number of Specimens	Average Strength	Standard Deviation	High	Low
Trial Batch					
5					
6					
13-14					
39 Inside Lane	2	2550	N/A	2570	2530
39 Outside Lane					
53 Inside Lane					
85 Inside Lane					
85 Outside Lane					
89 Inside Lane					
89 Outside Lane					

Cell	Specimens	Strength	Deviation	High	Low
Trial Batch	1	4280	N/A		
5	4	3760	191	4040	3620
6	1	4320	N/A		
13-14	1	3850	N/A		
39 Inside Lane	2	2915	N/A	2990	2840
39 Outside Lane	2	2395	N/A	2400	2390
53 Inside Lane	2	4445	N/A	4470	4420
85 Inside Lane	2	3220	N/A	3230	3200
85 Outside Lane	2	4160	N/A	4270	4040
89 Inside Lane	2	3410	N/A	3460	3350
89 Outside Lane	2	3120	N/A	3160	3070

<b>Average Compressive Strength @ 21 Days(psi):</b>					
Cell	Number of Specimens	Average Strength	Standard Deviation	High	Low
Trial Batch					
5	4	4530	67	4600	4470
6					
13-14					
39 Inside Lane	2	4255	N/A	4380	4130
39 Outside Lane	2	3020	N/A	3120	2920
53 Inside Lane	2	5465	N/A	5560	5370
85 Inside Lane	2	3450	N/A	3560	3340
85 Outside Lane	2	5005	N/A	5060	4950
89 Inside Lane	2	4130	N/A	4160	4090
89 Outside Lane	2	3520	N/A	3610	3430

<b>Average Compressive Strength @ 28 Days(psi):</b>					
Cell	Number of Specimens	Average Strength	Standard Deviation	High	Low
Trial Batch					
5	4	5200	85	5300	5100
6	2	5670	N/A	5750	5580
13-14	2	5030	N/A	5130	4920
39 Inside Lane	2	4750	N/A	4780	4720
39 Outside Lane	2	4020	N/A	4060	3980
53 Inside Lane	2	5895	N/A	5950	5840
85 Inside Lane	2	3850	N/A	3880	3810
85 Outside Lane	2	5200	N/A	5240	5150
89 Inside Lane	2	4290	N/A	4330	4240
89 Outside Lane	2	4250	N/A	4300	4200

### **Concrete Flexural Strength**

A total of 57 6" x 6" x 22" flexural beam specimens were cast on the project. The specimens were tested in accordance with ASTM C78, primarily at 3, 7, and 28 days, with a few exceptions. The results are summarized in Table 5 below. It can be seen from the data that there was a significant variability in flexural strength between the HPC concrete mix (Cells 5 and 53) at 7 and 28 days (and 47 days for Cell 53 outside lane), however all of the strengths are very high relative to a normal HPC mix on a Mn/DOT project (typical range of 650 to 800 psi at 28 days).

A review of the flexural strength data from the pervious pavement shows an even larger variation in test results. The 28 day breaks from Cell 39 Inside Lane average 855 psi, with Cell 39 Outside Lane averaged 465 psi. The only difference between these two sets of specimens was the dates they were cast, October 17, 2008 and October 1, 2008 respectively. It is recommended that the pavement be cored and the samples be tested for compressive strength and/or splitting tensile strength to determine the actual pavement strength.

**Table 5 - Concrete Flexural Strength Summary**

<b>Average Flexural Strength @ 1 Day(psi):</b>					
Cell	Number of Specimens	Average Strength	Standard Deviation	High	Low
Trail Batch					
5	2	490	N/A	490	490
6					
13-14					
39 Inside Lane					
39 Outside Lane	1	90	N/A	90	90
53 Inside Lane	1	280	N/A	280	280
53 Outside Lane					
85 Inside Lane					
85 Outside Lane					
89 Inside Lane					
89 Outside Lane					
<b>Average Flexural Strength @ 3 Days(psi):</b>					
Cell	Number of Specimens	Average Strength	Standard Deviation	High	Low
Trail Batch					
5	2	565	N/A	560	570
6					
13-14					
39 Inside Lane					
39 Outside Lane	1	360	N/A	360	360
53 Inside Lane	1	580	N/A	580	580
53 Outside Lane					
85 Inside Lane	2	295	N/A	310	280
85 Outside Lane	2	440	N/A	460	420
89 Inside Lane	2	435	N/A	460	410
89 Outside Lane	2	330	N/A	350	310

<b>Average Flexural Strength @ 4 Days(psi):</b>					
Cell	Number of Specimens	Average Strength	Standard Deviation	High	Low
Trail Batch					
5					
6					
13-14					
39 Inside Lane	2	380	N/A	390	370
39 Outside Lane					
53 Inside Lane					
53 Outside Lane					
85 Inside Lane					
85 Outside Lane					
89 Inside Lane					
89 Outside Lane					
<b>Average Flexural Strength @ 7 Days(psi):</b>					
Cell	Number of Specimens	Average Strength	Standard Deviation	High	Low
Trail Batch					
5	4	620	26.3	640	580
6					
13-14					
39 Inside Lane	2	575	N/A	590	570
39 Outside Lane	2	400	N/A	410	390
53 Inside Lane	2	760	N/A	790	730
53 Outside Lane	1	710	N/A	710	710
85 Inside Lane	2	320	N/A	320	320
85 Outside Lane	2	450	N/A	480	420
89 Inside Lane	2	425	N/A	450	400
89 Outside Lane	2	390	N/A	400	380

<b>Average Flexural Strength @ 28 Days(psi):</b>					
Cell	Number of Specimens	Average Strength	Standard Deviation	High	Low
Trail Batch					
5	4	930	87.3	1010	830
6					
13-14					
39 Inside Lane	2	855	N/A	890	820
39 Outside Lane	2	465	N/A	470	460
53 Inside Lane	2	1115	N/A	1150	1080
53 Outside Lane					
85 Inside Lane	2	325	N/A	330	320
85 Outside Lane	2	490	N/A	520	460
89 Inside Lane	2	490	N/A	520	450
89 Outside Lane	2	440	N/A	460	410
<b>Average Flexural Strength @ 47 Days(psi):</b>					
Cell	Number of Specimens	Average Strength	Standard Deviation	High	Low
Trail Batch					
5					
6					
13-14					
39 Inside Lane					
39 Outside Lane					
53 Inside Lane					
53 Outside Lane	2	885	N/A	930	840
85 Inside Lane					
85 Outside Lane					
89 Inside Lane					
89 Outside Lane					

**STANDARD OF CARE**

Our services for your project have been conducted to those standards considered normal for services of this type at this time and location. Other than this, no warranty, either express or implied, is intended.

**SIGNATURES**

Report Prepared by:

**American Engineering Testing, Inc.**

---

David L. Rettner, PE  
Principal Engineer, Geotechnical Division  
MN Reg #20458

Report Reviewed by:

**American Engineering Testing, Inc.**

---

Joseph Korzilius, PE  
Principal Engineer

Attachments:

Appendix A – Data Report

**APPENDIX F: RELEVANT EXCERPT OF CONSTRUCTION  
ENGINEER'S NOTES**

## **Relevant Construction notes**

2008 MnROAD Reconstruction (ML & LVR)

SP 8680-157

### **4/16/2008**

Pre-Construction meeting held in Golden Valley. Representatives from MnROAD, Golden Valley Mn./DOT, Contractor and Sub-Contractor were in attendance. (See minutes sent by Bob Rabine for details.

### **4/21/2008**

[9:00 A.M.] 1<sup>st</sup> job meeting at MnROAD site, MnROAD, GV, PCI staff present.

See meeting notes for details

Discussed erosion control measures needed. (Silt fence culvert protection, bale logs, etc.)

Discussed location of stockpiles in stockpile area

No erosion control needed.

Will start with removals later this week

Start on cell 5 and work east, then LVR

PCC first, HMA milling next week

Removals first, then grading, and then paving

PCI plans on reusing the PCC pavement as Class 7 wherever they can

We need to determine where Class 5 virgin is required (cell and quantities) and get back to GV & PCI; work order (price adjustments)

### **4/22/2008**

Rich N. on site - working with PCI and subs (Dousettes) to get erosion control measures in place.

TRC – met with Dave Rettner (AET) to discuss contract for PCC “research” sampling, testing, and reporting

### **6/19/2008**

Geoprobe demo at 10:00 A.M. on cell 25, 26, 30 people. Confirmed the following:

Clay at 6ft depth and down to 32 ft in former cell 26 cell 89 and 88 Pervious concrete and porous asphalt respectively

TC took samples to Maplewood Lab for gradation, proctor

2108SG011, 012	1I, 2I
2108SG019, 020	1J, 2J
2208SG011, 012	1K, 2K
2208SG019, 020	1L, 2L

Doug and crew handholes and conduit cell 21

\*2 paragraphs of taconite stuff to Maureen Friday

**9/5/2008**

CA-15 aggregate gradation passed. Approved for use in cells 85-89

AET sampled class 5 from cell 6 & 13 to Maplewood Lab:

0608GR001, 002	1, 2 CD
0608GR 019, 020	1, 2 CE
1308GR001, 002	1, 2 CF
1308GR009, 010	1, 2 CG

**10/6/2008**

Monday morning construction meeting, see notes

PCI getting ready to pave concrete on cell 5

Setting up paver, texturing, stringline

PCI backfilling behind curbs on cell 85-89

MnROAD busy instrumenting cell 5, 6, 13, 14

Doug L. saw cut West end of cell 5 to provide smooth face for adjacent concrete paving

Took WMA samples to Maplewood for TSR testing:

1608BM011, 025	Wear
1608BM038, 039	Non-wear

**10/8/2008**

PCI concrete paving on cell 5 East to West 27' wide. Lots of helpers on hand, no dowels, tie bars inserted by paver. MnROAD packed concrete and vibrated around wires and sensors in 4 areas. Bernard wanted long tining, 1/2' on center per his most recent texture allocation. TC failed to pass along to PCI so they tined 1.0" on center. (Trouble getting depth on tining) After tining, Len floated on man lift to install surface CE sensors. Cut groove for wires with a trowel, will epoxy the wires in later. Curing compound sprayed on, had to hand form West end and along some edges because of holes in slab. Broke down paver afterwards and set to 24' for tomorrow. PCI began laying out dowel baskets in cell 6.

PCI crew finished grading rock on cells 88 to 85 still unstable, backfilled black dirt behind curbs.

Installed TC tree in cell 88. ECH20s too (5 in sub-grade) careful not to contaminate rock with clay

Hardrives grading crew here to blade shoulder (PL) on cells 2-4. No roller will roll tomorrow, will also clean up gravel on (DL) shoulder around cabinets with blade or skidder. Jeff Palmer on site.

Lane shoulder drop-off on cells 2-4 is 3/4" 1 1/4" right at 12' lane. Called Randy Reznik (MnDOT Maintenance) Mini Mac will come tomorrow to fill in gap.

Diamond surfacing Inc. here to diamond grind cell 9 for PF study, new and improved next generation diamond grinding

Ben 2:00 P.M. radio interview with St. Cloud station

PCI set form for concrete paving on cell 39 (IL) and cell 53 (OL)

**10/14/2008**

PCI grading crew touched up rock on cells 85-89. Cleaned up along shoulders on cells 5, 6, 13, and 14.

MnROAD crew installed TC trees in 24, 85-89. Prepared instrumentation for pervious paving. Tom and crew worked on routing lead wires, other instrumentation on cells 5, 6, 13, and 14

Metro design crew out to MnROAD to look it over for 2009 job

TC and Bev sampled HMA agg and RAP for NCAT:

Loken 3/4" rock - 8 buckets

Martin Marietta washed sand – 8 pails

Martin Marietta 1/2" chip – 8 pails

Coarse RAP – 5 pails

Fine RAP – 6 pails

Standard RAP – 4 pails

Got ready 56 (?) buckets from cell 6 HMA for UC Davis

### **10/15/2008**

PCI cleaning up, grading shoulder cells 5, 6

Jeff Palmer (Sem) out to look at shoulder on cells 2-4, outside shoulder looks good with Mini Mac and grading. Inside shoulder on cells 2-3 looks good, inside shoulder on cell 4 is bad, missing material on East end, large (18") drop off to ditch. Hardrives will come back to fix. Also need to pull silt fence.

Steve O. and JP measured PALPS and JT opening on cells 5, 6, 13,14, early age PCC testing

Hardrives paved (3,B)mix on cell 87, 20% extra mix sunk into rock, 5 hour delay before paving porous agg came wet from quarry, had to run through the plant dry, then binder line clogged up, finally got running and paved cells 86 & 88. Paved 7-8" thick hot so that it (rolled rock behind trucks) would roll to 5" finished. Paved in 1 lift. Started rolling at about 220° F, still too soft, had to wait for 94° F on surface. Only 1-2 passes with large double drum steel roller (no vibration) very sticky, gooey mix with 70-28. Lots of samples for MnROAD.

Doug broke PCC beams on cell 5 (550 lbs) and cell 6 (435 lbs). Cell 6 is too low to run traffic and equipment on yet.

### **10/17/2008**

More instrumentation work on concrete cells by MnROAD crew

PCI poured other half of cell 39. Air content (by air pot) 6 to 8%, too low. Agg Industries staff on hand, they ran unit weight instead of air content came out ok. 2 different methods of 8 tests.

### **10/20/2008**

PCI poured outside lane of cells 85 & 89. Vibrating plate compactor cleaned up ruts from PCC trucks in agg base. Hand poured in forms, rolling compactor. Immediately after roller, special curing compound, tooled joints with pizza cutter, covered with white plastic, light hand roller to take out wrinkles. Inspectors ran unit weight (not air). Everything looked good.

PCI added agg shoulder (class 5) to cells 53, 14, 13, cleaned up shoulders around site.

MnROAD crews instrumenting concrete cells. Shrink wrap around exposed CE wires on cell 5. LVDT boxes on cells 53, 6

Saw cut flat edge along slab. Excavate gravel along edge, mark holes for boxed, hammer drill, anchors. Auger invar rod sleeves, install rods. Bolt boxes onto slab (each one is custom made).

Put covers on boxes (gasket and screws). Backfill class 5 around boxes and conduit connecting box to box. 30 boxes to install total.

### **10/21-24/2008**

PCI poured concrete shoulder on cell 53 Tuesday 3"x8'

PCI grading crew added class 5-agg shoulder to cells 5, 6, 13, 14, 39, and 53. Wick drains on cell 5.

7 drains on each side 75' apart, 15' wide on driving lane, 8' wide on passing lane. Daylighted to ditch, topsoil to cover.

MnROAD crews to install sensors in cells 85 & 89. LVDT boxes & invar rods in cells 5, 6, 13, 14, 53

Pervious PCC had trouble setting up. 1 beam crumbled when Doug S. tried to de-mold. Put other 2 in warm garage for another day, Could still move agg on surface- soft just like slab. Agg Industries (Tom Schmidt) said be patient and wait. After a 2<sup>nd</sup> day, slab and beams were cured well. AET got flexural strength of 400-500 psi at 3 days. Poured inside lane of cells 85,89 on Friday. Lane (?) around sensors Edge was solid. Metal flashing prevented chipping by screed. Cut retarder dosage in half on Friday. Again very good paving experience.

Japanese delegation (Intelligent Construction) visited MnROAD with Glen E., CAT, Sakai

### **10/28/2008**

PCI continued grading shoulders, filling in crossovers, sweeping

MnROAD crew raised LVDT boxes on cell 6 (forgot about 2" HMA overlay). Installed conduits and pulled lead wires.

### **10/30/2008**

PCI cleaned up gravel, crossovers, etc.

Hardrives here for last of HMA paving. 4.75mm mix on cell 6, Paved in (1) 2" 1.4 Dynatest HMA strain gauges (thinner profile). Marked joints with spray paint, will test FWD as a concrete cell. Very tough mix, everything went well. Paved 5% Mfr waste shingle mix on the rest, 10' outside shoulder and 4' inside shoulder (with shoulder machine). Lots of obstacles, PALPS bolts (covered up) LVDT boxes (taped screws and diesel fuel on covers) & IK wires and open conduits (taped tops) Paved ramps on cell 39 4" down to 2" (notch milled earlier). Paved cell 15, 14 transition. Tack along PCC edges on PCC pavement like "typical" MnDOT job. Also tacked (heavy) 100' on East end of cell 24 fog seal for aging study.

Sample buckets from cell 6 for MnROAD (30) UC Davis (56) and NCAT (15). Sampled shoulder mix from cells 5 & 6 (no cell 14 & 14 buckets)

NCAT here to observe cell 6 paving. took measurements for sound impedance, texture, and friction from several cells. Took 6 cores from cell 6 for lab permeability, rut testing

MnDOT made permeability measurements on cells 85-89.

Greg F. skid testing passing lane on cells 23-15 (ribbed, smooth). Will copy data for DL, should be same before traffic. Greg will finish testing tomorrow.

Painted transverse lines at start and end of each cell.

Drilled cores along ML & cell 24. Bob stuck TCs into HMA at appropriate depths. Filled all core holes with shoulder mix.

**10.31/2008**

PCI added millings to shoulder on cells 5, 6, 13, 14 Swept site to prepare for striping

MnROAD installed HCs in cell 5

General site cleanup; cores, barrels, plastic, conduit, garbage, etc.

Painted transverse lines at start & end of each cell

Sand patch on new PCC

Greg F. ran skid trailer around site

LVR inside rib            cell 24 to 27    missed 52

LVR O-rib                cell 27 to 24 – cell 37TS3 (left grind)

LVR I-smooth            cell 24 to 27

ML Driving-rib           cell 23 to 1     dirt on cell 5& 6

Low #s on new PCC, especially cell 5.

Cell 86- 8608BM031 PG64-34

8608BM032 PG70-28

\*\*\*\*\*End of Notes\*\*\*\*\*

### **Week of October 13 (Relevant Activity)**

PCI was on site Thursday to pave the outside lane of Cell 53 (60-year concrete). We had no sensors to place in that lane, so everything went smoothly on our end. PCI also filled in the hole they left on the West end of Cell 6. On Friday morning they paved the inside lane of Cell 39 (pervious concrete overlay). Staff from the CP Tech Center at Iowa State University were on hand to observe the paving. We had some sensors to mount as they were paving, but much fewer than we put on the Mainline last week. All in all, things went quite smoothly.

The most noteworthy activity this week was paving of the porous asphalt on Cells 86 & 88. The HMA plant had a number of problems getting started including drying the aggregate, cooling down the baghouse, and unclogging the binder line. Once they got those issues resolved and mix delivered to MnROAD, the paving went relatively smoothly. Hardrives paved the mat in a single lift in order to minimize compaction and the loss of air voids. The asphalt binder (PG 70-28) was heavily polymerized and quite sticky, which made handwork rather difficult. Both the contractor and MnDOT field staff had to shift our thinking. Normally we want to compact the mat well and get proper density. Here we needed to minimize the rolling effort so that we could maintain 18% design air voids and let rainwater flow through the pavement into the underlying base. In order to do that, the roller operator had to wait about 5 hours after paving to let the surface cool down to 94°F before he could roll it. The paver laid the mix at about 8" hot so that it would compact to 5" at the finished surface. At the end of the day the porous pavement came out looking quite good.

PCI was on site Thursday to pave the outside lane of Cell 53 (60-year concrete). We had no sensors to place in that lane, so everything went smoothly on our end. PCI also filled in the hole they left on the West end of Cell 6. On Friday morning they paved the inside lane of Cell 39 (pervious concrete overlay). Staff from the CP Tech Center at Iowa State University were on hand to observe the paving. We had some sensors to mount as they were paving, but much fewer than we put on the Mainline last week. All in all, things went quite smoothly.

The most noteworthy activity this week was paving of the porous asphalt on Cells 86 & 88. The HMA plant had a number of problems getting started including drying the aggregate, cooling down the baghouse, and unclogging the binder line. Once they got those issues resolved and mix delivered to MnROAD, the paving went relatively smoothly. Hardrives paved the mat in a single lift in order to minimize compaction and the loss of air voids. The asphalt binder (PG 70-28) was heavily polymerized and quite sticky, which made handwork rather difficult. Both the contractor and MnDOT field staff had to shift our thinking. Normally we want to compact the mat well and get proper density. Here we needed to minimize the rolling effort so that we could maintain 18% design air voids and let rainwater flow through the pavement into the underlying base. In order to do that, the roller operator had to wait about 5 hours after paving to let the surface cool down to 94°F before he could roll it. The paver laid the mix at about 8" hot so that it would compact to 5" at the finished surface. At the end of the day the porous pavement came out looking quite good.

## **APPENDIX G: MORE PICTURES**



**Figure G1: Grip Tester**



**Figure G2: Covered Cross drains showing Curb and Gutter Boundary**



**Figure G3: Cross Drains and Grating**



**Figure G4: Grip Tester**



**Figure G5: Cross-Drain Cell 88 and 89 Interface**



**Figure G6: Cross-Drain Cell 85/Cell 86 Forming and Placement**

**APPENDIX H: ADDITIONAL RIDE DATA FOR PERVIOUS  
CELLS**

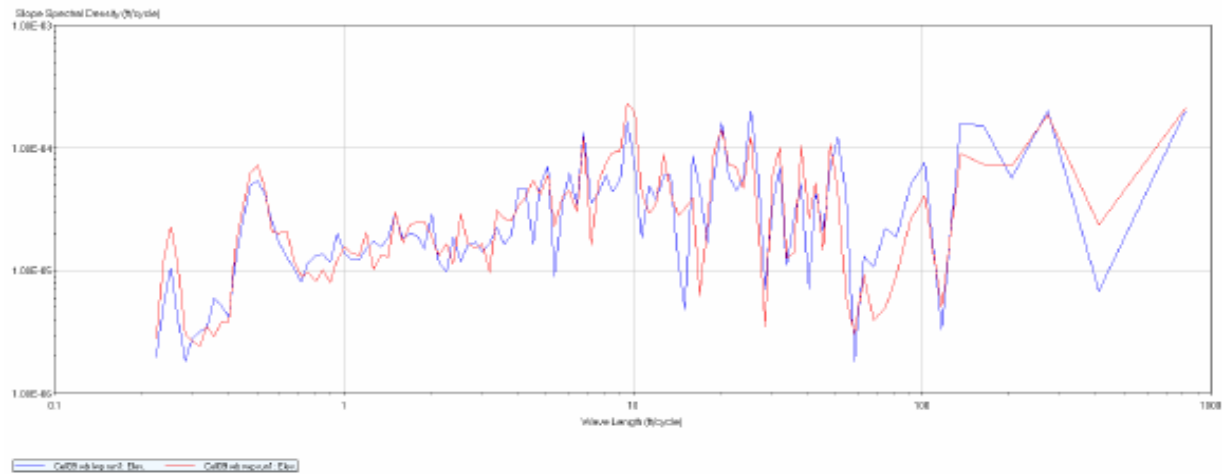
# MnROAD Low Volume Road Cells 39, 85, 86, 87, 88, 98

Pervious Pavements  
ProVal Analysis of April 2009 Data

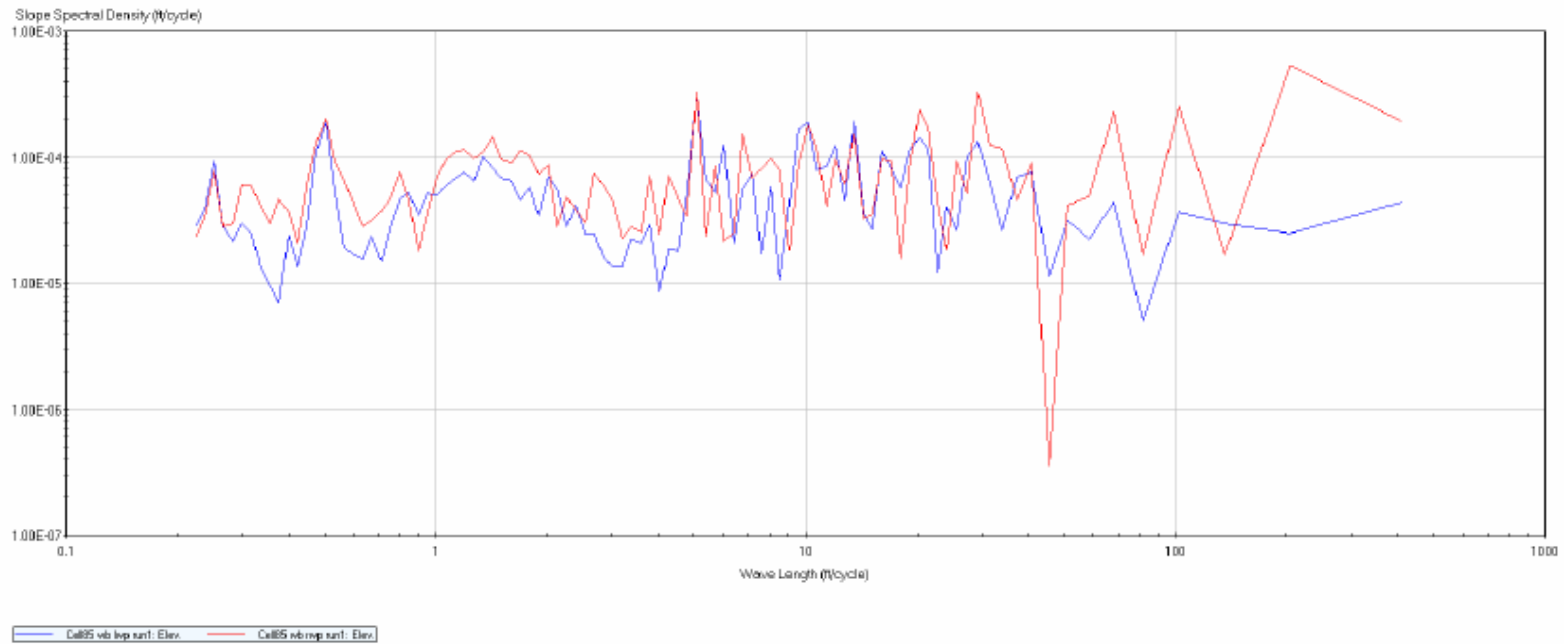
**Table H1: Porous pavement Ride Summary**

Cell	date	direction	wp	run1	run2	WP avg	Direction avg
39	9-Apr	eb	lwp	211.6	214.4	213.1	212.7
39	9-Apr	eb	rwp	208.5	216.1	212.3	
39	9-Apr	wb	lwp	227.5	227.9	227.7	233.3
39	9-Apr	wb	rwp	240.1	237.6	238.9	
85	9-Apr	eb	lwp	184.3	202.1	193.2	213.9
85	9-Apr	eb	rwp	235.4	233.6	234.5	
85	9-Apr	wb	lwp	253.6	255	254.3	261.3
85	9-Apr	wb	rwp	265.6	270.9	268.3	
89	9-Apr	eb	lwp	134.2	128	131.1	129
89	9-Apr	eb	rwp	127.9	125.9	126.9	
89	9-Apr	wb	lwp	213.6	202.7	208.3	172.6
89	9-Apr	wb	rwp	139.4	135.1	137.3	
87	9-Apr	eb	lwp	144.6	147.9	146.4	145
87	9-Apr	eb	rwp	146.1	141.2	143.7	
87	9-Apr	wb	lwp	126.6	162.7	162.9	147.4
87	9-Apr	wb	rwp	135.1	126.6	132	
86	9-Apr	eb	lwp	196	206.6	202.3	168.8
86	9-Apr	eb	rwp	134.4	136.3	135.4	
86	9-Apr	wb	lwp	194.6	188	191.3	177
86	9-Apr	wb	rwp	166	157.2	162.6	
89	9-Apr	eb	lwp	161.7	162.2	162	200.5
89	9-Apr	eb	rwp	222.4	215.7	219.1	
89	9-Apr	wb	lwp	241.7	235	238.4	262.5
89	9-Apr	wb	rwp	326.6	324.4	326.6	

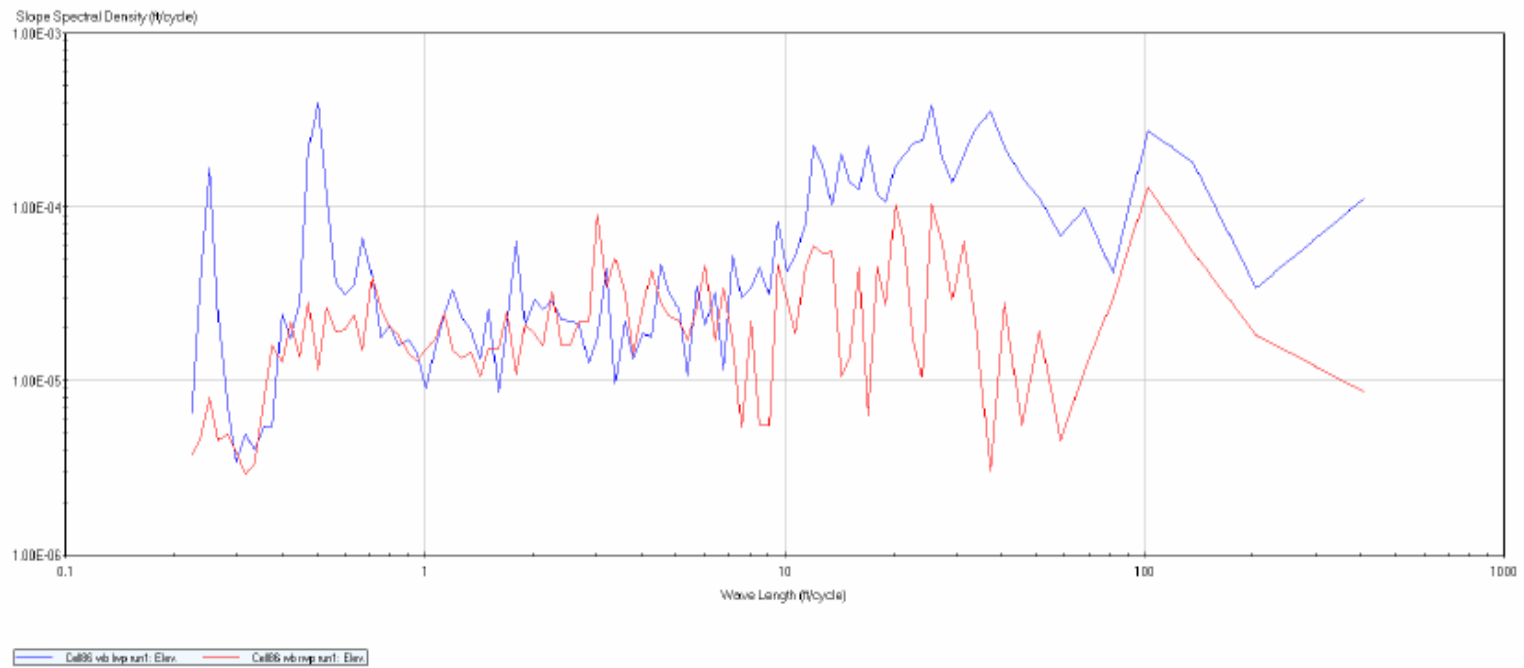
# Cell 39 PSD – 80K lane



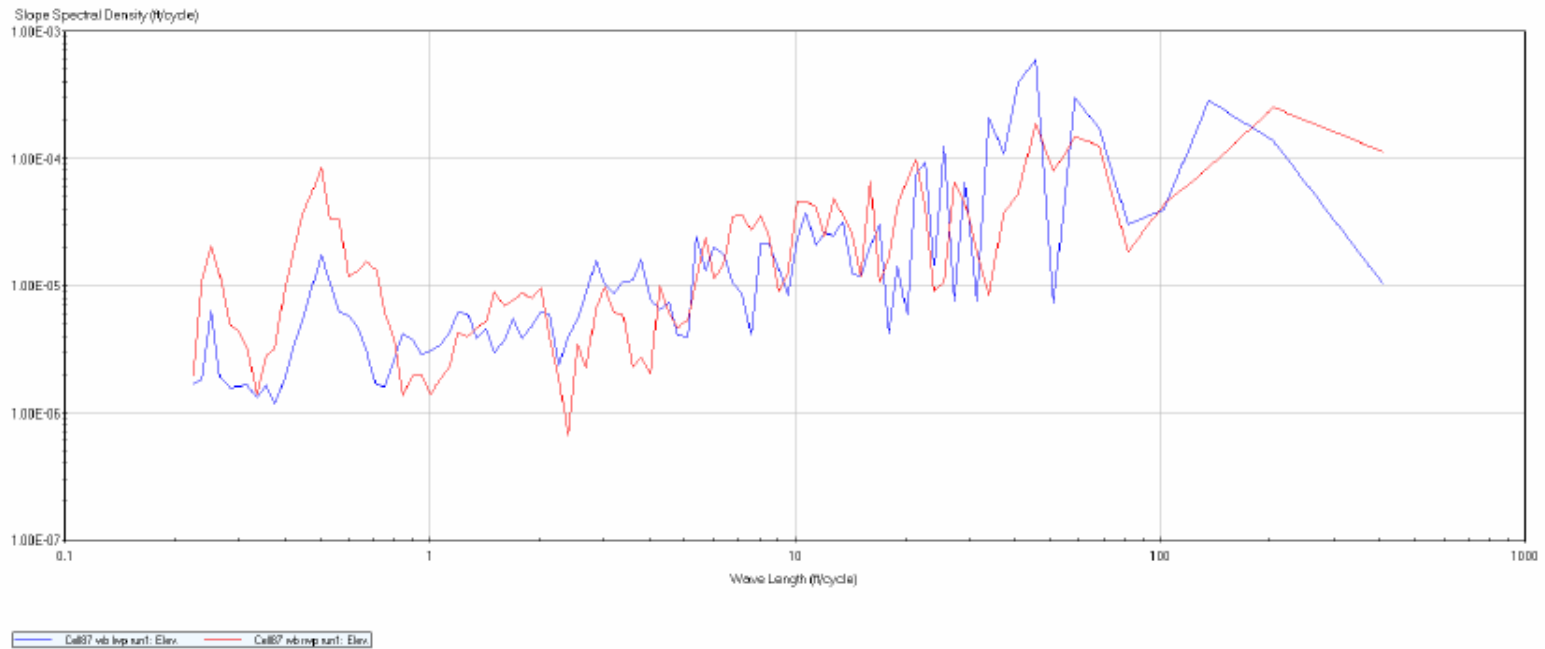
# Cell 85 PSD – 80K lane



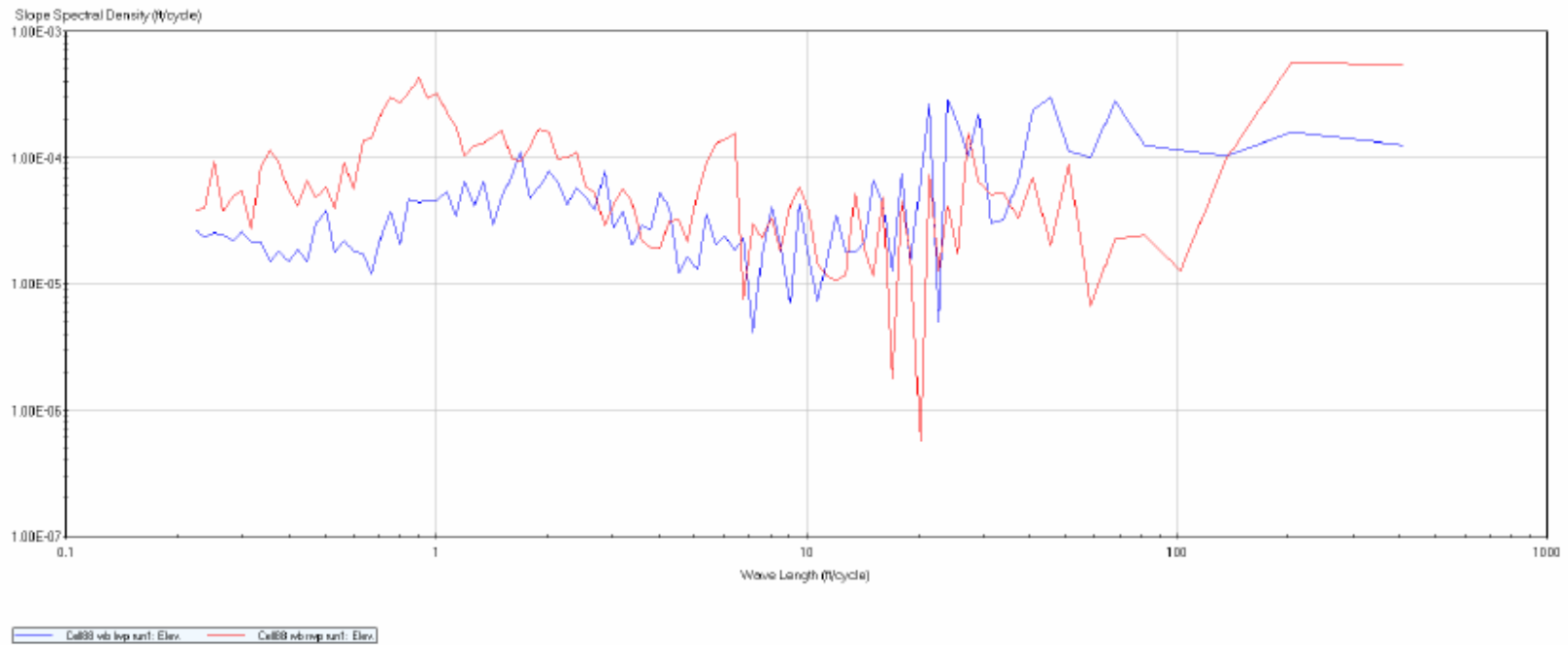
# Cell 86 PSD – 80K lane



# Cell 87 PSD – 80K lane



# Cell 88 PSD – 80K lane



**APPENDIX I: SA PLOTS WITH DATA FROM ALL  
EQUIPMENT**

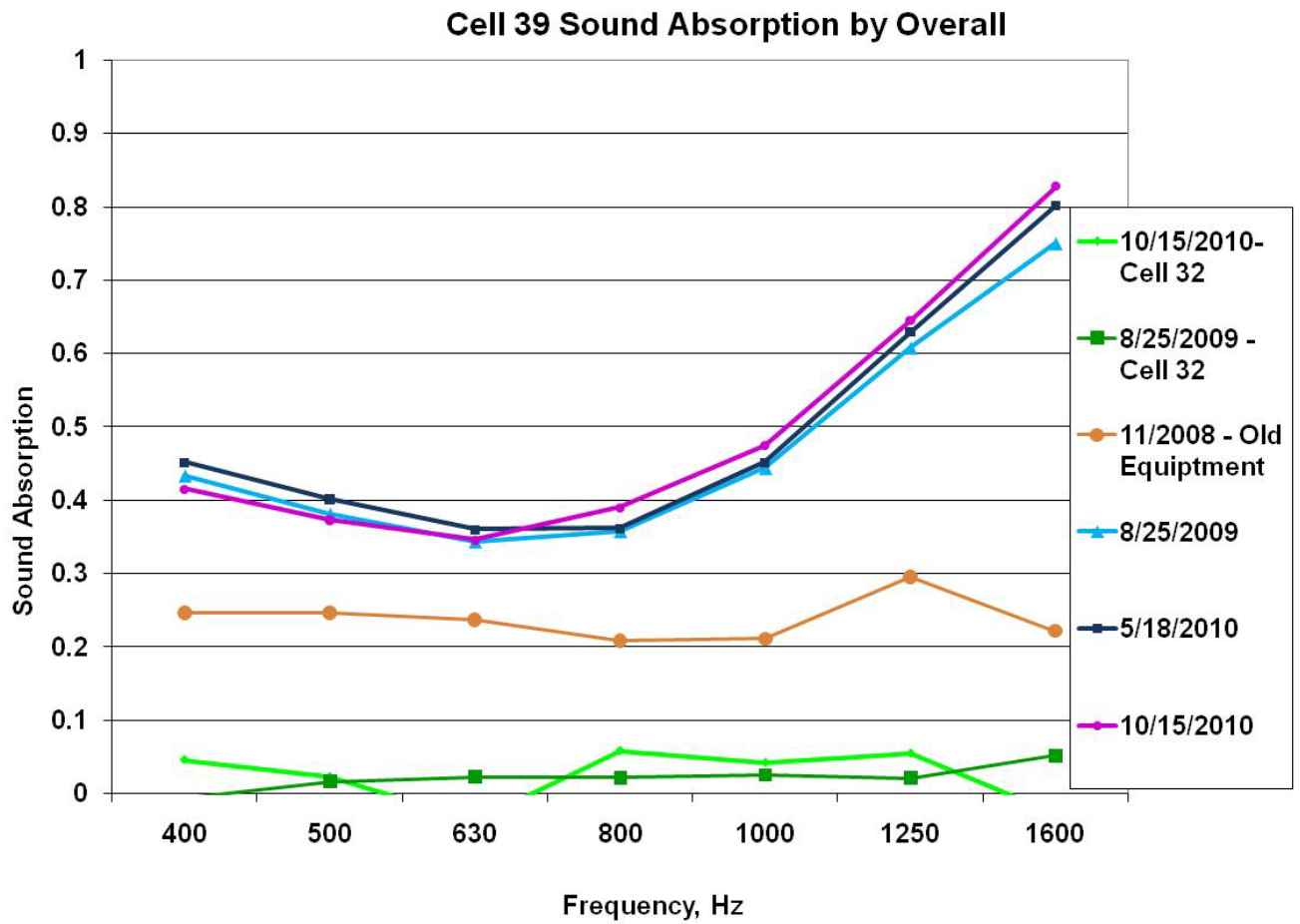


Figure I1: Cell 39 SA – All Equipment

### Cell 85 Sound Absorption by Overall

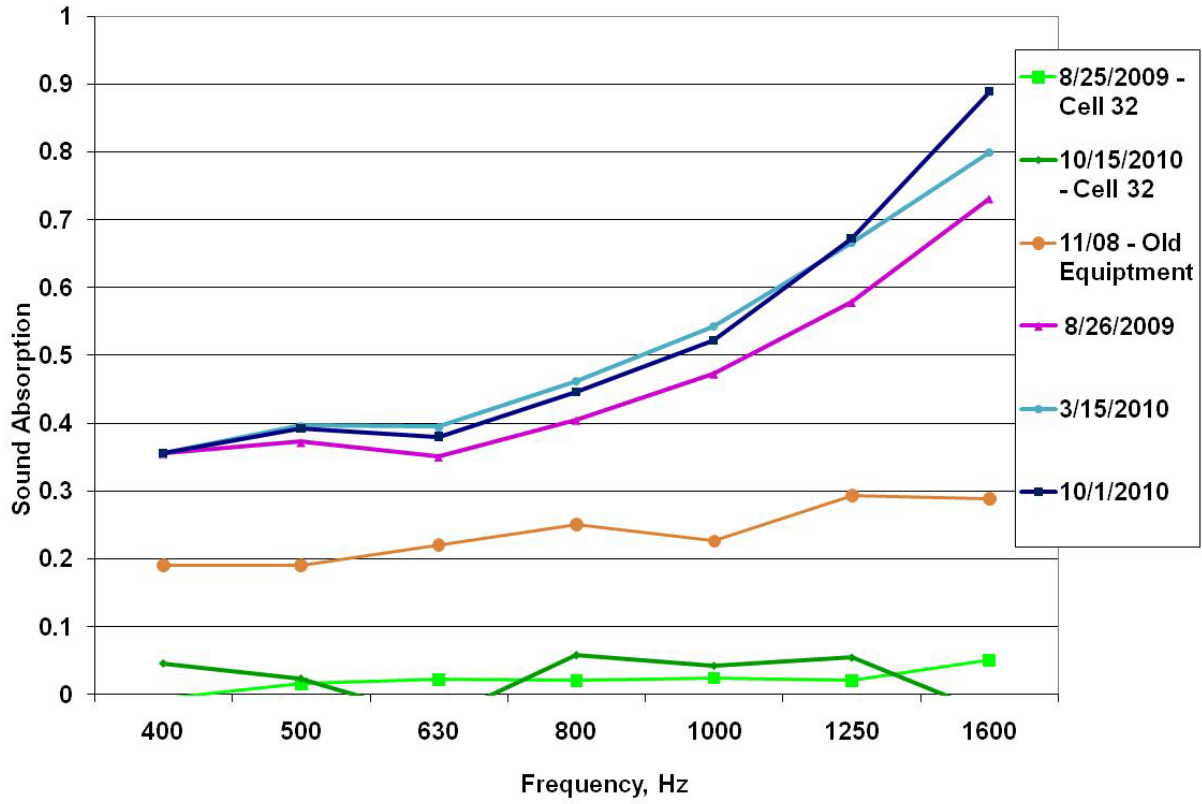


Figure I2: Cell 85 SA – All Equipment

### Cell 89 Sound Absorption by Overall

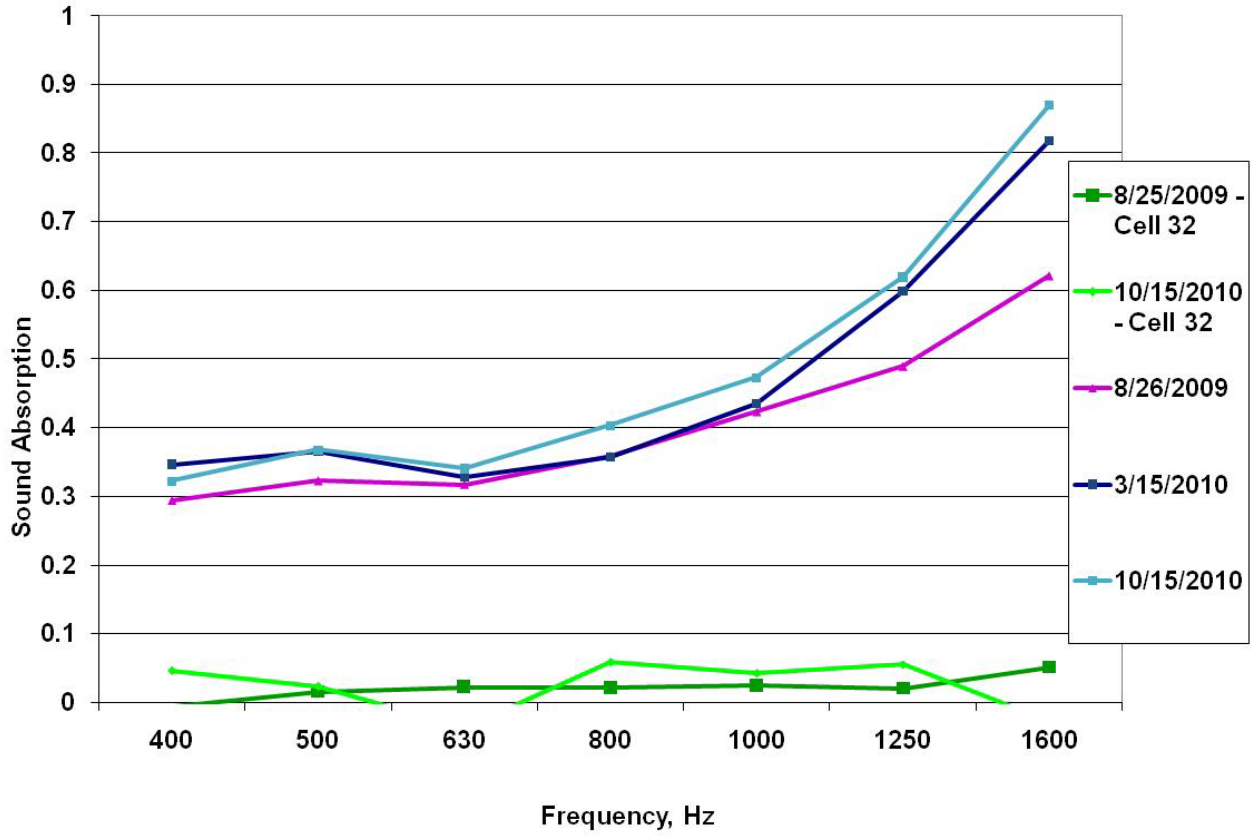


Figure I3: Cell 89 SA – All Equipment

**APPENDIX J: TIME SERIES PLOTS FOR SA DATA**

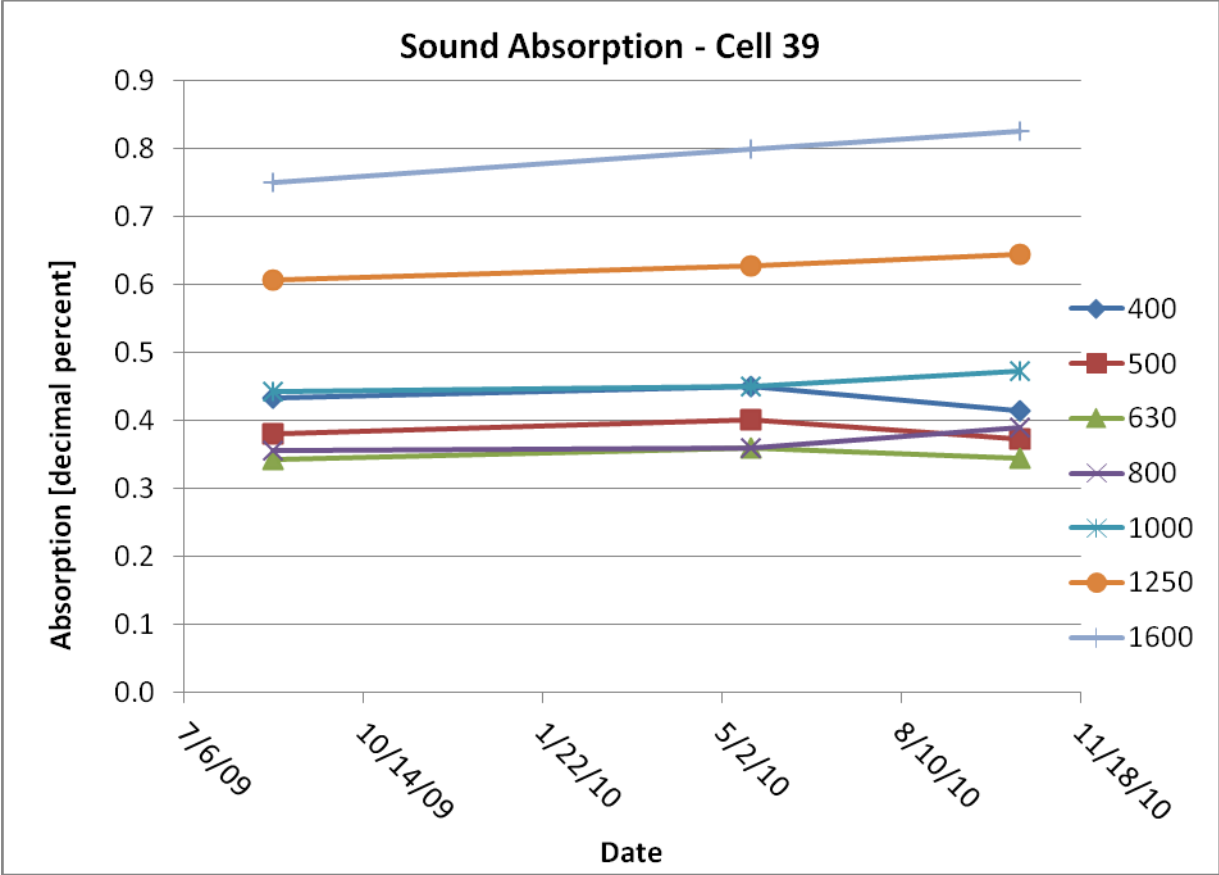
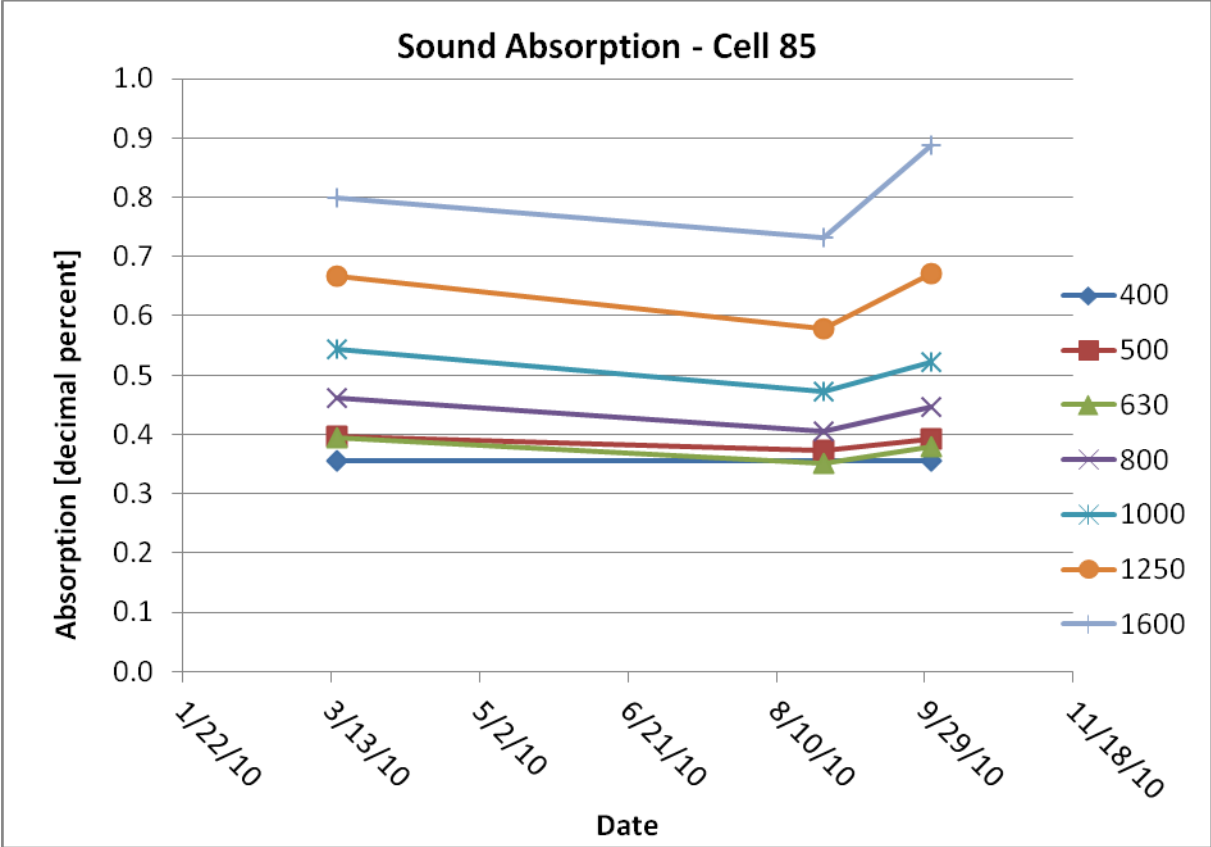
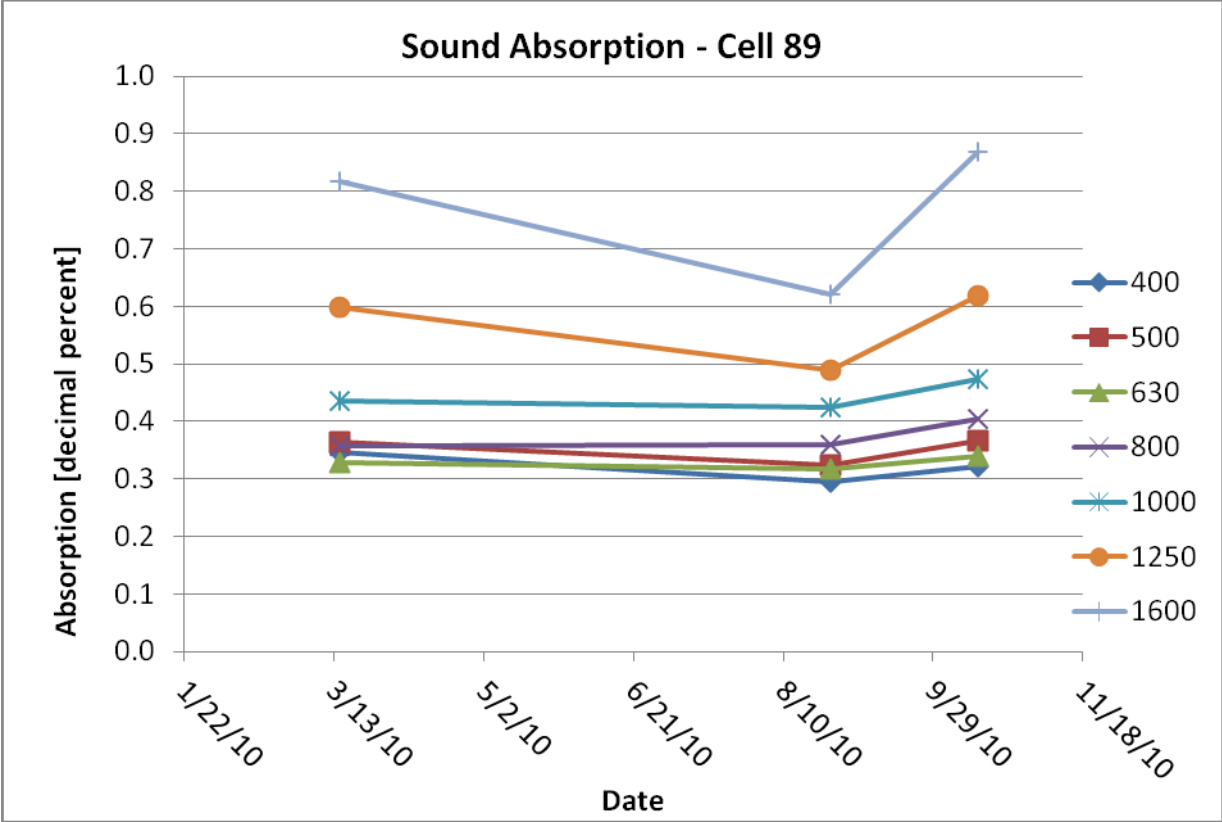


Figure J1: Cell 39 SA Time Series



**Figure J2: Cell 85 SA Time Series**



**Figure J3: Cell 89 SA Time Series**

## **APPENDIX K: RIDE CHARACTERISTIC DATA**

**Table K1: IRI Data**

Date	Inside Lane		Outside Lane	
	LWP	RWP	LWP	RWP
Cell 39 IRI				
4/2/09	3.43	3.41	3.66	3.84
6/30/09	3.53	3.47	3.68	3.94
11/18/09	3.44	3.67	3.80	4.19
3/9/10	3.58	3.59	3.78	4.12
6/24/10	3.87	3.74	4.02	4.32
10/13/10	3.69	3.68	3.86	4.03
Cell 85 IRI				
4/2/09	4.10	4.31	3.13	3.80
7/2/09	3.99	4.39	3.53	3.99
11/18/09	4.31	5.11	3.78	4.33
3/9/10	4.39	5.13	3.41	4.21
6/24/10	3.92	4.87	3.37	4.33
10/13/10	4.09	5.26	3.69	4.26
Cell 89 IRI				
4/2/09	3.84	5.23	2.94	3.52
7/2/09	3.99	5.47	3.00	3.48
11/18/09	5.09	6.72	3.60	4.37
3/9/10	4.97	6.68	3.29	4.81
6/24/10	5.14	6.76	3.33	4.37
10/13/10	5.28	6.84	3.14	4.47

**Table K2: SR Data**

DATE	Inside	Outside
Cell 39 SR		
27-Apr-09	3.8	3.8
28-Oct-09	3.8	3.8
12-Oct-10	3.6	3.7
Cell 85 SR		
27-Apr-09	4	3.8
28-Oct-09	3.8	3.8
12-Oct-10	3.8	3.8
Cell 89 SR		
27-Apr-09	3.8	4
28-Oct-09	3.8	4
12-Oct-10	3.7	4

## **APPENDIX L: NOISE CHARACTERISTIC DATA**

**Table L1: OBSI Data**

<b>Date</b>	<b>Cell 39 - Average OBSI</b>		<b>Cell 85 - Average OBSI</b>		<b>Cell 89 - Average OBSI</b>	
	<b>Outside</b>	<b>Inside</b>	<b>Outside</b>	<b>Inside</b>	<b>Outside</b>	<b>Inside</b>
3/17/2009	97.9	100.4	100.0	99.3	99.0	100.1
7/22/2009	97.6	100.1	99.4	99.1	98.2	99.3
9/15/2009	96.8	100.5	98.5	98.2	98.0	98.9
11/19/2009	100.8	101.1	99.8	99.5	99.4	100.1
3/15/2010	99.8*	101.89*	99.8	99.7	100.0	100.0
8/2/2010	98.1**	100.3**	98.7	98.1	98.5	98.5
9/17/2010	99.5	102.1	100.4	100.4	100.1	101.2
	* 3/8/10 **7/30/10					

**Table L2: SA Data**

Cell 32		
Frequency	8/25/2009	10/15/2010
400	-0.00625	0.0458333
500	0.0158333	0.0229167
630	0.0225	-0.0375
800	0.02125	0.0583333
1000	0.0245833	0.0420833
1250	0.0204167	0.0545833
1600	0.05125	0.0283333

Cell 39			
Frequency	8/26/2009	5/18/2010	10/15/2010
400	0.4329545	0.4511364	0.415
500	0.3806818	0.4015909	0.3728409
630	0.3429545	0.36	0.3457955
800	0.3570833	0.3610227	0.3894318
1000	0.4433712	0.4511364	0.4742045
1250	0.6076894	0.62875	0.6443182
1600	0.7501894	0.8005682	0.8271591

Cell 85			
Frequency	8/27/2009	10/1/2010	3/15/2010
400	0.3548333	0.3555	0.35525
500	0.3720833	0.39125	0.39575
630	0.3504167	0.37975	0.395
800	0.4046667	0.4455	0.46225
1000	0.4729167	0.52175	0.543
1250	0.5785	0.67225	0.66675
1600	0.7310833	0.8885	0.7995

Cell 89			
Frequency	8/28/2009	10/15/2010	3/15/2010
400	0.2945	0.32225	0.34625
500	0.32325	0.36725	0.365
630	0.31775	0.3405	0.32775
800	0.359	0.40325	0.35725
1000	0.4235	0.47275	0.435
1250	0.48975	0.619	0.59925
1600	0.6215	0.86925	0.818

**Table L3: SA Comparison Data**

	Cell 32 to 39	Cell 32 to 85	Cell 32 to 85
Frequency	8/25/2009 and 8/26/2009	8/25/2009 and 8/27/2009	8/25/2009 and 8/28/2009
500	24.04	23.50	20.42
630	15.24	15.57	14.12
800	16.80	19.04	16.89
1000	18.04	19.24	17.23
1250	29.76	28.33	23.99
1600	14.64	14.27	12.13

	Cell 32 to 39	Cell 32 to 85	Cell 32 to 85
Frequency	10/15/10 and 10/15/10	10/1/10 and 10/15/10	10/15/10 and 10/15/10
400	9.05	7.76	7.03
500	16.27	17.07	16.03
800	6.68	7.64	6.91
1000	11.27	12.40	11.23
1250	11.80	12.32	11.34

## **APPENDIX M: PHYSICAL PROPERTY DATA**

**Table M1: Nuclear Density Data**

Date	6/4/2009	8/4/2009	3/17/2010
Cell 39 (pcf)			
Lo 95% CI	116.3	117.87	104.28
Mean	120.33	120.92	107.51
Up 95% CI	124.35	123.98	110.74
Minimum	115	116.4	102.2
Maximum	128.4	125.1	114
Cell 85 Nuclear Density (pcf)			
Lo 95% CI	122.37	121.29	108.38
Mean	125.11	127.74	111.19
Up 95% CI	127.85	134.18	114
Minimum	120.9	112	105.5
Maximum	131.5	134.3	115.1
Cell 89 Nuclear Density (pcf)			
Lo 95% CI	119.65	118.89	106.16
Mean	122.6	123.75	108.46
Up 95% CI	125.55	128.61	110.77
Minimum	117.1	111.8	102.3
Maximum	128.9	129.4	111.1

**Table M2: Dissipated Volumetric Rata Data**

Cell 39					
Date	6/11/09	10/7/09	4/5/10	9/1/10	9/27/10
Number	9	18	10	3	44
Lo 95% CI	68.62	152.39	95.851	-1.6518	183.99
Mean	229.07	234.36	200.31	179.41	229.77
Up 95% CI	389.51	316.33	304.78	360.47	275.55
SD	208.73	164.83	146.03	72.886	150.58
Minimum	0.11	5.9	4.21	125.18	7.82
Maximum	698.04	586.36	398.52	262.26	714.92

Cell 89								
	9/19/08	7/24/09	10/7/09	4/5/10	9/1/10	9/16/10	9/29/10	10/12/10
Number	12	4	12	8	4	16	8	9
Lo 95% CI	160.83	-45.794	264.81	158.12	87.509	219.65	75.227	226.25
Mean	192.24	172.62	374.52	372.85	353.09	295.8	196.73	297.73
Up 95% CI	223.65	391.03	484.22	587.57	618.67	371.95	318.24	369.2
SD	49.44	137.26	172.67	256.84	166.90	142.90	145.34	92.99
Minimum	121.29	50.41	94.9	78.73	176.79	72.74	22.34	170.68
Maximum	257.24	317.43	576.16	650.3	525.88	579.91	379.31	415.1

Cell 85								
Date	9/13/08	6/11/09	10/7/09	4/5/10	9/9/10	9/14/10	9/29/10	10/12/10
Number	13	15	11	5	4	37	3	8
Lo 95% CI	241.57	391.79	409.36	473.55	77.411	256.03	178.03	186.2
Mean	339.71	470.55	545.29	699.96	198.86	369.11	458.46	338.33
Up 95% CI	437.85	549.3	681.21	926.37	320.3	482.19	738.89	490.45
SD	162.400	142.210	202.320	182.340	76.323	339.160	112.890	181.960
Minimum	170.51	286.29	197.99	491.53	96.67	49.94	347.03	165.99
Maximum	638.21	695.63	871.16	975.9	278.66	2174.1	572.75	609.85

**Table M3: Post Vacuum Data**

Location in Test Cell 39, 85, and 89	Difference in Sound Absorption Coefficient	Difference in Dissipated Volumetric Rate (cm <sup>3</sup> /s)
1	0.02	48.41
2	0	-36.66
3	0.065	7.87
4	-0.015	41.14
5	0	-43.08
6	-0.08	9.14
7	-0.055	-12.61
8	0.065	64.49
9	-0.02	4.91
10	0.015	118.71
11	-0.015	-1.06
12	0.06	-64.53